AD-A163 215 CORTICAL THOUGHT THEORY: A WORKING MODEL OF THE HUMAN GESTALT MECHANISM(U) AIR FORCE INST OF TECH WRIGHT-PATTERSON AFB OH SCHOOL OF ENGINEERING 1/5

UNCLASSIFIED R L ROUTH JUL 85 AFIT/DS/EE/85-1 F/G 5/10 NL

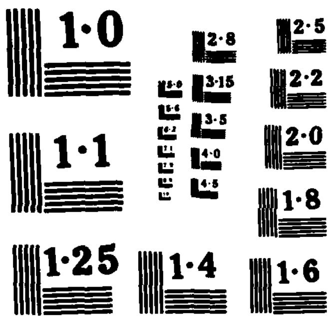

NATIONAL BUREAU OF STANDARDS
MICROCOPY RESOLUTION TEST CHART

CORTICAL THOUGHT THEORY: A WORKING MODEL OF THE HUMAN GESTALT MECHANISM

DISSERTATION

AFIT/DS/EE/85-1 Richard LeRoy Routh
Captain U.S.A.

DEPARTMENT OF THE AIR FORCE
AIR UNIVERSITY
AIR FORCE INSTITUTE OF TECHNOLOGY

Wright-Patterson Air Force Base, Ohio

AFIT/DS/EE/85-1

CORTICAL THOUGHT THEORY:
A WORKING MODEL OF THE HUMAN GESTALT MECHANISM

DISSERTATION

AFIT/DS/EE/85-1 Richard LeRoy Routh
Captain U.S.A.

AFIT/DS/EE/85-1

CORTICAL THOUGHT THEORY:

A WORKING MODEL OF THE HUMAN

GESTALT MECHANISM

DISSERTATION

Presented to the Faculty of the School of Engineering

of the Air Force Institute of Technology

Air University

In Partial Fulfillment of the

Requirements for the Degree of

Doctor of Philosophy

by

Richard LeRoy Routh, B.S., M.A.M., M.S.
Captain U.S. Army, Signal Corps

July 1985

Approved for public release; distribution unlimited.

AFIT/DS/EE/85-1

CORTICAL THOUGHT THEORY:
A WORKING MODEL OF THE HUMAN
GESTALT MECHANISM

by

Richard LeRoy Routh, B.S., M.A.M., M.S.
Captain U.S. Army, Signal Corps

Approved:

Matthew Kabrisky, Chairman	22 Aug 85
David A. Lee	29 August 1985
Stephen E. Cross	3 Sept 85
Robert W. Milne	27 Aug 85
Theodore E. Luke	29 August 1985

Accepted:

Dean, School of Engineering	3 Sep. 85

Acknowledgments and Preface

> "Every good thing bestowed and every perfect gift is from above, coming down from the Father of lights, with whom there is no variation or shifting shadow."
>
> James 1:17, NAS

A scientific work stands or falls on the basis of the verification of its hypotheses through repeatable experiments in a controlled environment. In addition, any derivations which lead to any of its hypotheses must be deductively, mathematically correct. If a scientific work does not meet these standards, then it is unacceptable regardless of the "good intentions" or the sincerity of its researcher(s). That standard, and no other, must be the standard against which this dissertation is measured. However, it is appropriate to acknowledge the significant source(s) of assistance in any research work. It is also useful to understand the motivation and perspective of the researcher (commonly the subject of the preface). In the case of this research, which has been attempting to find the answer to the very general and vague question, "How does the brain work?", the acknowledgments and the motivation and perspective of the researcher are so intertwined that they have been combined in this one section. Some will balk at what they are about to read, and some will become so overenthusiastic about it that, in both cases, there will be a tendency to prejudice one way or the other, the objective analysis of this research. Of both groups, I request that this scientific work, like any other, stand or fall on the basis of the verification of its hypotheses through repeatable experiments in a controlled environment and on the mathematical correctness of its derivations; it should not depend, in the slightest way, on the perspective and intentions of the researcher.

When I went to pick up my three-year-old son from his Sunday school class, he showed me a beautiful, full color, printed picture of trees, birds, people, rocks, and flowers, and exclaimed in great excitement, "Daddy, look! Look what I made!" I delighted in making a big-to-do over his great accomplishment, because I genuinely shared his joy in his artful creation, even though his part in its production amounted to nothing more than scotch-taping the pre-made colorful central figure to its pre-made elaborate, colorful printed background. My son did not consider the work of the teacher who cut out the central figure and tore off the piece of scotch tape. He did not consider the church secretary, the retail distributor, the design company, the U.S. Postal Service, or the hundreds of others who played a vital role in supplying him with the needed, finished materials. He did not consider the hours the artist, or the printer, put into designing and producing the colorful picture. He did not consider those who made the paper, or those who planted and cut the trees so the paper could be made, or those who supplied the tools and technology for cutting the trees and making the paper. He knew nothing of the thousands of years of the history behind man's search for the technology to produce colorful paints. He did not consider the dedication and the sacrifice of the thousands who trained, educated, and motivated those people who provided all these services. He did not stop to consider the God who created the very matter out of which all these tools and materials were made, who gave life to all those who contributed to the project, who lovingly and masterfully orchestrated all these efforts so that my son could "make" his picture, because my son had not yet learned that "every good thing...is from above, coming down from the Father of lights." Yet I know that that same infinite God has an even greater joy in my son's accomplishment than I did.

He tells us in His word that, "It is the glory of God to conceal a matter, but the glory of kings is to search out a matter" (Prov. 25:2). God delights in "concealing" things because He delights in the excitement of men when they find those things. We, as men, have the same attitude; that is why we wrap gifts when we give them -- the concealing of the gift adds surprise, and hence enjoyment for both the giver and the recipient.

In the same way, even though I have poured much of my creative energies and commitment, over the past few years, into the research presented in this dissertation, I am acutely aware that I have not done much more than scotch-tape a piece of the picture into place (and I expect that some will say I put it in the wrong place -- and they may be right). As I reflect on the efforts of the thousands of famous, and unknown, people who have been used by the Lord to lay the foundations, provide the support, and give the direction, encouragement, and motivation, which were all necessary for this work to be done, I am struck by the relative insignificance of my efforts. And yet this realization has not detracted from the delight and the awe that I have experienced over and over again throughout this research as another profound aspect of the purpose and design of the human brain came into view.

When the Lord Jesus Christ implemented the design of the universe at creation (see Collosians 1:16, or John 1:10), he did so in such a way that much of the beauty and profound awesomeness was concealed (or "gift wrapped"). Each of these concealed beauties reflects a different aspect of the character of God. As we unwrap each new gift, the thrilling awe we experience is because we see a new aspect of the glory of God. And in that turning of our attention to the Creator, we are glorified. That is the meaning of the verse which says:

> "It is the glory of God to conceal a matter,
> But the glory of kings is to search out a
> matter" (Prov. 25:2).

God has designed this search for the concealed beauties of creation, as a divine courtship in which our admiration of Him increases and His enjoyment of us increases. For these reasons, being involved in this search is a most thrilling, satisfying, and rewarding adventure.

It is important for us to remember that each of these divinely concealed matters reflects a part of the character of its Creator; in everything He does, there is a multiplicity of function and a singularity of purpose. This should not be surprising considering that even in His own person there is a multiplicity of function, but a singularity of identity. And each of His creations reflects His own nature. This results in the observation that one of the hallmark's of God's design of anything is that the more generally a matter is understood, the more simple is the statement of its complete expression; and conversely, the more its functions are explored, the more diverse its domain appears. For this reason, all of mechanics can be simply expressed as E = mv.

It is because this principle of creation is so evident that physicists are so expectantly pursuing the simple singular statement of the nature of matter, referred to as the unified field theory. It is also because of this understanding of the way God has created the universe that I have never for a moment doubted that the principle which underlies the function of the human brain at its most general level of description is simple and singular. Each of the constrained derivations of that most general principle of human brain function will be as simple as its constraints are broad. For example, the physical constraint that a system operates at non-relativistic velocities is very broad. It dictates that the time derivative of mass is negligibly significant, and, therefore, the derivation F = ma is a simple expression. (What could be a better picture of trading off the specificity of expression for the breadth of constraint than the Heisenberg uncertainty principle?)

Another example of this phenomenon is the existence of the four Maxwell's equations which represent the complete expression of the singular most general expression of electromagnetism -- but from the principle just stated, one suspects that each is a simple expression of the singular most general expression of electromagnetism which has been, in each of the four equations, broadly constrained in two ways. It follows then that the symmetry -- and completeness -- of the four equations is due to using two broad constraints and their complete complements to generate the four possible derivations of the single general electromagnetism expression.

Therefore, two of four foundational presuppositions of this research have been:

(1) The answer(s) to how the human brain works are as simple as E = MV and F = MA at the general level(s) of understanding, and

(2) It is the Lord's desire that we discover these answers through a diligent search process that recognizes the fact that we are searching for the blueprints of His design.

The third and fourth foundational presuppositions of this research are direct outgrowths of my personal relationship with God through the atoning mediation of His Son, Jesus Christ. God tells us that it is pleasing to Him for us to rely on the fact that "He is [He lives], and that He is a rewarder of those who seek Him" (Hebrews 11:6). In other words, He delights in supporting (making successful and not disappointing) those who rely on Him. I have learned that one very necessary part of relying on him is searching for the basic principles in His word and then taking them very seriously when they are found. This activity is characteristic of "those who seek Him." It is appropriate to note at this point that a reliance on the principles contained in the Bible does not compromise an objective scientific quest into the nature of the physical universe. It is encouraging to learn that the reliability of the Bible is intellectually supportable at a standard which is acceptable to any who care to review the evidence (regardless of their religious beliefs). (The interested reader is referred to the works of Josh McDowell, and then Francis Schaeffer, for the support of this statement.)

Therefore, the third and fourth foundational presuppositions of this research have been:

(3) I have relied heavily on the Lord to provide the direction and insights, through a diverse variety of people and events, which have been necessary to the successful progression of this research, and

(4) I have considered the great many references in the Bible to the purpose, function, and proper use of the human brain as inviolatible constraints on the form of the solution to the question: "How does the human brain work?" Some of the key principles (constraints) extracted from these Biblical references are listed as follows:

(a) There are two parts to the human mind: (1) the physical part (the brain), and (2) the spiritual part. I see no reason to doubt that the physical part can be characterized like any other physical system -- that is: it functions deterministically in accordance with simple physical principles which can be completely quantified. (This characterization requires the spiritual part to be able to generate physical inputs into the completely physical brain.)

(b) The physical part of the mind (the brain) performs a function which

(i) is designed to support (not control) the spiritual part of the mind. This leads one to suspect that its physical architecture is designed to elicit a function which is physically similar to the spiritual function. Navigation in the spiritual world is done by discernment which is the comparison of the spirit of a matter with the spirit of the prototype (God). Similarities are encouragements to be involved in the matter; dissimilarities are warnings to avoid the matter. Therefore, one expects to find the physical brain architectured in such a manner so as to be able to compare inputs to stored prototypes -- in order to be able to classify an input on the basis of its similarity to the stored prototypes.

(ii) The brain, operating apart from the spirit, is a blind system which lacks direction and therefore defaults to obtaining direction from its physical inputs. Since most people function in this manner (spiritually dead), it is reasonable to expect to be able to completely reduplicate their mental faculties with a deterministic, physical device.

(c) The more a person is exposed to something, the more he begins to conform to it (regardless of his intention to do otherwise).

(d) I suspected that the brain functions so as to compare pictures. This was suspected because God primarily uses pictures and their analogical comparisons in the Bible to convey new concepts to people.

There has come to be a great injustice in our society because we have forgotten that God defines the value of a person on the basis of his moral response to God, and not on the basis of his intellectual (physical brain) capabilities. It is an abominable thing to consider a human being as dead because his cortex has quit functioning. It is an abominable thing to consider a human fetus as inviable because it has not yet developed a fully functioning cortex. It is an abominable thing to consider one person as a more valuable human being because he has greater intellectual capabilities. I believe that God wants to remind us that the human brain needs to be understood as a simple, deterministic, physical device which no more houses the essence of a person than does his big toe. God has made it clear in his word that the quintessential value of a person is determined by his spiritual existence, not his mental abilities. The human brain was designed for the subordinate function of implementing in the physical world what was being communicated to it from God in the spiritual realm. When it is not functioning in this capacity, then it is either being misguided by lesser, malevolent spirits, or it is being driven bottom up by its sensory inputs (instead of top down by God's spirit). In either of these other two non-intended modes, the consequences are increasing inconsistency and malfunction of the system. (This is the subject and meaning of the eighth chapter of Paul's Epistle to the Romans.)

One way for God to remind us of this is to reveal to us, through solid and generally accepted scientific research, that the human brain is indeed a simple, deterministic, physical device; and that this device, in its entirety, is inadequate to explain all the phenomena which the human mind (not only brain) can elicit. Such a scientific discovery would most certainly have impact on the current social and legal trend to determine a person's value on the basis of how his cortex works. It is toward this end that this research is directed. This research does not pretend to accomplish the goal of completely defining the deterministic, physical functions of the human brain. It does not even claim to begin this search, because much fine research has already gone before this toward that accomplishment. This dissertation will provide a valuable new perspective which will have significant impact on how future research in the neurosciences is pursued.

This has been exciting research. Although it contains flaws and oversimplifications (at this point, no one knows its weaknesses better than I), as a whole, it is my hope that it will offer some valuable new insights as to how the brain works. I also hope that it will be a testimony of the faithfulness of the Lord in giving success to those who delight in, and meditate day and night on, His Word. I hope that others will see that He greatly delights in sharing His secrets with those who "believe that He is [He lives], and is a rewarder of those who seek Him".

I know that "every good thing bestowed and every perfect gift is from above, coming down from the Father of Lights, with whom there is no variation or shifting shadow." So I am particularly thankful to the Lord for giving me my wife, Edie, who has been used by Him to give much needed support and wise counsel throughout this research. I am thankful to the Lord for the tremendous honor he has given me by choosing for me the most capable person alive to be used by Him to advise me on this research -- that is, Dr. Matthew Kabrisky. I am thankful to the Lord for giving guidance and support to me in this research through people like Dr. David Lee, Dr. Rob Milne, James Holten, Robert Russel, Dan Zambon, and many others too numerous to all name here. I am particularly thankful to the Lord for providing me with such a conscientious typist, Sheryl Michel, who has worked very hard at producing high-quality drafts and final copies of this dissertation.

Richard LeRoy Routh
Dayton, Ohio
July 1985

Contents

ABSTRACT

This dissertation is addressed to the development of a new theory for an A.I. architecture. It is needed because of the requirement to have human-like recall. This dissertation addresses the shortfalls of previous theories and advances a new theory that attempts to integrate more of what is known from neurophysiology and perceptual psychology into a new approach. The theoretical necessity of using a computing machine which uses reasoning primitives of analogy as opposed to reasoning primitives of deduction in order to accomplish the real time integration of a human-adult-sized knowledge base into the semantic analysis process is discussed. The assertion is made that the primitives of analogy must perform input classifications and comparisons like the human brain if human-like reasoning is to be performed.

The systems approach was used to develop a new unified theory of human brain function called Cortical Thought Theory (CTT). The analysis integrates the disciplines of Artificial Intelligence, neurophysiology, perceptual psychology, and theory of computation, to develop the theoretical constraints which determine the form of the solution of the computing architecture which the human brain uses to process information. It was shown that the human gestalt mechanism is probably a singular mechanism of classification and comparison which is used in all domains and at all levels of abstraction of human information processing in the cortex. This gestalt mechanism is central to the operation of human memory access and human inferencing. Most significantly, it was shown that the cardinality of the gestalt feature

vector set is two.

This new computing architecture was implemented by simulation and used to process audio (speech) and visual (human face images) inputs. The results were shown to be psychologically compatible with human speech and image perception. A variety of human perceptual phenomena are accounted for by this new architecture. One of these was the prediction of a new class of audio-illusions which have since been synthesized and verified as true human audio-illusions.

When the CTT gestalt mechanism is integrated with the cortex association mechanisms hypothesized by Goldschlager, the result is a complete human-like information processing architecture capable of multiple levels of abstract human inferencing. It also accounts for the human characteristic of direct memory access to the desired information or inference. A natural language example is presented which illustrates how the sentence, "John shot the buck," can be unambiguously interpreted using a seven abstraction level CTT computing architecture.

The theory also identifies and accounts for the three types of human learning.

CORTICAL THOUGHT THEORY: A WORKING MODEL OF THE HUMAN GESTALT MECHANISM

1. Introduction

1.1 Definitions of "Artificial Intelligence" and "Gestalt Mechanism"

The engineering side of Artificial Intelligence can be thought of as being concerned with producing software which is capable of solving some specific problem that human experts can solve, without showing much regard for whether or not the method of solution is similar to that being used by the human expert. On the other hand, the science of Artificial Intelligence is concerned with discovering the algorithms which the human brain uses to classify its environment and then to compare these classifications to previous classifications of its environment in order to plan and direct actions which allow the human organism to change its environment. A more precise way to view this definition is to examine the concept which Elaine Rich [106] (certainly not unique to Rich) develops: "Artificial Intelligence is the study of techniques for solving exponentially hard[1] problems in polynomial time by exploiting knowledge about the problem domain." This definition of A.I. by Rich is so general that it includes both the scientific and engineering approaches to A.I. This dissertation is not concerned with

----

[1] An exponentially hard problem is one which appears to require exponential time to solve. By exponential time, Rich means that the time is proportional to K^N, where K is some number and N is the number of pertinent pieces of information in the database (or size of the input). Polynomial time is when the exponent is bounded (not allowed to increase with increases in N).

the engineering approach to A.I., but rather with discovering the particular implementations used by the human brain to process information. Therefore, the working definition for A.I. which will be used in this dissertation is:

> Artificial Intelligence is the study of how the human brain solves exponentially hard search problems in polynomial time.

It is evident that the human brain solves speech recognition/understanding, image analysis, natural language understanding, and knowledge representation exponentially hard problems in polynomial time. This reduction of the otherwise exponential nature of the search problem is so drastic that it provides for apparently direct (or at worst, deterministic) access to a single characterization of the environment or any subset thereof (Fahlman [36], Milne [85], Waltz and Pollack [126]).

This single characterization, referred to by Waltz and Pollack [126] as a "single interpretation" and also as the "universal will to disambiguate", is referred to traditionally in the perceptual psychology literature as the "Gestalt". Gestalt is the quintessential human identification of an object, or of a situation, or of an uttered word, or of a concept. Any event or environment which occurs at any level of abstraction in human perception can be given a single identification (name). The essence of the object which is necessary to elicit this single identification is the gestalt [60]. The human being has a preference to classify, compare, and, in general, to deal with events, concepts, and environments in terms of the gestalts of these events, concepts, and environments.

The algorithm which the human brain uses to arrive at these single names which characterize perceptual events will be termed the "gestalt mechanism."

1.2 Purpose and Scope

In conformance with the definition of artificial intelligence (as was just defined) this dissertation is concerned with discovering how the human brain does direct memory access. To do this, it seems necessary to find a gestalt mechanism which is mathematically reasonable, and which is, in perceptual psychological terms, indistinguishable from the human gestalt mechanism, and which is conceivably implementable by the human brain in accordance with what is known about the brain's neurophysiological structure and function (this is required by the definition of A.I.).

1.3 Standards

This dissertation proposes a new unified view of human brain function termed herein as Cortical Thought Theory (CTT). In compliance with the purpose and scope of this work, the following requirements have been met:

1. Mathematically, the gestalt algorithm is required to reduce input sets of very large cardinality to output sets of cardinality one (i.e. - the single name of the input). The gestalt mechanism must, therefore, exhibit a function which maps many sets into one set such that the many sets which will

all map into any given set all exhibit a similarity so obvious to the human observer that the human would easily identify them all as belonging to the same group. (This group name is then the gestalt of the group and is given the name of the output set of cardinality one.) Furthermore, this mapping must be group-wise invertible -- that is, given the gestalt of the group, a typical group member can be produced.

2. In perceptual psychology, it is common (as explained by Maher [78]) to experimentally measure the distance between perceived events by requiring a large number of human observers to assign a distance number to the difference of these events [78]. These distance numbers are then statistically analyzed in order to produce a mean and a standard deviation. A working model of the human gestalt mechanism should predict the same mean for every such experiment to within some acceptable measure such as a fraction of a standard deviation. The perceptual psychology standard, then, is that this model of the human gestalt mechanism must classify events so that these classifications are psychologically indistinguishable from the human classification system.

3. The neurosciences have compiled a vast set of experimentally observed phenomena which comprise, at best, a sketchy picture of the physiological structure and function of the human brain. Much data from experimental observations are needed, which are not yet available, in order to arrive at a clear understanding

of how the human brain processes information. This fact does not prevent significant progress now toward that end because many important clues have already been discovered. The nature of these clues, taken as a whole, form a set of constraints complete enough to estimate the reasonableness of any theory which purports to be a cohesive unifying explanation of the mechanisms by which the brain processes information. The standard for a unifying theory is that it explains previously apparently contradictory phenomena as the predicted result of taking measurements on the theorized system comprised of the operation of a few simple principles. For example, one such unification for which CTT seems to present is the simultaneous prediction of the Hubel and Wiesel [57] results and the DeValois [28,30] results. (These results are commonly considered to be apparently contradictory.) CTT shows how they are both consistent with a simple mechanism which operates to find the proper windows of visual field images in order to apply the gestalt mechanism for visual identification (described in Section 3.3.9 of this dissertation).

4. A second standard of interest to both perceptual psychologists and neurophysiologists is that this mechanism make at least one previously unmeasured prediction which can be experimentally verified. CTT predicts, among others, a new class of audio illusions. This prediction has been synthesized and verified at AFIT.

5. In order for CTT to be useful in the field of Artifical Intelligence, it should offer algorithms which are useful in explaining the structures used by the human brain to represent knowledge and the accessing of information in these structures in a manner which is direct and relatively effortless when compared with doing deductive inferencing within these same structures (this requirement developed by Fahlman [36]). It appears to do so. In addition, it suggests a new and interesting model for three kinds of human learning and also for the associational organization of the syntax and semantic interfaces of interest to natural language understanding.

1.4 Sequence of Presentation

The next chapter (Chapter Two) presents the motivation for the development of CTT from an A.I. perspective. Previous developments in knowledge representation structures and their inadequacies are reviewed. The overall systems characteristics of the human knowledge representation system are reviewed. An algorithm is proposed which meets the constraints posed by these human knowledge representation system characteristics. An example architecture, based on CTT, is presented which seems to be able to integrate several levels of syntax and semantic constraint in order to resolve the sentence "John shot the buck." The chapter concludes with a discussion on some of the implications of the new architecture as it relates to human inferencing capabilities.

Chapter Three presents the development of CTT from both the neurophysiological and perceptual psychological perspective. This chapter discusses the reasonableness of the proposition that the human cortex could be manipulating information in the manner prescribed by the CTT algorithm. A model is offered which describes the function of cortical columns which is needed to support the CTT algorithm. The literature of the two fields of neurophysiology and perceptual psychology is reviewed for the purpose of extracting a diverse set of constraints (comprised of the experimental findings of some of the most significant research in these areas). These constraints are used as the criteria for judging the goodness of the CTT model from neurophysiological and perceptual psychological perspectives. In addition, some discussion is presented which shows how this model might explain away the apparent contradiction of some significant experiments cited in the literature.

The fourth chapter is a detailed mathematical development of the CTT gestalt mechanism. This chapter demonstrates the bounds of performance of the algorithm used for extracting gestalt and discusses the mathematical reasonableness of the development of the algorithm.

The experimental verification of the CTT gestalt mechanism is presented in Chapter Five. The experimental verification includes the computer simulation which demonstrates that the high frequency roll-off of the visual contrast sensitivity curve can be explained as a result of the function which CTT ascribes to the cortical columns. Also included is the description and results of the simulation of part of the theorized functioning of the audio-cortex regions. (This simulation produced a speech recognition machine which behaves psychologically like the human word recognition system.) The third section of this chapter includes the prediction and experimental verification of the audio-illusions which were predicted by the CTT model. The fourth section reviews the preliminary results being obtained by Robert Russel at the Air Force Institute of Technology in follow-on research to this dissertation in which he uses the identically same software (algorithms) used in the audio simulation to perform human visual face recognition and to explain various optical illusions.

Chapter Six presents recommendations for the future development and applications of Cortical Thought Theory. Included in this chapter is a discussion of the current technological shortfalls which prevent a large human-like CTT system from being developed.

The conclusions and summary comments of this research are presented in the seventh chapter.

The appendices follow, which contain supporting discussions, pertinent software listings, and some of the computer generated data from the simulations (which were presented in Chapter Five).

2. The Artificial Intelligence Perspective

2.1 Introduction: Chapter Overview

This chapter addresses the development of a new theory for an A.I. machine architecture. It is needed because of the requirement to have human-like recall [Fahlman [36]). The shortfalls of previous theories of knowledge representation are addressed and a new theory is advanced which attempts to integrate more of what is known from neurophysiology and perceptual psychology into a new approach. The theoretical necessity of using a computing machine which uses reasoning primitives of analogy as opposed to reasoning primitives of deduction in order to accomplish the real time integration of a human-adult-like knowledge base into the semantic analysis process is discussed. It is argued that these primitives of analogy must perform input classifications and comparisons like the human brain if human-like reasoning is to be performed. The mechanisms for doing this human-like reasoning are stated in the form of a new computing architecture called Cortical Thought Theory (CTT). Its implementation and testing (by computer simulation) has been accomplished and is reported in later chapters of this dissertation.

2.2 The Problem

One definition of Artificial Intelligence says that A.I. is the pursuit of using knowledge about the problem to solve an exponentially hard problem in polynomial time (Rich [106]). It is evident that the human system does this (Rich [106], Manna [80], Routh [107]). The question which the science side of the A.I. community is asking is: "How does the human system solve exponentially hard search problems in polynomial time?" Cortical Thought Theory is seeking to discover the mechanism which the human system uses to reduce its exponentially hard search problems. This chapter begins by reviewing the A.I. literature to develop the assertion that any search strategy based on a sequential search algorithm (such as all algorithms which are run on a Turing machine) could not perform human-like reasoning in real-time. It is argued that a new approach to computing architectures, one radically different from the Turing approach, needs to be used. Since we are concerned with developing a mechanism (algorithm) which solves exponetially hard search problems in polynomial time the way the human brain does, it will be shown that the following appear to be required characteristics of the mechanism:

1. The mechanism needs to be able to directly or nearly directly access the particular data regardless of the size of the knowledge base.

2. It seems that the mechanism must be based on primitives of analogy which allow for human-like classification and comparison of sensory inputs - it must not be based on deductive logic primitives. (Primitives of deductive logic are the well defined constructs of first order predicate calculus. Primitives of analogy are the as yet unspecified basic constructs of inductive logic -- those constructs which, taken together as a set, comprise the mechanism(s) for doing human-like analogy.)

3. The classification mechanism is probably similar to a low pass two-dimensional Fourier transform of the information displayed on the properly windowed sensory input cortex surface (this assertion is developed in more detail in Chapter Three).

4. This classification is probably required to be reduced to a very small set (perhaps a single point) and then used for comparison simultaneously to all previous similarly classified sensory input data.

5. This information is then associated by the same mechanism (operating higher in the abstraction hierarchy) to produce single and immediate charcterizations of the semantic environment. This characterization is called the semantic gestalt and is probably analyzed with the same classification and comparison mechanism used at all other levels to recommend a prioritized list of inferences and responses which are the human appropriate inferences and responses in the situation.

6. This mechanism and its associated architecture should account for other characteristics of the human system such as trait inheritance (Quillian [103]), planning processes, expectation phenomena, and learning.

To be able to describe technically the mechanisms which account for these characteristics in the human brain is to be able to describe the blueprint of a significant subset of the operation of a human brain.

This operation description is independent of the medium of implementation. In other words, the chemistry and use of neurons is no more necessary to the human thinking process than feathers are to flight.

Keeping in mind that our aim is to describe the human gestalt mechanism and the system architecture which employs this mechanism to elicit human-like recall and reasoning, this chapter will begin by discussing the inadequacies of conventional approaches and conventional architectures.

2.3 The Inadequacies of Conventional Approaches

Slowly emerging from A.I. research is the realization that we probably have inadequate machines to solve the hard artificial intelligence problems which face us. What follows is a discussion which reviews the limitations which those in the forefront of A.I. research have discovered are hampering our progress. An analysis indicates that current computer architectures are fundamentally inadequate to address these limitations because they function with the primitives of deductive logic. Primitives of human-like analogy will be developed which are believed to be required to solve the problems which incorporate the semantics of a human-adult world-view.

In this discussion it will be established (through an analysis of a literature review) that:

1. Large semantic knowledge-bases (information in the knowledge-base necessary for semantic constraint) must be used to solve the artificial intelligence probl ms of speech recognition/

understanding (among others);

2. Turing-like (sequential boolean-logic-based) computing machines are fundamentally inadequate to be used for the purpose of integrating semantic constraints into the human information processing problems (such as speech and vision) if real time solutions are desired; and
3. No search-strategy/machine-architecture has yet been proposed which promises a solution to this problem.

It seems unlikely, in light of contemporary theory and technology, that it would ever be possible to develop the capability to organize and perform real-time searches of a semantic domain which models an adult human's world view (knowledge base). Probably the only thing that stands in the way of most of the A.I. community's accepting that it is an impossible task is that the human brain is an existence proof that it can be done. So, making the assumption that this capability can be realized with purely physical means, we press on looking for a solution.

Most researchers on the forefront of the quest for this solution would agree that it would make sense to mimic the mechanisms used by the human brain to solve these problems, if only they were known and could be fabricated non-biologically. Among these are: Schank and Riesbeck [111], who attempt to specify the structure of their theory of semantic knowledge-base organization on the basis of their best understanding of the human system; Fahlman [36], following in the footsteps of Quillian [102], [103], has abandoned the traditional approach of predicate calculus based (deductive logic) structures implemented on sequential processors in favor of a massively parallel spreading activation network which he reasons must function more like the human system than do the sequential processor based approaches; and Pollack and Waltz [99], [100], [126], who are attempting to incorporate the advantages that lateral inhibition offer (which they find present in the human system) into Falhman's spreading activation nets.

Unfortunately, science has not yet formulated even one theory of how thought (not just biochemically generated electric impulses) is processed at the neurophysiological level; let alone, how the human system builds a superstructure which incorporates the bits and pieces of what are already known from A.I., psychology, neurophysiology, neuroanatomy, and theory of computation, into one single coherent theory of how thought is processed in the human brain -- this is the purpose and scope of Cortical Thought Theory (CTT). Goldschlager [49] has recently proposed a very interesting, although severely limited, model which is the first theory of this type. His model is interesting principally because it accounts for the immediate association of the most pertinent information in the data base (memory). It is limited because in its present form it seems it can resolve only a relatively small number of concepts and apparently does not resolve abstract concepts well enough to allow for their use as fundamental concepts in building higher levels of abstraction.

CTT is based on the work of Kabrisky [59,60], Maher [78], and Ginsburg [47,48] which apparently identifies a successful approach for finding the gestalt (essence of identification) of human form perception. It incorporates the work done by Marcus [81], and Milne

[85], concerning the deterministic characteristics of the search strategies of hierarchically ordered syntax and semantic constraint spaces (Routh and Milne [108]) into the semantic structure prescribed by Schank and Riesbeck [111]. CTT is a theory which is consistent with the experimental data of neurophysiology, neuroanatomy, and psychology.

For the sake of gaining some historical perspective and understanding of the requirement to search large semantic domain knowledge bases in real time (which is a requirement for most advanced A.I. areas of interest), the following discussion considers the problem of developing a machine which types out text when the input is common spoken English.

2.3.1 One history of the semantic search problem:

Speech understanding is an area of study in artificial intelligence. Initially it was widely and apparently naively thought that a successful speech recognition machine could be built which was capable of typing common conversational speech by analyzing the acoustic characteristics of the speech signal. As progress toward the solution of a working speech recognition machine was made, the complexities of the problem became increasingly apparent. Gradually the speech recognition community became aware of the need to apply the constraints of syntax and semantics in the speech recognition. An example is the HEARSAY II system [34,70]. As speech recognition merged with the areas of linguistics and natural language to solve this very complex problem, the study of speech understanding emerged.

Milne [85] showed that during human analysis of English text the process of syntax constraint operated independently of any semantic considerations and appealed to the semantic levels of constraint only when there was insufficient information in the syntax to resolve the syntax ambiguities. This observation was implemented in the SPEREXSYS blackboard speech understanding expert system with encouraging results [107]. From that work, it was hypothesized that there exist three separate levels of semantic constraint hierarchically ordered above the syntax level in the human speech recognition system [108] as shown in Figure 2.1.

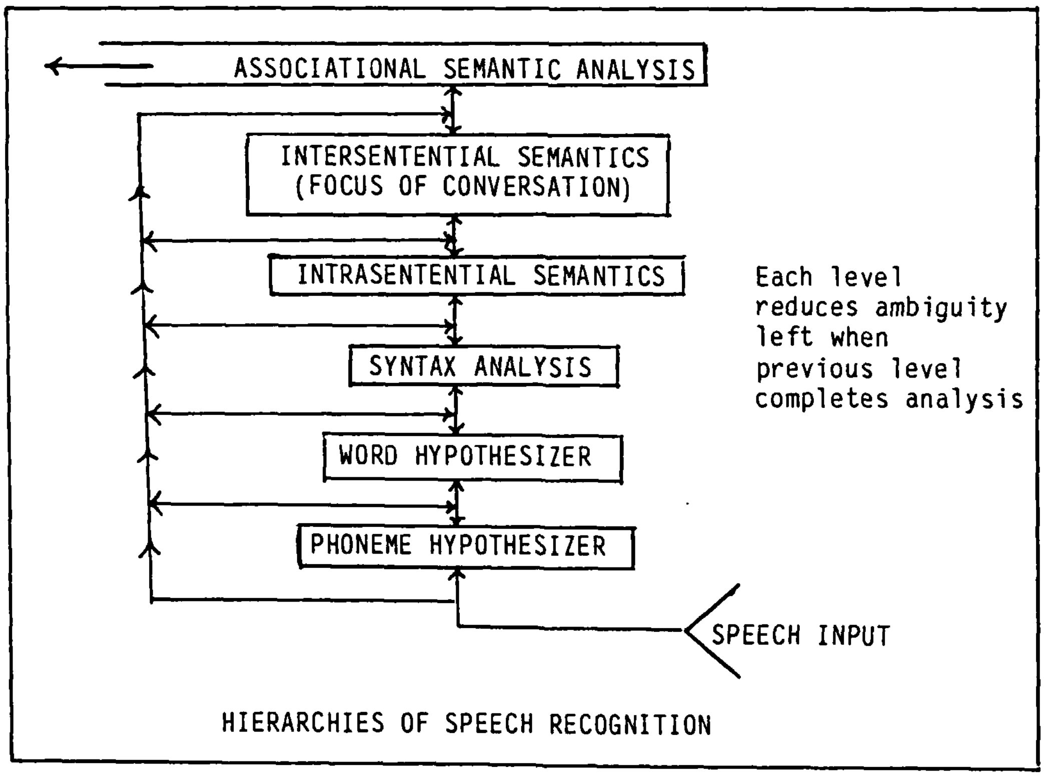

Figure 2.1

One of the conclusions of this work was that speech recognition/ understanding (for other than trivially small vocabularies and domains) is not possible without the application of all three semantic levels of constraint. Otherwise, there would remain ambiguities (which the human speech recognition system could resolve) which are unresolvable in the speech recognition/understanding process.

A similar conclusion had already been reached in regard to pure natural language problems. The following figure first appeared in the Bobrow and Winograd overview of KRL in 1976. They state, "A complete understander system demands the integration of a number of complex components, each resting on ones below, as illustrated in [the] figure" (Bobrow and Winograd [9, p. 1]):

TASK DOMAINS:
Travel Arrangements, Medical Diagnosis, Story Analysis, etc

LINGUISTIC DOMAINS:
Syntax and Parsing Strategies; Morphological and Lexical Analysis; Discourse Structures; Semantic Structures, etc.

COMMON SENSE DOMAINS:
Time, Events and States; Plans and Motivations; Actions and Causes; Knowledge and Belief Structures; Hypothetical Worlds

BASIC STRATEGIES.
Reasoning, Knowledge Representation; Search Strategies

UNDERLYING COMPUTER PROGRAMMING LANGUAGE AND ENVIRONMENT
Representation Language; Debugging Tools; Monitoring Tools

Figure 1. A layered view of a language understanding system

Figure 2.2 (From Bobrow and Winograd)

It illustrates the recognition (seven years prior to the SPEREXYS work) of the need for the complex interaction of large semantic domains in solving the natural language problems of speech understanding.

Fahlman [36, pp. 1,5] sums up his views on this requirement in the following way:

> The human mind can do remarkable things. Of these, perhaps the most remarkable is the mind's ability to store a huge quantity and variety of knowledge about its world, and to locate and retrieve whatever it needs from this storehouse at the proper time. This retrieving is very quick, very flexible, and in most cases seems almost effortless. If we are ever to create an artificial intelligence with human-like abilities, we will have to endow it with a comparable knowledge-handling facility; current knowledge-base systems fall far short of this goal... This impressive ability to store and access a large and diverse body of knowledge is a central feature of human intelligence. The knowledge-base system provides essential support for the other components of intelligence: the peripheral processes that handle such things as vision and speech understanding, and the linear, sequential, conscious kinds of thinking that characterize our problem solving behavior. The knowledge base is the common ground for these diverse elements, the glue that holds everything else together.

Milne argues that the search through this semantic knowledge-base (which is a model of a human world view -- from which we determine the sense, or common sense, of a proposition) must be either deterministic or direct, partially in order to function at the speed necessary for human speech communication. As will be shown here, this characteristic of deterministic or direct searches in real-time through the necessarily large semantic spaces is not possible with von Neumann-like (sequential boolean logic based) computing machines.

2.3.2 Semantic knowledge-base systems for sequential processing machines:

In an effort to build the semantic knowledge-base necessary to perform artificial intelligence tasks, knowledge representation systems such as Minsky's frames [86], Hawkinson's OWL [54], Bobrow and Winograd's KRL [9], Brachman, Ciccarelli, Greenfield, and Yonke's KLONE [11], Greiner's RLL [51], Hendrix's Partitioned Networks [55], and Schank and Riesbeck's Conceptual Dependency networks [111], have been built. All of these knowledge representation systems have three things in common: (1) They were all designed so they can be run on sequential processor machines; (2) They all were designed by researchers who understood the need to distribute knowledge in an ordered structure (as opposed to storing all knowledge explicitly) by relating various facts, concepts, and events through relational links; and (3) They all performed sequential searches by deduction (and sometimes analogy simulated with deduction) through this structure in order to find pertinent information which might help to solve the problem at hand.

Minsky saw the need to be able immediately to infer many key facts about a situation without being able to verify each of them. For example, when the words "living room" enter a conversation, one envisions a fairly large room (as compared to say a kitchen, bedroom, or bath) with some combination of different size sitting furniture arranged around the periphery of the room. A few small tables punctuate this sitting furniture. These tables are decorated with "knick knacks," and lamps appear on some of them. Near the center of the room is a large elongated table which is more sparsely decorated. One wall may or may not sport a fireplace. Pictures and other wall decorations hang on the walls at irregular intervals. One wall is predominantly decorated with a large window with drapes hanging from the sides. Some sort of carpet covers at least part of the floor. And on and on this stereotypical description goes. This all appears in a single memory structure called a frame and is diagramatically represented as is shown in Figure 2.3.

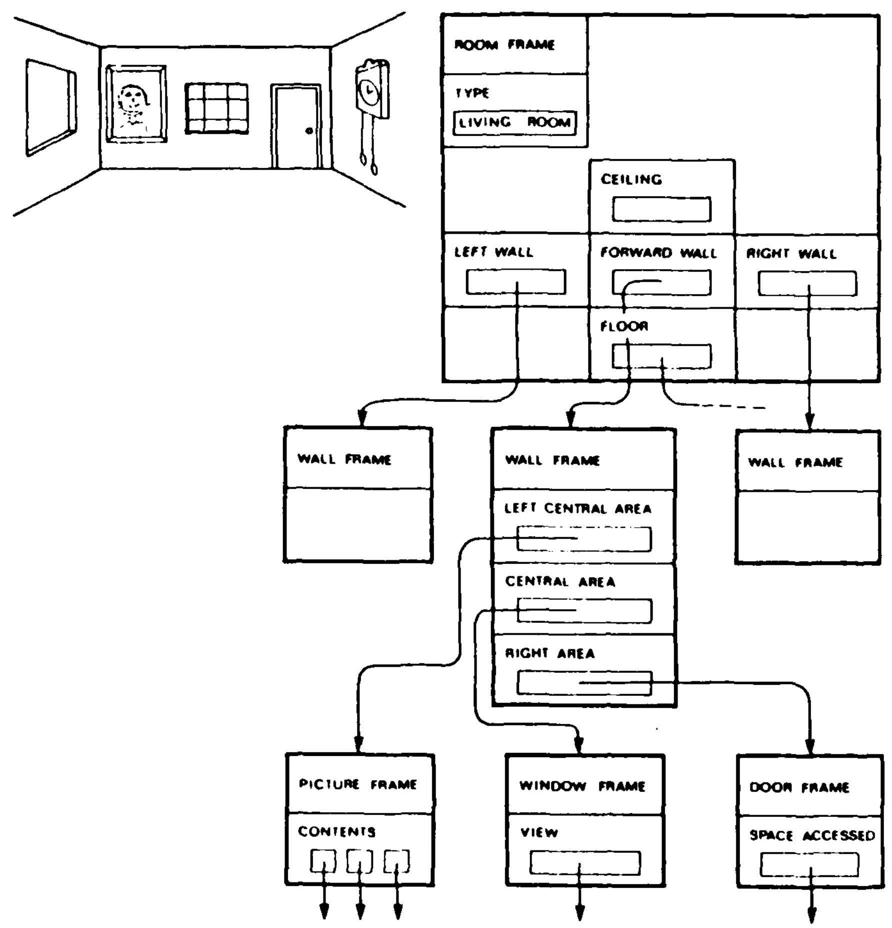

Describing a room requires many frames on many levels. Each frame could contain considerable detail.

Figure 2.3 (From Winston)

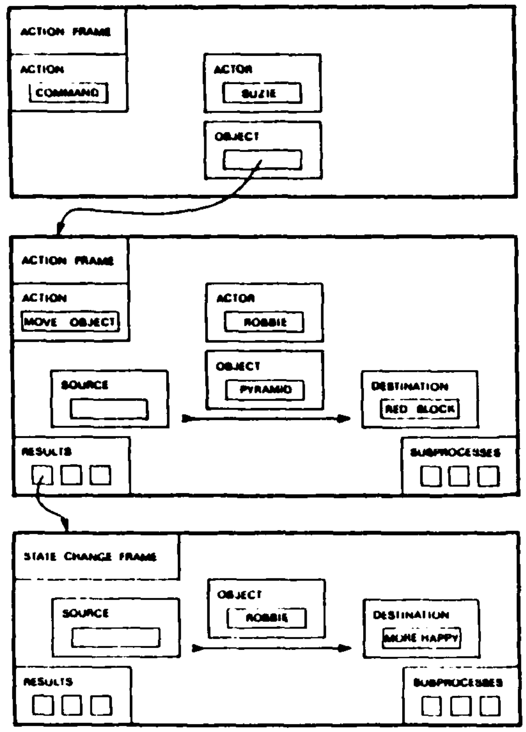

One act can cause another as when Suzie tells Robbie to do something

Figure 2.3b (From Winston)

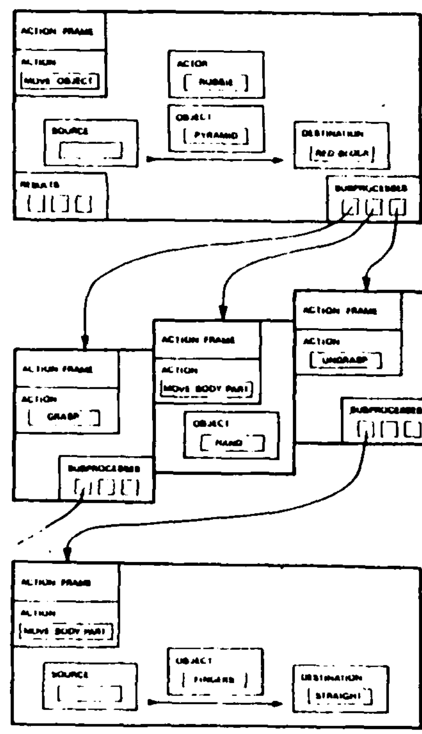

Subprocess slots offer another way of linking action frames together. This simple arrangement shows that moving a pyramid is ultimately accomplished by a sequence of body movements

Figure 2.3c (From Winston)

Note that each frame has a frame title and several slots which represent pieces of information which elaborate the character of the frame. There are object frames and action frames. Each slot is allowed to point to a separate complete frame. (And so large trees of frames can be built.) Each slot may contain a single piece of information and, in the absence of verified information, contains default information. This collection of default information (which was just previously listed for a "living room" frame) represents the generic essence (which will later be shown to be closely related to, but not the same as, the gestalt) of a living room. It is obvious that the common sense of many propositions can be determined by using trait inheritance deductions with such a structure. The problem arises in that one does not know how many levels (and their associated sub-branches) must be searched before all information, pertinent to the proper conclusion, is retrieved. As the knowledge-base increases in size, it can be shown that the number of structures which must be reviewed becomes unmanageably large in order to obtain real-time (for purposes of use in uninterrupted spoken conversation with a human) system response.

Hendrix's Partitioned Networks knowledge representation system is the richest and most versatile of a second type (although not really conceptually distinct from frames) of approach to building a knowledge base. It is the newest (and incorporates most of the advantages of the older ones) of the node-link structures which are also characteristic of OWL, KRL, and KLONE (KL1) knowledge representation systems. In the Partitioned Networks scheme, nodes, which denote objects (physical, conceptual, situations, sets, etc.), are linked diagramatically by arcs which represent logical relationships (such as element-of, subset-of, agent-of, object-of, theme-of, etc.). Hendrix offers a diagram to illustrate a simple representation which is reproduced here (Figure 2.4) [55, p. 5].

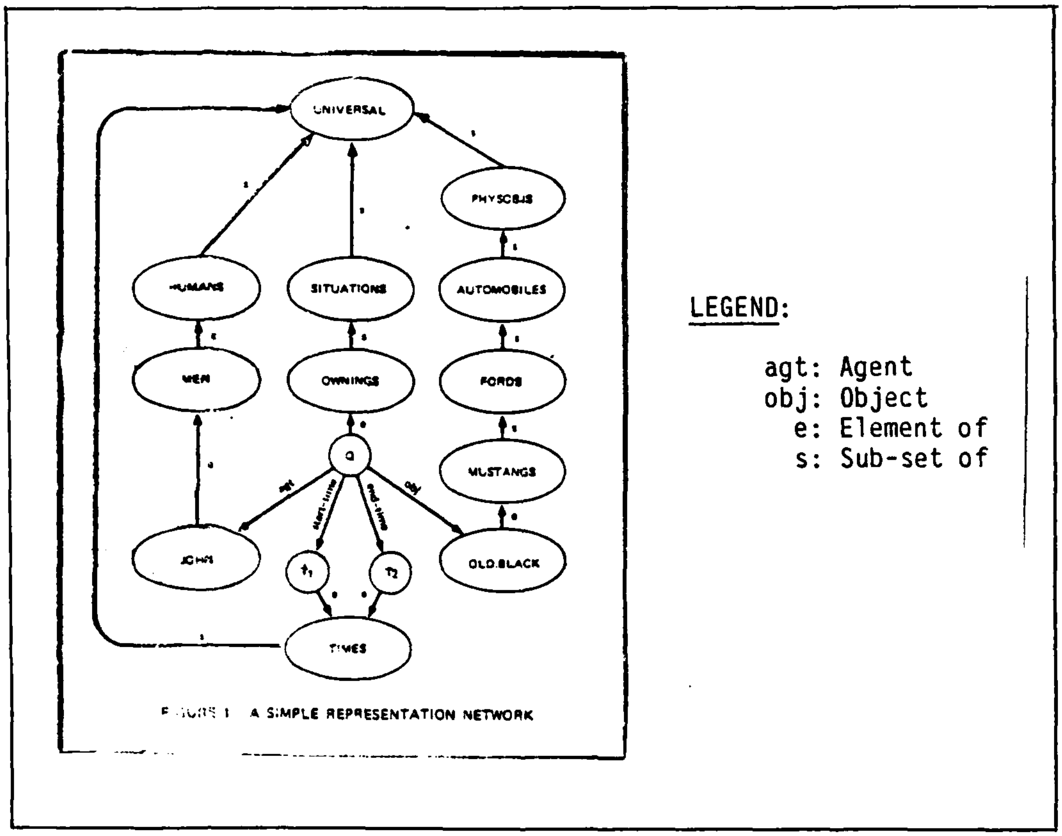

Figure 2.4 (From Hendrix)

He was able to represent certain types of information, such as disjunction and conjunction, quantifiers, and time, more adequately than some of the precursor systems. He accomplished these representations by explicitly storing this information as arcs which resulted in a a larger and richer set of arcs (links) than the other systems of this type. This gave his system more versatility than the others.

The old problem of deduction through trait inheritance was potentially still a very large search problem if the relevant knowledge base was large. A typical query on a very small knowledge base helps to illustrate the expanding nature of the problem (which increases with knowledge base size). This query: "What company built old.black" (from the previous diagram) is diagramatically shown in Hendrix and is reproduced here as Figure 2.5 [55, p. 9].:

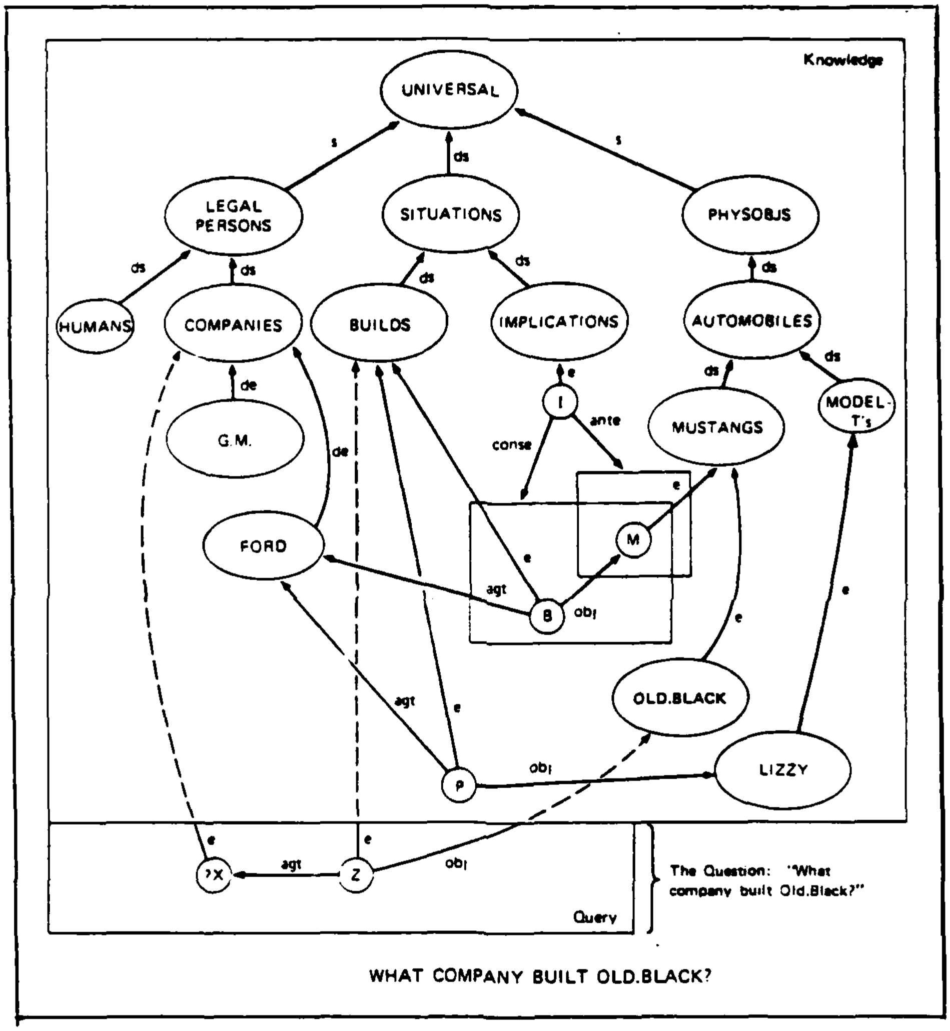

Figure 2.5 (From Hendrix)

The reader should note that the number of relationships (node-arc-node) which must be searched to answer a specific simple question increases significantly with the size of the pertinent knowledge base. The determination of what parts of the knowledge base are "pertinent" increases in difficulty with the complexity of the question asked. This characteristic is typical (universal) of all knowledge representation systems of this type.

The advent of RLL-1 was a simple, but useful, addition to the world of node-link structured knowledge base systems. In order to assure the advantages of all the foregoing systems of this type, RLL-1 used all of their techniques and buried them as RLL-1 primitives which the user could not directly access. Instead, the user constructed his own new node-link relationships by designing them through the use of "Type of Slots". These "Type of Slots" or "frames", as Greiner also calls them, define node functions and relationship characteristics declaratively (ultimately in terms of the primitives of the other subsumed systems). This allows the user to define his own semantics to be as rich or poor as any combination of the other systems' semantics will allow. This solution, although it offers the user a richer set of tools, only increases the complexity of the structure of the knowledge base. This increased complexity results in exponential increases in search times. Hence it is seen that this conceptual approach, although producing a knowledge base which is easier for humans to use, compounds (not solves) the search time problem.

The approach used by the aforementioned designers of node-link structured knowledge base systems has been to solve each new representation-type deficiency by inventing new mechanisms to augment the old systems. Schank and Riesbeck [111] have approached the problem from a more fundamental viewpoint. The result was the system, built on semantic primitives, known as conceptual dependency.

Schank and Riesbeck asked the question: "What is the smallest set of semantic relationships which can be used to describe every kind of relationship which might occur in English?" They found that if they used only the following eleven "primitive actions" that they could, from this set, describe many possible actions which can be expressed in English [111, p. 17]:

ATRANS	MTRANS	SPEAK	INGEST
PTRANS	MBUILD	GRASP	EXPEL
PROPEL	ATTEND	MOVE.	

ATRANS -- Transfer possession. MTRANS -- Mental transfer. PTRANS -- Physical transfer. MBUILD -- Mental build (learn).

They further found that all events have the same form which consists of the following four slots (although some may be implied or unknown) [111, p. 11]:

Every EVENT has:

an ACTOR

an ACTION performed by that actor

an OBJECT that the action is performed upon

a DIRECTION in which that action is oriented

(and potentially lots more).

Schank and Riesbeck further argued that events stereotypically orient themselves into rigid syntax structures called "scripts" from which expectation is inferred. "Plans" then become system-originated scripts to achieve "goals". Goals are the result of meta-plans to achieve "themes".

The drawback comes when these fundamental building blocks are implemented as a system on a sequential processor. The result is a hybrid cross between Minsky's frames and the more common node-link structure. And all of the disadvantages of these systems are then incorporated into the implementation of conceptual dependency.

2.3.3 The argument against knowledge-representation systems based on sequential processors:

Over the many years of research which were spent developing and working with these and other such sequential processor based knowledge representation systems, it became increasingly apparent that there was something fundamentally wrong with attempting to build a human-like knowledge representation system on a boolean logic based sequential processor. The larger these systems got, the slower they got. In fact, even with a relatively small knowledge-base (a few thousand structures) it became apparent that no search optimization technique would ever allow these systems to be able to operate in real-time (for communicating in normal conversation with a human being). This realization, in light of the fact that electronic device switching times are already about a million times faster than neuron switching times, gave rise to serious doubt that the human system was functioning this way and caused speculation that no working model with human-like capabilities could ever operate on a sequential processor based machine.

Further speculation and analysis began to focus serious doubt on ever arriving at a workable solution to this problem by using large numbers of boolean logic based processors cooperating in parallel. Minsky expresses his thoughts on this:

> Would parallel processing help? This is a more technical question than it might seem. At the level of detecting elementary visual [or any peripheral processing] features,... it is obvious that parallel processing might be useful. At the level of grouping features into objects, it is harder to see exactly how to use parallelism, but one can at least conceive of the aggregation of connected "nuclei", or the application of boundary line constraint semantics, performed in a special parallel network. At "higher" levels of cognitive processing, however, I suspect fundamental limitations in the usefulness of parallelism [86, p. 214].

It seems the basic problem is the use of boolean logic based processors. (Note: Even though the Turing theorem is probably applicable to this problem, Turing just guaranteed us it could be done; his theory makes no guarantees as to how long it would take.) We have become so engrossed in the digital world that for a moment we forget that there was once a host of very fast (at the cost of precision) differential equation solving machines, called analog computers, which knew nothing of boolean logic. This, of course, is only one example of an alternative computing logic. CTT introduces another.

Minsky's reservations are not unique. Pollack examines this problem and concludes:

> The processing of natural language requires the cooperative application of many kinds of knowledge, both language specific knowledge about word use, word order and phrase structure, and "real-world" knowledge about stereotypical situations, events, and roles. And even though these knowledge systems are nearly decomposable, enabling the circumscription of individual knowledge areas for scrutiny, it is not clear that this modularity can be extended into the realm of computation, that is, that a natural language processor can be constructed by serially conjoining a "syntax module" with various "semantic modules." Indeed, evidence is accumulating for parallel, integrated language processing in humans..., and some "integrated" computational models are being offered..., but, unfortunately, these are just top-down semantics-first processors.

Furthermore, Pollack claims that "binary [two-state boolean logic] and serial decision-making" machines are unsatisfactory for implementing the solution to this problem. An excerpt from his summary of this analysis is included here:

> The problem in integrating language processing, in making concurrent and cooperative decisions about syntax and semantics is that current computers do not like to! The modern style of computation, what Backus [1978] calls the "von Neumann" style, uses a strictly serial primitive operation sequencer, and this organization underlies the models which cognitive researchers offer. As Pylyshyn [1980, p. 124] points out:
>
>> Now, what is typically overlooked when we [use a computational system as a cognitive model] is the extent to which the class of algorithms that can even be considered is conditioned by the assumptions we make regarding what basic operations are possible, how these may interact, how operations are sequenced, what data structures are possible, and so on. Such assumptions are an intrinsic part of our choice of descriptive formalism...
>
> To build the kinds of integrated computational models needed for natural language understanding, then, the tacit assumption of binary and serial decision-making must be revoked [underlining Routh's] [pp. 1, 2].

Fahlman makes an interesting case for the inadequacy of sequential processors to be used in the building of human-like knowledge representation systems. He begins by illustrating the problem with an example which is included here because it so aptly reveals the magnitude and nature of the challenge which lies before us:

> Suppose I tell you that a certain animal -- let's call him Clyde -- is an elephant. You accept this simple assertion and file it away with no apparent display of mental effort. And yet, as a result of this transaction, you suddenly appear to know a great deal about Clyde. You can tell me, with a fair degree of certainty, how many legs he has, what color he is, and whether he would be a good pet in a small third-floor apartment. You know not only that he has eyes, but what they are used for, and what it implies if they are closed. If I try to tell you that Clyde builds his nest in a tree or that he is a virtuoso on the piano or that he amuses himself by hiding in a teacup, you will immediately begin to doubt my credibility. And you can do this very quickly and easily, with none of the sort of apparent mental effort that would accompany, say, adding two four-digit numbers. This effortlessness may be an illusion, but it is a compelling one [36, p. 4].

Not only is the human thinking apparatus capable of knowing a great deal about Clyde, but it appears that it is keeping track of the single most significant inference which characterizes the semantic environment. An informal experiment with about twelve people was done to help illustrate this. Suppose one is told only three facts: (1) Clyde is an elephant; (2) Clyde's eyes are closed; and (3) Clyde is very still. Normally, one will infer in the absence of further information, even without being asked, that Clyde is dead or asleep. If one is asked to "say something new about Clyde -- the first thing that popped into your head," one would usually say either Clyde is dead (most common response) or Clyde is sleeping (next most common response). (These two responses accounted for over ninety percent of the answers given.) Two things are significant here. Firstly, a <u>single</u> fact was inferred (there was a "first thing that popped into your head"). Secondly, the "new" response was not a general property of elephant, eyes, closed, or still. It was an inferred characterization of the semantic environment. It is very important to notice that the response does not produce statements like: (1) Clyde has flat feet; (2) Clyde has four legs; (3) Clyde has a tail; (4) Clyde has mammary glands; (5) Clyde's right upper eyelid is touching his right lower eyelid; or (6) Clyde's feet are not moving.

Fahlman goes on to elaborate on several characteristics of a system which is able to perform this amazing feat of semantically orienting Clyde. The remainder of this section is a summary and analysis of his arguments.

As Fahlman argues, when the search is concerned with deducing the relevance of particular details about a subject, it is important for this deduction process to not become cluttered with irrelevant, but associated, trivia (Clyde has flat feet, etc.). This, of course, implies a search strategy based on inference.

Once a complicated concept such as integration (in calculus) is built from large amounts of detail linked together with complicated inferences, this new concept is then bandied around (apparently effortlessly) as a single entity which is available as a building block for even more complicated concepts. But once this new conceptual entity is formed, the system must be able to quickly (and again apparently effortlessly) search through this new maze of detail for precisely the pertinent fact needed without being interfered with by all the other non-pertinent details. "If, hidden away somewhere, there is a sequential search for this [pertinent detail], that search is remarkably quick and efficient, and it does not become noticeably slower as the knowledge base expands to its adult proportions" [36, p. 5]. Since this search is required to find all pertinent data, and since the retrieval time does not increase noticeably, regardless of the size of the data-base, then one can conclude that a search method is not being used which looks at only one datum at a time. This conclusion is particularly striking when one considers that neurons have switching times on the order of one millisecond and electronic sequential processor computing machines have logical component switching times on the order of one nanosecond. Hence, the conclusion is arrived at which states that a boolean logic based sequential processor cannot be used to implement a real-time solution to the semantic search problem (remembering Minsky's comments on the unlikelihood of the suitable use of multiple parallel processors for this task).

Fahlman goes on to observe that the current techniques of forward and backward chaining search strategies, predicate calculus based systems, and the procedural approach to building knowledge-bases (such as frames, FRL, KRL, and so forth) are inadequate.

2.3.4 The insufficient results of other approaches:

Knowing the solution to the problem lies elsewhere (other than sequential processor based systems), Fahlman saw that it was necessary to abandon this classical A.I. approach in favor of some revolutionary new architecture. He opted to extend the Quillian work on spreading activation nets and developed NETL [36].

Falhman points out in his concluding chapter, there are still several "minor" bugs in the system, but he says, "Still, if there is a system-killer in this group of problems, it has yet to make its identity known" [36, p. 231].

The "system-killer" is NETL's inability to deal with conceptual gestalt (i.e., his system will not converge to a single environmental characterization). Not only does the human brain "classify" its sensor inputs in terms of the input's gestalt, but it also classifies entire concepts and questions in terms of their gestalt. This classification of higher level semantic concepts in terms of the gestalt of the concept is defined here as "conceptual gestalt."

The requirement to classify a concept (or query) in terms of its gestalt is evident in the fact that when we are told that Clyde's eyes are closed we infer that he is asleep (without any additional information). We do not infer, unless we are pressed to do so, a myriad of other equally plausible conclusions such as Clyde's right upper eyelid is now touching his right lower eyelid. However, if additional context is added such as, "Clyde has an infection on his right lower eyelid which causes him pain everytime his right upper eyelid touches it and our job is to relay the existence of this condition telephonically to the zoo veterinarian," and then when we are told that Clyde's eyes are shut, we may indeed infer that Clyde's right upper eyelid is now touching his right lower eyelid. What is significant here is, that in each case, <u>only</u> <u>one</u> conclusion was reached. It is the conclusion for which the conceptual gestalt most closely matches the conceptual gestalt of the semantic environment after the new information is added. Since the background information is different in each of the above two situations, a different conclusion is reached for each situation given the same piece of new information. Fahlman's NETL will not consider conceptual and situational gestalt in looking for the single most significant inference given the new information. It is therefore insufficient for searching a semantic knowledge-base in a human-like manner.

Although Pollack's and Waltz's work is interesting in that it seeks to reduce the number of intersections remaining after a search by employing lateral inhibition, it also falls short. The main problem is that it does not minimize those intersections based on conceptual gestalt.

2.4 Recapitulation

By employing a literature review to examine the problem, it has been established that:

1. In order to do speech recognition/understanding, it is necessary to incorporate human adult semantics (world view) in the process.

2. In order to incorporate real time human adult semantics in speech recognition/understanding, it is necessary to have human-like recall (rapid access to the most significant information in the knowledge base).

3. Human-like recall cannot be implemented using a sequential boolean based processing scheme.

Hence it is established that speech recognition/understanding, in real time, is not possible if the algorithm to do so is implemented on a sequential boolean based processor. (The obvious exception to this argument is speech recognition/understanding using a very small vocabulary and limited semantics based on a restricted small-domain world-view -- but this is not considered to be adult speech recognition/understanding and therefore is not included in the scope of this discussion.

The foregoing argument is not a proof, nor is it intended to be. Its conclusion is being believed by a growing number of researchers involved in the arena. It is presented here only to serve as a background for the following discussion which attempts to identify the fundamental weakness of these past approaches and to outline the solution to overcoming this weakness.

2.5 The Nature of the Proper Solution

Primitives of deduction or analogy?

There seems to be only three fundamentally different approacnes to arriving at a conclusion to a problem. These are: (1) deduction, (2) analogy (the mechanism for doing induction), and (3) revelation. When one thinks of reasoning logically to a conclusion, one normally thinks of deductive logic. This is the realm of first order predicate calculus, boolean algebra, etc. Indeed, when one asserts that an argument is illogical, one normally means that the argument has violated some commonly accepted premise of deductive logic. Deductive logic is the sequential application of "logical" rules on nodes of information (or facts).

The second approach to arriving at a conclusion to a problem is through the use of analogy. Analogy is commonly considered to be an inferior approach (when compared to deduction) because experience tells us that conclusions reached by analogy are not as reliable as conclusions which are reached through deductive processes. The use of analogy does not include any consideration of the sufficiency of information required to arrive at a reliable conclusion. An example will help to illustrate this. If one is shown a box with a door on which is painted a yellow stripe and inside the box is found a live cat, then one is shown a second box with a yellow-striped door, analogy allows one to conclude that there is a cat inside the second box. Experience warns us about trusting that conclusion if only one previous example has been seen. But if 500 consecutive such previous examples had been presented, we would be more inclined to trust the conclusion. On the other hand, even with one million consecutive identical examples, deductive logic would refuse to arrive at that conclusion on the grounds that insufficient information was presented.

The third approach to arriving at a conclusion to a problem is through revelation, or obtaining the answer from sources outside the system. A consideration of this approach is beyond the scope of this discussion. It is mentioned here for completeness.

Modern technology would probably not have developed (at least as soon as it did) if reasoning by analogy were always used. Aristotle reasoned by analogy to conclude that a ten pound ball falls to the ground ten times faster than a one pound ball. We would not advance very far with that kind of science.

It is important to note that the characteristic which prevents a sequential boolean based computer from solving, in real time, the human-like recall problem is also the fundamental characteristic of deductive logic. That is, it has already been shown in this discussion that human-like recall cannot be done in real time if it is to be implemented by performing operations sequentially on isolated facts. It should have become apparent by now that since deductive logic is the sequential performance of operations on isolated facts, then it follows that human-like recall cannot be done in real time using deductive logic. Therefore, we have challenged ourselves with a technological problem (build a speech recognition/understanding machine) which cannot be solved with the reasoning processes which have been used to build our technology. The philosophical considerations which grow from this conclusion are fascinating, but they are beyond the scope of this discourse.

The following situation presents itself: the initial assumption has been made that this speech recognition/understanding capability can be performed with entirely physical mechanisms, but these mechanisms are not allowed to work according to the traditional rules of deductive logic. Only one conclusion can be drawn if our initial assumption is correct -- the reasoning primitives for accomplishing this task must be primitives of analogy, not primitives of deduction.

Therefore, in order to solve the speech recognition/understanding problem, a computer which reasons by analogy, rather than by deduction, must be developed. Furthermore, since analogy relies on mechanisms of comparison in order to arrive at conclusions, it is most likely necessary to compare the same sorts of things (features) in this new computer which the human system compares.

2.6 In Search of Gestalt

Computations based on primitives of analogy must be concerned with finding the gestalt classification mechanism of the computing system. To hear the word "bird", one must first know what to extract from the acoustic event before one knows that the word "bird" is the consequence of the extraction. Researchers working on the speech recognition problem over the past thirty years have discovered that the number of features which can be extracted from a single utterance of "bird" is infinite. The question then arises: "Which finite subset of this infinite set of features is being extracted by the Human Speech Recognition System (HSRS)?" Without knowing the essential features which must be extracted in order to do the comparison (which analogy requires) between the received utterance and the stored vocabulary (these essential features are referred to as the gestalt of the utterance), the proper (human-like) analogy cannot be made. Because no speech recognition system has yet been built which has the speaker-independent capabilities of the human listener, it is evident that none has yet implemented the appropriate gestalt extraction.

The work of Kabrisky [59,60], Maher [78], and Ginsburg [47,48] have shown that certain behavior of the human brain is indistinguishable from a mechanism which extracts the two-dimensional low-spatial-frequency Fourier harmonics as the gestalt feature set of the first level of cortical analysis in vision. It is therefore suggested that speech be classified by extracting the two-dimensional low-spatial-frequency Fourier harmonics of sound as it appears on the primary audio cortex. This appears to be reasonable since it is apparently part of the mechanism in operation for the visual system; and, in addition, the neurophysiology of the speech areas in the brain is remarkably similar to the neurophysiology of the visual areas which suggests the information processing mechanism is similar for both vision and speech. This leads to the speculation that the mechanism of low harmonic feature extraction is part of the fundamental mechanism for gestalt extraction throughout the hierarchies of abstraction in the brain. If this is true, then the architecture of the analogy mechanism will have been discovered and we should be able to implement human-like recall on a machine.

The following approach outlines the scope and methodology of Cortical Thought Theory (CTT) which seeks to develop a new computing architecture based on primitives of analogy. A simulation of this new CTT architecture has been developed and tested. A more detailed account of its development and testing is found in later chapters of this dissertation.

2.7 Outline of the Solution

2.7.1 Cortical Thought Theory -- a possible architecture based on primitives of analogy:

A new computer architecture which is based on primitives of analogy has been developed. This new architecture, called Cortical Thought Theory (CTT), is intended to be an embodiment of the basic thought mechanisms which are physiologically present in the human brain.

One of the basic assumptions of CTT is that all information is displayed as a pattern on a local cortex surface (meaning a relatively small subsection of the entire cortex surface). In the neurophysiology literature, it is well established that the senses of sight, touch, and audition are mapped as two-dimensional patterns on anatomically specific local cortex surfaces, so it seems a reasonable extension (since the neurophysiology of all areas of the cortex is quite similar) to allow that all information, no matter how high it is in the hierarchy of abstraction, is displayed as a two-dimensional pattern on a local cortex surface (which corresponds to the appropriate syntax or semantic function at the appropriate level of abstraction in the hierarchy).

The analogical primitive is defined by the function of the structure which follows. A two-dimensional image on a local cortex surface is classified by computing the low frequency harmonics of that two dimensional image. The set of these harmonics is reduced to a subset of smaller cardinality and reprojected (through cortical-to-cortical axons) onto a second local cortex surface (the next one up in the abstraction hierarchy). This second local cortex surface "remembers" the temporal/procedural/positional sequencing (or syntax) of the classifications of the images on the first local cortex surface. By allowing multiple lower level local cortex 1 surface (including syntax surfaces) classifications to be simultaneously reprojected onto another single local cortex surface (referred to as a semantic surface), comparisons and associations can be made. Since these comparisons and associations are made on the basis of the low spatial frequency harmonics of the lower level images composing this higher level semantic analysis, then the pattern displayed on the semantic surface represents the semantic gestalt of the situation/environment. A lengthy two part illustrative example follows. The first part of this example is a brief keypoint technical description of the gestalt classification and comparison mechanism. The second part of this example shows how a collection of these gestalt classification and comparison mechanisms might be linked together to emulate abstract human reasoning.

2.7.2 Illustrative example, part-one: keypoint technical description of the gestalt mechanism:

A brief keypoint technical description of the human classification and comparison (gestalt) mechanism is presented here for the purpose of clarification. It will be developed in more detail in Chapter Four. (This may not be the precise mechanism, but it is indistinguishable from the precise human mechanism according to the testing done during the course of this dissertation.) The simulation, reported on in Chapter Five, implements a working model of this human classification and comparison mechanism for the speech domain of audio sensory inputs. For this discussion, its techniques are extended to also show how a simulation for visual image classification domain would work.

As has already been stated, neurophysiological data is sufficient to describe, with a reasonable confidence to useful detail, the cortex surface mappings for the primary audio and primary visual cortex surfaces. Specifically, the primary audio cortex is a two dimensional display of what can bascially be described as the log-amplitude versus log-frequency plot of sound at the eardrum. The primary visual cortex is basically a projection of the image on the retina which is warped according to well documented cortical magnification and composed locally of its spatial frequency components.

The first step in classifying an image displayed on one of these two surfaces is to properly window it. This is the most difficult part of the entire process. The proposed neurophysiological mechanism for doing this for vision is beyond the scope of current technology (in the current face recognition machine using CTT, this part of the process is being done manually). This visual windowing mechanism is a well defined process which will be described in detail in Chapter Three. The mechanism for properly windowing the image on the primary audio cortex appears to be well within the capability of current technology. It has been approximated in the simulation by using a rectangular window with the left boundary at 100 hz and the right boundary at 4 khz (see Figure 2.8). The height of the window (distance between upper boundary and lower boundary) is always 60 dB (1dB = 20 LOG $\frac{V_o}{V_i}$). But the exact location of the upper boundary (and hence lower boundary) is variable. It changes logarithmically in time following the instantaneous normalized energy. This windowed image represents the spectrum of a 20 millisecond time slice of speech which changes every two milliseconds (i.e., - a 20 millisecond sliding window image is digitized in a 64 x 64 array). Each of the 64 rows is multiplied by a Hamming window; then each of the 64 columns is multiplied by a Hamming window. The following transform is then performed on this windowed matrix-image (this transform will be derived in Chapter Four):

Given: M_{kl} ; k, l=1,...,64,

Then: $$S_{kj} = \sum_{l=1}^{64} M_{kl} \sin\left(\frac{2\pi j(l-1)}{4096}\right) ; \quad k,j=1,\ldots 64 \qquad (1)$$

$$T_{ij} = \sum_{k=1}^{64} S_{kj} \left(\sin \frac{2\pi i(k-1)}{4096} \right); \ i,j=1,\ldots 64 \qquad (2)$$

NOTE: This is a discrete Fourier-sine transform; it is not a complete Fourier transform. Based on the work of Kabrisky, Maher, and Ginsburg, it seems it should be a Fourier-like transform which provides only real answers (not complex) and has a DC component ($T_{1,1}$) of zero, as well as having the characteristic of being phase variant (i.e., - changes in the phase of the image, M_{ij}, produce changes in T).

The set reduction (characteristic number four listed in the first part of this chapter) is performed by setting $\max_{i,j} T_{ij} = 1, \forall_{i,j}$; and all other $T_{ij}=0$. This set reduction mechanism is startlingly simple. At first appearance it seemed quite absurd. However, testing and analysis has shown that it is sufficient to elicit all measurable phonemic psychological behavior of the human system.

RESTATED: It appears that the two-dimensional psychological mapping of phonemes by the human system is explained by this one simple mechanism. In addition, this model predicts as yet unknown classes of audio illusions which we have synthesized, tested, and verified (reported on in Chapter Five). This is compelling evidence for concluding that this single simple mechanism is solely responsible for the human ability to classify and compare speech inputs at the phonemic level.

As each new 20 milliseconds time slice (updated every 2 msec) is analyzed in this manner, the single points on this phoneme cortex surface trace out a track which forms a new two-dimensional image on a second cortex surface. This entire new image is again transformed, and set-reduced in the identical manner as was the primary audio cortex (windowing on this surface occurs differently -- preliminary indications are that each speaker has his own unique window; if this is true, then speaker recognition would result from finding the appropriate window to provide a speaker-independent recognition system). The single point resulting from this classification and set-reduction is the location/identity of the word spoken. It has the property of being close to all other words which sound similar to the human ear. The more similar the other words sound, the closer is the distance between this word and those.

This mechanism, continued in its application for higher levels in the abstraction hierarchy and using multiple surface inputs, is predicted to have the property of classifying the semantic environment as a human would and eliciting the single characteristic most expressive of the semantic environment. This mathematically guarantees the convergence of a set of inputs to the single most significant (most human like) inference -- a property which eludes spreading activation net (Fahlman) machines and constraint propagation (Boltzman) machines.

The mathematics of the model guarantees that the resolution of cortex images will increase with increasing matrix sizes from 64 x 64 to N x N, N > 64. The increased resolution of the image surface guarantees (by the mathematics of the model) increased resolution on the transform surface. Increased resolution on the transform surface allows for a greater vocabulary. Convergence continues to be guaranteed by the nature of the process.

A step by step example of the process just described is provided.

STEP 1: Digitize a speech file and divide it into 40 msec windowed segments. (See Figure 2.6 of Time Domain of Long "E" Sound.)

STEP 2: Multiply each 40 msec sample by a Hamming [104] window and take the Fourier transform of it. The magnitude plot of this transform is the linear plot of the spectral content of the 40 msec Time Domain Sample. (See Figure 2.7.)

STEP 3: Replot the Linear Spectrum on a Log-Log Plot. (See Figure 2.8.)

STEP 4: Window the Log-Log Plot and perform the transform of the 64 x 64 resolution image of this plot. (Example of one of these transforms is Figure 2.9.) The identity of the phoneme is the set of coordinates of the point of maximum amplitude of this low pass transform.

STEP 5: Continue Steps 1 through 4 until the entire word has been processed by plotting each phoneme name for all 40 msec windows of the utterance; a phoneme track will have been traced out on the phoneme cortex surface. (An example of a track resulting from processing the word "ELM" is in Figure 2.10.)

STEP 6: Perform transform of phoneme track (shown in Figure 2.11). The identity of the word is the set of coordinates of the point of maximum amplitude of the absolute value of this low pass transform. In this example, the world "ELM" is stored on the word cortex surface at location (38,36). The closer any future word location is to (38,36), the more it will sound like the word "ELM" to the human listener.

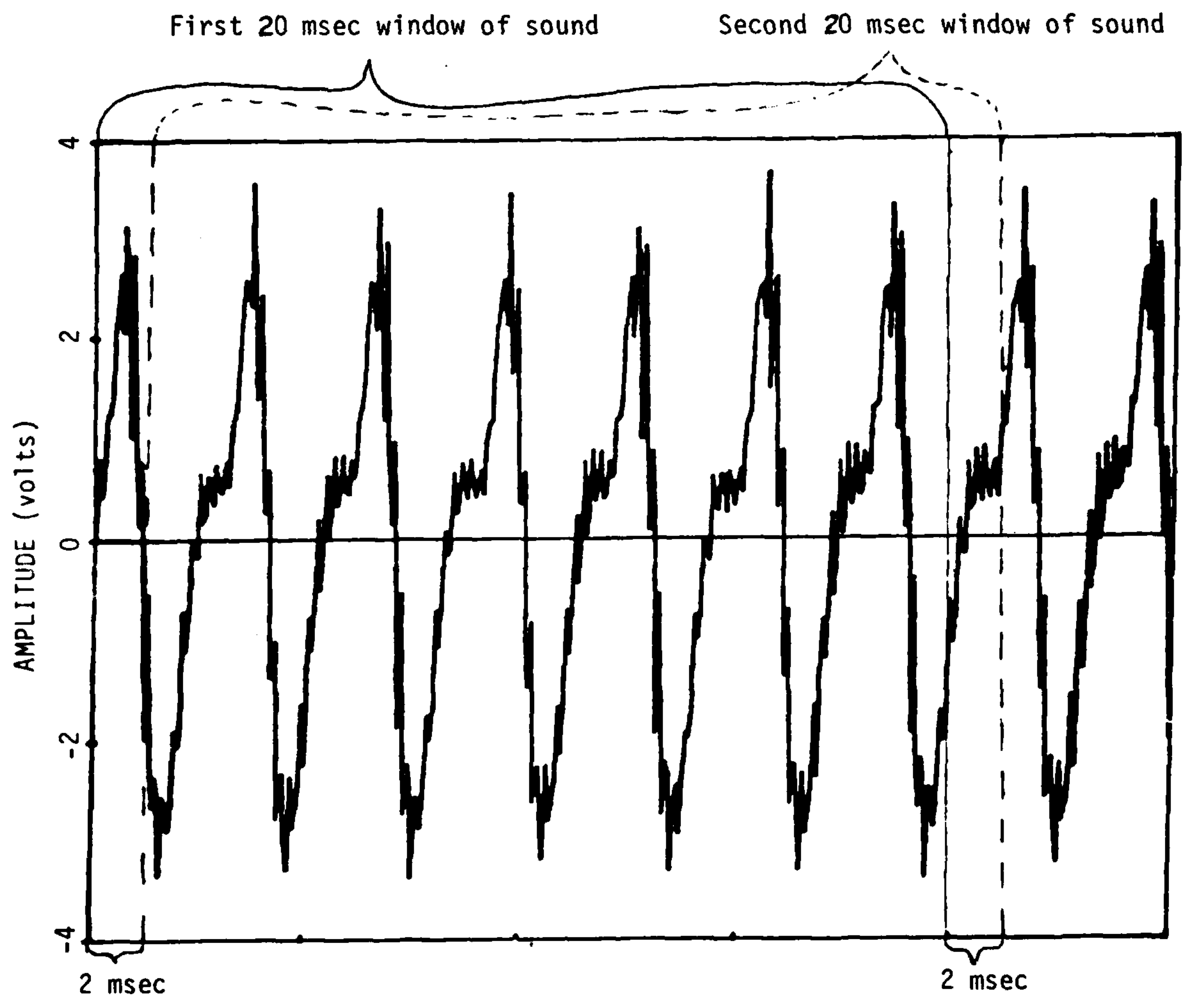

Figure 2.6 - Time Domain Plot of a Vowel

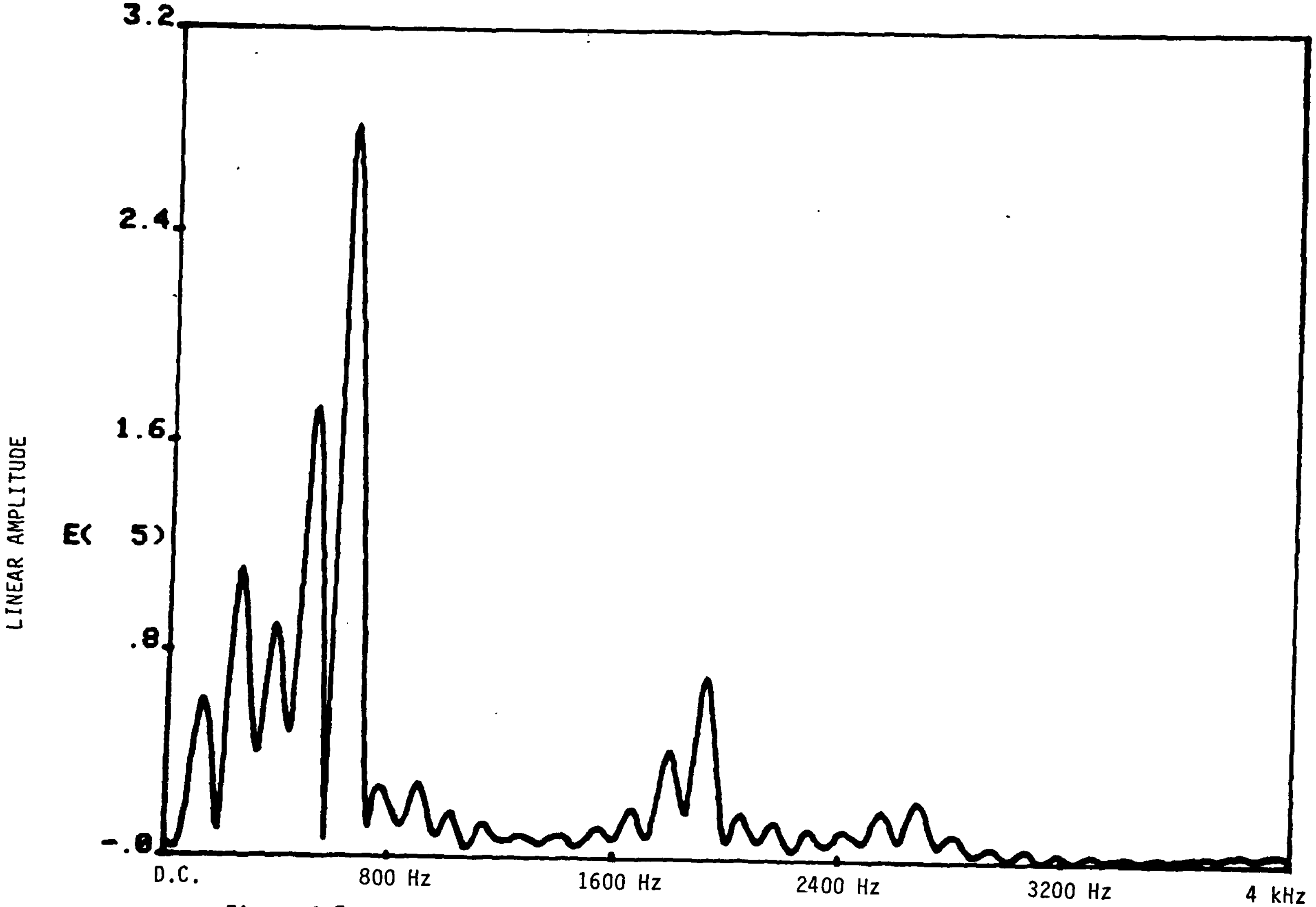

Figure 2.7 - Magnitude Spectrum of 20 msec Hamming Window of ĕ

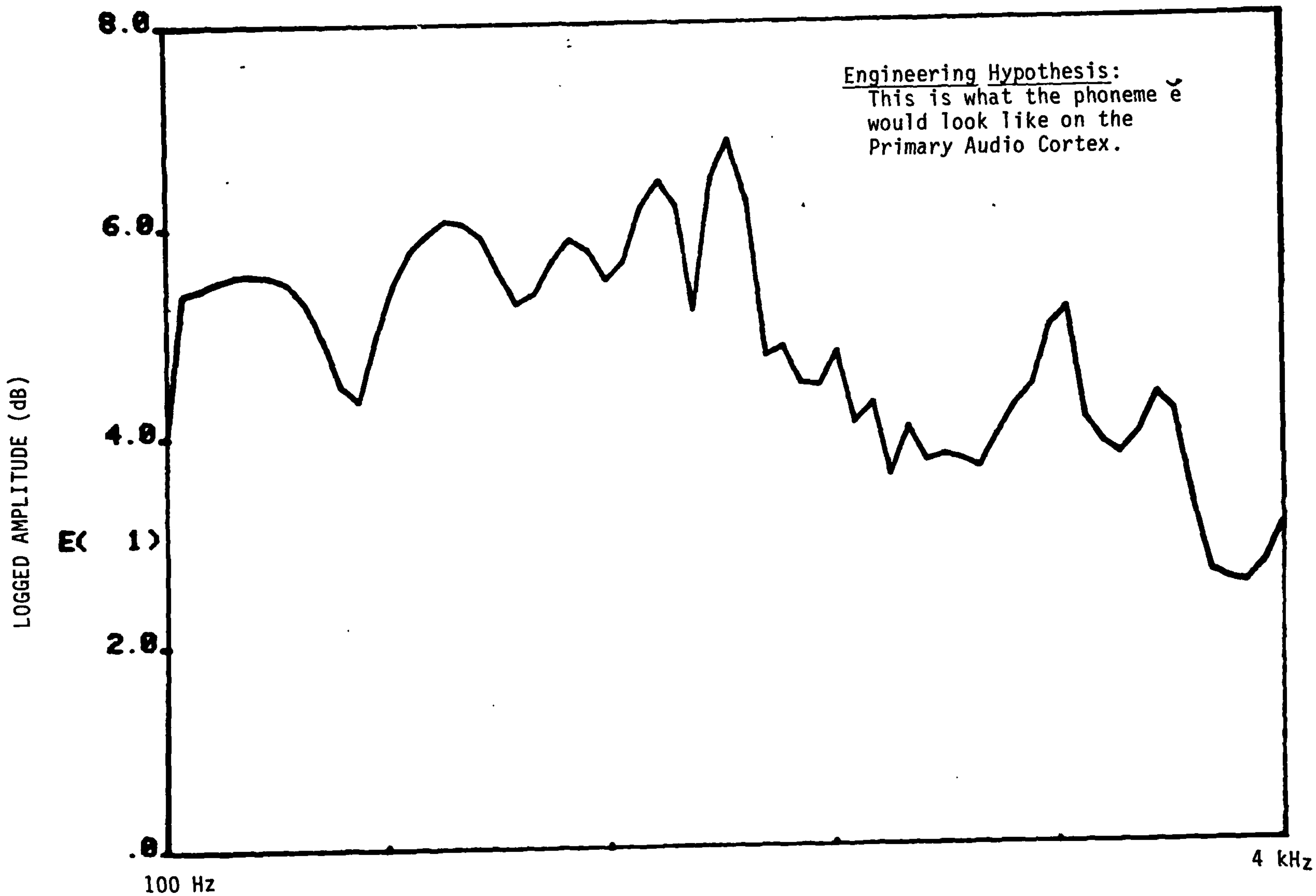

Figure 2.8 - Log Plot (Both Axes) of Curve in Figure 2.7

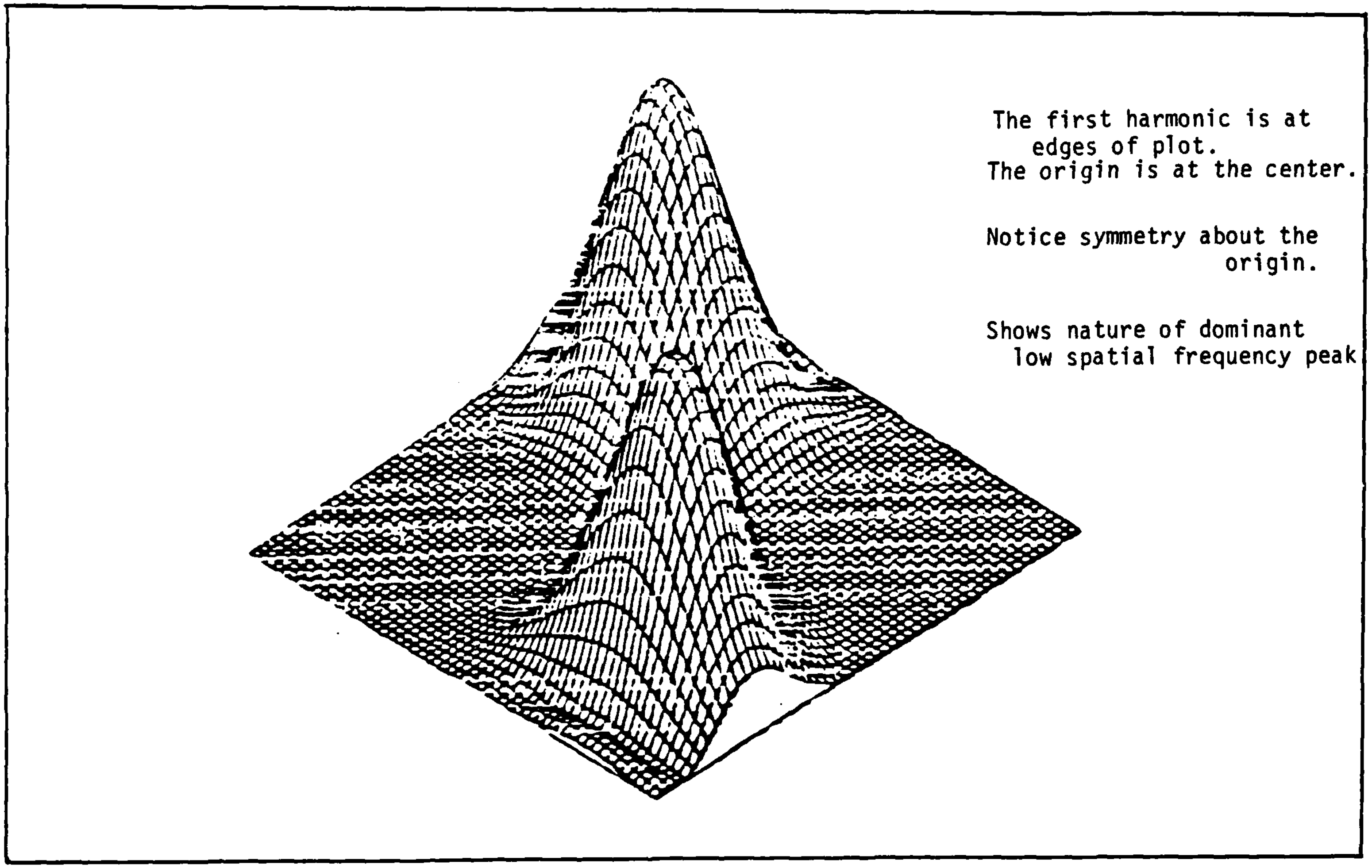

Figure 2.9 - Low Spatial Frequency Characteristics of 2DDFST of Phoneme Displayed on Primary Audio Cortex

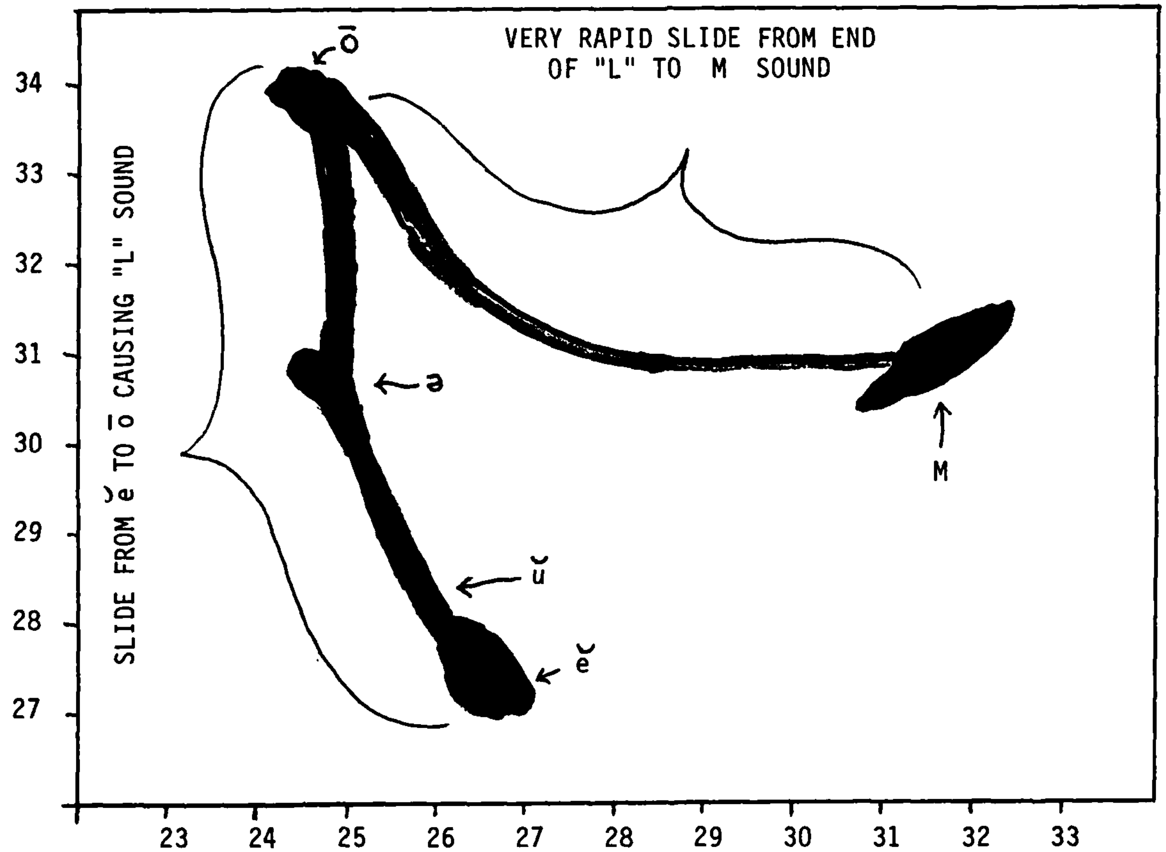

Figure 2.10 - Track Trail on Phoneme Cortex Surface of "Elm" (File SPQELM1.DA)

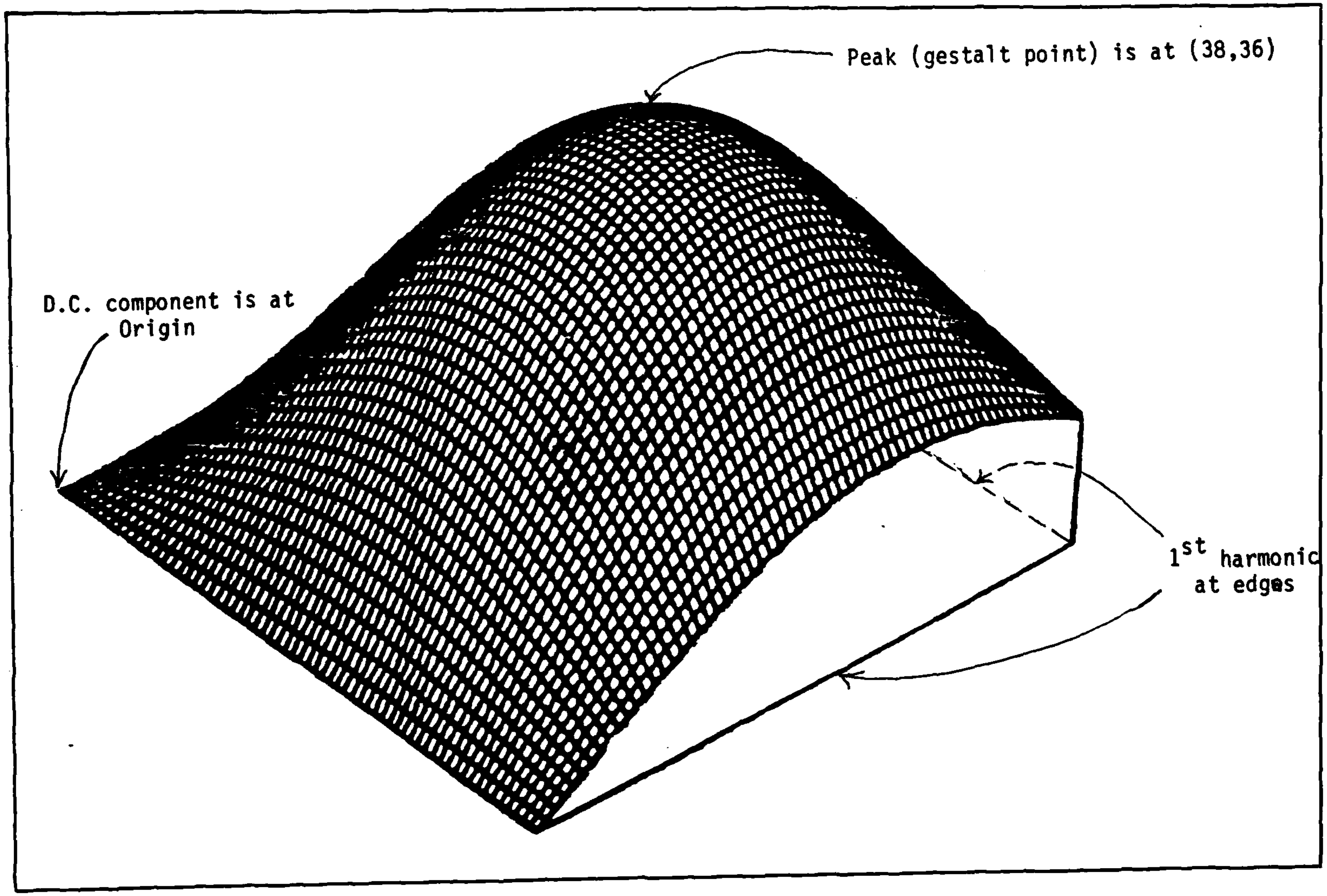

Figure 2.11 - Word-Surface Plot of "Elm" (File TSQELM1.DA)

2.7.3 Illustrative example, part two: extending the model to form a complete human reasoning system:

The following example is intentionally oversimplified. The astute observer, after reading Chapter Five of this dissertation, will argue (and rightly so) that the resolution and error requirements to accomplish the following example with the few surfaces shown are not justifiable on the basis of the simulation results. This example actually would require a great many more surfaces than shown, with significantly greater connectivity between surfaces (in order to interpret the example sentence, given the resolution and margin for error characteristics indicated by the simulation results). It is intentionally oversimplified in order to more clearly present the CTT system's salient characteristics.

The problem proposed to be solved in this example architecture is a modification of a conventional A.I. example (Waltz and Pollack [126] among others): Find the proper interpretation of the last word in the sentence: "John shot the buck." (There are some characteristics of this model which are an extension of the work done by Waltz and Pollack.)

In order to present this example, it is first necessary to review work which has been done by Leslie Goldschlager [49] and is being continued by Janet Wiles and Leslie Goldschlager at the University of Sydney in Sydney, Australia.

In analyzing theoretical connectionist models, Goldschlager has found a way to trade the number of connections between elements in a node structure for time. He shows that if one is willing to allow the communication to be slower, one can essentially connect every node in the structure to every other node in the structure by using a simple set of communication rules that he shows fit quite nicely into the neuroanatomy of the cortex. The most attractive part of his proposed structure is that the number of actual physically direct connections from any single node are relatively few and are restricted to those nodes which are physically adjacent (or very near) it. He shows how using this structure, the simple communication rules he proposes, and the chemical properties of neuron synapses, a local cortex surface, will elicit the following properties (among others):

(1) <u>The Goldschlager Set Completion Mechanism</u>: Goldschlager [49] shows that if a given set of points on a local cortex surface is often active at the same time, then the set will form a corporate memory. In the future, when only a small subset of those points becomes active, this set completion mechanism will operate in such a manner so as to cause all points in the set to become active.

(2) <u>The Goldschlager Sequence Completion Mechanism</u>: Goldschlager shows that if a given sequence (in time) of points on a local cortex surface often become active (in a given sequential order in time), then it will form a corporate memory of this sequence. In the future when part of the sequence becomes active, the sequence completion mechanism will operate in such a way so as to cause the remainder of the sequence to become active [49].

As has been mentioned earlier in this dissertation, these mechanisms do not work well when the number of points on the local cortex surface is very large. Also, these mechanisms cannot adequately account for the brain's ability to deal with abstract concepts. For relatively small local cortex surfaces, these mechanisms fit in quite well with CTT (CTT provides a structure which allows for dealing well with abstract concepts and for connecting many small domains into a larger, loosely hierarchically-ordered system).

In Chapter Five, it will be seen that in order to find phonemes in speech, it is probably necessary to include a vocal-tract local cortex surface (the spectrum plot on the primary audio cortex) and an audio-energy local cortex surface in the gestalt calculation for phonemes. Other surfaces may also be required. The gestalt of the spectrum, displayed on the primary audio cortex, is calculated and projected onto the intermediate audio phoneme cortex surface. At the same time, the gestalt of the energy of the speech (displayed on the energy cortex surface) is calculated and also projected onto the intermediate audio cortex surface (see Figures 2.12 through 2.14).

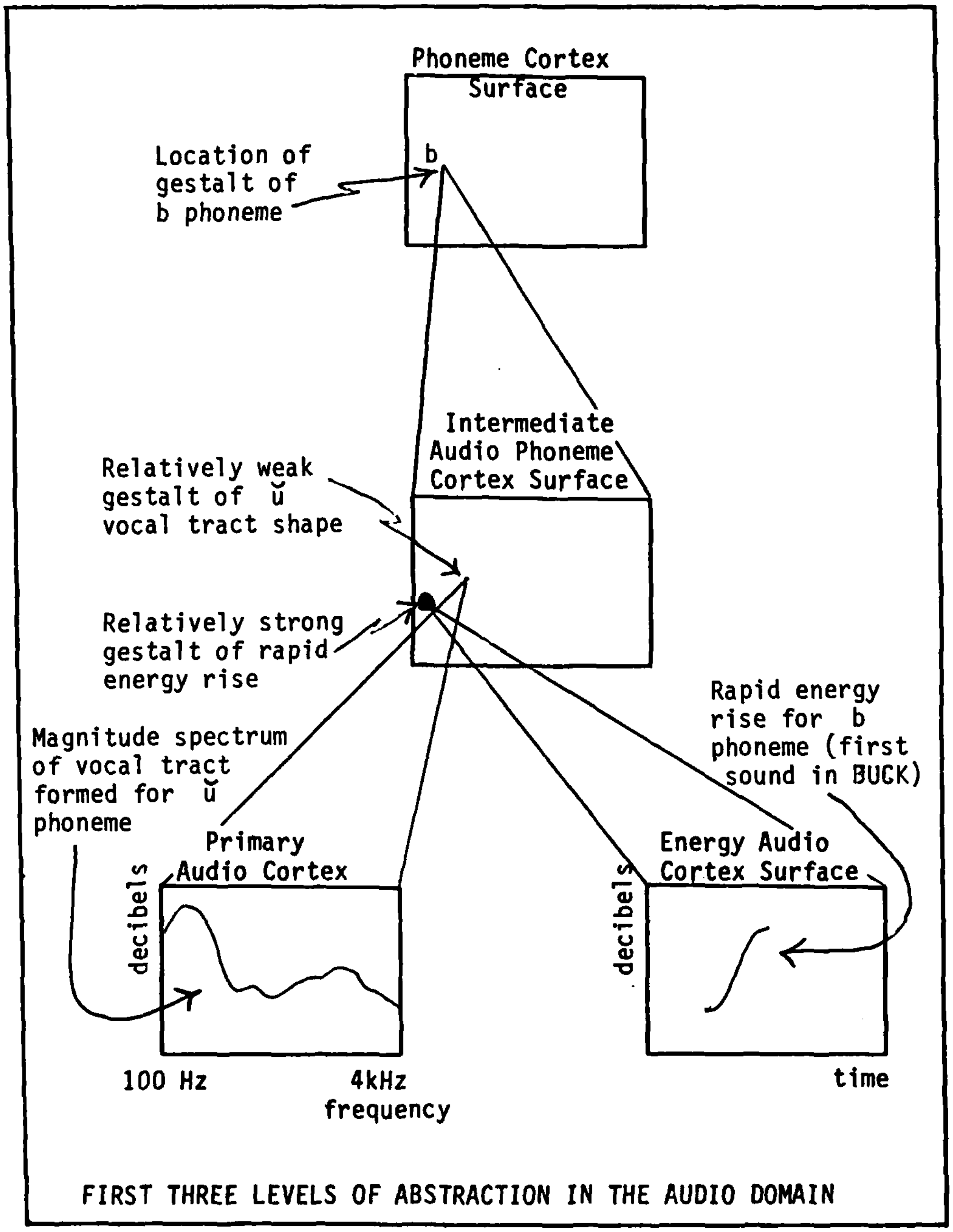
Phoneme Cortex Surface
Location of gestalt of b phoneme
b
Intermediate Audio Phoneme Cortex Surface
Relatively weak gestalt of ŭ vocal tract shape
Relatively strong gestalt of rapid energy rise
Magnitude spectrum of vocal tract formed for ŭ phoneme
Rapid energy rise for b phoneme (first sound in BUCK)
Primary Audio Cortex
Energy Audio Cortex Surface
decibels
decibels
100 Hz
4kHz
frequency
time
FIRST THREE LEVELS OF ABSTRACTION IN THE AUDIO DOMAIN

Figure 2.12

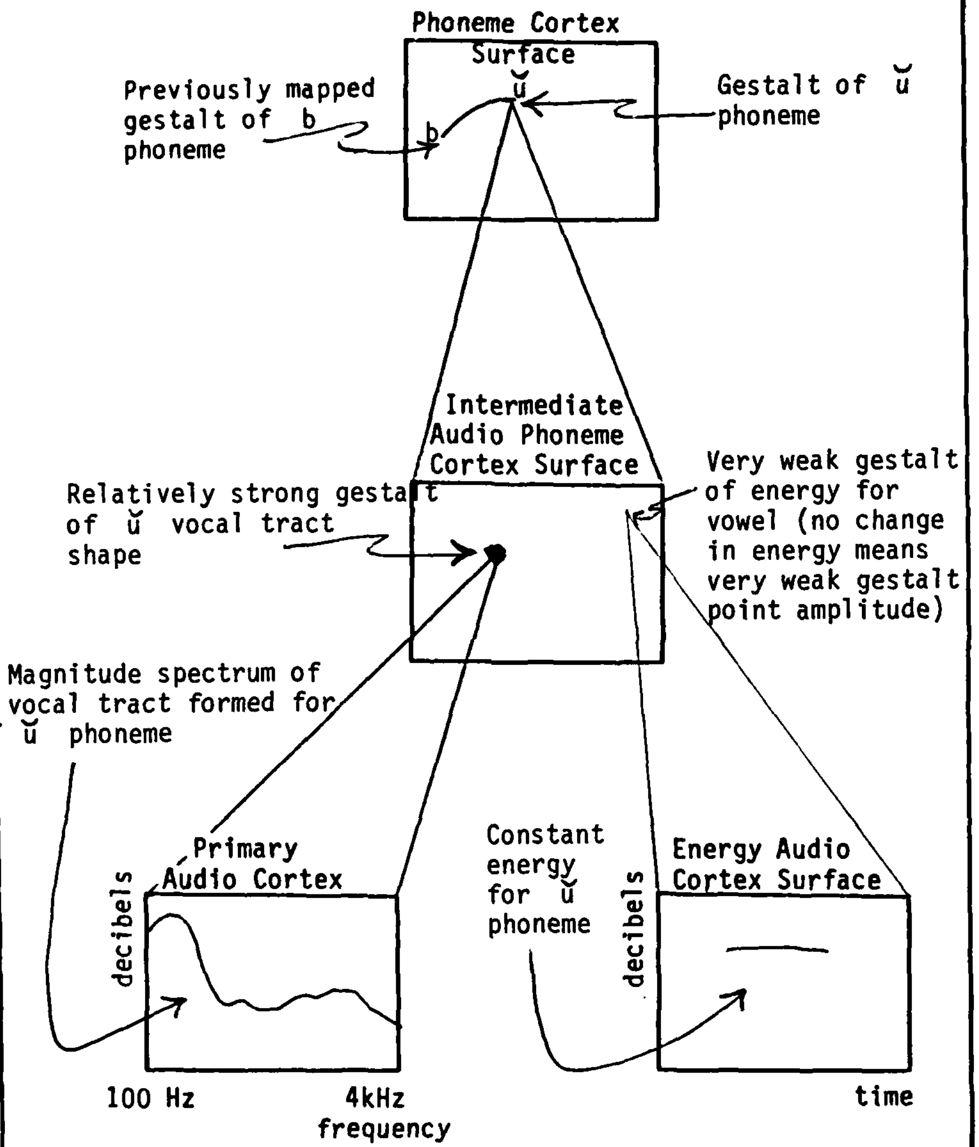

FIRST THREE LEVELS OF ABSTRACTION IN THE AUDIO DOMAIN

Figure 2.13

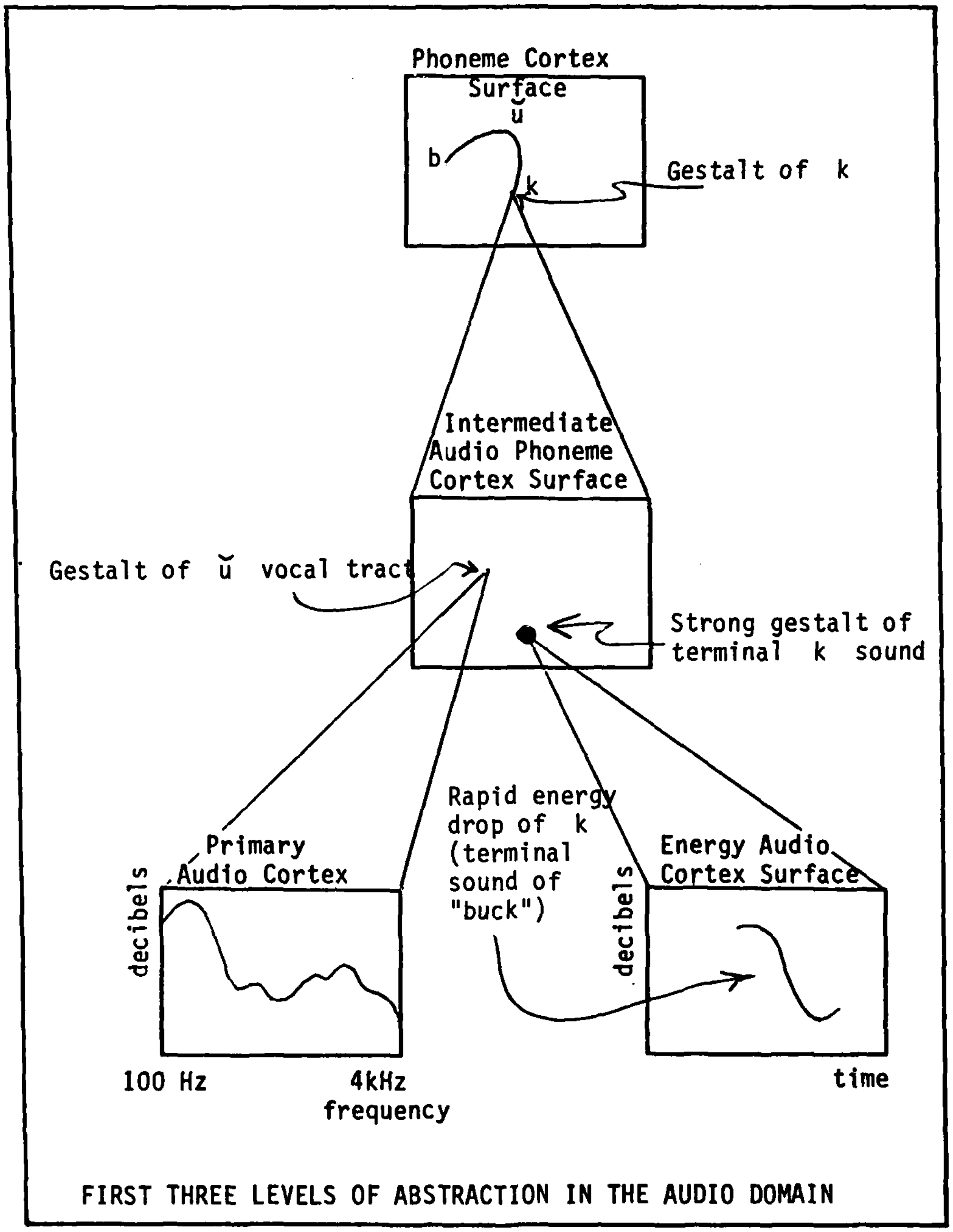
Phoneme Cortex
Surface
ŭ
b
k
Gestalt of k
Intermediate
Audio Phoneme
Cortex Surface
Gestalt of ŭ vocal tract
Strong gestalt of
terminal k sound
Rapid energy
drop of k
(terminal
sound of
"buck")
Primary
Audio Cortex
decibels
100 Hz
4kHz
frequency
Energy Audio
Cortex Surface
decibels
time
FIRST THREE LEVELS OF ABSTRACTION IN THE AUDIO DOMAIN

Figure 2.14

It seems necessary (see Sections 5.2 and 5.3) to increase the amplitude of the energy gestalt point, which is displayed on the intermediate audio phoneme surface, in accordance with the absolute value of the first derivative of the energy. If there is a very rapid change in energy, then the amplitude of the energy-gestalt needs to be much greater than the amplitude of the gestalt of the spectrum (the spectrum is the image on the primary audio cortex). If there is no change in the energy, then the amplitude of the energy-gestalt needs to be relatively insignificant when compared to the amplitude of the gestalt of the spectrum.

Analysis has shown that the spectrum of the "b" phoneme at the beginning of "buck" looks very similar to the spectrum of "u" phoneme in the middle of "buck". (The same is true of the "k" phoneme at the end of buck.) The information in the start and stop consonant phonemes is in the rapidity of the energy change.

The image (set of points) on the intermediate audio phoneme cortex surface is the input image for the second abstract level gestalt mechanism. The gestalt of this image (on the intermediate audio phoneme surface) is calculated and projected onto the phoneme cortex surface.

In Figure 2.12, the phoneme "b" at the beginning of "buck" is found. At the first level of abstraction, the gestalts for the spectrum and energy are calculated and projected onto the intermediate audio phoneme cortex surface (the second level of abstraction). The gestalt of these two points is then calculated and projected onto the phoneme cortex surface (the third level of abstraction). The location of this gestalt on the phoneme surface is the memory location of the "b" phoneme.

Similarly, in Figure 2.13, the same process continues until the "u" phoneme is identified. This continues until the "k" phoneme on the phoneme surface is found. The temporal record of this phoneme surface trace is the sequential image (script) for the audio input "buck."

The algorithms used in the SPEREXSYS expert system (Routh [107]) show how to find the beginning and end of words in connected speech. Relying on the principles used in SPEREXSYS, the beginning and end of the word "buck" would be identified on the phoneme cortex surface. The gestalt of the phoneme-track on this surface would be projected to the syntax surface. (The terminus of this projection is a grandmother cell (Barlow [6,7]) for the audio form of "buck"). The surface on which it is projected is the syntax surface (see Figure 2.15).

The syntax surface shown in Figure 2.15 is hypothesized for this example. It could be constructed using CTT and is a necessary element, in light of CTT, of the language acquisition device hypothesized by Chomsky [21], [22]. Hypothetically, the gestalt locations of the various syntax types shown on the syntax surface were previously learned. Other hierarchically ordered surfaces (not shown here) were responsible for generalizing the repeated exposure to each syntax type. The gestalts of each of these syntax-type-generalizations were repeatedly projected onto the syntax surface until it learned the labelled syntax points, and the legal syntax sequences, shown in Figure 2.15.

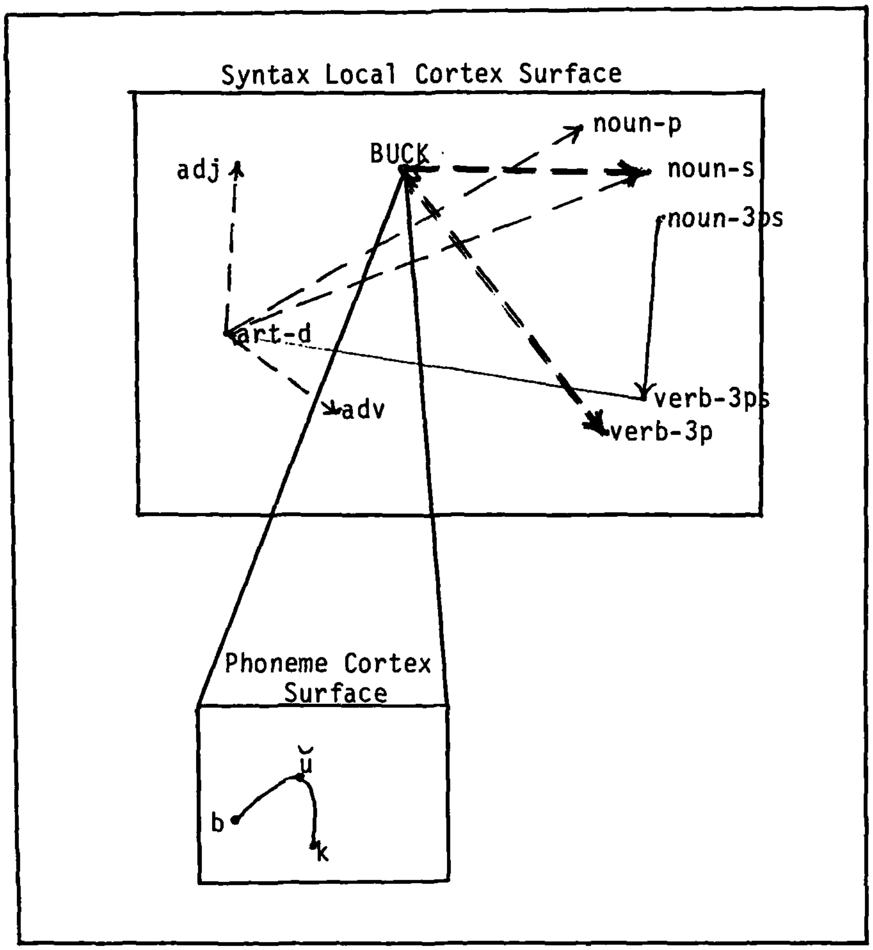

Figure 2.15

Two mechanisms are simultaneously in operation on this syntax surface. The first is the Goldschlager set completion mechanism (shown by the red, dashed-line arrows) which is operating to indicate the grammar-type which the system has associated previously with the word "buck". Two of these (the only two shown here) are: singular noun (noun-s), and third-person plural verb (verb-3p). Since noun-s and verb-3p are not part of the same set, neither will become dominant over the other (on the basis of this set completion mechanism alone).

Goldschlager [49] shows how only one set can complete (activate the entire set) on any given surface at any one time. This characteristic is useful in that it will tend to refuse to arbitrarily resolve an outstanding ambiguity. Therefore, neither set (the "buck-verb-3p" set, or the "buck-noun-s" set) will complete unless something else in the system tends to want to activate either verb-3p or noun-s.

Also in operation on this surface is the Goldschlager sequence completion mechanism. It is operating to complete the syntax sequence (or syntax script -- see Schank and Riesbeck [111]) which has been started by the words "John shot the." This sequence has activated (in turn) the gestalt points for (1) noun-third-person-singular (noun-3ps), then (2) third-person-singular-verb (verb-3ps), then (3) definite-article (art-d). The next grammar type in the sequence is allowed to be either noun-singular (noun-s), noun-plural (noun-p), adjective (adj), or adverb (adv). Again, the sequence completion mechanism alone is unwilling to arbitrarily resolve this ambiguity. The set completion mechanism and the sequence completion mechanism intersect only at the gestalt point for noun-singular. (Note - if this were a more complete example, buck would also point to adjective, and the ambiguity -- between adjective and the noun-singular -- would not be resolvable until the next word. This mechanism precisely models the one word look-ahead deterministic parsing mechanism which Milne [85] found to be characteristic of the Human Speech Recognition System.) The gestalt of the noun-singular grammar type and the gestalt of the audio version of "buck" are gestalt classified and projected to the word-association semantics surface (see Figure 2.16).

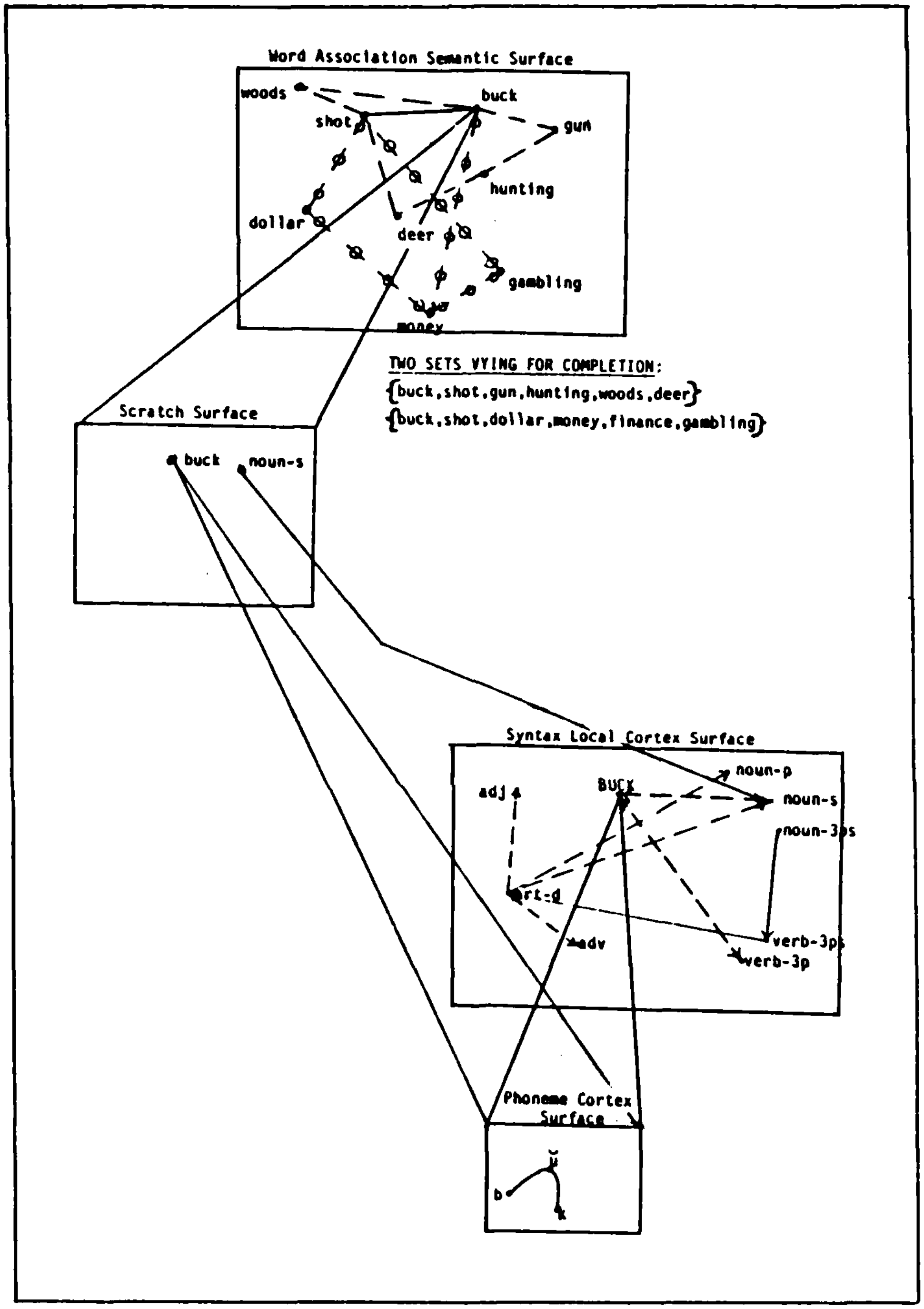
Word Association Semantic Surface
woods
buck
shot
gun
hunting
dollar
deer
gambling
money
TWO SETS VYING FOR COMPLETION:
{buck,shot,gun,hunting,woods,deer}
{buck,shot,dollar,money,finance,gambling}
Scratch Surface
buck
noun-s
Syntax Local Cortex Surface
noun-p
adj
BUCK
noun-s
noun-3ps
adv
verb-3ps
verb-3p
Phoneme Cortex Surface
b
k

Figure 2.16

The Goldschlager set completion mechanism is in operation on this (word-association-semantics) surface. It is acting to complete the set of associations of which buck is a part. It finds that two association sets are in contention for completion -- the money/finance set and the hunting set. This ambiguity would not exist if there had been previous discourse which identified other elements in either (but not both) set.

In Figure 2.17, the entire example hierarchy is shown.

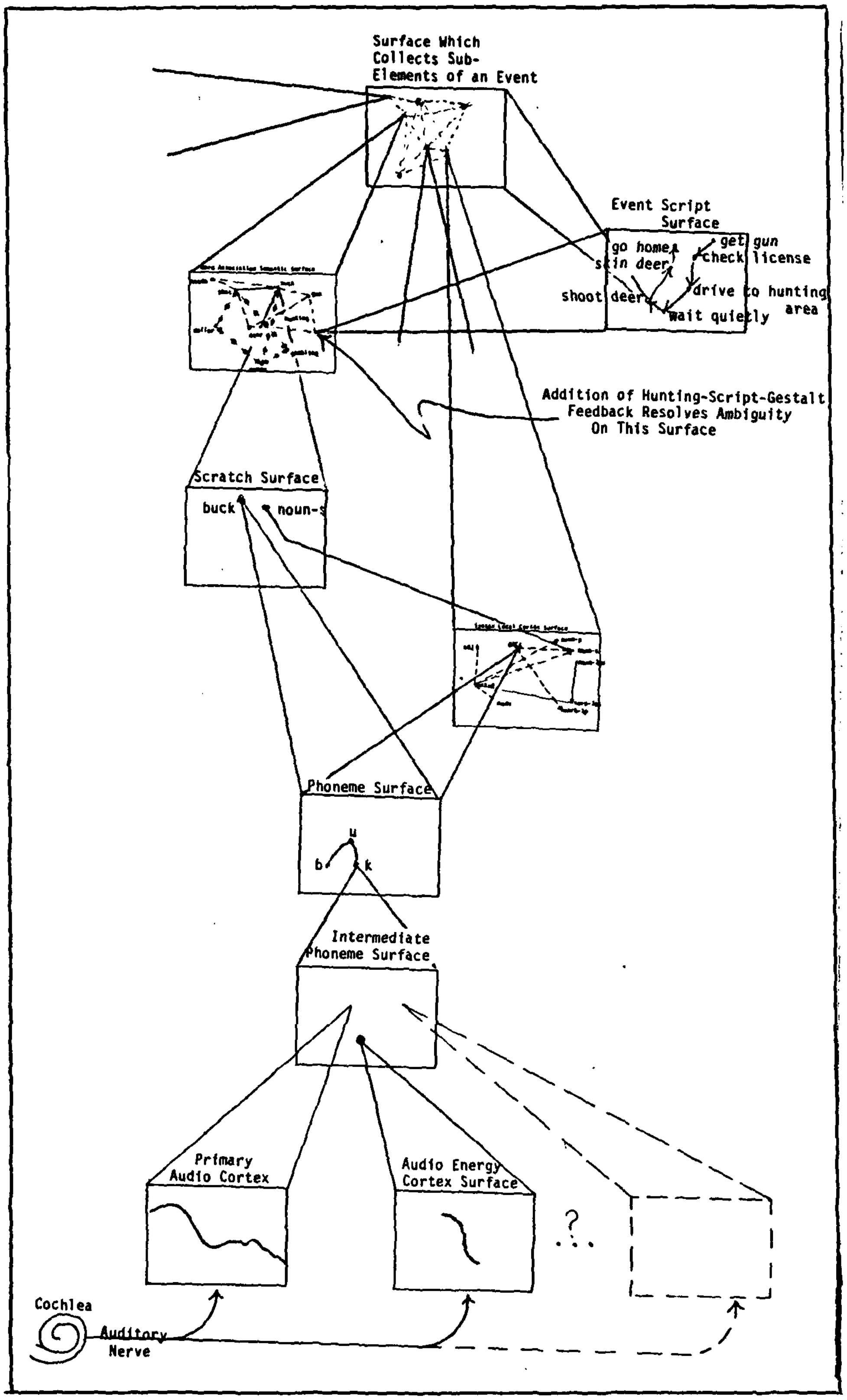
Surface Which Collects Sub-Elements of an Event
Event Script Surface
go home
get gun
skin deer
check license
shoot deer
drive to hunting area
wait quietly
Addition of Hunting-Script-Gestalt Feedback Resolves Ambiguity On This Surface
Scratch Surface
buck
noun-s
Phoneme Surface
u
b
k
Intermediate Phoneme Surface
Primary Audio Cortex
Audio Energy Cortex Surface
?
Cochlea
Auditory Nerve

Figure 2.17

In Figure 2.17, one sees that several subordinate surfaces combine on a seventh surface (the sub-element event surface). The gestalt classification of this surface produces the gestalt of the event: "A deer got shot," and is projected onto the event-script-surface. This surface is busily using the Goldschlager sequence completion mechanism to complete the script for hunting. Hypothetically, this hunting script exists on this surface because the sequence of hunting events (which define the hunting script) have been previously seen and recorded on this script surface. Expectations for future events are established by feeding back the gestalt of the hunting script to lower surfaces in the hierarchy (such as the word-association-semantics surface). The Goldschlager set completion mechanism, which is already in operation on these lower surfaces, will use this feedback gestalt point to reinforce the association sets where ambiguities might otherwise exist.

It can be seen that by using extensive feedback back down the abstraction hierarchy (such as the scripts-gestalt feeding back to the word-association-semantic surface), and relying on the Goldschlager set completion and sequence completion mechanisms, one can move up and down the hierarchy to fill in the missing information at all levels of the hierarchy as desired.

By alternating syntax (script) with semantic (association) local cortex surfaces in the hierarchy of abstraction (conceptually very similar to Schank and Riesbeck's [111] scripts, goals, meta-plans, themes), two properties of the system emerge. The first is that reasoning occurs through a nested application of the process of: classification, set reduction, association and comparison, and generalization to reach a conclusion. The second is that conclusions are most likely reached which least modify the gestalt of the semantic environment -- in other words, this mechanism directly accesses the single piece of information which is most significant in the situation. This algorithm for convergence is the mechanism which gives the system the human-like recall capability which is essential for human-like intelligence. This algorithm for convergence is believed to be (or very similar to) the human gestalt mechanism.

The aforegoing example of this reasoning system based on the described primitives of analogy is, in a nutshell, what CTT is all about. A simulation of the lower three abstraction levels (up to word identification) of CTT in the speech area has been implemented and is reported on in the second section of Chapter Five. In addition, a simulation of the lower three abstraction levels of CTT in the vision area is being carried out by Robert Russel and is reported on in the fourth section of Chapter Five.

2.7.4 Doing deduction with primitives of analogy:

It is interesting to examine how such a system based on primitives of analogy might perform reasoning with deductive logic. It is certainly the case that the human system is capable of reasoning with deductive logic. This leads one to suspect, even require, that a system like CTT which is based on analogical primitives must be capable of reasoning deductively.

The mechanism of deduction requires: (1) that facts be associated with logic states of true and false, and (2) that rules (e.g., modus ponens) relating pairs of these facts be able to be applied according to a prescribed sequence.

In an analogically based system such as CTT, facts are "learned" by observation (internally or externally originated). The ability to do association occurs as a result of merging multiple local cortex surfaces onto a single higher level (in the abstraction hierarchy) local cortex surface. The ability to apply rules in a prelearned sequence is a property of the syntax surfaces. So we see that all components of the deduction mechanism are present in the system. It is also now apparent that performing deductive reasoning with such a system proceeds slowly and with effort (compared to "looking up" information) which is demonstrated by performing the task of adding two four-digit numbers "in your head." This task is performed deductively typically by "picturing" two four-digit numbers, one written above the other, and adding the columns and performing the carries (the sequential application of the rules) to obtain the result as if one were doing the task on a chalkboard or paper.

The axioms of deduction are usually experientially derived (that is, they are seen often enough to "make sense" to the human analogy classification system). That, of course, is the fundamental property of an axiom. When in the course of human experience no counter example can be observed which violates an axiom of deductive logic, then the axiom is accepted if it proves helpful in arriving at useful conclusions. Hence the irony that the entire "reliable" system of deductive logic sits on top of a foundation of axioms which have been arrived at through the use of the "unreliable" system of analogy. Is it any wonder then that people are continually arguing about the nature of fundamental truth?

2.8 The Significance of the Solution

A broader view:

It has been shown that the weakness in solving the speech recognition/understanding problem is the current inability to incorporate an adult world-view semantic analysis into the problem. This is due to the inability to provide the system with human-like recall capability which allows it to search, in a very short time, the entire data base and find the single most important piece of information. But this constraint is not unique to speech understanding. Remembering Fahlman's words, "If we are ever to create an artificial intelligence with human-like abilities, we will have to endow it with a comparable knowledge-handling facility [a human-like recall ability]."

The inability to implement human-like recall is becoming a limiting factor in several areas of artificial intelligence research. This leads to the position, in light of the entire aforegoing discussion, that continued advances in artificial intelligence depend on the development of a computing machine based on primitives of analogy which function in terms of human gestalt.

This chapter has discussed how a collection of the herein described "gestalt mechanisms" could be networked together to both explain and artificially reduplicate the human reasoning process. A few of the significant advantages of this particular solution are:

1. Reasoning with a CTT system is supposedly done in the same way that the human brain does it. This results in the CTT reasoned conclusions being more consistent with the real human conclusions and therefore more satisfactory to the human user.

2. This reasoning process can be done in real-time (or faster) with hardware specifically designed to perform the prescribed gestalt mechanism calculation.

3. The human learning mechanism is explained as a result of implementing this CTT system with neurons. This will be described in further detail in the next chapter.

3. The Neurophysiological and Psychological Perspectives

3.1 The Problem

At one time in history, the disciplines of chemistry and physics were considered to be fairly distant from each other. Chemists were concerned with how different substances react with each other under various conditions. Physicists were concerned with the basic nature of matter and how it reacts to various forces. As each of these two disciplines matured, the boundary between the two became less well defined. With the advent of quantum mechanics, significant parts of physics became indistinguishable from significant parts of chemistry. It had turned out that the answers to important questions for both fields could be found by understanding electron shell activity.

In the same way, it is thought that many of the questions posed by neurophysiology, psychology, neurology, and artificial intelligence can be answered by understanding the physical mechanisms used by the human brain in processing information (how it thinks). The recent increased usage of the term "neurosciences" reflects the growing realization that several of these fields are cooperating together to answer the question: "How does the brain work?"

Therefore, the end goal is to come to an understanding of how the brain works. But what does this mean? When will we know that we have discovered how the brain works? How much detail is enough? How should we go about pursuing that discovery? What approaches are reasonable for us to follow in that quest?

This chapter develops a neurophysiological description of a new unified theory of thought-processing as it might occur in the human brain. It uses the top-down systems approach[1] to develop a hierarchical description of human brain function down to (and including) the level of neuron functions in the cortex and cortical-to-cortical nerves. Previous work in this realm, which is characterized by the approach and results of investigation teams such as Hubel and Wiesel [57], DeValois et al. [28,29], DeMott [26], and Ervin [35], has sought only to explain the function of the lowest level elements (the neurons) of the system without seriously addressing how the elements might be integrated into a system which is capable of intelligent thought.

Much data from experimental observations are needed which are not yet available in order to arrive at a clear understanding of how the human brain processes information. This fact does not prevent significant progress now toward that end because many important clues have already been discovered. The nature of these clues taken as a whole is that they form a set of constraints complete enough to judge the reasonableness of any theory which purports to be a cohesive and complete explanation of the mechanisms by which the brain processes

---

[1] The systems approach to solving a problem has been likened to peeling off the layers of skin from an onion. The entire onion represents the top level of abstraction of a solution to a problem. Each new peeled layer of onion skin represents the elaboration of the solution with increasing detail. By approaching the solution to a problem in this manner, one only investigates down to the level of detail necessary to solve the problem. This systems approach to problem solving tends to eliminate the consideration of unnecessary detail that will normally only confuse the investigation and obscure the pertinent information necessary for obtaining the proper solution.

information. It is because Cortical Thought Theory incorporates and satisfies these constraints that one is able to have some degree of confidence in it. The fact that it is also a fairly simple system (having been shaved many times by Occam's razor) which seems to account for so many as yet unaccounted for phenomena, adds to its attractiveness.

3.1.1 Selected key system developmental constraints:

In the development of a new and radically different general theory, it is necessary to have checkpoints which are known (experimentally determined) phenomena which serve as intermediate test points for assessing the validity of the new theory.

The following is a list of such checkpoints (or theory-anchors) drawn from the neurosciences, psychology, and artificial intelligence. This list is not complete. A complete list would be too long to be practical to produce here. This list is diverse and represents some of the critical, and in some cases trivial but interesting, generally accepted phenomena of human brain characteristics. Taken together, it is hoped they form a reasonable set of constraints for the intermediate developmental testing of CTT. It is also hoped that the informed reader will note the many other experimental results, which cannot all be covered in the restricted written length of this dissertation, but which also neatly fit into the framework of this theory.

CTT is a single theory which accounts for and incorporates the following phenomena:

1. Lorente de Nó [75] found several separable levels of distinctly different neuron types in the cerebral cortex.

2. Lorente de Nó [75] noted, and it has since been confirmed, that there are no nodes of Ranvier in either the grey or white matter.

3. Cortical-to-cortical nerves apparently communicate in only one direction.

4. It has been reported by many independent researchers (among the first was Luria [76]) that common functional areas exist on the surface of the cortex which map the sensory and motor areas onto the two-dimensional cortex surface.

5. The existence of a logarithmic frequency versus decibel map in the primary audio cortex region [98].

6. Bok [10] observed that there are structural differences between the communities of glial cells and the communities of neurons. He hypothesized that this was due to the fact that glial cells are not responsible for the thinking functions (calculations).

7. As a result of the findings of several researchers ([28],[57]), it has been generally accepted that the cortex is a collection of isofunctional columnar cells of activity organized in a honeycomb fashion. These cells are commonly referred to as cortical columns.

8. Hubel and Weisel [57] report the finding that the cortical columns in the striate cortex seem to respond to specific angular orientations of straight lines in the visual field.

9. DeValois et al. ([28],[29]) have shown evidence (which seems, to many observers, to counter the Hubel and Wiesel results) that the single neurons in the primary visual cortex (Area 17) are responsible for processing visual information from large retinal regions. A model will be presented which shows this finding does not contradict the Hubel and Wiesel results.

10. Ervin [35] observed that the function of a neuron in the cortex seems to change in a predictable and periodic manner over short periods of time (a few milliseconds).

11. Ervin [35] also observed that the response of a single neuron has a significant correlation to the output of a nearby macro surface electrode.

12. The results of the AFIT brain electrode experiments (Hayes, Movie) suggest small (on the order of 100 microns) cortical columns which exhibit high frequency activity.

13. DeMott ([26],[27]) reported the existence of cortical electrical surface waves.

14. Barlow et al. [7] report on the existence of single cortex neurons (or cortical columns) which appear to have the function of going active only when a particular complex visual image is presented. These cells are sometimes referred to as grandmother cells.

15. The human thinking system degrades gracefully with random neuron deaths and catastrophically with massive local death.

16. When the hippocampus in a human brain in vivo is removed, the ability to store new facts in permanent memory is lost without losing the ability to learn, and remember, new skills.

17. The work of Kabrisky [59], [60] (and later Maher [78] and Ginsburg [47],[48]) linked the gestalt of a visual image to its low spatial frequency Fourier harmonics.

18. Apparently there exists the capability to simultaneously window a few (five or six) visual images distributed asymmetrically on the primary visual cortex [conversations with Kabrisky about AFIT thesis work].

19. Ginsburg's [47],[48] results apparently explain static two-dimensional optical illusions.

20. It has been experimentally observed that lower spatial frequency harmonic content of a visual image is apparently computed before higher spatial frequency harmonic content [13],[124],[129].

AD-A163 215 CORTICAL THOUGHT THEORY: A WORKING MODEL OF THE HUMAN GESTALT MECHANISM(U) AIR FORCE INST OF TECH WRIGHT-PATTERSON AFB OH SCHOOL OF ENGINEERING 2/5

UNCLASSIFIED R L ROUTH JUL 85 AFIT/DS/EE/85-1 F/G 5/10 NL

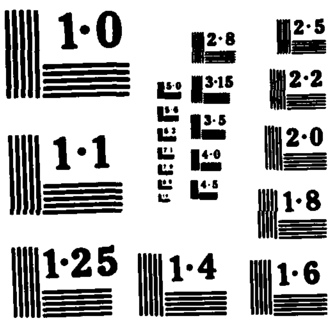
1·0
2·8
2·5
3·2
3·6
2·2
4·0
2·0
1·8
1·1
1·25
1·4
1·6

21. The nervous system contributes to the high frequency and low frequency rolloff of the contrast sensitivity curve [65],[18].

22. Milne's [85] work concludes that English syntax is deterministically computed in the human speech recognition system.

23. There is a growing realization among A.I. researchers in Natural Language that syntax and semantic levels are hierarchically oriented [71],[9],[70],[107].

24. The upper hierarchical semantic levels are able to override lower level decisions [107],[108].

25. The human brain has the ability to very rapidly search an enormous knowledge base [36].

26. The maximum information throughput for an alert human brain is approximately 50 bits per second [conversations with Kabrisky].

3.2 Assumptions:

Every theory is built on assumptions. The following is an exposition of the major assumptions which were used to develop Cortical Thought Theory. It is understood by this researcher that some may consider some of these assumptions as oversimplified, but it is hoped that final judgment on their reasonableness will be reserved until the predictions of CTT have been experimentally tested.

The first, and most bold, of these major assumptions is:

1. Thought, that which is commonly considered to be conscious thought, is processed only in the upper brain -- that part of the brain consisting of cortex and cortical-to-cortical trunks (the white and gray matter). Its formation/calculation/processing is independent of the lower brain organs (except for those functions which will be stated in the other assumptions).

2. The only impact on the thought processes that any lower brain organ is allowed to have is that of preprocessing the afferent sensory signals before they are displayed on the first (primary) sensory cortex. Similar efferent post processing is allowed. Otherwise the functions of the lower brain organs, as they relate to thought processing, are to provide the chemical support required for higher brain functions.

An example to illustrate this last point is as follows in this hypothetical (not within the scope of CTT) mechanism:

> The pituitary gland is responsible for maintaining adequate amounts of epinephrine because epinephrine is one of the primary catalysts used in the conversion of short-term memory

to long-term memory. When the cortex thought-functions detect a situation which requires emergency attention, the amounts of activity on the surfaces of the cortex increase. This causes the cortex to use more epinephrine than is normally required in the steady state calculation mode. This reduces the epinephrine in the blood system at a more rapid rate than is normal and hence a deficit in epinephrine is the result. The pituitary gland senses this deficit and signals the adrenal glands to increase epinephrine output beginning with an initial surge to compensate for the deficit. This has the indirect effect of temporarily increasing the thought processing capability of the cortex regions and of increasing the intensity of the memory of the situation at the current time. But no direct contribution to the calculations of the cortex regions is made by the pituitary gland.

3. The upper brain is homeofunctional. That is, the mechanisms for processing visual information on the striate cortex are essentially the same as the mechanisms to process information on the primary audio cortex and essentially the same as the mechanisms to process information on any other cortex surface.

This last assumption, of course, prefers to ignore the minor structural differences between major areas of the cortex such as the increased structure and activity (detected by glucose consumption) of level four in the striate cortex. CTT discards these differences as insignificant in the establishment of the basic functions and mechanisms which process thought on the cortex surfaces.

4. Cortical-to-cortical trunks function only as unidirectional massive parallel communication trunks which are only capable of transferring the output image of a cortex surface to be the input image of another cortex surface. No calculation or transformation of information takes place in the white matter. (This assumption does not include the role that cortical-to-cortical trunks play in the windowing of images on the cortex surfaces.)

5. Cortical columns, as are commonly referred to by the literature, exist.

6. A cortical column functions as an averaging element which weighs the importance of the input signal strengths of neighboring cortical columns in accordance with a decreasing distribution of dendrites emanating from the cortical column. Its output is the averaged calculation.

The exact nature of this distribution may be able to be determined experimentally and will be reported on in Chapter Five. This assumption will be more fully justified later in this chapter and in the next chapter.

7. Bok's observations and justification are accepted as sufficient grounds for assuming that the glial cells are not participating in the calculation.

These aforegoing seven assumptions comprise the major assumptions on which the neuron level description of CTT is built. It is recognized by this researcher that if any of these assumptions is incorrect (with the possible exception of number five), then the usefulness of the <u>neuron level</u> systems description of CTT will be severely limited if not completely invalidated.

3.3 Why A Systems Approach

> "In the systems approach, concentration is on the analysis and design of the whole, as distinct from . . . the components or parts. The systems approach relates the technology to the need; it insists on a clear understanding of exactly what the problem is, and the goals that should dominate the solution and lead to the criteria for evaluating alternative avenues. The systems approach . . . provides for simulation and modeling so as to make possible predicting the performance before the entire system is brought into being . . . it makes feasible the selection of the best approach from the many alternatives."
>
> - Simon Ramo, "Cure For Chaos"

A review of the neurophysiology literature seems to point to the underlying philosophy that we are involved in a quest not unlike the construction of a giant jigsaw puzzle composed of millions of pieces. Each new experiment is designed to present us with at least one more new jigsaw puzzle piece which was not previously available to us. It seems to be thought that the more pieces we have, the more likely we will be able to fit them together in some way which will give us greater understanding of what the entire picture looks like. Although there is some merit to this approach, it is the contention of this researcher that this is not the best approach. An alternate analogy to the jigsaw puzzle approach is offered in order to underscore some of the weaknesses in the approach of the investigations currently being carried on by neurophysiology:

> If one desires to understand how the human body works, one might begin by studying the behavior of a single cell. After much investigation, let us suppose that we finally understand everything there is to know about a single cell (any cell). From that information, can we then design a human being? One thinks not because all of the systems information is still missing. What does a blood cell tell you about the structure and inter-relation of the circulatory system with other systems? Not much. What does a muscle cell tell you about the structure and function of the various muscle groups? Not much, else there would be only one muscle group. What does one bone cell tell you about skeletal organization? Not much. And so on and so forth. So we see that if our goal is to understand the workings of the human body, it is insufficient for us to undertake an investigation of single cells.

When anatomy and physiology are taught, a systems approach is used. That is, one first learns about the inputs and outputs of the human body. (It takes in oxygen and outputs carbon dioxide and water vapor; it takes in food and water and outputs energy and specific kinds of waste; it "takes in" specific kinds of muscular tensions and "outputs" specific changes in its muscular structure; etc.) From the knowledge gained about the inputs and outputs, further questions are asked as to the nature of the systems which cause the observed input-output behavior. Now one is interested in learning about the major systems in the body. So the skeletal system is studied, the cardiovascular system is studied, etc. Then one begins to be concerned with the inter-relation of these systems. This leads to studying the endocrine system, the connective tissue structures, etc. Now one observes that anomalies can occur in each of these systems, so one investigates deeper down this system's abstraction hierarchy and discovers the existence of and interworkings of the blood cell manufacture systems, the immune systems, etc. Now one <u>needs</u> to know how single cells work in order to understand how they malfunction and can be prevented from doing so. Now it is understood how the function (or malfunction) of the single cell impacts the entire body.

It is important to notice that the function of single cells did not tell us how the body works, but an understanding of how the body works made it important to understand how single cells work. And how is it that we came to an understanding of how the body works? We came to that understanding by using the systems approach: we developed a top-down (in the abstraction hierarchy) understanding of the principles in operation in the body.

In this same way, it is argued that an understanding of how the human brain works is not to come from a detailed investigation of neuron behavior. It is not even to come from an understanding of the input-output mechanisms in operation in the neurons of the brain. This would be no more helpful than trying to arrive at an understanding of the function and inter-relation of all the various muscle groups given that all we are allowed to investigate are the input-output characteristics of a single muscle cell. There will be a time in our investigation when it will be desirable to understand all there is to know about neurons, but it is probably premature to undertake an investigation at this level of detail before understanding the levels of abstraction in the system's description of the function of the brain which are above the neuron level.

Therefore, a systems approach was used to develop Cortical Thought Theory. To begin a systems approach to this problem, one needs to know the top level systems requirements in terms of the inputs, the basic nature of the transfer function, and the outputs.

In Chapter Two, the argument was presented which concluded that the brain must reason with primitives of analogy. This is the top physical level in the abstraction hierarchy. Once this top level has been identified, the next step is to characterize its function by describing the transformation it performs on its inputs to produce its outputs. To do that requires the identification of its inputs and outputs.

An analogy mechanism requires that information be presented to it using some standardized representation scheme. The analogy mechanism must then extract the essence of identification (gestalt) of the input. This gestalt is then compared to all other stored-image-gestalts in order to determine the best match. It is thought that the previous three sentences describe all possible analogy mechanisms. So we can conclude from all of the aforegoing argument that this description must subsume the description of the top level systems function of the brain.

3.3.1 The three crucial questions:

We continue to proceed logically in this systems analysis to see that we must now answer these three questions:

1) What is the standardized representation scheme that is used to present input?

2) How is the gestalt extracted from one of these input representatives?

3) How is the gestalt, which is extracted from a single input representation, compared to all other stored-image-gestalts (remembering that the comparison must elicit the best match)?

It will be shown in the remainder of this chapter that enough information exists in the literature to strongly support reasonable answers to these questions. The answers to these questions form the foundation of Cortical Thought Theory; they define the top level of the systems description of the human gestalt mechanism.

3.3.2 The first question:

The first question which needs to be answered from the literature is: "What is the standardized representation scheme that is used to present input?" There is a great richness and variety in the literature which points to the use of the cerebral cortex as a two-dimensional sheet on which are "drawn" two-dimensional pictures representing sensory inputs. For example, the radioactive metabolite experiments performed by Tootell et al. [119] show that the two-dimensional visual images on the retina are mapped to two-dimensional cortically magnified images on the striate cortex. An example from the auditory sensory inputs is the work reported by Woolsey [132] which shows that mammalian brains "draw" two-dimensional images on the cortex to present frequency domain audio information. This local cortex surface (sometimes referred to as the primary audio cortex) appears to be a two-dimensional map with ordinate axis calibrated in decibels and abscissa axis calibrated in logarithm units of frequency. A third example is that the motor output information appears to be "drawn" as a two-dimensional image (an elongated strip) across the perietal lobe. From these examples it is evident, at least for some input representation schemes, that the brain uses two-dimensional pictures. From Krieg [67], Lorente de Nó [75], and Kabrisky [59], in addition to the ground swell of neuropathology literature, since function is dependent on structure, it can be argued that since the neurophysiological structure is so similar for all areas of the cortex that the function in all areas of the cortex is similar. It seems unreasonable to suspect that input information, at any level in the abstraction hierarchy, is presented in any form other than two-dimensional pictures "drawn" on the cortex surface.

3.3.3 The second question:

Having answered the first question, the second question: "How is the gestalt extracted from one of these input representations?" can now be reworded as: "How is the gestalt extracted from two-dimensional images?" The perceptual psychology literature provides a very reasonable answer to this second question.

In the late 1950s, Kabrisky began the search for an algorithm which was able to detect the essence of the shape of a written symbol (its gestalt) without paying attention to the non-essential detail of the symbol. He noted that a low-pass two-dimensional Fourier transform had the characteristic of preserving the general shape of a written symbol without paying attention to its non-essential detail. After this thinking, modern Fourier analysis theories of visual perception emerged. Kabrisky et al. [60] showed that a machine which defined the gestalt of an image as the complex set of its first three Fourier harmonics and used this gestalt as the basis for classification comparison of simple visual symbols, performed in a manner which was psychologically indistinguishable from a human attempting to identify the same symbols. Maher [78] showed a similar result using only the first two harmonics of the more complicated visual images of black and white photographs of animal crackers. Ginsburg [47,48] showed that all static two-dimensional optical illusions could be explained by this same technique of low-pass two-dimensional Fourier analysis of images. This work by Ginsburg was extremely compelling evidence in support of the hypothesis that the human brain is calculating gestalt on the basis of low frequency Fourier transforms. Pantle and Sekuler [93] found evidence for the existence of size detection mechanisms (which are crucial for the preprocessing stage of windowing before the Fourier transform can be calculated -- this will be expanded on later in this chapter).

The combined results of the entire body of work in the area of Fourier analysis of visual perception establishes a compelling case to support the conclusion that the human brain is classifying its two-dimensional input representations in terms of low frequency Fourier harmonics. At this point, many researchers would cite results like the Hubel and Wiesel [57] findings which seem to point to a different feature extraction process. It will be shown later in this chapter that the Hubel and Wiesel results appear to be better interpreted as evidence to suggest a preprocessing windowing mechanism which must necessarily occur before an image is Fourier analyzed.

3.3.4 The third question:

Having now answered the first two questions, the third question can be reworded as: "How are the low frequency Fourier harmonics, which are extracted from a single two-dimensional input representation, compared to the stored Fourier harmonics of all other previously encountered images (remembering that the comparison must elicit the best match)?" The answer to this third question as it now is worded is more obvious than it might first appear. The range of theoretically possible options which will fit the experimental data available is quite narrow. In order to arrive at this narrow range of feasible options, let us examine an argument which will force the conclusion through a process of elimination by examining the unreasonableness of large classes of other options.

All the theoretical possibilities which might be examined to answer this question can be divided into groups based on the cardinality of their gestalt feature sets. Either the cardinality of the gestalt feature vector set (GFVS) is two or it is not two.

It is critical that the reader remember at this point that we have already accepted the phenomenon that the human perception mechanism tends to attach a single name to any observation, regardless of its complexity. In the last chapter this was referred to as "the requirement for convergence" and also as the "universal will to disambiguate" [126]. In the psychology literature it is simply known as gestalt finding. This requirement for convergence is a requirement to converge to a single name. It is the result of a universal will to disambiguate any naming set with more than one name in it to a set with, at most, one name in it. It is the characteristic of finding a single gestalt. In the neurophysiology literature, this shows up as the concept of the grandmother cell [6,7]. In the audio domain, the gestalt of an acoustical disturbance is a sound. The gestalts of the sounds of speech are called phonemes. The gestalt of a particular sequence of phonemes is a particular word. The gestalt of a particular sequence of words is the gestalt of the phrase or sentence they form. A particular sequence of these sentence gestalts forms the gestalt of a more abstract semantic environment (sometimes this more abstract environment is called a paragraph or a story, etc.). The central concept to be conveyed here is that at each level of abstraction in the human brain, a single gestalt of the environment is available. This requires a best-match-comparison between an input to any level (of the abstraction hiearchy) and all the previously stored gestalts at that level. Given that we understand this requirement, we are now in a position to more precisely describe the comparison mechanism which must be in operation.

If the cardinality of the gestalt feature vector set is zero, then the system does not function. This is a trivial and unreasonable case and will not be considered further.

If the cardinality of the gestalt feature vector set is one, then all gestalts can be arranged on a linear continuum for any given domain. Bush [14] showed that this is not so for the domain of alphanumeric symbols. Since we have assumed a unique gestalt mechanism, we conclude that the cardinality of the gestalt feature vector set cannot be one.

If the cardinality of the gestalt feature vector set (GFVS) is two, then all gestalts in a given domain can be arranged on a surface. Comparison would occur as a result of physical proximity on the cortex surface of the domain in question. There are considerable advantages to this mechanism. It will be shown (in Appendix A) that this mechanism seems to be the only theoretically reasonable one. (A brief review of the discussion in Appendix A appears as follows.)

If the cardinality of the GFVS is more than two, then in order to position the gestalts physically relative to their actual distances (using any known distance rule that yields distances other than one or zero), we would need an N-dimensional (N is the cardinality of the GFVS) system where N is greater than two. For N greater than three, this is obviously impossible. For N equal to three, it becomes necessary to neuroanatomically demonstrate a system which has three-dimensional homogeneity. It has been demonstrated (Lorente de Nó [75]) neuroanatomically that the brain does not have three-dimensional homogeneity. (We have already shown that input images are presented as two-dimensional pictures.)

So for N greater than two, it becomes necessary to store every classified image gestalt as an N-dimensional vector. For comparison purposes, this does not theoretically present a problem. However, it will be shown that such a model seems to have major faults. Apparently, it could not learn in the manner that the human system learns. Also, it is argued that the number of associational links would increase exponentially with linear increases in the number of stored pieces of information. Finally, the control structure necessary to do so is thought not to be supported by any experimental neurophysiology findings. These will be more fully elaborated on in Appendix A. The following example is presented for the purpose of understanding a feature vector storage system where N is greater than two (in this case N equals 49).

3.3.5 Example

To begin with, consider a model which stores some discretized version of the low-pass two-dimensional Fourier transform of every image which is ever remembered by the brain. If we use the simplest of discretization schemes and allow for a cartesian grid with only enough resolution to differentiate the orthogonal harmonics of a three harmonic low-pass Fourier 2DDFT, then we see that we require a 49 point (seven by seven) grid:

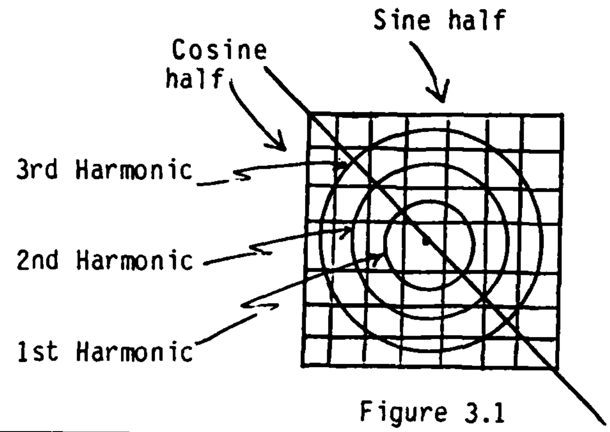

Figure 3.1

Note that the cardinality of this GFVS is 49. It matters not where and how these 49 samples are stored as long as they are stored in such a fashion that they can be recalled as a unit without ambiguity as to which sample represents which harmonic.

Now, if we use the simplest possible distance measure, Minkowski-one distance, it becomes evident that for each newly perceived image the system (brain) must: (1) calculate its 49-sample gestalt feature vector from its two-dimensional Fourier transform, (2) propogate this 49-point feature vector to all other previously stored (remembered) 49-point feature vectors (in the domain), (3) calculate the Minkowski-one distance between all other stored feature vectors and the new one, (4) compare all the distances, and (5) identify the lowest distance (best match) and point back to the feature vector which elicited that best match. The best-matched feature vector is the name of the gestalt. Its links (associations) are associated with the links of the newly acquired (and newly stored) feature vector.

So far we have not identified a control mechanism which would allow for this process of feature vector comparison. We have only stated that it must exist and must perform in the described manner -- there is no other alternative. We do not yet care how long this propagation and comparison would take, so we do not yet consider a description of the propagation and comparison mechanism. We have also not addressed the mechanism for associating the stored links of the best-matched gestalt with the newly acquired gestalt. We only state that if the distance between the gestalts is close enough (distance is less than some threshold), then at least a partial transfer of linked associations must take place or the newly stored gestalt will remain isolated and meaningless.

This is a systems description of not only the example 49-sample GFVS, *but of all gestalt feature vector sets which cannot* be stored proximally in their domain space (i.e., all gestalt feature sets with cardinality N greater than two).

For the purpose of not diverging too far from the central development of this chapter, Appendix A contains the remainder of the analysis of the structures which must exist to support the processing of information in a system with gestalt feature set cardinalities of two and three or more. The reader is referred to Appendix A for the justification of the following conclusions.

(1) Human memory is believed to behave non-linearly in the way it increases in proportion to the number of exposures to an event (image, concept, sequence of sounds, etc.).

(2) For N greater than two, it seems that an extremely complex system of association-links must exist which connects to previously stored gestalt feature vector sets.

(3) If it is the case that an extremely complex system of association-links exists which connects to previously stored gestalt feature sets, then: (a) not only would a mechanism be required which can simultaneously propagate the data for a desired comparison to all previously stored gestalt feature sets in the domain (a mechanism to do this is difficult to imagine, although no argument is forwarded to deny its theoretical possibility), but, (b) it is argued that the system would not have a memory which behaves the way the human memory behaves (regardless of the memory decay function used). It is possible to posit a mechanism which would elicit human memory behavior with this complex-association-link system, but it is so inordinately complicated that it seems to be unreasonable.

(4) The above conclusions argue strongly against the theoretical possibility that the cardinality of the gestalt feature vector set could be greater than two.

(5) If the gestalt feature vector set has a cardinality of two, then the gestalts could be stored in their domain space on the surface of the cortex at the location specified by the two numbers in the gestalt feature vector set. This scheme stores all gestalts proximally to all like gestalts. The simple known

chemical mechanisms (what little is known or accepted about the chemical mechanisms) for dendritic synapse increase and decay are sufficient to explain non-linear human memory behavior using this storage and access scheme. The storage access control mechanism for this scheme is trivial since every time a new gestalt feature vector set is calculated, its address is the feature vector set and all association links are strengthened inversely proportional to their distance from the new gestalt's location. The establishment of the direction and terminus of all association links is simply a consequence of calculating the gestalt of an image on a local cortex surface and then the projecting that gestalt feature vector set to other local cortex surfaces as dictated by the preformed cortical-to-cortical nerves. So we see that the apparently complex system behaviors which arise when the GFVS has a cardinality greater than two, become trivially implementable when the gestalt feature vector set has cardinality two.

Therefore, part of the answer to the third question is apparent. The question was: "How are the low frequency Fourier harmonics, which are extracted from a single two-dimensional input representation, compared to the stored Fourier harmonics of all other previously encountered images (remembering that the comparison must elicit the best match)?" The answer is: The low frequency Fourier harmonics are reduced in some way to a GFVS with cardinality two. This GFVS acts as the domain address (location coordinates) of the gestalt of the input image and is, therefore, the direct, single-step pointer to the appropriate location of the storage area for the newly calculated image gestalt. The best match is the previously stored gestalt location which is closest to this new gestalt location. This solves the direct memory access problem. Not only do we now know the best match, but we simultaneously know the degree to which this new image matches each of the other previously stored image gestalts.

3.3.6 The fourth question:

The new question which has been generated by answering the third question this way is: "What is the mechanism for reducing the low frequency two-dimensional Fourier harmonics to a feature vector set of cardinality two?" The proposed answer to this fourth question was discovered experimentally by simulating a system which performed two-dimensional low-pass Fourier transforms of the images of human speech as they would appear on the primary audio cortex. Using a three-dimensional graphics package, many two-dimensional Fourier transforms of speech phonemes were analyzed in an attempt to find some obvious single-point (on a two-dimensional surface) classification scheme. A single-point classification scheme was found which appears to work. It is the same as that presented in summary form in Chapter Two. The experimental work which constituted the development and psychological justification of this scheme are reported on in detail in the second and fourth sections of Chapter Five. The mathematical justification of this reduction mechanism is the subject of Chapter Four. It will be covered further later in this chapter. This simple scheme has proved sufficient to separate English phonemes, separate simple and complex visual images (the work done by Robert Russel [110a]) and account for particularly difficult optical illusions. In short, it seems that it is not too simple to be sufficient to distinguish those things which the human system can distinguish.

3.3.7 The systems level which is of interest to A.I.:

As we continue in our top-down systems analysis, we are led next to addressing the structure in which these analogy-gestalt-finding-mechanisms are organized. In Chapter Two, it was shown that if these gestalt mechanisms are structured hierarchically with any level being fed by multiple other surfaces, then: (1) trait inheritance is explained, (2) scripts are implemented, (3) deductive logic analysis can be simulated, (4) memory access to any pertinent fact in memory is direct (deterministic if each of the sequentially accessed layers in the abstraction hierarchy is considered a separate step), and (5) human-like inferencing is accomplished. Since this level of the top-down systems analysis has already been accomplished in Chapter Two, it will not be dealt with here.

3.3.8 The cortical-column-function systems level:

The next level of detail to be investigated in our top-down systems analysis is the cortical-column-function systems level. It is at this level of detail that we see how the cortical columns function to perform the gestalt calculation.

The requirement is that some calculation be performed which finds the local maximum which is closest to the zeroeth harmonic of the continuous two-dimensional Fourier transform. The answer to the question of how the cortical columns are doing this is not obvious and this research has failed to develop an analysis which points to the uniqueness of the solution that is about to be presented. It should be understood that the discovery of the precise description of the way the cortical columns function in order to perform the already identified calculation is of relatively little significance to Cortical Thought Theory. Because before we inquire into the level of detail which reveals the manner in which neurons are used to implement the system which has already been developed, we already can completely define the human calculation; we have all the necessary building blocks to develop a duplication of the functions of human perception, human memory storage and retrieval, human inferencing, and we are in a position to develop a complete model of how these functions are integrated so that we can predict and explain all types of higher thought phenomena (that are physically implementable). We see at this point that we have arrived at the same position that aerodynamics found itself when it conceded that feathers were not required in order to fly -- neither did the flying machine have to look or work like a bird -- because the principles of flight were independent of the biological implementation. In the same sense it can now be seen that the principles of human thought appear to be independent of the biological implementation -- that is, the neuron.

After having stated the reasons for the unimportance of exploring the neuron level of detail, it is recognized that it is important to demonstrate that the neurons are capable of performing the required calculation. In other words, feasibility must be demonstrated. Two possible solutions to this neuron implementation requirement are proposed -- there are probably others. The first is a solution proposed by Dr. David Lee which assumes the same type of cortical column function (which will be described later) as is assumed for the second model, but shows how the harmonic of interest can be determined by adjusting the gain on a collection of networked cortical columns -- the harmonics are determined by the eigen values of the integral-equation model of a network of cortical columns. Dr. Lee's model is described in Appendix B and will not be further discussed in this chapter.

Another possible solution to the question of "How do neurons work to extract the required gestalt?" is now presented.

Of the seven levels in a cortical column, the only levels which have substantial communication with other cortical columns are levels one and four. It has been shown in Chapter Two that it is desirable for the communications of one of these levels to be assigned the message transmission requirements hypothesized by Goldschlager [49] for the purpose of completing partially identified association sets on local cortex surfaces. (This would be level four). The other layer (level one) could be assigned the task of sampling the input activities of neighboring cortical columns and then averaging these samples. The result of this averaging activity would then be the output of that cortical column. This function is portrayed diagrammatically as follows:

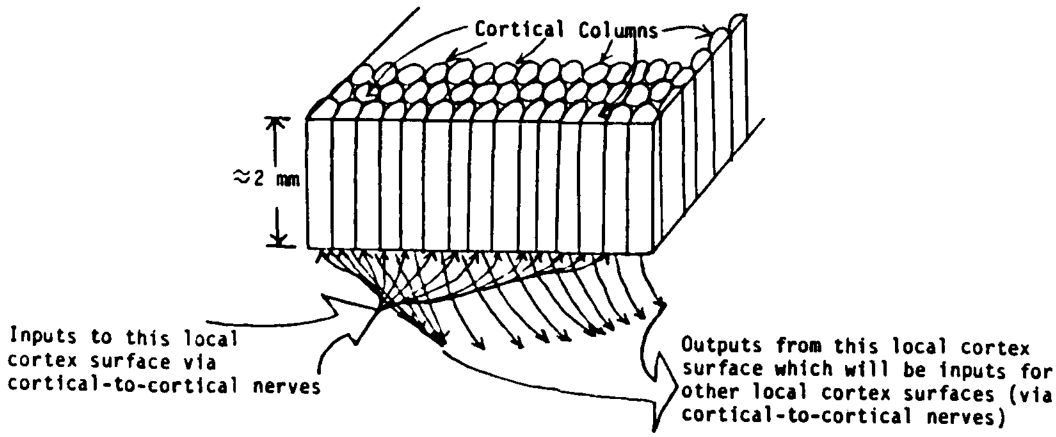

Figure 3.2 - Cut-Away Side View of Cortex Showing "Two-Dimensional Sheet" (3rd Dimension of 2 mm Depth is not Considered)

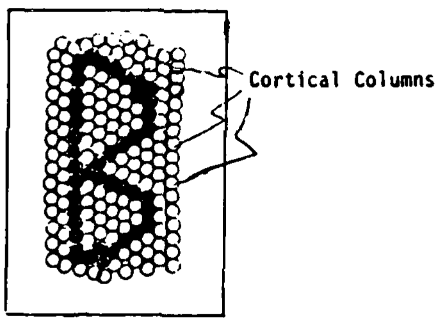

Figure 3.3 - Top View of Primary Visual Cortex with Visual Image of Letter "B" as Input (Shows 2-D Picture) (Greatly Simplified to Illustrate Basic Concept)

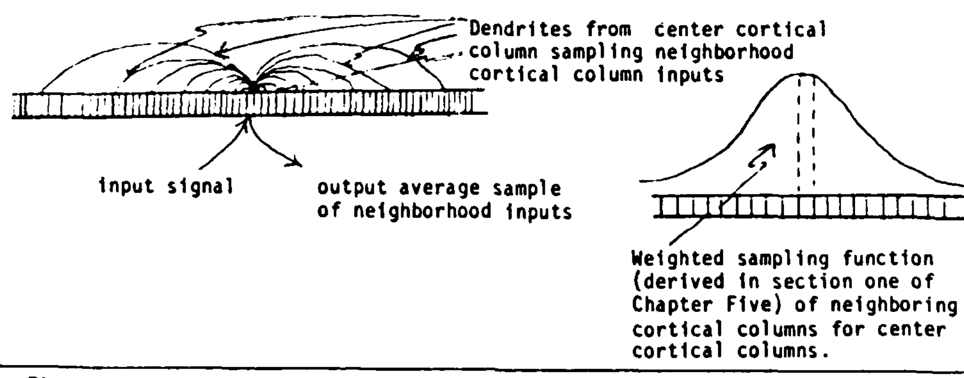

Figure 3.4 - Shows Sample-Average Function of a Typical Cortical Column

Note that the farther away a neighboring cortical column is, the less it will impact the sample average.

Evidence to substantiate this proposed activity of the cortical columns as well as the experimentally justified and mathematically described sampling distribution function is reported on in Section One of Chapter Five.

One common algorithm for calculating the Fourier transform of an NxN discretized two-dimensional image is to first calculate the one-dimensional Fourier transform for each row, building a new NxN matrix out of the N rows of N elements in each row, and then calculate the one-dimensional Fourier transforms of each column of this new matrix. The NxN matrix of these transformed columns is the two-dimensional Fourier transform of the original two-dimensional image. Mathematically, this is given by:

<u>Given</u>: NxN matrix M_{xy}; $x,y = 1,\ldots,N$

<u>Then</u>: The two-dimensional Fourier transform T_{wz} ($w,z = 1,\ldots,N$) is given by:

$$S_{wy} = \sum_{x=1}^{N} M_{xy} \exp\left(\frac{i2\pi w(x-1)}{N}\right) \quad w,y = 1,\ldots,64 \tag{3}$$

$$T_{wz} = \sum_{y=1}^{N} S_{wy} \exp\left(\frac{i2\pi z(y-1)}{N}\right) \quad ; \quad w,z = 1,\ldots,64 \tag{4}$$

The problem with this calculation is that the matrix T_{wz} is made up of complex terms (i.e., each term has a real part and an imaginary part). In the next chapter, justification is given for resolving this problem by taking the Fourier sine transform so that T_{wz} ends up with only all real terms.

Now if the requirement is to find only the low pass sine Fourier transform, and we are content to find the harmonics (to include fractional harmonics) between the D.C. term (which is the zeroeth harmonic) and the first harmonic, then we can use equations (1) and (2) in Chapter Two to describe the procedure that might be followed. The nature of this transform is that it is blind below the 1/4 harmonic (see Chapter Four). The 1/4 harmonic component of a one-dimensional transform can be obtained by doing the point by point correlation of the function with $g(x) = \sin\frac{2\pi x}{4}$:

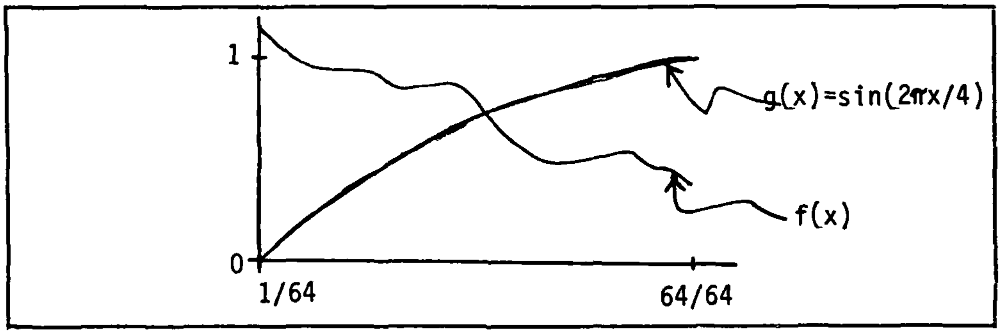

Figure 3.5

So that the value of the 1/4 harmonic is:

$$\frac{1}{64}\sum_{k=1}^{64}\left(\sin\frac{2\pi k}{64}\right)\left(f(k/64)\right) \tag{5}$$

If the dendrites have the distribution shown in Figure 3.4, then the point by point correlation of Equation (5) can be simultaneously approximated in all radial directions by the averaged sample value (the output) of the cortical column which is centered at x=1 (if f(x) = 0 for x > 1). Likewise, the 1/2 harmonic would be approximated by the output of the cortical column centered at x = 1/2, $(x = \frac{32}{64})$, etc. The degree to which approximations like this are in error can be shown to exactly predict the difference between the experimentally measured high frequency roll-off of the visual contrast sensitivity curve and the calculated high frequency roll-off due to airy disk diffraction. This is reported on in detail in section one of Chapter Five.

If the rows are all replaced by the approximations of their one-dimensional Fourier transforms in this way and then the same process is applied to the columns and then the largest cortical column output is identified, its location will be the location of the highest local peak of the estimated two-dimensional Fourier transform.

More specifically, if, for example, the equation to describe the weighted sampling function to compute the neighborhood average (performed by dendritic distribution of Figure 3.4) is given by $D(x) = \exp -(\frac{x}{\sigma})^2$, where x is measured in cortical column diameters (or in this case, discretization units), then Equations (1) and (2) would become:

Given: M_{kl} ; $k,l=1,\ldots,64$

Then: $$S'_{kj} = \sum_{l=1}^{64} M_{kl} \exp -\left(\frac{l-j}{\sigma}\right)^2 \quad ; k,j=1,\ldots,64 \qquad (1a)$$

$$T'_{ij} = \sum_{k=1}^{64} S'_{kj} \exp -\left(\frac{k-i}{\sigma}\right)^2 \quad ; i,j=1,\ldots,64 \qquad (2a)$$

$$\Rightarrow \quad GFVS = \{(i,j): \max_{ij} T_{ij}\}.$$

Although Equations (1a) and (2a) comprise a tetrahedral approximation of the circular theoretical hypothethesized weighted-neighborhood-sampled-averaging-function, it is a better approximation than Equations (1) and (2). (Russel [110a] has implemented this better approximation in both the speech and visual domains, and has obtained as good, if not better, results than the approximation of Equations (1) and (2) which were used throughout the research of this dissertation.)

Careful analysis shows that there is a continuous one-to-one and onto mapping between all such schemes and the location of the largest cortical column output of the original non-transformed input image. This means that the calculation to compute the two-dimensional feature vector from the two-dimensional Fourier transform of the two-dimensional input image needs to be no more complicated than identifying the location of the single cortical column which has the largest output (neighborhood sample average) of the windowed image on the input image local cortex surface. This certainly is a trivial calculation for the cortex to perform.

The cortical-to-cortical nerves, connected at their afferent ends to the local cortex surface on which the input image is displayed, project this location (of the cortical column on that surface with the largest output) to the same respective location (as if two transparencies were laid on top of each other) on the local cortex surface at the efferent end of that cortical-to-cortical nerve. To do this, each cortical-to- cortical nerve must be a bundle of fully insulated (and hence no nodes of Ranvier) parallel communication channels where each communication channel is responsible for transmitting the output of the cortical column on the afferent local cortex surface to the input of the cortical column in the efferent local cortex surface where both cortical columns are in the same respective locations on each of their local cortex surfaces.

3.3.9 The visual windowing mechanism:

In order to complete the systems description of this level of detail, it is necessary to describe the mechanism for windowing the proper portion of an input image. It is crucial that the system has the ability to properly do multiple windowing for any given image. The ability to discriminate on the basis of fine detail is dependent on the ability to window and analyze the various sub-components of an image. James Holten, a doctoral candidate doing research in visual image processing at the Air Force Institute of Technology, helped in the development of the following analysis. To demonstrate how windowing might work, the following possible mechanism for finding windows on the primary visual cortex is offered:

Consider attempting to window the red square in the following figure:

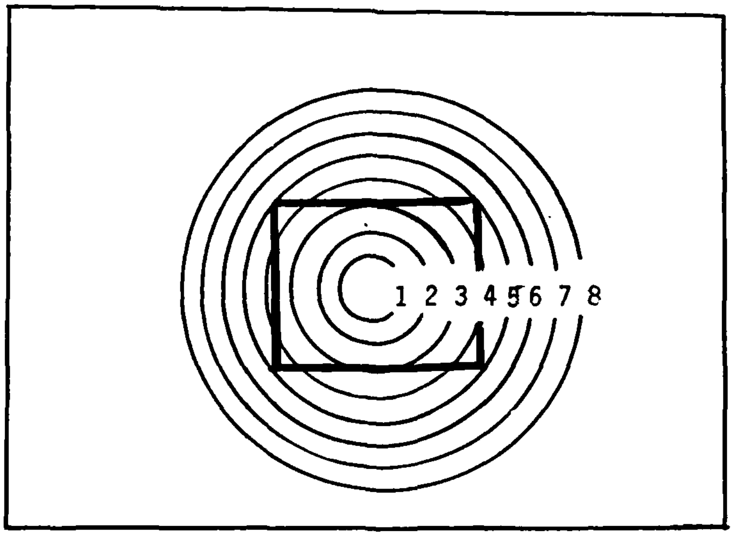

Figure 3.6

Eight candidate windows appear. Each of these windows is circular and centered at the center of the square. It is obvious that windows 1, 2, and 3 are inadequate for windowing the square. Window 4 contains part of the square, but cannot see its corners. Window 5 is the first window which completely contains the square. For windows larger than 5 (6, 7, 8,...), the larger the window, the less significant is the event which is trying to be measured (the square). The square begins to become nothing more than a small detail which is lost in the background noise. In addition, we have already seen that our classification scheme does not do well if the object being classified is much smaller than the window. So it would be most desirable to find a window which contained most or all of the image of interest, but not much more. In this example, this would be window number 5.

One way to find this window number 5 (assuming reasonable brightness statistics for the scene) is to perform the following calculation. Average the visual field in window number one (V_1). Subtract from this average value, V_1, the average of the area outside window 1 but inside window 2 (E_2). Now compute the value W_2 according to the following equation:

$$W_2 = V_1 - E_2 \tag{6}$$

The value for W_3 is:

$$W_3 = V_2 - E_3 \tag{7}$$

where V_2 is the averaged value inside all of window 2 (to include the area inside window 1), and E_3 is the average value of the area outside window 2 but inside window 3. In general, the value for W_n is given by:

$$W_n = V_{n-1} - E_n \ . \tag{8}$$

If we plot the values for W_n, n=1,...8, we have the following figures:

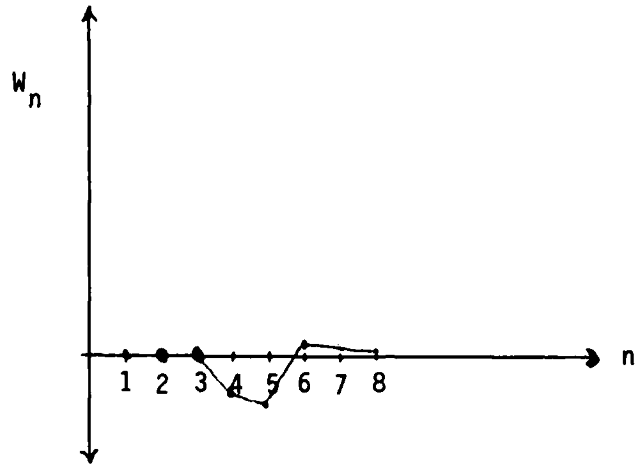

Plot of W_n if inside of square is same amplitude as outside of square and square edges are more positive than background.

Figure 3.7

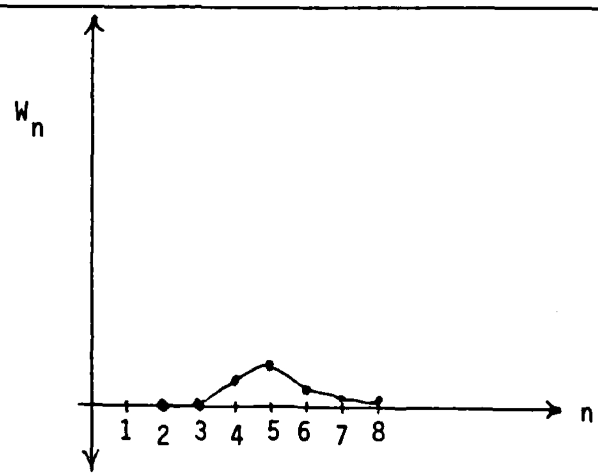

Plot of W_n if inside and outside are same amplitude but square edges are more negative than background.

Figure 3.8

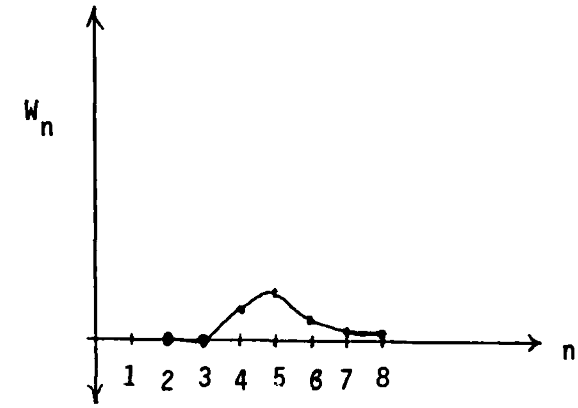

Plot of W_n if inside of square is more positive than outside of square.

Figure 3.9

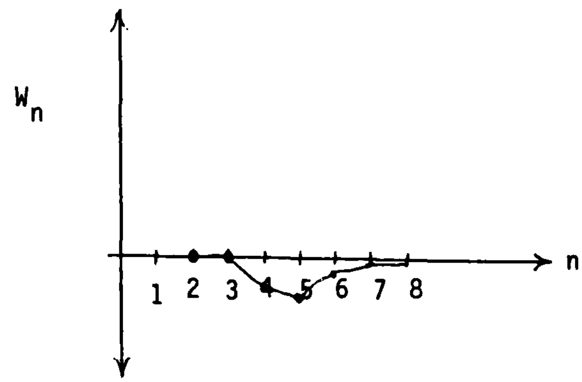

Plot of W_n if inside of square is more negative than outside of square.

Figure 3.10

All curves will have a local positive peak at the desired window (window 5) if the general equation shown in Equation 8 is:

$$W_n = | V_{n-1} - E_n | \quad . \tag{9}$$

If the volume of E_n is equal to the volume of V_{n-1}, then it will not matter what the average brightness is for any V_n. If the average brightness remains the same, the values for W_n will be zero inside an edge boundary and will quickly tend to zero outside the edge boundary. In order to accommodate this requirement for equal boundaries, it will be necessary to either have increasingly large E_n areas, or weigh the averaging operation on V_{n-1} and E_n so that their volumes are equal for relatively small E_n:

This requirement would dictate a weighting function which has a two-dimensional cross-section diagram which looks like this:

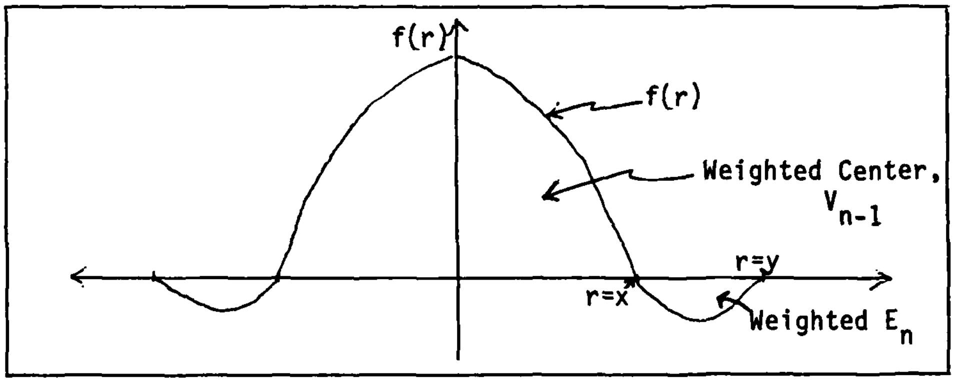

Figure 3.11

(Note that because the area of the end region is so much greater than the area of the V_n region, the magnitude of the negative amplitude of the E_n region does not need to be as great as the magnitude of the amplitude of the V_{n-1} region.) In other words:

$$\int_0^{2\pi} \int_0^{x} f(r)\, r dr d\theta = - \int_0^{2\pi} \int_x^{y} f(r)\, r dr d\theta \qquad (10).$$

The weighting function necessary to perform this calculation is the center-surround weighting function which is known to be characteristic of retinal output channels.

This mechanism for finding the appropriate window appears to be trivial and is supported by the neurophysiology. It is reliant on having the candidate windows centered concentrically on the center of the image to be windowed. This requires that the retina be fairly dense with such concentric sets. It will be the case that there will be significant overlap of the center-surround areas. Will this overlap complicate the requirement of finding the best window for an object? This can be answered by examining the W_n graph for the performance of a set of concentric circular windows which is off-centered.

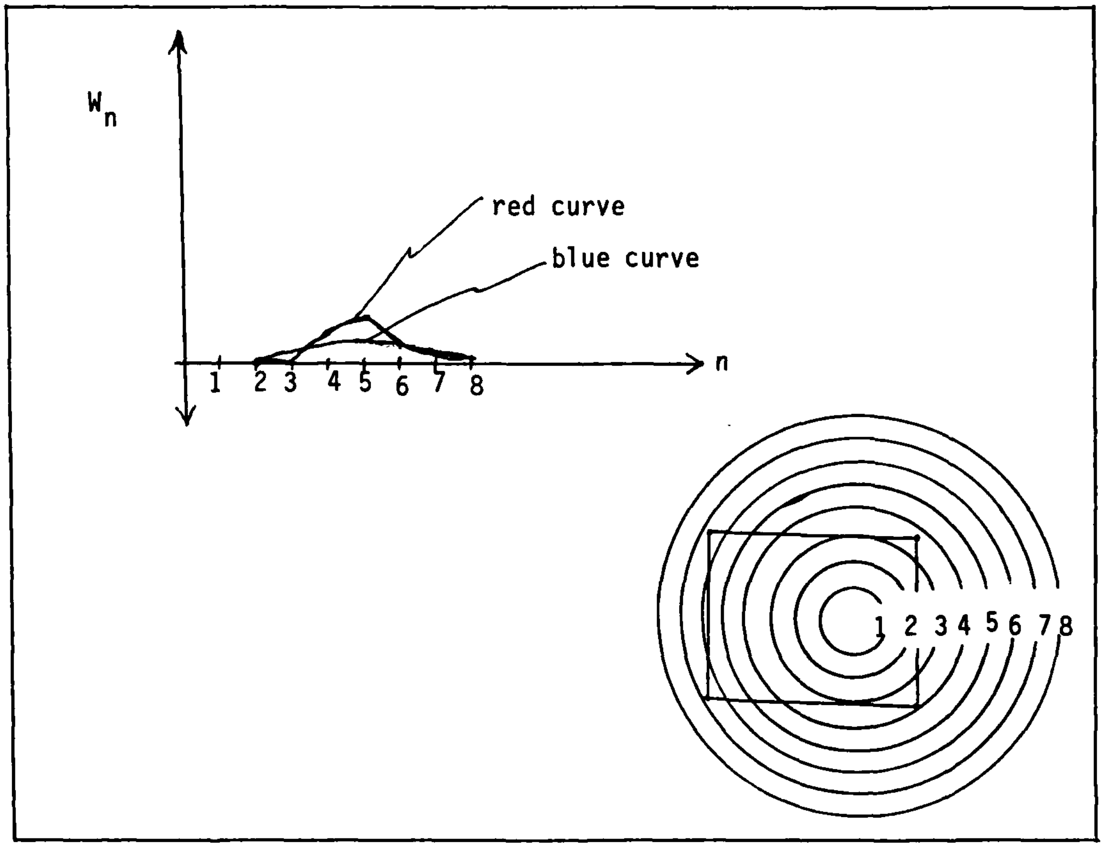

Figure 3.12

The red curve is a replot of the previous results when the concentric windows were centered. The blue curve shows the results of an off-centered set of concentric circular windows. It is still clearly a simple decision scheme which identifies the proper window (i.e., the largest local peak points to the proper window).

Now the question arises as to how to best window an object which is not essentially circular, but instead is elongated. The answer to this question is obviously to use elongated windows which are arranged in the same sort of concentric sets as are the circular windows. So in order to find the rectangle below, we would need to use the window indicated:

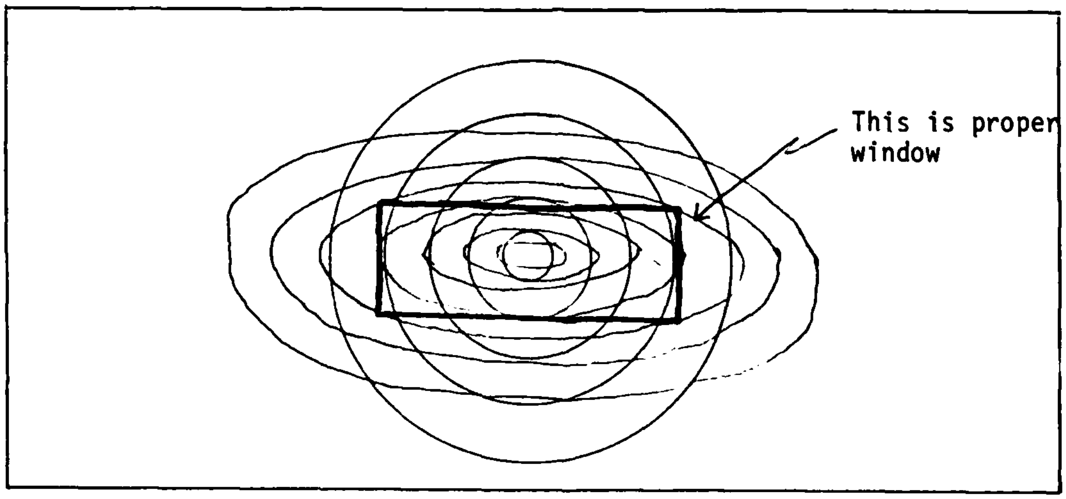

Figure 3.13

It is evident that several sets of elongated windows of different eccentricities which are also co-centered are needed. In addition, each set of different eccentricity elongated windows must appear reduplicated with a different angular offset of its major axis every 15 degrees.

With a grid of fairly densely distributed sets of these windows all across the retina, the set of local peaks in the W_n curves would identify all the windows of all the objects in the visual field.

Since the frequency response of each of the different windows is orthogonal to the frequency responses of all other windows, it is not necessary to recontruct a one-to-one continuous mapping of the visual field onto the primary visual cortex. It is sufficient to construct on the primary visual cortex the output of each of the windows so that windows with the same center are close to each other. This will give the macro effect of looking like a one-to-one continuous mapping of the visual field onto the primary visual cortex, and the micro effect of having small local areas composed of frequency and angle detectors. As long as the distance between co-centered window groups on the cortex is relatively small when compared to the span of the neighborhood averaging function being carried on by each cortical column, the results of the classification algorithm (Equations (1) and (2)) will be essentially unchanged.

In addition, each of the individual inputs to the individual cortical columns will behave like line and angle detectors (Hubel's and Weisel's results) and each will also respond to large, differently shaped areas in the visual field (DeValois's results). It is interesting to note that the "line detectors" will each respond maximally to a specific length line at a specific angular orientation -- this is precisely what Hubel and Weisel report [57]. (Note: If there are only eight different sets of elongated eccentricities, the elongated regions will be 96 times more numerous than the circular regions, which is why Hubel and Weisel did not find many cells which did not show an angular preference.)

3.4 The Human Learning Mechanisms

According to Dietterich [30a], four basic learning situations can be discerned: (1) rote learning (e.g., - Samuel's Checkers Player), (2) learning by taking advice (e.g., - Mostow's FOO), (3) learning from examples (e.g., - Soloway's BASEBALL, Michalski et al.'s AQ11, Buchanan and Mitchell's META-DENDRAL, and Lenat's AM), and (4) learning by analogy. CTT offers a single architecture which appears to account for these four types of learning (which, will be argued later, are really only two types of learning). In addition, Chomsky [21],[22] has hypothesized a precondition to human learning which is considered here as a third type of learning. He argues that hardware which is specific to the task it will perform (e.g., - his hypothesized language acquisition device which is an innate mechanism predisposed to detect certain events in the acoustics and syntax of speech) is a part of the human learning system. CTT generalizes this requirement so that it applies to the acquisition of all types of knowledge, not just the language skills.

It can be seen from the CTT model that the propensity to consider (or even detect) certain events and orderings is inherent in the connectivity structure between the various local cortex surfaces. For example, in order for the CTT system to perform deterministic syntax analysis (Milne [85] shows that the human system is doing deterministic syntax analysis), at least the following structural connectivity must exist:

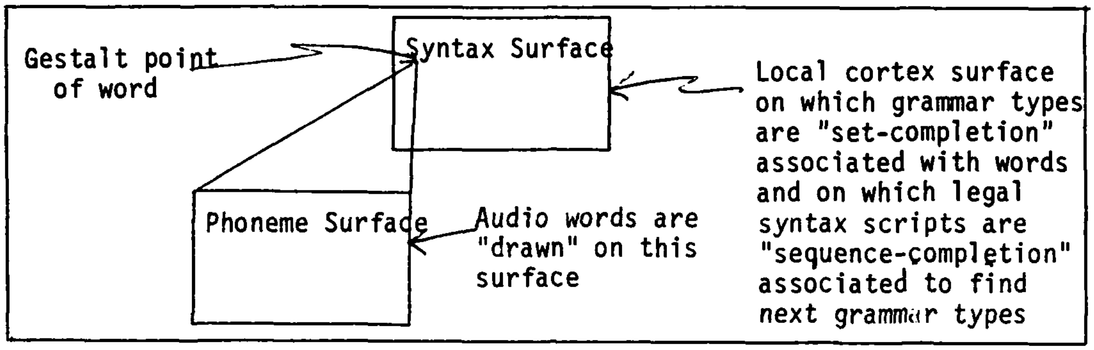

Figure 3.14 (See Figures 2.15 and 2.17)

When a word is hypothesized, it will be projected to the surface responsible for remembering grammar types. The Goldschlager set completion mechanism will complete the set of all grammar types which can be associated with that word. Already in operation on that surface will be the Goldschlager sequence completion mechanism attempting to complete a known legal-syntax sequence. The set completion operation will attempt to activate all grammar types that are associated with the hypothesized word while the syntax sequence completion mechanism will be attempting to complete a legal-syntax sequence. Both operations will intersect (doubly reinforce) the grammar type which most commonly completes the next step in the legal syntax sequence. That grammar type will be the grammar type associated with the hypothesized word. (See Routh [107] for more specifics on the algorithm used in this example.)

Before these two operations (set completion and sequence completion) can take place on the syntax surface, the gestalt of the audio word must be calculated on the phoneme suface and projected to the syntax surface. This gestalt projection is accomplished by the cortical-to-cortical nerve going from the phoneme surface to the syntax surface. If this particular cortical-to-cortical nerve were missing, then the system would not have the capability to learn the syntax of the language. As stated previously (in Section 2.7.3), this structure is oversimplified for the purpose of simply presenting the CTT architectural concept. In all likelihood, there are probably hundreds of local syntax surfaces all interconnected with these cortical-to-cortical nerves (and probably all located in Broca's area). There is neuroanatomical evidence to suggest great diversity, among people, in their relative local densities of cortical-to-cortical nerves throughout the cerebrum. Since the ability to do associations between two different areas of activity (on the cortex) is dependent on the density of cortical-to-cortical nerves between those areas, then we see that the existence of the ability to learn certain functions is dependent on the existence of the necessary cortical-to-cortical nerves; and furthermore, we see that the propensity to learn certain functions is dependent on the relative numbers and densities of the necessary cortical-to-cortical nerves. For example, a person with relatively many and diverse cortical-to-cortical connections between the motor and visual areas of the cortex can be expected to show a great innate ability to learn functions which require good hand-eye coordination; wheras, a person with relatively many and diverse cortical-to-cortical connections between the areas responsible for abstract symbol manipulation can be expected to show a great deal innate ability to learn mathematical subjects.

We see from the foregoing simplified example of Figure 3.14 (not shown in this example were the local cortex semantic surfaces which must also be linked in feedback with this operation) that learning can only take place if the structure exists to support it. Different types of learning require different connectivity structures. It can be seen from this that the location of cortical-to-cortical nerves will tend to dictate an individual's propensity to learn certain types of things. Since cortical-to-cortical nerves are hardwired in at birth (and probably decided genetically), this model helps to explain how natural tendencies and capabilities are passed on genetically.

In addition to explaining the existence of such things as Chomsky's language acquisition device, CTT provides an accurate model for the manner in which this existing knowledge acquisition structure can be programmed. Much of the background development of the following model is covered in the discussion in Appendix A. The characteristics pertinent to learning, from that development, will be reviewed here.

Neurons have multiple mechanisms at their disposal for increasing the propensity for firing (electro-chemical discharge across) previously used synapses. It is clear from this that often used synapses will be more easily excited with smaller stimuli than seldom used synapses. With a new system (i.e., a newborn infant), those events most often observed will begin to be remembered by the increasing of the propensity of the synapses to fire which correspond to the physical location of the gestalts of those observations. In this way, the system will become familiar with specific objects, patterns, sequences, and associations which have often been observed.

Thirdly, according to Goldschlager [49], as the Goldschalger sets and sequences (from the set and sequence completion operations) on local cortex surfaces become more clearly defined, their propensity to add new set members increases. This models the ability to quickly learn new things which have many associations already established in the system.

The increase in the propensity to make abstract associations (associations which occur by computing the gestalt of a set of points forming a two-dimensional pattern on a local cortex surface lower in the abstraction hierarchy) is due to the greater intensity of the key points on the lower cortex surface. They will have a greater intensity because they will produce greater cortical column outputs due to their increased propensity to fire their synapses.

Let us now examine how these three CTT learning mechanisms seem to account for the traditionally recognized types of learning (identified by Dietterich). Rote learning can be viewed in the CTT architecture as the observation of facts, at any level of abstraction, which are useful pieces of information in their observed form -- they do not need to be further analyzed and integrated with other information in order to be useful. A set or sequence of points on any surface at any level of abstraction is considered by the next higher level of abstraction in the CTT system as a raw, unprocessed input. It simply computes the gestalt of that input and "observes" the input by projecting the gestalt of the input onto the surface at the next higher level of abstraction. Since the degree of analogy is measured by the system as the closeness between the gestalt of the input and the gestalt of a remembered pattern, it seems that CTT provides a model which can answer the three questions posed by Dietterich [30a] as to the nature of analogy.

He first asks: "What is the nature of an analogy?" CTT answers this question by showing that the closeness of fit, or similarity of two patterns, is analogous to a human to the degree that their two gestalt points are physically close to each other.

His second question is: "How are analogies recognized?" The answer to this question is evident. When two gestalt points are close to each other, the input patterns which generated them are analogous (even though the input patterns may have originated on two different surfaces which both project the gestalts calculated on their surfaces to the same next higher abstraction surface).

His third question is: "How is the relevant knowledge transferred from the analogous knowledge base and applied to accomplish the desired tasks?" The answer to this third question is more difficult to explain and requires a better undestanding of the feedback nature of the cortical-to-cortical nerves connectivity than is presented in this dissertation. Lacking this more elaborate presentation of the interconnectivity of the several involved surfaces, this author asserts that the analogy is not complete unless the effect of the actions dictated by the input in one realm are also analogous to the effect of the actions dictated by the input in the other realm.

Therefore, the second type of learning defined here and accounted for by CTT is learning by multiple exposure to the gestalt of a pattern. This multiple exposure is accomplished at all levels of abstraction by the analogy mechanism which was just reviewed and the memory of these multiple exposures is described in Appendix A by the mechanism which neurons, and hence cortical columns, use to increase their propensity to activate in accordance with their use.

The third type of learning is to be attributed to Goldschlager [49]. He describes a learning mechanism which will be called here "learning by attaching multiple associations." He shows how the memory of a new fact (gestalt point) is reinforced in proportion to the number of elements in the set with which it is being associated. If the number of elements in a set is large, then the addition of a new point to that set will be much easier than if that new point is not set associated with many points.

This third learning mechanism, when operating so as to attempt to complete a set with only partial information, can be shown to prefer to complete the set which best matches the data given. This appears to account for the inductive learning phenomenom which the previously mentioned "learning from examples" A.I. systems attempted to model.

The only type of learning situation identified by Dietterich which has not yet been explicitly accounted for, is learning by taking advice. An examination of Mostow's FOO (a typical advice-taking system) reveals that advice given could only be integrated into the system when: (1) the advice was first translated into a form recognizable by the system, (2) assoicated with other pertinent facts in the system by (3) a pre-existing association mechanism which was predisposed to look for certain prioritized associations, and finally, (4) a new fact was inferred from these discovered associations which was then added to the knowledge-base. CTT can be seen to account for this type of learning by: (1) first finding the gestalt of an input, then (2) using the Goldschlager set and sequence completion mechanisms to associate it with the most relative information already in the system. This is done by

(3) the pre-existing association mechanisms which are predisposed to look for associations in accordance with the priorities established by the most relatively densely connected (by cortical-to-cortical nerves) cortex surfaces. Finally, (4) the gestalt of these new associations and analogies is computed and added to the knowledge-base.

Therefore, it is seen that CTT models the three types of learning: learning in accordance with innate ability, learning by multiple exposure to the same (or similar) cortex image, and learning by attaching multiple associations to new observations.

3.5 Chapter Summary

In this chapter, a systems analysis approach was taken in order to define that which is and is not theoretically plausible in the quest for a complete unified systems description of the information processing architecture and operation of the human brain. This chapter (along with the argument in Appendix A) developed a line of reasoning which, given that the brain is using analogy (rather than deduction mechanisms) to do its reasoning, concluded:

(1) It is likely the case that the same gestalt classification mechanism is used throughout the brain at all levels of abstraction in all domains.

(2) This gestalt classification mechanism uses two-dimensional images "drawn" on small local areas of the cortex to represent its input.

(3) It is argued that it processes these images by first calculating their two-dimensional Fourier transforms.

(4) It was shown that only two numbers are extracted from this two-dimensional transform which are used to identify the physical storage location (on another local cortex surface) of the gestalt identification of the image. This was shown in Appendix A and is considered to be the most significant single contribution of this dissertation to the neurosciences.

(5) A windowing mechanism for visual image processing was hypothesized which explains the results reported by both Hubel and Weisel and DeValois et al.

(6) It was shown how Cortical Thought Theory provides a model sufficient to account for the three kinds of human learning.

4. Some Mathematical Reflections on the CTT Gestalt Mechanism

This chapter discusses the mathematical reasonableness of the CTT gestalt mechanism which is described in Equations (1) and (2) of Chapter Two. This discussion, although it specifically addresses Equations (1) and (2), is also valuable for understanding the performance of approximations to Equations (1) and (2) such as equations (1a) and (2a) or such as the true theoretical gestalt mechanism described in Section 3.3.8.

Some mathematical analysis is in order, at this point in the development of this dissertation, which seeks to understand the theoretical boundaries of the spectrum of possible solutions to the following problem:

> Find the algorithmic mechanisms which perform consistent classifications of two-dimensional Fourier-like transforms so that the cardinality of the classification set is two, and such that the distance between the two-space vectors (from the two members of the classification set) for any two input images (before being Fourier transformed) agrees with the human assessment of the distance between the two input images. (The "images" referred to here are the input sensory cortex images and are therefore not restricted to the visual image domain.)

This is basically a three-part problem. It can be divided into the following three questions:

(1) What two-dimensional Fourier-like transform is being calculated by the cortex?

(2) What two measurements are being extracted?

(3) How are these two measurements indicative of human distance measures?

Let us first consider a partial answer to question number three. In general, the support of a two-dimensional Fourier transform is the entire plane. The high frequency terms change more perceptibly with minor-detail changes in the image. The low frequency terms characterize the general shape of an image. The more two images differ in general shape, the more disparate they appear to a human observer. This tends to indicate that the human observer is paying more attention to the low spatial frequencies of an image. (This is verified by the perceptual psychology experiments of Kabrisky [59], Maher [78], Ginsburg [48], and others.) The exception to this generalization is the lowest (zeroeth) harmonic. The value of the D.C. term seems not to make much difference in determining the psychologically perceived similarity between two images. This characteristic of human perception suggests that we extract the two measurements from the very low frequency harmonics *without considering the D.C. term.*

We will further consider the answer to the third question later. Let us now turn our attention to question number one: "What two-dimensional Fourier-like transform is being calculated on the cortex?"

It is required only that a transform be used which characterizes an image in terms of its frequency components. There are so many transforms which do this that they are too numerous to list here. Some of the more popular ones are: Fourier, Fourier-sine, Fourier-cosine, Laplace, Mellin, and Walsh.

The Walsh transform is an example of a class of transforms which do provide orthogonal basis sets which completely represent (is completely invertible) the image. However, it does not continuously map the frequency components from the lowest to highest frequencies. Also, its computation would require point-by-point correlations with the square wave basis functions. Square waves are very difficult (impossible if approximations are not allowed) to produce in the real world. It seems that a biological system would have considerable difficulty producing them. For these two reasons, although neither reason is sufficient to rigorously discount the Walsh class of transforms, this class of transforms will not be further discussed.

Another fairly popular class of transforms is represented by the Mellin transform. The most significant advantage of this transform is that it handles scaling fairly easily. Scaling is not a required operation because CTT has already displayed a window function which frames every image identically regardless of its size. Since the Mellin class of transforms represents a more complicated calculation than the straight Fourier transform, and since the advantage (scaling) of the Mellin class of transforms is not an advantage if the system already has the CTT windowing mechanism, this class of transforms will not be considered further. (Occam's razor must be viewed as an indispensible tool in this type of modeling analysis.)

The next class of transforms to be considered is the class of transforms represented by the Laplace transform. This class of transform first multiplies the input image by some window which goes to zero at infinity (to guarantee integrability) and then takes the pure Fourier transform of the windowed image. Since the multiplication of the image by a window function is viewed by CTT (see Chapter Five) as a necessary, but separate, preprocessing operation before an image is displayed on a cortex surface, the Laplace transform can be considered as essentially the same as the Fourier transform for CTT purposes.

Consideration of all other classes of transforms in this manner will make it evident that it is only necessary to consider an analysis of the pure Fourier transforms (to include the sine and cosine transforms). The other classes of transforms are either unnecessary modifications of the Fourier transform, or they offer advantages which are not necessary within the framework of CTT, or they do not meet the requirement to present a simple scheme for performing (or approximating) a continuous mapping of the frequency characteristics of an image from the lowest to the highest harmonics.

Therefore, we consider the Fourier transform. For the moment, let us not consider the difficulty of representing complex numbers at the same location on the cortex. If we examine the two-dimensional Fourier passes through the D.C. term (a diameter). Therefore, half of the image is redundant. It seems that it would be convenient, in light of the difficulty of representing complex numbers, to use one half of the plane to store the coefficients of the cosine harmonics and the other half of the plane to store the coefficients of the sine harmonics. This is indeed what Kabrisky, Maher, and O'Hair [90] have done in their work.

O'Hair shows that although phase variance is preserved by using this method, dyslexia can be explained by calculating and storing the magnitude transform (i.e., $(a_n^2 + b_n^2)^{\frac{1}{2}}$). Although this discards one half of the information (the phase information), it does explain the common natural tendency of the human image classification system to be dyslectic. It was decided, since it seemed best at the time (and may well have been right), to consider only a transform which could distinguish phase variations of an image. For this reason, the magnitude transform was not pursued (beyond early graphical analysis which will be described later).

It seems to be an awkward requirement to expect the cortex to perform two calculations, the sine function correlations and the cosine function correlations, and then store them in separate locations (even if on either side of a diameter). For this reason, the Fourier sine transform and the Fourier cosine transform were considered. Each is completely invertible and achieves this property by assuming the even symmetry (in the case of the cosine transform) or the odd symmetry (in the case of the sine transform) of the image.

When faced with the choice of either the sine or the cosine transforms, we choose the sine transform because, as we have already pointed out, we will not be considering the D.C. term. The D.C. term for the sine transform is always zero; but in order to drive the D.C. term of the cosine transform to zero, an initial D.C. offset of the original image is generally required. This requirement to provide an initial D.C. offset requires a set of fairly complicated preprocessing operations. Occam's razor is again employed to make our decision for us.

It has now been demonstrated that it is reasonable to use the Fourier sine transform and to only have to calculate the low frequency harmonics. But how high must we go to insure we have calculated the proper number of harmonics? Kabrisky's work shows us that the third harmonic is a sufficiently high low-pass filter cut-off; Maher's work shows us that the second harmonic is a sufficiently high low-pass filter cut-off.

At this point, a three dimensional graphics plotter was used to confirm the reasoning thus far (which resulted in settling on the Fourier-sine transform) and to help find an answer to question number two: "What two measurements are being extracted?"

A map of the primary audio cortex was built. This cortex is essentially a plot of the amplitude spectrum of the acoustical excitation of the eardrum plotted on a log-log cartesian coordinate system. (See Chapter Five, section two for more details.) The log-log spectrum of a phoneme was displayed on this surface. This image was then discretized into a 64 x 64 matrix. A Hamming window was applied to every row, and then a Hamming window was applied to every column. This image was then treated as the input cortex image which was to be transformed. (The technique of zero-filling was used to approximate a continuous transform.) A three-dimensional plotting program was used to examine hundreds of low-pass two-dimensional transforms. Many different types of transforms were used. Two things were being looked for in this process. The first was: "How did each of the different types of transforms behave compared to the other transforms?" The second was: "What two measurements seem to be reasonable choices for the two member gestalt feature vector set?"

Some examples of these plots are presented in Figures 4.1 through 4.4 and also in Figure 2.8. Figure 4.1 shows a typical picture of the plot of the magnitude of the Fourier transform. The D.C. term is the peak in the center. The eighth harmonic is at the edges. The sort of measurements that might be taken from this are: (1) average gradient along two different orthogonal axes, (2) direction and distance to second highest peak, (3) direction and distance to the local minimum closest to the D.C. term, etc. There is obviously an infinite number of sets of two measurements which can be taken from this data, but none of them appears to be very valuable in characterizing the low frequency behavior of the image on the input surface.

Figure 4.2 shows a typical picture of the plot of the phase of the first eight harmonics of the Fourier transform. The plot of the phase was investigated because the inverse of the phase (setting the magnitude to one everywhere) is reported to produce a cartoon of the original picture. But again, no two readily apparent measurements of the phase plot seem to be very valuable in characterizing the low frequency behavior of the image on the input surface.

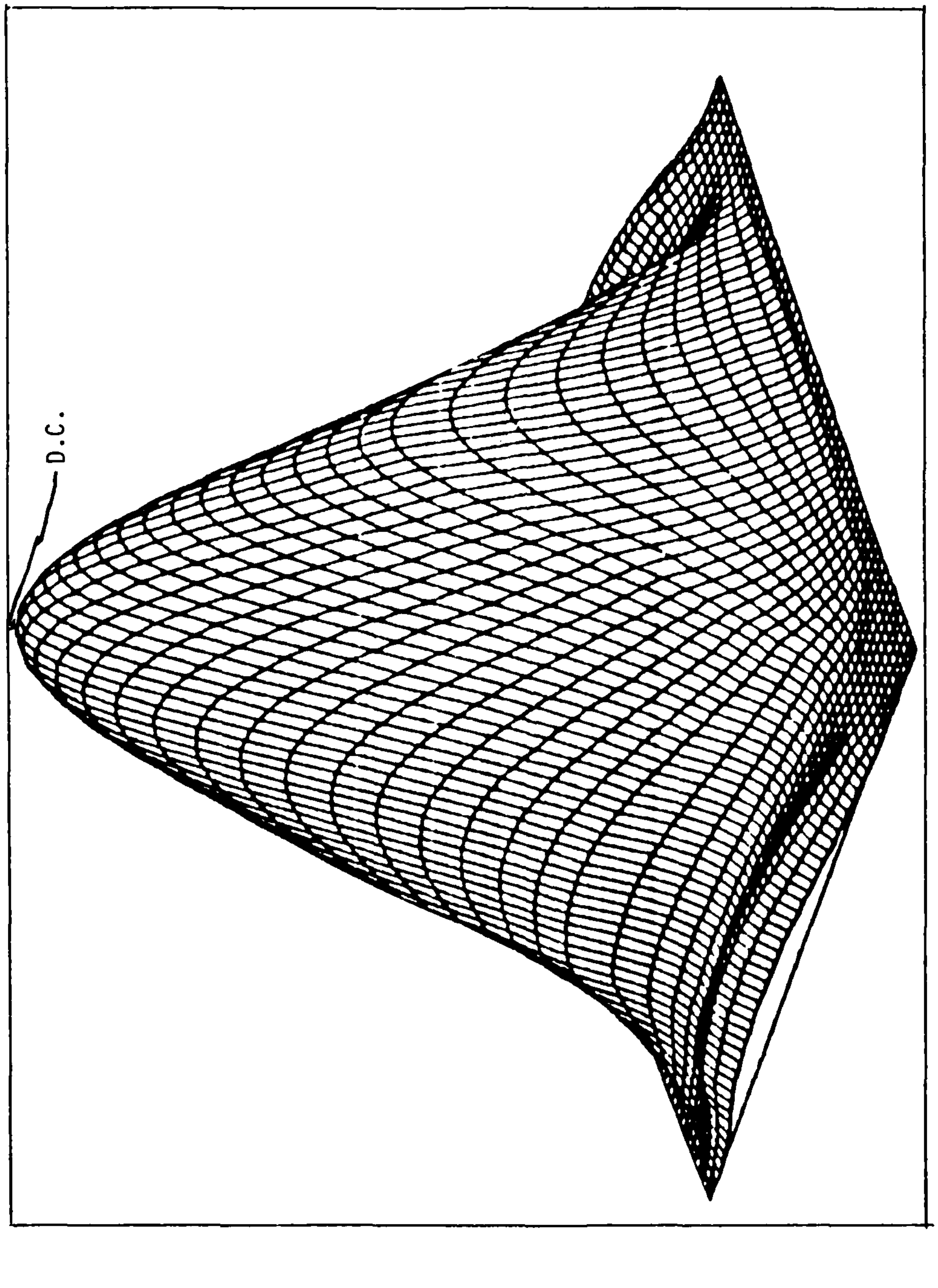

Figure 4.1

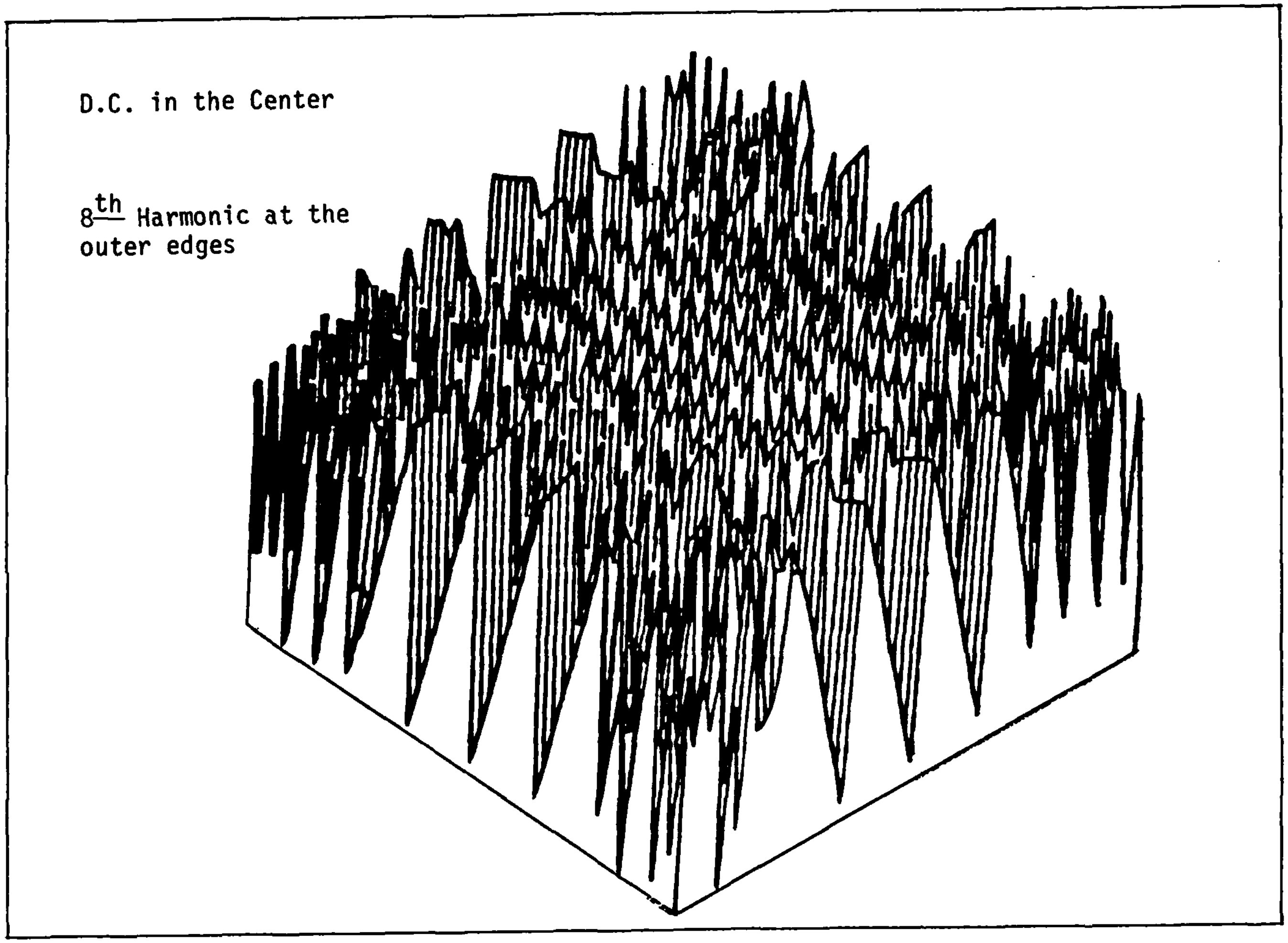

Figure 4.2

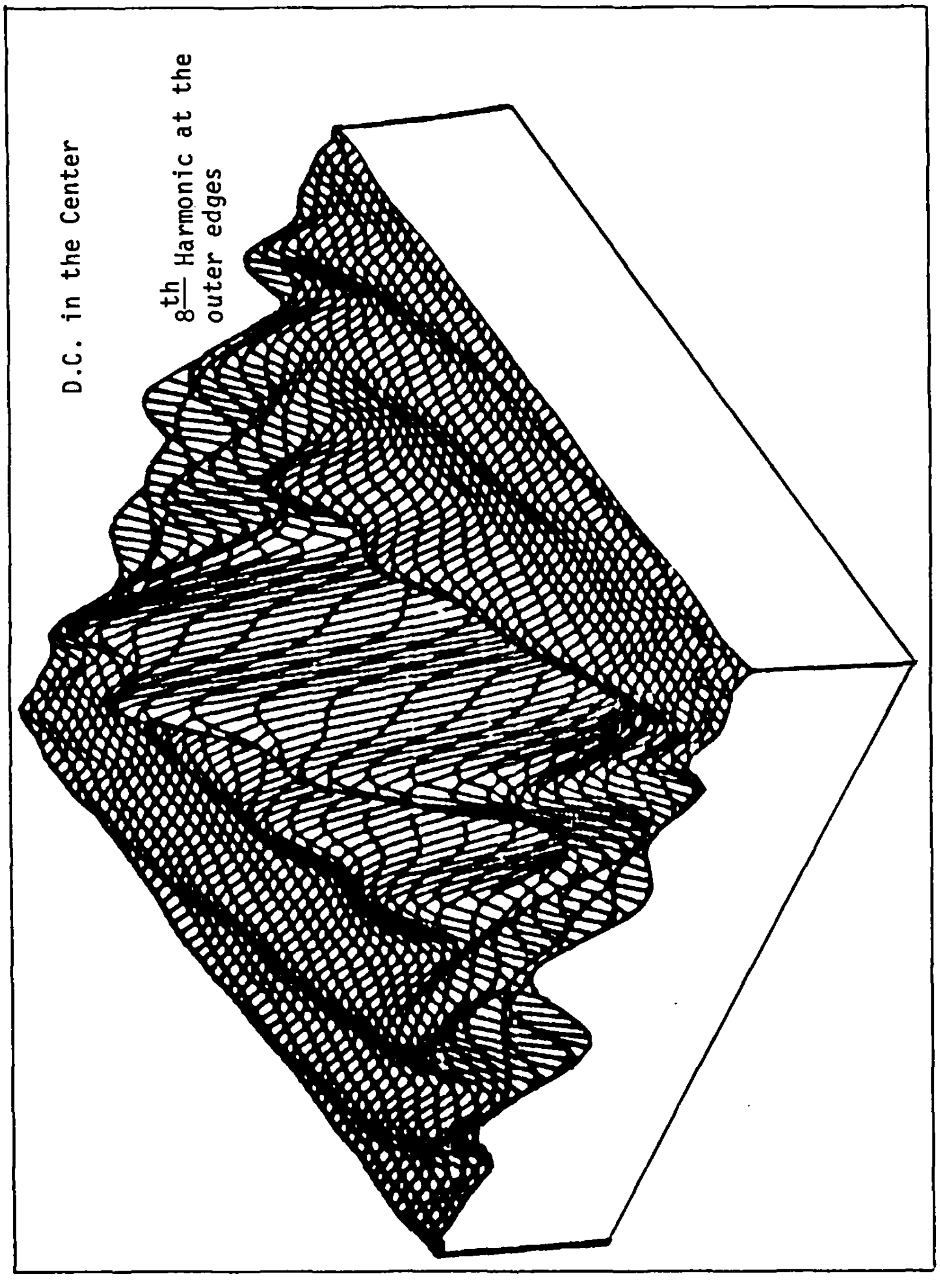

Figure 4.3

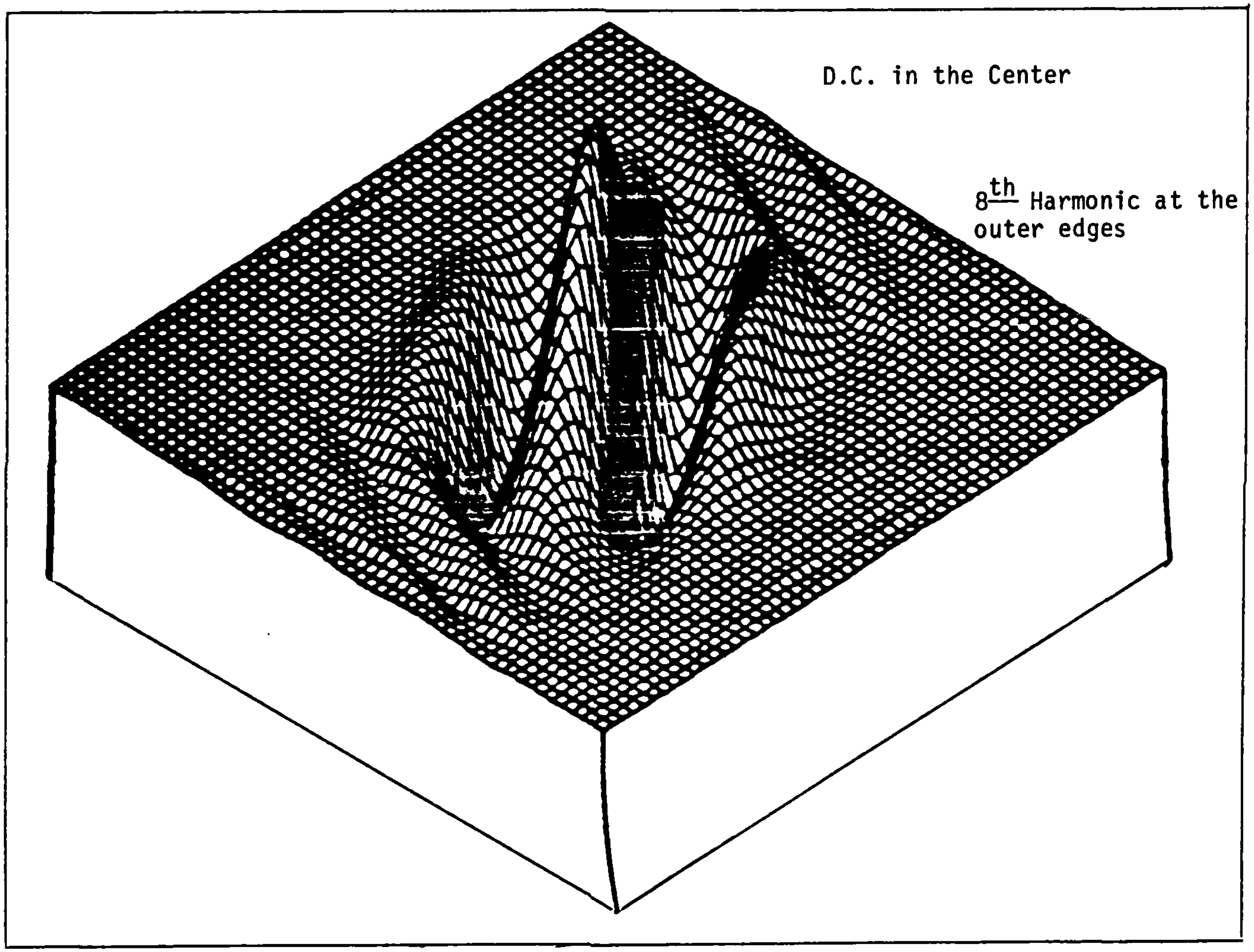

Figure 4.4

Figure 4.3 shows a typical picture of the plot of the first eight harmonics of the Fourier-cosine transform. (The lower harmonics are expanded and the higher harmonics are reduced in scale.) Two possible sets of two measurements are immediately apparent when one looks at this picture. The first is to find the local peak of the first derivative (calculated radially in all directions from the center) which is closest to the D.C. term (but not at the D.C. term). Its coordinates would be two extractable measurements that indicate a significant feature of the behavior of the low frequency harmonics. Experiments showed that this was not a consistent indicator of the phonemic identity of the input image. The second immediately apparent possible set of two measurements is the distance and direction to the peak across the deep valley descending sharply from the D.C. term. Since this is the location of the highest peak of the magnitude transform of this transform, one asks, *"Why not just find the highest peak of the sine transform of the original image?"*

The sine transform was investigated and it was found that the local peak which is closest to the D.C. term is also usually the highest and usually occurs between the D.C. term and the first harmonic. (Figure 2.9 is a plot of the sine transform out to the first harmonic.) Since the location of this peak represents the single most significant characteristic of the low frequency behavior of the input image, it makes sense to consider this as a reasonable candidate solution of the set of two measurements (the coordinates of the point) which comprise the gestalt feature set.

For the sake of thoroughness of the investigation, many other representation schemes for the transform were examined. For instance, consider plotting the cosine transform on one half plane and the sine transform on the other, or plot the cosine plus sine value at all points. (A typical plot of this appears in Figure 4.4), or plot the magnitude of one half plane and the phase on the other, or plot the absolute value of all of these already mentioned plotting schemes, etc.

None of the schemes that were tried appeared to present a technique as simple and straight-forward as finding the location of the first dominant peak in the sine transform. This seems to be the most reasonable solution of those tried.

Let us now turn our attention to examining the robustness of this solution. The news here is, at first, not very encouraging. Let us use the simplified representation scheme of allowing any single pixel in the 64 x 64 input matrix to be either on or off (one or zero). This is not at all unreasonable for the primary audio cortex. We see that we have a many-to-one mapping scheme. Quantitatively, we have N different possible image input pictures and only 4096 possible answers, or gestalts (assuming a transform output matrix of 64 x 64 = 4096), where N is given by:

$$N = \frac{4096!}{4906!\,0!} + \frac{4096!}{4095!\,1!} + \frac{4096!}{4094!\,2!} + \ldots + \frac{4096!}{0!\,4096!} \qquad (11)$$

This yield, on the average, an N/4096 to one mapping ratio, R.

$$R = N/4096 \gg 10^{100} \qquad (12)$$

This means that, on the average, there will be more than 10^{100} different input images that all map into the same gestalt point.

Further analysis shows that the situation is not really as ill-conditioned as it might appear.

In matrix notation, the transform expressed by Equations (1) and (2) in Chapter Two is:

$$(AB)^T B = S \tag{13}$$

where A is the 64 x 64 input matrix, S is the 64 x 64 solution matrix, and B is the 64 x 64 transform matrix given by:

$$B = \begin{bmatrix} \sin\left(\frac{2\pi\cdot 1\cdot 1}{4096}\right) & \sin\left(\frac{2\pi\cdot 1\cdot 2}{4096}\right) & \cdots & \sin\left(\frac{2\pi\cdot 1\cdot 64}{4096}\right) \\ \sin\left(\frac{2\pi\cdot 2\cdot 1}{4096}\right) & \sin\left(\frac{2\pi\cdot 2\cdot 2}{4096}\right) & \cdots & \sin\left(\frac{2\pi\cdot 2\cdot 64}{4096}\right) \\ \sin\left(\frac{2\pi\cdot 3\cdot 1}{4096}\right) & \sin\left(\frac{2\pi\cdot 3\cdot 2}{4096}\right) & \cdots & \sin\left(\frac{2\pi\cdot 3\cdot 64}{4096}\right) \\ \vdots & & & \\ \sin\left(\frac{2\pi\cdot 64\cdot 1}{4096}\right) & \sin\left(\frac{2\pi\cdot 64\cdot 2}{4096}\right) & \cdots & \sin\left(\frac{2\pi\cdot 64\cdot 64}{4096}\right) \end{bmatrix} \tag{14}$$

One nice property of B is that it is not singular. That means that given any matrix S, it is completely invertible; that is, given S, one can reproduce A without ambiguity in any term.

Since the three-dimensional plot of S (see Figure 4.5) is always (by experience) a single simply-shaped hill which peaks at $\max_{i,j} S_{ij}$, and since the gestalt only tells us the location of $\max_{i,j} S_{ij}$, and no other information, it is tempting to say that we need only know the location of the peak, and then we can interpolate between the peak and the first row and first column (since we know they are very near zero), and we can extrapolate from the peak to the 64th row and the 64th column (assuming they are a small fraction of the peak amplitude -- unless, of course, the peak is near the outer border). In order to be able to do this interpolation and extrapolation with any degree of confidence that the inverse of the result ($\hat{A}$):

$$(S\ B^{-1})^T\ B^{-1} = \hat{A} \tag{15}$$

will have the same basic shape as A, we must demonstrate a fairly low condition number for B.

As it turns out, B is an ill-conditioned matrix. This is due primarily to the fact that the first 16 rows of B (especially the first two rows of B) are nearly linear multiples of each other.

The situation gets considerably better when we realize that B (and, therefore, Equations (1) and (2)) is not a very accurate model of the function which Chapter Three proposes is being approximated by surface averaging functions (see Figures 3.2, 3.3, and 3.4) operating across the entire span of A.

To further explain this last statement, consider that each dot product (a row of A dotted with a column of B to produce a single term in AB) represents the point-by-point correlation of the first one-sixty-fourth of the particular sine-wave harmonic with the particular row of A.

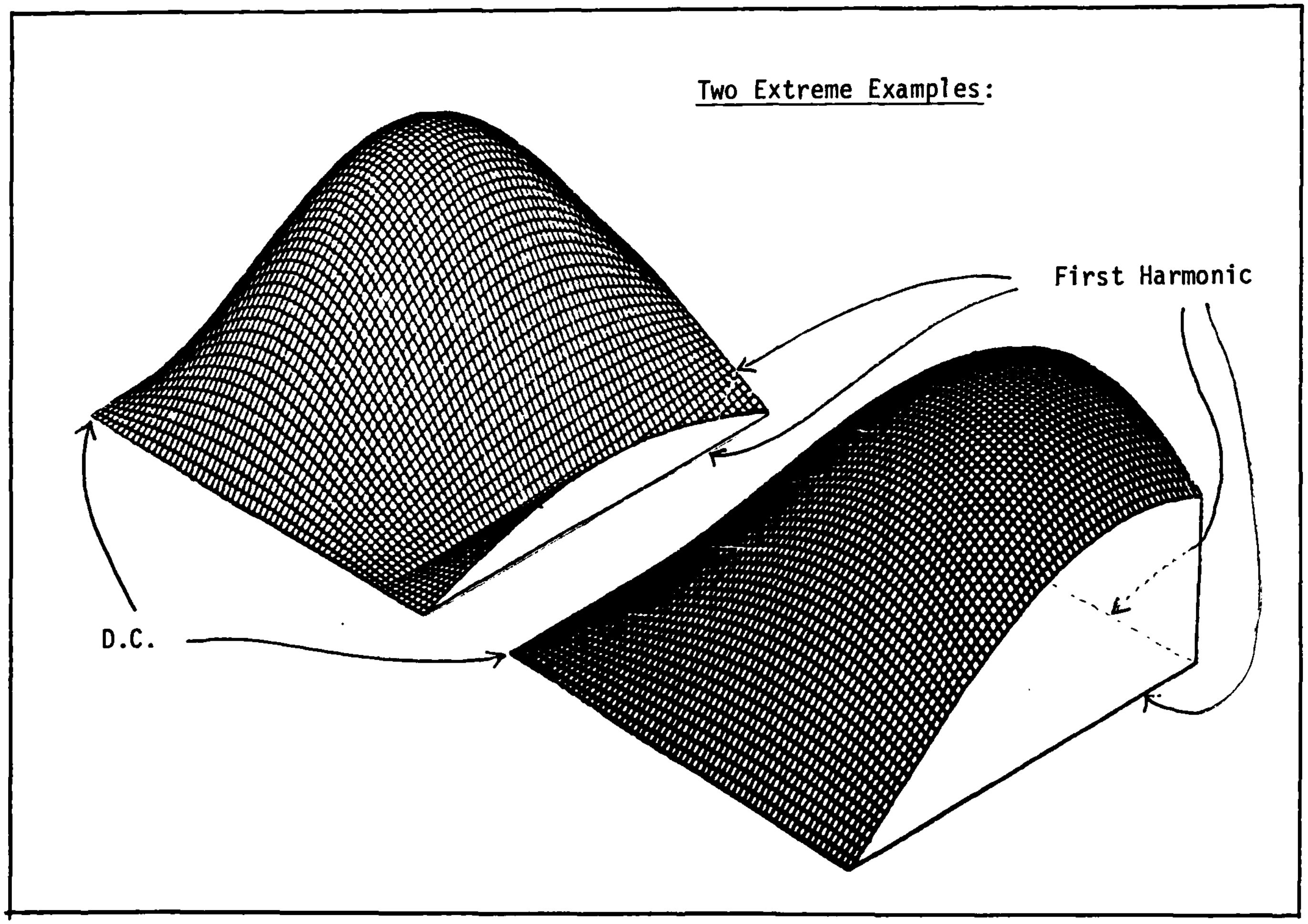

Figure 4.5

Since this point-by-point correlation for the first 15 columns (or rows -- it is symmetric) of B can never exceed the point-by-point correlation of the 16th column (a term-by-term comparison shows that every term in the 16th column exceeds every corresponding term in the first 15 columns), we conclude that the transform is blind for all parts of images which exist in the first 15 rows (and first 15 columns) of A.

This is not true of the proposed neurophysiological transform estimation operation, carried out by the surface averaging function of the cortical columns, which is proposed in Chapter Three. If, instead of using B, we construct a B' such that each column is a point-by-point correlation of the sample averaging function (which will be derived in the next chapter), we find that the condition number of B' is on the order of 64.

This appears to be considerably better than "astronomical". But as it turns out, it is not better. Experience shows that our estimation of S will often yield errors which are one pixel size or larger. This means that this may produce errors which are 64 pixels off between A and $\hat{A}$. Since this is the entire span of A, the condition number of B' might as well be infinite.

Further analysis can show that the maximum error under normal conditions (an actual speech-produced input image, rather than a contrived example to test the limits of robustness) is 32 pixels, and that the average error is closer to 16 pixels. But all of this is still rather discouraging because an error of even 16 pixels allows for vastly disparate shapes on the image surface.

The following example will illustrate an extreme instance of this phenomenon. Consider an input image given by A_1:

$$A_1 = \begin{bmatrix} 0\ 0\ 0\ 0 & \cdots & 0 \\ 0\ 0\ 0\ 0 & \cdots & 0 \\ \vdots & & \\ 0\ 0\ 0\ 0\ 0 & \cdots & 0 \\ 1\ 1\ 1\ 1 & \cdots & 1\ 1 \\ 0\ 0\ 0\ 0\ 0 & \cdots & 0 \\ \vdots & & \\ 0\ 0\ 0\ 0\ 0 & \cdots & 0 \end{bmatrix} \begin{matrix} \\ \\ \\ \\ \leftarrow \text{32nd row} \\ \\ \\ \\ \end{matrix} \tag{16}$$

And an input image A_2:

$$A_2 = \begin{bmatrix} 0\ 0\ 0\ 0\ 0 & \cdots & 0 \\ 0\ 0\ 0\ 0\ 0 & \cdots & 0 \\ 0\ 0\ 0\ 0\ 0 & \cdots & 0 \\ \vdots & & \\ 0\ 0\ 0\ 0\ 0 & \cdots & 0 \\ 0\ 0\ 0\ 0 & \ldots 0\ 1\ 0 \ldots & 0 \\ 0\ 0\ 0\ 0\ 0 & \cdots & 0 \\ \vdots & & \\ 0\ 0\ 0\ 0\ 0 & \cdots & 0 \end{bmatrix} \begin{matrix} \\ \\ \\ \\ \\ \leftarrow \text{32nd row} \\ \\ \\ \\ \end{matrix} \tag{17}$$

$$\uparrow \text{32nd column}$$

In A_1, the entire input matrix is zero except the 32nd row which is all one. In A_2, the entire input matrix is all zero except the single term, $A_{32,32}$, which is one. The gestalt for both of these images will be the same, which is S_1. (S_1 will be equal to A_2.)

So, does all this mean that the proposed gestalt mechanism is useless? No, it does not. It does show very vividly that more than one window of an object is necessary. This means that subportions of an image need to be treated as entire images and classified separately in order to characterize an image in terms of the gestalts of its whole and its parts. This multiple windowing characteristic is illustrated repeatedly in the example given in Chapter Two (with Figures 2.11 through 2.1).

Therefore, all the characteristics which were listed at the beginning of this chapter as requirements for a reasonable gestalt mechanism are met by this hypothesized mechanism. Specifically, this mechanism does meet the requirement to extract a two-element feature vector set which significantly characterizes the low frequency behavior of the two-dimensional Fourier-sine transform. Since it extracts the gestalt from the most dominant feature of the low spatial frequencies, it is a consistent measure of the elements in what a human would consider a group of similar images. It is conceivably implementable, even suggested, by the neurophysiological structure of the cortex and cortical-to-cortical nerves. It becomes a semi-smart mechanism when it works in conjunction with the windowing mechanism proposed in Chapter Three, in that only significant subsets of the image will also be windowed (for the purpose of further discrimination and categorization). The next chapter offers experimental evidence which suggests that this mechanism does indeed elicit psychological distance measurements which are characteristic of the human system.

5. Experimental Verification

Perhaps this chapter is mistitled because it is not possible to verify a general theory. It has been said that in order to prove a hypothesis, it must be demonstrated that the hypothesis is consistent with all the axioms of the system. In the case of a general theory, the "system" is the real universe. We cannot yet completely list the set of axioms sufficient to account for the real universe. So, no general theory can be proven (and so never verified). Confidence in, and hence acceptance of, a general theory is achieved through the gradual process of demonstrating that a theory is consistent with a wide variety of the axioms of the real universe, while, at the same time, avoiding any demonstration of its inconsistency with any of these axioms. To accomplish this fact is far beyond the scope of any single dissertation. However, it is certainly reasonable for the necessarily critical scientific community to expect some fairly significant demonstration that any new theory is consistent with an important subset of these axioms. This is usually accomplished by failing, after many attempts, to find some inconsistency between the new theory and any observed behavior of the real world.

There are at least three broad categories of test types which are commonly considered significant indicators of the usefulness and consistency of a new theory. The first category is made up of those experimental observations which have not yet been explained by any pre-existing theory. The second category is made up of those observations, which can be explained to some extent by existing

5. Experimental Verification

Perhaps this chapter is mistitled because it is not possible to verify a general theory. It has been said that in order to prove a hypothesis, it must be demonstrated that the hypothesis is consistent with all the axioms of the system. In the case of a general theory, the "system" is the real universe. We cannot yet completely list the set of axioms sufficient to account for the real universe. So, no general theory can be proven (and so never verified). Confidence in, and hence acceptance of, a general theory is achieved through the gradual process of demonstrating that a theory is consistent with a wide variety of the axioms of the real universe, while, at the same time, avoiding any demonstration of its inconsistency with any of these axioms. To accomplish this fact is far beyond the scope of any single dissertation. However, it is certainly reasonable for the necessarily critical scientific community to expect some fairly significant demonstration that any new theory is consistent with an important subset of these axioms. This is usually accomplished by failing, after many attempts, to find some inconsistency between the new theory and any observed behavior of the real world.

There are at least three broad categories of test types which are commonly considered significant indicators of the usefulness and consistency of a new theory. The first category is made up of those experimental observations which have not yet been explained by any pre-existing theory. The second category is made up of those observations, which can be explained to some extent by existing theories, which must continue to be explained by any new theory. The third category is made up of those observations which are experimentally measurable, but which have not yet been measured because no one has yet thought to look for them -- a new theory should predict some of these observations. This chapter presents experimental results which belong in each of these three categories.

In Section One of this chapter, it is shown how the dendritic distributions, hypothesied by CTT, in layer one of the primary visual cortex might account for the high frequency roll-off of the visual contrast sensitivity curve.

In Section Two of this chapter, the first three levels of abstraction of the CTT architecture are implemented for the audio domain. This simulation is then shown to be able to do speech recognition in a manner which is perceptually psychologically similar to the human speech recognition system. In the process of implementing this simulation, it became evident that the simulation predicted a new class of audio-illusions. One audio-illusion from this class was synthesized and was verified to be a true human audio-illusion -- this is reported on in Section Three.

Section Four is a preliminary report on the work done by Robert L. Russel. Russel is doing a masters thesis which is attempting to demonstrate that CTT also works for the visual domain. His work applies the simulation developed for the audio areas of the cortex to the visual areas (by exchanging the primary audio cortex image for the primary visual cortex image -- the rest of the simulation remains unchanged). He shows that this CTT visual system is capable of doing human face recognition. In addition, a new explanation for static two-dimensional optical illusions is forwarded and the preliminary results of the testing of this explanation are presented.

5.1 Section One

The contrast sensitivity curve for a human is typified by the experimental results obtained by Campbell, Kulikowski, and Levinson [18], averaged by Ginsburg [48], and reproduced in Figure 5.1.

The high-frequency roll-off characteristic of this curve is peculiar in that its shape cannot be explained by the optics of the eye (which would account only for the high-frequency roll-off due to the Airy disk interference). The difference between the high-frequency roll-off due to the optics and the experimentally observed high-frequency roll-off must be due to some mechanism(s) between the retina and the recognition area in the brain inclusive. D.H. Kelly [65] presents some exceptionally fine work which shows how the neural-distribution on the retina may account for this behavior. He shows that statistically-averaged overlapping areas of summation on the retina can explain this type of high-frequency roll-off behavior. The mechanism which he describes as being in operation as a consequence of the statistically-averaged retinal area-summation structure is equivalent to the mechanism which CTT hypothesizes is present in layer one of the primary visual cortex (see Figures 3.2 and 3.4), only the CTT model on the cortex is simpler because it assumes all the area-summation distributions are the same (instead of statistically-averaged as Kelly did for the retina).

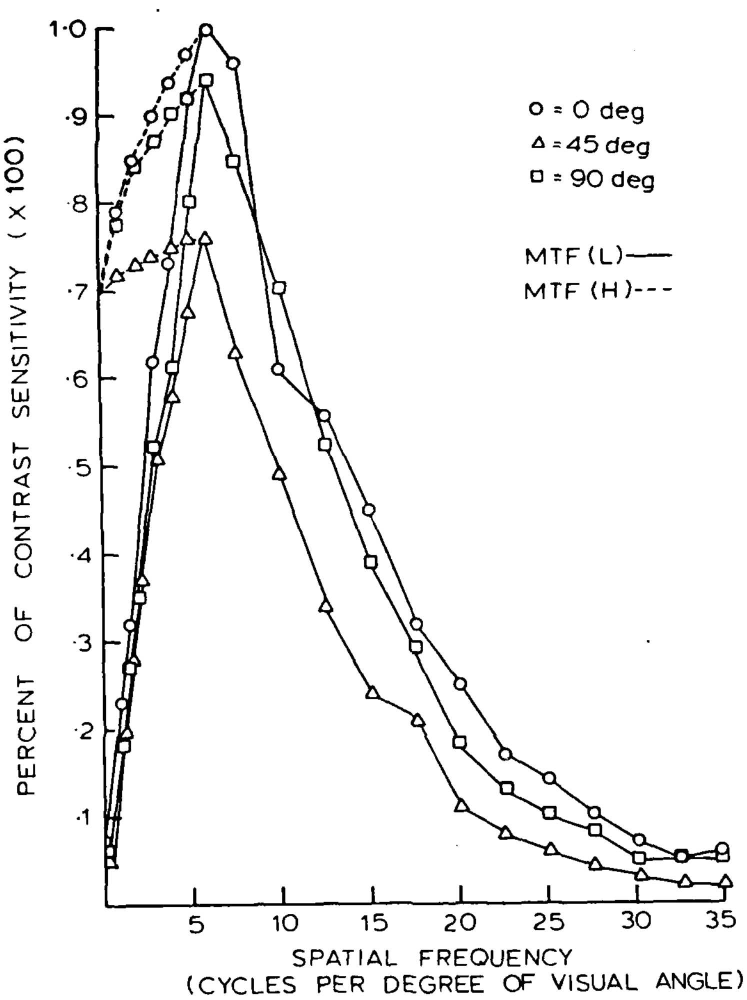

Normalized Contrast Sensitivity Functions for 0, 45, 90 Degrees from the Averaged Data of Campbell, Kulikowski, and Levinson (1966).

Figure 5.1 (From Ginsburg)

When discussing the effect that the Airy disk interference has on the high frequency roll-off of the contrast sensitivity curve, one considers the following model:

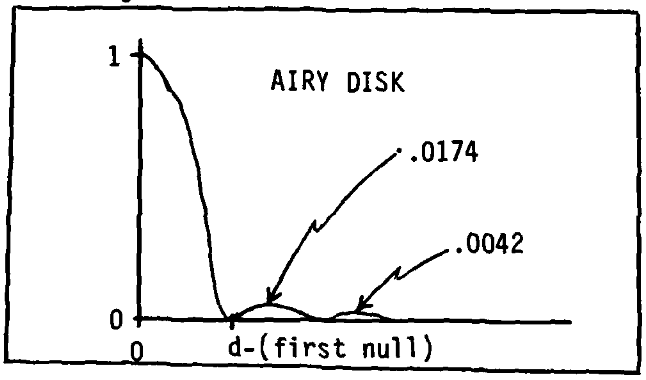

Figure 5.2

according to Hausmann & Slack [53, p. 690],

$$d = \frac{2.44\, f\lambda}{D} \qquad (16)$$

where: $f = 1.4 \times 10^{-2}$ meters

$\lambda = (3.8 \times 10^{-7}, \underline{5.5 \times 10^{-7}}, 7.8 \times 10^{-7})$

$D = 2 \times 10^{-3}$ meters

$$d = \frac{(2.44)\ (1.4 \times 10^{-2})\ (5.5 \times 10^{-7})}{2 \times 10^{-3}} \qquad (17)$$

$$= 9.4 \times 10^{-6} \text{ or about 10 microns.}$$

According to Polyak [101, p. 269], the smallest cones are about 1 to 1.5 microns. Considering the dead space in between cones, and referencing the plates in Polyak [101, p. 268], three cones span about a ten micron distance in the central area of the fovea.

We now have the following picture:

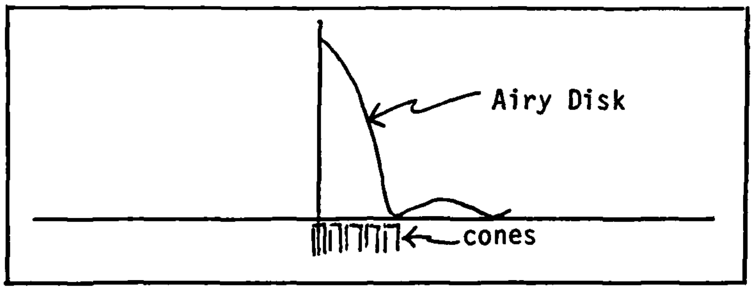

Figure 5.3

In order for resolution to occur, the Rayleigh criterium must be met which, as can be seen from the diagram above, is not going to occur between two adjacent cones because there will be too much interference between the Airy disks.

According to Polyak [101, p. 269], 500 microns corresponds to about 1°50' of arc in the field of view. This means that 10 microns (the distance, d, from the center to the first null of the Airy disk) corresponds to about 132 seconds of arc. (Note: If the pupil opens to seven millimeters instead of two millimeters, then the first null occurs at about 38 seconds of arc for 5500 Å green light. According to the Rayleigh criteria, resolution should begin to occur at about 28 seconds of arc for 7800 Å blue light and at about 38 seconds of arc for 5500 Å green light. This agrees with conventional experiments that suggest that resolution first occurs at about 30 seconds of arc.)

To determine the high frequency roll-off in the human eye due to the Airy disk interference, an experiment (by way of computer simulation) was performed. The following is a description of that experiment.

One micron corresponds to about 13.2 seconds of arc. The normalized contrast sensitivity curve compiled from the data of Campbell, Kulikowski, and Levinson [18, p. 138], records human contrast sensitivity out to 35 cycles per degree of visual angle. Sixty (60) cycles per degree (cpd) has a wavelength of 60 seconds of arc. Thirty (30) cpd has a wavelength of 120 seconds of arc.

Diagramatically, the problem looks like this:

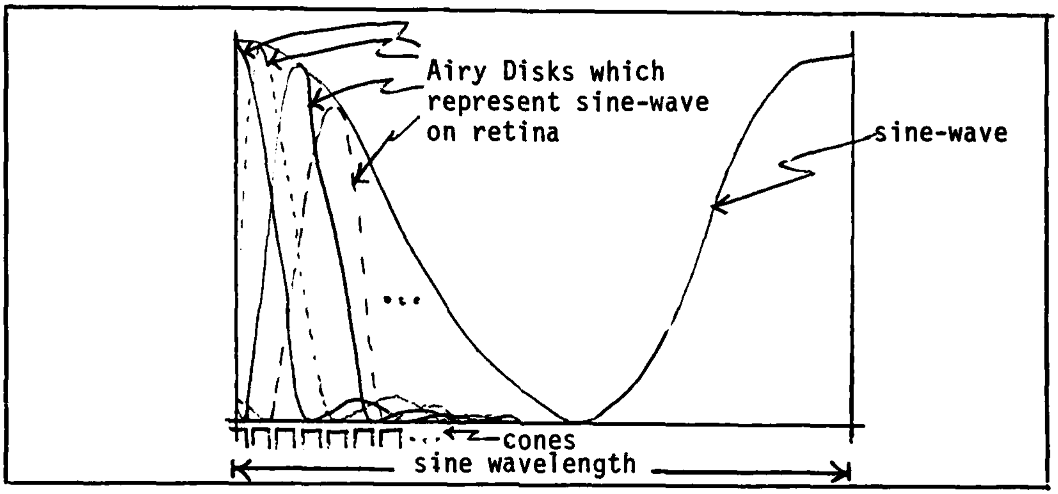

Figure 5.4

A simulation was built which represented a sine wave of the appropriate (and varying) frequencies in terms of Airy disks of appropriate (and varying due to pupil size and light wavelength) sizes. All the Airy disk components for a given sine wave frequency and Airy disk size must be added for each of many points per wavelength along the abscissa. The contrast sensitivity can then be determined by the following equation:

$$\text{Cont. sens.} = \frac{\text{Intensity}_{max} - \text{Intensity}_{min}}{\text{Intensity}_{max} + \text{Intensity}_{min}} \qquad (18)$$

The Airy disk used in this model was calculated out to the third null and set to zero beyond the third null.

The expression for the Airy disk is:

$$I/I_0 = (2\ J_1(x)/x)^2\ , \qquad (19)$$

and $J_1(x)$ was approximated by Equation 20 [6, p. 534] (truncated to 17 terms):

$$J_1\ (x) = \frac{x}{2} - \frac{x^3}{2^3 \cdot 1!2!} + \frac{x^5}{2^5 \cdot 2!3!} - \frac{x^7}{2^7 \cdot 3!4!} + \dots + \frac{x^{33}}{2^{33} \cdot 16!17!} \qquad (20)$$

This produced a first maximum of .01748 (.0174 is correct), a second maximum of .0042 (.0042 is correct), and a third maximum of .0009 (.0016 is correct). This is far in excess of the precision required for this experiment.

The documented Fortran program which simulated this problem, to include one complete sample run and the results of the others, is found in Appendix C.

The results are shown graphically here:

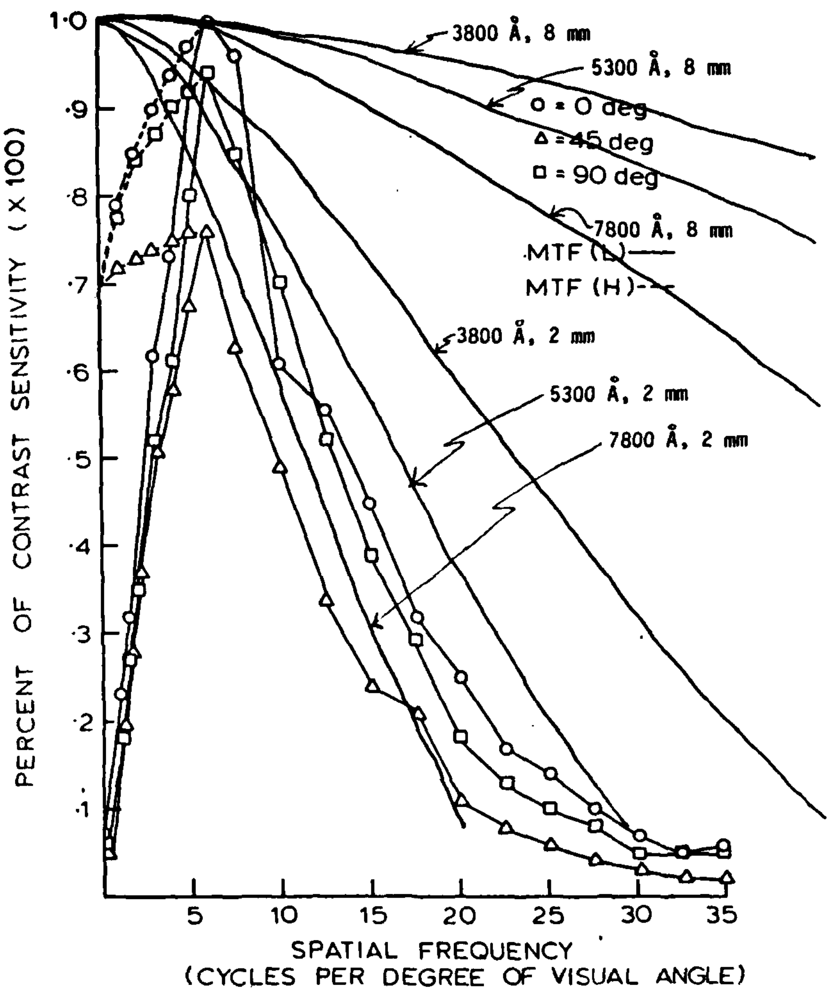

Normalized Contrast Sensitivity Functions for 0, 45, 90 Degrees from the Averaged Data of Campbell, Kulikowski, and Levinson (1966).

Figure 5.5

Two conclusions can now be reached. The first is that Airy disk interference is not entirely responsible for the contrast sensitivity high frequency roll-off. The second is that the other, as yet unexplained, component can be calculated. One must only find which curve, when multiplied by the Airy disk curve, produces the measured contrast sensitivity curve. In the experiment which produced the contrast sensitivity curve shown in Figure 5.1, the wavelength of the light was 5300 Å and the pupil diameter was 2.8 millimeters. This produces the following curves:

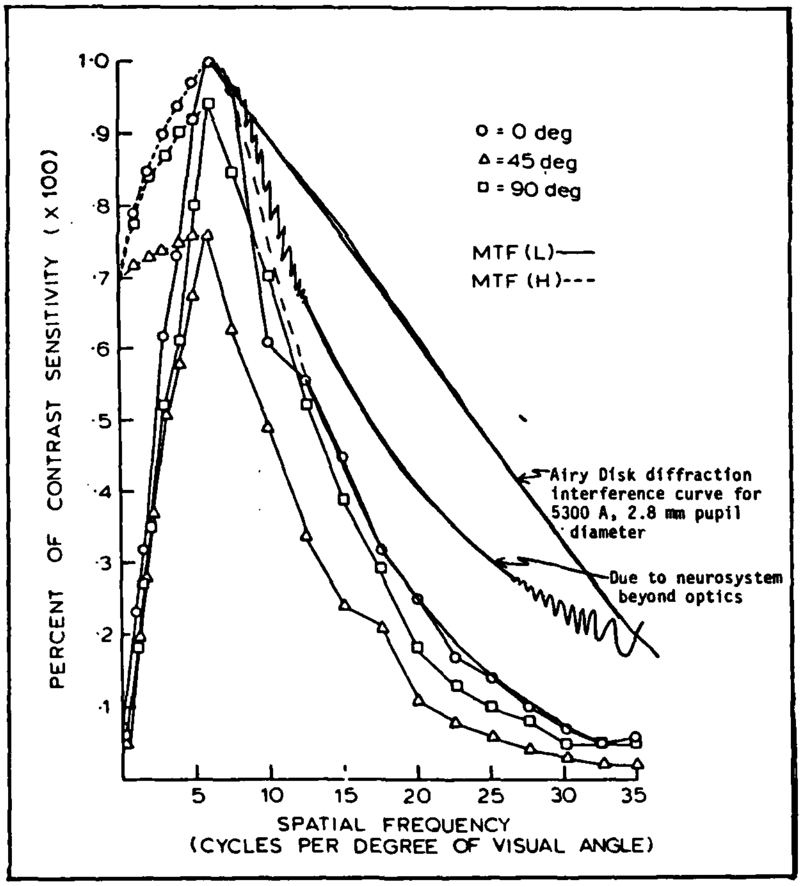

Figure 5.6

If half (half is arbitrarily chosen to demonstrate how the following calculation would be performed) of this difference curve is accounted for by the Kelly hypothesis and the other half of it is accounted for by the CTT cortex dendritic distribution model, then the curve which the CTT cortex dendritic distribution summation mechanism must account for is shown in Figure 5.7.

At this point, a new simulation program was written (and is contained in Appendix D along with a sample run) which calculated the high frequency roll-off characteristics due to the error in the approximation between the shape of the dendritic neighborhood-sample-averaging function (see Figure 3.4) and the shape of a sine wave. This is illustrated in Figure 5.8.

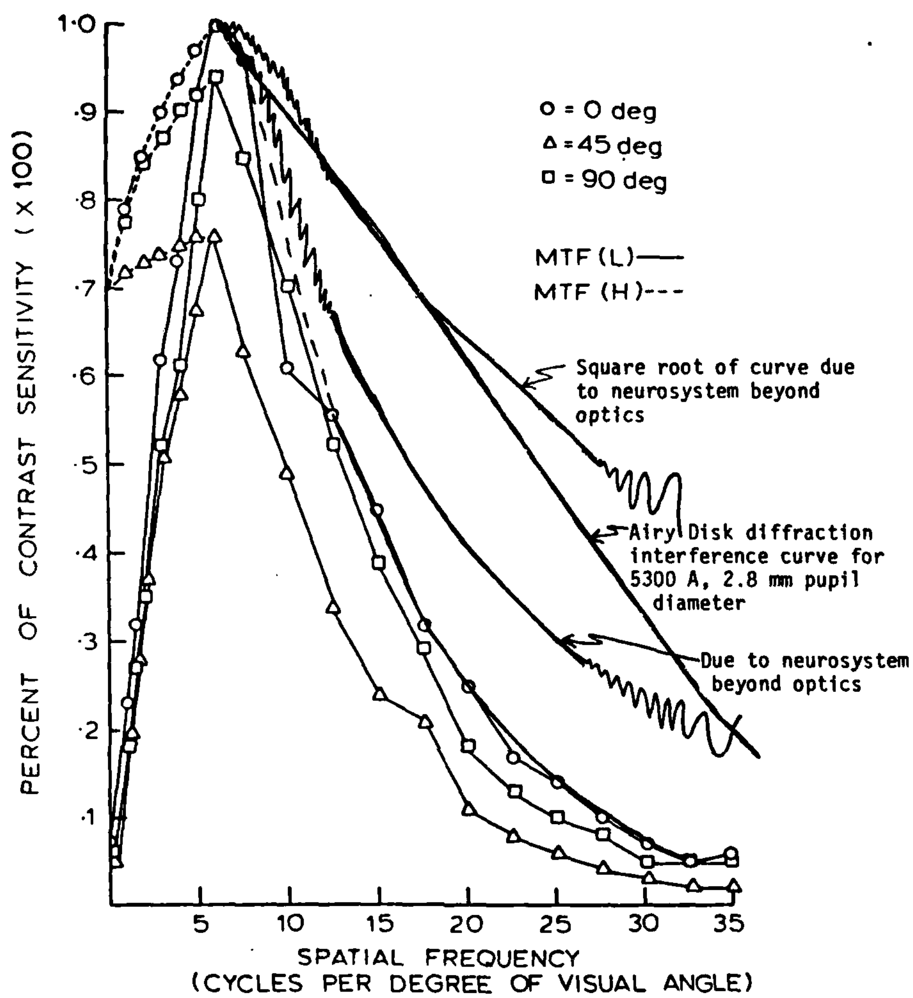

Normalized Contrast Sensitivity Functions for 0, 45, 90 Degrees from the Averaged Data of Campbell, Kulikowski, and Levinson (1966).

Figure 5.7

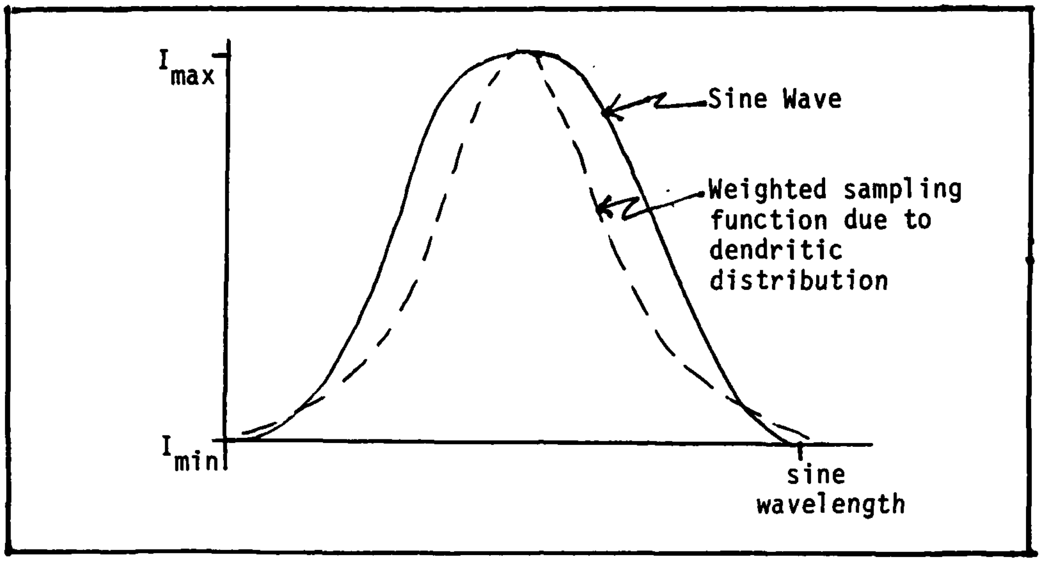

Figure 5.8

A point-by-point correlation calculation between the dendritic distribution function and sine waves of frequencies from 1 cycle-per-degree (cpd) to 35 cpd will yield a particular high-frequency roll-off curve. (This is in accordance with the 2DDFT cortex approximation mechanism hypothesized in Chapter Three.) By adjusting the dendritic distribution curve (shape and width) and using Equation (18) to calculate the contrast sensitivity, a dendritic distribution curve was found which precisely predicts the required high-frequency roll-off curve. This distribution, D(x), is given by the equation

$$D(x) = \exp(-|x|/.9), \qquad (21)$$

where x is measured in cortical column widths.

The reader is reminded that this calculation assumes the width of the curve is large compared to the distance between the mapping of the centers onto the cortex of the concentric window regions from the retina. Equation (21) does not indicate that that condition holds true unless there is some sort of averaging in the preprocessing stages of the lower brain which perform a combination of the amplitudes from several windows of a single concentric retinal region into a single amplitude for a single cortical column (after it has extracted the windowing information from that concentric retinal region).

5.2 Section Two

If the model described by CTT is correct, then one should be able to do human sensory input processing in any domain if one is able to describe the form of the input sensory information on the primary local cortex surface of that domain. More specifically, if one knows how the audio information is displayed on the primary audio cortex, then one should be able to use a computerized emulation of the proposed CTT architecture to do speech recognition. This seemed like an interesting engineering challenge which would be sufficient to provide a preliminary indication of the correctness of the theory. So, that is what was done. The first three levels of abstraction were emulated according to the following basic scheme:

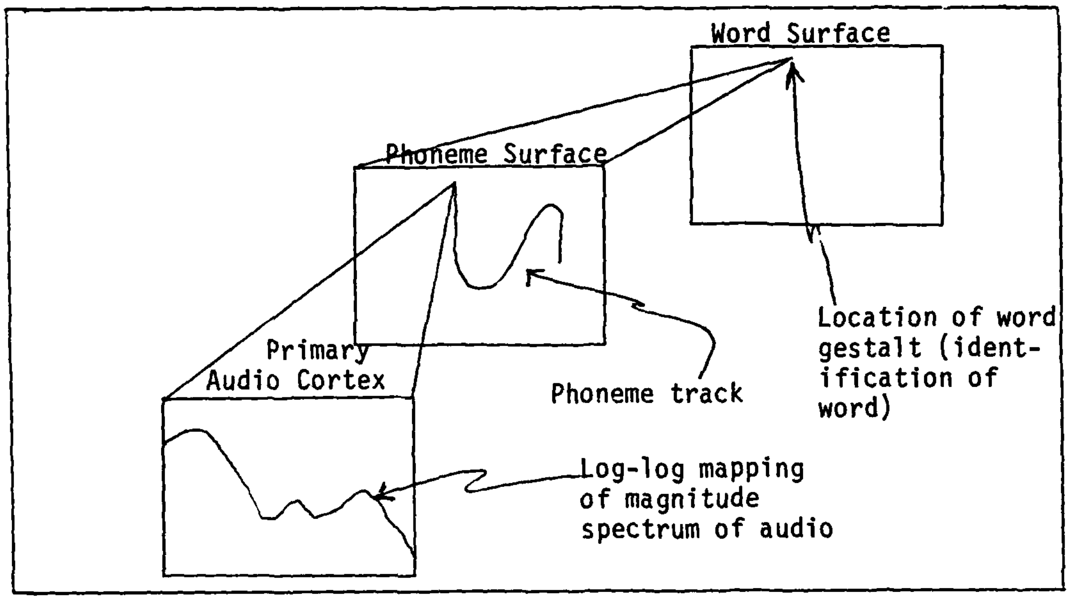

Figure 5.9

It was later learned that this architecture is oversimplified. An improved architecture appears in Figure 2.17, based on the lessons learned from the analysis of the simulation which was built.

In reading the description of the development of the simulation, which follows, the reader may want to consult the program listings of this simulation. They are contained in Appendix F.

The primary audio cortex in cats and monkeys (and hence, presumably in humans) is basically a mapping of the magnitude spectrum of the acoustical disturbance of the eardrum onto a cartesian coordinates plot. One axis displays the logarithm of the amplitude (decibels -- dB). The other axis displays the logarithm of the frequency. In the human, the primary audio cortex is physically located in a fissure on the cortex and hence cannot be easily experimented with in vivo (and has not been experimented with in vivo). The structure of the audio preprocessing mechanisms and cortex for all mammals is so similar that there is no reason to suspect that the human primary audio cortex is not mapped in the same manner as those of the cat and monkey. The major questions regarding the engineering duplication of the human primary audio cortex are:

(1) What are the low frequency and high frequency cut-offs of this mapping scheme?

(2) Are all the frequencies weighted equally, or is there some weighting function (e.g., - the threshold and supra-threshold set of audiological mel-sone curves) applied across the spectrum?

(3) Is there an adequate simplified way to represent the complex right ear/left ear interwoven mapping scheme (see Figure 5.10)?

For this engineering duplication, the foregoing questions were answered in the following way:

(1) Since human speech is intelligible at the quality of a conventional telephone communication if the frequency cut-offs are 100 Hertz and 4 Kilo-hertz, then the frequency cut-offs for this engineering model were chosen to be 100 Hertz and 4 Khz.

(2) The non-linear weighting function of the audiological threshold mel-sone curve transitions to be nearly linear far into

the supra-threshold region. Since most of speech occurs far into the supra-threshold region, and since one is not aware of any other evidence to suggest otherwise, it was decided that there would be no weighting function across the frequency band.

(3) One fortuitous property of the low frequencies of the 2DDFT is that they do not change much between an underlying image which is a solid region and an underlying image which is a cartoon (just the border outline) of a region of the same shape. Therefore, it does not much matter whether a region under the magnitude transform plot is partially "filled in" or completely "filled in". That property of the 2DDFT used in this way (as CTT prescribes) helps to explain why a sound sounds the same, regardless of which ear hears it the louder, in spite of the complex left ear/right ear interleaved property shown in the mapping in Figure 5.10b. For this reason, only the cartoon was used. (Experimentation was carried out to insure that it truly did not make any difference whether this region was solid or just "cartooned". The experiments showed a slight, but consistent, translation in the results. This was interpreted to mean thas as long as all images were either "cartooned" or solid -- the same representation scheme was consistently used -- there would be no difference in the performance of the system. Therefore, this simplification assumption was considered validated.)

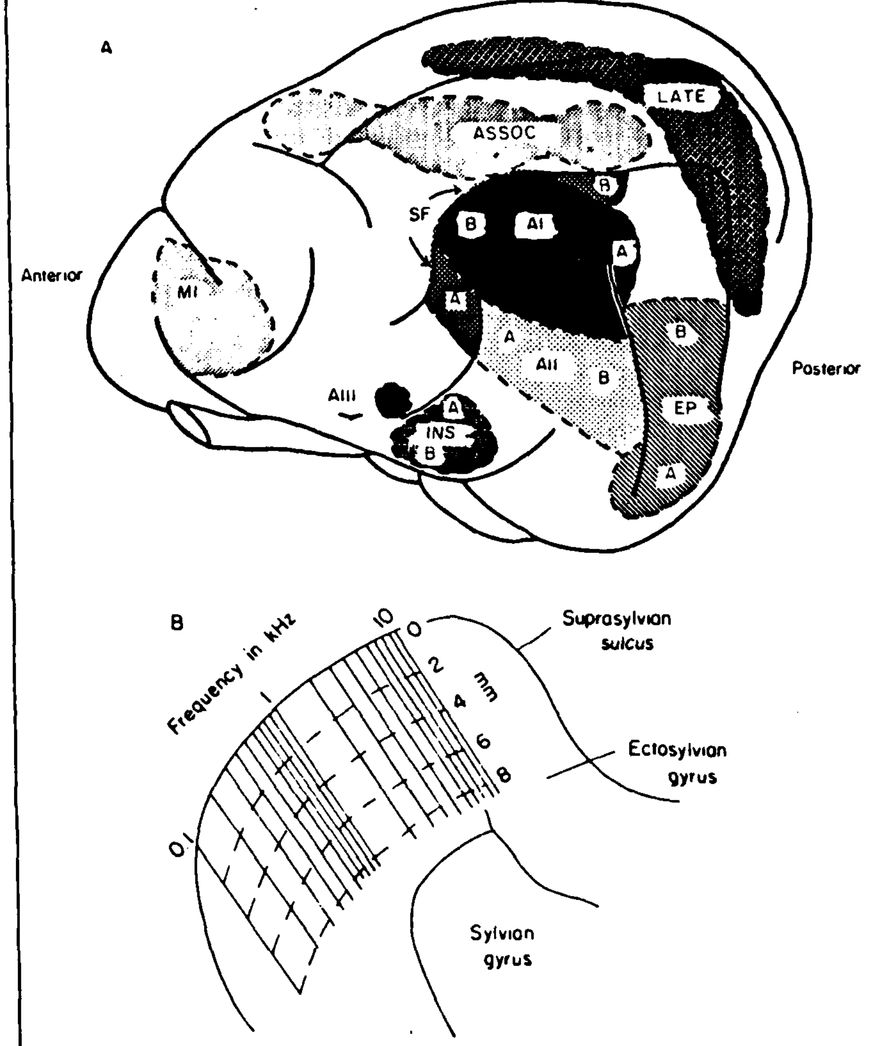

Auditory areas and their tonotopic organization were shown with gross evoked potentials by Woolsey (1960) in the cat. Where the areas are organized tonotopically, the representation of the high frequency base of the cochlea (B), and of the low frequency apex (A), are indicated. MI: precentral motor area. AIII is now called SII. Other abbreviations as in Fig. 7.1. From Woolsey (1960), *Neural Mechanisms of the Auditory and Vestibular Systems* (G. L. Rasmussen and W. F. Windle, eds) Courtesy of Charles C. Thomas, Publisher, Springfield, Illinois.
B. Isofrequency strips in the dog auditory cortex. From Tunturi (1952), Fig. 2.

Figure 5.10a (From Pickles)

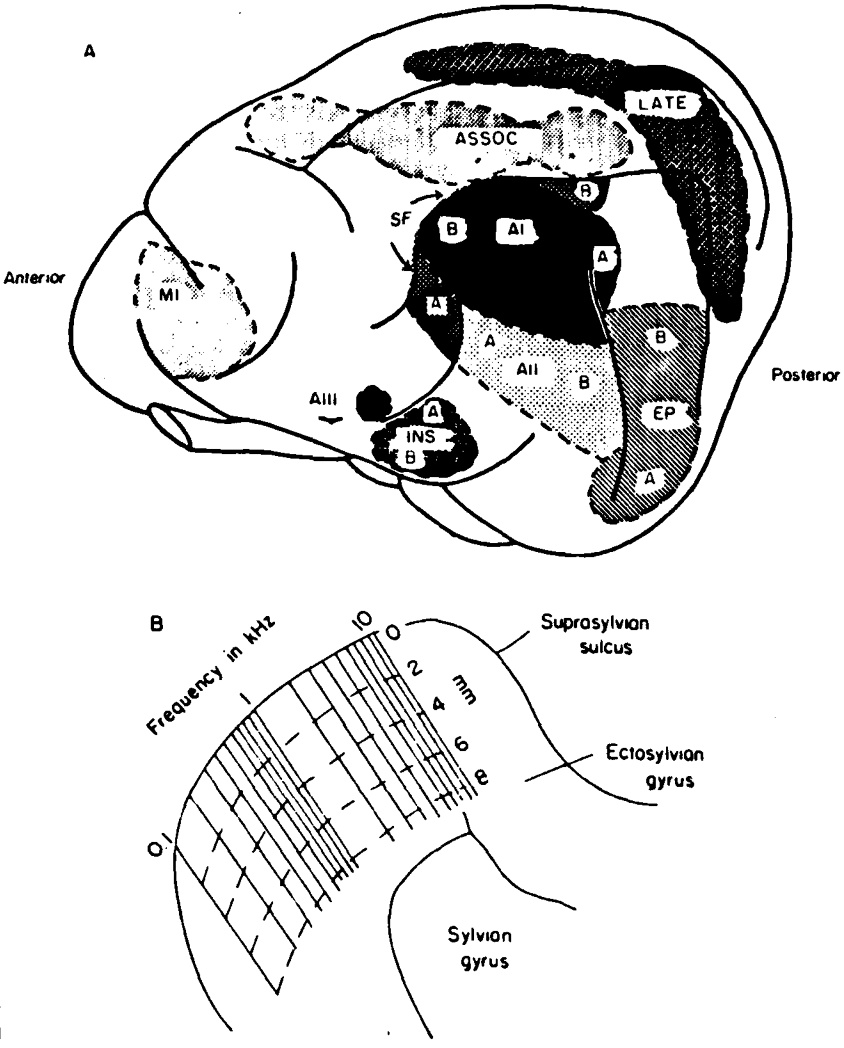

Auditory areas and their tonotopic organization were shown with gross evoked potentials by Woolsey (1960) in the cat. Where the areas are organized tonotopically, the representation of the high frequency base of the cochlea (B), and of the low frequency apex (A), are indicated. MI: precentral motor area. AIII is now called SII. Other abbreviations as in Fig. 7.1. From Woolsey (1960), *Neural Mechanisms of the Auditory and Vestibular Systems* (G. L. Rasmussen and W. F. Windle, eds) Courtesy of Charles C. Thomas, Publisher, Springfield, Illinois.
B. Isofrequency strips in the dog auditory cortex. From Tunturi (1952), Fig. 2.

Figure 5.10a (From Pickles)

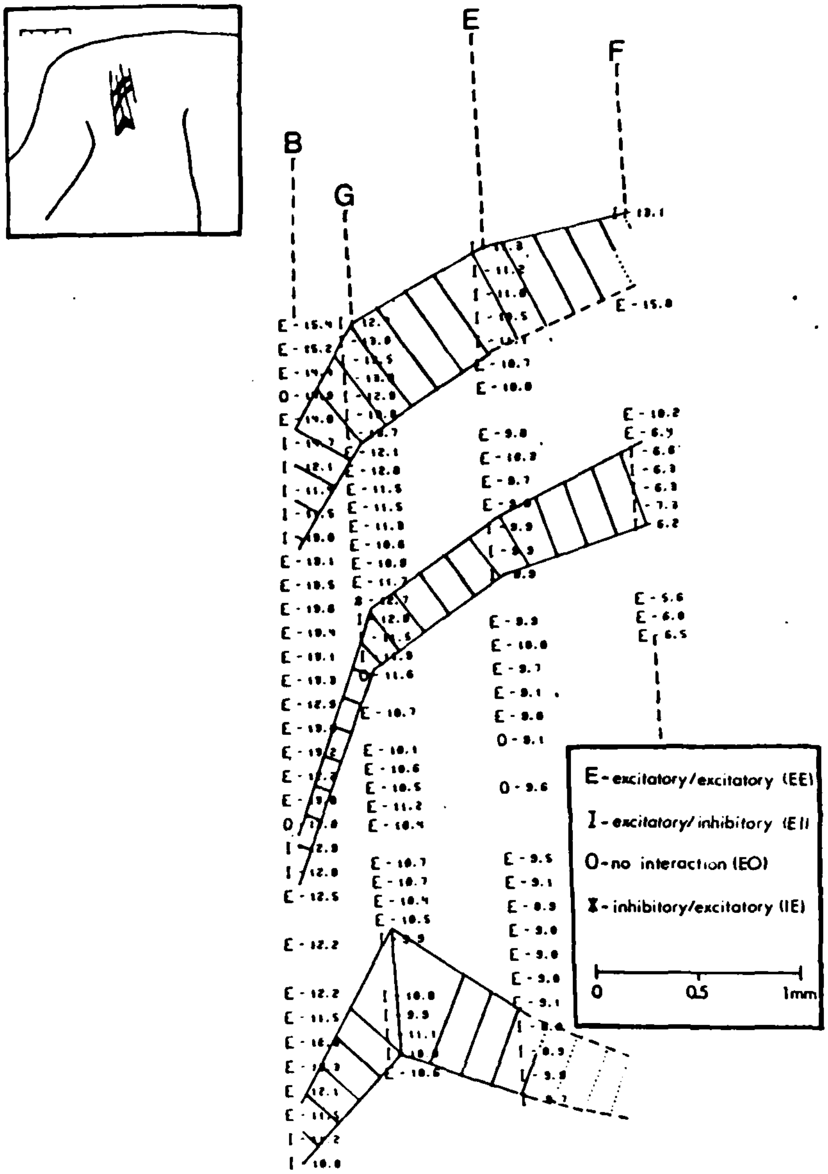

Columns of cells that are excited by one ear and inhibited by the other (EI cells, shown in crosshatched areas) are segregated from columns of cells that are excited by both ears (EE cells). The cell CFs are indicated by numbers along the electrode tracks. Inset shows the cortical area sampled. From Middlebrooks *et al.* (1980), Fig. 4.

Figure 5.10b (From Pickles)

The next step was to window a particular region of this display in order to discretize and digitize it. This turned out to be a difficult and fascinating problem.

First, one had to consider the nature of the magnitude transform which would be displayed on this primary audio cortex (PAC) map. The time duration and the shape of the window of the time domain audio signal affected the shape of the magnitude transform. Time durations of 5, 8, 10, 15, 20, 30, 40, and 50 milliseconds were tried. Window shapes of rectangular, Hamming, Hanning, and Blackmann were explored. After much simulation and experimentation of different combinations of window length and window shapes, a window length of 20 milliseconds (sampled at 8 Khz, this was 160 samples) and the Hamming window shape were chosen. Forty milliseconds and Blackmann would have given a better signal to window-noise response while still maintaining about the same frequency response (equivalent slope of formant peaks or "Q" of the frequency filters), but phonemes change too rapidly (25 Hertz) to allow for a 40 millisecond window length.

Since the Hamming signal to window-noise ratio is typically 40 dB, it made sense to want to view about a 40 dB span of the magnitude transform mapping as shown in Figure 5.11. However, in order to find the significant 40 dB part of the mapping, it was necessary to posit a framing (two-dimensional windowing) mechanism which always knew the exact maximum amplitude of the mapping. It could then set the top of its frame at this window height (and the bottom of its frame 40 dB lower). It seemed, at the time, that this requirement had two disadvantages. First, it required a fairly complex algorithm to insure

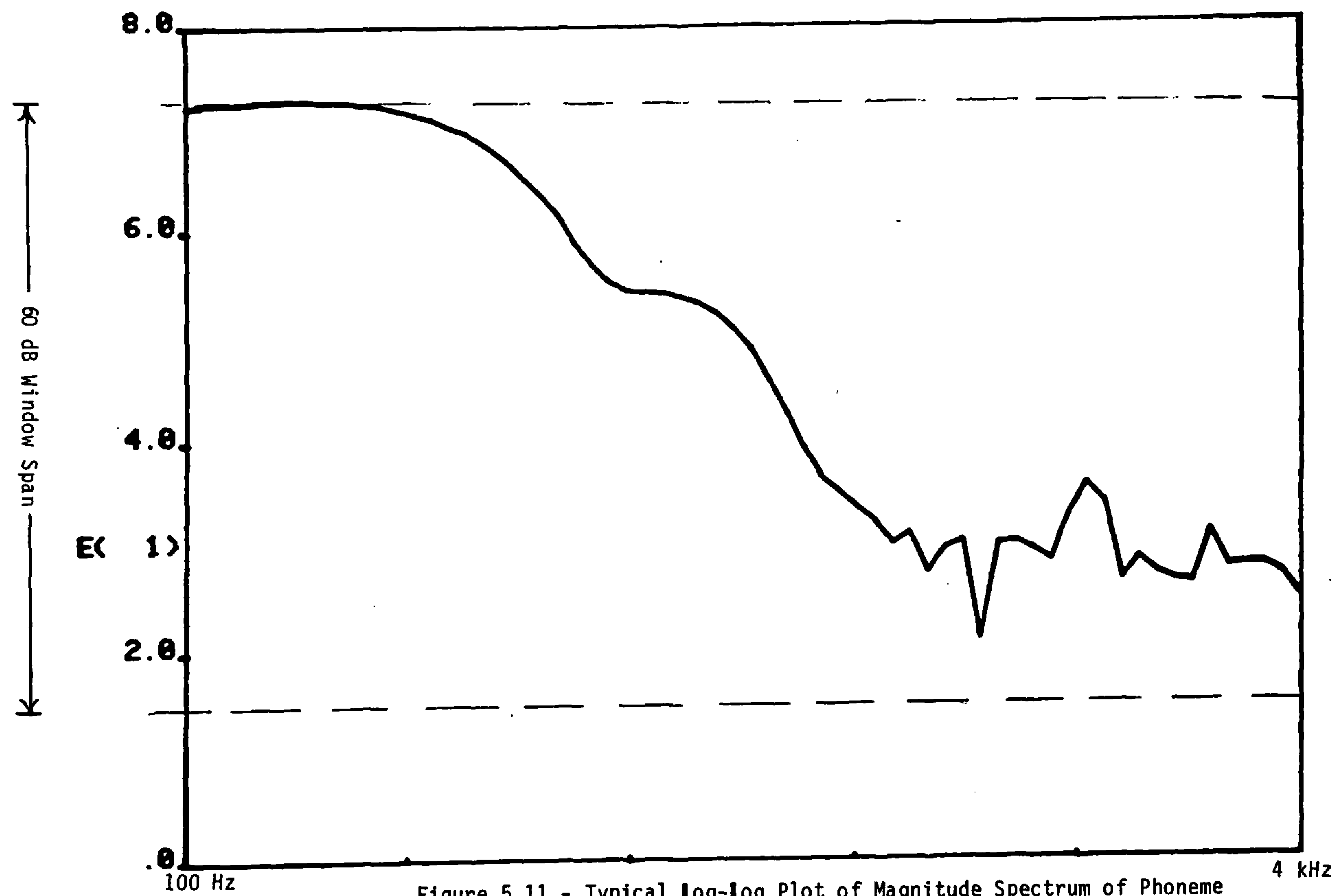

Figure 5.11 - Typical Log-Log Plot of Magnitude Spectrum of Phoneme

that this mechanism did not get fooled by narrow-band, high-amplitude background noise. A high-amplitude sine-wave in the background would cause such a mechanism to set the frame height too high to properly window the PAC map. The second disadvantage was that this mechanism would be unable to differentiate on the basis of signal energy between sounds like "sh" and long "e" which have very similar magnitude transforms on a log-log map, but significantly different energy distribution across the linear frequency map.

For these two reasons, it was decided that the maximum frame height should be decided by the energy of the signal, which was easy for the system to measure and was not significantly disturbed by high amplitude, narrow band noise. (Refer to Appendix F for the precise algorithm used.) Since this mechanism could result in setting the top of the frame as much as 20 dB above the maximum formant amplitude (this is typically the case for "s" and "sh" sounds), the amplitude range was increased to 60 dB.

This two-dimensional window was discretized by a 64 x 64 matrix. To complete the two-dimensional window, a Hamming window was applied to each of the 64 rows and then to each of the resultant 64 columns. (This was to reduce the 2DDFT window noise.) Before the 2DDFT was calculated, the 64 x 64 matrix was zero-filled out to a 4096 x 4096 matrix (that is, all rows from 65 to 4096 were set to zero, and all columns from 65 to 4096 were set to zero -- the first 64 x 64 elements of this 4096 x 4096 matrix were the same as the original 64 x 64 matrix). This allowed for the approximation of the continuous two-dimensional Fourier-sine transform (in discretized steps of 1/64th harmonics).

For reasons that were discussed in Chapter Four, only the first 64 x 64 elements (out to the first harmonic of the original 64 x 64 matrix) were kept of the resulting 4096 x 4096 element 2DDFT. According to the analysis presented in Chapter Four, the entire 64 x 64 matrix was set to zero except for the maximum value which was set to one. The physical location of the single non-zero element in this matrix is the gestalt of the original 20 millisecond sound.

A chart of the gestalts (calculated in this manner) for the English vowel sounds (five utterances each) for the speaker, RLR, is presented in Figure 5.12. The sounds shown in Figure 5.12 are:

beat	(ɨ)	
bit	(i)	
bet	(e)	
bat	(æ)	
bot	(a)	
but	(ə)	
Spanish "ọ"	(ọ)	(without ū part of dipthong)
bush	(ü)	
boot	(ū)	

In Figure 5.13, the Tragerian vowel rectangle, which shows the preference for vowel alternation in English, is shown and is indicative of the psychological distance between vowels [127a]. Since the order of these is equally valid for the mirror image (either is an arbitrary choice), the mirror image of Figure 5.13, when overlayed on Figure 5.12, reveals a correspondence which is startling. This result is considered as strong supporting evidence for the correctness of CTT. It helps to illustrate how CTT makes human-like classifications and, at the same time, proposes a mechanism to explain the tendency in humans to make the phoneme substitutions which are linguistically observed.

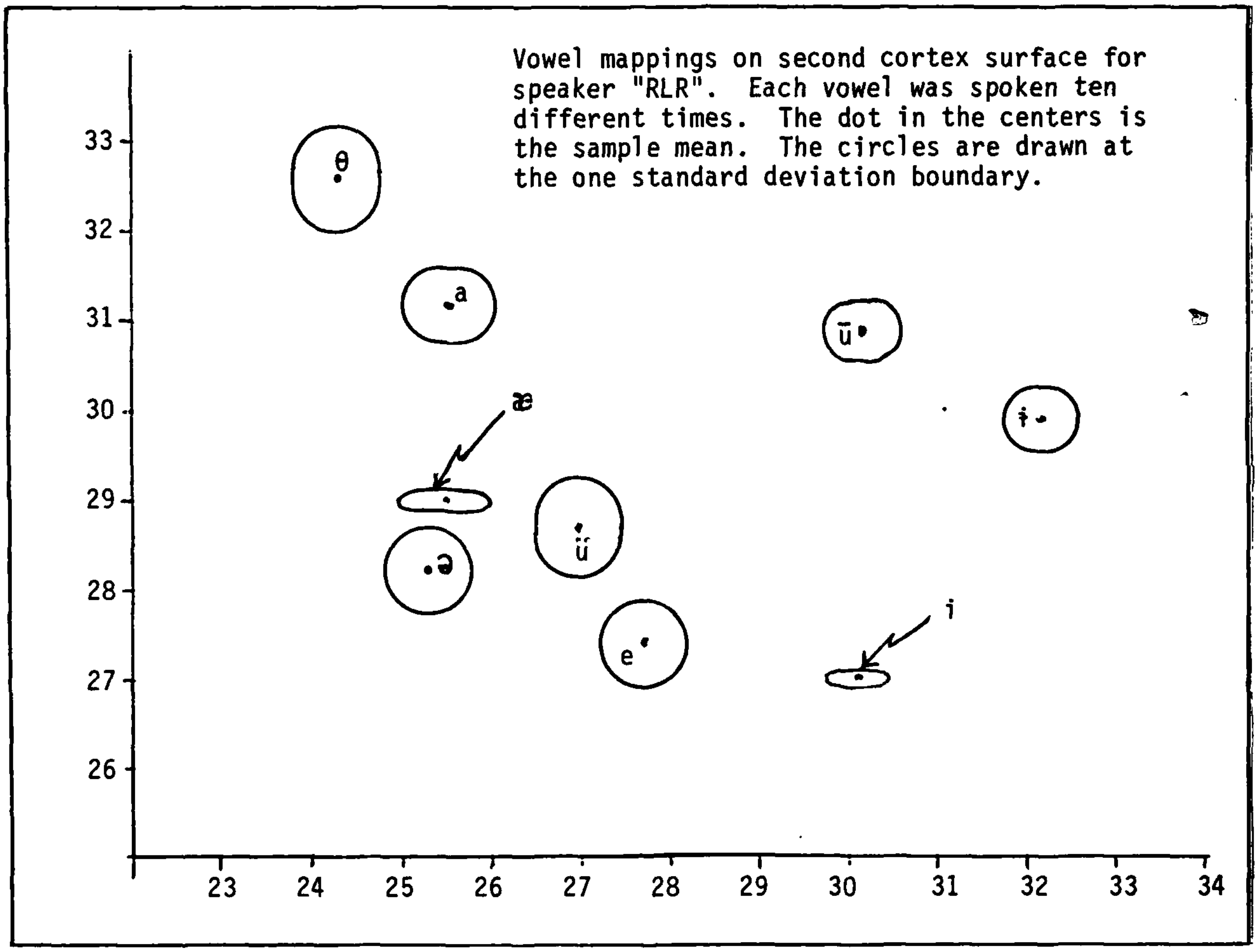
Vowel mappings on second cortex surface for speaker "RLR". Each vowel was spoken ten different times. The dot in the centers is the sample mean. The circles are drawn at the one standard deviation boundary.
33
32
31
30
29
28
27
26
23
24
25
26
27
28
29
30
31
32
33
34
θ
a
æ
ə
ü
e
ū
ɨ
i

Figure 5.12

TYPES OF VOWEL ALTERNATION IN ENGLISH

i	ɨ	u
e	ə	o
æ	a	ɔ

Figure 1

TABLE 1. ONE-STEP MONOPHTHONGAL VOWEL ALTERNANTS IN AMERICAN ENGLISH

Alternating Vowels	Exemplificatory Word
i – ɨ	whip
i – e	get
ɨ – u	sure
ɨ – ə	just
u – o	your
e – ə	err
e – æ	catch
ə – o	owe
ə – a	of
o – ɔ	awe
æ – a	aunt
a – ɔ	or

Similarly allologous vowel alternants differing from one another by two steps on the Trager-Smith square are rarer; about half as many of them as of the one-step alternants can be found, as illustrated in table 2.

TABLE 2. TWO-STEP MONOPHTHONGAL VOWEL ALTERNANTS IN AMERICAN ENGLISH

Alternating Vowels	Exemplificatory Word
i – a	either
i – u	dew
i – ə	Missouri (final vowel)
e – a	resin
æ – ɔ	haunt
ə – ɔ	was

Figure 5.13 (From Wescott)

Encouraged by this success, it was speculated that perhaps all phonemes could be mapped in this way onto a specific point (or small region) on the vowel phoneme surface. In order to test this hypothesis, and expecting that it would result in the physical proximity of words that sound similar to humans, four different speakers were asked to utter the following fifteen words: elm (three times each for each speaker), helm (one time per speaker), bell (1), cot (3), cop (1), tot (1), sash (3), ash (1), sass (1). To test the psychological consistency, the base word of each group (elm, cot, sash) were each spoken three times. To test psychological closeness, each group has two other words which sound close to the base word (by human judgement). As each word was spoken, the 20 millisecond window (of the audio) was used to produce a single point on the phoneme surface. Then it was shifted two milliseconds and the calculation was done again (see the example in Chapter Two). This produced a phoneme track on the phoneme surface. This track was treated as a two-dimensional input image for the next level of abstraction (see Figure 5.9). The gestalt was calculated identically to that of the lower level. It projected its gestalt point onto a word surface. The plot of 15 test words for speaker, RLR, are shown in Figure 5.14. The plots for the other three speakers are shown in Appendix G. Both the consistency and expected human-like psychological closeness of the results are as predicted.

A closer scrutiny of the phoneme track data (contained in Appendix E) shows that the start and stop phonemes are not being seen by the system. The more rapid the energy change is, the less properly sensitive this CTT model seems to be ("t" and "d" have more rapid energy changes than "k" and "g" which have more rapid energy changes than "j"

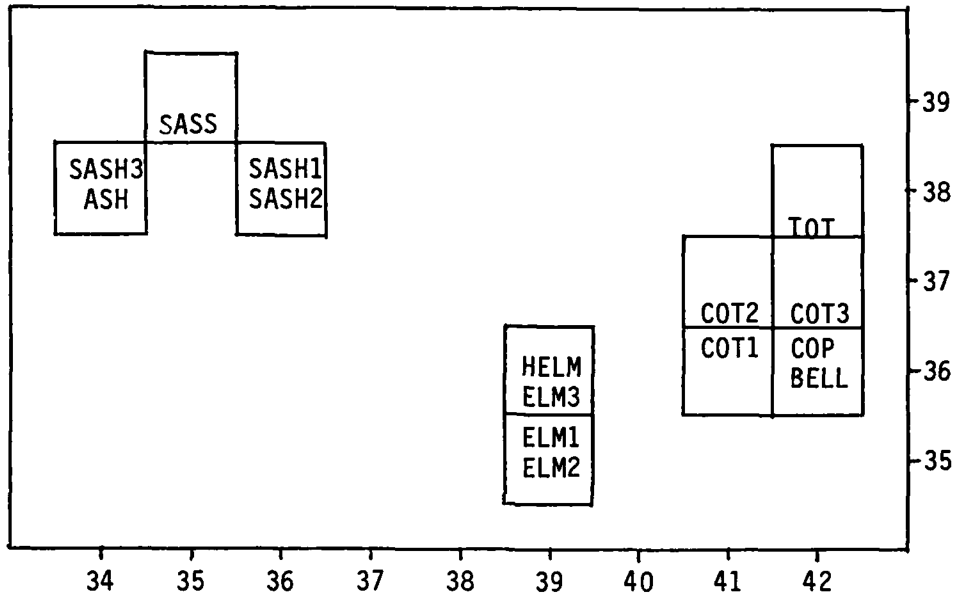

Figure 5.14 - Word Gestalt Plots on the Word Local Cortex Surface for Speaker "RLR"

or "ch" which have more rapid energy changes than "m" or "n" which have more rapid energy changes than "s" or "sh" or "z" or "zh" which have more rapid energy changes than the vowels which essentially have no energy change). The data indicate that some other mechanism must be in operation which watches the instantaneous time derivative of the energy and weights that more significantly, in proportion to the magnitude of the derivative, than the mechanism which watches the spectrum of a sound. This hypothesis changes the model shown in Figure 5.9 to the model shown in Figures 2.12 through 2.14 and 2.17.

This new model predicts a new class of audio illusions which will be discussed in the next section.

It is interesting to note that this mechanism would be very useful for resolving the ambiguity of all types of phoneme substitutions, omissions, and insertions (see Routh [108], and Zue [137]), since it predicts that such modifications are of little consequence as long as they do not significantly modify the basic shape of the phoneme track of the otherwise intended utterance. An example of this is offered in Appendix H. In Appendix H, the phoneme tracks for the two utterances "did you" and "dijew" and "want to" and "wanna" are compared to show that there is a preliminary indication that the CTT model can perform human-like speech recognition for mangled phoneme strings.

5.3 Section Three

In the previous section, it was hypothesized that a phoneme is identified on the basis of both its spectrum and its energy change. It was also suggested, based on analysis of the data in Appendix D, that the mechanism which watches the energy change must exercise more influence (proportional to the magnitude of the energy derivative) on phoneme identification than the mechanism which watches the spectrum. This suggests that an audio-illusion will occur when the energy of an otherwise normally stable energy phoneme is rapidly changed. The following experiment was hypothesized and performed:

> The utterance for "cow" was recorded. The utterance was about 500 msecs long. A forty millisecond portion in the middle of the vowel portion was extracted, its amplitude reduced to one tenth (20 dB down) of its original amplitude, and reinserted back into its original position in the utterance. It would be expected that this new (20 dB down) 40 msec portion of the utterance, when played by itself (in isolation from the rest of the utterance "cow") would sound like one of the vowel sounds in "cow". It did. It sounded like the "o" in bot. But the CTT model presented in the previous section, and recapitulated in Figures 2.12 through 2.14, would predict that this sound would sound like a "t" when played in the context of the entire utterance. This is a somewhat surprising prediction due to the fact that the spectrum of the sound never changes (even when the 20 msec sliding audio window is across the boundaries of the beginning or the end of the (20 dB down) 40 msec portion), and the fact that the energy throughout its duration remains high enough for the vowel to be heard. Several people listened to the modified utterance. All of them heard the "t" sound in the middle of the word "cow". As a matter of fact, since the speaker had a slight

AD-A163 215 CORTICAL THOUGHT THEORY: A WORKING MODEL OF THE HUMAN GESTALT MECHANISM(U) AIR FORCE INST OF TECH WRIGHT-PATTERSON AFB OH SCHOOL OF ENGINEERING 3/5

UNCLASSIFIED R L ROUTH JUL 85 AFIT/DS/EE/85-1 F/G 5/10 NL

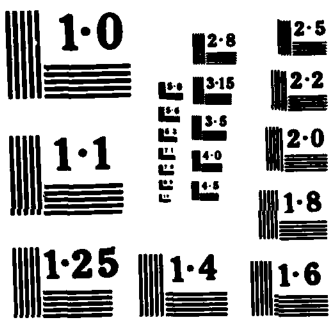
1·0
2·8
2·5
3·15
2·2
3·5
2·0
1·1
4·0
1·8
1·25
1·4
1·6

western twang, the original utterance consisted of the following phoneme string: "k", "a" (as in cat), "u" (as in cut), "o" (as in bot), "ou" (as in bought), and "u" (as in lute). Since the "o" was the part that was removed (and hence interpreted as a "t"), and since the energy utterance faded near its end, the modified utterance sounded like the English word "cattle" without a clearly ennunciated "l". The naive listeners were asked to identify the word they heard. All said that it was the word "cattle". They were also asked to identify the original (unmodified) utterance. All of them heard the word "cow".

This result is considered to be a significant one in that the prediction seemed to be unreasonable, but nevertheless was verified experimentally as an accurate prediction.

5.4 Section Four

CTT claims to be a generic model for sensory information analysis, regardless of the domain or entry level of abstraction. Robert L. Russel decided to test this hypothesis by using the speech recognition program to do face recognition. He removed the 64 x 64 primary audio cortex map and inserted in its place a 64 x 64, sixteen gray level, digitized image of a human face. All the rest of the program remained unchanged. The preliminary results of this analysis, applied to five images each of sixteen different people, are shown mapped in Figure 5.15. A sample digitized image of each person is contained in Appendix J. The only bearded man, also partially balding, was significantly at

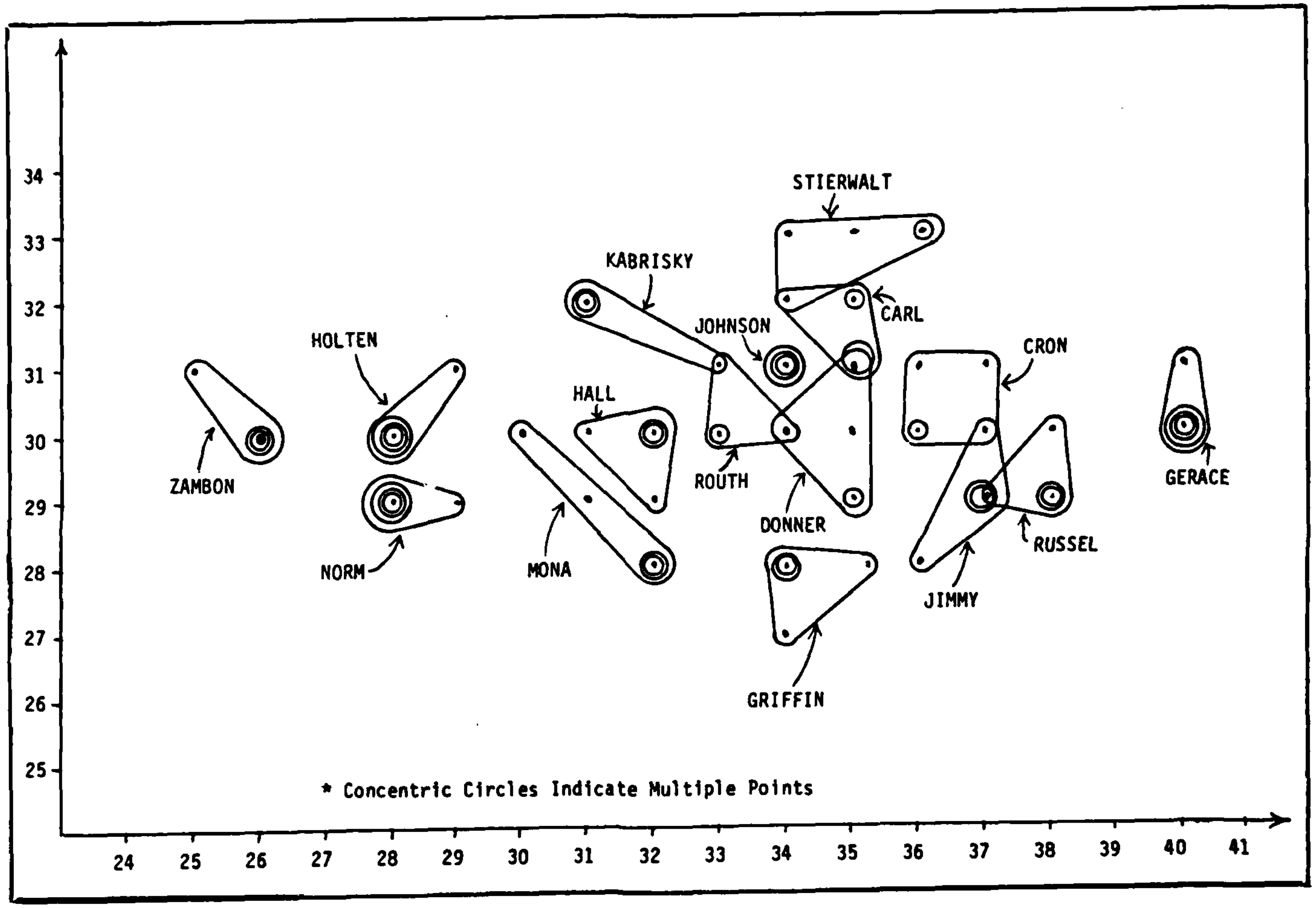

Figure 5.15 - Full Face Gestalt Plots (From Russel)

one extreme of the spread. Those closest to him are partially balding. Two identical twins (separable by a first-time human observer -- but nevertheless admittedly quite similar in appearance) were classified by the CTT system as similar.

The preliminary indication of these results is that CTT is indeed a generic human classification architecture which produces psychologically similar results to that of a human.

In addition, the illusory triangle [47] optical illusion was drawn, first without the triangle being explicitly "drawn in" and then with the triangle being explicitly "drawn in". The CTT image recognition machine classified the two only one memory (gestalt) location apart. This is a preliminary indication that CTT might be a new mechanism for explaining optical illusions.

6. Recommendations for Future Development and Applications

6.1 Current Technology Shortfalls for the Full-Scale Implementation of a Human Brain Sized CTT System

Cortical Thought Theory is as much an approach to discovering the architecture of the human brain as it is the engineering specification of that architecture. CTT is intended as much to provide a new way of approaching the answer to the question, "How does the human brain think?" as it is the answer to that question. As an approach, it is fairly complete; as a set of answers, it is quite incomplete -- only the framework for the answers is offered in this dissertation. This chapter is presented in three parts. The first part tries to convey some of the reasons why it is important to continue to develop our information processing capabilities as rapidly as we can -- even though these new capabilities may present significant management challenges. The second part briefly reviews CTT's credentials as an approach which should be seriously considered in an attempt to improve our information processing capabilities. The third part is an overview of a strategy which might be followed to span the gap between current technology and a technology which is capable of building a full-scale implementation of human brain sized CTT system.

6.1.1 The requirement to increase our information processing capabilities:

There is a requirement to continue to increase our information processing capabilities. This requirement has no forseeable limit.

Even if there were no other market for an unlimited information processing capability, the requirement for national defense will always demand the most sophisticated information processing capabilities possible.

There will no doubt emerge various political and social action groups from time to time throughout the future which will express concern about developing machines with information processing capabilities that exceed those of the human brain. History has already seen some who have offered philosophical reservations about the development of the modern digital electronic computer which is far more capable than the human brain for performing certain types of information processing tasks (such as mathematical calculations, deductive inferencing, etc.).

As computing architectures are developed which promise to exceed all physical aspects of human information processing capabilities, there will likely be an increase in the reticence, on the part of some segments of society, to participate in the development of these capabilities. Certainly there will be some developments which will present new challenges in the proper management of this new technology. One foreseeable such challenge will occur when the interconnectivity between some of the semantic surfaces will allow the machine to first impact its environment as a result of its own planning (this is already being done in some applications), then to measure (observe) the effect of this planned impact on its environment, and then to make longer range plans, as a result of lessons learned from the previous two steps, which allow it to more efficiently impact its environment (than it did in its previous attempts). This algorithm is a simple control-feedback algorithm applied by providing the proper interconnectivity and feedback links between the cortex surfaces responsible for the semantic association and script planning functions (reference Figure 2.17) of the system. Psychologists and sociologists have described this algorithm as self-awareness and self-preservation.

6.1.2 CTT's credentials:

When the human gestalt mechanism is found and when it is learned how the human brain networks these gestalt mechanisms together to form a human-like memory and inferencing system, then it will be reasonable to suspect that a new era in information processing has begun. The research presented in this dissertation does not claim to have the final answers to these questions. It does claim to have presented a reasonable approach, which has developed a consistent theoretical framework, which is supported by significant experimental data, for identifying both the human gestalt mechanism and the architecture for networking a collection of these mechanisms together so that both human-like memory and human-like inferencing capabilities are elicited. In light of these preliminary successes, CTT should be further developed and investigated.

6.1.3 A strategy for improving the technology:

The cautious observer will note that the breadth of this research is greater than that of the average dissertation, and that breadth and depth are usually inversely proportional. Therefore, the depth of the experimental support for several assertions made in this dissertation is expectedly less than average. It seems prudent to begin reducing the technology gap by increasing our understanding of the foundation upon which a large CTT system would be built. This calls for further experimentation of various types which will provide the massive amounts of data which will be required to foster both a broader confidence and a deeper understanding of the assertions made in this dissertation. A rapid, but potentially more expensive, way to proceed down this road is to begin building a large CTT system with a view toward identifying and solving problems as they become obstacles.

Specifically, special-purpose hardware modules should be developed (after further software simulation) which function as local cortex surfaces that perform the prescribed gestalt calculation. These modules must be built of elements which communicate at two different levels. One of these communication levels must be dedicated to performing the gestalt neighborhood-sample-averaging calculation. For the other level of communication, the individual elements must have the simple functions which Goldschlager and Wiles prescribe in order for these cortex-surface-modules to perform the necessary set completion and sequence completion operations. These modules must provide multiple sets of massive parallel communication ports (one channel per cortical column per set) for both input and output image transfers. The region of activity of these ports must be adjustable; the control mechanism for performing this regional adjustment (for windowing) must still be hypothesized (this is a necessary part of CTT which has not yet been specified).

Once these modules are mass-produced, then an entire new field of study can begin which addresses itself to the effects of the interconnectivity of these local cortex surfaces on the potential capabilities of a large CTT system. It is anticipated that, at most, a system can contain only three (any three) of the following four attributes:

(1) Lateral consistency of inferences: A richness of lateral interconnectivity between local cortex surfaces of the same hierarchical abstraction level will result in an inferencing capability which is as devoid of contradictions as the information in the system will allow.

(2) Creativity and ability to generalize: A richness of vertical interconnectivity between local cortex surfaces of differing hierarchical abstraction levels (to include feedback links) will result in an ability to synthesize new hypotheses, which are characteristic of creative generalizations, which increases with increases in the density of the interconnectivity.

(3) Ability to update memory: If the basic computing elements (those elements with the equivalent function of the cortical columns) are built so that their propensity to activate is modifiable, then this will add a significant degree of complexity to the system which will then trade adaptability for speed. If this were not a requirement of the system, inferences could be performed many orders of magnitude faster than the human brain could perform them. All the facts and associations would have to be preprogrammed.

(4) Inferencing speed which exceeds that of the human brain: The less lateral interconnectivity there is, the faster will be the inferencing -- but it may not be very consistent with the information in the system. The less vertical interconnectivity there is, the faster will be the inferencing -- but it may not be very creative. The more creativity, consistency, and ability to learn new facts and associations, that are required by the system, the slower will be its inferencing capability.

Beyond these macro system characteristics, due to the nature of the interconnectivity patterns, the micro system interconnectivity characteristics will need to be researched. There still remain questions like: "How much interconnectivity is required to provide for a large vocabulary with poor resolution surfaces?", and "What are the minimum, maximum, and optimal interconnectivity patterns and densities for eliciting specific types of inferences?"

Initially these local cortex surface modules should probably be built with a minimal capability to modify their stored propensities to activate (on both communication levels). This will facilitate the quantification of effects due to various patterns of interconnectivity. Eventually, these local cortex surface modules will have to be built so that they can modify their propensities to activate. Goldschlager and Wiles have found that the problems of specifying the coefficients for habituation, reinforcement, exposure times, etc., are very complex. The answers to these sorts of questions will not come easily.

Additionally, hardware should be designed which functions according to the CTT description of the retinal and lower brain preprocessing architecture and function for identifying visual image windows.

6.2 Current and Near Term Applications of CTT

If the architecture proposed in this dissertation is actually the architecture of the human brain, then the medical and psychological impacts of this knowledge could be significant and immediate. But before CTT could be responsibly applied to solving the problems facing these two fields of study, it will have to be further studied and verified. This work will have to be left to medical and psychological researchers.

However, there are engineering applications of CTT which are significant, inexpensive, and can be accomplished in the near term. Some of these are listed as follows:

(1) A real-time, connected-word, few hundred word speech recognizer when speech conforms to formal English grammar or other programmed syntax: An acoustic analyzer with the property of plotting the phoneme tracks of words is ideally suited as a front end for the Spoken English Recognition Expert System (SPEREXSYS) [107]. This would produce a system which is capable of performing real-time, connected-word, multi-hundred word vocabulary, speech recognition. Speaker independencies, and speaker recognition capabilities will have to wait on a better understanding of how the primary audio cortex windowing mechanism works.

(2) Low-bit speech transmission: Because the intelligibility of speech is affected by the energy level, the vocal tract shape, and the method of vocal tract excitation, and since the vocal tract shapes are all quantifiable on a grid with about 300 locations, it should be possible to transmit speech, with proper information coding techniques, at about 100 bits per second.

(3) Rudimentary image analysis and/or face recognition machine: This application is currently being developed at AFIT by Robert L. Russel. It is called "rudimentary" because it will require human intervention to set the windows until the herein prescribed visual image windowing mechanism is built (see Chapter Three).

(4) When the Wiles/Goldschlager research is completed, it would be very interesting for A.I. research purposes to build a small domain, several tier, abstract human reasoning system (software simulation) to perform the reasoning processes outlined by Figure 2.17.

7. Summary and Conclusions

This dissertation has used the systems approach to unify the disciplines of Artificial Intelligence, perceptual psychology, neurophysiology, and various branches of mathematics, into a new theory of human brain function. This theory has been experimentally supported by:

(1) Producing a computer simulation (emulation of the hypothesized neurostructure and neurofunction) of the first three levels of the abstraction hierarchy of the human brain and showing that this architecture is capable of doing both speech recognition and visual image analysis,

(2) Predicting and verifying a new class of audio-illusions and offering an alternate explanation of the class of static, two-dimensional optical illusions, and

(3) Showing that the high frequency roll-off of the visual contrast sensitivity curve could be explained by attributing to the cortical columns in the cortex the neighborhood sample and average function hypothesized by CTT.

In addition, this new theory has been able to account for a wide diversity of experimental phenomena from the neurosciences by offering a few simple principles of operation and architecture of the human brain.

The development of CTT began with a review of the lessons which have been learned by Artificial Intelligence in the area of knowledge representation. Specifically, it is becoming commonly acceptable that in order to produce a system capable of the direct memory accessing of the most pertinent information and inferences in a very large knowledge-base (which appears to be characteristic of human intelligence), traditional sequential deductive reasoning strategies are inadequate. This leads to the conclusion that it is necessary to abandon the conventional mindset of attempting to solve the problems of human reasoning by using the conceptual framework of deductive logic. Instead, the conceptual framework of inductive logic should be used. This means, that conceptually, the primitives of deductive logic (first order predicate calculus) must be abandoned in favor of primitives of analogy.

An examination of the neurophysiological structure of the cortex reveals that for the most part, it is two-dimensionally homogeneous; that is, a small region of cortex in one area of the brain is structurally very similar to a small region of cortex in any other part of the brain. Since function is predicated on structure, it is reasonable to assume that the computational function of one region of the cortex is essentially the same as the computational function of any other region of the cortex. This leads to the expectation that if one can describe the analogical mechanism which is in operation in one part of the cortex, one can then describe the analogical mechanisms which are in operation in all regions of the cortex because they will all be the same.

A systems approach was used to find the analogical (also called gestalt) mechanism. It was argued that the general description of any analogy mechanism is embodied in a three-part description:

(1) An analogy mechanism requires that information be presented to it using some standardized representation scheme.

(2) The analogy mechanism must then extract the essence of identification (gestalt) of the input.

(3) This gestalt must then be compared to all other stored-image-gestalts in order to determine the best match.

This leads to the requirement to answer the following three questions:

(1) What is the standardized representation scheme that is used to present input?

(2) How is the gestalt extracted from one of these input representations?

(3) How is the gestalt, which is extracted from a single input representation, compared to all other stored-image-gestalts (remembering that the comparison must elicit the best match)?

It was shown that the answer to the first question is likely that input information, at any level in the abstraction hierarchy, is presented as a two-dimensional image "drawn" on a small region of the cortex surface (local cortex surface).

In answering the second question, it was argued that the gestalt feature vector set is probably extracted from a low-pass, two-dimensional, Fourier-like transform of the input image. Appendix A contains a mathematical argument that shows that it is reasonable only to conclude that the cardinality of this gestalt feature vector set is two. This is considered to be the most significant contribution of this research. Further analysis indicates that the two members of this gestalt feature vector set might be the two-space coordinates of the location of the local maximum of the two-dimensional Fourier-sine transform (of the input image) which is closest to the D.C. term.

The answer to the third question is a consequence of the answer to the second question. Since the answer to the second question is a physical two-dimensional location, the similarity of an image-gestalt to all other stored-image-gestalts is directly proportional to the distance between the physical locations of the two gestalts being compared. Finding the stored gestalt location closest to the inquiry-gestalt location elicits the behavior of direct memory access to the most pertinent information or inference in the knowledge base.

Having developed a detailed description of the gestalt mechanism, it was shown how to combine this mechanism with the

Goldschlager results to obtain a computing architecture which is capable of all levels of abstract human reasoning. A detailed example of the architecture of the natural language domain was presented to show how the system would interpret the meaning of: "John shot the buck."

A neurologically-based model for computing the prescribed gestalt calculation was presented. This model is capable of only approximating the prescribed calculation. An analysis of the error between the prescribed calculations and the neurologically implemented approximation was shown to be able to exactly predict the high frequency roll-off of the visual contrast sensitivity curve.

A computer simulation was built to emulate the hypothesized function of the first three levels of abstraction of sensory analysis. It was shown that human-like speech recognition and image analysis could be performed with this simulation. Only the initial input image needs to be changed in order to do either speech recognition or image analysis.

The model predicts an as yet unknown class of audio-illusions. An audio-illusion from this class was sythesized and verified as a true human audio-illusion.

The experimental results of both Hubel and Wiesel and DeValois et al. were reconciled and are both the predicted results of the simple hypothesized visual image windowing mechanism.

It was shown how the three types of human learning are accounted for by this model.

A rationale and strategy were presented for the continued development of the work presented in this dissertation. This discussion included recommendations for further research, and some proposed near-term and long-range applications of Cortical Thought Theory.

Bibliography

1. Ackley, David H.; and Geoffrey E. Hinton, and Terrence J. Sejnowski. "A Learning Algorithm for Boltzmann Machines." Cognitive Science, Vol 9, No. 1, pp 147-169, Jan-Mar 1985.

2. Aho, Alfred V., John E. Hopcroft, and Jeffrey D. Ullman. The Design and Analysis of Computer Algorithms. Addison-Wesley: Reading, Mass. 1974.

3. Akmajan, A., and F. Heny. An Introduction to the Principles of Transformational Syntax. Cambridge, Mass: MIT Press, 1975.

4. Arend, Lawrence E., Jr. "Response of the Human Eye to Spatially Sinusoidal Gratings at Various Exposure Durations." Vision Research, Vol 16, No. 11, pp 1311-1315, 1976.

5. Bach, Emmon. An Introduction to Transformational Grammars. New York: Holt, Rinehart and Winston, 1964.

6. Barlow, H.B. "Some Possible Principles Underlying the Transformations of Sensory Messages," in Sensory Communications, W.A. Rosenblith, ed., New York: John Wiley, pp. 217-234, 1961.

7. Barlow, H.B.; Narashimhan, R.; and Rosenfeld, A. "Visual Pattern Analysis in Machines and Animals." Science, Vol 177, pp. 567-575, 1972.

8. Barr, Avron, and James Davidson. "Representation of Knowledge," Handbook of Artificial Intelligence, edited by Avron Barr and Edward A. Feigenbaum. DTIC document number AD A074078, 1980.

9. Bobrow, Daniel G., and Terry Winograd. An Overview of KRL, A Knowledge Representation Language. Stanford Artificial Intelligence Laboratory Memo AIM-293, November 1976. DTIC document number ADA042508.

10. Bok, S. T. Histonomy of the Cerebral Cortex. Elsevier: New York, 1959.

11. Brachman, R., et al. KLONE Reference Manual. BBN Report No. 3848, Bolt Beranek and Newman, Inc., July 1978. DTIC document number ADA122437.

12. Breitmeyer, Bruno; Dennis M. Levi; and Ronald S. Harwerth. "Flicker Masking in Spatial Vision." Vision Research, Vol 21, pp. 1377-1385, 1981.

13. Breitmeyer, Bruno G. "Letter to the Editors: Simple Reaction Time as a Measure of the Temporal Response Properties of Transient and Sustained Channels." Vision Research, Vol 15, pp. 1411-1412, 1975.

14. Bush, Larry F. The Design of an Optimum Alphanumeric Symbol Set For Cockpit Displays. AFIT M.S. Thesis, AFIT/GE/EE/77-11, Air Force Institute of Technology. DTIC Document ADA053447, 1977.

15. Campbell, Fergus W. "The Human Eye As An Optical Filter." Proceedings of the IEEE, Vol 56, No. 6, pp. 1009-1014, June 1968.

16. Campbell, F.W. and D.G. Green. "Optical and Retinal Factors Affecting Visual Resolution." In Journal of Physiology, No. 181, pp. 576-593, Nov-Dec 1965.

17. Campbell, F.W., and R.W. Gubisch. "Optical Quality of the Human Eye." Journal of Physiology, Vol 186, pp. 558-578, 1966.

18. Campbell, F.W., and J.J. Kulikowski, and J.Z. Levinson. "The Effect of Orientation on the Visual Resolution of Gratings." In Journal of Physiology, No. 187, pp. 427-436, Nov-Dec 1966.

19. Campbell, F.W., and L. Maffei. "Electrophysiological Evidence for the Existence of Orientation and Size Detectors in the Human Visual System." Journal of Physiology, Vol 207, pp. 635-652, 1970.

20. Cannon, Mark W., Jr. "Evoked Potential Contrast Sensitivity in the Parafovea: Spatial Organization." Vision Research, Vol 23, No. 12, pp. 1441-1449, 1983.

21. Chomsky, N. The Logical Structure of Linguistic Theory. New York: Pelnum Press, 1975.

22. Chomsky, N. Aspects of the Theory of Syntax. Cambridge, Mass: MIT Press, 1965.

23. Christofides, Nicos. Graph Theory: An Algorithm Approach. Academic Press: London, 1975.

24. Crick, F.H.C. "Thinking About the Brain." Scientific American, Vol 241, No. 3, pp. 219-232, Sep 1979.

25. DeGroot, Doug. PROLOG and Knowledge Information Processing: A Tutorial. IBM Research, T.J. Watson Research Center, Yorktown Heights, NY, 1984.

26. DeMott, Donald W. "Microtoposcopic Investigation of the Peristriate Cortex of the Squirrel Monkey." Medical Research Engineering, Vol 10, No. 2, April-May 1971.

27. DeMott, Donald W. "Cortical Micro-Toposcopy." Medical Research Engineering, Fourth Quarter 1966.

28. DeValois, Russell L., Duane G. Albrecht, and Lisa G. Thorell. "Spatial Frequency Selectivity of Cells in Macaque Visual Cortex." Vision Research, Vol 22, No. 5, pp. 545-559, 1982.

29. DeValois, Russell L., Herman Morgan, and D. Max Snodderly. "Psychophysical Studies of Monkey Vision - III. Spatial Luminance Contrast Sensitivity Tests of Macaque and Human Observers." Vision Research, Vol 14, No. 1, pp. 75-81, 1974.

30. DeValois, Russell L., E. William Yund, and Norva Hepler. "The Orientation and Direction Selectivity of Cells in Macaque Visual Cortex." Vision Research, Vol 22, No. 5, pp. 531-544, 1982.

30a. Dietterich, Thomas G. "Learning and Inductive Inference," Handbook of Artificial Intelligence, Vol III, edited by Paul R. Cohen and Edward A. Feigenbaum. 1982.

31. Ditchburn, R.W. Light. Blackie & Son: Glasgow, 1953.

32. Doddington, George R., and Thomas B. Schalk. "Speech Recognition, Turning Theory to Practice," IEEE Spectrum, 18:26-32 (September 1981).

33. Enroth-Cugell, C., and J.G. Robson. "The Contrast Sensitivity of Retinal Ganglion Cells of the Cat." Journal of Physiology, Vol 187, pp. 517-552, 1966.

34. Erman, Lee D. Fredrick Hayes-Roth, Victor R. Lesser, and D. Raj Reddy. "The Hearsay II Speech Understanding System: Integrating Knowledge to Resolve Uncertainty." Computing Surveys, 12: 213-253 (June 1980).

35. Ervin, Frank R. "On-Line Computer Techniques for Analysis of the Visual System." Symposium on the analysis of central nervous system and cardiovascular data using computer methods. NASA SP-72. Washington, D.C., October 29-30, 1964.

36. Fahlman, Scott E. NETL: A System For Representing and Using Real-World Knowledge. The MIT Press: Cambridge, Massachusetts, 1979.

37. Feldman, Jerome A. "Connections Models and Their Applications Introduction." Cognitive Science, Vol 9, No. 1, pp. 1,2, Jan-Mar 1985.

38. Ferber, Leon, et al. Continuously Automatic Speaker Adaptation. DTIC document number ADA082620, January 1980.

39. Ferber, Leon, et al. Speech Perception. DTIC document number ADA018442, November 1975.

40. Fowles, Grant R. Introduction to Modern Optics. Holt, Rinehart and Winston: New York, 1968.

41. Franzén, Ove and Mark Berkley. "Apparent Contrast As A Function of Modulation Depth and Spatial Frequency: A Comparison Between Perceptual and Electrophysiological Measures." In Vision Research, Vol 15, No. 6, pp. 655-660, June 1975.

42. Gallager, Robert G. Information Theory And Reliable Communication. Wiley and Sons: New York, 1968.

43. Gardner, Anne. "Search," Handbook of Artificial Intelligence, edited by Avron Barr and Edward A. Feigenbaum, DTIC document number AD A074078, 1979.

44. Gardner, Anne, et al. "Natural Language Understanding," Handbook of Artificial Intelligence, edited by Avron Barr and Edward A. Feigenbaum. DTIC document number AD A076873, 1979.

45. Gelfand, Stanley A. Hearing: An Introduction to Psychological and Physiological Acoustics. Dekker: New York, 1981.

46. Geschwind, Norman. "Specialization of the Human Brain." Scientific American, Vol 241, No. 3, pp. 180-199, Sep 1979.

47. Ginsburg, A.P. "Is the Illusory Triangle Physical or Imaginary?" Nature, 257, pp. 219-220, 1975.

48. Ginsburg, Arthur P. Visual Information Processing Based On Spatial Filters Constrained By Biological Data. PhD Dissertation. University of Cambridge (Library of Congress Catalog Card Number 79-600156), 1978.

49. Goldschlager, Leslie M. A Computational Theory of Higher Brain Function. Stanford University: STAN-CS-84-1004, April 1984.

50. Graham, Norma. "The Visual System Does a Crude Fourier Analysis of Patterns." SIAM-AMS Proceedings, Vol 13, pp. 1-16, 1981.

51. Greiner, Russell. RLL-1: A Representation Language Language. Stanford Heuristic Programming Project, HPP-80 8 (Working Paper), October 1980. DTIC document number ADA096510.

52. Harwerth, R.S., et al. "Behavioral Studies on the Effect of Abnormal Early Visual Experience In Monkeys: Spatial Modulation Sensitivity." Vision Research, Vol 23, No. 12, pp. 1501-1510, 1983.

53. Hausmann, Erich and Edgar P. Slack. Physics. 2nd Ed. Van Nostrand: New York, 1947.

54. Hawkinson, Lowell. The Representation of Concepts In OWL. Automatic Programming Group Internal memo 17, MIT, July 3, 1975.

55. Hendrix, Gary G. Encoding Knowledge In Partitioned Networks. Technical Note 164, SRI Project 5844, A.I. Center, SRI International, Menlo Park, CA, June 28, 1978.

56. Hubel, David H. "The Brain." Scientific American, Vol 241, No. 3, pp. 44-53, Sep 1979.

57. Hubel, David H. and Torsten N. Wiesel. "Brain Mechanisms of Vision." Scientific American, Vol 241, No. 3, pp. 150-162, Sep 1979.

58. Isaacson, Robert L. Basic Readings in Neuropsychology, editor. Harper and Row: New York, 1964.

59. Kabrisky, Matthew. A Proposed Model for Visual Information Processing In The Human Brain. University of Illinois Press: Urbana, 1966.

60. Kabrisky, M., et al. "A Theory of Pattern Perception Based on Human Physiology." Contemporary Problems In Perception. Edited by A.T. Welford and L.H. Houssiadas. Taylor and Francis Ltd: London, pp. 129-147, 1970.

61. Kandel, Eric R. "Small Systems of Neurons." Scientific American, Vol 241, No. 3, pp. 66-84, Sep 1979.

62. Kanerva, Pentti. Self-Propagating Search: A Unified Theory of Memory. PhD Dissertation, Report Number CSLI-84-7. Ventura Hall; Stanford University: Stanford, CA. March 1984.

63. Keidel, Wolf D.; S. Kallert; and M. Korth. The Physiological Basis of Hearing. Thieme-Stratton: New York, 1983.

64. Kelly, D.H. "Adaptation Effects on Saptio-Temporal Sine-Wave Thresholds." Vision Research, Vol 12, No. 1, pp. 89-101, 1972.

65. Kelly, D.H. "Spatial Frequency Selectivity in the Retina." Vision Research. Vol 15, No. 6, pp. 665-672, June 1975.

66. Koutsoudas, A. Writing Transformational Grammars: An Introduction. New York: McGraw-Hill, 1966.

67. Krieg, Wendell J.S. Functional Neuroanatomy. Blackiston: New York, 1953.

68. Kronauer, Richard E. and Yehoshua Y. Zeevi. "Reorganization and Diversification of Signals in Vision." IEEE Transactions on Systems, Man, and Cybernetics, Vol. SMC-15, No. 1, pp. 91-101, Jan-Feb 1985.

69. Kulikowski, J.J. "Apparent Fineness of Briefly Presented Gratings: Balance Between Movement and Pattern Channels." Vision Research, Vol 15, No. 6, pp. 673-680, June 1975.

70. Lesser, Victor R., Richard D. Fennel, Lee D. Erman, and D. Raj Reddy. "Organization of the Hearsay II Speech Understanding System," IEEE Transactions on Acoust., Speech, and Signal Processing, ASSP-23: 11-24 (February 1975).

71. Levinson, Stephen E., and Mark Y. Liberman. "Speech Recognition by Computer," Scientific American. New York: Scientific American, April 1981: 64-76.

72. Lin, Shu, and Daniel J. Costello, Jr. Error Control Coding. Prentice-Hall: Englewood Cliffs, N.J., 1983.

73. Linsenmeier, R.A.; L.J. Frishman, H.G. Jakiela, and C. Enroth-Cugell. "Receptive Field Properties of X and Y Cells in the Cat Retina Derived From Contrast Sensitivity Measurements." Vision Research, Vol 22, No. 9, pp. 1173-1183, 1982.

74. Longhurst, R.S. Geometrical And Physical Optics 2nd Ed. Wiley & Sons: New York, 1967.

75. Lorente de Nó, R. "Cerebral Cortex: Architecture, Intracortical Connections, Motor Projections." In Physiology of the Nervous System, 3rd ed., by J.F. Fulton, Oxford University Press: Oxford, 1949.

76. Luria, Aleksandr Romanovich. Higher Cortical Functions In Man. Basic Books: New York, 1966.

77. Maffei, Lamberto, and Adriana Fiorentini. "The Visual Cortex As A Spatial Frequency Analyser." Vision Research, Vol 13, pp. 1255-1267, 1973.

78. Maher, Frank A. "A Correlation of Human and Machine Pattern Discrimination." Processing of the IEEE 1970 NAECON Conference, pp. 260-264, 1970.

79. Makhoul, John. "Linear Prediction: A Tutorial Review." Proceedings of the IEEE, Vol 63, pp. 561-580, 1975.

80. Manna, Zohar. Mathematical Theory of Computation. McGraw-Hill: New York, 1974.

81. Marcus, Mitchell P. A Theory of Syntactic Recognition for Natural Language. Cambridge, Mass: MIT Press, 1980.

82. Markel, J.D. and A.H. Gray, Jr. Linear Prediction Of Speech. Springer-Verlag: New York, 1976.

83. Marr, David C. Vision. Freeman: New York, 1982.

84. Martin, William A. Descriptions and the Specialization of Concepts. Laboratory for Computer Science, MIT. Not published.

85. Milne, Robert W. Handling Lexical Ambiguity In A Deterministic Parser. PhD Dissertation University of Edinburgh, Edinburgh, Scotland, 1983.

86. Minsky, Marvin A. "Framework for Representing Knowledge." In The Psychology of Computer Vision, edited by P.H. Winston. McGraw Hill: New York, 1975.

87. Moore, Thomas J. and John L. Cashin, Jr. "Response of Cochlear-Nucleus Neurons to Synthetic Speech." Journal Acoustical Society of America, Vol 59, No. 6, pp. 1443-1449, 1976.

88. Moore, Thomas J. and John L. Cashin, Jr. "Response Patterns of Cochlear Nucleus Neurons to Excerpts From Sustained Vowels." Journal Acoustical Society of America, Vol 56, No. 5, pp. 1565-1576, November 1974.

89. Nilsson, Nils J. Principles of Artificial Intelligence. Tioga: Palo Alto, CA, 1980.

90. O'Hair, Mark A. Whole Word Recognition [written] Based on Low Frequency Fourier Complex and Amplitude Spectrums. Masters Thesis, AFIT/GEO/ENG/84D-4, DTIC Document, Dec 1984.

91. Oppenheim, A.V., and R.W. Schafer. Digital Signal Processing. Prentice-Hall: Englewood Cliffs, N.J., 1975.

92. Pantle, A. "Visual Information Processing of Complex Imagery." Research Report AMRL-TR-74-43, Aerospace Medical Research Laboratory, Wright-Patterson AFB, OH, 1974.

93. Pantle, A. and R. Sekuler. "Size Detecting Mechanisms In Human Vision." Science, 162, pp. 1146-1148, 1968.

94. Pasternak, Tatiana, et al. "The Role of Area Centralis in the Spatial Vision of the Cat." Vision Research, Vol 23, No. 12, pp. 1409-1416, 1983.

95. Patel, A.S. "Spatial Resolution By The Human Visual System. The Effect of Mean Retinal Illuminance." Journal of the Optical Society of America, Vol 56, No. 5, May 1966.

96. Penfield, Wilder, and Lamar Roberts. Speech and Brain - Mechanisms. Princeton University Press: Princeton, N.J., 1959.

97. Pick, Arnold. APHASIA. Thomas: Springfield, Illinois, 1973.

98. Pickles, James O. An Introduction to the Physiology of Hearing. Academic Press: New York, 1982.

99. Pollack, Jordan. "An Activation/Inhibition Network Cell." Working Paper 31, Advanced Automation Research Group, Coordinated Science Laboratory, University of Illinois, Urbana, January 1982.

100. Pollack, Jordan B. "Massively Parallel Parsing." ACL 1983 Summary, Coordinated Science Laboratory, University of Illinois, Urbana, 1983.

101. Polyak, Stephen. The Vertebrate Visual System. University of Chicago Press: Chicago, 1957.

102. Quillian, M.R. "The Teachable Language Comprehender: A Simulation Program and the Theory of Language." CACM, Vol 12, pp. 459-476, 1969.

103. Quillian, M.R. "Semantic Memory," in Semantic Information Processing, M. Minksy, Cambridge, Mass: MIT Press, pp. 227-270, 1968.

104. Rabiner, L.R., and R.W. Schafer. Digital Processing of Speech Signals. Prentice-Hall: Englewood Cliffs, N.J., 1978.

105. Regan, D. "Spatial Frequency Mechanisms in Human Vision Investigated by Evoked Potential Recording." Vision Research, Vol 23, No. 12, pp. 1401-1407, 1983.

106. Rich, Elaine. Artificial Intelligence. McGraw-Hill: New York, 1983.

107. Routh, Richard LeRoy. A Spoken English Recognition Expert System. MS Thesis GCS/EE/83S-01. Air Force Institute of Technology; Wright-Patterson AFB, OH, September 1983. DTIC document number ADA136835.

108. Routh, R.L. and R. Milne. "Continous Speech Recognition Using Natural Language Constraints." Proceedings of the IEEE NAECON 1984 Conference, pp. 916-923, May 1984.

109. Rovamo, J. and V. Virsu. "An Estimation and Application of the Human Cortical Magnification Factor." Experimental Brain Research, Vol 37, pp. 495-510, 1979.

110. Ruch, Theodore C. and John F. Fulton. Medical Physiology and Biophysics. Saunders: Philadelphia, 1960.

110a. Russel, Robert L. Jr. Performance of a Face Recognition Machine Using Cortical Thought Theory. MS Thesis. Wright-Patterson AFB, Ohio: School of Engineering, AFIT, TBP December 1985.

111. Schank, Roger C. and Cristopher K. Riesbeck. Inside Computer Understanding. Lawrence Erlbaum Associates: Hillsdale, NJ, 1981.

112. Seelandt, Karl G. Computer Analysis and Recognition of Phoneme Sounds in Connected Speech. MS Thesis GE/EE/81D-53. Wright-Patterson AFB, Ohio: School of Engineering, Air Force Institute of Technology, December 1981.

113. Sekuler, Robert. "Spatial Vision." Annual Review of Psychology, Vol 25, pp. 195-232, 1974.

114. Shepherd, Gordon M. "Microcircuits in the Nervous System." Scientific American.

115. Sinex, Donal G., and C. Daniel Geisler. "Responses of Auditory-Nerve Fibers to Consonant-Vowel Syllables." Journal Acoustical Society of America, Vol 73, No. 2, pp. 602-615, February 1983.

116. Stevens, Charles F. "The Neuron." Scientific American, Vol 241, No. 3, pp. 54-65, Sep 1979.

117. Stevens, S.S. "The Measurement of Loudness." Journal of the Acoustical Society of America, Vol 27, No. 5, pp. 815-829, September 1955.

118. Tobias, Jerry V. Foundations of Modern Auditory Theory, editor. Volumes I & II. Academic Press: New York, 1972.

119. Tootell, R.B.H.; M.S. Silverman; E. Switkes; and R.L. DeValois. "Deoxyglucose Analysis of Retinotopic Organization in Primate Striate Cortex." Science, Vol. 218, pp. 902-904, 1982.

120. Trejo, Leonard J. and Carol M. Cicerone. "Retinal Sensitivity Measured by the Pupillary Light Reflex in RCS and Albino Rats." Vision Research, Vol 22, No. 9, pp. 1163-1171, 1982.

121. Tyc, Raymond J. An Improved Linear Predictive Vocoder and Isolated Word Recognizer Using LPC. Masters Thesis AFIT/GE/EE/84J-9. Air Force Institute of Technology: WPAFB. DTIC document, June 1984.

122. Uttal, William R. The Psychobiology of Sensory Coding. Harper and Row: New York, 1973.

123. Van Nes, F.L. and M.A. Bouman. "Spatial Modulation Transfer in the Human Eye." Journal of Optical Society of America, 57, pp. 401-407, 1967.

124. Vassilev, A. and D. Mitov. "Perception Time and Spatial Frequency." Vision Research, Vol 16, pp. 89-92, 1976.

125. Virsu, Veijo; Jyrki Rovamo; and Risto Näsänen. "Temporal Contrast Sensitivity and Cortical Magnification." Vision Research, Vol 22, No. 9, pp. 1211-1217, 1982.

126. Waltz, David L., and Jordan B. Pollack. "Massively Parallel Parsing: A Strongly Interactive Model of Natural Language Interpretation." Cognitive Science, Vol 9, No. 1, pp. 51-74, Jan-Mar 1985.

127. Werblin, Frank S. "The Control of Sensitivity in the Retina." Scientific American,

127a. Wescott, Roger W. "Types of Vowel Alternation in English." Word, Vol 26, No. 3, pp. 309-343, Dec 1970.

128. Wilks, Yorick. "Good and Bad Arguments About Semantic Primitives." D.A.I. Research Report No. 42, University of Edinburgh, Edinburgh, Scotland, May 1977.

129. Williamson, S.J.; L. Kaufman; and D. Brenner. "Research Note: Latency of the Neuromagnetic Response of the Human Visual Cortex." Vision Research, Vol 18, pp. 107-110, 1978.

130. Winston, Patrick Henry. Artificial Intelligence. Addison-Wesley: Reading, Massachusetts, 1977.

131. Woods, William A. "What's In A Link: Foundations For Semantic Networks." In RV, pp. 35-82, 1975.

132. Woolsey, C.N. "Organization of Cortical Auditory System: A Review and a Synthesis." In Neural Mechanisms of the Auditory and Vestibular Systems; Rasmussen, G.L., and W.F. Windle, editors, pp. 165-180, Thomas, Springfield, 1960.

133. Yilmaz, H., et al. Speaker Adaptation Test and Evaluation. DTIC document number ADA071675, May 1979.

134. Yilmaz, H., et al. Automatic Speaker Adaptation. DTIC document number ADA032592, September 1976.

135. Yilmaz, H., et al. Perceptual Continuous Speech Recognition. DTIC document number ADA783899, July 1974.

136. Yilmaz, H., et al. A Real-Time, Small-Vocubulary, Connected-Word Speech Recognition System. DTIC document number AD753176, November 1972.

137. Zue, V.W. Speech Recognition: Acoustic Phonetic and Lexical Knowledge Representation. Pp. 79. Res. Lab. Electron., MIT, Cambridge, MA (February 1984). ADA 137697/9 (No. 10, 1984).

Appendix A

This appendix presents the single most significant contribution that this research and dissertation have to make to the neurosciences, to wit: If the cardinality of the Gestalt Feature Vector Set (GFVS) is allowed to be greater than two, then it appears that we must overcome some ominous obstacles and accept some difficult system performance criteria. If on the other hand the cardinality of the GFVS is two, then the difficulties which accompany the larger cardinalities are easily overcome, and other important system performance criteria, such as direct accessing of memory, are simply accounted for.

One of the corollaries of the argument presented in this appendix is a clear, definitive understanding of the theoretical limitations of using a Turing machine to attempt to model the human inference processes. Chapter Two asserted, based on the review of the opinions appearing in the A.I. literature, that a computing machine built on the sequential application of the primitives of deductive logic is theoretically insufficient for implementing a large scale real-time model of the human information processing mechanisms. This assertion can now seem to be justified solely on the basis of the argument developed in this appendix (if the reader is willing to accept the assumptions on which it is based).

This argument was developed to answer the following question which was posed in Chapter Three:

"How are the low frequency Fourier harmonics, which are extracted from a single two-dimensional input representation, compared to the stored Fourier harmonics of all other previously encountered images (remembering that the comparison must elicit the best match)?"

Prior to posing this question in Chapter Three, it was argued that the gestalt feature vector set (GFVS) was to be extracted from a two-dimensional Fourier-like transform. This is not a required assumption for the following argument. This argument only assumes that the storage area has dimension two (from neuroanatomical observation of the cortex structure).

Another fundamental assumption used in this argument is that human memory is non-linear with respect to the number of exposures of an object. More specifically, if the strength of the memory of an event after a single exposure is: $M_1 = f_1(t)$, where $f_1(t)$ is some function of time (for a single event), and if the strength of the memory of an event after the second exposure (occuring t_0 after the first exposure) is M_2, then $M_2 > f_1(t) + f_1(t+t_0)$. It is asserted from common observation that there exists at least one t_0 such that this inequality is true. (Due to the phenomenon of habituation, it is conceivable that it may not be true for all t_0).

A sensory input (and presumably any level of abstraction input) to the gestalt classification and comparison process is represented as a two-dimensional image. The gestalt must be some set of features extracted from that (or some function of that -- e.g., 2DDFT) 2-D image. The cardinality of the GFVS is the dimension of the feature vector.

If the cardinality of the gestalt feature set is zero, then the system does not function. This is a trivial and unreasonable case and will not be considered further.

If the cardinality of the gestalt feature set is one, tnen, for any given domain, all gestalts can be arranged on a linear continuum so that they are physically close to the gestalts which are distant-measure-wise close. Bush [14] showed that this could not possibly be so for the domain of alphanumeric symbols. Since we have assumed a unique gestalt mechanism, we conclude that the cardinality of the GFVS cannot be one.

If the cardinality of the gestalt feature set is two, then all gestalts in a given domain can be arranged on a surface. Comparison could occur as a result of physical proximity on the cortex surface of the domain in question. There are considerable advantages to this mechanism. It will be shown later that this mechanism is the only theoretically possible one. To show this, let us continue to examine the other possibilities.

If the cardinality of the gestalt feature set is more than two, then in order to position the gestalts physically relative to their actual distances (using any known distance rule that yields distances other than one or zero), we would need an N-dimensional system where N is greater than two. For N greater than three, this is obviously impossible. For N equal to three, it becomes necessary to neurophysiologically demonstrate a system which has three-dimensional homogeneity. It has been demonstrated (Lorente de Nó [75]) neurophysiologically that the brain does not have three-dimensional homogeneity. (We have already shown that input images are probably presented as two-dimensional pictures.)

So for N greater than two, it becomes necessary to store every classified image gestalt as an N-dimensional vector. For comparison purposes, this does not theoretically present a problem. However, it will be shown that such a model appears to have two major faults. The first and most important is that it seems to be unable to learn in the manner that the human system learns. The second is that the control structure necessary to do so is not supported by any experimental neurophysiology findings. These will both be explained after the following example is presented for the purpose of understanding a feature vector storage system where N is greater than two (in this case N equals 49).

Example:

To begin with, consider a model which stores some discretized version of the low-pass two-dimensional Fourier transform of every image which is ever remembered by the brain. If we use the simplest of discretization schemes and allow for a cartesian grid with only enough resolution to differentiate the orthogonal harmonics of a three harmonic low-pass Fourier 2DDFT, then we see that we require a 49 point (seven by seven) grid:

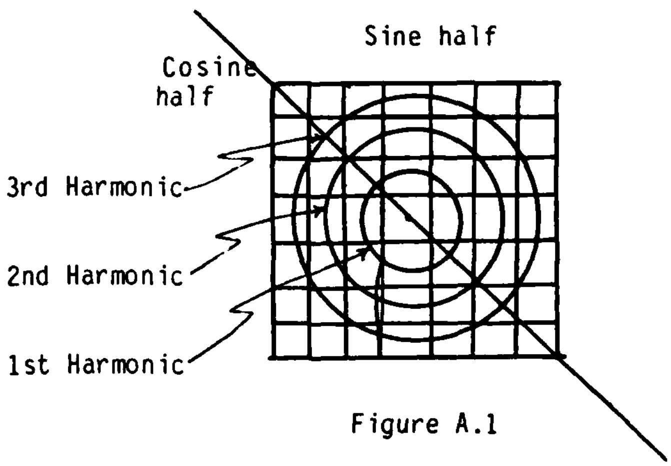

Figure A.1

Note that the cardinality of this gestalt feature set is 49. It matters not where and how these 49 samples are stored as long as they are stored in such a fashion that they can be recalled as a unit without ambiguity as to which sample represents which harmonic.

Now if we use the simplest possible distance measure, Minkowski-one distance, it becomes evident that for each newly perceived image the system (brain) must: (1) calculate its 49-sample gestalt feature vector from its two-dimensional Fourier transform, (2) propogate this 49-point feature vector to all other previously stored (remembered) 49-point feature vectors (in the domain), (3) calculate the Minkowski-one distance between all other stored feature vectors and the new one, (4) compare all the distances, and (5) identify the lowest distance (best match) and point back to the feature vector which elicited that best match. The best-matched feature vector is the name of the gestalt. It links (associations) are associated with the links of the newly acquired (and newly stored) feature vector.

So far we have not identified a control mechanism which would allow for this process of feature vector comparison. We have only stated that it must exist and must perform in the described manner -- there seems to be no alternative. (We do not yet care how long this propagation and comparison would take, so we do not yet consider a description of the propagation and comparison mechanism.) We have also not addressed the mechanism for associating the stored links of the best-matched gestalt with the newly acquired gestalt. We only state that if it is close enough (distance is less than some threshold), then at least a partial transfer of linked associations must take place or the newly stored gestalt will remain isolated and meaningless.

This is a systems description of not only the example 49-sample gestalt feature set, but of all gestalt feature sets which cannot be stored proximally in their domain space (i.e., all gestalt features sets with cardinality N greater than two).

Now that we have seen an example of how a gestalt classification and comparison system works, let us review some of the theoretical points which were quickly presented or alluded to in the foregoing example.

Since the dimension of the storage medium is two, and since we are considering all cases where the dimension of the GFVS is greater than two, it is impossible to store all gestalts so that they are physically closest to the other stored gestalts to which they are distance-measure-wise closest. This dictates that the storage order must be, at best, pseudo-random.

Since the memory of a given domain is composed of gestalts which are pseudo-randomly stored, then the gestalt of the newly classified input image must be propagated simultaneously to all previously stored gestalt_. This is required if real-time operation of the system is to occur. A mechanism to do this is conceivable.

The distance-measure must be determined at each stored gestalt location. There are too many previously stored gestalts in memory, and not enough time available, to perform the gestalt distance calculations at some central location. It is not difficult to conceive of the cortical columns being able to individually, or in small groups, perform the calculations necessary to determine the distance-measure between the stored gestalt and a new one.

Each newly calculated distance-measure must then be compared to all the other newly calculated distance-measures in order to find the stored gestalt which is closest to the newly calculated gestalt (for the input image). A mechanism to simultaneously do this is also conceivable.

So far, it has been stated that the system must simultaneously propagate the gestalt for a new input image to all stored gestalts in the domain, perform distance-measure calculations at each gestalt storage site, and simultaneously compare all the newly calculated distance measures to find the stored gestalt which is closest to the gestalt of the new input image. One can envision an architecture which can accomplish this. This is not a difficult requirement. The problem arises from the fact that the strength of the association links for gestalts which are randomly stored cannot easily satisfy the constraint $M_2 > f_1(t) + f_1(t+t_0)$. A little elaboration on this problem is in order.

Conceptually, the gestalts for various visual images are stored as follows:

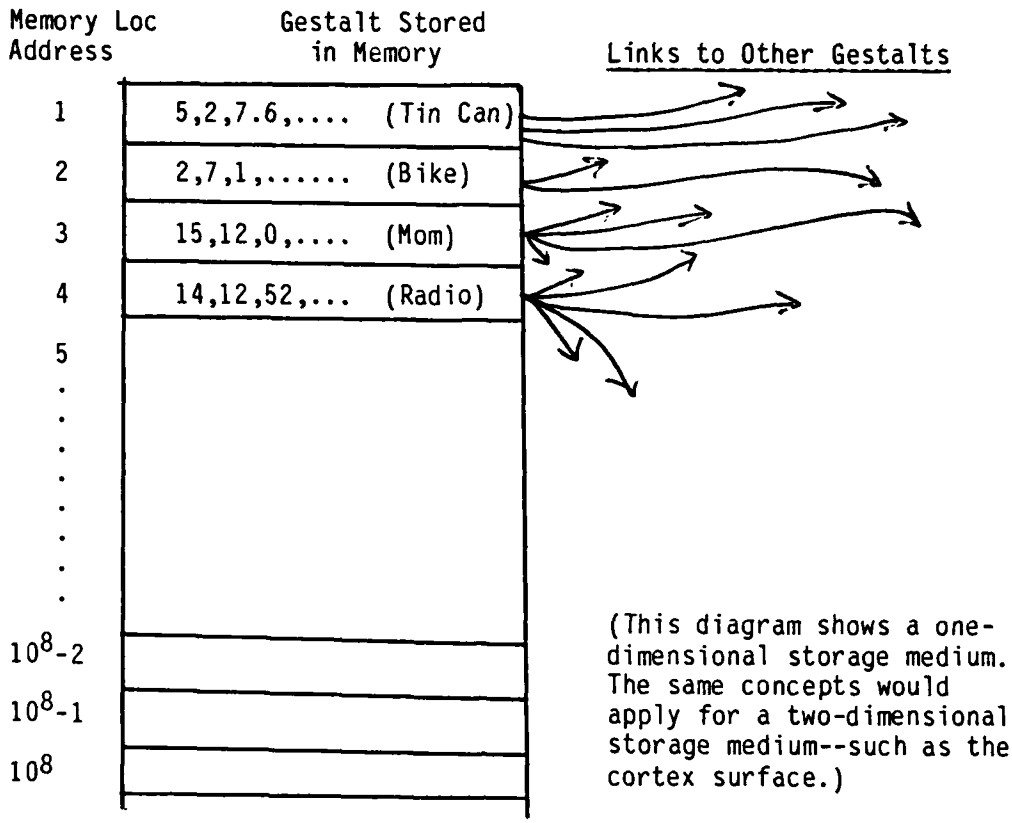
Memory Loc Address
Gestalt Stored in Memory
Links to Other Gestalts
1
5,2,7.6,.... (Tin Can)
2
2,7,1,...... (Bike)
3
15,12,0,.... (Mom)
4
14,12,52,... (Radio)
5
10^8-2
10^8-1
10^8
(This diagram shows a one-dimensional storage medium. The same concepts would apply for a two-dimensional storage medium--such as the cortex surface.)

Figure A.2

Each stored gestalt has a memory strength. This memory strength, as has already been stated, decays in time given by $M_1 = f_1(t)$.

Either each new gestalt is stored in a previously unused memory location, or it is stored on top of (not stored, just reinforces) a previously stored gestalt.

If it is the case that it gets stored on top of (not stored, just reinforces) a previously stored gestalt if the distnace measure is beneath some threshold, then the system will have discrete prototypes. The following diagram helps to illustrate this concept:

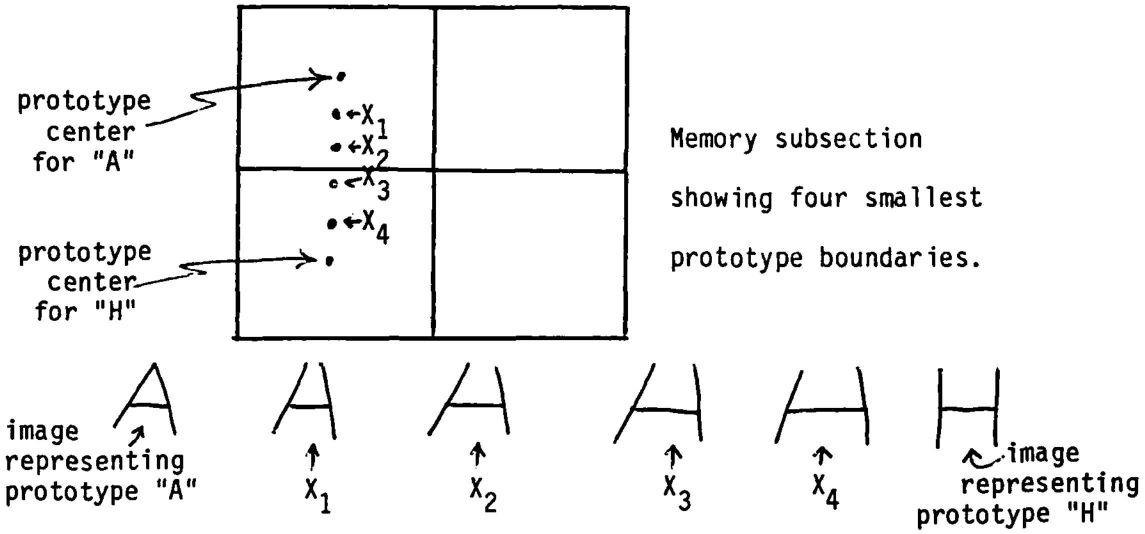

We see that X_1 and X_2 will be classified as an "A" since they are closest to the "A" prototype. Since they will not be stored, but only reinforce the strength of the memory of prototype "A", any memory of them will be lost--and along with that, any naming of them as events separate from "A". We also see that X_3 and X_4 will be classified as "H" since they are closest to the "H" prototype. Since they will not be stored, but only reinforce the strength of the memory of prototype "H", any memory of them will be lost -- and along with that, any naming of them as events separate from "H". This would dictate that sample X_2 is indistinguishable from prototype "A", and that sample X_3 is indistinguishable from prototype "H". This dictates that the X_2 sample would look as much different from the X_3 sample as the "A" prototype does from the "H" prototype. This type of predicted behavior is clearly not indicative of the human system. Therefore, the human memory system must be able to store and name all gestalts from newly observed input images.

Therefore, each new gestalt is stored in a previously unused memory location.

It has been stated that the problem with this model is that it appears that the strength of the association links for gestalts which are randomly stored cannot satisfy the constraint $M_2 > f_1(t) + f_1(t+t_0)$. We see that so far our model will allow that only the closest (distance-measure) stored gestalt will be identified. That gestalt will have some strength of memory, $M_1 = f_1(t)$. If t is very large, the strength of the memory will be significantly faded. This characteristic will elicit behavior which is extremely atypical of the human system. For example, if you look at your ten-year-old car in the driveway, and the image on your retina and primary visual cortex best matches the first image you ever saw of your car (ten years ago), regardless of the fact that there might be 52,761 other image gestalts of your car in the system, your reaction would be that you were no more familiar with that car (your car) than with any other car you saw ten years ago. In other words, you would probably not recognize it because $M_1 = f_1$ (ten years) which is a very small number. So we see that our model seems to be inadequate. There are two ways (that are apparent to this researcher) to modify the model in order to attempt to overcome this shortcoming.

The first is to find all occurrences (not just the closest) of gestalts which have distance-measures below some threshold and add their memory strengths in order to determine the familiarity of the input image. This would yield:

$$M_{input\ image} = f_1(t+t_0) + f(t+t_1) + f(t+t_2) + \ldots + f_1(t+t_n)$$

for the n gestalts in memory which lie below the acceptance threshold. This cannot work because we have observed that the following must be satisfied.

$$M_{input\ image} > f_1(t+t_0) + f(t+t_1) + f(t+t_2) + \ldots + f_1(t+t_n)$$

If we are going to use this mechanism, then we must hypothesize some combination function which performs a more complex calculation on the stored gestalt strengths in order to present the illusion that the system remembers an object better than the combined strengths of all the stored memory strengths of the observations of that object. At this point, one wants to question the validity of a model which would require such complex contortions.

The other mechanism which might be hypothesized to fix the "ten-year-old-car-problem" is to establish pointer-links between all similar stored gestalts which reinforce (increase) the strength of the memory of each gestalt. The reinforcement would be inversely proportional to the distance-measure difference between the gestalts. If gestalts are not stored physically closest to those gestalts to which they are distance-measure-wise closest, then this would seem to require the establishment of a number of links which increases exponentially with the number of gestalts in the memory. Each link would be quickly established and be capable of pointing to any location in the domain regardless of the physical distance to the extremities of the domain. Again, one wants to question the validity of a model which requires these sorts of characteristics. A similar set of requirements and objections are made when one considers the apparent requirement to establish association links for each new gestalt to the other information in other domains which make an observation relevant to the rest of the system's experience (the number of these association links also increases exponentially and must be quickly established and be able to physically span the distance of the cortex).

So we see that if we allow the cardinality of the GFVS to exceed the physical dimension of the storage medium, then it appears that we must overcome some ominous obstacles and accept some apparently difficult system performance criteria.

Let us now consider the case when the cardinality of the GFVS is two. This allows for the use of the feature vector also as the physical address on a two-dimensional storage medium. All gestalts can be stored physically closest to those gestalts to which they are distance-measure closest.

This model provides for the direct one-step trivially simple access to the stored GFVS which is most like the new GFVS. In addition, the distance measure to all stored gestalts in that domain is immediately available. If one allows for the dendritic sampling distribution hypothesized in the dissertation (see Figures 3.2 through 3.4), then each gestalt has a grade of membership (from fuzzy set theory) of all other gestalts in that domain determined by the sensitivity dictated by the shape and extent of the dendritic distribution. (In this way, the probability that any gestalt is intended to be any other gestalt is simultaneously available to all other stored gestalts.)

If we remember that these gestalt address locations are made of neurons and that they are "pointed to" by firing the appropriate synapses at that gestalt address location, and if we remember that the more a neuron synapse is used, the greater is its propensity to be used again, then we can hypothesize a chemical function which reinforces the propensity to fire across a particular synapse junction in such a way that it produces the effect stated by:

$$M_2 > f_1(t) + f_1(t+t_0).$$

If we also realize that a synapse's propensity to fire causes an increase in the propensity of an often-used gestalt location to be identified, then we see that the system will prefer to identify those gestalts which it has most often seen before -- thus accounting for the psychological phenomenon of selective perception. (See also Goldschlager's explanation of selective perception.)

If one has only seen the capital block letter "B" thousands of times, then the first exposure to the greek letter "β" will elicit the identification "B". This is because the gestalt point for β has never been used, but is very near the gestalt point for "B". As the observer is exposed to many more "β"'s, then the "β" gestalt point will have had its synapses fired so often that it will eventually be recognizable as a separate gestalt.

Notice that all the problems and complexities which were raised when the cardinality of the GFVS was larger than two, are now very simply accounted for by a system made of neurons with local neighborhood sampling functions when we allow the cardinality of GFVS to be two.

The reasonableness of simplicity, often referred to as Occam's razor, compels us to favor a system in which the cardinality of the GFVS is two, if such a system can account for the high resolution of differentiation demonstrated by the human system. The concept of using multiple windows in both space and time (as demonstrated by Figure 2.17) appears to be able to account for this high-resolution characteristic of human differentiation. Therefore, we conclude that the cardinality of human gestalt feature vector set is two.

The foregoing analysis is helpful for understanding why a Turing machine is unable to be used to produce real-time human inferencing with a large knowledge-base. The foregoing analysis suggests that the number of associational links must increase exponentially whenever the dimension of the problem space exceeds the dimension of the simulation space. Since the human knowledge-base is represented in a two-dimensional space, and since a Turing machine is a one-dimensional simulation machine, then we can use the same foregoing analysis to conclude that any Turing-machine-based simulation of a human knowledge-base increases the number of its associational links exponentially (and so also its search times) as the size of the knowledge-base increases linearly. This is exactly what experience shows. Now we can more clearly see why this is.

Appendix B

Lee's Cortical DFT Model

This appendix presents one of many theoretical alternatives to the neurophysiological mechanism presented in this dissertation for calculating the Fourier transform of an image displayed on the cortex surface. This model is an outgrowth of discussions between Dr. David Lee, Head, Department of Mathematics, Air Force Institute of Technology, and myself regarding the theoretical possibility of calculating discrete Fourier transforms given a very simple model (presented later in this appendix) of connectivity on the cortex.

Since a 2DDFT can be calculated if one has a mechanism for calculating a one-dimensional DFT and the control to apply this mechanism first to all the "rows" and then to all the "columns" of a discretized two-dimensional image, and since a 1DDFT can be thought of as being an ordered set of harmonics from D.C. to the $N/2^{nd}$ harmonic (N being the number of discretizations in the linear direction), then it is only necessary to display a mechanism which is capable of calculating any desired harmonic of a linear set, in order to demonstrate the theoretical possibility of the existence of a mechanism which is capable of calculating a 2DDFT. Lee presents such a mechanism capable of calculating any desired harmonic. The remainder of this appendix is the presentation of his mathematical model for doing so.

Lee gave it as his opinion that this work presents some examples of integral equations relevant to CTT. In his words, "The most interesting thing ... is, that characteristic frequencies (or wave numbers) occur, which may, for a given distribution of dendrites on top [layer one of the cortex], be varied continuously over broad ranges by varying a gains parameter."

D. Lee
30 Apr 84

Some Integral Equations

1. Let us re-visit Routh's cortex model in a 1-d setting:

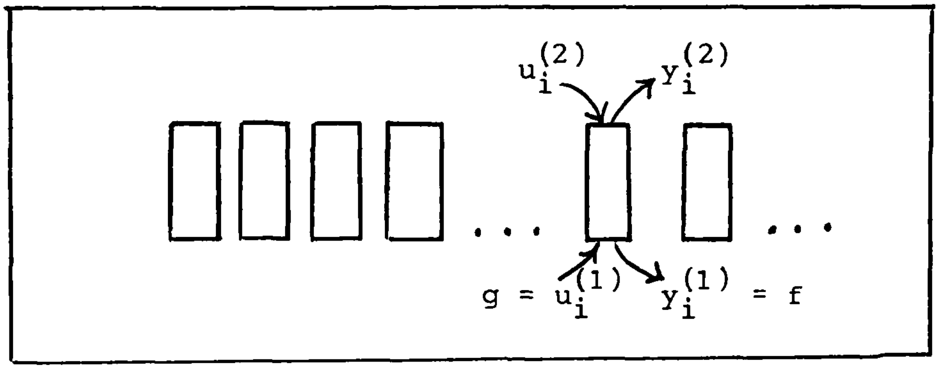

$$y_i^{(1)} = r_{11}u_i^{(1)} + r_{12}u_i^{(2)}$$

$$y_i^{(2)} = r_{21}u_i^{(1)} + r_{22}u_i^{(2)}$$

$$u_i^{(2)} = \sum_{\ell} K_{i,\ell}y_\ell^{(2)}$$

If we move to continuum model, and call $y_i^{(1)}$, f and $u_i^{(1)}$, g, we would find

$$g(x) = r_{11}f(x) + r_{12}\int_a^b K(x,z)\, y_{(z)}^{(2)}\, dz \qquad (1)$$

$$y_{(x)}^{(2)} = r_{21}f(x) + r_{22}\int_a^b K(x,z)\, y_{(z)}^{(2)}\, dz \qquad (2)$$

Where the cortex "runs" from $x = a$ to $x = b$, and $K(x,z)$ denotes the top input at x resulting from the top output at z.

From (2) we see that

$$\int_a^b K(x,z)y^{(2)}(z)dz = \frac{y^{(2)}_{(x)} - r_{21}f(x)}{r_{22}} ,$$

and then from (1) we have

$$g(x) = r_{11}f(x) + \frac{r_{12}}{r_{22}} y^{(2)}_{(x)} - \frac{r_{12}r_{21}}{r_{22}} f(x)$$

$$= (r_{11} - \frac{r_{12}r_{21}}{r_{22}}) f(x) + \frac{r_{12}}{r_{22}} y^{(2)}_{(x)} \qquad (3)$$

so that finding the cortex output $g(x)$ in terms of its input $f(x)$ amounts to finding $y^{(2)}_{(x)}$ in terms of $f(x)$, i.e., to solving

$$y^{(2)}_{(x)} = r_{21}f(x) + r_{22} \int_a^b K(x,z)\, y^{(2)}_{(z)}\, dz \qquad (2)$$

for $y^{(2)}_{(x)}$.

Let us get a notion of the behavior of this system for an <u>un-bounded</u> cortex, where

$$K(x,z) = e^{-\frac{(x-z)^2}{L^2}}$$

Then, dropping the superscript from $y^{(2)}_{(x)}$, we would have

$$y(x) = r_{21}f(x) + r_{22} \int_{-\infty}^{\infty} e^{-\frac{(x-z)^2}{L^2}}\, y_{(z)}dz \qquad (4)$$

In asking for the solution of (4), we need to ask if there are any functions $v(x)$ such that

$$v(x) = r_{22} \int_{-\infty}^{\infty} e^{-\frac{(x-z)^2}{L^2}} v(z)dz \ ; \quad v \ \underline{\text{not}} = 0. \qquad (5)$$

If there are such functions $v(x)$, then (4) does not have a unique solution, because if y_o was a solution, $y_o + v$ would be another solution.

There is another problem, too, when (5) has non-trivial solutions. Suppose that (4) <u>and</u> (5) <u>both</u> have solutions:

$$y(x) = r_{21}f(x) + r_{22} \int_{-\infty}^{\infty} e^{-\frac{(x-z)^2}{L^2}} y(z)dz$$

$$v(x) = r_{22} \int_{-\infty}^{\infty} e^{-\frac{(x-z)^2}{L^2}} y(z)dz$$

Then

$$y(x)v(x) = r_{21}f(x)v(x) + r_{22}v(x) \int_{-\infty}^{\infty} e^{-\frac{(x-z)^2}{L^2}} y(z)dz$$

$$y(x)(v(x)) = r_{22}y(x) \int_{-\infty}^{\infty} e^{-\frac{(x-z)^2}{L^2}} v(z)dz$$

$$0 = r_{21}f(x)v(x) + r_{22}\left[v(x) \int_{-\infty}^{\infty} e^{-\frac{(x-z)^2}{L^2}} y(z)dz \right.$$

$$\left. - \ y(x) \int_{-\infty}^{\infty} e^{-\frac{(x-z)^2}{L^2}} v(z)dz\right]$$

Now, let us assume $\int_{-\infty}^{\infty} f(x)v(x)dx \ \exists$, and see what its value is, also assuming that $\int_{-\infty}^{\infty}\int_{-\infty}^{\infty} e^{-\frac{(x-z)^2}{L^2}} v(x)y(z)\, dxdz \ \exists$:

$$0 = r_{21}\int_{-\infty}^{\infty} f(x)v(x)dx + r_{22}\Big[\int_{-\infty}^{\infty} v(x)\int_{-\infty}^{\infty} e^{-\frac{(x-z)^2}{L^2}} y(z)dzdx$$

$$-\int_{-\infty}^{\infty} y(x)\int_{-\infty}^{\infty} e^{-\frac{(x-z)^2}{L^2}} v(z)dzdx\Big]$$

<u>But</u> both iterated integrals are equal to the same double integral,

so $$\int_{-\infty}^{\infty} f(x)v(x)dx = 0 \qquad (6)$$

<u>That is</u>: When (5) has non-trivial solutions, the condition (6) may <u>restrict</u> the set of functions f(x) for which (4) has any solutions at all!

I claim that (5) <u>does</u> have solutions, provided $r_{22}L$ is sufficiently large.

<u>Proof</u>:

$$\int_{z=-\infty}^{\infty} e^{-\frac{(x-z)^2}{L^2}} \cos Kz\, dz \overset{u=z-x}{=} \int_{u=-\infty}^{\infty} e^{-u^2/L^2} \cos K(u+x)du$$

$$= \int_{-\infty}^{\infty} e^{-u^2/L^2} \cos Ku \cos Kxdu$$

$$= \sqrt{\pi}\, L\, e^{-\frac{K^2L^2}{4}} \cos Kx$$

So, if

$$1 = r_{22} \sqrt{\pi}\, L\, e^{-\frac{K^2L^2}{4}} \qquad (7)$$

then (5) has the solution: $v = \cos Kx$.

But (7) implies

$$K\, L = 2 \sqrt{\ell n(\sqrt{\pi} r_{22} L)} \qquad (8)$$

Thus as long as $\sqrt{\pi}\, r_{22}L > 1$,

$$v = \cos\left(\frac{2}{L} \sqrt{\ell n(\sqrt{\pi} r_{22} L)}\;\; x\right) \qquad (9)$$

solves (5).

It is worth noting that the characteristic wave number of these solutions (these eigenfunctions) is

$$K_o L = 2 \sqrt{\ell n(\sqrt{\pi} r_{22} L)}$$

which is a function of r_{22}: increasing r_{22} from $\frac{1}{\sqrt{\pi}L}$ increases K_o from 0 and, for <u>any</u> fixed L , <u>any</u> K_o can be produced, by taking r_{22} sufficiently large. (This makes me ask, "Is it possible that the density of dendritic connections, characterized by L , is uniform all right, but the 'gain' r_{22} varies to vary the critical frequency?")

A formal transfer function for (4) is easy to produce:

Let capital letters denote Fourier transforms; then

$$y(x) = r_{21}f(x) + r_{22}\int_{-\infty}^{\infty} e^{-\frac{(x-z)^2}{L^2}}\, y(z)dz \qquad (4)$$

$$\Rightarrow$$

$$Y(K) = r_{21}F_{(K)} + r_{22}\, e^{-\frac{K^2L^2}{4}}\; Y(K)\, \sqrt{\pi}L$$

or

$$Y(K) = \frac{r_{21}\; F(K)}{1 - \sqrt{\pi}\; L\; r_{22}\; e^{-\frac{K^2L^2}{4}}} \qquad (10)$$

or

$$Y(K) = r_{21}F(K) + \frac{r_{21}r_{22}\sqrt{\pi}\; L\; e^{-\frac{K^2L^2}{4}}}{1 - \sqrt{\pi}\; L\; r_{22}\; e^{-\frac{K^2L^2}{4}}}\; F(K) \qquad (11)$$

The transfer fcn of (10) has, of course, the form of the following sketch, when $\sqrt{\pi}Lr_{22} > 1$:

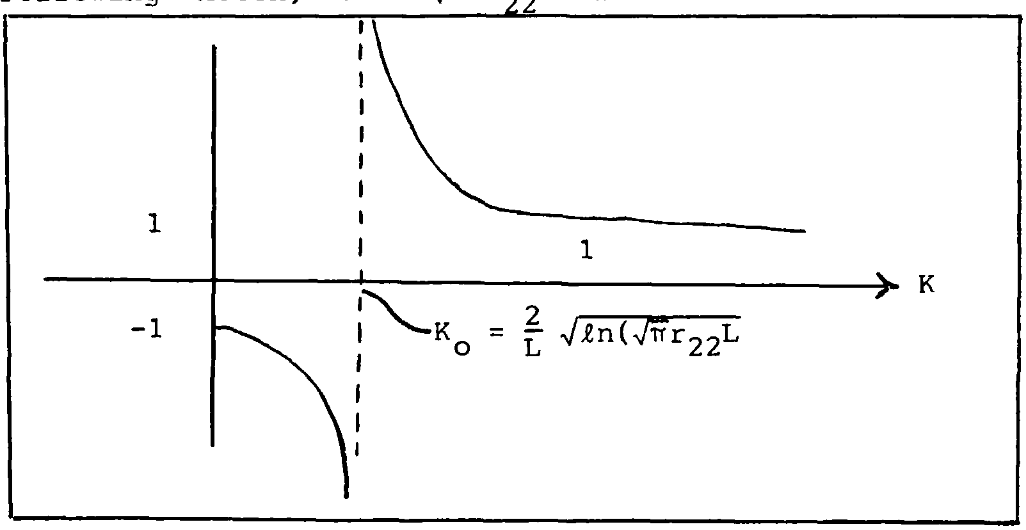

The results above are pretty robust to the exact shape of the kernel. For example, suppose that in (2),

$$K(x,z) = \left\{ L\ M_{x-L,\ 2}(z) \right\}$$

i.e. $K(x,z)$ has the following graph:

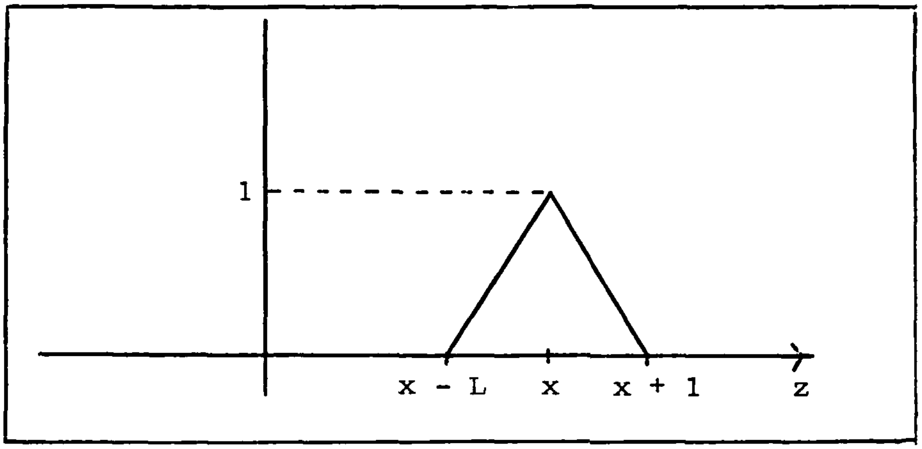

Again, we ask after eigenfunctions. Note that for this K,

$$\int_{-\infty}^{\infty} K(x,z) \cos Kz\, dz = L \int_{x-L}^{x+L} M_{x-L,\ 2}(z) \cos Kz$$

$$u = z - x$$

$$= L \int_{-L}^{L} M_{-L,2}(u) \,[\cos Ku \cos Kx$$

$$- \sin Ku \sin Kx]\, du$$

$$= L \cos Kx \int_{-L}^{L} M_{-L,2}(u) \cos Ku du$$

$$= \cos Kx \cdot \frac{L}{\frac{K^2L^2}{4}} \sin^2\left(\frac{KL}{2}\right)$$

so that $\cos Kx = V$ is an eigenfunction if

$$1 = r_{22}L \left(\frac{\sin(KL/2)}{KL/2}\right)^2 ,$$

i.e. if

$$\frac{1}{r_{22}L} = \left(\frac{\sin(KL/2)}{(KL/2)}\right)^2 \qquad (12)$$

Here again, $\cos Kx$ is an eigenfunction only if $r_{22}L$ is sufficiently large $(r_{22}L > 1)$. Critical wave-numbers follow from (12), as from this graph

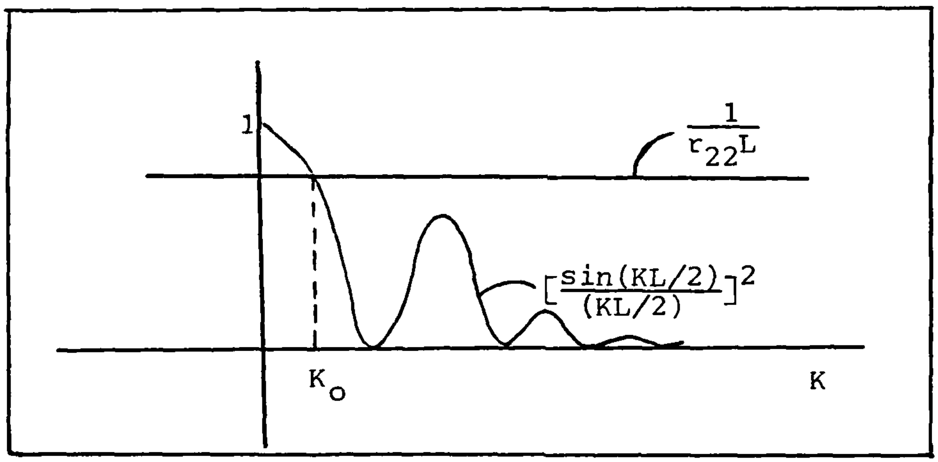

It is interesting to see that, here too <u>any</u> wave number can be made a critical wave number, by taking r_{22} sufficiently large, although the set of critical K's is more complicated than it was for the Gaussian kernel.

As a final e.g. which illustrates the effect of boundaries, let us look at

$$y = r_{21}f + r_{22} \int_o^1 K(x,z)y(z)dz \qquad (12)$$

when

$$K(x,z) = \begin{cases} z(1-x) & , \quad o \le z \le x \\ x(1-z) & , \quad x \le z \le 1 \end{cases}$$

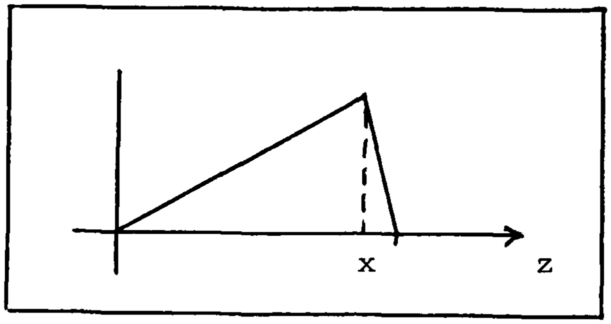

If $y = \sin n\pi x$, we have an eigenfunction if

$$1 = \frac{r_{22}}{n^2\pi^2} \quad , \quad \text{or,} \quad \frac{1}{r_{22}} = \frac{1}{n^2\pi^2} \, , \, \underline{r_{22}\ n^2\pi^2} \qquad (13)$$

Here again, r_{22} controls the proper frequencies. If we ask after a transfer function for (12):

expand all functions in $\left\{\sin n\pi x\right\}_1^\infty$

$$y = \sum_1^\infty y_i \sin i\pi x \; , \quad f = \sum_1^\infty f_i \sin i\pi x;$$

then (12)

$$y_i = r_{21}f_i + \frac{r_{22}}{n^2\pi^2} \; y_i$$

$$y_i = \frac{r_{21} f_i}{1 - \frac{r_{22}}{n^2 \pi^2}} = \frac{n^2 \pi^2 r_{21} f_i}{n^2 \pi^2 - r_{22}}$$

Thus, again, by appropriate choice of the gain, r_{22}, one can "emphasize" any desired frequency in the response.

Appendix C

Airy Disk Interference Program Listings

This appendix contains the program listings and computer generated data to support the claims made in section one of Chapter Five referring to the high frequency roll-off of the contrast sensitivity curve, due to airy disk diffraction interference, which were presented in Figure 5.5

```
cccccccccccccccccccccccccccccccccccccccccccccccccccccccccccccccccccccccc
C                                                                      C
C        PROGRAM NAME:  AIRY                                           C
C        PURPOSE:  TO COMPUTE HIGH FREQUENCY ROLL-OFF CHARACTERISTICS  C
C                  OF THE CONTRAST SENSITIVITY CURVE DUE TO AIRY DISK  C
C                  INTERFERENCE ON THE RETINA                          C
C        AUTHOR: R.L.  ROUTH                                           C
C        DATE:  25 OCT 84                                              C
C        LOAD COMMAND:  RLDR AIRY @FLIB@                               C
C                                                                      C
C        COMMENTS:                                                     C
C                                                                      C
C                 1 DEGREE =  272 7 MICRONS                            C
C                 AMPAD MEANS AMPLITUDE OF AIRY DISK (EVERY .1 MICRONS) C
C                 WVLNCC MEANS WAVELENGTH OF IMAGE IN CONES            C
C                            (1 CONE = 3 MICRONS)                      C
C                                                                      C
C                                                                      C
C                                                                      C
cccccccccccccccccccccccccccccccccccccccccccccccccccccccccccccccccccccccc

      DIMENSION ARRAY(8500),CONSEN(125),AMPAD(2000),WVLNCC(20)

      WVLNCC(1) =  120.
      WVLNCC(2) =  60.
      WVLNCC(3) =  40.
      WVLNCC(4) =  30.
      WVLNCC(5) =  24.
      WVLNCC(6) =  20.
      WVLNCC(7) =  15.
      WVLNCC(8) =  12.
      WVLNCC(9) =  10.
      WVLNCC(10) =  8.
      WVLNCC(11) =  6.
      WVLNCC(12) =  4.8
      WVLNCC(13) =  4.
      WVLNCC(14) =  3.428571
      WVLNCC(15) =  3.
      WVLNCC(16) =  2.
      WVLNCC(17) =  1.

      IENDRN = 17

      DO 5 I=1,2000
 5    AMPAD(I)=0.

      ACCEPT "ENTER LIGHT WAVELENGTH IN ANGSTRUMS (3800-7800) ",LTWVLN
        RLTWVL=LTWVLN*1.0E-10   ; RLTWVL = LIGHT WAVELENGTH IN METERS

      ACCEPT "ENTER PUPIL DIAMETER IN MILIMETERS (2-7) ",PUPDIA
        RPUPDI=PUPDIA*1.0E-3    ; RPUPDI = PUPIL DIAMETER IN METERS
```

```
        TYPE "DO YOU WANT A SHORT RUN (ENTER 4), OR A LONG RUN (ENTER 1)"
        ACCEPT "                                                > ",INITRN
        TYPE " "

        DNULL1 = 2.44*1.4E-2*RLTWVL/RPUPDI*1.0E7
             , DNULL1 = DISTANCE TO FIRST NULL OF AIRY DISK IN TENTHS OF MICRONS

        IDSTMX=3*DNULL1   ; IDSTMX IS BEYOND THIRD NULL WHERE ALL AIRY DISK
                          ; VALUES ARE ZERO.  THIS IS USED AS A SHORTCUT CHECK
                          ; IN STATEMENT 25.

        WRITE(12,2222)LTWVLN,PUPDIA,DNULL1/10.
2222    FORMAT(1X,"For LIGHT WAVELENGTH = ",I4," ANGSTRUMS, and PUPIL DIAMETER",
     &  " = ",F3.1," mm.,",/,10x," the DISTANCE to the first null of the Airy ",
     &  "disk is",F6.2," MICRONS.",///)

C   CALCULATE AIRY DISK FOR DISTANCE ALONG R-AXIS IN TENTH MICRON INTERVALS
        DO 10 I=1,1200
          X=I
          R=X/DNULL1*3.829   ; SCALES AIRY DISK SO FIRST NULL OCCURS AT
                             ;  AMPAD(DNULL1) -- DNULL1/10 MICRONS FROM CENTER
          IF(R .GT. 12.3) GO TO 10

            TIMP=(R**28/6.12037E31)-(R**30/5.87556E34)+(R**32/6.39261E37)
              IF(TIMP .GT. .5) TIMP=0.
            TUMP=-(R**22/1.60392E23)+(R**24/1.00085E26)-(R**26/7.28616E28)
            TOMP=(R**16/1.9176E15)-(R**18/6.9040E17)+(R**20/3.0377E20)
            TEMP=-(R**10/1.769472E8)+(R**12/2.9727E10)-(R**14/6.6589E12)
            TAMP=.5-(R*R/16.)+(R**4/384)-(R**6/18432.)+(R**8/1.47456E6)
            RVAR=2*(TEMP+TAMP+TOMP+TUMP+TIMP)
          AMPAD(I)=RVAR*RVAR    ,AMPAD(I)=I/IO=(2*J1(R)/R)**2
         TYPE "AMPAD(",I,")  = ",AMPAD(I)
         WRITE(12,1111)I,AMPAD(I)
1111     FORMAT(5X,"AMPAD(",I4,") = ",F10.6)
10       CONTINUE

         TYPE " "

C   WRITE NEW HEADER AT THE TOP OF A NEW PAGE
         WRITE(12,2221)
2221     FORMAT(1H1,5X)
         WRITE(12,2222)LTWVLN,PUPDIA,DNULL1/10.


         DO 100 INVFRE=INITRN,IENDRN
           W=WVLNCC(INVFRE)
           FREQ=120./W

           P2PDST=2727/FREQ   ; PEAK TO PEAK DISTANCE IN TENTHS OF MICRONS
                              ; FOR ONE CYCLE AT THIS FREQUENCY (FREQ)
                              ; ( .1 DEGREE = 2727 MICRONS, POLYAK,P.169)
           NUMPTS = P2PDST*3
           NINNUL = 9.*DNULL1                ; THIS ENSURES THAT THE MIDDLE
```

```
          IF(NUMPTS .LT. NINNUL)NUMPTS=NINNUL  ; THIRD OF THE ARRAY HAS COMP-
                                               ; LETE REPRESENTATION OF ALL
                                               ; CONTRIBUTING AIRY DISKS.

          DO 20 I=1,NUMPTS
20        ARRAY(I)=0.           ; INITIALIZE ALL ARRAY VALUES

          DO 30 IR=1,NUMPTS
            R=IR                  ; CALCULATE COSINE (OF LIGHT) AMPLITUDE FOR
            X=6.2831853*R/P2PDST  ; THE POINT WHICH  IS IR TENTH MICRONS FROM
            A=COS(X)+1.           ; LEFT EXTREME (ZERO ON R-AXIS)

            DO 30 IC=1,NUMPTS
              IDIST = ABS(IC-IR)                ; IDIST IS DISTANCE IN TENTH MIC-
25            IF(IDIST .GT. IDSTMX)GO TO 30   ; RONS FROM POINT IR TO POINT IC.
              ARRAY(IC)=ARRAY(IC)+(A*AMPAD(IDIST)) ; ARRAY(IC) IS RUNNING SUM OF
                                                   ; ALL COMPONENTS OF AIRY DISKS
                                                   ; CENTERED AT POINT IR AT ALL
                                                   ; POINTS IC.
30        CONTINUE

          AMIN=50000.
          AMAX=0
          ISTART=NUMPTS/3.333   ; ONLY CHECK MIDDLE THIRD OF ARRAY FOR MAX AND
          IEND=ISTART*2.1       ; MIN INTENSITIES (LIGHT AMPLITUDES)
          DO 40 I=ISTART,IEND
            IF(ARRAY(I) .LT. AMIN)AMIN=ARRAY(I)   ; FIND MINIMUM INTENSITY
            IF(ARRAY(I) .GT. AMAX)AMAX=ARRAY(I)   ; FIND MAXIMUM INTENSITY
40        CONTINUE

          CONSEN(INVFRE)=(AMAX-AMIN)/(AMAX+AMIN)   ; COMPUTE CONTRAST SENSITIVITY
                                                   ; FOR THIS FREQUENCY
        TYPE "FOR FREQ =",FREQ," cpd,  CONT SENS =",CONSEN(INVFRE)

100     CONTINUE


C   PRINT OUT RESULTS

        DO 220 I=INITRN,IENDRN
          W=WVLNCC(I)
          FREQ=120./W
          WRITE(12,301)FREQ,CONSEN(I)
301       FORMAT(/,5X,"FOR A SPATIAL FREQ IN CYCLES PER DEGREE OF ",
     &       F6.2,/,15X,"CONTRAST SENSITIVITY DUE TO AIRY DISK INTERFERENCE IS",
     &       F6.3)
220     CONTINUE

        END
```

For LIGHT WAVELENGTH = 5300 ANGSTRUMS, and PUPIL DIAMETER = 2.8 mm., the DISTANCE to the first null of the Airy disk is 6.47 MICRONS.

AMPAD(	1) =	.999124
AMPAD(	2) =	.996498
AMPAD(	3) =	.992136
AMPAD(	4) =	.986055
AMPAD(	5) =	.978282
AMPAD(	6) =	.968851
AMPAD(	7) =	.957804
AMPAD(	8) =	.945187
AMPAD(	9) =	.931055
AMPAD(	10) =	.915469
AMPAD(	11) =	.898496
AMPAD(	12) =	.880206
AMPAD(	13) =	.860678
AMPAD(	14) =	.839992
AMPAD(	15) =	.818235
AMPAD(	16) =	.795494
AMPAD(	17) =	.771864
AMPAD(	18) =	.747437
AMPAD(	19) =	.722312
AMPAD(	20) =	.696587
AMPAD(	21) =	.670360
AMPAD(	22) =	.643730
AMPAD(	23) =	.616798
AMPAD(	24) =	.589662
AMPAD(	25) =	.562418
AMPAD(	26) =	.535162
AMPAD(	27) =	.507987
AMPAD(	28) =	.480984
AMPAD(	29) =	.454240
AMPAD(	30) =	.427838
AMPAD(	31) =	.401858
AMPAD(	32) =	.376375
AMPAD(	33) =	.351459
AMPAD(	34) =	.327178
AMPAD(	35) =	.303590
AMPAD(	36) =	.280751
AMPAD(	37) =	.258710
AMPAD(	38) =	.237512
AMPAD(	39) =	.217195
AMPAD(	40) =	.197790
AMPAD(	41) =	.179325
AMPAD(	42) =	.161820
AMPAD(	43) =	.145291
AMPAD(	44) =	.129746
AMPAD(	45) =	.115190
AMPAD(	46) =	.101621
AMPAD(	47) =	.089033
AMPAD(	48) =	.077415
AMPAD(	49) =	.066752
AMPAD(	50) =	.057022
AMPAD(	51) =	.048201
AMPAD(	52) =	.040263
AMPAD(	53) =	.033175
AMPAD(	54) =	.026903
AMPAD(	55) =	.021410
AMPAD(	56) =	.016658
AMPAD(	57) =	.012604
AMPAD(	58) =	.009206
AMPAD(	59) =	.006419
AMPAD(	60) =	[illegible]

```
AMPAD( [illegible]) = [illegible]
AMPAD(  61) =   .002502
AMPAD(  62) =   .001279
AMPAD(  63) =   .000487
AMPAD(  64) =   .000080
AMPAD(  65) =   .000013
AMPAD(  66) =   .000244
AMPAD(  67) =   .000731
AMPAD(  68) =   .001432
AMPAD(  69) =   .002309
AMPAD(  70) =   .003325
AMPAD(  71) =   .004446
AMPAD(  72) =   .005638
AMPAD(  73) =   .006872
AMPAD(  74) =   .008120
AMPAD(  75) =   .009356
AMPAD(  76) =   .010556
AMPAD(  77) =   .011703
AMPAD(  78) =   .012777
AMPAD(  79) =   .013765
AMPAD(  80) =   .014651
AMPAD(  81) =   .015428
AMPAD(  82) =   .016087
AMPAD(  83) =   .016623
AMPAD(  84) =   .017032
AMPAD(  85) =   .017312
AMPAD(  86) =   .017465
AMPAD(  87) =   .017493
AMPAD(  88) =   .017400
AMPAD(  89) =   .017190
AMPAD(  90) =   .016871
AMPAD(  91) =   .016450
AMPAD(  92) =   .015936
AMPAD(  93) =   .015338
AMPAD(  94) =   .014667
AMPAD(  95) =   .013932
AMPAD(  96) =   .013144
AMPAD(  97) =   .012314
AMPAD(  98) =   .011454
AMPAD(  99) =   .010573
AMPAD( 100) =   .009682
AMPAD( 101) =   .008791
AMPAD( 102) =   .007909
AMPAD( 103) =   .007046
AMPAD( 104) =   .006210
AMPAD( 105) =   .005408
AMPAD( 106) =   .004647
AMPAD( 107) =   .003932
AMPAD( 108) =   .003269
AMPAD( 109) =   .002663
AMPAD( 110) =   .002117
AMPAD( 111) =   .001633
AMPAD( 112) =   .001212
AMPAD( 113) =   .000855
AMPAD( 114) =   .000563
AMPAD( 115) =   .000333
AMPAD( 116) =   .000166
AMPAD( 117) =   .000057
AMPAD( 118) =   .000006
AMPAD( 119) =   .000007
AMPAD( 120) =   .000058
AMPAD( 121) =   .000153
AMPAD( 122) =   .000289
AMPAD( 123) =   .000460
AMPAD( 124) =   .000662
AMPAD( 125) =   .000888
AMPAD( 126) =   .001124
```

```
AMPAD( 127) =    .001395
AMPAD( 128) =    .001665
AMPAD( 129) =    .001939
AMPAD( 130) =    .002213
AMPAD( 131) =    .002482
AMPAD( 132) =    .002741
AMPAD( 133) =    .002988
AMPAD( 134) =    .003218
AMPAD( 135) =    .003429
AMPAD( 136) =    .003612
AMPAD( 137) =    .003778
AMPAD( 138) =    .003913
AMPAD( 139) =    .004020
AMPAD( 140) =    .004101
AMPAD( 141) =    .004146
AMPAD( 142) =    .004166
AMPAD( 143) =    .004159
AMPAD( 144) =    .004122
AMPAD( 145) =    .004057
AMPAD( 146) =    .003968
AMPAD( 147) =    .003849
AMPAD( 148) =    .003713
AMPAD( 149) =    .003563
AMPAD( 150) =    .003387
AMPAD( 151) =    .003195
AMPAD( 152) =    .002998
AMPAD( 153) =    .002786
AMPAD( 154) =    .002567
AMPAD( 155) =    .002355
AMPAD( 156) =    .002129
AMPAD( 157) =    .001906
AMPAD( 158) =    .001694
AMPAD( 159) =    .001477
AMPAD( 160) =    .001279
AMPAD( 161) =    .001082
AMPAD( 162) =    .000903
AMPAD( 163) =    .000740
AMPAD( 164) =    .000590
AMPAD( 165) =    .000456
AMPAD( 166) =    .000340
AMPAD( 167) =    .000238
AMPAD( 168) =    .000157
AMPAD( 169) =    .000092
AMPAD( 170) =    .000045
AMPAD( 171) =    .000016
AMPAD( 172) =    .000001
AMPAD( 173) =    .000002
AMPAD( 174) =    .000018
AMPAD( 175) =    .000046
AMPAD( 176) =    .000085
AMPAD( 177) =    .000131
AMPAD( 178) =    .000196
AMPAD( 179) =    .000254
AMPAD( 180) =    .000320
AMPAD( 181) =    .000394
AMPAD( 182) =    .000465
AMPAD( 183) =    .000536
AMPAD( 184) =    .000596
AMPAD( 185) =    .000664
AMPAD( 186) =    .000727
AMPAD( 187) =    .000774
AMPAD( 188) =    .000811
AMPAD( 189) =    .000846
AMPAD( 190) =    .000865
AMPAD( 191) =    .000884
AMPAD( 19[illegible]) =    .000[illegible]
```

AMPAD(192) = [illegible]
AMPAD(193) = .000872
AMPAD(194) = .000841
AMPAD(195) = .000817
AMPAD(196) = .000766
AMPAD(197) = .000707
AMPAD(198) = .000619
AMPAD(199) = .000550
AMPAD(200) = .000467
AMPAD(201) = .000398
AMPAD(202) = .000328
AMPAD(203) = .000240
AMPAD(204) = .000160
AMPAD(205) = .000088
AMPAD(206) = .000044
AMPAD(207) = .000013

For LIGHT WAVELENGTH = 5300 ANGSTRUMS, and PUPIL DIAMETER = 2.8 mm.,
the DISTANCE to the first null of the Airy disk is 6.47 MICRONS.

FOR A SPATIAL FREQ IN CYCLES PER DEGREE OF 1.00
CONTRAST SENSITIVITY DUE TO AIRY DISK INTERFERENCE IS .998

FOR A SPATIAL FREQ IN CYCLES PER DEGREE OF 2.00
CONTRAST SENSITIVITY DUE TO AIRY DISK INTERFERENCE IS .993

FOR A SPATIAL FREQ IN CYCLES PER DEGREE OF 3.00
CONTRAST SENSITIVITY DUE TO AIRY DISK INTERFERENCE IS .984

FOR A SPATIAL FREQ IN CYCLES PER DEGREE OF 4.00
CONTRAST SENSITIVITY DUE TO AIRY DISK INTERFERENCE IS .973

FOR A SPATIAL FREQ IN CYCLES PER DEGREE OF 5.00
CONTRAST SENSITIVITY DUE TO AIRY DISK INTERFERENCE IS .959

FOR A SPATIAL FREQ IN CYCLES PER DEGREE OF 6.00
CONTRAST SENSITIVITY DUE TO AIRY DISK INTERFERENCE IS .942

FOR A SPATIAL FREQ IN CYCLES PER DEGREE OF 8.00
CONTRAST SENSITIVITY DUE TO AIRY DISK INTERFERENCE IS .902

FOR A SPATIAL FREQ IN CYCLES PER DEGREE OF 10.00
CONTRAST SENSITIVITY DUE TO AIRY DISK INTERFERENCE IS .857

FOR A SPATIAL FREQ IN CYCLES PER DEGREE OF 12.00
CONTRAST SENSITIVITY DUE TO AIRY DISK INTERFERENCE IS .809

FOR A SPATIAL FREQ IN CYCLES PER DEGREE OF 15.00
CONTRAST SENSITIVITY DUE TO AIRY DISK INTERFERENCE IS .731

FOR A SPATIAL FREQ IN CYCLES PER DEGREE OF 20.00
CONTRAST SENSITIVITY DUE TO AIRY DISK INTERFERENCE IS .591

FOR A SPATIAL FREQ IN CYCLES PER DEGREE OF 25.00
CONTRAST SENSITIVITY DUE TO AIRY DISK INTERFERENCE IS .446

FOR A SPATIAL FREQ IN CYCLES PER DEGREE OF 30.00
CONTRAST SENSITIVITY DUE TO AIRY DISK INTERFERENCE IS .309

FOR A SPATIAL FREQ IN CYCLES PER DEGREE OF 35.00
CONTRAST SENSITIVITY DUE TO AIRY DISK INTERFERENCE IS .188

FOR A SPATIAL FREQ IN CYCLES PER DEGREE OF 40.00
CONTRAST SENSITIVITY DUE TO AIRY DISK INTERFERENCE IS .087

FOR A SPATIAL FREQ IN CYCLES PER DEGREE OF 60.00
CONTRAST SENSITIVITY DUE TO AIRY DISK INTERFERENCE IS .017

FOR A SPATIAL FREQ IN CYCLES PER DEGREE OF 120.00
CONTRAST SENSITIVITY DUE TO AIRY DISK INTERFERENCE IS .018

For LIGHT WAVELENGTH = 5300 ANGSTRUMS, and PUPIL DIAMETER = 8.0 mm.,
the DISTANCE to the first null of the Airy disk is 2.26 MICRONS.

FOR A SPATIAL FREQ IN CYCLES PER DEGREE OF 4.00
CONTRAST SENSITIVITY DUE TO AIRY DISK INTERFERENCE IS .996

FOR A SPATIAL FREQ IN CYCLES PER DEGREE OF 5.00
CONTRAST SENSITIVITY DUE TO AIRY DISK INTERFERENCE IS .994

FOR A SPATIAL FREQ IN CYCLES PER DEGREE OF 6.00
CONTRAST SENSITIVITY DUE TO AIRY DISK INTERFERENCE IS .992

FOR A SPATIAL FREQ IN CYCLES PER DEGREE OF 8.00
CONTRAST SENSITIVITY DUE TO AIRY DISK INTERFERENCE IS .986

FOR A SPATIAL FREQ IN CYCLES PER DEGREE OF 10.00
CONTRAST SENSITIVITY DUE TO AIRY DISK INTERFERENCE IS .978

FOR A SPATIAL FREQ IN CYCLES PER DEGREE OF 12.00
CONTRAST SENSITIVITY DUE TO AIRY DISK INTERFERENCE IS .969

FOR A SPATIAL FREQ IN CYCLES PER DEGREE OF 15.00
CONTRAST SENSITIVITY DUE TO AIRY DISK INTERFERENCE IS .953

FOR A SPATIAL FREQ IN CYCLES PER DEGREE OF 20.00
CONTRAST SENSITIVITY DUE TO AIRY DISK INTERFERENCE IS .920

FOR A SPATIAL FREQ IN CYCLES PER DEGREE OF 25.00
CONTRAST SENSITIVITY DUE TO AIRY DISK INTERFERENCE IS .882

FOR A SPATIAL FREQ IN CYCLES PER DEGREE OF 30.00
CONTRAST SENSITIVITY DUE TO AIRY DISK INTERFERENCE IS .840

FOR A SPATIAL FREQ IN CYCLES PER DEGREE OF 35.00
CONTRAST SENSITIVITY DUE TO AIRY DISK INTERFERENCE IS .795

FOR A SPATIAL FREQ IN CYCLES PER DEGREE OF 40.00
CONTRAST SENSITIVITY DUE TO AIRY DISK INTERFERENCE IS .749

FOR A SPATIAL FREQ IN CYCLES PER DEGREE OF 60.00
CONTRAST SENSITIVITY DUE TO AIRY DISK INTERFERENCE IS .547

FOR A SPATIAL FREQ IN CYCLES PER DEGREE OF 120.00
CONTRAST SENSITIVITY DUE TO AIRY DISK INTERFERENCE IS .022

For LIGHT WAVELENGTH = 5300 ANGSTRUMS, and PUPIL DIAMETER = 7.0 mm.,
the DISTANCE to the first null of the Airy disk is 2.59 MICRONS.

FOR A SPATIAL FREQ IN CYCLES PER DEGREE OF 4.00
CONTRAST SENSITIVITY DUE TO AIRY DISK INTERFERENCE IS .995

FOR A SPATIAL FREQ IN CYCLES PER DEGREE OF 5.00
CONTRAST SENSITIVITY DUE TO AIRY DISK INTERFERENCE IS .993

FOR A SPATIAL FREQ IN CYCLES PER DEGREE OF 6.00
CONTRAST SENSITIVITY DUE TO AIRY DISK INTERFERENCE IS .990

FOR A SPATIAL FREQ IN CYCLES PER DEGREE OF 8.00
CONTRAST SENSITIVITY DUE TO AIRY DISK INTERFERENCE IS .982

FOR A SPATIAL FREQ IN CYCLES PER DEGREE OF 10.00
CONTRAST SENSITIVITY DUE TO AIRY DISK INTERFERENCE IS .972

FOR A SPATIAL FREQ IN CYCLES PER DEGREE OF 12.00
CONTRAST SENSITIVITY DUE TO AIRY DISK INTERFERENCE IS .961

FOR A SPATIAL FREQ IN CYCLES PER DEGREE OF 15.00
CONTRAST SENSITIVITY DUE TO AIRY DISK INTERFERENCE IS .940

FOR A SPATIAL FREQ IN CYCLES PER DEGREE OF 20.00
CONTRAST SENSITIVITY DUE TO AIRY DISK INTERFERENCE IS .899

FOR A SPATIAL FREQ IN CYCLES PER DEGREE OF 25.00
CONTRAST SENSITIVITY DUE TO AIRY DISK INTERFERENCE IS .853

FOR A SPATIAL FREQ IN CYCLES PER DEGREE OF 30.00
CONTRAST SENSITIVITY DUE TO AIRY DISK INTERFERENCE IS .803

FOR A SPATIAL FREQ IN CYCLES PER DEGREE OF 35.00
CONTRAST SENSITIVITY DUE TO AIRY DISK INTERFERENCE IS .750

FOR A SPATIAL FREQ IN CYCLES PER DEGREE OF 40.00
CONTRAST SENSITIVITY DUE TO AIRY DISK INTERFERENCE IS .695

FOR A SPATIAL FREQ IN CYCLES PER DEGREE OF 60.00
CONTRAST SENSITIVITY DUE TO AIRY DISK INTERFERENCE IS .460

FOR A SPATIAL FREQ IN CYCLES PER DEGREE OF 120.00
CONTRAST SENSITIVITY DUE TO AIRY DISK INTERFERENCE IS .034

For LIGHT WAVELENGTH = 5300 ANGSTRUMS, and PUPIL DIAMETER = 6.0 mm.,
the DISTANCE to the first null of the Airy disk is 3.02 MICRONS.

FOR A SPATIAL FREQ IN CYCLES PER DEGREE OF 4.00
CONTRAST SENSITIVITY DUE TO AIRY DISK INTERFERENCE IS .994

FOR A SPATIAL FREQ IN CYCLES PER DEGREE OF 5.00
CONTRAST SENSITIVITY DUE TO AIRY DISK INTERFERENCE IS .990

FOR A SPATIAL FREQ IN CYCLES PER DEGREE OF 6.00
CONTRAST SENSITIVITY DUE TO AIRY DISK INTERFERENCE IS .986

FOR A SPATIAL FREQ IN CYCLES PER DEGREE OF 8.00
CONTRAST SENSITIVITY DUE TO AIRY DISK INTERFERENCE IS .976

FOR A SPATIAL FREQ IN CYCLES PER DEGREE OF 10.00
CONTRAST SENSITIVITY DUE TO AIRY DISK INTERFERENCE IS .963

FOR A SPATIAL FREQ IN CYCLES PER DEGREE OF 12.00
CONTRAST SENSITIVITY DUE TO AIRY DISK INTERFERENCE IS .948

FOR A SPATIAL FREQ IN CYCLES PER DEGREE OF 15.00
CONTRAST SENSITIVITY DUE TO AIRY DISK INTERFERENCE IS .921

FOR A SPATIAL FREQ IN CYCLES PER DEGREE OF 20.00
CONTRAST SENSITIVITY DUE TO AIRY DISK INTERFERENCE IS .870

FOR A SPATIAL FREQ IN CYCLES PER DEGREE OF 25.00
CONTRAST SENSITIVITY DUE TO AIRY DISK INTERFERENCE IS .813

FOR A SPATIAL FREQ IN CYCLES PER DEGREE OF 30.00
CONTRAST SENSITIVITY DUE TO AIRY DISK INTERFERENCE IS .752

FOR A SPATIAL FREQ IN CYCLES PER DEGREE OF 35.00
CONTRAST SENSITIVITY DUE TO AIRY DISK INTERFERENCE IS .688

FOR A SPATIAL FREQ IN CYCLES PER DEGREE OF 40.00
CONTRAST SENSITIVITY DUE TO AIRY DISK INTERFERENCE IS .621

FOR A SPATIAL FREQ IN CYCLES PER DEGREE OF 60.00
CONTRAST SENSITIVITY DUE TO AIRY DISK INTERFERENCE IS .349

FOR A SPATIAL FREQ IN CYCLES PER DEGREE OF 120.00
CONTRAST SENSITIVITY DUE TO AIRY DISK INTERFERENCE IS .039

For LIGHT WAVELENGTH = 5300 ANGSTRUMS, and PUPIL DIAMETER = 5.0 mm., the DISTANCE to the first null of the Airy disk is 3.62 MICRONS.

FOR A SPATIAL FREQ IN CYCLES PER DEGREE OF 4.00
CONTRAST SENSITIVITY DUE TO AIRY DISK INTERFERENCE IS .991

FOR A SPATIAL FREQ IN CYCLES PER DEGREE OF 5.00
CONTRAST SENSITIVITY DUE TO AIRY DISK INTERFERENCE IS .986

FOR A SPATIAL FREQ IN CYCLES PER DEGREE OF 6.00
CONTRAST SENSITIVITY DUE TO AIRY DISK INTERFERENCE IS .980

FOR A SPATIAL FREQ IN CYCLES PER DEGREE OF 8.00
CONTRAST SENSITIVITY DUE TO AIRY DISK INTERFERENCE IS .966

FOR A SPATIAL FREQ IN CYCLES PER DEGREE OF 10.00
CONTRAST SENSITIVITY DUE TO AIRY DISK INTERFERENCE IS .948

FOR A SPATIAL FREQ IN CYCLES PER DEGREE OF 12.00
CONTRAST SENSITIVITY DUE TO AIRY DISK INTERFERENCE IS .927

FOR A SPATIAL FREQ IN CYCLES PER DEGREE OF 15.00
CONTRAST SENSITIVITY DUE TO AIRY DISK INTERFERENCE IS .892

FOR A SPATIAL FREQ IN CYCLES PER DEGREE OF 20.00
CONTRAST SENSITIVITY DUE TO AIRY DISK INTERFERENCE IS .826

FOR A SPATIAL FREQ IN CYCLES PER DEGREE OF 25.00
CONTRAST SENSITIVITY DUE TO AIRY DISK INTERFERENCE IS .754

FOR A SPATIAL FREQ IN CYCLES PER DEGREE OF 30.00
CONTRAST SENSITIVITY DUE TO AIRY DISK INTERFERENCE IS .677

FOR A SPATIAL FREQ IN CYCLES PER DEGREE OF 35.00
CONTRAST SENSITIVITY DUE TO AIRY DISK INTERFERENCE IS .597

FOR A SPATIAL FREQ IN CYCLES PER DEGREE OF 40.00
CONTRAST SENSITIVITY DUE TO AIRY DISK INTERFERENCE IS .515

FOR A SPATIAL FREQ IN CYCLES PER DEGREE OF 60.00
CONTRAST SENSITIVITY DUE TO AIRY DISK INTERFERENCE IS .209

FOR A SPATIAL FREQ IN CYCLES PER DEGREE OF 120.00
CONTRAST SENSITIVITY DUE TO AIRY DISK INTERFERENCE IS .033

For LIGHT WAVELENGTH = 5300 ANGSTRUMS, and PUPIL DIAMETER = 4.0 mm.,
the DISTANCE to the first null of the Airy disk is 4.53 MICRONS.

FOR A SPATIAL FREQ IN CYCLES PER DEGREE OF 4.00
CONTRAST SENSITIVITY DUE TO AIRY DISK INTERFERENCE IS .986

FOR A SPATIAL FREQ IN CYCLES PER DEGREE OF 5.00
CONTRAST SENSITIVITY DUE TO AIRY DISK INTERFERENCE IS .979

FOR A SPATIAL FREQ IN CYCLES PER DEGREE OF 6.00
CONTRAST SENSITIVITY DUE TO AIRY DISK INTERFERENCE IS .970

FOR A SPATIAL FREQ IN CYCLES PER DEGREE OF 8.00
CONTRAST SENSITIVITY DUE TO AIRY DISK INTERFERENCE IS .948

FOR A SPATIAL FREQ IN CYCLES PER DEGREE OF 10.00
CONTRAST SENSITIVITY DUE TO AIRY DISK INTERFERENCE IS .922

FOR A SPATIAL FREQ IN CYCLES PER DEGREE OF 12.00
CONTRAST SENSITIVITY DUE TO AIRY DISK INTERFERENCE IS .893

FOR A SPATIAL FREQ IN CYCLES PER DEGREE OF 15.00
CONTRAST SENSITIVITY DUE TO AIRY DISK INTERFERENCE IS .844

FOR A SPATIAL FREQ IN CYCLES PER DEGREE OF 20.00
CONTRAST SENSITIVITY DUE TO AIRY DISK INTERFERENCE IS .755

FOR A SPATIAL FREQ IN CYCLES PER DEGREE OF 25.00
CONTRAST SENSITIVITY DUE TO AIRY DISK INTERFERENCE IS .659

FOR A SPATIAL FREQ IN CYCLES PER DEGREE OF 30.00
CONTRAST SENSITIVITY DUE TO AIRY DISK INTERFERENCE IS .559

FOR A SPATIAL FREQ IN CYCLES PER DEGREE OF 35.00
CONTRAST SENSITIVITY DUE TO AIRY DISK INTERFERENCE IS .456

FOR A SPATIAL FREQ IN CYCLES PER DEGREE OF 40.00
CONTRAST SENSITIVITY DUE TO AIRY DISK INTERFERENCE IS .357

FOR A SPATIAL FREQ IN CYCLES PER DEGREE OF 60.00
CONTRAST SENSITIVITY DUE TO AIRY DISK INTERFERENCE IS .047

FOR A SPATIAL FREQ IN CYCLES PER DEGREE OF 120.00
CONTRAST SENSITIVITY DUE TO AIRY DISK INTERFERENCE IS .026

For LIGHT WAVELENGTH = 5300 ANGSTRUMS, and PUPIL DIAMETER = 2.0 mm.,
the DISTANCE to the first null of the Airy disk is 9.05 MICRONS.

FOR A SPATIAL FREQ IN CYCLES PER DEGREE OF 4.00
CONTRAST SENSITIVITY DUE TO AIRY DISK INTERFERENCE IS .949

FOR A SPATIAL FREQ IN CYCLES PER DEGREE OF 5.00
CONTRAST SENSITIVITY DUE TO AIRY DISK INTERFERENCE IS .923

FOR A SPATIAL FREQ IN CYCLES PER DEGREE OF 6.00
CONTRAST SENSITIVITY DUE TO AIRY DISK INTERFERENCE IS .894

FOR A SPATIAL FREQ IN CYCLES PER DEGREE OF 8.00
CONTRAST SENSITIVITY DUE TO AIRY DISK INTERFERENCE IS .829

FOR A SPATIAL FREQ IN CYCLES PER DEGREE OF 10.00
CONTRAST SENSITIVITY DUE TO AIRY DISK INTERFERENCE IS .758

FOR A SPATIAL FREQ IN CYCLES PER DEGREE OF 12.00
CONTRAST SENSITIVITY DUE TO AIRY DISK INTERFERENCE IS .683

FOR A SPATIAL FREQ IN CYCLES PER DEGREE OF 15.00
CONTRAST SENSITIVITY DUE TO AIRY DISK INTERFERENCE IS .564

FOR A SPATIAL FREQ IN CYCLES PER DEGREE OF 20.00
CONTRAST SENSITIVITY DUE TO AIRY DISK INTERFERENCE IS .366

FOR A SPATIAL FREQ IN CYCLES PER DEGREE OF 25.00
CONTRAST SENSITIVITY DUE TO AIRY DISK INTERFERENCE IS .192

FOR A SPATIAL FREQ IN CYCLES PER DEGREE OF 30.00
CONTRAST SENSITIVITY DUE TO AIRY DISK INTERFERENCE IS .059

FOR A SPATIAL FREQ IN CYCLES PER DEGREE OF 35.00
CONTRAST SENSITIVITY DUE TO AIRY DISK INTERFERENCE IS .006

FOR A SPATIAL FREQ IN CYCLES PER DEGREE OF 40.00
CONTRAST SENSITIVITY DUE TO AIRY DISK INTERFERENCE IS .013

FOR A SPATIAL FREQ IN CYCLES PER DEGREE OF 60.00
CONTRAST SENSITIVITY DUE TO AIRY DISK INTERFERENCE IS .013

FOR A SPATIAL FREQ IN CYCLES PER DEGREE OF 120.00
CONTRAST SENSITIVITY DUE TO AIRY DISK INTERFERENCE IS .013

For LIGHT WAVELENGTH = 3800 ANGSTRUMS, and PUPIL DIAMETER = 8.0 mm.,
the DISTANCE to the first null of the Airy disk is 1.62 MICRONS.

AMPAD(1) =	.986158
AMPAD(2) =	.945589
AMPAD(3) =	.881059
AMPAD(4) =	.796888
AMPAD(5) =	.698539
AMPAD(6) =	.592115
AMPAD(7) =	.483815
AMPAD(8) =	.379411
AMPAD(9) =	.283796
AMPAD(10) =	.200648
AMPAD(11) =	.132248
AMPAD(12) =	.079441
AMPAD(13) =	.041747
AMPAD(14) =	.017599
AMPAD(15) =	.004653
AMPAD(16) =	.000145
AMPAD(17) =	.001234
AMPAD(18) =	.005310
AMPAD(19) =	.010218
AMPAD(20) =	.014396
AMPAD(21) =	.016917
AMPAD(22) =	.017444
AMPAD(23) =	.016124
AMPAD(24) =	.013434
AMPAD(25) =	.010017
AMPAD(26) =	.006533
AMPAD(27) =	.003532
AMPAD(28) =	.001381
AMPAD(29) =	.000231
AMPAD(30) =	.000029
AMPAD(31) =	.000564
AMPAD(32) =	.001534
AMPAD(33) =	.002614
AMPAD(34) =	.003519
AMPAD(35) =	.004066
AMPAD(36) =	.004143
AMPAD(37) =	.003795
AMPAD(38) =	.003109
AMPAD(39) =	.002261
AMPAD(40) =	.001399
AMPAD(41) =	.000678
AMPAD(42) =	.000206
AMPAD(43) =	.000009
AMPAD(44) =	.000058
AMPAD(45) =	.000280
AMPAD(46) =	.000550
AMPAD(47) =	.000781
AMPAD(48) =	.000889
AMPAD(49) =	.000799
AMPAD(50) =	.000530
AMPAD(51) =	.000239
AMPAD(52) =	.000005

For LIGHT WAVELENGTH = 3800 ANGSTRUMS, and PUPIL DIAMETER = 8.0 mm., the DISTANCE to the first null of the Airy disk is 1.62 MICRONS.

FOR A SPATIAL FREQ IN CYCLES PER DEGREE OF 4.00
CONTRAST SENSITIVITY DUE TO AIRY DISK INTERFERENCE IS .998

FOR A SPATIAL FREQ IN CYCLES PER DEGREE OF 5.00
CONTRAST SENSITIVITY DUE TO AIRY DISK INTERFERENCE IS .997

FOR A SPATIAL FREQ IN CYCLES PER DEGREE OF 6.00
CONTRAST SENSITIVITY DUE TO AIRY DISK INTERFERENCE IS .996

FOR A SPATIAL FREQ IN CYCLES PER DEGREE OF 8.00
CONTRAST SENSITIVITY DUE TO AIRY DISK INTERFERENCE IS .993

FOR A SPATIAL FREQ IN CYCLES PER DEGREE OF 10.00
CONTRAST SENSITIVITY DUE TO AIRY DISK INTERFERENCE IS .988

FOR A SPATIAL FREQ IN CYCLES PER DEGREE OF 12.00
CONTRAST SENSITIVITY DUE TO AIRY DISK INTERFERENCE IS .983

FOR A SPATIAL FREQ IN CYCLES PER DEGREE OF 15.00
CONTRAST SENSITIVITY DUE TO AIRY DISK INTERFERENCE IS .974

FOR A SPATIAL FREQ IN CYCLES PER DEGREE OF 20.00
CONTRAST SENSITIVITY DUE TO AIRY DISK INTERFERENCE IS .956

FOR A SPATIAL FREQ IN CYCLES PER DEGREE OF 25.00
CONTRAST SENSITIVITY DUE TO AIRY DISK INTERFERENCE IS .933

FOR A SPATIAL FREQ IN CYCLES PER DEGREE OF 30.00
CONTRAST SENSITIVITY DUE TO AIRY DISK INTERFERENCE IS .907

FOR A SPATIAL FREQ IN CYCLES PER DEGREE OF 35.00
CONTRAST SENSITIVITY DUE TO AIRY DISK INTERFERENCE IS .879

FOR A SPATIAL FREQ IN CYCLES PER DEGREE OF 40.00
CONTRAST SENSITIVITY DUE TO AIRY DISK INTERFERENCE IS .848

FOR A SPATIAL FREQ IN CYCLES PER DEGREE OF 60.00
CONTRAST SENSITIVITY DUE TO AIRY DISK INTERFERENCE IS .714

FOR A SPATIAL FREQ IN CYCLES PER DEGREE OF 120.00
CONTRAST SENSITIVITY DUE TO AIRY DISK INTERFERENCE IS .267

For LIGHT WAVELENGTH = 3800 ANGSTRUMS, and PUPIL DIAMETER = 5.0 mm.,
the DISTANCE to the first null of the Airy disk is 2.60 MICRONS.

FOR A SPATIAL FREQ IN CYCLES PER DEGREE OF 4.00
CONTRAST SENSITIVITY DUE TO AIRY DISK INTERFERENCE IS .995

FOR A SPATIAL FREQ IN CYCLES PER DEGREE OF 5.00
CONTRAST SENSITIVITY DUE TO AIRY DISK INTERFERENCE IS .993

FOR A SPATIAL FREQ IN CYCLES PER DEGREE OF 6.00
CONTRAST SENSITIVITY DUE TO AIRY DISK INTERFERENCE IS .990

FOR A SPATIAL FREQ IN CYCLES PER DEGREE OF 8.00
CONTRAST SENSITIVITY DUE TO AIRY DISK INTERFERENCE IS .982

FOR A SPATIAL FREQ IN CYCLES PER DEGREE OF 10.00
CONTRAST SENSITIVITY DUE TO AIRY DISK INTERFERENCE IS .972

FOR A SPATIAL FREQ IN CYCLES PER DEGREE OF 12.00
CONTRAST SENSITIVITY DUE TO AIRY DISK INTERFERENCE IS .960

FOR A SPATIAL FREQ IN CYCLES PER DEGREE OF 15.00
CONTRAST SENSITIVITY DUE TO AIRY DISK INTERFERENCE IS .940

FOR A SPATIAL FREQ IN CYCLES PER DEGREE OF 20.00
CONTRAST SENSITIVITY DUE TO AIRY DISK INTERFERENCE IS .899

FOR A SPATIAL FREQ IN CYCLES PER DEGREE OF 25.00
CONTRAST SENSITIVITY DUE TO AIRY DISK INTERFERENCE IS .852

FOR A SPATIAL FREQ IN CYCLES PER DEGREE OF 30.00
CONTRAST SENSITIVITY DUE TO AIRY DISK INTERFERENCE IS .802

FOR A SPATIAL FREQ IN CYCLES PER DEGREE OF 35.00
CONTRAST SENSITIVITY DUE TO AIRY DISK INTERFERENCE IS .749

FOR A SPATIAL FREQ IN CYCLES PER DEGREE OF 40.00
CONTRAST SENSITIVITY DUE TO AIRY DISK INTERFERENCE IS .694

FOR A SPATIAL FREQ IN CYCLES PER DEGREE OF 60.00
CONTRAST SENSITIVITY DUE TO AIRY DISK INTERFERENCE IS .458

FOR A SPATIAL FREQ IN CYCLES PER DEGREE OF 120.00
CONTRAST SENSITIVITY DUE TO AIRY DISK INTERFERENCE IS .035

For LIGHT WAVELENGTH = 3800 ANGSTRUMS, and PUPIL DIAMETER = 2.0 mm.,
the DISTANCE to the first null of the Airy disk is 6.49 MICRONS.

FOR A SPATIAL FREQ IN CYCLES PER DEGREE OF 4.00
CONTRAST SENSITIVITY DUE TO AIRY DISK INTERFERENCE IS .973

FOR A SPATIAL FREQ IN CYCLES PER DEGREE OF 5.00
CONTRAST SENSITIVITY DUE TO AIRY DISK INTERFERENCE IS .958

FOR A SPATIAL FREQ IN CYCLES PER DEGREE OF 6.00
CONTRAST SENSITIVITY DUE TO AIRY DISK INTERFERENCE IS .941

FOR A SPATIAL FREQ IN CYCLES PER DEGREE OF 8.00
CONTRAST SENSITIVITY DUE TO AIRY DISK INTERFERENCE IS .902

FOR A SPATIAL FREQ IN CYCLES PER DEGREE OF 10.00
CONTRAST SENSITIVITY DUE TO AIRY DISK INTERFERENCE IS .856

FOR A SPATIAL FREQ IN CYCLES PER DEGREE OF 12.00
CONTRAST SENSITIVITY DUE TO AIRY DISK INTERFERENCE IS .807

FOR A SPATIAL FREQ IN CYCLES PER DEGREE OF 15.00
CONTRAST SENSITIVITY DUE TO AIRY DISK INTERFERENCE IS .729

FOR A SPATIAL FREQ IN CYCLES PER DEGREE OF 20.00
CONTRAST SENSITIVITY DUE TO AIRY DISK INTERFERENCE IS .589

FOR A SPATIAL FREQ IN CYCLES PER DEGREE OF 25.00
CONTRAST SENSITIVITY DUE TO AIRY DISK INTERFERENCE IS .444

FOR A SPATIAL FREQ IN CYCLES PER DEGREE OF 30.00
CONTRAST SENSITIVITY DUE TO AIRY DISK INTERFERENCE IS .306

FOR A SPATIAL FREQ IN CYCLES PER DEGREE OF 35.00
CONTRAST SENSITIVITY DUE TO AIRY DISK INTERFERENCE IS .185

FOR A SPATIAL FREQ IN CYCLES PER DEGREE OF 40.00
CONTRAST SENSITIVITY DUE TO AIRY DISK INTERFERENCE IS .084

FOR A SPATIAL FREQ IN CYCLES PER DEGREE OF 60.00
CONTRAST SENSITIVITY DUE TO AIRY DISK INTERFERENCE IS .017

FOR A SPATIAL FREQ IN CYCLES PER DEGREE OF 120.00
CONTRAST SENSITIVITY DUE TO AIRY DISK INTERFERENCE IS .018

For LIGHT WAVELENGTH = 7800 ANGSTRUMS, and PUPIL DIAMETER = 2.0 mm.,
the DISTANCE to the first null of the Airy disk is 13.32 MICRONS.

AMPAD(1) =	.999793
AMPAD(2) =	.999174
AMPAD(3) =	.998143
AMPAD(4) =	.996700
AMPAD(5) =	.994848
AMPAD(6) =	.992588
AMPAD(7) =	.989923
AMPAD(8) =	.986855
AMPAD(9) =	.983388
AMPAD(10) =	.979525
AMPAD(11) =	.975270
AMPAD(12) =	.970628
AMPAD(13) =	.965603
AMPAD(14) =	.960200
AMPAD(15) =	.954424
AMPAD(16) =	.948283
AMPAD(17) =	.941781
AMPAD(18) =	.934926
AMPAD(19) =	.927725
AMPAD(20) =	.920184
AMPAD(21) =	.912311
AMPAD(22) =	.904115
AMPAD(23) =	.895602
AMPAD(24) =	.886783
AMPAD(25) =	.877666
AMPAD(26) =	.868259
AMPAD(27) =	.858571
AMPAD(28) =	.848613
AMPAD(29) =	.838394
AMPAD(30) =	.827925
AMPAD(31) =	.817214
AMPAD(32) =	.806273
AMPAD(33) =	.795112
AMPAD(34) =	.783741
AMPAD(35) =	.772172
AMPAD(36) =	.760415
AMPAD(37) =	.748481
AMPAD(38) =	.736382
AMPAD(39) =	.724128
AMPAD(40) =	.711731
AMPAD(41) =	.699203
AMPAD(42) =	.686553
AMPAD(43) =	.673795
AMPAD(44) =	.660939
AMPAD(45) =	.647996
AMPAD(46) =	.634979
AMPAD(47) =	.621897
AMPAD(48) =	.608763
AMPAD(49) =	.595588
AMPAD(50) =	.582383
AMPAD(51) =	.569159
AMPAD(52) =	.555926
AMPAD(53) =	.542695
AMPAD(54) =	.529478
AMPAD(55) =	.516285
AMPAD(56) =	.503126
AMPAD(57) =	.490010
AMPAD(58) =	[illegible]

```
AMPAD(  59) =    .463952
AMPAD(  60) =    .451029
AMPAD(  61) =    .438188
AMPAD(  62) =    .425440
AMPAD(  63) =    .412793
AMPAD(  64) =    .400256
AMPAD(  65) =    .387837
AMPAD(  66) =    .375544
AMPAD(  67) =    .363386
AMPAD(  68) =    .351369
AMPAD(  69) =    .339503
AMPAD(  70) =    .327792
AMPAD(  71) =    .316245
AMPAD(  72) =    .304867
AMPAD(  73) =    .293665
AMPAD(  74) =    .282645
AMPAD(  75) =    .271812
AMPAD(  76) =    .261172
AMPAD(  77) =    .250728
AMPAD(  78) =    .240487
AMPAD(  79) =    .230453
AMPAD(  80) =    .220629
AMPAD(  81) =    .211018
AMPAD(  82) =    .201625
AMPAD(  83) =    .192452
AMPAD(  84) =    .183502
AMPAD(  85) =    .174777
AMPAD(  86) =    .166279
AMPAD(  87) =    .158011
AMPAD(  88) =    .149973
AMPAD(  89) =    .142166
AMPAD(  90) =    .134592
AMPAD(  91) =    .127251
AMPAD(  92) =    .120143
AMPAD(  93) =    .113267
AMPAD(  94) =    .106625
AMPAD(  95) =    .100214
AMPAD(  96) =    .094033
AMPAD(  97) =    .088083
AMPAD(  98) =    .082361
AMPAD(  99) =    .076866
AMPAD( 100) =    .071595
AMPAD( 101) =    .066546
AMPAD( 102) =    .061718
AMPAD( 103) =    .057107
AMPAD( 104) =    .052710
AMPAD( 105) =    .048524
AMPAD( 106) =    .044547
AMPAD( 107) =    .040774
AMPAD( 108) =    .037202
AMPAD( 109) =    .033827
AMPAD( 110) =    .030645
AMPAD( 111) =    .027652
AMPAD( 112) =    .024844
AMPAD( 113) =    .022216
AMPAD( 114) =    .019764
AMPAD( 115) =    .017483
AMPAD( 116) =    .015369
AMPAD( 117) =    .013416
AMPAD( 118) =    .011620
AMPAD( 119) =    .009975
AMPAD( 120) =    .008478
AMPAD( 121) =    .007122
AMPAD( 122) =    .005902
AMPAD( 123) =    .004814
```

```
AMPAD( 125) =     .003010
AMPAD( 126) =     .002284
AMPAD( 127) =     .001668
AMPAD( 128) =     .001158
AMPAD( 129) =     .000748
AMPAD( 130) =     .000432
AMPAD( 131) =     .000206
AMPAD( 132) =     .000065
AMPAD( 133) =     .000004
AMPAD( 134) =     .000017
AMPAD( 135) =     .000099
AMPAD( 136) =     .000247
AMPAD( 137) =     .000454
AMPAD( 138) =     .000717
AMPAD( 139) =     .001031
AMPAD( 140) =     .001391
AMPAD( 141) =     .001793
AMPAD( 142) =     .002233
AMPAD( 143) =     .002705
AMPAD( 144) =     .003208
AMPAD( 145) =     .003735
AMPAD( 146) =     .004285
AMPAD( 147) =     .004852
AMPAD( 148) =     .005434
AMPAD( 149) =     .006026
AMPAD( 150) =     .006626
AMPAD( 151) =     .007230
AMPAD( 152) =     .007836
AMPAD( 153) =     .008441
AMPAD( 154) =     .009041
AMPAD( 155) =     .009634
AMPAD( 156) =     .010218
AMPAD( 157) =     .010791
AMPAD( 158) =     .011349
AMPAD( 159) =     .011892
AMPAD( 160) =     .012417
AMPAD( 161) =     .012923
AMPAD( 162) =     .013407
AMPAD( 163) =     .013869
AMPAD( 164) =     .014307
AMPAD( 165) =     .014720
AMPAD( 166) =     .015107
AMPAD( 167) =     .015467
AMPAD( 168) =     .015798
AMPAD( 169) =     .016102
AMPAD( 170) =     .016376
AMPAD( 171) =     .016621
AMPAD( 172) =     .016835
AMPAD( 173) =     .017020
AMPAD( 174) =     .017174
AMPAD( 175) =     .017298
AMPAD( 176) =     .017393
AMPAD( 177) =     .017457
AMPAD( 178) =     .017491
AMPAD( 179) =     .017497
AMPAD( 180) =     .017473
AMPAD( 181) =     .017422
AMPAD( 182) =     .017342
AMPAD( 183) =     .017236
AMPAD( 184) =     .017105
AMPAD( 185) =     .016947
AMPAD( 186) =     .016766
AMPAD( 187) =     .016560
AMPAD( 188) =     .016332
AMPAD( 189) =     .016083
```

```
AMPAD( 191) =    .015525
AMPAD( 192) =    .015218
AMPAD( 193) =    .014894
AMPAD( 194) =    .014555
AMPAD( 195) =    .014201
AMPAD( 196) =    .013834
AMPAD( 197) =    .013454
AMPAD( 198) =    .013064
AMPAD( 199) =    .012664
AMPAD( 200) =    .012256
AMPAD( 201) =    .011840
AMPAD( 202) =    .011419
AMPAD( 203) =    .010992
AMPAD( 204) =    .010563
AMPAD( 205) =    .010131
AMPAD( 206) =    .009698
AMPAD( 207) =    .009265
AMPAD( 208) =    .008834
AMPAD( 209) =    .008403
AMPAD( 210) =    .007976
AMPAD( 211) =    .007554
AMPAD( 212) =    .007137
AMPAD( 213) =    .006726
AMPAD( 214) =    .006321
AMPAD( 215) =    .005925
AMPAD( 216) =    .005537
AMPAD( 217) =    .005159
AMPAD( 218) =    .004791
AMPAD( 219) =    .004433
AMPAD( 220) =    .004087
AMPAD( 221) =    .003753
AMPAD( 222) =    .003432
AMPAD( 223) =    .003124
AMPAD( 224) =    .002829
AMPAD( 225) =    .002547
AMPAD( 226) =    .002281
AMPAD( 227) =    .002029
AMPAD( 228) =    .001791
AMPAD( 229) =    .001568
AMPAD( 230) =    .001360
AMPAD( 231) =    .001167
AMPAD( 232) =    .000990
AMPAD( 233) =    .000828
AMPAD( 234) =    .000680
AMPAD( 235) =    .000548
AMPAD( 236) =    .000430
AMPAD( 237) =    .000328
AMPAD( 238) =    .000240
AMPAD( 239) =    .000166
AMPAD( 240) =    .000106
AMPAD( 241) =    .000060
AMPAD( 242) =    .000027
AMPAD( 243) =    .000007
AMPAD( 244) =    .000000
AMPAD( 245) =    .000005
AMPAD( 246) =    .000022
AMPAD( 247) =    .000049
AMPAD( 248) =    .000088
AMPAD( 249) =    .000137
AMPAD( 250) =    .000195
AMPAD( 251) =    .000262
AMPAD( 252) =    .000338
AMPAD( 253) =    .000422
AMPAD( 254) =    .000513
AMPAD( 255) =    .000611
```

AMPAD(257)	=	.000826
AMPAD(258)	=	.000940
AMPAD(259)	=	.001060
AMPAD(260)	=	.001183
AMPAD(261)	=	.001309
AMPAD(262)	=	.001438
AMPAD(263)	=	.001568
AMPAD(264)	=	.001701
AMPAD(265)	=	.001834
AMPAD(266)	=	.001967
AMPAD(267)	=	.002100
AMPAD(268)	=	.002233
AMPAD(269)	=	.002364
AMPAD(270)	=	.002494
AMPAD(271)	=	.002621
AMPAD(272)	=	.002746
AMPAD(273)	=	.002867
AMPAD(274)	=	.002985
AMPAD(275)	=	.003098
AMPAD(276)	=	.003208
AMPAD(277)	=	.003313
AMPAD(278)	=	.003414
AMPAD(279)	=	.003505
AMPAD(280)	=	.003596
AMPAD(281)	=	.003678
AMPAD(282)	=	.003756
AMPAD(283)	=	.003829
AMPAD(284)	=	.003893
AMPAD(285)	=	.003951
AMPAD(286)	=	.004003
AMPAD(287)	=	.004046
AMPAD(288)	=	.004088
AMPAD(289)	=	.004116
AMPAD(290)	=	.004142
AMPAD(291)	=	.004156
AMPAD(292)	=	.004166
AMPAD(293)	=	.004171
AMPAD(294)	=	.004166
AMPAD(295)	=	.004153
AMPAD(296)	=	.004134
AMPAD(297)	=	.004111
AMPAD(298)	=	.004087
AMPAD(299)	=	.004046
AMPAD(300)	=	.004004
AMPAD(301)	=	.003958
AMPAD(302)	=	.003904
AMPAD(303)	=	.003841
AMPAD(304)	=	.003780
AMPAD(305)	=	.003710
AMPAD(306)	=	.003636
AMPAD(307)	=	.003562
AMPAD(308)	=	.003476
AMPAD(309)	=	.003389
AMPAD(310)	=	.003301
AMPAD(311)	=	.003206
AMPAD(312)	=	.003106
AMPAD(313)	=	.003017
AMPAD(314)	=	.002916
AMPAD(315)	=	.002813
AMPAD(316)	=	.002712
AMPAD(317)	=	.002601
AMPAD(318)	=	.002496
AMPAD(319)	=	.002388
AMPAD(320)	=	.002282
AMPAD(321)	=	.002178

AMPAD(322)	=	.002072
AMPAD(323)	=	.001957
AMPAD(324)	=	.001851
AMPAD(325)	=	.001749
AMPAD(326)	=	.001645
AMPAD(327)	=	.001544
AMPAD(328)	=	.001440
AMPAD(329)	=	.001340
AMPAD(330)	=	.001246
AMPAD(331)	=	.001151
AMPAD(332)	=	.001058
AMPAD(333)	=	.000973
AMPAD(334)	=	.000888
AMPAD(335)	=	.000805
AMPAD(336)	=	.000726
AMPAD(337)	=	.000651
AMPAD(338)	=	.000580
AMPAD(339)	=	.000515
AMPAD(340)	=	.000453
AMPAD(341)	=	.000392
AMPAD(342)	=	.000339
AMPAD(343)	=	.000289
AMPAD(344)	=	.000241
AMPAD(345)	=	.000201
AMPAD(346)	=	.000161
AMPAD(347)	=	.000126
AMPAD(348)	=	.000096
AMPAD(349)	=	.000071
AMPAD(350)	=	.000050
AMPAD(351)	=	.000033
AMPAD(352)	=	.000019
AMPAD(353)	=	.000008
AMPAD(354)	=	.000003
AMPAD(355)	=	.000000
AMPAD(356)	=	.000001
AMPAD(357)	=	.000005
AMPAD(358)	=	.000013
AMPAD(359)	=	.000023
AMPAD(360)	=	.000037
AMPAD(361)	=	.000054
AMPAD(362)	=	.000073
AMPAD(363)	=	.000095
AMPAD(364)	=	.000116
AMPAD(365)	=	.000141
AMPAD(366)	=	.000173
AMPAD(367)	=	.000201
AMPAD(368)	=	.000232
AMPAD(369)	=	.000263
AMPAD(370)	=	.000294
AMPAD(371)	=	.000329
AMPAD(372)	=	.000358
AMPAD(373)	=	.000396
AMPAD(374)	=	.000433
AMPAD(375)	=	.000462
AMPAD(376)	=	.000502
AMPAD(377)	=	.000536
AMPAD(378)	=	.000566
AMPAD(379)	=	.000600
AMPAD(380)	=	.000637
AMPAD(381)	=	.000667
AMPAD(382)	=	.000692
AMPAD(383)	=	.000722
AMPAD(384)	=	.000749
AMPAD(385)	=	.000772
AMPAD(386)	=	.000795
AMPAD(387)	=	.000808

```
AMPAD( 388) =     .000851
AMPAD( 389) =     .000845
AMPAD( 390) =     .000854
AMPAD( 391) =     .000866
AMPAD( 392) =     .000879
AMPAD( 393) =     .000879
AMPAD( 394) =     .000885
AMPAD( 395) =     .000880
AMPAD( 396) =     .000880
AMPAD( 397) =     .000883
AMPAD( 398) =     .000877
AMPAD( 399) =     .000851
AMPAD( 400) =     .000850
AMPAD( 401) =     .000812
AMPAD( 402) =     .000808
AMPAD( 403) =     .000771
AMPAD( 404) =     .000756
AMPAD( 405) =     .000725
AMPAD( 406) =     .000688
AMPAD( 407) =     .000657
AMPAD( 408) =     .000627
AMPAD( 409) =     .000596
AMPAD( 410) =     .000552
AMPAD( 411) =     .000526
AMPAD( 412) =     .000490
AMPAD( 413) =     .000471
AMPAD( 414) =     .000423
AMPAD( 415) =     .000371
AMPAD( 416) =     .000326
AMPAD( 417) =     .000310
AMPAD( 418) =     .000268
AMPAD( 419) =     .000213
AMPAD( 420) =     .000160
AMPAD( 421) =     .000125
AMPAD( 422) =     .000097
AMPAD( 423) =     .000072
AMPAD( 424) =     .000042
AMPAD( 425) =     .000034
AMPAD( 426) =     .000016
AMPAD( 427) =     .000006
```

For LIGHT WAVELENGTH = 7800 ANGSTRUMS, and PUPIL DIAMETER = 8.0 mm.,
the DISTANCE to the first null of the Airy disk is 3.33 MICRONS.

FOR A SPATIAL FREQ IN CYCLES PER DEGREE OF 4.00
CONTRAST SENSITIVITY DUE TO AIRY DISK INTERFERENCE IS .992

FOR A SPATIAL FREQ IN CYCLES PER DEGREE OF 5.00
CONTRAST SENSITIVITY DUE TO AIRY DISK INTERFERENCE IS .988

FOR A SPATIAL FREQ IN CYCLES PER DEGREE OF 6.00
CONTRAST SENSITIVITY DUE TO AIRY DISK INTERFERENCE IS .983

FOR A SPATIAL FREQ IN CYCLES PER DEGREE OF 8.00
CONTRAST SENSITIVITY DUE TO AIRY DISK INTERFERENCE IS .971

FOR A SPATIAL FREQ IN CYCLES PER DEGREE OF 10.00
CONTRAST SENSITIVITY DUE TO AIRY DISK INTERFERENCE IS .955

FOR A SPATIAL FREQ IN CYCLES PER DEGREE OF 12.00
CONTRAST SENSITIVITY DUE TO AIRY DISK INTERFERENCE IS .937

FOR A SPATIAL FREQ IN CYCLES PER DEGREE OF 15.00
CONTRAST SENSITIVITY DUE TO AIRY DISK INTERFERENCE IS .906

FOR A SPATIAL FREQ IN CYCLES PER DEGREE OF 20.00
CONTRAST SENSITIVITY DUE TO AIRY DISK INTERFERENCE IS .847

FOR A SPATIAL FREQ IN CYCLES PER DEGREE OF 25.00
CONTRAST SENSITIVITY DUE TO AIRY DISK INTERFERENCE IS .782

FOR A SPATIAL FREQ IN CYCLES PER DEGREE OF 30.00
CONTRAST SENSITIVITY DUE TO AIRY DISK INTERFERENCE IS .714

FOR A SPATIAL FREQ IN CYCLES PER DEGREE OF 35.00
CONTRAST SENSITIVITY DUE TO AIRY DISK INTERFERENCE IS .641

FOR A SPATIAL FREQ IN CYCLES PER DEGREE OF 40.00
CONTRAST SENSITIVITY DUE TO AIRY DISK INTERFERENCE IS .566

FOR A SPATIAL FREQ IN CYCLES PER DEGREE OF 60.00
CONTRAST SENSITIVITY DUE TO AIRY DISK INTERFERENCE IS .274

FOR A SPATIAL FREQ IN CYCLES PER DEGREE OF 120.00
CONTRAST SENSITIVITY DUE TO AIRY DISK INTERFERENCE IS .035

For LIGHT WAVELENGTH = 7800 ANGSTRUMS, and PUPIL DIAMETER = 2.0 mm.,
the DISTANCE to the first null of the Airy disk is 13.32 MICRONS.

FOR A SPATIAL FREQ IN CYCLES PER DEGREE OF 4.00
CONTRAST SENSITIVITY DUE TO AIRY DISK INTERFERENCE IS .898

FOR A SPATIAL FREQ IN CYCLES PER DEGREE OF 5.00
CONTRAST SENSITIVITY DUE TO AIRY DISK INTERFERENCE IS .851

FOR A SPATIAL FREQ IN CYCLES PER DEGREE OF 6.00
CONTRAST SENSITIVITY DUE TO AIRY DISK INTERFERENCE IS .801

FOR A SPATIAL FREQ IN CYCLES PER DEGREE OF 8.00
CONTRAST SENSITIVITY DUE TO AIRY DISK INTERFERENCE IS .693

FOR A SPATIAL FREQ IN CYCLES PER DEGREE OF 10.00
CONTRAST SENSITIVITY DUE TO AIRY DISK INTERFERENCE IS .577

FOR A SPATIAL FREQ IN CYCLES PER DEGREE OF 12.00
CONTRAST SENSITIVITY DUE TO AIRY DISK INTERFERENCE IS .459

FOR A SPATIAL FREQ IN CYCLES PER DEGREE OF 15.00
CONTRAST SENSITIVITY DUE TO AIRY DISK INTERFERENCE IS .293

FOR A SPATIAL FREQ IN CYCLES PER DEGREE OF 20.00
CONTRAST SENSITIVITY DUE TO AIRY DISK INTERFERENCE IS .075

FOR A SPATIAL FREQ IN CYCLES PER DEGREE OF 25.00
CONTRAST SENSITIVITY DUE TO AIRY DISK INTERFERENCE IS .009

FOR A SPATIAL FREQ IN CYCLES PER DEGREE OF 30.00
CONTRAST SENSITIVITY DUE TO AIRY DISK INTERFERENCE IS .008

FOR A SPATIAL FREQ IN CYCLES PER DEGREE OF 35.00
CONTRAST SENSITIVITY DUE TO AIRY DISK INTERFERENCE IS .008

FOR A SPATIAL FREQ IN CYCLES PER DEGREE OF 40.00
CONTRAST SENSITIVITY DUE TO AIRY DISK INTERFERENCE IS .009

FOR A SPATIAL FREQ IN CYCLES PER DEGREE OF 60.00
CONTRAST SENSITIVITY DUE TO AIRY DISK INTERFERENCE IS .009

FOR A SPATIAL FREQ IN CYCLES PER DEGREE OF 120.00
CONTRAST SENSITIVITY DUE TO AIRY DISK INTERFERENCE IS .009

Appendix D

Dendritic Distribution Calculation Program Listings

This appendix is organized into two sections. The first section contains the listings of the program which was used to find the high frequency roll-off due to the statistically averaged retinal distribution. Applicable computer generated results are also included. This first section presents the retinal distributions required to both: (1) completely account for the nervous system component of the high-frequency roll-off of the contrast sensitivity curve, and (2) account for half of this component.

The second section of this appendix contains the listing of the program that was used to calculate the dendritic distribution of layer one of the primary visual cortex which would account for the other half of the high frequency roll-off of the nervous system component of the contrast sensitivity curve.

The retinal distribution which completely accounts for the high-frequency roll-off of the contrast sensitivity curve can be seen from the computer run results to be approximately:

$$D(x) = \exp\left(-(X/2.2)^2\right). \qquad \text{(D-1)}$$

The dendritic distribution which accounts for half of this effect can be seen from the computer run results to be approximately:

$$D(x) = \exp\left(-|X|/.9\right). \qquad \text{(D-2)}$$

```
CCCCCCCCCCCCCCCCCCCCCCCCCCCCCCCCCCCCCCCCCCCCCCCCCCCCCCCCCCCCCCCCCCCCCCCCCC
C                                                                        C
C       PROGRAM NAME:  RETDIS                                            C
C       PURPOSE:  TO COMPUTE HIGH FREQUENCY ROLL-OFF CHARACTERISTICS     C
C              OF THE CONTRAST SENSITIVITY CURVE DUE TO THE RETINAL      C
C              DISTRIBUTION OF REGIONAL SENSITIVITY.                     C
C       AUTHOR: R.L. ROUTH                                               C
C       DATE:  03 NOV 84                                                 C
C       LOAD COMMAND:  RLDR RETDIS @FLIB@                                C
C                                                                        C
C       COMMENTS:                                                        C
C                                                                        C
C               100 CENTICONES=1 CONE DIAMETER                           C
C               AMPDD MEANS AMPLITUDE OF AVERAGING FUNCTION ON THE       C
C                     RETINA SURFACE DUE TO THE RETINAL DISTRIBUTION     C
C                     OF REGIONAL SENSITIVITES.                          C
C                                                                        C
C                                                                        C
C                                                                        C
CCCCCCCCCCCCCCCCCCCCCCCCCCCCCCCCCCCCCCCCCCCCCCCCCCCCCCCCCCCCCCCCCCCCCCCCCC

        DIMENSION ARRAY(10000),CONSEN(125),AMPDD(2000),WVLNCC(20)

CCCCCCCCCCCCCCCCCCCCCCCCCCCCCCCCCCCCCCCCCCCCCCCCCCCCCCCCCCCCCCCCCCCCCCCCCC
C
C  INITIALIZE ARRAY VARIABLES
C
CCCCCCCCCCCCCCCCCCCCCCCCCCCCCCCCCCCCCCCCCCCCCCCCCCCCCCCCCCCCCCCCCCCCCCCCCC
        DO 1001 I=1,10000
          ARRAY(I)=0.
1001    CONTINUE
        DO 1002 I=1,125
          CONSEN(I)=0.
1002    CONTINUE
        DO 1003 I=1,2000
          AMPDD(I)=0.
1003    CONTINUE
        DO 1004 I=1,20
          WVLNCC(I)=0.
1004    CONTINUE

        WVLNCC(1) = 120.
        WVLNCC(2) =  60.
        WVLNCC(3) =  40.
        WVLNCC(4) =  30.
        WVLNCC(5) =  24.
        WVLNCC(6) =  20.
        WVLNCC(7) =  15.
        WVLNCC(8) =  12.
        WVLNCC(9) =  10.
        WVLNCC(10) =  8.
        WVLNCC(11) =  6.
```

```
        WVLNCC(12) =  4.8
        WVLNCC(13) =  4.
        WVLNCC(14) =  3.428571
        WVLNCC(15) =  3.
        WVLNCC(16) =  2.
        WVLNCC(17) =  1.


        DO 5 I=1,2000
5       AMPDD(I)=0.


CCCCCCCCCCCCCCCCCCCCCCCCCCCCCCCCCCCCCCCCCCCCCCCCCCCCCCCCCCCCCC
C
C  INPUT USER DESIGNATED PARAMETERS
C
CCCCCCCCCCCCCCCCCCCCCCCCCCCCCCCCCCCCCCCCCCCCCCCCCCCCCCCCCCCCCC
        ACCEPT "ENTER THE SCALING DIVIDER FOR EXPONENT ",S

        ACCEPT "ENTER EXPONENT OF EXPONENT ",XPONNT

        TYPE "DO YOU WANT A SHORT RUN (ENTER 8) OR A LONG RUN (ENTER 1) "
        ACCEPT "                                                      > ",INITRN
        TYPE " "

        TYPE "DO YOU WANT TO SEND THE RETINAL DISTRIBUTION TO THE PRINTER?"
        ACCEPT "                              (1-YES;   0-NO)    > ",XPRINT

        IENDRN = 17
        IF(INITRN .GT. 7)IENDRN=12

        TYPE "COMPUTE ONLY AT CONE CENTERS (ENTER 100) OR CONTINUOUSLY "
        ACCEPT "                                         (ENTER 1)   > ",INCALC



        IF(XPRINT .GE. .5)WRITE(12,2222)S,XPONNT



C   CALCULATE DISTRIBUTION FOR DISTANCE ALONG R-AXIS IN CENTICONE INTERVALS

        IDSTE =0
        DO 10 I=1,1999
          IF(IDSTE .GT. 1)GO TO 10
          X=I
          AMPDD(I)=EXP(-(X/S)**XPONNT)
        TYPE "AMPDD(",I,")  = ",AMPDD(I)
        IF(XPRINT .GE. .5)WRITE(12,1111)I,AMPDD(I)
        IF(AMPDD(I) .LT. .0000001)IDSTE=I
1111    FORMAT(5X,"AMPDD(",I4,") = ",F11.8)
10      CONTINUE
        IF(IDSTE .LT. 1)IDSTE=1999
        IDSTMX = IDSTE *4
```

```
C       WRITE(12,5555)(AMPDD(I),I=1,2000)
5555    FORMAT(1X,10F12.8)


        DO 100 INVFRE=INITRN,IENDRN
          W=WVLNCC(INVFRE)
          FREQ=120./W
          P2PDST=12000/FREQ  ; PEAK TO PEAK DISTANCE IN CENTICONES FOR ONE CYCLE
                             ; AT THIS FREQUENCY(FREQ) (1 CONE = 100 CENTICONES)
          NUMPTS = P2PDST*4
          IF(NUMPTS .LT. IDSTMX)NUMPTS=IDSTMX
          IF(NUMPTS .LT. 10000)GO TO 19
          TYPE " "
          TYPE "*******************************************************"
          TYPE "*******************************************************"
          TYPE " "
          TYPE "FREQ =",FREQ,",  NUMPTS (MUST BE LESS THAN 10000) =",NUMPTS
          TYPE "NUMPTS HAS EXCEDED BOUNDS.  NUMPTS NOW = 9999. "
          NUMPTS = 9999
          TYPE "***  ANSWERS MAY NOT BE RIGHT  ***"
          TYPE " "
          TYPE "*******************************************************"
          TYPE "*******************************************************"
          TYPE " "
19        CONTINUE

CCCCCCCCCCCCCCCCCCCCCCCCCCCCCCCCCCCCCCCCCCCCCCCCCCCCCCCCCCCCCCCC
C
C  SET UP OUTPUT COPY HEADERS
C
CCCCCCCCCCCCCCCCCCCCCCCCCCCCCCCCCCCCCCCCCCCCCCCCCCCCCCCCCCCCCCCC
        IF(XPRINT .GE. .5)WRITE(12,3331)
3331    FORMAT(1X,"**********************************************",/,1H1)
        IF(XPRINT .GE. .5)WRITE(12,3332)FREQ
3332    FORMAT(1X,"***************************  FOR FREQ =",F10.6,/////////////)
3333    FORMAT(1X,20F6.3)


CCCCCCCCCCCCCCCCCCCCCCCCCCCCCCCCCCCCCCCCCCCCCCCCCCCCCCCCCCCCCCCC
C
C   BEGIN CORTEX RESOLUTION CALCULATIONS
C
CCCCCCCCCCCCCCCCCCCCCCCCCCCCCCCCCCCCCCCCCCCCCCCCCCCCCCCCCCCCCCCC
          DO 30 IR=1,NUMPTS,INCALC
            R=IR                   ; CALCULATE COSINE (OF LIGHT) AMPLITUDE FOR
            X=6.2831853*R/P2PDST   ; THE POINT WHICH  IS IR CENTICONES FROM
            A=COS(X)+1.            ; LEFT EXTREME (ZERO ON R-AXIS)

            DO 30 IC=1,NUMPTS
              IDIST = ABS(IC-IR)              ; IDIST IS DISTANCE IN CENTICONES
25            IF(IDIST .GT. IDSTE) GO TO 30   ; FROM POINT IR TO POINT IC.
```

```
                ARRAY(IC) = ARRAY(IC)+(A*AMPDD(IDIST)) ; ARRAY(IC) IS RUNNING SUM
                                                 ; OF ALL COMPONENTS OF AIRY DISKS
                                                 ; CENTERED AT POINT IR AT ALL POINTS IC.
30          CONTINUE

            AMIN=50000.
            AMAX=0.
            ISTART=NUMPTS/3.333  ; ONLY CHECK MIDDLE THIRD OF ARRAY FOR MAX AND
            IEND=ISTART*2.1      ; MIN INTENSITIES (LIGHT AMPLITUDES)
            DO 40 I=ISTART,IEND
              IF(ARRAY(I) .LT. AMIN)AMIN=ARRAY(I)   ; FIND MINIMUM INTENSITY
              IF(ARRAY(I) .GT. AMAX)AMAX=ARRAY(I)   ; FIND MAXIMUM INTENSITY
40          CONTINUE
          WRITE(12,3334)ISTART,IEND,NUMPTS
3334      FORMAT(16X,3I10)
          IF(XPRINT .GE. .5)WRITE(12,3333)(ARRAY(I),I=ISTART,IEND)


            CONSEN(INVFRE)=(AMAX-AMIN)/(AMAX+AMIN)   ; COMPUTE CONTRAST SENSITIVTY
                                                     ; FOR THIS FREQUENCY
          TYPE "FOR FREQ =",FREQ," cpd,  THE CONT SENS =",CONSEN(INVFRE)

100       CONTINUE


CCCCCCCCCCCCCCCCCCCCCCCCCCCCCCCCCCCCCCCCCCCCCCCCCCCCCCCCCCCCCCCCCCCC
C
C   PRINT OUT RESULTS
C
CCCCCCCCCCCCCCCCCCCCCCCCCCCCCCCCCCCCCCCCCCCCCCCCCCCCCCCCCCCCCCCCCCCC

C   WRITE NEW HEADER AT THE TOP OF A NEW PAGE
          WRITE(12,2221)
2221      FORMAT(1H1,5X,///,5x)
          WRITE(12,2222)S,XPONNT
2222      FORMAT(11X,"For EXPONENT DIVISOR =",F10.4," and an EXPONENT TO THE ",
     &           "EXPONENT =",F7.4)
          WRITE(12,2223)INCALC
2223      FORMAT(30X,"and the intensity of the sine image recomputed at ",
     &           "INTERVALS of",I4," centicones :",////)

          DO 220 I=INITRN,IENDRN
            W=WVLNCC(I)
            FREQ=120./W
            WRITE(12,301)FREQ,CONSEN(I)
301         FORMAT(/,5X,"FOR A SPATIAL FREQ IN CYCLES PER DEGREE OF ",
     &        F6.2,/,15X,"CONTRAST SENSITIVITY DUE TO RETINAL AVERAGING =",F6.3)
220       CONTINUE

          END
```

```
CCCCCCCCCCCCCCCCCCCCCCCCCCCCCCCCCCCCCCCCCCCCCCCCCCCCCCCCCCCCCCCCCCCCCCC
C                                                                     C
C       PROGRAM NAME:  DENDIS                                         C
C       PURPOSE:  TO COMPUTE HIGH FREQUENCY ROLL-OFF CHARACTERISTICS  C
C              OF THE CONTRAST SENSITIVITY CURVE DUE TO THE DENDRITIC C
C              DISTRIBUTION IN LAYER ONE OF THE STRIATE CORTEX.       C
C       AUTHOR: R.L. ROUTH                                            C
C       DATE:  03 NOV 84                                              C
C       LOAD COMMAND:  RLDR DENDIS @FLIB@                             C
C                                                                     C
C       COMMENTS:                                                     C
C                                                                     C
C               1 COCO = 100 MICRONS                                  C
C               AMPDD MEANS AMPLITUDE OF AVERAGING FUNCTION ON THE    C
C                     CORTEX SURFACE DUE TO THE DENDRITIC DISTRIBUTION C
C                                                                     C
C                                                                     C
C                                                                     C
C                                                                     C
CCCCCCCCCCCCCCCCCCCCCCCCCCCCCCCCCCCCCCCCCCCCCCCCCCCCCCCCCCCCCCCCCCCCCCC

        DIMENSION ARRAY(10000),CONSEN(125),AMPDD(2000),WVLNCC(20)

CCCCCCCCCCCCCCCCCCCCCCCCCCCCCCCCCCCCCCCCCCCCCCCCCCCCCCCCCCCCCCCCCCCCCCC
C
C  INITIALIZE ARRAY VARIABLES
C
CCCCCCCCCCCCCCCCCCCCCCCCCCCCCCCCCCCCCCCCCCCCCCCCCCCCCCCCCCCCCCCCCCCCCCC
        DO 1001 I=1,10000
          ARRAY(I)=0.
1001    CONTINUE
        DO 1002 I=1,125
          CONSEN(I)=0.
1002    CONTINUE
        DO 1003 I=1,2000
          AMPDD(I)=0.
1003    CONTINUE
        DO 1004 I=1,20
          WVLNCC(I)=0.
1004    CONTINUE

        WVLNCC(1) = 120.
        WVLNCC(2) =  60.
        WVLNCC(3) =  40.
        WVLNCC(4) =  30.
        WVLNCC(5) =  24.
        WVLNCC(6) =  20.
        WVLNCC(7) =  15.
        WVLNCC(8) =  12.
        WVLNCC(9) =  10.
        WVLNCC(10) =  8.
        WVLNCC(11) =  6.
```

```
        WVLNCC(12) =  4.8
        WVLNCC(13) =  4.
        WVLNCC(14) =  3.428571
        WVLNCC(15) =  3.
        WVLNCC(16) =  2.
        WVLNCC(17) =  1.


        DO 5 I=1,2000
5       AMPDD(I)=0.


CCCCCCCCCCCCCCCCCCCCCCCCCCCCCCCCCCCCCCCCCCCCCCCCCCCCCCCCCCCCCCCC
C
C  INPUT USER DESIGNATED PARAMETERS
C
CCCCCCCCCCCCCCCCCCCCCCCCCCCCCCCCCCCCCCCCCCCCCCCCCCCCCCCCCCCCCCCC
        ACCEPT "ENTER THE SCALING DIVIDER FOR EXPONENT ",S

        ACCEPT "ENTER EXPONENT OF EXPONENT ",XPONNT

        TYPE "DO YOU WANT A SHORT RUN (ENTER 8) OR A LONG RUN (ENTER 1) "
        ACCEPT "                                                  > ",INITRN
        TYPE " "

        TYPE "DO YOU WANT TO SEND THE DENDRITIC DISTRIBUTION TO THE PRINTER?"
        ACCEPT "                                   (1-YES;   0-NO)    > ",XPRINT

        IENDRN = 17
        IF(INITRN .GT. 7)IENDRN=12

        TYPE "COMPUTE ONLY AT COCO CENTERS (ENTER 100) OR CONTINUOUSLY "
        ACCEPT "                                           (ENTER 1)  > ",INCALC



        IF(XPRINT .GE. .5)WRITE(12,2222)S,XPONNT



C   CALCULATE DISTRIBUTION FOR DISTANCE ALONG R-AXIS IN MICRON INTERVALS

        IDSTE =0
        DO 10 I=1,1999
          IF(IDSTE .GT. 1)GO TO 10
          X=I
          AMPDD(I)=EXP(-(X/S)**XPONNT)
        TYPE "AMPDD(",I,")  = ",AMPDD(I)
        IF(XPRINT .GE. .5)WRITE(12,1111)I,AMPDD(I)
        IF(AMPDD(I) .LT. .0000001)IDSTE=I
1111    FORMAT(5X,"AMPDD(",I4,") = ",F11.8)
10      CONTINUE
        IF(IDSTE .LT. 1)IDSTE=1999
        IDSTMX = IDSTE *4
```

```
C       WRITE(12,5555)(AMPDD(I),I=1,2000)
5555    FORMAT(1X,10F12.8)


        DO 100 INVFRE=INITRN,IENDRN
          W=WVLNCC(INVFRE)
          FREQ=120./W
          P2PDST=12000/FREQ   ; PEAK TO PEAK DISTANCE IN MICRONS FOR ONE CYCLE
                              ; AT THIS FREQUENCY (FREQ)  (1 COCO = 100 MICRONS)
          NUMPTS = P2PDST*4
          IF(NUMPTS .LT. IDSTMX)NUMPTS=IDSTMX
          IF(NUMPTS .LT. 10000)GO TO 19
          TYPE " "
          TYPE "*******************************************************"
          TYPE "*******************************************************"
          TYPE " "
          TYPE "FREQ =",FREQ,",  NUMPTS (MUST BE LESS THAN 10000) =",NUMPTS
          TYPE "NUMPTS HAS EXCEDED BOUNDS.  NUMPTS NOW = 9999. "
          NUMPTS = 9999
          TYPE "***  ANSWERS MAY NOT BE RIGHT  ***"
          TYPE " "
          TYPE "*******************************************************"
          TYPE "*******************************************************"
          TYPE " "
19        CONTINUE

CCCCCCCCCCCCCCCCCCCCCCCCCCCCCCCCCCCCCCCCCCCCCCCCCCCCCCCCCCCCCCCCCCCCCC
C
C  SET UP OUTPUT COPY HEADERS
C
CCCCCCCCCCCCCCCCCCCCCCCCCCCCCCCCCCCCCCCCCCCCCCCCCCCCCCCCCCCCCCCCCCCCCC
        IF(XPRINT .GE. .5)WRITE(12,3331)
3331    FORMAT(1X,"**************************************************",/,1H1)
        IF(XPRINT .GE. .5)WRITE(12,3332)FREQ
3332    FORMAT(1X,"***************************  FOR FREQ =",F10.6,////////////)
3333    FORMAT(1X,20F6.3)


CCCCCCCCCCCCCCCCCCCCCCCCCCCCCCCCCCCCCCCCCCCCCCCCCCCCCCCCCCCCCCCCCCCCCC
C
C   BEGIN CORTEX RESOLUTION CALCULATIONS
C
CCCCCCCCCCCCCCCCCCCCCCCCCCCCCCCCCCCCCCCCCCCCCCCCCCCCCCCCCCCCCCCCCCCCCC
            DO 30 IR=1,NUMPTS,INCALC
              R=IR                  ; CALCULATE COSINE (OF LIGHT) AMPLITUDE FOR
              X=6.2831853*R/P2PDST  ; THE POINT WHICH  IS IR MICRONS FROM
              A=COS(X)+1.           ; LEFT EXTREME (ZERO ON R-AXIS)

              DO 30 IC=1,NUMPTS
                IDIST = ABS(IC-IR)                ; IDIST IS DISTANCE IN MICRONS
25              IF(IDIST .GT. IDSTE) GO TO 30     ; FROM POINT IR TO POINT IC.
```

```
                ARRAY(IC) = ARRAY(IC)+(A*AMPDD(IDIST)) ; ARRAY(IC) IS RUNNING SUM
                                                ; OF ALL COMPONENTS OF AIRY DISKS
                                                ; CENTERED AT POINT IR AT ALL POINTS IC.
30          CONTINUE

            AMIN=50000.
            AMAX=0.
            ISTART=NUMPTS/3.333  ; ONLY CHECK MIDDLE THIRD OF ARRAY FOR MAX AND
            IEND=ISTART*2.1      ; MIN INTENSITIES (LIGHT AMPLITUDES)
            DO 40 I=ISTART,IEND
              IF(ARRAY(I) .LT. AMIN)AMIN=ARRAY(I)   ; FIND MINIMUM INTENSITY
              IF(ARRAY(I) .GT. AMAX)AMAX=ARRAY(I)   ; FIND MAXIMUM INTENSITY
40          CONTINUE
          WRITE(12,3334)ISTART,IEND,NUMPTS
3334      FORMAT(16X,3I10)
          IF(XPRINT .GE. .5)WRITE(12,3333)(ARRAY(I),I=ISTART,IEND)


            CONSEN(INVFRE)=(AMAX-AMIN)/(AMAX+AMIN)   ; COMPUTE CONTRAST SENSITIVTY
                                                     ; FOR THIS FREQUENCY
          TYPE "FOR FREQ =",FREQ," cpd,  THE CONT SENS =",CONSEN(INVFRE)

100       CONTINUE


CCCCCCCCCCCCCCCCCCCCCCCCCCCCCCCCCCCCCCCCCCCCCCCCCCCCCCCCCCCCCC
C
C   PRINT OUT RESULTS
C
CCCCCCCCCCCCCCCCCCCCCCCCCCCCCCCCCCCCCCCCCCCCCCCCCCCCCCCCCCCCCC

C   WRITE NEW HEADER AT THE TOP OF A NEW PAGE
          WRITE(12,2221)
2221      FORMAT(1H1,5X,///,5x)
          WRITE(12,2222)S,XPONNT
2222      FORMAT(11X,"For EXPONENT DIVISOR =",F10.4," and an EXPONENT TO THE ",
     &           "EXPONENT =",F7.4)
          WRITE(12,2223)INCALC
2223      FORMAT(30X,"and the intensity of the sine image recomputed at ",
     &           "INTERVALS of",I4," microns :",////)

          DO 220 I=INITRN,IENDRN
            W=WVLNCC(I)
            FREQ=120./W
            WRITE(12,301)FREQ,CONSEN(I)
301         FORMAT(/,5X,"FOR A SPATIAL FREQ IN CYCLES PER DEGREE OF ",
     &        F6.2,/,15X,"CONTRAST SENSITIVITY DUE TO DENDRITIC AVERAGING =",F6.3)
220       CONTINUE

          END
```

Appendix E

Phoneme Track Listings

This appendix contains the "TRP" files generated by the second stage ("TRACKSR3") of the CTT audio simulation. They are included here for the reader who desires to critically evaluate the data which supports the results presented in section two of Chapter Five.

Each "TRP" file for speaker "RLR" from the TRACKSR3 program is presented in its entirety. They are listed here in the following order organized by utterance:

For speaker: RLR (R.L. Routh), male, 31 years old:

ELM1 - SPQELM1.DA

ELM2 - SPQELM2.DA

ELM3 - SPQELM3.DA

HELM - SPQHELM.DA

BELL - SPQBELL.DA

SASH1 - SPZSASH.DA

SASH2 - SPQSASH2.DA

SASH3 - SPZSASH3.DA

ASH - SPZASH.DA

SASS - SPZSASS.DA

COT1 - SPQCOT1.DA

COT2 - SPQCOT2.DA

COT3 - SPQCOT3.DA

COP - SPQCOP.DA

TOT - SPQTOT.DA

Space considerations preclude the inclusion of the "TRP" files for all speakers. The "TRP" files for the other three speakers are on file at the digital signal processing laboratory of the Air Force Institute of Technology. They are filed in the following order and, if desired, should be requested by their "SP-.DA" filename.

For speaker: BLR (Robert L. Russel), male, 29 years old:

ELM1 - SPTBELM1.DA
ELM2 - SPTBELM2.DA
ELM3 - SPTBELM3.DA
HELM - SPTBHELM.DA
BELL - SPTBBELL.DA
SASH1 - SPTBSASH.DA
SASH2 - SPTBSASH2.DA
SASH3 - SPTBSASH3.DA
ASH - SPTBASH.DA
SASS - SPTBSASS.DA
COT1 - SPTBCOT1.DA
COT2 - SPTBCOT2.DA
COT3 - SPTBCOT3.DA
COP - SPTBCOP.DA
TOT - SPTBTOT.DA

For speaker: ENR (Edith N. Routh), female, 31 years old:

ELM1 - SPTEELM2.DA

ELM2 - SPTEELM2.DA

ELM3 - SPTEELM3.DA

HELM - SPTEHELM.DA

BELL - SPTEBELL.DA

SASH1 - SPTESASH.DA

SASH2 - SPTESASH2.DA

SASH3 - SPTESASH3.DA

ASH - SPTEASH.DA

SASS - SPTESASS.DA

COT1 - SPTECOT1.DA

COT2 - SPTECOT2.DA

COT3 - SPTECOT3.DA

COP - SPTECOP.DA

TOT - SPTETOT.DA

For speaker: AH (Ahni Holten), female, 7 years old:

ELM1 - TAELM1.DA

ELM2 - TAELM2.DA

ELM3 - TAELM3.DA

HELM - SPTAHELM.DA

BELL - SPTABELL.DA

SASH1 - SPTASASH.DA

SASH2 - SPTASASH2.DA

SASH3 - SPTASASH3.DA

ASH - SPTAASH.DA

SASS - SPTASASS.DA

COT1 - SPTACOT1.DA

COT2 - SPTACOT2.DA

COT3 - SPTACOT3.DA

COP - SPTACOP.DA

TOT - SPTATOT.DA

See Appendices F, G, and H for further information and analysis of these data.

TRACK TRAIL FOR SPGELM1.DA

BLOCK	(IR3D, JR3D)	AMAX	AMAXUP	RSUM	LOG COORD'S	POWER
29	(26,27)	90.6	97.7	2677.3	(20,21)	92613460.
30	(25,27)	94.7	101.9	2675.9	(19,21)	246811400.
31	(26,26)	97.0	104.6	2686.8	(20,20)	460595700.
32	(26,27)	98.4	106.0	2680.0	(20,21)	634152200.
33	(26,27)	99.4	106.4	2661.8	(20,21)	695650800.
34	(26,27)	100.2	106.6	2636.7	(20,21)	728269800.
35	(26,27)	101.3	107.3	2625.3	(20,21)	857833700.
36	(26,27)	102.2	108.2	2612.7	(20,21)	1053853000.
37	(26,27)	102.8	108.6	2608.1	(20,21)	1142378000.
38	(27,27)	102.8	108.2	2589.3	(20,20)	1042668000.
39	(27,27)	102.3	107.5	2595.7	(20,20)	883129600.
40	(26,27)	101.5	107.1	2649.6	(20,21)	815564500.
41	(26,27)	101.5	107.2	2682.2	(20,21)	838700800.
42	(27,27)	101.6	107.3	2664.0	(20,20)	854636000.
43	(27,27)	102.0	107.4	2622.6	(20,20)	863657500.
44	(27,27)	102.3	107.7	2618.3	(20,20)	928985600.
45	(26,27)	102.5	108.2	2636.8	(20,21)	1052089000.
46	(26,27)	103.0	108.6	2632.4	(20,21)	1150758000.
47	(27,27)	103.6	108.7	2587.9	(20,20)	1170195000.
48	(27,28)	104.1	108.7	2551.3	(20,21)	1186441000.
49	(27,27)	104.6	109.1	2580.4	(20,20)	1286086000.
50	(27,27)	104.8	109.5	2613.1	(20,20)	1421245000.
51	(26,28)	104.4	109.6	2609.2	(20,21)	1440965000.
52	(27,28)	104.6	109.3	2582.6	(20,21)	1349447000.
53	(26,28)	104.9	109.3	2570.5	(20,21)	1341624000.
54	(26,28)	105.1	109.8	2603.3	(20,21)	1519265000.
55	(26,28)	105.1	110.3	2616.6	(20,21)	1690403000.
56	(27,27)	104.9	110.1	2614.8	(20,20)	1618933000.
57	(27,27)	105.0	109.6	2624.1	(20,20)	1445090000.
58	(26,27)	105.5	109.8	2618.1	(20,21)	1527153000.
59	(26,28)	106.3	110.8	2604.8	(20,21)	1914701000.
60	(27,28)	107.0	111.5	2557.9	(20,21)	2230998000.
61	(27,28)	107.1	111.5	2546.5	(20,21)	2213392000.
62	(26,28)	106.5	111.2	2594.4	(20,21)	2084126000.
63	(25,28)	105.6	111.3	2678.1	(19,21)	2161432000.
64	(25,28)	105.3	111.7	2704.7	(19,21)	2351309000.
65	(25,28)	104.9	111.6	2685.9	(19,21)	2312623000.
66	(25,28)	104.6	111.2	2675.4	(19,21)	2087761000.
67	(25,28)	104.3	111.2	2685.6	(19,21)	2084023000.
68	(25,28)	104.8	111.8	2728.3	(19,21)	2417637000.
69	(25,28)	105.0	112.3	2714.4	(19,21)	2673256000.
70	(25,28)	105.4	112.0	2669.7	(19,21)	2490660000.
71	(25,28)	105.6	111.3	2647.6	(19,21)	2161147000.
72	(25,29)	105.9	111.4	2610.0	(19,22)	2208165000.
73	(24,29)	106.4	112.2	2616.7	(18,22)	2608920000.
74	(25,29)	106.8	112.5	2575.9	(19,22)	2808319000.
75	(25,29)	107.2	112.2	2520.8	(19,22)	2605763000.
76	(25,30)	107.7	112.0	2494.6	(19,23)	2484945000.
77	(24,30)	108.2	112.6	2477.1	(18,23)	2909409000.
78	(25,30)	108.8	113.5	2475.9	(19,23)	3578569000.
79	(25,30)	109.4	113.8	2448.4	(19,23)	3842554000.
80	(26,29)	110.1	113.8	2462.0	(20,22)	3825395000.
81	(25,29)	110.7	114.3	2442.6	(19,22)	4270326000.
82	(25,30)	111.2	115.2	2447.2	(19,23)	5275578000.
83	(25,30)	111.4	115.7	2430.3	(19,23)	5922517000.
84	(25,30)	111.4	115.5	2370.4	(19,23)	5608440000.
85	(25,31)	111.3	115.1	2359.8	(19,23)	5165789000.
86	(25,30)	111.3	115.6	2354.9	(19,23)	5710590000.
87	(24,31)	111.5	116.4	2376.3	(18,23)	6847902000.
88	(25,31)	111.6	116.5	2388.4	(19,23)	7118877000
89	(25,31)	111.6	116.1	2366.3	(19,23)	6395699000

AD-A163 215 CORTICAL THOUGHT THEORY: A WORKING MODEL OF THE HUMAN GESTALT MECHANISM(U) AIR FORCE INST OF TECH WRIGHT-PATTERSON AFB OH SCHOOL OF ENGINEERING

UNCLASSIFIED R L ROUTH JUL 85 AFIT/DS/EE/85-1 F/G 5/10 NL

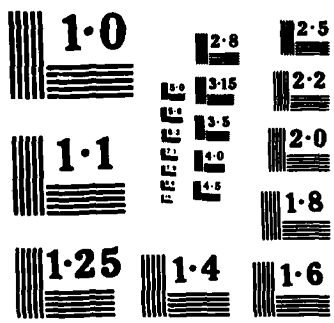

NATIONAL BUREAU OF STANDARDS
MICROCOPY RESOLUTION TEST CHART

90	(25,30)	111.6	115.9	2379.0	(19,23)	6103482000.
91	(24,30)	111.4	116.4	2380.9	(18,23)	6976143000.
92	(24,31)	111.3	116.9	2377.3	(18,23)	7825392000.
93	(25,31)	110.9	116.6	2361.2	(19,23)	7286313000.
94	(25,31)	110.5	116.0	2355.1	(19,23)	6251102000.
95	(24,31)	110.6	116.2	2353.5	(18,23)	6542746000.
96	(24,30)	110.8	117.1	2377.8	(18,23)	8074588000.
97	(24,31)	110.6	117.5	2366.3	(18,23)	8821514000.
98	(25,31)	110.1	116.9	2362.4	(19,23)	7764849000.
99	(25,31)	109.9	116.1	2355.6	(19,23)	6509945000.
100	(24,30)	109.8	116.4	2356.7	(18,23)	6898516000.
101	(24,30)	110.0	117.2	2371.7	(18,23)	8302522000.
102	(25,31)	110.2	117.3	2353.0	(19,23)	8547066000.
103	(25,31)	109.8	116.5	2324.2	(19,23)	7134978000.
104	(25,31)	109.4	115.7	2336.5	(19,23)	5920301000.
105	(25,30)	109.2	116.0	2334.8	(19,23)	6377218000.
106	(25,30)	109.9	116.8	2374.1	(19,23)	7549075000.
107	(25,31)	110.2	116.8	2328.6	(19,23)	7505277000.
108	(25,31)	110.3	116.0	2291.2	(19,23)	6288355000.
109	(25,31)	110.5	115.6	2264.6	(19,23)	5794619000.
110	(25,31)	110.9	116.4	2254.0	(19,23)	6956130000.
111	(25,31)	111.3	117.2	2283.6	(19,23)	8322601000.
112	(25,32)	111.2	117.0	2234.6	(19,24)	8018354000.
113	(25,32)	111.1	116.2.	2214.8	(19,24)	6595105000.
114	(25,32)	111.0	115.9	2214.8	(19,24)	6233047000.
115	(25,31)	111.2	116.8	2222.2	(19,23)	7635681000.
116	(25,31)	111.5	117.5	2267.0	(19,23)	8972104000.
117	(25,32)	111.5	117.2	2204.9	(19,24)	8388194000.
118	(25,33)	111.3	116.3	2182.5	(18,24)	6748672000.
119	(25,32)	111.2	116.1	2161.9	(19,24)	6428111000.
120	(25,32)	111.5	117.0	2165.0	(19,24)	7985754000.
121	(25,32)	111.8	117.7	2220.2	(19,24)	9354416000.
122	(25,33)	112.0	117.4	2170.3	(18,24)	8689983000.
123	(25,33)	111.8	116.4	2122.5	(18,24)	6949282000.
124	(25,33)	111.7	116.2	2110.8	(18,24)	6637457000.
125	(25,33)	111.8	117.2	2087.3	(18,24)	8282771000.
126	(25,33)	111.9	117.8	2145.7	(18,24)	9613361000.
127	(25,33)	111.7	117.4	2125.2	(18,24)	8643113000.
128	(25,34)	111.2	116.0	2076.2	(18,25)	6319731000.
129	(25,33)	110.8	115.2	2068.8	(18,24)	5287166000.
130	(24,33)	110.8	116.1	2067.2	(18,25)	6388093000.
131	(25,33)	110.9	116.8	2148.0	(18,24)	7631127000.
132	(25,33)	110.5	116.5	2111.7	(18,24)	7044227000.
133	(25,34)	109.9	115.2	2057.7	(18,25)	5265531000.
134	(25,33)	109.5	114.6	2060.5	(18,24)	4534039000.
135	(25,33)	109.8	115.5	2042.6	(18,24)	5639168000.
136	(25,32)	110.1	116.4	2125.9	(19,24)	6877540000.
137	(25,33)	109.8	116.1	2084.8	(18,24)	6452404000.
138	(25,34)	109.1	114.9	2011.8	(18,25)	4869485000.
139	(25,33)	108.5	114.2	2022.1	(18,24)	4162091000.
140	(24,33)	108.7	115.1	2054.6	(18,25)	5115118000.
141	(25,32)	109.3	116.0	2150.6	(19,24)	6246339000.
142	(25,34)	109.3	115.7	2084.1	(18,25)	5914173000.
143	(25,34)	108.5	114.6	2019.6	(18,25)	4545647000.
144	(25,33)	108.2	114.0	2018.4	(18,24)	3975104000.
145	(24,33)	108.6	114.9	2044.9	(18,25)	4911833000.
146	(25,32)	109.1	115.8	2164.8	(19,24)	5999120000.
147	(25,34)	109.2	115.6	2074.4	(18,25)	5715800000.
148	(24,35)	109.2	114.5	2016.0	(18,26)	4438905000.
149	(25,34)	109.2	113.9	1996.6	(18,25)	3854682000.
150	(24,34)	109.6	114.7	2016.5	(18,25)	4646109000.
151	(25,33)	110.0	115.5	2127.4	(18,24)	5608657000.
152	(25,34)	110.2	115.3	2054.2	(18,25)	5367194000.
153	(24,34)	110.3	114.3	2015.0	(18,25)	4281427000.
154	(25,34)	110.5	113.9	1989.5	(18,25)	3877396000.
155	(24,33)	110.8	114.7	2004.5	(18,25)	4711559000

156	(25,33)	111.1	115.5	2086.8	(18,24)	5603918000.
157	(25,34)	111.1	115.2	2035.7	(18,25)	5291713000.
158	(24,34)	111.0	114.2	1983.3	(18,25)	4168093000.
159	(25,34)	110.9	113.6	1960.6	(18,25)	3625070000.
160	(24,34)	110.8	114.2	1978.1	(18,25)	4122256000.
161	(25,33)	110.8	114.7	2094.9	(18,24)	4649214000.
162	(25,34)	110.6	114.3	2034.9	(18,25)	4259768000.
163	(25,34)	110.3	113.3	1987.3	(18,25)	3413158000.
164	(25,33)	110.1	113.1	1963.5	(18,24)	3206191000.
165	(25,33)	109.9	113.8	2012.2	(18,24)	3765221000.
166	(25,33)	109.8	114.1	2074.6	(18,24)	4116631000.
167	(25,34)	109.5	113.6	2022.3	(18,25)	3625028000.
168	(25,34)	109.1	112.7	1960.2	(18,25)	2924518000.
169	(25,34)	108.9	112.7	1940.9	(18,25)	2930304000.
170	(24,34)	108.8	113.5	1982.7	(18,25)	3516858000.
171	(25,33)	108.7	113.7	2071.2	(18,24)	3725881000.
172	(24,34)	108.2	113.0	2011.6	(18,25)	3171831000.
173	(25,34)	107.7	112.2	1958.2	(18,25)	2603570000.
174	(24,34)	107.4	112.4	1970.8	(18,25)	2756785000.
175	(25,32)	107.7	113.2	2134.3	(19,24)	3319732000.
176	(25,33)	107.7	113.3	2093.9	(18,24)	3399629000.
177	(24,35)	107.4	112.6	1970.1	(18,26)	2883849000.
178	(24,35)	107.0	112.1	1961.9	(18,26)	2574414000.
179	(24,34)	107.1	112.7	1977.1	(18,25)	2982899000.
180	(24,34)	107.5	113.5	1993.9	(18,25)	3560795000.
181	(24,34)	107.4	113.4	1990.4	(18,25)	3464358000.
182	(24,34)	107.1	112.5	1989.9	(18,25)	2827410000.
183	(25,34)	106.5	112.0	1982.8	(18,25)	2484605000.
184	(24,33)	106.5	112.4	2023.0	(18,25)	2768811000.
185	(25,31)	106.7	112.9	2165.7	(19,23)	3076458000.
186	(24,34)	106.4	112.5	2001.3	(18,25)	2817643000.
187	(25,33)	106.0	111.7	2007.6	(18,24)	2330929000.
188	(25,33)	105.5	111.6	1988.4	(18,24)	2265757000.
189	(25,32)	105.2	112.2	2046.0	(19,24)	2600623000.
190	(25,32)	105.4	112.3	2061.7	(19,24)	2705882000.
191	(25,32)	105.3	111.7	2072.4	(19,24)	2319012000.
192	(25,32)	105.3	110.9	2037.8	(19,24)	1935025000.
193	(26,32)	105.6	111.0	2019.5	(19,24)	1990615000.
194	(26,31)	105.7	111.5	2147.5	(19,23)	2236090000.
195	(26,31)	105.7	111.3	2182.3	(19,23)	2139561000.
196	(26,32)	105.6	110.4	2089.6	(19,24)	1720252000.
197	(27,31)	105.6	109.6	2089.0	(20,23)	1458168000.
198	(26,31)	105.8	110.0	2112.0	(19,23)	1575446000.
199	(26,31)	106.0	110.4	2120.1	(19,23)	1749804000.
200	(26,31)	105.9	110.0	2117.9	(19,23)	1598637000.
201	(26,32)	105.5	108.9	2099.3	(19,24)	1217053000.
202	(27,32)	105.0	107.7	2080.7	(20,24)	938333700.
203	(26,32)	104.3	107.5	2101.4	(19,24)	896047900.
204	(27,30)	103.4	107.5	2263.1	(20,22)	900467500.
205	(27,31)	102.2	106.8	2178.9	(20,23)	761486300.
206	(28,31)	100.9	105.2	2178.5	(21,23)	519847700.
207	(29,31)	101.0	103.4	2122.5	(21,23)	349735700.
208	(30,31)	101.2	103.3	2168.8	(22,23)	338966300.
209	(31,32)	101.5	104.1	2116.3	(22,23)	406059500.
210	(32,32)	101.8	104.3	2102.8	(23,23)	430594000.
211	(33,31)	102.1	103.9	2098.9	(24,22)	389136900.
212	(32,31)	102.3	103.6	2083.5	(23,22)	365733100.
213	(33,31)	102.4	104.2	2085.1	(24,22)	418462000.
214	(33,31)	102.5	104.9	2076.5	(24,22)	490180600.
215	(33,32)	102.5	104.9	2061.0	(24,23)	485978400.
216	(33,31)	102.5	104.2	2060.3	(24,22)	412209700.
217	(33,31)	102.4	103.7	2065.0	(24,22)	368495100.
218	(33,31)	102.2	104.1	2071.4	(24,22)	403212000.
219	(34,31)	102.1	104.5	2068.8	(24,22)	446843100.
220	(33,32)	101.9	104.2	2061.1	(24,23)	418527700.
221	(32,31)	101.8	103.5	2112.4	(23,22)	350935800

222	(31, 31)	101. 7	103. 3	2130. 2	(23, 23)	335465700.
223	(32, 31)	101. 7	103. 9	2138. 9	(23, 22)	386548200.
224	(33, 31)	101. 7	104. 3	2125. 1	(24, 22)	423037400.
225	(34, 30)	101. 6	103. 9	2093. 1	(24, 22)	389028600.
226	(34, 30)	101. 5	103. 3	2141. 5	(24, 22)	335978800.
227	(34, 30)	101. 5	103. 3	2142. 5	(24, 22)	336577000.
228	(34, 30)	101. 4	103. 8	2147. 8	(24, 22)	377949400.
229	(33, 31)	101. 5	103. 9	2150. 5	(24, 22)	387043100.
230	(32, 31)	101. 6	103. 4	2182. 4	(23, 22)	345392100.
231	(31, 31)	101. 6	103. 0	2201. 3	(23, 23)	317549600.
232	(32, 30)	101. 7	103. 4	2189. 3	(23, 22)	349570800.
233	(33, 30)	101. 6	104. 0	2148. 2	(24, 22)	396806400.
234	(34, 31)	101. 6	103. 9	2103. 4	(24, 22)	387250200.
235	(34, 31)	101. 7	103. 2	2079. 2	(24, 22)	329125100.
236	(33, 31)	101. 6	102. 7	2085. 2	(24, 22)	297118200.
237	(34, 31)	101. 4	103. 1	2090. 4	(24, 22)	322388500.
238	(34, 31)	101. 2	103. 4	2116. 6	(24, 22)	349804000.
239	(33, 31)	100. 9	103. 1	2119. 5	(24, 22)	322036000.
240	(32, 30)	100. 7	102. 2	2166. 1	(23, 22)	265029900.
241	(32, 30)	100. 4	101. 8	2187. 3	(23, 22)	240146200.
242	(32, 30)	100. 0	102. 0	2202. 3	(23, 22)	253991900.
243	(33, 30)	99. 8	102. 1	2208. 5	(24, 22)	255971600.
244	(33, 30)	99. 5	101. 4	2175. 3	(24, 22)	219814200.
245	(33, 30)	99. 3	100. 7	2177. 4	(24, 22)	187202700.
246	(33, 30)	99. 3	101. 0	2175. 8	(24, 22)	200406300.
247	(33, 30)	99. 4	101. 8	2167. 1	(24, 22)	238763400.
248	(34, 31)	99. 5	101. 9	2138. 5	(24, 22)	247326300.
249	(34, 31)	99. 6	101. 3	2094. 2	(24, 22)	215468100.
250	(34, 31)	99. 6	100. 8	2047. 1	(24, 22)	192586200.
251	(35, 31)	99. 5	101. 3	2040. 6	(25, 22)	214566400.
252	(36, 31)	99. 3	102. 0	2029. 6	(25, 22)	250303800.
253	(38, 31)	99. 0	101. 9	2011. 0	(27, 22)	244002000.
254	(37, 31)	98. 7	100. 9	2014. 4	(26, 22)	193093400.
255	(35, 30)	98. 1	99. 7	2032. 5	(25, 21)	149497900.
256	(34, 31)	97. 6	99. 7	2106. 6	(24, 22)	148634600.
257	(33, 31)	97. 2	100. 2	2147. 0	(24, 22)	166647600.
258	(33, 31)	96. 8	100. 1	2165. 9	(24, 22)	160806600.
259	(32, 30)	96. 4	99. 1	2223. 8	(23, 22)	130218800.
260	(31, 30)	95. 9	98. 4	2265. 8	(23, 22)	108450000.
261	(32, 30)	95. 7	98. 6	2256. 8	(23, 22)	114027300.
262	(32, 30)	95. 8	99. 1	2251. 4	(23, 22)	127384100.
263	(32, 30)	95. 8	98. 9	2206. 7	(23, 22)	121920800.
264	(31, 31)	95. 8	98. 1	2228. 3	(23, 23)	102449500.
265	(31, 30)	95. 8	97. 7	2241. 4	(23, 22)	92716340.
266	(31, 30)	95. 8	98. 0	2224. 9	(23, 22)	101103000.
267	(32, 30)	95. 7	98. 4	2239. 3	(23, 22)	109589900.
268	(32, 30)	95. 4	98. 0	2237. 3	(23, 22)	100099400.
269	(32, 30)	95. 2	97. 0	2264. 9	(23, 22)	79378270.
270	(32, 29)	94. 9	96. 3	2277. 5	(23, 21)	67164860.
271	(31, 29)	94. 4	96. 4	2298. 3	(23, 21)	68858050.
272	(31, 29)	93. 8	96. 5	2304. 2	(23, 21)	70392110.
273	(31, 30)	93. 2	95. 8	2275. 0	(23, 22)	60378050.
274	(31, 29)	92. 7	94. 6	2262. 0	(23, 21)	45202080.
275	(31, 29)	92. 3	93. 9	2272. 9	(23, 21)	38553410.
276	(31, 29)	92. 0	94. 3	2298. 7	(23, 21)	42574740.
277	(31, 29)	91. 9	94. 7	2315. 2	(23, 21)	46706180.
278	(32, 29)	91. 8	94. 4	2310. 3	(23, 21)	43378030.
279	(31, 29)	91. 7	93. 8	2333. 3	(23, 21)	37763760.
280	(31, 29)	91. 5	93. 8	2342. 1	(23, 21)	38414530.
281	(31, 29)	91. 3	94. 5	2331. 2	(23, 21)	44483920.
282	(31, 29)	91. 1	94. 7	2319. 5	(23, 21)	46490830.
283	(31, 29)	90. 6	93. 9	2319. 9	(23, 21)	39145810.
287	(31, 29)	88. 5	92. 8	2368. 3	(23, 21)	30503180.

TRACK TRAIL FOR SPGELM2.DA

BLOCK	(IR3D, JR3D)	AMAX	AMAXUP	RSUM	LOG COORD'S	POWER
43	(26, 27)	87.0	93.8	2682.8	(20, 21)	38239660.
44	(27, 27)	90.6	97.1	2659.4	(20, 20)	80589100.
45	(27, 27)	93.7	99.9	2587.4	(20, 20)	154041700.
46	(27, 27)	95.7	101.8	2521.7	(20, 20)	237952800.
47	(27, 28)	96.9	102.6	2485.0	(20, 21)	289679400.
48	(27, 28)	97.5	102.7	2517.7	(20, 21)	293311200.
49	(27, 28)	98.0	102.8	2544.3	(20, 21)	298612000.
50	(26, 28)	98.6	103.5	2578.5	(20, 21)	358219800.
51	(26, 28)	99.5	104.5	2585.8	(20, 21)	447339000.
52	(26, 28)	100.3	104.9	2545.1	(20, 21)	490382600.
53	(27, 28)	101.1	104.9	2518.6	(20, 21)	494407400.
54	(26, 28)	101.9	105.6	2524.6	(20, 21)	568915200.
55	(26, 28)	102.7	106.8	2559.5	(20, 21)	756131800.
56	(26, 28)	103.3	107.7	2545.0	(20, 21)	928409100.
57	(27, 28)	103.6	107.7	2511.4	(20, 21)	938606100.
58	(27, 28)	104.0	107.4	2515.3	(20, 21)	874760200.
59	(26, 28)	104.4	107.8	2525.2	(20, 21)	962893100.
60	(26, 28)	104.9	108.9	2548.1	(20, 21)	1229979000.
61	(26, 28)	105.3	109.5	2518.6	(20, 21)	1426931000.
62	(27, 28)	105.4	109.4	2495.0	(20, 21)	1380716000.
63	(26, 28)	105.2	109.0	2513.0	(20, 21)	1270936000.
64	(25, 28)	105.1	109.3	2566.2	(19, 21)	1350081000.
65	(25, 28)	104.9	109.9	2579.7	(19, 21)	1545540000.
66	(26, 28)	104.4	110.0	2552.7	(20, 21)	1567081000.
67	(26, 28)	103.4	109.4	2530.4	(20, 21)	1377967000.
68	(25, 28)	102.7	109.0	2528.6	(19, 21)	1253217000.
69	(25, 28)	102.9	109.3	2571.9	(19, 21)	1343183000.
70	(25, 28)	103.2	109.7	2564.0	(19, 21)	1462520000.
71	(25, 29)	103.5	109.6	2518.7	(19, 22)	1430509000.
72	(25, 29)	103.9	109.6	2496.9	(19, 22)	1457093000.
73	(25, 28)	104.4	110.5	2496.3	(19, 21)	1788648000.
74	(25, 29)	104.9	111.5	2493.4	(19, 22)	2228881000.
75	(25, 29)	105.4	111.7	2469.1	(19, 22)	2329267000.
76	(25, 29)	105.5	111.2	2426.0	(19, 22)	2096003000.
77	(25, 29)	105.6	111.1	2398.5	(19, 22)	2033414000.
78	(25, 29)	106.1	111.8	2414.8	(19, 22)	2375191000.
79	(25, 29)	106.9	112.3	2415.7	(19, 22)	2711503000.
80	(25, 30)	107.6	112.2	2375.7	(19, 23)	2609171000.
81	(25, 30)	108.1	111.9	2347.0	(19, 23)	2436296000.
82	(25, 30)	108.5	112.5	2323.3	(19, 23)	2806887000.
83	(25, 30)	108.9	113.5	2371.0	(19, 23)	3558745000.
84	(25, 30)	109.1	113.9	2322.5	(19, 23)	3859732000.
85	(25, 31)	109.1	113.4	2311.3	(19, 23)	3430004000.
86	(25, 31)	109.1	112.8	2308.7	(19, 23)	3022162000.
87	(25, 30)	109.0	113.2	2342.5	(19, 23)	3298074000.
88	(25, 30)	109.1	113.8	2349.6	(19, 23)	3839264000.
89	(25, 30)	108.9	113.8	2344.6	(19, 23)	3769618000.
90	(25, 31)	108.6	113.0	2320.2	(19, 23)	3177320000.
91	(25, 30)	108.4	112.7	2329.1	(19, 23)	2938562000.
92	(24, 30)	108.3	113.3	2353.3	(18, 23)	3363423000.
93	(25, 30)	108.3	113.7	2367.8	(19, 23)	3743635000.
94	(25, 31)	108.2	113.4	2323.9	(19, 23)	3444446000
95	(25, 31)	108.1	112.7	2317.1	(19, 23)	2949651000.
96	(24, 30)	107.9	112.8	2333.9	(18, 23)	3025019000
97	(24, 30)	107.7	113.5	2382.9	(18, 23)	3525239000
98	(24, 31)	107.6	113.6	2352.1	(18, 23)	3609976000.
99	(24, 31)	107.4	112.9	2330.4	(18, 23)	3104013000.
100	(25, 31)	107.5	112.5	2317.3	(19, 23)	2807974000.
101	(24, 30)	107.5	113.1	2316.6	(18, 23)	3240818000.
102	(24, 30)	108.0	113.8	2333.6	(18, 23)	3826176000.
103	(25, 31)	108.3	113.7	2298.2	(19, 23)	3716019000

104	(25,31)	108.5	113.0	2254.2	(19,23)	3177312000.
105	(25,31)	108.7	113.0	2240.2	(19,23)	3130074000.
106	(24,31)	108.9	113.7	2256.7	(18,23)	3742036000.
107	(25,31)	109.3	114.2	2288.6	(19,23)	4153530000.
108	(25,32)	109.5	113.8	2214.0	(19,24)	3783244000.
109	(25,32)	109.7	113.2	2195.5	(19,24)	3342532000.
110	(25,31)	110.0	113.7	2210.1	(19,23)	3676688000.
111	(25,31)	110.2	114.5	2254.6	(19,23)	4452852000.
112	(24,32)	110.4	114.6	2218.6	(18,24)	4596638000.
113	(25,32)	110.6	114.0	2182.9	(19,24)	3996365000.
114	(25,32)	110.8	113.7	2155.7	(19,24)	3712197000.
115	(25,31)	111.0	114.4	2160.2	(19,23)	4343992000.
116	(25,31)	111.2	115.1	2191.4	(19,23)	5086634000.
117	(25,32)	111.4	114.9	2144.3	(19,24)	4891562000.
118	(25,32)	111.5	114.2	2136.4	(19,24)	4190981000.
119	(25,32)	111.6	114.2	2151.7	(19,24)	4181311000.
120	(25,32)	111.7	115.0	2173.4	(19,24)	5011636000.
121	(25,31)	111.9	115.4	2195.5	(19,23)	5517894000.
122	(25,33)	111.9	115.0	2109.7	(18,24)	4980171000.
123	(25,32)	111.9	114.4	2104.0	(19,24)	4358357000.
124	(25,32)	112.0	114.8	2125.2	(19,24)	4735025000.
125	(25,32)	112.0	115.5	2186.8	(19,24)	5661630000.
126	(25,32)	111.9	115.6	2158.6	(19,24)	5770572000.
127	(25,33)	111.7	114.9	2116.2	(18,24)	4862042000.
128	(25,33)	111.6	114.3	2105.9	(18,24)	4258990000.
129	(25,32)	111.5	114.8	2120.9	(19,24)	4784607000.
130	(25,32)	111.6	115.5	2136.9	(19,24)	5594087000.
131	(25,33)	111.5	115.3	2098.6	(18,24)	5407986000.
132	(25,33)	111.4	114.6	2059.3	(18,24)	4534686000.
133	(25,33)	111.3	114.3	2080.4	(18,24)	4304409000.
134	(25,33)	111.6	115.1	2100.4	(18,24)	5110620000.
135	(25,32)	111.9	115.7	2175.1	(19,24)	5823136000.
136	(25,34)	111.8	115.3	2071.1	(18,25)	5405786000.
137	(25,34)	111.7	114.5	2056.2	(18,25)	4502196000.
138	(25,33)	111.6	114.4	2054.9	(18,24)	4374278000.
139	(25,33)	111.7	115.1	2084.8	(18,24)	5098824000.
140	(25,33)	111.9	115.4	2123.0	(18,24)	5486035000.
141	(25,34)	112.0	114.8	2026.5	(18,25)	4841337000.
142	(25,34)	112.0	114.0	2023.5	(18,25)	4011047000.
143	(25,33)	111.9	114.1	2015.9	(18,24)	4088984000.
144	(25,33)	112.0	114.9	2039.7	(18,24)	4858855000.
145	(25,33)	112.0	115.1	2100.3	(18,24)	5119271000.
146	(25,34)	111.8	114.4	1986.3	(18,25)	4413719000.
147	(25,34)	111.7	113.6	1989.8	(18,25)	3663891000.
148	(25,33)	111.5	113.8	1989.0	(18,24)	3778708000.
149	(25,33)	111.5	114.4	2055.7	(18,24)	4406088000.
150	(25,33)	111.4	114.5	2074.7	(18,24)	4473700000.
151	(25,34)	111.1	113.7	1972.4	(18,25)	3756670000.
152	(25,34)	110.7	112.9	2004.4	(18,25)	3107573000.
153	(25,33)	110.4	113.0	2004.4	(18,24)	3185910000.
154	(25,32)	110.3	113.5	2091.5	(19,24)	3586234000.
155	(25,34)	110.2	113.4	2010.5	(18,25)	3491261000.
156	(25,34)	109.8	112.7	1972.8	(18,25)	2930681000.
157	(25,33)	109.5	112.2	1981.8	(18,24)	2634356000.
158	(25,33)	109.3	112.7	1987.8	(18,24)	2933266000.
159	(25,33)	109.3	113.2	2053.5	(18,24)	3286734000.
160	(25,34)	109.0	112.9	2000.2	(18,25)	3068392000.
161	(25,34)	108.5	112.0	1980.6	(18,25)	2528809000.
162	(25,33)	107.9	111.7	2001.4	(18,24)	2344359000.
163	(25,33)	108.0	112.2	2046.9	(18,24)	2644410000.
164	(26,31)	107.8	112.5	2160.7	(19,23)	2846691000.
165	(25,33)	107.3	112.1	2033.6	(18,24)	2543598000.
166	(25,33)	106.9	111.3	2046.3	(18,24)	2150510000.
167	(25,32)	106.8	111.5	2061.9	(19,24)	2219556000.
168	(25,32)	106.8	112.2	2102.9	(19,24)	2613079000.
169	(25,33)	106.7	112.3	2073.8	(18,24)	2694034000

170	(25, 33)	106.2	111.6	2064.0	(18, 24)	2281008000.
171	(25, 33)	105.6	110.9	2045.5	(18, 24)	1950964000.
172	(25, 32)	105.3	111.3	2065.2	(19, 24)	2137003000.
173	(25, 32)	105.3	112.0	2125.0	(19, 24)	2507253000.
174	(25, 32)	105.0	111.9	2162.8	(19, 24)	2441027000.
175	(25, 33)	104.8	111.0	2050.2	(18, 24)	1988330000.
176	(25, 33)	104.6	110.3	2062.8	(18, 24)	1715004000.
177	(25, 32)	104.2	110.7	2102.7	(19, 24)	1847330000.
178	(25, 31)	104.5	111.0	2161.2	(19, 23)	1987791000.
179	(25, 32)	104.4	110.4	2106.2	(19, 24)	1746225000.
180	(26, 32)	104.6	109.3	2153.1	(19, 24)	1337651000.
181	(26, 31)	104.6	108.6	2156.7	(19, 23)	1150015000.
182	(26, 31)	104.5	108.8	2180.0	(19, 23)	1202391000.
183	(26, 30)	104.2	108.7	2226.1	(19, 22)	1172069000.
184	(26, 31)	103.6	107.6	2210.9	(19, 23)	909151200.
185	(27, 30)	102.5	105.7	2285.6	(20, 22)	582757100.
186	(28, 29)	100.8	104.0	2339.6	(21, 22)	397398300.
187	(29, 29)	99.0	103.6	2389.4	(22, 22)	359677400.
188	(29, 29)	99.6	103.4	2361.2	(22, 22)	346723300.
189	(30, 30)	100.3	102.8	2279.3	(22, 22)	304333800.
190	(31, 31)	100.9	102.3	2218.7	(23, 23)	271504100.
191	(32, 30)	101.2	102.6	2172.3	(23, 22)	290708200.
192	(32, 31)	101.3	103.3	2156.9	(23, 22)	338609400.
193	(32, 31)	101.5	103.5	2129.8	(23, 22)	356108500.
194	(32, 31)	101.6	103.1	2144.6	(23, 22)	327164900.
195	(32, 30)	101.5	102.8	2168.5	(23, 22)	299616500.
196	(33, 30)	101.4	102.9	2162.0	(24, 22)	308377300.
197	(33, 30)	101.2	103.1	2170.4	(24, 22)	325271600.
198	(34, 30)	101.1	102.9	2156.7	(24, 22)	308944600.
199	(33, 30)	101.1	102.4	2189.4	(24, 22)	276499200.
200	(33, 29)	101.0	102.4	2201.9	(24, 21)	276010200.
201	(33, 30)	101.0	102.9	2197.6	(24, 22)	307299600.
202	(32, 30)	101.0	103.1	2180.4	(23, 22)	320712700.
203	(32, 30)	100.9	102.7	2174.4	(23, 22)	293722100.
204	(31, 30)	100.9	102.2	2213.5	(23, 22)	265967800.
205	(31, 30)	100.8	102.3	2230.1	(23, 22)	271763500.
206	(32, 30)	100.7	102.6	2225.1	(23, 22)	289592300.
207	(32, 30)	100.6	102.5	2224.8	(23, 22)	280469800.
208	(31, 30)	100.6	102.0	2233.3	(23, 22)	251829900.
209	(30, 30)	100.5	101.9	2261.7	(22, 22)	243722600.
210	(31, 30)	100.4	102.2	2242.9	(23, 22)	262874100.
211	(32, 30)	100.4	102.4	2201.9	(23, 22)	273816800.
212	(33, 30)	100.5	102.1	2190.9	(24, 22)	257545700.
213	(33, 30)	100.6	101.9	2195.1	(24, 22)	245627600.
214	(33, 30)	100.7	102.2	2188.9	(24, 22)	265968500.
215	(34, 30)	100.7	102.7	2168.0	(24, 22)	295692000.
216	(34, 31)	100.7	102.7	2141.7	(24, 22)	292418000.
217	(32, 31)	100.6	102.2	2155.9	(23, 22)	260793500.
218	(32, 30)	100.4	101.9	2179.9	(23, 22)	246969300.
219	(32, 30)	100.3	102.2	2171.8	(23, 22)	265585700.
220	(32, 31)	100.1	102.5	2144.7	(23, 22)	278937600.
221	(32, 31)	99.8	102.1	2136.4	(23, 22)	255298100.
222	(32, 31)	99.6	101.4	2110.8	(23, 22)	218342500.
223	(32, 32)	99.2	101.1	2077.3	(23, 23)	204945900.
224	(32, 31)	98.9	101.3	2085.2	(23, 22)	211455500.
225	(33, 31)	98.7	101.1	2087.3	(24, 22)	204472300.
226	(33, 32)	98.5	100.5	2049.4	(24, 23)	176163800.
227	(33, 31)	98.3	99.9	2063.8	(24, 22)	155167500.
228	(33, 31)	98.1	100.0	2062.5	(24, 22)	158686300.
229	(34, 31)	97.8	100.2	2068.1	(24, 22)	167395300.
230	(34, 31)	97.3	99.9	2082.2	(24, 22)	155410000.
231	(33, 31)	97.0	99.2	2122.5	(24, 22)	131050800.
232	(32, 30)	96.6	98.8	2152.3	(23, 22)	119473500.
233	(33, 30)	96.1	99.0	2183.4	(24, 22)	125950100.
234	(32, 31)	95.9	99.1	2160.0	(23, 22)	129864200.
235	(31, 31)	95.8	98.7	2136.7	(23, 23)	117922300.

236	(31,31)	95.6	98.2	2174.0	(23,23)	103973400.
237	(31,31)	95.5	98.2	2163.0	(23,23)	104064800.
238	(32,31)	95.3	98.5	2151.7	(23,22)	112948600.
239	(33,31)	95.2	98.5	2122.5	(24,22)	112866000.
240	(34,31)	95.3	98.0	2103.6	(24,22)	101147400.
241	(33,31)	95.2	97.5	2079.1	(24,22)	90119120.
242	(33,31)	95.1	97.5	2074.1	(24,22)	88596610.
243	(33,31)	94.9	97.5	2101.4	(24,22)	89742670.
244	(33,31)	94.6	97.2	2109.9	(24,22)	83168350.
245	(33,31)	94.4	96.5	2137.9	(24,22)	71283380.
246	(34,31)	94.2	96.1	2105.3	(24,22)	63907250.
247	(35,31)	93.9	96.0	2066.4	(25,22)	63786420.
248	(35,31)	93.5	96.0	2092.4	(25,22)	62657280.
249	(35,31)	92.9	95.3	2090.6	(25,22)	53841630.
250	(34,31)	92.3	94.2	2131.6	(24,22)	41236400.
251	(32,31)	91.5	93.3	2179.3	(23,22)	33854420.
252	(31,31)	90.7	93.2	2219.3	(23,23)	33146080.
253	(31,31)	89.8	93.1	2216.8	(23,23)	32264540.

TRACK TRAIL FOR SPGELM3.DA

BLOCK	(IR3D, JR3D)	AMAX	AMAXUP	RSUM	LOG COORD'S	POWER
87	(24, 28)	87.2	96.7	2631.1	(18, 21)	73323200.
88	(24, 28)	92.4	100.2	2667.2	(18, 21)	166723800.
89	(25, 28)	96.2	102.5	2666.6	(19, 21)	279729900.
90	(25, 28)	99.0	104.0	2659.6	(19, 21)	393867000.
91	(25, 28)	100.9	105.2	2618.8	(19, 21)	522235600.
92	(26, 28)	101.8	106.3	2574.4	(20, 21)	677214700.
93	(27, 27)	101.9	107.6	2557.7	(20, 20)	904088300.
94	(26, 27)	102.5	108.8	2630.3	(20, 21)	1215291000.
95	(26, 27)	103.1	109.8	2655.0	(20, 21)	1507710000.
96	(26, 27)	103.3	110.1	2653.2	(20, 21)	1616161000.
97	(26, 27)	103.6	110.0	2623.6	(20, 21)	1584529000.
98	(26, 28)	104.0	110.3	2597.9	(20, 21)	1685820000.
99	(26, 27)	104.7	111.1	2629.7	(20, 21)	2031496000.
100	(26, 28)	105.3	111.7	2620.7	(20, 21)	2346323000.
101	(26, 28)	105.9	111.8	2607.2	(20, 21)	2413935000.
102	(26, 28)	106.5	112.0	2615.8	(20, 21)	2526440000.
103	(25, 28)	106.9	112.8	2647.3	(19, 21)	2986601000.
104	(25, 28)	107.4	113.5	2648.0	(19, 21)	3526975000.
105	(26, 28)	107.7	113.6	2624.9	(20, 21)	3670110000.
106	(26, 28)	108.0	113.6	2624.5	(20, 21)	3637134000.
107	(25, 28)	108.2	114.0	2648.9	(19, 21)	3972481000.
108	(25, 28)	108.3	114.6	2676.4	(19, 21)	4571210000.
109	(25, 28)	108.4	114.8	2663.9	(19, 21)	4744270000.
110	(26, 28)	108.6	114.5	2645.8	(20, 21)	4467122000.
111	(25, 28)	108.5	114.5	2664.1	(19, 21)	4481278000.
112	(25, 28)	108.5	115.0	2707.5	(19, 21)	5006062000.
113	(25, 28)	108.4	115.2	2705.7	(19, 21)	5258330000.
114	(25, 28)	108.1	114.7	2674.6	(19, 21)	4721586000.
115	(25, 28)	107.7	114.1	2646.9	(19, 21)	4038029000.
116	(25, 28)	107.0	114.0	2671.2	(19, 21)	3952647000.
117	(25, 28)	106.5	114.2	2661.3	(19, 21)	4186230000.
118	(25, 28)	106.3	114.0	2625.6	(19, 21)	3968771000.
119	(25, 28)	106.4	113.3	2594.0	(19, 21)	3399178000.
120	(25, 28)	106.5	113.0	2581.7	(19, 21)	3147756000.
121	(25, 28)	106.4	113.2	2607.7	(19, 21)	3315938000.
122	(25, 28)	106.3	113.3	2610.5	(19, 21)	3361678000.
123	(25, 28)	106.7	113.2	2579.7	(19, 21)	3280342000.
124	(25, 28)	106.9	113.6	2562.1	(19, 21)	3662929000.
125	(24, 28)	107.1	114.6	2590.5	(18, 21)	4536496000.
126	(25, 29)	107.4	115.0	2562.9	(19, 22)	5051060000.
127	(25, 29)	107.8	114.8	2521.8	(19, 22)	4807041000.
128	(25, 29)	108.4	114.7	2485.6	(19, 22)	4720452000.
129	(24, 29)	109.0	115.4	2468.5	(18, 22)	5552685000.
130	(24, 29)	109.5	116.2	2469.4	(18, 22)	6563426000.
131	(24, 30)	109.3	116.1	2443.3	(18, 23)	6474199000.
132	(25, 30)	109.4	115.5	2430.9	(19, 23)	5609996000.
133	(24, 30)	109.6	115.3	2432.7	(18, 23)	5421433000.
134	(24, 29)	110.0	116.0	2457.2	(18, 22)	6249239000.
135	(24, 30)	110.4	116.3	2454.6	(18, 23)	6809211000.
136	(25, 30)	110.6	116.0	2397.9	(19, 23)	6242697000.
137	(25, 30)	110.7	115.5	2378.7	(19, 23)	5621211000.
138	(24, 30)	110.9	115.9	2376.2	(18, 23)	6213456000.
139	(24, 30)	111.4	116.7	2395.5	(18, 23)	7482614000.
140	(24, 31)	111.5	116.9	2357.3	(18, 23)	7730569000.
141	(25, 31)	111.5	116.3	2318.4	(19, 23)	6803272000.
142	(25, 31)	111.4	115.9	2317.3	(19, 23)	6208295000.
143	(24, 31)	111.5	116.4	2327.1	(18, 23)	6858744000.
144	(24, 31)	111.7	116.9	2350.2	(18, 23)	7714836000.
145	(24, 31)	111.6	116.7	2308.8	(18, 23)	7340216000.
146	(25, 32)	111.3	116.0	2281.8	(19, 24)	6257705000.
147	(25, 31)	111.1	115.8	2272.6	(19, 23)	6066627000

148	(24, 31)	111.2	116.5	2284.7	(18, 23)	7061254000.
149	(25, 31)	111.4	116.9	2304.9	(19, 23)	7773602000.
150	(25, 32)	111.4	116.5	2239.3	(19, 24)	7090512000.
151	(25, 32)	111.2	115.7	2227.6	(19, 24)	5824823000.
152	(25, 31)	111.1	115.4	2224.2	(19, 23)	5480362000.
153	(25, 31)	111.5	115.9	2244.7	(19, 23)	6149562000.
154	(25, 31)	111.8	116.2	2258.7	(19, 23)	6545605000.
155	(25, 32)	111.9	115.7	2192.4	(19, 24)	5926486000.
156	(26, 32)	111.8	115.1	2178.9	(19, 24)	5145403000.
157	(25, 32)	111.8	115.3	2136.6	(19, 24)	5379990000.
158	(25, 32)	112.0	116.1	2152.7	(19, 24)	6410134000.
159	(25, 32)	112.0	116.4	2180.5	(19, 24)	6868898000.
160	(26, 33)	111.7	115.8	2089.0	(19, 24)	6072152000.
161	(26, 34)	111.0	114.9	2071.5	(19, 25)	4889231000.
162	(25, 33)	111.0	114.7	2060.9	(18, 24)	4667048000.
163	(25, 33)	111.3	115.3	2088.9	(18, 24)	5417693000.
164	(25, 33)	111.5	115.7	2098.5	(18, 24)	5886579000.
165	(26, 34)	111.4	115.2	2086.7	(19, 25)	5256815000.
166	(26, 34)	111.1	114.1	2084.4	(19, 25)	4063773000.
167	(25, 34)	110.9	113.5	2014.0	(18, 25)	3555894000.
168	(25, 34)	110.9	114.1	2000.9	(18, 25)	4059327000.
169	(26, 33)	110.8	114.6	2114.4	(19, 24)	4604850000.
170	(26, 35)	110.6	114.3	1994.9	(19, 25)	4281823000.
171	(26, 35)	110.2	113.1	1996.9	(19, 25)	3253842000.
172	(26, 34)	109.7	112.0	2024.9	(19, 25)	2540236000.
173	(25, 33)	109.5	112.4	2035.8	(18, 24)	2745520000.
174	(25, 33)	109.5	113.2	2065.4	(18, 24)	3318953000.
175	(25, 34)	109.4	113.3	2092.5	(18, 25)	3375557000.
176	(25, 35)	109.0	112.4	2006.2	(18, 26)	2739670000.
177	(25, 34)	108.6	111.2	1982.8	(18, 25)	2084999000.
178	(25, 34)	108.4	111.2	1970.6	(18, 25)	2079825000.
179	(25, 33)	108.6	112.1	2083.6	(18, 24)	2550725000.
180	(25, 34)	108.4	112.4	2072.7	(18, 25)	2766223000.
181	(25, 35)	108.0	111.7	1989.9	(18, 26)	2365744000.
182	(25, 35)	107.6	110.3	1998.5	(18, 26)	1717249000.
183	(25, 33)	107.3	109.7	2040.7	(18, 24)	1467794000.
184	(25, 33)	107.4	110.5	2097.6	(18, 24)	1772958000.
185	(25, 33)	107.5	111.3	2110.9	(18, 24)	2141110000.
186	(25, 34)	107.3	111.2	2086.3	(18, 25)	2078258000.
187	(25, 34)	106.7	110.0	2044.8	(18, 25)	1578931000.
188	(25, 34)	105.8	108.4	2036.2	(18, 25)	1089546000.
189	(25, 33)	105.1	107.9	2076.7	(18, 24)	971738600.
190	(25, 31)	104.5	108.5	2216.7	(19, 23)	1118113000.
191	(24, 33)	103.8	108.7	2171.4	(18, 25)	1184418000.
192	(24, 34)	102.7	108.0	2088.3	(18, 25)	1001050000.
193	(24, 33)	101.1	106.4	2127.0	(18, 25)	695471100.
194	(25, 32)	100.1	105.0	2156.2	(19, 24)	497778400.
195	(25, 31)	100.0	104.8	2204.2	(19, 23)	476380200.
196	(25, 31)	99.8	105.0	2297.3	(19, 23)	506632200.
197	(25, 31)	99.5	104.7	2240.2	(19, 23)	467165700.
198	(25, 31)	99.0	103.4	2269.5	(19, 23)	342791700.
199	(26, 30)	98.4	101.4	2326.4	(19, 22)	216510100.
200	(27, 30)	98.1	100.3	2315.8	(20, 22)	170803400.
201	(28, 29)	98.3	101.0	2373.1	(21, 22)	201373600.
202	(28, 30)	98.5	101.8	2317.8	(21, 22)	240559400.
203	(28, 31)	98.6	101.8	2264.0	(21, 23)	237445100.
204	(29, 32)	98.3	100.7	2201.7	(21, 23)	187117400.
205	(30, 31)	97.8	99.1	2194.7	(22, 23)	128887600.
206	(31, 30)	97.6	98.4	2205.8	(23, 22)	109832500.
207	(31, 31)	98.0	99.6	2188.7	(23, 23)	143000600.
208	(31, 31)	98.[illegible]	101.0	2153.6	(23, 23)	201607400.
209	(31, 32)	99.6	101.9	2076.4	(22, 23)	244481100.
210	(32, 32)	99.9	101.9	2014.2	(23, 23)	244105500.
211	(32, 32)	99.8	101.2	2080.7	(23, 23)	209418000.
212	(31, 31)	99.6	100.5	2149.8	(23, 23)	178569400
213	(31, 31)	99.5	100.5	2152.9	(23, 23)	178190200

214	(32, 31)	99.4	101.0	2116.4	(23, 22)	198801100.
215	(33, 32)	99.4	101.2	2053.3	(24, 23)	210120700.
216	(34, 32)	99.1	100.8	2035.2	(24, 23)	190963900.
217	(33, 31)	98.6	99.8	2084.5	(24, 22)	151982200.
218	(32, 30)	98.0	98.9	2151.9	(23, 22)	124265700.
219	(32, 30)	97.9	98.9	2162.9	(23, 22)	124189200.
220	(32, 31)	97.7	99.4	2123.5	(23, 22)	139296800.
221	(34, 31)	97.6	99.6	2102.6	(24, 22)	145036300.
222	(35, 31)	97.1	99.1	2078.2	(25, 22)	127625600.
223	(34, 30)	96.5	98.0	2111.7	(24, 22)	99099600.
224	(34, 30)	95.9	97.2	2122.4	(24, 22)	83517790.
225	(33, 30)	95.7	97.5	2147.9	(24, 22)	89667090.
226	(33, 31)	95.8	98.2	2107.3	(24, 22)	104410100.
227	(34, 31)	95.8	98.3	2106.4	(24, 22)	108350600.
228	(33, 31)	95.6	97.8	2138.9	(24, 22)	96533410.
229	(32, 30)	95.6	97.4	2201.5	(23, 22)	87307630.
230	(31, 30)	96.0	98.0	2237.2	(23, 22)	100589200.
231	(32, 30)	96.5	99.2	2214.1	(23, 22)	131514000.
232	(32, 31)	96.8	99.9	2150.9	(23, 22)	153496200.
233	(32, 31)	96.8	99.6	2126.9	(23, 22)	144962400
234	(33, 31)	95.9	98.4	2167.0	(24, 22)	110744800
235	(32, 30)	95.1	97.0	2278.4	(23, 22)	79598510.
236	(31, 29)	94.8	96.8	2306.4	(23, 21)	75292460.
237	(31, 29)	95.0	97.8	2311.2	(23, 21)	95882020.
238	(31, 30)	95.6	98.8	2241.8	(23, 22)	118977800.
239	(32, 31)	95.8	98.8	2185.5	(23, 22)	121442200.
240	(33, 30)	95.1	98.0	2181.5	(24, 22)	100111400.
241	(33, 29)	94.3	96.7	2253.5	(24, 21)	74096370.
242	(33, 28)	93.8	96.1	2256.6	(24, 20)	64738880.
243	(34, 28)	93.6	96.7	2236.5	(25, 20)	74629540.
244	(35, 29)	93.9	97.5	2129.3	(25, 21)	88214620.
245	(35, 30)	94.4	97.4	2082.6	(25, 21)	87943440
246	(33, 30)	93.7	96.5	2103.4	(24, 22)	71567100.
247	(32, 29)	92.1	95.1	2207.7	(23, 21)	51873760.
248	(32, 29)	91.5	94.3	2299.2	(23, 21)	43123820.
249	(32, 29)	91.5	94.8	2327.2	(23, 21)	48260460.
250	(32, 29)	91.5	95.6	2279.7	(23, 21)	58063200.
251	(33, 30)	91.4	95.6	2230.6	(24, 22)	60292800.
252	(32, 30)	91.0	95.1	2248.0	(23, 22)	50747760.
253	(31, 29)	89.9	93.6	2354.5	(23, 21)	36570210
256	(29, 29)	88.5	93.0	2396.8	(22, 22)	31609330.
257	(30, 29)	89.1	93.0	2317.6	(22, 21)	31368060.

TRACK TRAIL FOR SPQHELM.DA

BLOCK	(IR3D, JR3D)	AMAX	AMAXUP	RSUM	LOC COORD'S	POWER
63	(25,28)	86.4	92.8	2678.9	(19,21)	30209090.
64	(25,28)	87.4	94.1	2717.9	(19,21)	40832300.
65	(24,28)	89.8	97.2	2682.3	(18,21)	82621220.
66	(24,28)	92.2	100.2	2663.0	(18,21)	164761300.
67	(24,28)	94.0	102.1	2664.9	(18,21)	257693900.
68	(25,28)	95.6	103.1	2685.3	(19,21)	322480400.
69	(25,28)	97.6	104.1	2700.5	(19,21)	409374000.
70	(24,28)	99.4	105.8	2689.4	(18,21)	601110800.
71	(24,28)	100.5	107.3	2716.1	(18,21)	854189300.
72	(24,28)	100.6	108.0	2700.3	(18,21)	1002847000.
73	(25,28)	101.3	108.0	2659.5	(19,21)	1004500000.
74	(25,28)	102.0	108.3	2636.2	(19,21)	1077198000.
75	(25,28)	102.9	109.4	2619.7	(19,21)	1366491000.
76	(25,28)	104.0	110.3	2615.6	(19,21)	1685674000.
77	(25,28)	104.8	110.5	2589.3	(19,21)	1777420000.
78	(25,28)	105.7	110.6	2568.8	(19,21)	1831075000.
79	(25,28)	106.5	111.4	2564.8	(19,21)	2201857000.
80	(25,28)	107.1	112.4	2576.7	(19,21)	2776780000.
81	(25,29)	107.5	112.8	2554.5	(19,22)	3015659000.
82	(25,29)	107.8	112.5	2512.4	(19,22)	2820924000.
83	(25,29)	108.1	112.5	2500.6	(19,22)	2800506000.
84	(25,29)	108.4	113.2	2510.3	(19,22)	3329856000.
85	(25,29)	108.8	113.9	2506.2	(19,22)	3923718000.
86	(25,29)	109.2	114.0	2477.8	(19,22)	3955418000.
87	(25,29)	109.7	113.8	2454.8	(19,22)	3844150000.
88	(25,29)	110.2	114.4	2466.0	(19,22)	4401238000.
89	(25,29)	110.4	115.3	2472.6	(19,22)	5427986000.
90	(25,29)	110.1	115.6	2449.7	(19,22)	5795058000.
91	(26,30)	110.2	115.1	2402.9	(19,22)	5177528000.
92	(25,30)	110.2	114.7	2411.5	(19,23)	4664467000.
93	(25,29)	110.4	115.1	2436.0	(19,22)	5138579000.
94	(25,29)	110.8	115.7	2437.5	(19,22)	5931819000.
95	(25,30)	110.9	115.7	2407.7	(19,23)	5839966000.
96	(26,30)	110.9	115.1	2374.1	(19,22)	5186314000.
97	(25,30)	110.9	115.2	2397.5	(19,23)	5224714000.
98	(25,30)	111.2	115.9	2413.5	(19,23)	6142530000.
99	(25,30)	111.5	116.3	2402.7	(19,23)	6693876000.
100	(26,30)	111.6	115.9	2347.7	(19,22)	6127690000.
101	(25,30)	111.6	115.3	2339.1	(19,23)	5432021000.
102	(25,30)	111.7	115.6	2360.1	(19,23)	5730796000.
103	(25,30)	111.9	116.2	2365.5	(19,23)	6574948000.
104	(25,31)	111.9	116.2	2335.8	(19,23)	6635434000.
105	(26,31)	111.8	115.7	2290.2	(19,23)	5948482000.
106	(25,31)	111.6	115.6	2302.4	(19,23)	5698429000.
107	(25,30)	111.8	116.0	2327.7	(19,23)	6320865000.
108	(25,31)	112.0	116.3	2322.5	(19,23)	6798729000.
109	(26,31)	111.9	116.0	2274.2	(19,23)	6280782000.
110	(26,31)	111.7	115.5	2265.2	(19,23)	5570830000.
111	(25,31)	111.6	115.6	2287.6	(19,23)	5718381000.
112	(25,31)	111.7	116.1	2295.0	(19,23)	6428668000.
113	(25,31)	111.6	116.1	2285.7	(19,23)	6475682000.
114	(26,32)	111.4	115.6	2229.1	(19,24)	5745353000
115	(26,31)	111.1	115.2	2233.9	(19,23)	5301305000.
116	(25,31)	111.0	115.5	2257.9	(19,23)	5672116000
117	(25,31)	111.2	115.8	2261.2	(19,23)	6035624000.
118	(25,32)	111.0	115.4	2222.1	(19,24)	5512544000.
119	(26,32)	110.7	114.7	2190.4	(19,24)	4670575000.
120	(26,31)	110.3	114.5	2207.8	(19,23)	4494979000.
121	(25,31)	110.1	114.9	2254.8	(19,23)	4908569000.
122	(25,32)	110.0	114.9	2224.1	(19,24)	4880032000
123	(25,32)	109.6	114.2	2197.2	(19,24)	4155168000

124	(25,32)	109.3	113.6	2182.7	(19,24)	3658782000.
125	(25,32)	109.0	114.0	2190.8	(19,24)	3985716000.
126	(25,32)	108.8	114.5	2217.9	(19,24)	4464878000.
127	(25,33)	108.7	114.2	2175.3	(18,24)	4147526000.
128	(25,33)	108.7	113.3	2154.5	(18,24)	3378024000.
129	(25,32)	108.7	113.0	2170.1	(19,24)	3195646000
130	(25,32)	108.6	113.7	2183.2	(19,24)	3734991000.
131	(25,32)	108.6	114.0	2221.7	(19,24)	4022995000.
132	(25,33)	108.4	113.4	2138.2	(18,24)	3466965000.
133	(25,33)	108.2	112.4	2137.0	(18,24)	2783074000.
134	(25,32)	108.0	112.5	2153.3	(19,24)	2828743000.
135	(25,32)	108.0	113.2	2205.2	(19,24)	3347247000.
136	(25,32)	107.8	113.3	2189.8	(19,24)	3385346000.
137	(25,33)	107.7	112.5	2118.8	(18,24)	2792566000.
138	(25,33)	107.6	111.8	2118.9	(18,24)	2390942000.
139	(25,32)	107.6	112.3	2134.3	(19,24)	2684353000.
140	(25,32)	107.7	113.0	2149.4	(19,24)	3133568000.
141	(25,33)	107.6	112.7	2135.5	(18,24)	2969131000.
142	(25,33)	107.4	111.8	2080.7	(18,24)	2380745000.
143	(25,33)	107.3	111.3	2091.2	(18,24)	2131986000.
144	(25,32)	107.3	111.8	2129.6	(19,24)	2412185000.
145	(25,32)	107.2	112.2	2188.8	(19,24)	2616753000.
146	(25,33)	107.0	111.6	2072.2	(18,24)	2310126000.
147	(25,33)	106.8	110.8	2069.4	(18,24)	1906792000.
148	(25,32)	106.7	110.9	2079.0	(19,24)	1952539000.
149	(25,32)	106.7	111.6	2170.6	(19,24)	2297736000.
150	(25,33)	106.5	111.7	2123.6	(18,24)	2332834000.
151	(25,33)	106.2	110.9	2104.1	(18,24)	1937887000.
152	(25,33)	105.9	110.1	2082.6	(18,24)	1638216000.
153	(25,32)	105.8	110.5	2100.5	(19,24)	1781624000.
154	(25,32)	105.7	111.1	2126.6	(19,24)	2048052000.
155	(25,33)	105.5	110.9	2109.4	(18,24)	1945405000.
156	(25,33)	105.2	110.0	2061.1	(18,24)	1588457000.
157	(25,33)	105.0	109.7	2076.0	(18,24)	1462431000.
158	(25,32)	104.9	110.3	2109.1	(19,24)	1686940000.
159	(25,31)	104.9	110.7	2199.4	(19,23)	1852823000.
160	(25,33)	104.6	110.2	2072.9	(18,24)	1643254000.
161	(25,33)	104.2	109.2	2091.0	(18,24)	1318951000.
162	(25,32)	104.0	109.1	2110.4	(19,24)	1274323000.
163	(25,31)	103.9	109.7	2194.7	(19,23)	1467282000.
164	(25,32)	103.8	109.8	2130.9	(19,24)	1512186000.
165	(25,32)	103.6	109.1	2152.3	(19,24)	1286831000.
166	(25,32)	103.3	108.4	2117.9	(19,24)	1086153000.
167	(25,32)	103.0	108.6	2137.2	(19,24)	1141144000.
168	(25,31)	102.9	109.1	2156.9	(19,23)	1287028000.
169	(25,32)	102.4	108.9	2163.9	(19,24)	1226903000.
170	(25,32)	102.1	108.0	2130.7	(19,24)	1007771000.
171	(25,32)	101.5	107.5	2141.3	(19,24)	900202000.
172	(25,31)	101.1	107.9	2179.7	(19,23)	987294700.
173	(25,30)	101.1	108.2	2261.2	(19,23)	1053721000.
174	(25,32)	101.0	107.7	2162.0	(19,24)	923670500.
175	(26,31)	101.0	106.6	2190.8	(19,23)	724174300.
176	(26,31)	101.1	106.2	2198.8	(19,23)	657772500.
177	(26,30)	101.2	106.6	2248.3	(19,22)	716783100.
178	(26,30)	101.1	106.6	2235.3	(19,22)	721587500.
179	(26,31)	101.2	105.8	2239.0	(19,23)	604530900.
180	(27,31)	101.1	104.8	2222.7	(20,23)	476523300.
181	(27,30)	100.8	104.5	2221.4	(20,22)	444059400.
182	(27,30)	100.4	104.7	2253.2	(20,22)	463573000.
183	(27,30)	99.5	104.3	2278.9	(20,22)	423489300
184	(27,31)	98.1	102.9	2245.1	(20,23)	306815700
185	(29,30)	97.5	100.8	2264.0	(21,22)	188907400.
186	(30,30)	97.3	99.4	2243.8	(22,22)	137934400.
187	(31,30)	97.3	99.6	2296.6	(23,22)	144433500.
188	(32,30)	97.5	99.9	2225.7	(23,22)	155956900.
189	(32,30)	97.9	99.7	2175.8	(23,22)	147374200.

190	(32, 30)	98.1	99.4	2205.2	(23, 22)	137704200.
191	(32, 30)	98.3	99.8	2208.6	(23, 22)	150843200.
192	(32, 30)	98.4	100.5	2181.1	(23, 22)	176607500.
193	(33, 30)	98.5	100.6	2168.3	(24, 22)	183181100.
194	(33, 30)	98.4	100.1	2198.7	(24, 22)	162491100.
195	(32, 30)	98.2	99.6	2235.7	(23, 22)	143740700.
196	(32, 30)	98.0	99.7	2238.2	(23, 22)	149245900.
197	(32, 30)	97.8	100.1	2216.3	(23, 22)	162643500.
198	(32, 30)	97.6	99.9	2197.9	(23, 22)	154995600.
199	(32, 30)	97.4	99.1	2183.4	(23, 22)	129643000.
200	(32, 30)	97.2	98.6	2209.9	(23, 22)	116068000.
201	(32, 30)	97.0	99.0	2220.4	(23, 22)	125552400.
202	(32, 30)	96.8	99.3	2225.1	(23, 22)	135648900.
203	(32, 30)	96.6	99.0	2238.4	(23, 22)	124625400.
204	(31, 30)	96.4	98.2	2286.9	(23, 22)	104544800.
205	(31, 30)	96.2	98.0	2293.2	(23, 22)	99851940.
206	(32, 30)	96.0	98.5	2261.2	(23, 22)	111282000.
207	(32, 30)	95.9	98.6	2213.2	(23, 22)	116114100.
208	(33, 30)	95.6	98.1	2157.9	(24, 22)	102960000.
209	(32, 30)	95.4	97.5	2174.3	(23, 22)	88619820.
210	(32, 30)	95.3	97.6	2182.4	(23, 22)	90366260.
211	(32, 30)	95.2	98.0	2185.6	(23, 22)	100716300.
212	(32, 30)	95.1	98.0	2188.1	(23, 22)	99541440.
213	(32, 30)	95.1	97.3	2206.0	(23, 22)	84277180.
214	(32, 30)	95.0	96.6	2227.6	(23, 22)	72419230.
215	(32, 30)	94.8	96.8	2223.0	(23, 22)	75293520.
216	(33, 30)	94.6	97.2	2190.0	(24, 22)	82422240.
217	(34, 30)	94.3	96.9	2168.0	(24, 22)	77664850.
218	(34, 30)	94.0	96.0	2195.4	(24, 22)	62725410.
219	(33, 30)	93.6	95.2	2219.4	(24, 22)	52279260.
220	(33, 29)	93.2	95.2	2216.0	(24, 21)	52978930.
221	(32, 30)	92.8	95.5	2201.4	(23, 22)	55651840.
222	(32, 30)	92.3	95.0	2187.3	(23, 22)	50473460.
223	(32, 30)	92.0	94.2	2186.4	(23, 22)	41346260.
224	(32, 30)	91.7	93.8	2228.2	(23, 22)	37594670.
225	(32, 30)	91.4	94.0	2240.7	(23, 22)	40225630.
226	(32, 30)	91.2	94.2	2243.8	(23, 22)	41623260.
227	(32, 30)	90.9	93.7	2199.7	(23, 22)	37457760.
228	(32, 30)	90.7	93.2	2214.3	(23, 22)	33094190.
229	(33, 30)	90.6	93.3	2201.2	(24, 22)	34195200.
230	(33, 30)	90.5	93.8	2205.9	(24, 22)	38274060.
231	(33, 30)	90.5	93.8	2187.4	(24, 22)	38455220.
232	(34, 30)	90.5	93.3	2174.6	(24, 22)	33767140.
233	(33, 30)	90.5	92.9	2168.2	(24, 22)	30762770.
234	(33, 29)	90.5	93.3	2150.2	(24, 21)	33759980.
235	(33, 30)	90.4	93.8	2136.0	(24, 22)	38246540.
236	(34, 30)	90.2	93.7	2131.5	(24, 22)	36815360.

TRACK TRAIL FOR SPQBELL.DA

BLOCK	(IR3D, JR3D)	AMAX	AMAXUP	RSUM	LOG COORD'S	POWER
83	(31,27)	91.0	96.1	2430.8	(23,20)	64225020.
84	(29,27)	93.8	98.2	2453.8	(22,20)	105504800.
85	(28,27)	96.0	100.0	2465.5	(21,20)	158297600.
86	(28,27)	97.9	103.1	2488.9	(21,20)	323441400.
87	(28,27)	101.2	106.6	2466.6	(21,20)	722389500.
88	(28,27)	104.3	109.2	2436.9	(21,20)	1323906000.
89	(29,28)	107.4	110.9	2358.5	(22,21)	1934262000.
90	(29,28)	109.6	112.0	2335.7	(22,21)	2488385000.
91	(29,28)	110.9	113.0	2393.0	(22,21)	3187068000.
92	(28,28)	111.5	114.1	2435.0	(21,21)	4055571000.
93	(28,28)	111.4	114.7	2427.5	(21,21)	4639805000.
94	(28,28)	110.6	114.5	2412.2	(21,21)	4451533000.
95	(28,28)	110.5	113.7	2422.5	(21,21)	3730891000.
96	(27,27)	110.2	113.1	2465.0	(20,20)	3221791000.
97	(27,27)	109.8	113.1	2495.8	(20,20)	3241991000.
98	(28,27)	109.7	113.3	2479.7	(21,20)	3372150000.
99	(28,28)	109.9	113.1	2439.4	(21,21)	3242620000.
100	(28,28)	110.2	113.0	2452.2	(21,21)	3178479000.
101	(27,27)	110.6	113.5	2456.5	(20,20)	3569703000.
102	(28,27)	111.1	114.2	2443.7	(21,20)	4174134000.
103	(28,28)	111.4	114.4	2395.7	(21,21)	4377145000.
104	(28,28)	111.6	114.2	2364.3	(21,21)	4180346000.
105	(28,28)	111.7	114.2	2376.4	(21,21)	4151002000.
106	(27,28)	111.8	114.6	2405.1	(20,21)	4526875000.
107	(28,28)	112.0	114.9	2392.6	(21,21)	4852052000.
108	(28,28)	111.9	114.7	2345.9	(21,21)	4678664000.
109	(28,28)	111.7	114.3	2356.0	(21,21)	4264072000.
110	(27,28)	111.5	114.1	2413.0	(20,21)	4066774000.
111	(27,28)	111.3	114.1	2450.5	(20,21)	4089615000.
112	(27,28)	110.9	113.9	2433.1	(20,21)	3923434000.
113	(28,28)	110.5	113.5	2412.4	(21,21)	3523621000.
114	(27,28)	110.2	113.1	2450.8	(20,21)	3231974000.
115	(26,28)	109.9	113.1	2509.6	(20,21)	3234041000.
116	(27,27)	109.6	113.1	2525.4	(20,20)	3273253000.
117	(27,28)	109.1	112.8	2483.6	(20,21)	3042632000.
118	(27,28)	108.6	112.3	2465.6	(20,21)	2708673000.
119	(26,28)	108.1	112.2	2517.3	(20,21)	2606403000.
120	(26,27)	107.7	112.4	2565.9	(20,21)	2739876000.
121	(26,28)	107.3	112.4	2552.1	(20,21)	2754644000.
122	(27,28)	107.0	112.0	2504.2	(20,21)	2493447000.
123	(27,28)	106.5	111.5	2494.0	(20,21)	2214656000.
124	(26,28)	106.0	111.4	2518.5	(20,21)	2196120000.
125	(26,28)	105.7	111.7	2550.9	(20,21)	2319162000.
126	(26,28)	105.4	111.5	2527.9	(20,21)	2249933000.
127	(27,28)	105.8	111.1	2491.5	(20,21)	2039548000.
128	(26,28)	106.5	111.2	2512.8	(20,21)	2083592000.
129	(26,28)	107.2	112.0	2521.8	(20,21)	2532806000.
130	(26,28)	107.7	112.7	2512.8	(20,21)	2972353000.
131	(26,28)	107.9	112.6	2474.1	(20,21)	2894779000.
132	(27,29)	107.8	111.8	2443.6	(20,22)	2401743000.
133	(26,28)	107.3	111.1	2494.1	(20,21)	2046694000.
134	(26,28)	107.1	111.2	2518.7	(20,21)	2105749000.
135	(26,28)	107.3	111.5	2525.2	(20,21)	2263428000.
136	(27,28)	107.6	111.3	2480.9	(20,21)	2149138000.
137	(27,29)	107.6	110.8	2438.5	(20,22)	1905851000.
138	(26,28)	107.7	110.9	2463.1	(20,21)	1957545000.
139	(26,28)	108.2	111.7	2445.5	(20,21)	2343523000.
140	(26,29)	108.6	112.2	2430.1	(20,22)	2612555000.
141	(27,29)	108.8	111.9	2391.3	(20,22)	2431956000.
142	(26,29)	108.7	111.2	2384.8	(20,22)	2065661000.
143	(26,29)	108.7	111.1	2423.3	(20,22)	2019455000.

144	(25,29)	108.7	111.7	2408.5	(19,22)	2335868000.
145	(26,29)	108.7	112.1	2392.7	(20,22)	2542899000.
146	(26,29)	108.3	111.6	2359.3	(20,22)	2311773000.
147	(26,30)	107.8	110.8	2337.2	(19,22)	1927010000.
148	(26,29)	107.5	110.8	2371.5	(20,22)	1901324000.
149	(25,29)	107.6	111.6	2389.8	(19,22)	2273069000.
150	(26,29)	107.9	112.0	2373.3	(20,22)	2540009000.
151	(26,30)	107.8	111.7	2337.8	(19,22)	2333060000.
152	(26,30)	107.3	110.8	2321.2	(19,22)	1920337000.
153	(25,30)	106.9	110.7	2358.5	(19,23)	1844082000.
154	(25,29)	107.1	111.4	2409.5	(19,22)	2187878000.
155	(25,30)	107.5	111.9	2395.3	(19,23)	2463612000.
156	(26,30)	107.4	111.6	2364.6	(19,22)	2280020000.
157	(26,30)	106.9	110.8	2330.7	(19,22)	1894247000.
158	(25,30)	106.5	110.7	2359.0	(19,23)	1868510000.
159	(25,30)	107.0	111.6	2354.7	(19,23)	2302546000.
160	(25,30)	107.5	112.3	2340.9	(19,23)	2681737000.
161	(25,31)	107.4	112.1	2299.0	(19,23)	2542455000.
162	(25,32)	106.4	111.2	2260.4	(19,24)	2072099000.
163	(25,31)	106.0	110.7	2296.3	(19,23)	1841569000.
164	(24,31)	106.3	111.1	2294.8	(18,23)	2056025000.
165	(24,31)	106.5	111.6	2311.5	(18,23)	2313081000.
166	(25,31)	106.6	111.4	2288.3	(19,23)	2175764000.
167	(25,32)	106.5	110.4	2256.6	(19,24)	1738431000.
168	(24,31)	106.1	109.7	2319.1	(18,23)	1479959000.
169	(24,30)	105.9	110.1	2311.6	(18,23)	1617434000.
170	(24,30)	105.9	110.6	2330.9	(18,23)	1835012000.
171	(25,31)	105.9	110.4	2271.3	(19,23)	1755920000.
172	(25,31)	105.8	109.6	2232.3	(19,23)	1450711000.
173	(25,31)	105.6	109.3	2231.5	(19,23)	1351844000.
174	(24,31)	105.7	110.1	2254.6	(18,23)	1639333000.
175	(25,30)	106.0	111.0	2317.7	(19,23)	1983132000.
176	(25,32)	106.2	111.0	2207.6	(19,24)	1988660000.
177	(25,32)	106.4	110.4	2180.9	(19,24)	1745802000.
178	(25,31)	106.6	110.4	2181.9	(19,23)	1720745000.
179	(25,31)	107.0	111.2	2209.7	(19,23)	2038536000.
180	(25,30)	107.3	111.9	2298.2	(19,23)	2466135000.
181	(25,32)	107.2	111.8	2162.5	(19,24)	2412237000.
182	(25,32)	107.0	111.1	2162.8	(19,24)	2056378000.
183	(25,32)	106.9	110.9	2172.7	(19,24)	1932516000.
184	(24,32)	106.9	111.5	2166.4	(18,24)	2244708000.
185	(25,31)	107.1	112.1	2272.6	(19,23)	2588039000.
186	(24,33)	107.0	112.0	2157.9	(18,25)	2505583000.
187	(25,32)	106.8	111.3	2169.7	(19,24)	2133510000.
188	(25,32)	106.7	111.0	2167.2	(19,24)	2009105000.
189	(24,32)	106.8	111.7	2136.0	(18,24)	2321274000.
190	(24,32)	107.0	112.2	2216.3	(18,24)	2658143000.
191	(24,33)	107.1	112.1	2105.9	(18,25)	2583442000.
192	(25,33)	107.1	111.5	2119.5	(18,24)	2263205000.
193	(24,33)	107.0	111.5	2116.4	(18,25)	2225058000.
194	(24,33)	107.1	112.2	2092.5	(18,25)	2603144000.
195	(24,32)	107.2	112.7	2160.1	(18,24)	2950928000.
196	(24,34)	107.2	112.6	2058.2	(18,25)	2862156000.
197	(25,33)	107.2	112.1	2081.8	(18,24)	2549582000.
198	(24,33)	107.3	112.0	2039.9	(18,25)	2521617000.
199	(24,33)	107.5	112.5	2038.3	(18,25)	2843036000.
200	(24,32)	107.6	112.8	2129.3	(18,24)	3052812000.
201	(24,34)	107.6	112.5	2026.6	(18,25)	2838366000.
202	(25,33)	107.7	112.0	2030.8	(18,24)	2522847000.
203	(25,33)	107.8	112.1	2006.9	(18,24)	2582853000.
204	(24,33)	107.9	112.7	2042.0	(18,25)	2954324000.
205	(24,33)	108.0	112.9	2074.9	(18,25)	3098115000.
206	(24,34)	108.0	112.4	2016.5	(18,25)	2770084000.
207	(25,34)	108.0	111.8	2008.2	(18,25)	2417893000.
208	(24,34)	108.1	112.0	2003.3	(18,25)	2527344000.
209	(24,34)	108.2	112.7	2050.5	(18,25)	2923660000.

210	(24,33)	108.3	112.8	2130.3	(18,25)	2986878000
211	(24,34)	108.1	112.1	2033.5	(18,25)	2554752000.
212	(25,34)	108.1	111.4	2018.7	(18,25)	2193674000.
213	(24,34)	108.2	111.8	2019.6	(18,25)	2393772000.
214	(24,33)	108.3	112.6	2092.3	(18,25)	2855251000.
215	(24,34)	108.3	112.6	2076.1	(18,25)	2877338000.
216	(24,35)	108.1	111.7	2021.7	(18,26)	2344257000.
217	(25,34)	107.8	110.7	1997.0	(18,25)	1859368000.
218	(24,34)	107.6	110.8	1989.3	(18,25)	1903944000.
219	(24,33)	107.5	111.4	2104.1	(18,25)	2210516000.
220	(24,35)	107.3	111.4	2009.1	(18,26)	2185611000.
221	(25,34)	106.9	110.5	2027.6	(18,25)	1765449000.
222	(25,34)	106.4	109.5	2021.3	(18,25)	1397157000.
223	(25,33)	106.1	109.5	2015.5	(18,24)	1399541000.
224	(25,33)	106.2	110.0	2084.8	(18,24)	1573353000.
225	(25,33)	106.0	109.9	2057.1	(18,24)	1539064000.
226	(25,34)	105.7	109.1	1995.9	(18,25)	1301626000.
227	(25,33)	105.2	108.5	2002.3	(18,24)	1130406000.
228	(25,33)	104.9	108.7	2013.8	(18,24)	1161482000.
229	(25,32)	104.8	108.9	2161.9	(19,24)	1221545000.
230	(24,34)	104.5	108.5	2002.7	(18,25)	1109580000.
231	(25,33)	103.9	107.5	2048.4	(18,24)	881319200.
232	(25,33)	103.0	106.5	2012.5	(18,24)	713639200.
233	(24,33)	102.2	106.2	2045.3	(18,25)	663744800.
234	(24,33)	101.6	105.9	2112.8	(18,25)	617499100.
235	(24,33)	101.1	104.9	2080.3	(18,25)	492986100.
236	(25,33)	100.2	103.3	2121.3	(18,24)	341482000.
237	(25,33)	99.1	102.0	2055.8	(18,24)	250219600.
238	(24,32)	97.9	101.5	2139.3	(18,24)	224101400.
239	(25,30)	96.5	101.0	2300.1	(19,23)	199253300.
240	(24,32)	94.9	99.8	2224.6	(18,24)	149786900.
241	(25,31)	93.3	98.1	2249.7	(19,23)	102700500.
242	(26,30)	92.0	97.3	2270.5	(19,22)	85948530.
243	(26,30)	90.5	97.5	2340.3	(19,22)	88246700.
244	(26,29)	89.0	97.0	2379.4	(20,22)	80266190.
245	(26,30)	87.9	95.8	2355.5	(19,22)	60202510.
246	(26,30)	87.2	94.7	2354.4	(19,22)	46304260.
247	(26,29)	87.0	94.8	2391.0	(20,22)	47956910.
248	(26,29)	87.3	95.3	2416.5	(20,22)	54031220.
249	(26,29)	86.8	95.0	2409.2	(20,22)	49621100
250	(26,29)	86.6	93.4	2418.8	(20,22)	34860370

TRACK TRAIL FOR SPQCOT1.DA

BLOCK	(IR3D, JR3D)	AMAX	AMAXUP	RSUM	LOG COORD'S	POWER
60	(25, 29)	85.4	92.9	2514.3	(19, 22)	31042450.
61	(25, 29)	88.0	95.3	2390.1	(19, 22)	53468080.
62	(25, 29)	89.7	96.7	2440.0	(19, 22)	73845140.
63	(25, 29)	90.5	97.2	2490.3	(19, 22)	82517440.
64	(25, 29)	90.4	97.1	2512.0	(19, 22)	82059260.
65	(25, 29)	90.6	97.2	2536.8	(19, 22)	82784450.
66	(25, 29)	91.3	97.4	2538.8	(19, 22)	87377070.
67	(25, 29)	92.0	97.4	2507.3	(19, 22)	87551860.
68	(25, 29)	92.0	96.8	2520.4	(19, 22)	76329410.
69	(26, 28)	90.5	95.6	2557.6	(20, 21)	57304400.
70	(26, 28)	87.7	93.9	2612.0	(20, 21)	38741980.
75	(26, 29)	87.1	93.1	2496.1	(20, 22)	32324020.
76	(27, 29)	86.0	93.4	2459.1	(20, 22)	34332000.
77	(27, 30)	85.9	93.4	2455.1	(20, 22)	34758540.
78	(26, 30)	86.8	93.1	2476.1	(19, 22)	32302480.
85	(26, 29)	84.2	93.0	2650.3	(20, 22)	31639980.
86	(26, 30)	86.2	93.5	2602.3	(19, 22)	35607760.
87	(27, 30)	87.8	93.6	2524.6	(20, 22)	36234180.
88	(28, 30)	88.4	93.3	2436.5	(21, 22)	33526460.
99	(25, 28)	85.1	93.5	2675.8	(19, 21)	35619390.
100	(25, 28)	88.6	97.6	2611.7	(19, 21)	91321440.
101	(25, 29)	94.8	102.7	2538.7	(19, 22)	296169200.
102	(25, 29)	99.1	106.5	2464.1	(19, 22)	714619400.
103	(25, 29)	101.7	108.8	2438.6	(19, 22)	1193328000.
104	(25, 30)	102.6	109.6	2407.2	(19, 23)	1449578000.
105	(25, 30)	103.1	109.4	2364.1	(19, 23)	1395504000.
106	(26, 30)	103.3	109.3	2330.3	(19, 22)	1342386000.
107	(25, 30)	103.6	110.0	2316.8	(19, 23)	1589541000.
108	(25, 30)	104.1	111.0	2328.0	(19, 23)	1975855000.
109	(25, 31)	104.5	111.2	2298.4	(19, 23)	2082319000.
110	(26, 31)	104.6	110.7	2260.2	(19, 23)	1880681000.
111	(26, 31)	104.7	110.6	2258.5	(19, 23)	1817613000.
112	(26, 30)	104.9	111.3	2261.1	(19, 22)	2141207000.
113	(26, 31)	105.1	112.0	2266.4	(19, 23)	2498946000.
114	(26, 31)	105.4	111.8	2264.4	(19, 23)	2416979000.
115	(26, 31)	104.9	111.2	2239.9	(19, 23)	2079912000.
116	(26, 31)	104.7	111.1	2249.8	(19, 23)	2042071000.
117	(26, 30)	105.1	111.8	2260.4	(19, 22)	2408373000.
118	(26, 30)	105.6	112.3	2280.6	(19, 22)	2662134000.
119	(26, 31)	105.2	111.8	2248.0	(19, 23)	2415113000.
120	(26, 31)	104.4	111.1	2235.2	(19, 23)	2050842000.
121	(26, 30)	104.3	111.2	2251.2	(19, 22)	2113270000.
122	(26, 30)	104.8	112.0	2279.8	(19, 22)	2506203000.
123	(26, 31)	105.1	112.2	2267.0	(19, 23)	2626511000.
124	(26, 31)	104.7	111.6	2246.7	(19, 23)	2292644000.
125	(26, 31)	104.0	111.1	2238.5	(19, 23)	2019850000.
126	(26, 30)	104.4	111.5	2260.2	(19, 22)	2229586000.
127	(26, 31)	105.2	112.2	2275.5	(19, 23)	2614813000.
128	(26, 31)	105.3	112.1	2272.1	(19, 23)	2585440000.
129	(26, 31)	105.4	111.5	2226.3	(19, 23)	2254763000.
130	(26, 31)	105.4	111.5	2223.1	(19, 23)	2229705000.
131	(26, 31)	105.7	112.3	2254.1	(19, 23)	2693336000.
132	(26, 31)	106.0	112.9	2264.3	(19, 23)	3078839000.
133	(26, 31)	105.9	112.6	2241.0	(19, 23)	2881080000.
134	(26, 31)	105.7	112.0	2220.7	(19, 23)	2498504000.
135	(26, 31)	105.8	112.1	2240.6	(19, 23)	2588681000.
136	(26, 31)	106.3	112.9	2263.4	(19, 23)	3088614000.
137	(26, 31)	106.8	113.2	2250.2	(19, 23)	3292755000.
138	(26, 31)	107.1	112.7	2223.7	(19, 23)	2966757000.
139	(26, 31)	107.2	112.4	2215.0	(19, 23)	2733360000.
140	(26, 31)	107.4	112.9	2235.6	(19, 23)	3101723000.

141	(26,31)	107.8	113.6	2259.5	(19,23)	3657970000.
142	(26,31)	108.0	113.6	2238.5	(19,23)	3649538000.
143	(27,31)	108.1	113.1	2208.7	(20,23)	3237423000.
144	(26,31)	108.3	113.0	2216.4	(19,23)	3192320000.
145	(26,31)	108.4	113.7	2252.9	(19,23)	3712390000.
146	(26,31)	108.5	114.1	2245.1	(19,23)	4085778000.
147	(27,31)	108.4	113.8	2220.8	(20,23)	3820878000.
148	(27,31)	108.3	113.5	2222.7	(20,23)	3515752000.
149	(27,30)	108.6	113.8	2243.2	(20,22)	3845169000.
150	(26,31)	108.9	114.5	2255.9	(19,23)	4469068000.
151	(27,31)	108.8	114.5	2248.8	(20,23)	4483703000.
152	(27,31)	108.3	114.0	2215.5	(20,23)	3952282000.
153	(27,30)	108.0	113.7	2232.2	(20,22)	3756018000.
154	(26,30)	108.3	114.2	2267.1	(19,22)	4215973000.
155	(27,31)	108.5	114.6	2265.1	(20,23)	4578566000.
156	(27,31)	108.1	114.3	2240.5	(20,23)	4268083000.
157	(27,30)	107.6	113.9	2246.1	(20,22)	3890538000.
158	(26,30)	107.8	114.2	2278.7	(19,22)	4168051000.
159	(26,30)	108.2	114.8	2283.9	(19,22)	4751512000.
160	(27,31)	108.4	114.8	2266.2	(20,23)	4733600000.
161	(27,30)	108.4	114.3	2255.6	(20,22)	4243263000.
162	(27,30)	108.5	114.2	2280.5	(20,22)	4166506000.
163	(27,30)	108.8	114.7	2293.5	(20,22)	4712178000.
164	(27,30)	109.1	115.0	2300.3	(20,22)	5015826000.
165	(27,30)	109.4	114.7	2271.0	(20,22)	4648399000.
166	(27,30)	107.5	114.4	2289.9	(20,22)	4343058000.
167	(27,30)	109.6	114.7	2312.4	(20,22)	4713828000.
168	(27,30)	109.8	115.2	2313.4	(20,22)	5202739000.
169	(27,30)	109.9	115.0	2296.7	(20,22)	5007929000.
170	(27,30)	110.0	114.6	2281.0	(20,22)	4545667000.
171	(27,30)	110.2	114.7	2299.0	(20,22)	4705628000.
172	(27,30)	110.5	115.3	2299.5	(20,22)	5367312000.
173	(27,30)	110.8	115.4	2277.2	(20,22)	5537014000.
174	(27,30)	111.0	115.1	2259.1	(20,22)	5096165000.
175	(27,30)	111.2	114.9	2284.3	(20,22)	4930593000.
176	(27,30)	111.3	115.4	2311.4	(20,22)	5440324000.
177	(27,30)	111.5	115.7	2306.9	(20,22)	5856551000.
178	(28,30)	111.8	115.5	2265.3	(21,22)	5598089000.
179	(28,30)	112.0	115.2	2250.0	(21,22)	5252522000.
180	(27,30)	112.0	115.4	2283.2	(20,22)	5498110000.
181	(27,30)	111.9	115.7	2295.3	(20,22)	5949157000.
182	(27,30)	111.7	115.6	2277.2	(20,22)	5756375000.
183	(27,30)	111.5	115.0	2266.3	(20,22)	5019578000.
184	(27,29)	111.0	114.5	2308.4	(20,22)	4504982000.
185	(26,29)	110.3	114.5	2362.3	(20,22)	4466086000.
186	(27,29)	109.3	114.4	2357.2	(20,22)	4359885000.
187	(27,29)	108.5	113.8	2333.5	(20,22)	3837908000.
188	(26,29)	107.9	113.0	2401.4	(20,22)	3175644000.
189	(25,29)	107.6	112.4	2469.3	(19,22)	2737338000.
190	(25,29)	108.1	112.0	2490.4	(19,22)	2499679000.
191	(26,29)	108.5	111.7	2433.7	(20,22)	2325176000.
192	(26,29)	108.9	111.6	2387.5	(20,22)	2287869000.
193	(26,29)	109.4	111.8	2378.3	(20,22)	2415454000.
194	(27,29)	109.5	112.0	2372.4	(20,22)	2497200000.
195	(27,29)	109.1	111.6	2325.5	(20,22)	2296536000.
196	(28,29)	108.1	110.8	2265.7	(21,22)	1886685000.
197	(27,29)	107.3	109.8	2287.3	(20,22)	1513433000.
198	(27,29)	106.8	109.1	2289.1	(20,22)	1275035000.
199	(27,29)	105.9	108.3	2288.8	(20,22)	1066559000.
200	(28,29)	104.5	107.1	2237.7	(21,22)	812109100.
201	(28,30)	102.8	105.5	2182.7	(21,22)	561211900.
202	(28,29)	100.5	103.9	2240.7	(21,22)	389719800.
203	(27,28)	97.1	102.7	2401.5	(20,21)	298101200.
204	(26,27)	96.5	101.7	2419.4	(20,21)	232583900.
205	(26,27)	96.0	100.2	2486.7	(20,21)	164160900.
206	(27,28)	94.7	98.0	2501.8	(20,21)	99475970.
207	(27,28)	92.3	95.2	2442.9	(20,21)	52415330.

TRACK TRAIL FOR SPGCOT2.DA

BLOCK	(IR3D, JR3D)	AMAX	AMAXUP	RSUM	LOG COORD'S	POWER
61	(25,30)	86.4	94.8	2494.0	(19,23)	47701360.
62	(26,29)	89.5	97.7	2508.4	(20,22)	92445540.
63	(25,29)	91.0	99.2	2569.1	(19,22)	130388500.
64	(25,28)	90.8	99.5	2632.2	(19,21)	141492900.
65	(25,28)	90.7	99.3	2646.6	(19,21)	135249400.
66	(25,28)	91.7	100.4	2610.2	(19,21)	172255000.
67	(24,28)	93.1	102.6	2564.1	(18,21)	290361100.
68	(24,29)	95.4	104.4	2569.6	(18,22)	437578800.
69	(24,29)	97.1	105.1	2569.2	(18,22)	510922200.
70	(24,29)	97.6	104.6	2555.6	(18,22)	458501900.
71	(25,29)	97.1	103.1	2534.9	(19,22)	325777700.
72	(26,29)	95.1	100.9	2500.2	(20,22)	197160400.
73	(26,29)	92.2	98.6	2490.5	(20,22)	115228000.
74	(26,29)	88.6	96.6	2581.9	(20,22)	72405260.
75	(25,29)	86.6	95.6	2594.9	(19,22)	57822270.
76	(26,29)	87.9	95.7	2587.1	(20,22)	59357410.
77	(26,30)	88.6	96.3	2516.9	(19,22)	67896850.
78	(27,30)	90.1	96.8	2425.0	(20,22)	76479460.
79	(27,30)	90.8	97.0	2398.6	(20,22)	80068030.
80	(27,30)	92.3	96.9	2355.8	(20,22)	77566560.
81	(27,30)	92.9	96.6	2302.3	(20,22)	72841360.
82	(28,30)	92.9	96.5	2340.1	(21,22)	70021140.
83	(27,30)	92.8	96.4	2406.8	(20,22)	69079700.
84	(27,30)	92.4	96.2	2479.9	(20,22)	65987520.
85	(27,30)	91.4	95.6	2537.1	(20,22)	57860260.
86	(25,29)	89.6	95.2	2614.4	(19,22)	51954220.
87	(24,28)	88.4	96.6	2631.4	(18,21)	73032180.
88	(24,28)	92.2	100.1	2573.6	(18,21)	163882200.
89	(24,28)	94.9	103.4	2543.2	(18,21)	344051700.
90	(25,28)	99.3	106.1	2503.6	(19,21)	649246500.
91	(25,29)	103.2	109.1	2487.3	(19,22)	1296673000.
92	(25,29)	106.0	111.8	2477.8	(19,22)	2381097000.
93	(25,29)	107.5	113.5	2464.2	(19,22)	3507630000.
94	(25,29)	108.9	114.1	2425.9	(19,22)	4038186000.
95	(26,30)	109.8	114.1	2388.7	(19,22)	4048137000.
96	(26,29)	110.5	114.4	2395.1	(20,22)	4368323000.
97	(25,29)	111.0	115.3	2394.3	(19,22)	5393711000.
98	(25,30)	111.1	116.0	2379.4	(19,23)	6343197000.
99	(26,30)	110.4	116.0	2336.0	(19,22)	6314885000.
100	(26,30)	110.5	115.7	2300.1	(19,22)	5841863000.
101	(26,30)	110.6	115.8	2305.7	(19,22)	6067343000.
102	(26,30)	111.3	116.4	2333.6	(19,22)	6988669000.
103	(26,30)	111.7	116.7	2309.0	(19,22)	7369236000.
104	(27,30)	111.9	116.3	2253.1	(20,22)	6744326000.
105	(27,30)	112.0	115.9	2223.5	(20,22)	6108697000.
106	(26,30)	112.0	116.0	2234.0	(19,22)	6334218000.
107	(26,30)	112.0	116.3	2256.4	(19,22)	6804427000.
108	(26,31)	111.7	116.0	2253.4	(19,23)	6362055000.
109	(27,31)	111.0	115.2	2226.4	(20,23)	5240398000.
110	(26,31)	110.2	114.6	2254.6	(19,23)	4614484000.
111	(26,30)	109.7	114.9	2305.0	(19,22)	4861432000.
112	(26,31)	109.3	115.0	2335.8	(19,23)	5068423000.
113	(26,31)	108.4	114.5	2311.3	(19,23)	4495167000.
114	(26,31)	107.7	113.7	2296.9	(19,23)	3677266000.
115	(26,30)	107.3	113.5	2317.1	(19,22)	3509888000.
116	(25,30)	107.1	113.9	2367.3	(19,23)	3897564000.
117	(26,30)	106.9	114.0	2358.5	(19,22)	3945339000.
118	(26,31)	106.5	113.3	2319.5	(19,23)	3380589000.
119	(26,31)	106.2	112.7	2289.8	(19,23)	2935278000.

120	(26, 30)	106. 3	113. 1	2303. 7	(19, 22)	3232333000.
121	(26, 30)	107. 3	113. 8	2332. 0	(19, 22)	3832438000.
122	(26, 31)	107. 7	113. 8	2302. 8	(19, 23)	3837285000.
123	(27, 31)	107. 6	113. 1	2272. 2	(20, 23)	3220414000.
124	(27, 30)	107. 2	112. 5	2281. 2	(20, 22)	2838498000.
125	(26, 30)	107. 6	113. 0	2294. 4	(19, 22)	3196514000.
126	(26, 30)	108. 3	113. 7	2317. 6	(19, 22)	3748895000.
127	(26, 31)	108. 5	113. 6	2292. 4	(19, 23)	3664392000.
128	(27, 31)	108. 1	112. 7	2250. 2	(20, 23)	2981316000.
129	(27, 30)	107. 6	111. 9	2266. 7	(20, 22)	2437153000.
130	(26, 30)	107. 3	111. 9	2301. 3	(19, 22)	2438808000.
131	(26, 30)	107. 5	112. 2	2346. 4	(19, 22)	2613435000.
132	(26, 30)	107. 4	111. 9	2321. 2	(19, 22)	2447913000.
133	(27, 30)	107. 3	111. 2	2281. 7	(20, 22)	2100776000.
134	(27, 30)	107. 3	111. 2	2305. 6	(20, 22)	2105975000.
135	(26, 30)	107. 5	112. 1	2288. 6	(19, 22)	2558230000.
136	(26, 30)	107. 8	112. 7	2298. 7	(19, 22)	2923831000.
137	(27, 30)	107. 9	112. 4	2274. 9	(20, 22)	2753450000.
138	(27, 30)	107. 8	111. 7	22[illegible]6. 0	(20, 22)	2332953000.
139	(27, 30)	107. 7	111. 6	2270. 6	(20, 22)	2287852000.
140	(26, 30)	107. 8	112. 3	2292. 7	(19, 22)	2704029000.
141	(26, 30)	107. 9	112. 8	2300. 4	(19, 22)	3011331000.
142	(27, 30)	107. 9	112. 5	2271. 0	(20, 22)	2789678000.
143	(27, 30)	107. 6	111. 7	2246. 4	(20, 22)	2363868000.
144	(26, 30)	107. 5	111. 7	2270. 2	(19, 22)	2328704000.
145	(26, 30)	107. 5	112. 3	2321. 4	(19, 22)	2715037000.
146	(26, 30)	107. 7	112. 7	2326. 4	(19, 22)	2958994000.
147	(27, 31)	107. 7	112. 3	2292. 3	(20, 23)	2716453000.
148	(27, 30)	107. 6	111. 7	2271. 2	(20, 22)	2341137000.
149	(26, 30)	107. 5	111. 7	2306. 4	(19, 22)	2365296000.
150	(26, 30)	107. 5	112. 4	2353. 7	(19, 22)	2750218000.
151	(26, 30)	107. 4	112. 7	2354. 3	(19, 22)	2943479000.
152	(27, 30)	107. 0	112. 2	2309. 0	(20, 22)	2635422000.
153	(27, 30)	106. 5	111. 3	2293. 0	(20, 22)	2113880000.
154	(26, 30)	105. 9	110. 6	2363. 9	(19, 22)	1839671000.
155	(26, 30)	105. 2	110. 7	2419. 5	(19, 22)	1862243000.
156	(26, 30)	104. 4	110. 7	2435. 8	(19, 22)	1843344000.
157	(26, 30)	104. 3	110. 0	2394. 8	(19, 22)	1598544000.
158	(27, 30)	103. 6	109. 2	2373. 4	(20, 22)	1326310000.
159	(26, 30)	103. 9	109. 2	2400. 1	(19, 22)	1305424000.
160	(26, 30)	104. 2	109. 7	2407. 4	(19, 22)	1494911000.
161	(26, 30)	104. 3	110. 0	2410. 5	(19, 22)	1569633000.
162	(27, 30)	103. 8	109. 3	2367. 8	(20, 22)	1360166000.
163	(27, 30)	103. 3	108. 2	2376. 0	(20, 22)	1052724000.
164	(27, 29)	102. 8	107. 7	2423. 4	(20, 22)	939084500.
165	(26, 29)	102. 5	108. 2	2412. 7	(20, 22)	1048746000.
166	(27, 29)	103. 3	108. 6	2407. 6	(20, 22)	1140055000.
167	(27, 30)	103. 8	108. 2	2360. 4	(20, 22)	1040397000.
168	(28, 30)	103. 4	107. 2	2315. 4	(21, 22)	835237900.
169	(27, 29)	103. 0	106. 6	2328. 1	(20, 22)	732572900.
170	(27, 29)	103. 3	107. 0	2356. 9	(20, 22)	785538800.
171	(27, 29)	103. 8	107. 3	2364. 0	(20, 22)	854322200.
172	(28, 30)	104. 0	107. 1	2315. 4	(21, 22)	813997300.
173	(28, 30)	103. 8	106. 4	2282. 4	(21, 22)	686740000.
174	(27, 29)	103. 2	105. 7	2330. 1	(20, 22)	585464600.
175	(27, 29)	102. 5	105. 5	2361. 9	(20, 22)	558203900
176	(27, 29)	101. 2	105. 4	2418. 2	(20, 22)	546438100.
177	(27, 29)	101. 2	104. 9	2397. 4	(20, 22)	490196500.
178	(28, 29)	101. 0	104. 0	2352. 8	(21, 22)	401234400
179	(27, 29)	100. 7	103. 3	2372. 0	(20, 22)	339362300.
180	(27, 29)	101. 0	103. 3	2390. 2	(20, 22)	337514800.
181	(27, 29)	101. 0	103. 6	2385. 2	(20, 22)	361578000.
182	(27, 29)	100. 6	103. 5	2320. 3	(20, 22)	354959600
183	(28, 29)	99. 8	102. 7	2235. 7	(21, 22)	297189900.
184	(29, 30)	98. 6	101. 2	2163. 1	(21, 22)	210902200.
185	(32, 31)	96. 9	99. 2	1991. 1	(23, 22)	130788100.
186	(33, 32)	94. 8	96. 7	1845. 9	(24, 23)	74342740
187	(34, 31)	92. 3	94. 0	1923. 5	(24, 22)	39977550

TRACK TRAIL FOR SPQCOT3.DA

BLOCK	(IR3D, JR3D)	AMAX	AMAXUP	RSUM	LOG COORD'S	POWER
113	(26, 29)	86.9	94.9	2536.8	(20, 22)	49535980.
114	(26, 29)	91.3	99.1	2431.3	(20, 22)	129867100.
115	(27, 29)	94.0	101.8	2365.8	(20, 22)	239579300.
116	(27, 29)	95.8	103.1	2387.4	(20, 22)	324274900.
117	(27, 29)	96.2	103.2	2442.4	(20, 22)	333084900.
118	(26, 29)	95.4	102.3	2520.7	(20, 22)	268585200.
119	(25, 29)	93.0	100.6	2571.4	(19, 22)	180417400.
120	(25, 29)	88.8	98.5	2609.6	(19, 22)	112851200.
121	(24, 28)	87.2	96.6	2666.4	(18, 21)	72927920.
122	(24, 28)	85.5	94.9	2713.1	(18, 21)	48785230.
123	(25, 28)	85.8	93.8	2700.8	(19, 21)	38261460.
124	(25, 28)	86.3	94.1	2678.5	(19, 21)	40646160.
125	(25, 28)	87.5	94.9	2672.0	(19, 21)	49256940.
126	(25, 28)	89.2	95.4	2656.6	(19, 21)	55291440.
127	(26, 28)	90.1	95.4	2641.5	(20, 21)	55571280.
128	(26, 28)	89.7	95.1	2626.2	(20, 21)	51531170.
129	(26, 29)	88.2	94.6	2628.9	(20, 22)	45668340.
130	(25, 29)	86.0	94.1	2674.2	(19, 22)	40887380.
131	(24, 28)	86.0	94.0	2731.0	(18, 21)	39538290.
132	(24, 28)	85.9	94.1	2746.7	(18, 21)	41128060.
133	(25, 28)	85.5	94.2	2741.9	(19, 21)	41732080.
134	(25, 29)	84.6	93.9	2736.9	(19, 22)	39037120.
135	(25, 29)	84.2	93.4	2726.3	(19, 22)	35063550.
136	(25, 29)	84.2	93.3	2674.1	(19, 22)	33636450.
137	(25, 28)	86.2	94.7	2763.9	(19, 21)	46416480.
138	(24, 28)	89.7	98.4	2706.6	(18, 21)	110153000.
139	(24, 28)	94.8	103.8	2655.9	(18, 21)	383957500.
140	(24, 28)	99.5	107.9	2639.9	(18, 21)	980739600.
141	(24, 28)	102.0	110.3	2630.5	(18, 21)	1690015000.
142	(24, 28)	104.0	111.2	2615.4	(18, 21)	2095941000.
143	(24, 28)	105.4	111.3	2587.7	(18, 21)	2149198000.
144	(25, 29)	106.4	111.8	2548.3	(19, 22)	2375425000.
145	(25, 29)	107.1	112.9	2541.5	(19, 22)	3061521000.
146.	(25, 29)	107.2	113.7	2548.7	(19, 22)	3707315000.
147	(25, 29)	106.9	113.7	2529.2	(19, 22)	3698864000.
148	(25, 29)	107.6	113.4	2484.1	(19, 22)	3461476000.
149	(25, 29)	108.2	113.9	2466.6	(19, 22)	3892747000.
150	(25, 29)	108.6	114.9	2470.4	(19, 22)	4907090000.
151	(25, 30)	108.5	115.3	2451.1	(19, 23)	5419880000.
152	(26, 30)	109.1	115.0	2407.7	(19, 22)	5020180000.
153	(26, 30)	109.7	114.8	2379.3	(19, 22)	4809036000.
154	(26, 29)	110.2	115.5	2391.0	(20, 22)	5669736000.
155	(26, 30)	110.9	116.4	2392.2	(19, 22)	6863733000.
156	(26, 30)	111.3	116.5	2370.6	(19, 22)	7002513000.
157	(27, 30)	111.6	116.0	2338.8	(20, 22)	6355198000.
158	(26, 30)	111.8	116.1	2350.0	(19, 22)	6460658000.
159	(26, 30)	111.9	116.9	2358.1	(19, 22)	7696380000.
160	(26, 30)	111.7	117.3	2364.6	(19, 22)	8543347000.
161	(26, 30)	112.0	116.9	2346.1	(19, 22)	7708561000.
162	(27, 30)	111.6	115.9	2310.3	(20, 22)	6190698000.
163	(26, 31)	111.1	115.6	2290.8	(19, 23)	5778981000.
164	(26, 31)	111.0	116.1	2297.8	(19, 23)	6524473000.
165	(26, 31)	110.7	116.3	2303.5	(19, 23)	6745371000.
166	(26, 31)	109.6	115.4	2284.0	(19, 23)	5493461000.
167	(26, 31)	107.9	113.7	2284.3	(19, 23)	3708153000.
168	(26, 30)	106.3	112.5	2330.5	(19, 22)	2800259000.
169	(25, 30)	106.1	112.6	2357.3	(19, 23)	2891332000.
170	(25, 30)	106.3	112.7	2371.8	(19, 23)	2970389000.
171	(26, 30)	105.9	111.9	2350.1	(19, 22)	2447677000.

172	(26, 31)	104. 9	110. 3	2330. 1	(19, 23)	1710128000.
173	(25, 30)	104. 1	109. 6	2352. 2	(19, 23)	1440534000.
174	(25, 30)	104. 3	110. 3	2339. 8	(19, 23)	1699536000.
175	(25, 30)	104. 3	110. 8	2369. 5	(19, 23)	1922503000.
176	(26, 31)	103. 9	110. 3	2340. 2	(19, 23)	1704540000.
177	(26, 31)	103. 0	108. 9	2329. 2	(19, 23)	1224280000.
178	(25, 30)	102. 2	107. 8	2365. 2	(19, 23)	965002200.
179	(25, 30)	102. 4	108. 4	2327. 8	(19, 23)	1098182000.
180	(25, 30)	103. 2	109. 2	2344. 6	(19, 23)	1318688000.
181	(25, 31)	103. 7	109. 1	2326. 9	(19, 23)	1289174000.
182	(26, 31)	103. 2	108. 0	2294. 3	(19, 23)	988577000.
183	(26, 30)	101. 6	106. 3	2292. 9	(19, 22)	668536300.
184	(26, 30)	100. 9	105. 3	2348. 9	(19, 22)	535432200.
185	(25, 29)	101. 2	105. 4	2454. 1	(19, 22)	550444000.
186	(26, 30)	101. 1	105. 5	2438. 4	(19, 22)	557836500.
187	(26, 30)	99. 9	104. 8	2386. 9	(19, 22)	483096600.
188	(27, 30)	100. 1	103. 9	2341. 4	(20, 22)	387172100.
189	(26, 30)	100. 0	103. 7	2334. 6	(19, 22)	369122800.
190	(26, 30)	99. 4	104. 3	2308. 9	(19, 22)	430161700.
191	(26, 30)	99. 4	104. 8	2349. 0	(19, 22)	474093100.
192	(26, 30)	100. 1	104. 4	2327. 6	(19, 22)	433147600.
193	(27, 30)	99. 5	103. 2	2328. 6	(20, 22)	328239400.
194	(27, 29)	97. 7	101. 6	2394. 1	(20, 22)	231420800.
195	(26, 29)	96. 9	100. 6	2436. 8	(20, 22)	181718600.
196	(26, 29)	95. 6	100. 0	2471. 0	(20, 22)	159258500.
197	(26, 29)	93. 5	99. 5	2511. 8	(20, 22)	140522800.
198	(26, 29)	92. 8	99. 0	2502. 1	(20, 22)	125277700.
199	(26, 29)	94. 2	99. 0	2482. 6	(20, 22)	126741100.
200	(26, 29)	94. 8	99. 7	2435. 5	(20, 22)	148529800.
201	(27, 29)	95. 6	100. 4	2367. 7	(20, 22)	172267700.
202	(28, 30)	96. 5	100. 4	2309. 5	(21, 22)	173684900.
203	(29, 30)	96. 3	99. 7	2257. 2	(21, 22)	146230700.
204	(30, 30)	95. 6	98. 1	2147. 4	(22, 22)	103264100.
205	(31, 31)	94. 0	96. 0	2070. 8	(23, 23)	63546000.
206	(30, 30)	91. 5	93. 8	2191. 4	(22, 22)	37586030.
209	(26, 28)	88. 8	93. 2	2548. 7	(20, 21)	32907680.
210	(26, 28)	89. 7	93. 8	2474. 7	(20, 21)	38127600.
211	(26, 28)	89. 8	93. 6	2460. 0	(20, 21)	36437470.

TRACK TRAIL FOR SPQCOP.DA

BLOCK	(IR3D, JR3D)	AMAX	AMAXUP	RSUM	LOG COORD'S	POWER
32	(25,29)	89.3	96.5	2653.0	(19,22)	71205300
33	(26,29)	94.6	100.4	2503.0	(20,22)	173746800.
34	(27,30)	98.4	103.5	2413.7	(20,22)	353160700.
35	(28,30)	100.8	105.7	2355.1	(21,22)	593794600.
36	(28,30)	101.9	107.1	2351.3	(21,22)	805394700.
37	(27,30)	101.6	107.4	2356.5	(20,22)	866770700.
38	(27,30)	100.0	106.7	2342.8	(20,22)	736831000.
39	(27,30)	98.6	105.1	2391.1	(20,22)	512230700.
40	(26,30)	96.4	103.4	2489.0	(19,22)	344127000.
41	(25,29)	93.8	103.0	2559.0	(19,22)	314185000.
42	(26,28)	96.4	104.1	2596.3	(20,21)	405606100.
43	(26,28)	98.3	105.4	2561.4	(20,21)	548193000.
44	(27,28)	100.8	106.2	2502.3	(20,21)	665245400.
45	(27,28)	102.1	106.4	2497.2	(20,21)	696489000.
46	(27,28)	102.3	106.0	2490.0	(20,21)	632469000.
47	(27,28)	101.5	105.1	2486.6	(20,21)	515139300
48	(27,28)	99.6	104.0	2456.5	(20,21)	395648500.
49	(26,28)	98.0	102.7	2481.3	(20,21)	294243600.
50	(26,28)	97.7	101.3	2558.0	(20,21)	214320500
51	(26,28)	97.2	100.2	2580.2	(20,21)	167359800.
52	(27,28)	97.0	100.2	2507.4	(20,21)	166181600.
53	(27,28)	97.4	101.0	2399.2	(20,21)	179758100
54	(28,28)	99.3	102.0	2347.9	(21,21)	250873000.
55	(28,28)	100.5	102.9	2318.8	(21,21)	307950600
56	(28,28)	100.9	103.5	2342.3	(21,21)	353918700.
57	(28,28)	100.7	103.6	2368.3	(21,21)	360329700.
58	(28,28)	99.7	102.9	2404.3	(21,21)	311158500
59	(27,28)	97.8	101.5	2489.6	(20,21)	225751100.
60	(27,28)	95.7	99.6	2613.1	(20,21)	145679700
61	(26,28)	93.1	97.8	2708.0	(20,21)	96514140.
62	(26,28)	89.9	96.6	2728.4	(20,21)	72661620.
63	(26,28)	88.9	95.7	2769.5	(20,21)	59565120.
64	(25,28)	87.6	95.4	2841.0	(19,21)	54367500.
65	(25,28)	89.5	95.6	2874.5	(19,21)	57045790.
66	(25,28)	90.9	96.1	2844.7	(19,21)	64942540.
67	(26,28)	91.5	96.7	2832.3	(20,21)	73384960
68	(25,28)	91.5	96.9	2843.9	(19,21)	77326850.
69	(26,28)	90.7	96.7	2819.2	(20,21)	74611680
70	(26,28)	89.7	96.3	2772.1	(20,21)	67826900.
71	(26,29)	88.7	95.9	2748.8	(20,22)	62000740.
72	(26,29)	87.4	95.7	2765.4	(20,22)	59303580.
73	(25,28)	86.4	95.7	2804.0	(19,21)	58588060.
74	(25,28)	86.5	95.7	2815.5	(19,21)	58768340.
75	(25,28)	87.1	95.9	2811.2	(19,21)	61485710.
76	(25,28)	87.9	96.3	2849.8	(19,21)	68380210.
77	(25,28)	88.7	96.8	2857.8	(19,21)	76247360.
78	(26,28)	89.2	97.0	2858.7	(20,21)	79848370.
79	(25,28)	90.1	96.9	2860.4	(19,21)	77625950
80	(25,28)	89.6	96.7	2844.6	(19,21)	74240130
81	(26,28)	89.0	96.6	2785.6	(20,21)	73010130
82	(26,28)	90.2	96.6	2725.3	(20,21)	72153300.
83	(25,28)	90.5	96.3	2741.6	(19,21)	67928020
84	(25,28)	90.3	95.8	2749.6	(19,21)	60666860
85	(25,28)	90.0	95.4	2764.4	(19,21)	54611780.
86	(26,28)	89.7	95.3	2728.2	(20,21)	54068960.
87	(26,29)	91.6	96.0	2638.0	(20,22)	63318990
88	(28,29)	93.9	97.4	2503.0	(21,22)	87096420
89	(28,29)	95.6	98.9	2421.3	(21,22)	122358400
90	(28,29)	96.2	99.8	2376.7	(21,22)	149961600

91	(28,29)	95.8	99.7	2372.3	(21,22)	149014600.
92	(27,29)	94.4	98.7	2382.1	(20,22)	118302500.
93	(27,29)	92.3	97.0	2488.0	(20,22)	79258050.
94	(27,29)	90.5	95.5	2550.2	(20,22)	55847710.
95	(27,29)	90.0	95.2	2534.1	(20,22)	52912590.
96	(27,29)	90.4	95.7	2527.8	(20,22)	59197250.
97	(26,29)	90.8	96.1	2568.3	(20,22)	64416830.
98	(26,29)	90.5	96.2	2603.8	(20,22)	65491520.
99	(25,29)	89.0	96.5	2627.7	(19,22)	70156750.
100	(24,28)	89.2	98.5	2596.7	(18,21)	112537700.
101	(24,28)	92.4	101.7	2581.4	(18,21)	235084400.
102	(24,28)	94.4	104.1	2588.9	(18,21)	407999500.
103	(24,29)	96.8	105.6	2563.0	(18,22)	580387300.
104	(25,29)	99.3	107.5	2505.1	(19,22)	881220100.
105	(25,29)	102.2	110.5	2441.3	(19,22)	1786366000.
106	(25,30)	104.9	113.2	2380.0	(19,23)	3317088000.
107	(25,30)	106.3	114.6	2376.6	(19,23)	4623163000.
108	(25,30)	107.2	114.8	2377.8	(19,23)	4787462000.
109	(26,30)	107.6	114.2	2350.5	(19,22)	4211134000.
110	(25,30)	108.2	114.2	2369.4	(19,23)	4189796000.
111	(25,30)	109.0	115.1	2362.5	(19,23)	5114397000.
112	(25,30)	109.3	115.7	2353.2	(19,23)	5900509000.
113	(26,30)	109.5	115.4	2321.0	(19,22)	5544088000.
114	(26,31)	109.9	114.8	2298.1	(19,23)	4738159000.
115	(26,30)	110.2	114.7	2341.0	(19,22)	4651246000.
116	(25,30)	110.5	115.2	2319.9	(19,23)	5289431000.
117	(26,30)	110.7	115.5	2290.9	(19,22)	5613834000.
118	(26,31)	111.0	115.2	2245.5	(19,23)	5286158000
119	(26,31)	111.2	115.1	2197.4	(19,23)	5116322000.
120	(26,31)	111.4	115.5	2200.0	(19,23)	5684711000.
121	(26,31)	111.6	116.0	2207.6	(19,23)	6367515000.
122	(26,32)	111.6	115.9	2183.0	(19,24)	6212792000.
123	(27,32)	111.7	115.4	2128.1	(20,24)	5542576000.
124	(26,31)	111.9	115.3	2152.6	(19,23)	5349728000.
125	(26,31)	112.0	115.7	2198.6	(19,23)	5822292000.
126	(26,31)	112.0	115.8	2213.7	(19,23)	6086570000.
127	(26,32)	111.8	115.5	2162.3	(19,24)	5635936000.
128	(26,32)	111.6	115.2	2131.0	(19,24)	5202821000.
129	(26,32)	111.5	115.4	2156.8	(19,24)	5504344000.
130	(26,32)	111.7	115.8	2183.7	(19,24)	6084485000.
131	(26,32)	111.7	115.7	2173.9	(19,24)	5922132000.
132	(27,32)	111.7	115.1	2128.9	(20,24)	5119521000.
133	(27,31)	111.5	114.7	2145.7	(20,23)	4660990000.
134	(26,31)	111.3	114.9	2201.3	(19,23)	4936270000.
135	(26,31)	111.2	115.2	2211.4	(19,23)	5207806000.
136	(26,32)	111.0	114.8	2174.4	(19,24)	4801802000.
137	(27,32)	110.9	114.3	2141.3	(20,24)	4283507000.
138	(26,31)	111.0	114.5	2170.7	(19,23)	4468740000.
139	(26,31)	111.1	115.1	2223.7	(19,23)	5133464000
140	(26,32)	111.1	115.2	2193.8	(19,24)	5286183000.
141	(27,32)	111.2	114.8	2169.5	(20,24)	4752753000.
142	(27,31)	111.1	114.4	2194.9	(20,23)	4381180000.
143	(26,31)	110.8	114.7	2218.7	(19,23)	4704494000.
144	(26,31)	110.7	115.1	2228.6	(19,23)	5099745000.
145	(26,31)	110.2	114.8	2223.4	(19,23)	4731744000.
146	(26,31)	109.9	114.1	2216.3	(19,23)	4037380000.
147	(26,31)	109.7	114.0	2257.3	(19,23)	3965163000.
148	(26,31)	109.6	114.6	2292.1	(19,23)	4524999000.
149	(26,31)	109.6	114.8	2301.3	(19,23)	4744634000.
150	(26,31)	109.6	114.2	2257.2	(19,23)	4211002000.
151	(26,31)	109.4	113.7	2249.4	(19,23)	3735769000.
152	(26,30)	109.3	114.0	2274.2	(19,22)	4023969000
153	(26,31)	109.3	114.6	2288.9	(19,23)	4564476000.
154	(26,31)	109.1	114.4	2277.2	(19,23)	4408586000.
155	(27,31)	108.9	113.8	2235.2	(20,23)	3773425000.
156	(26,31)	108.8	113.5	2240.4	(19,23)	3568911000.
[illegible]	[illegible]	[illegible]	[illegible]	[illegible]	[illegible]	

157	(26,31)	108.8	114.0	2255.5	(19,23)	3984327000
158	(26,31)	108.7	114.2	2253.5	(19,23)	4196678000.
159	(26,31)	108.1	113.7	2222.7	(19,23)	3680647000.
160	(27,31)	107.4	112.8	2200.9	(20,23)	3020631000.
161	(26,31)	107.0	112.6	2241.3	(19,23)	2879379000.
162	(25,31)	106.7	112.8	2274.8	(19,23)	3046705000.
163	(26,31)	105.8	112.6	2280.7	(19,23)	2883068000
164	(26,31)	105.8	111.9	2262.9	(19,23)	2454192000.
165	(25,31)	105.6	111.6	2282.5	(19,23)	2264968000.
166	(25,31)	105.4	111.8	2267.9	(19,23)	2409552000
167	(25,31)	105.2	111.9	2270.9	(19,23)	2434247000
168	(25,31)	105.3	111.3	2244.8	(19,23)	2157164000.
169	(25,31)	105.1	110.9	2264.7	(19,23)	1943762000.
170	(25,31)	105.6	111.1	2294.9	(19,23)	2030110000.
171	(25,31)	106.3	111.3	2296.1	(19,23)	2147832000
172	(25,31)	106.7	111.0	2264.9	(19,23)	1992950000
173	(25,31)	107.0	110.4	2236.1	(19,23)	1754044000.
174	(25,31)	107.0	110.4	2244.0	(19,23)	1724197000
175	(25,31)	106.8	110.6	2229.1	(19,23)	1825274000.
176	(25,32)	106.1	110.4	2218.3	(19,24)	1722711000
177	(26,32)	104.7	109.2	2153.8	(19,24)	1328138000
178	(26,32)	102.4	107.3	2154.5	(19,24)	859656200.
179	(25,32)	100.4	105.3	2223.5	(19,24)	534530000.
180	(25,30)	99.1	103.6	2330.4	(19,23)	362509800.
181	(25,30)	98.2	102.0	2355.7	(19,23)	252594900.
182	(25,31)	96.8	100.2	2326.2	(19,23)	164537400.
183	(27,31)	94.6	97.7	2267.0	(20,23)	94311680.
184	(28,30)	91.8	94.9	2269.4	(21,22)	48456560.

TRACK TRAIL FOR SPQTOT.DA

BLOCK	(IR3D,JR3D)	AMAX	AMAXUP	RSUM	LOG COORD'S	POWER
65	(25,27)	84.6	93.7	2817.2	(19,21)	36762690.
66	(26,27)	86.3	95.1	2816.3	(20,21)	50811180.
67	(27,27)	88.0	95.9	2799.1	(20,20)	61802380.
68	(27,26)	90.3	96.4	2784.5	(21,20)	60480770.
69	(27,26)	91.0	96.8	2755.9	(21,20)	75318460.
70	(27,27)	91.3	98.0	2747.7	(20,20)	101033200.
71	(27,27)	95.4	100.6	2672.8	(20,20)	181666300.
72	(28,27)	99.7	103.3	2608.8	(21,20)	342269200.
73	(29,28)	102.6	105.6	2521.4	(22,21)	574005800
74	(30,28)	104.5	107.2	2441.3	(22,21)	822951400.
75	(31,28)	105.6	108.0	2364.9	(23,21)	990907100.
76	(32,28)	105.8	108.0	2307.1	(23,21)	991112700.
77	(32,28)	105.4	107.2	2287.2	(23,21)	826276400.
78	(31,28)	104.5	105.8	2283.2	(23,21)	578571300.
79	(30,28)	103.3	104.4	2399.3	(22,21)	437212200.
80	(29,28)	102.4	103.9	2499.1	(22,21)	392451100
81	(28,28)	100.9	104.2	2533.1	(21,21)	414019600
82	(28,28)	100.1	104.6	2543.8	(21,21)	455648500
83	(28,28)	101.8	105.5	2539.3	(21,21)	563854600
84	(29,28)	102.8	106.9	2505.3	(22,21)	775469300.
85	(29,28)	103.2	108.0	2483.8	(22,21)	990020400
86	(29,28)	103.4	108.1	2497.8	(22,21)	1029876000
87	(28,28)	103.0	107.3	2547.8	(21,21)	841592800
88	(27,28)	101.5	105.5	2644.8	(20,21)	568709100.
89	(26,28)	99.6	103.9	2739.9	(20,21)	385459700.
90	(26,28)	99.0	103.3	2775.4	(20,21)	338586600.
91	(26,28)	99.4	103.7	2768.1	(20,21)	369339900.
92	(27,27)	99.4	104.1	2774.8	(20,20)	411346200.
93	(27,27)	99.3	104.2	2766.4	(20,20)	418521900.
94	(27,27)	98.8	103.7	2773.3	(20,20)	374761000.
95	(26,27)	97.5	102.9	2797.2	(20,21)	306706200.
96	(25,27)	95.2	102.2	2826.4	(19,21)	263214500.
97	(25,27)	94.9	102.2	2833.0	(19,21)	264241400.
98	(25,28)	95.3	102.5	2781.5	(19,21)	283091500.
99	(25,28)	96.0	102.5	2745.2	(19,21)	283137000.
100	(25,28)	95.5	102.0	2744.7	(19,21)	250717600.
101	(26,28)	94.3	100.9	2762.8	(20,21)	193958900.
102	(25,28)	93.1	99.4	2787.7	(19,21)	136461700.
103	(25,28)	91.9	97.8	2824.3	(19,21)	95115580.
104	(25,28)	90.3	96.7	2835.0	(19,21)	74529730.
105	(24,28)	88.4	97.2	2825.4	(18,21)	83553760
106	(24,28)	90.6	99.1	2812.0	(18,21)	127715000.
107	(24,28)	93.0	100.8	2730.7	(18,21)	192065000.
108	(25,28)	94.5	101.8	2704.4	(19,21)	241255400
109	(25,28)	95.9	102.3	2663.6	(19,21)	272164100.
110	(24,29)	97.3	104.0	2611.0	(18,22)	401687600
111	(24,29)	98.5	107.2	2486.3	(18,22)	837855000.
112	(24,29)	101.3	109.9	2483.2	(18,22)	1533361000.
113	(24,30)	104.2	111.3	2473.1	(18,23)	2157136000.
114	(25,29)	106.4	112.4	2494.7	(19,22)	2772048000.
115	(25,29)	108.4	114.3	2466.7	(19,22)	4217772000.
116	(26,29)	110.0	116.3	2422.6	(20,22)	6820434000.
117	(26,30)	111.4	117.7	2409.8	(19,22)	9271661000.
118	(26,30)	111.9	117.9	2373.7	(19,22)	9773781000.
119	(27,30)	112.0	117.3	2326.1	(20,22)	8578666000.
120	(26,30)	111.8	116.9	2333.0	(19,22)	7829254000.
121	(26,30)	111.8	117.3	2357.3	(19,22)	8551723000
122	(26,30)	112.0	117.7	2358.8	(19,22)	9323213000.
123	(26,30)	111.9	117.3	2322.9	(19,22)	8537006000

124	(27, 30)	111. 6	116. 4	2296. 5	(20, 22)	6937154000
125	(26, 30)	111. 2	116. 0	2343. 6	(19, 22)	6273774000.
126	(26, 29)	110. 8	116. 3	2392. 6	(20, 22)	6722740000.
127	(26, 30)	110. 6	116. 3	2371. 4	(19, 22)	6825042000.
128	(26, 30)	110. 4	115. 8	2329. 6	(19, 22)	5979300000.
129	(26, 30)	110. 3	115. 2	2318. 3	(19, 22)	5275513000.
130	(26, 30)	110. 3	115. 5	2340. 4	(19, 22)	5657489000.
131	(26, 30)	110. 2	116. 1	2350. 4	(19, 22)	6378525000.
132	(26, 30)	110. 1	115. 9	2329. 8	(19, 22)	6132666000.
133	(26, 31)	109. 7	115. 0	2298. 7	(19, 23)	5023728000.
134	(26, 30)	109. 0	114. 5	2326. 5	(19, 22)	4432499000.
135	(25, 30)	109. 0	114. 9	2362. 0	(19, 23)	4910879000.
136	(26, 30)	109. 5	115. 4	2372. 9	(19, 22)	5452333000.
137	(26, 31)	109. 7	115. 0	2337. 0	(19, 23)	5062562000.
138	(26, 30)	109. 5	114. 4	2326. 4	(19, 22)	4350726000.
139	(26, 30)	109. 5	114. 5	2356. 0	(19, 22)	4507988000.
140	(26, 30)	109. 9	115. 4	2369. 6	(19, 22)	5443375000.
141	(26, 30)	110. 2	115. 7	2363. 4	(19, 22)	5828444000.
142	(26, 30)	110. 0	115. 0	2327. 2	(19, 22)	4982260000.
143	(26, 30)	109. 4	113. 8	2323. 0	(19, 22)	3814700000.
144	(25, 30)	108. 8	113. 4	2359. 1	(19, 23)	3486393000.
145	(25, 30)	108. 5	113. 9	2386. 8	(19, 23)	3872181000.
146	(25, 30)	108. 3	113. 9	2375. 5	(19, 23)	3931162000.
147	(26, 31)	108. 2	113. 3	2341. 0	(19, 23)	3388949000.
148	(26, 30)	108. 3	112. 9	2349. 3	(19, 22)	3070262000.
149	(25, 30)	108. 4	113. 5	2355. 1	(19, 23)	3582970000.
150	(25, 30)	108. 7	114. 4	2368. 8	(19, 23)	4338700000.
151	(25, 30)	108. 7	114. 4	2345. 4	(19, 23)	4329415000.
152	(26, 30)	108. 7	113. 6	2332. 9	(19, 22)	3623226000.
153	(25, 30)	108. 6	113. 1	2368. 1	(19, 23)	3268636000.
154	(25, 30)	108. 6	113. 8	2382. 3	(19, 23)	3796956000.
155	(25, 30)	108. 9	114. 5	2404. 4	(19, 23)	4456808000.
156	(26, 30)	108. 8	114. 3	2383. 5	(19, 22)	4263988000.
157	(26, 30)	108. 6	113. 4	2339. 6	(19, 22)	3492391000.
158	(25, 30)	108. 3	113. 1	2347. 2	(19, 23)	3232248000.
159	(25, 30)	108. 3	113. 8	2381. 9	(19, 23)	3832728000.
160	(25, 30)	108. 5	114. 4	2400. 3	(19, 23)	4402315000.
161	(25, 30)	108. 4	114. 1	2380. 0	(19, 23)	4066936000.
162	(26, 30)	108. 2	113. 1	2367. 6	(19, 22)	3241520000.
163	(25, 30)	107. 9	112. 7	2415. 5	(19, 23)	29628[illegible]00.
164	(25, 30)	107. 8	113. 3	2440. 2	(19, 23)	3419250000.
165	(25, 30)	107. 8	113. 7	2456. 8	(19, 23)	3739597000.
166	(25, 30)	107. 8	113. 2	2441. 3	(19, 23)	3313247000.
167	(26, 30)	107. 7	112. 3	2418. 1	(19, 22)	2663464000.
168	(26, 29)	107. 8	112. 2	2439. 5	(20, 22)	2642238000.
169	(25, 29)	108. 1	113. 0	2464. 7	(19, 22)	3185719000.
170	(26, 29)	108. 1	113. 3	2455. 1	(20, 22)	3426985000.
171	(26, 30)	107. 7	112. 8	2427. 7	(19, 22)	3019268000.
172	(26, 29)	107. 1	112. 2	2434. 6	(20, 22)	2637540000.
173	(25, 29)	107. 1	112. 7	2463. 3	(19, 22)	2944815000.
174	(25, 29)	107. 5	113. 6	2466. 1	(19, 22)	3589287000.
175	(26, 29)	107. 4	113. 6	2455. 6	(20, 22)	3669761000.
176	(26, 30)	107. 3	113. 0	2420. 3	(19, 22)	3128769000.
177	(26, 29)	107. 2	112. 4	2436. 6	(20, 22)	2776991000.
178	(25, 29)	107. 3	112. 9	2437. 0	(19, 22)	3088607000.
179	(25, 29)	107. 5	113. 5	2436. 9	(19, 22)	3520145000.
180	(26, 30)	107. 7	113. 2	2414. 0	(19, 22)	3341272000.
181	(26, 30)	107. 7	112. 4	2389. 1	(19, 22)	2766186000.
182	(26, 29)	107. 7	112. 0	2420. 5	(20, 22)	2533964000.
183	(25, 29)	107. 7	112. 5	2431. 6	(19, 22)	2803762000.
184	(26, 29)	107. 3	112. 7	2433. 5	(20, 22)	2974340000.
185	(26, 29)	107. 7	112. 4	2415. 3	(20, 22)	2732502000.
186	(26, 29)	107. 8	112. 0	2432. 3	(20, 22)	2487828000.
187	(25, 29)	108. 0	112. 2	2436. 7	(19, 22)	2653211000.
188	(25, 29)	108. 3	112. 7	2432. 3	(19, 22)	2959658000.
189	(26, 29)	108. 1	112. 5	2395. 9	(20, 22)	2840769000.

190	(26, 30)	107.4	111.6	2335.1	(19, 22)	2278814000.
191	(25, 29)	105.8	110.4	2363.9	(19, 22)	1732521000.
192	(25, 29)	105.6	109.7	2400.4	(19, 22)	1488483000.
193	(25, 29)	105.6	109.4	2419.6	(19, 22)	1387464000.
194	(26, 29)	105.3	108.8	2377.3	(20, 22)	1203358000.
195	(26, 29)	104.5	107.7	2357.4	(20, 22)	937502700.
196	(26, 29)	103.2	106.6	2428.4	(20, 22)	716974100.
197	(25, 28)	101.9	105.7	2509.6	(19, 21)	584212700.
198	(25, 28)	100.8	104.8	2536.2	(19, 21)	483932200.
199	(26, 29)	99.9	103.8	2492.5	(20, 22)	383351000.
200	(27, 29)	98.2	102.6	2430.9	(20, 22)	291158300.
201	(27, 28)	96.3	101.6	2496.7	(20, 21)	227622200.
202	(26, 28)	94.4	100.8	2536.7	(20, 21)	191541600.
203	(26, 28)	93.8	100.1	2570.6	(20, 21)	162333400.
204	(26, 28)	93.2	99.1	2573.5	(20, 21)	128095300.
205	(27, 28)	93.0	97.5	2507.4	(20, 21)	89780910.
206	(28, 29)	92.3	95.5	2410.8	(21, 22)	56143310.
207	(28, 30)	90.5	93.3	2319.8	(21, 22)	33536590.

TRACK TRAIL FOR SPZSASH.DA

BLOCK	(IR3D, JR3D)	AMAX	AMAXUP	RSUM	LOG COORD'S	POWER
327	(31, 29)	80.9	92.9	2369.3	(23, 21)	30716270.
328	(30, 29)	82.0	92.9	2384.8	(22, 21)	30742980.
341	(31, 29)	81.8	92.9	2233.3	(23, 21)	30862750.
342	(32, 29)	81.7	93.2	2273.3	(23, 21)	33298350.
343	(32, 29)	82.6	93.7	2280.0	(23, 21)	37145740.
344	(33, 30)	83.8	94.2	2224.0	(24, 22)	41929390.
345	(34, 30)	84.0	94.6	2152.4	(24, 22)	45536640.
346	(34, 29)	83.7	94.7	2166.6	(25, 21)	47046180.
347	(34, 29)	84.1	94.8	2177.2	(25, 21)	47791840.
348	(34, 29)	84.8	94.9	2192.4	(25, 21)	48929170.
349	(35, 29)	85.6	95.0	2233.0	(25, 21)	49567620.
350	(35, 29)	86.6	95.0	2232.2	(25, 21)	49585780.
351	(37, 29)	86.6	95.1	2193.9	(26, 21)	50907860.
352	(38, 29)	85.9	95.4	2133.2	(27, 20)	54568340.
353	(37, 29)	85.7	95.7	2108.2	(26, 21)	58322700.
354	(37, 29)	85.4	95.6	2095.5	(26, 21)	57763680.
355	(36, 29)	84.5	95.1	2152.7	(26, 21)	51361330.
356	(35, 29)	83.6	94.3	2204.4	(25, 21)	42817650
357	(35, 29)	82.8	93.8	2228.9	(25, 21)	37802020.
358	(35, 29)	83.2	93.9	2263.0	(25, 21)	38571300.
359	(35, 29)	84.4	94.3	2273.8	(25, 21)	42358610.
360	(35, 29)	85.0	94.5	2273.9	(25, 21)	44662620.
361	(35, 29)	84.8	94.4	2315.9	(25, 21)	43805660.
362	(34, 29)	84.6	94.2	2323.4	(25, 21)	41637550.
363	(33, 29)	84.4	94.0	2325.4	(24, 21)	40207070.
364	(32, 29)	83.5	93.9	2351.7	(23, 21)	39295740.
365	(32, 29)	82.5	93.7	2372.8	(23, 21)	37456690.
366	(32, 29)	81.6	93.5	2362.6	(23, 21)	35254190.
367	(32, 29)	81.5	93.4	2346.7	(23, 21)	34903620.
368	(33, 29)	82.6	93.7	2323.0	(24, 21)	36956290.
369	(34, 29)	82.9	93.9	2324.0	(25, 21)	39234690.
370	(34, 29)	82.8	94.1	2313.8	(25, 21)	40468750.
371	(34, 29)	84.3	94.3	2275.1	(25, 21)	42471620.
372	(34, 29)	85.4	94.7	2218.4	(25, 21)	47064800.
373	(35, 29)	85.9	95.3	2217.5	(25, 21)	53194740.
374	(35, 29)	85.4	95.6	2219.3	(25, 21)	57324100.
375	(34, 29)	84.4	95.6	2253.1	(25, 21)	57743340.
376	(34, 29)	84.2	95.5	2302.4	(25, 21)	56125200.
377	(34, 29)	84.2	95.4	2290.7	(25, 21)	54694480.
378	(34, 29)	83.5	95.4	2232.1	(25, 21)	55112260.
379	(34, 29)	82.5	95.6	2240.6	(25, 21)	58183950.
380	(34, 29)	83.8	95.9	2248.4	(25, 21)	62240290.
381	(34, 29)	84.8	96.2	2289.4	(25, 21)	65791420.
382	(33, 29)	84.8	96.5	2348.5	(24, 21)	70305470.
383	(33, 29)	85.5	97.0	2357.4	(24, 21)	78753340.
384	(33, 29)	87.4	97.5	2324.5	(24, 21)	90039200.
385	(33, 29)	88.2	97.9	2309.0	(24, 21)	97792510.
386	(33, 29)	88.6	97.9	2275.9	(24, 21)	98847730.
387	(32, 29)	88.8	98.0	2244.3	(23, 21)	99650500.
388	(32, 29)	88.9	98.4	2199.7	(23, 21)	108838300.
389	(32, 29)	89.4	99.0	2158.5	(23, 21)	125062400.
390	(33, 29)	89.2	99.5	2100.4	(24, 21)	140690400.
391	(34, 29)	89.1	99.9	2122.8	(25, 21)	153583900.
392	(34, 29)	90.3	100.3	2155.7	(25, 21)	169105200.
393	(33, 29)	91.1	100.8	2260.9	(24, 21)	192090000.
394	(33, 29)	91.3	101.4	2302.8	(24, 21)	219601500.
395	(32, 29)	91.1	101.9	2360.2	(23, 21)	244492300.
396	(31, 29)	90.7	102.1	2410.4	(23, 21)	259552700.
397	(30, 29)	90.7	102.1	2432.0	(22, 21)	258698400.
398	(29, 29)	90.3	101.9	2401.9	(22, 22)	243390900.
399	(29, 29)	89.6	101.5	2380.6	(22, 22)	226070600.

400	(30,29)	89.6	101.4	2372.0	(22,21)	220128000.
401	(30,29)	89.8	101.5	2355.5	(22,21)	225701700.
402	(31,29)	89.7	101.7	2310.6	(23,21)	235689100.
403	(30,29)	90.0	101.8	2298.8	(22,21)	241343700.
404	(30,29)	90.3	101.8	2305.9	(22,21)	237194400.
405	(29,29)	90.1	101.4	2384.8	(22,22)	220158800.
406	(28,29)	89.2	100.9	2484.0	(21,22)	193336500.
407	(28,29)	88.4	100.3	2560.2	(21,22)	170545900.
408	(27,29)	91.5	100.2	2583.9	(20,22)	166450500.
409	(28,28)	94.5	100.8	2646.3	(21,21)	189045500.
410	(28,28)	97.2	101.8	2668.3	(21,21)	237790800.
411	(28,28)	99.2	102.8	2645.6	(21,21)	300144100.
412	(29,28)	100.3	103.4	2603.8	(22,21)	349357800.
413	(29,28)	101.3	104.0	2595.4	(22,21)	397413900.
414	(28,27)	102.1	105.5	2634.5	(21,20)	556175900.
415	(27,27)	102.8	108.1	2684.3	(20,20)	1014553000.
416	(28,27)	105.6	110.8	2664.6	(21,20)	1915163000.
417	(27,27)	108.6	113.5	2737.0	(20,20)	3565713000.
418	(27,27)	110.7	116.0	2768.4	(20,20)	6316524000.
419	(27,27)	111.5	117.7	2782.8	(20,20)	9416868000.
420	(27,27)	111.0	118.5	2775.7	(20,20)	11212420000.
421	(27,27)	111.5	118.5	2760.4	(20,20)	11180440000.
422	(27,27)	111.8	118.2	2742.8	(20,20)	10362010000.
423	(27,27)	111.9	117.9	2777.7	(20,20)	9787105000.
424	(27,27)	111.9	117.7	2779.6	(20,20)	9268040000.
425	(27,27)	112.0	117.2	2738.6	(20,20)	8340693000.
426	(27,27)	111.7	116.7	2717.5	(20,20)	7328891000.
427	(28,27)	111.5	116.3	2728.3	(21,20)	6793949000.
428	(28,27)	111.3	116.3	2729.7	(21,20)	6699790000.
429	(28,27)	111.0	116.6	2731.3	(21,20)	7185252000.
430	(27,27)	111.4	117.3	2756.7	(20,20)	8455746000.
431	(27,27)	111.7	117.8	2752.9	(20,20)	9653838000.
432	(27,27)	111.5	117.8	2719.1	(20,20)	9629925000.
433	(28,28)	110.8	117.3	2666.6	(21,21)	8431006000.
434	(28,28)	110.7	116.5	2672.1	(21,21)	7145226000.
435	(28,28)	110.4	116.0	2689.9	(21,21)	6256587000.
436	(28,28)	110.5	115.5	2685.7	(21,21)	5562843000.
437	(28,28)	110.2	115.0	2672.9	(21,21)	5049979000.
438	(28,28)	110.1	115.0	2716.8	(21,21)	4965958000.
439	(27,27)	109.8	115.0	2733.6	(20,20)	5026718000.
440	(27,28)	109.8	114.9	2733.5	(20,21)	4941459000.
441	(27,28)	109.7	115.0	2723.7	(20,21)	4980457000.
442	(27,27)	109.6	115.3	2767.9	(20,20)	5401141000.
443	(27,27)	109.4	115.6	2763.1	(20,20)	5714715000.
444	(27,28)	109.3	115.4	2729.7	(20,21)	5450682000.
445	(28,28)	109.3	115.0	2681.2	(21,21)	4973883000.
446	(27,28)	109.3	114.9	2703.3	(20,21)	4866224000.
447	(27,28)	109.6	115.0	2708.6	(20,21)	4987552000.
448	(28,27)	110.0	115.0	2696.6	(21,20)	5010407000.
449	(28,28)	110.4	115.1	2689.7	(21,21)	5165969000.
450	(27,27)	110.6	115.5	2725.7	(20,20)	5683274000.
451	(27,27)	110.9	115.8	2724.1	(20,20)	6080066000.
452	(27,28)	111.0	115.7	2691.3	(20,21)	5861356000.
453	(27,28)	110.9	115.3	2677.3	(20,21)	5382234000.
454	(27,28)	110.7	115.2	2724.6	(20,21)	5226258000.
455	(27,28)	110.5	115.2	2739.0	(20,21)	5240365000.
456	(27,28)	110.3	114.9	2705.4	(20,21)	4883034000.
457	(27,28)	110.1	114.4	2676.8	(20,21)	4316516000.
458	(27,28)	109.8	114.1	2711.9	(20,21)	4057895000.
459	(27,27)	109.5	114.1	2730.5	(20,20)	4094809000.
460	(27,27)	109.2	114.0	2713.0	(20,20)	3986345000.
461	(27,28)	109.2	113.8	2706.5	(20,21)	3830218000.
462	(27,27)	109.1	114.0	2753.2	(20,20)	3973512000.
463	(27,27)	109.0	114.3	2769.1	(20,20)	4265566000.
464	(27,28)	109.0	114.3	2739.1	(20,21)	4220513000.
465	(27,28)	109.0	114.0	2699.4	(20,21)	3959604000.

466	(27,28)	108.9	114.0	2731.7	(20,21)	3995057000.
467	(27,28)	108.8	114.3	2752.5	(20,21)	4290798000.
468	(27,28)	108.8	114.3	2732.8	(20,21)	4302103000.
469	(27,28)	108.7	114.1	2712.0	(20,21)	4033647000.
470	(27,28)	108.6	114.1	2732.5	(20,21)	4031830000.
471	(26,28)	108.5	114.4	2759.4	(20,21)	4337914000.
472	(27,28)	108.4	114.4	2743.4	(20,21)	4363420000.
473	(27,28)	108.2	114.0	2709.6	(20,21)	3982226000.
474	(27,28)	107.9	113.8	2719.8	(20,21)	3759677000.
475	(27,27)	107.3	113.9	2760.2	(20,20)	3925905000.
476	(27,27)	106.8	114.0	2763.1	(20,20)	3982619000.
477	(27,28)	107.0	113.6	2748.0	(20,21)	3633529000.
478	(27,28)	107.1	113.2	2749.4	(20,21)	3304489000.
479	(26,28)	107.0	113.2	2798.7	(20,21)	3327006000.
480	(26,28)	106.7	113.3	2801.3	(20,21)	3377213000.
481	(27,28)	106.3	112.9	2776.1	(20,21)	3116592000.
482	(27,28)	105.9	112.5	2762.9	(20,21)	2814089000.
483	(26,28)	105.5	112.5	2809.1	(20,21)	2803388000.
484	(26,28)	105.3	112.6	2820.8	(20,21)	2905857000.
485	(26,28)	105.3	112.5	2799.0	(20,21)	2808507000.
486	(26,28)	105.5	112.4	2783.3	(20,21)	2730001000.
487	(26,28)	105.8	112.8	2816.8	(20,21)	2988350000.
488	(26,28)	106.0	113.3	2826.3	(20,21)	3367389000.
489	(26,28)	105.9	113.3	2806.5	(20,21)	3367404000.
490	(26,28)	105.7	112.8	2793.3	(20,21)	3036706000.
491	(26,28)	105.2	112.5	2824.6	(20,21)	2839332000.
492	(25,28)	105.2	112.7	2865.5	(19,21)	2919672000.
493	(26,28)	105.1	112.6	2848.1	(20,21)	2912731000.
494	(26,28)	105.5	112.3	2795.3	(20,21)	2678856000.
495	(27,28)	105.8	112.1	2770.7	(20,21)	2554248000.
496	(26,28)	106.0	112.4	2802.5	(20,21)	2727539000.
497	(26,28)	106.1	112.6	2794.7	(20,21)	2911679000.
498	(27,28)	106.2	112.6	2760.8	(20,21)	2876690000.
499	(26,28)	106.5	112.6	2763.5	(20,21)	2890161000.
500	(26,28)	107.1	113.1	2785.7	(20,21)	3204307000.
501	(26,28)	107.5	113.5	2790.8	(20,21)	3554696000.
502	(26,28)	107.4	113.4	2764.7	(20,21)	3482980000.
503	(27,28)	107.0	112.9	2740.5	(20,21)	3090271000.
504	(26,28)	106.2	112.5	2774.0	(20,21)	2834913000.
505	(26,28)	105.7	112.6	2821.2	(20,21)	2865477000.
506	(26,28)	105.6	112.6	2803.3	(20,21)	2865154000.
507	(27,28)	106.0	112.4	2741.3	(20,21)	2730674000.
508	(27,28)	106.5	112.4	2709.4	(20,21)	2753486000.
509	(27,28)	107.0	112.9	2732.4	(20,21)	3073845000.
510	(27,28)	107.2	113.2	2726.8	(20,21)	3339134000.
511	(27,28)	107.0	113.0	2704.5	(20,21)	3196770000.
512	(27,28)	106.6	112.5	2731.1	(20,21)	2846092000.
513	(26,28)	105.9	112.3	2779.0	(20,21)	2690488000.
514	(26,28)	105.4	112.4	2813.0	(20,21)	2745364000.
515	(26,28)	104.9	112.3	2792.7	(20,21)	2664564000.
516	(27,28)	104.4	111.8	2753.2	(20,21)	2402298000.
517	(26,28)	104.0	111.5	2782.4	(20,21)	2236779000.
518	(26,28)	103.9	111.6	2827.7	(20,21)	2296926000.
519	(26,28)	103.9	111.7	2819.6	(20,21)	2334823000.
520	(27,28)	104.1	111.4	2769.2	(20,21)	2180222000.
521	(27,28)	104.6	111.1	2725.6	(20,21)	2058085000.
522	(27,28)	105.3	111.4	2740.5	(20,21)	2212167000.
523	(27,28)	106.1	111.9	2747.9	(20,21)	2477569000.
524	(27,28)	106.5	112.0	2715.9	(20,21)	2488014000.
525	(28,28)	106.4	111.6	2690.8	(21,21)	2266710000.
526	(27,28)	105.9	111.3	2736.1	(20,21)	2140176000.
527	(26,28)	105.5	111.5	2778.2	(20,21)	2239014000.
528	(27,28)	105.4	111.6	2770.4	(20,21)	2300401000.
529	(27,28)	105.1	111.3	2726.9	(20,21)	2121216000.
530	(27,28)	104.6	110.7	2712.2	(20,21)	1882085000.
531	(27,28)	104.2	110.7	2748.3	(20,21)	1847592000.

532	(26,28)	104.0	110.9	2773.9	(20,21)	1959095000.
533	(27,28)	103.8	110.9	2742.9	(20,21)	1935424000.
534	(27,28)	103.7	110.4	2706.5	(20,21)	1750747000.
535	(27,28)	103.7	110.1	2756.5	(20,21)	1630113000.
536	(26,28)	103.8	110.3	2794.6	(20,21)	1703426000.
537	(26,28)	104.0	110.6	2791.9	(20,21)	1799394000.
538	(27,28)	104.2	110.4	2738.8	(20,21)	1744656000.
539	(27,28)	104.6	110.2	2713.2	(20,21)	1668926000.
540	(27,28)	105.0	110.5	2720.4	(20,21)	1783986000.
541	(27,28)	105.4	111.1	2740.0	(20,21)	2022362000.
542	(27,28)	105.3	111.2	2719.4	(20,21)	2070366000.
543	(28,28)	104.8	110.6	2673.6	(21,21)	1814078000.
544	(27,28)	104.0	109.7	2690.7	(20,21)	1472051000.
545	(27,28)	103.0	109.2	2749.5	(20,21)	1309201000.
546	(26,28)	102.4	109.2	2784.0	(20,21)	1305866000.
547	(27,28)	102.3	109.0	2755.4	(20,21)	1269240000.
548	(27,28)	102.6	108.7	2718.4	(20,21)	1182244000.
549	(27,28)	103.0	108.7	2756.4	(20,21)	1186203000.
550	(26,28)	103.4	109.2	2787.1	(20,21)	1323577000.
551	(26,28)	103.7	109.5	2775.0	(20,21)	1422745000.
552	(27,28)	103.9	109.3	2721.1	(20,21)	1343954000.
553	(27,28)	103.9	108.8	2685.1	(20,21)	1191138000.
554	(27,28)	103.9	108.6	2707.4	(20,21)	1160292000.
555	(27,28)	103.8	109.0	2739.2	(20,21)	1249111000.
556	(27,28)	103.5	109.0	2719.9	(20,21)	1262173000.
557	(28,28)	103.2	108.5	2679.4	(21,21)	1119311000.
558	(27,28)	102.7	107.8	2686.5	(20,21)	948863500.
559	(27,28)	102.3	107.5	2719.9	(20,21)	899530500.
560	(27,27)	101.9	107.7	2737.9	(20,20)	928649700.
561	(27,28)	101.6	107.5	2703.8	(20,21)	892283400.
562	(28,28)	101.4	107.0	2634.7	(21,21)	798345200.
563	(27,28)	101.3	106.9	2615.1	(20,21)	780626900.
564	(27,28)	101.4	107.5	2627.9	(20,21)	882705200.
565	(27,28)	101.3	107.8	2621.6	(20,21)	957616600.
566	(27,28)	100.2	107.4	2593.3	(20,21)	864124400.
567	(27,28)	100.1	106.1	2582.4	(20,21)	647828500.
568	(27,28)	100.2	104.8	2597.2	(20,21)	483090200.
569	(27,28)	100.1	104.6	2640.6	(20,21)	455498500.
570	(27,28)	99.9	104.9	2640.6	(20,21)	487546400.
571	(27,28)	99.8	104.8	2605.0	(20,21)	477479200.
572	(27,28)	99.4	104.1	2581.9	(20,21)	410985700.
573	(27,28)	99.1	103.5	2546.8	(20,21)	352472100.
574	(27,28)	98.9	103.3	2556.8	(20,21)	335527700.
575	(27,28)	98.8	103.1	2560.6	(20,21)	326955800.
576	(27,28)	98.6	102.5	2556.6	(20,21)	284962800.
577	(27,28)	98.3	101.4	2565.6	(20,21)	219504800.
578	(27,28)	98.0	100.4	2598.4	(20,21)	175065000.
579	(27,28)	97.6	100.2	2589.2	(20,21)	167074400.
580	(27,28)	97.4	100.3	2596.1	(20,21)	170285600.
581	(27,28)	97.1	100.0	2597.5	(20,21)	159071500.
582	(27,28)	96.8	99.4	2633.3	(20,21)	137657400.
583	(27,28)	96.5	98.9	2666.6	(20,21)	123259200.
584	(27,28)	95.8	98.8	2662.4	(20,21)	119890000.
585	(27,28)	95.3	98.6	2663.7	(20,21)	115675300.
586	(26,28)	94.6	98.0	2697.2	(20,21)	100888800.
587	(26,28)	94.1	97.2	2704.6	(20,21)	83259970.
588	(27,28)	93.7	96.8	2660.8	(20,21)	76355840.
589	(28,29)	93.3	97.2	2651.3	(21,22)	82847100.
590	(28,29)	92.9	97.6	2632.6	(21,22)	90270910.
591	(28,28)	92.5	97.3	2623.3	(21,21)	85222000.
592	(28,28)	92.2	96.4	2639.4	(21,21)	69252990.
593	(28,28)	92.1	95.5	2694.5	(21,21)	56274530.
594	(27,28)	92.1	95.4	2741.5	(20,21)	54798780.
595	(28,28)	92.0	95.7	2725.8	(21,21)	58785810.
596	(27,28)	91.8	95.6	2726.3	(20,21)	57753900.
597	(27,28)	91.2	95.1	2762.0	(20,21)	50715950.

598	(26,28)	90.4	94.6	2804.2	(20,21)	46071730.
599	(27,28)	89.3	95.0	2753.5	(20,21)	50183140.
600	(27,28)	88.6	95.7	2768.9	(20,21)	59213980.
601	(27,28)	87.6	96.0	2803.3	(20,21)	63291220.
602	(26,28)	87.0	95.6	2817.9	(20,21)	57955140.
603	(26,28)	86.1	94.8	2806.7	(20,21)	47565820.
604	(27,28)	85.2	94.2	2749.6	(20,21)	41318220.
605	(27,28)	85.1	94.5	2767.7	(20,21)	44813540.
606	(27,28)	86.0	95.7	2774.3	(20,21)	59512740.
607	(28,28)	87.6	97.2	2729.7	(21,21)	83805760.
608	(28,29)	88.7	98.4	2721.3	(21,22)	109398400.
609	(28,29)	89.2	99.0	2726.8	(21,22)	125021800.
610	(28,29)	88.6	99.0	2723.5	(21,22)	126865500.
611	(28,29)	87.9	98.9	2726.4	(21,22)	121852100.
612	(28,29)	86.8	98.8	2696.6	(21,22)	120118100.
613	(28,29)	87.6	99.0	2634.5	(21,22)	125948200.
614	(29,29)	89.2	99.4	2598.7	(22,22)	136909600.
615	(29,29)	90.1	99.7	2568.8	(22,22)	148381700.
616	(29,29)	89.9	100.0	2543.8	(22,22)	159875200.
617	(30,29)	89.1	100.5	2511.1	(22,21)	177344900.
618	(30,29)	88.7	101.1	2532.6	(22,21)	203336500.
619	(30,29)	89.9	101.7	2539.7	(22,21)	233335800.
620	(31,29)	89.7	102.1	2511.3	(23,21)	255678200.
621	(31,29)	91.0	102.2	2484.3	(23,21)	260306600.
622	(31,29)	91.1	102.0	2476.3	(23,21)	251198500.
623	(31,29)	90.2	101.8	2547.7	(23,21)	240992900.
624	(30,29)	89.2	101.9	2589.5	(22,21)	245148300.
625	(30,29)	89.2	102.4	2569.5	(22,21)	274474500.
626	(30,29)	90.8	103.0	2524.8	(22,21)	314932500.
627	(30,29)	91.9	103.2	2464.4	(22,21)	333371600.
628	(30,29)	91.8	103.0	2498.7	(22,21)	315062500.
629	(30,29)	90.5	102.4	2536.2	(22,21)	277861600
630	(30,29)	90.3	102.1	2569.8	(22,21)	256338800.
631	(30,29)	90.6	102.3	2587.1	(22,21)	269252100.
632	(30,29)	91.6	102.8	2568.6	(22,21)	300159500.
633	(31,29)	91.8	103.1	2539.4	(23,21)	325923300.
634	(31,29)	92.7	103.3	2476.3	(23,21)	340881400.
635	(32,29)	93.3	103.4	2411.4	(23,21)	347500300.
636	(33,29)	93.0	103.4	2334.1	(24,21)	346082300.
637	(34,29)	92.3	103.2	2252.5	(25,21)	329857300.
638	(33,29)	91.2	102.8	2265.1	(24,21)	299381500.
639	(33,30)	89.9	102.3	2299.3	(24,22)	268002400.
640	(32,30)	89.4	102.0	2326.7	(23,22)	253349200
641	(32,30)	89.6	102.3	2319.9	(23,22)	269518100.
642	(33,30)	91.3	103.0	2291.0	(24,22)	318886900.
643	(34,30)	92.6	103.9	2297.6	(24,22)	390603300.
644	(34,29)	93.1	104.6	2318.3	(25,21)	453109800
645	(33,30)	93.1	104.8	2365.0	(24,22)	476250900.
646	(33,30)	93.2	104.6	2386.6	(24,22)	460631300.
647	(33,29)	93.2	104.4	2360.3	(24,21)	434608100
648	(33,30)	94.0	104.2	2332.8	(24,22)	418864600
649	(34,29)	94.0	104.2	2304.6	(25,21)	417335800
650	(34,30)	93.3	104.3	2293.3	(24,22)	426046000
651	(35,29)	92.8	104.5	2251.3	(25,21)	441945600
652	(35,30)	92.9	104.6	2234.8	(25,21)	455387100.
653	(35,30)	93.2	104.5	2233.5	(25,21)	443911700.
654	(34,30)	92.9	104.1	2208.4	(24,22)	402746900.
655	(33,29)	92.0	103.5	2260.5	(24,21)	352640500
656	(32,29)	91.4	102.9	2311.3	(23,21)	311569900.
657	(32,29)	90.3	102.4	2[illegible]38.0	(23,21)	276736800
658	(33,29)	89.1	101.8	2418.3	(24,21)	242241500
659	(33,29)	89.5	101.4	2410.1	(24,21)	220826500
660	(34,29)	89.5	101.8	2380.2	(25,21)	240759200
661	(35,29)	91.7	102.9	2320.0	(25,21)	309736400
662	(35,29)	93.0	104.0	2239.5	(25,21)	394107400
663	(35,29)	93.3	104.5	2185.0	(25,21)	441978600

664	(35, 29)	92.8	104.3	2192.0	(25, 21)	429250800.
665	(33, 29)	91.7	104.0	2316.8	(24, 21)	396949500.
666	(32, 29)	92.3	104.4	2389.3	(23, 21)	432342000.
667	(33, 29)	94.6	105.5	2371.8	(24, 21)	556478700.
668	(33, 30)	95.9	106.3	2335.2	(24, 22)	683153900.
669	(34, 30)	96.0	106.6	2308.2	(24, 22)	724655600.
670	(35, 30)	95.0	106.4	2275.7	(25, 21)	694019300.
671	(34, 30)	95.6	106.2	2239.2	(24, 22)	667657200.
672	(35, 30)	96.1	106.5	2248.4	(25, 21)	703551700.
673	(35, 29)	95.7	107.1	2246.8	(25, 21)	808123900.
674	(35, 29)	95.6	107.8	2189.3	(25, 21)	950937900.
675	(36, 29)	96.5	108.3	2127.2	(26, 21)	1065702000.
676	(37, 29)	96.5	108.3	2101.6	(26, 21)	1070738000.
677	(37, 30)	95.6	107.9	2149.9	(26, 21)	966490900.
678	(36, 30)	95.5	107.3	2233.4	(26, 21)	849774600.
679	(35, 30)	95.8	107.1	2298.8	(25, 21)	816768500.
680	(35, 30)	96.2	107.4	2304.9	(25, 21)	861797900.
681	(35, 30)	96.7	107.6	2313.4	(25, 21)	917298400.
682	(34, 30)	96.1	107.8	2309.9	(24, 22)	950396700.
683	(34, 30)	95.6	107.8	2278.9	(24, 22)	961038800.
684	(34, 30)	96.8	107.7	2213.9	(24, 22)	931545900.
685	(34, 30)	96.8	107.3	2221.9	(24, 22)	849529300.
686	(32, 29)	95.9	106.7	2351.8	(23, 21)	737056000.
687	(32, 29)	94.6	106.2	2442.0	(23, 21)	658821100.
688	(32, 29)	93.4	106.3	2440.3	(23, 21)	676542200.
689	(32, 30)	94.5	106.9	2382.9	(23, 22)	771213600.
690	(33, 30)	95.6	107.4	2333.1	(24, 22)	871556100.
691	(33, 30)	96.0	107.7	2287.1	(24, 22)	932806100.
692	(34, 30)	95.5	107.8	2263.9	(24, 22)	954978300.
693	(35, 30)	95.6	107.8	2236.1	(25, 21)	961893400.
694	(36, 30)	95.0	107.9	2191.8	(26, 21)	968356400.
695	(37, 30)	95.0	107.8	2148.7	(26, 21)	944959000.
696	(36, 30)	95.2	107.4	2164.1	(26, 21)	867580700.
697	(35, 30)	94.4	106.8	2230.5	(25, 21)	759135700.
698	(34, 29)	93.2	106.3	2271.7	(25, 21)	679145500.
699	(33, 29)	95.1	106.3	2295.0	(24, 21)	675537400.
700	(33, 29)	96.4	106.6	2347.7	(24, 21)	728302100.
701	(32, 29)	96.3	106.8	2385.2	(23, 21)	764087800.
702	(32, 29)	94.8	106.7	2412.2	(23, 21)	737164500.
703	(32, 29)	95.0	106.3	2410.3	(23, 21)	672652500.
704	(32, 29)	94.1	106.0	2407.2	(23, 21)	628486400.
705	(32, 29)	93.3	106.1	2387.0	(23, 21)	641368300.
706	(32, 29)	95.4	106.4	2421.4	(23, 21)	690063600.
707	(31, 29)	96.5	106.7	2461.3	(23, 21)	735993300.
708	(31, 29)	96.2	106.9	2485.1	(23, 21)	772594700.
709	(30, 29)	94.7	107.1	2514.7	(22, 21)	815511000.
710	(30, 29)	95.2	107.4	2517.9	(22, 21)	878596400.
711	(31, 29)	95.5	107.7	2475.1	(23, 21)	942982100.
712	(31, 29)	95.6	107.9	2402.5	(23, 21)	969834000.
713	(31, 30)	96.0	107.7	2354.5	(23, 22)	938497800.
714	(32, 30)	95.9	107.3	2323.3	(23, 22)	855688200.
715	(31, 29)	94.7	106.7	2363.2	(23, 21)	744487200.
716	(30, 29)	92.4	106.1	2432.5	(22, 21)	640601600.
717	(30, 29)	92.4	105.6	2463.2	(22, 21)	575268900.
718	(30, 29)	92.3	105.7	2460.3	(22, 21)	586011100.
719	(32, 29)	92.6	106.4	2428.6	(23, 21)	690923300.
720	(33, 29)	94.7	107.2	2394.8	(24, 21)	829219600.
721	(33, 29)	95.5	107.6	2365.9	(24, 21)	916230900.
722	(33, 29)	95.2	107.8	2369.2	(24, 21)	950671100.
723	(33, 29)	95.4	108.0	2401.5	(24, 21)	1000510000.
724	(33, 29)	96.4	108.4	2405.6	(24, 21)	1084648000.
725	(33, 29)	96.3	108.5	2410.1	(24, 21)	1123723000.
726	(33, 29)	95.4	108.2	2388.2	(24, 21)	1051928000.
727	(33, 30)	93.8	107.7	2394.1	(24, 22)	932258000.
728	(33, 30)	95.8	107.4	2413.3	(24, 22)	865074900.
729	(33, 30)	97.2	107.4	2397.0	(24, 22)	862383900.

730	(33,30)	97.9	107.4	2321.3	(24,22)	861974800.
731	(33,30)	97.7	107.2	2355.8	(24,22)	833397800.
732	(33,30)	97.0	107.0	2395.2	(24,22)	800053000
733	(33,30)	95.6	107.0	2416.2	(24,22)	787244300.
734	(33,30)	95.6	107.0	2398.0	(24,22)	797263100.
735	(33,30)	96.1	107.3	2328.7	(24,22)	843720700.
736	(34,30)	96.6	107.7	2295.8	(24,22).	923132700.
737	(35,30)	96.6	107.9	2305.5	(25,21)	985853700.
738	(34,30)	96.8	107.9	2327.2	(24,22)	973301000.
739	(33,29)	96.4	107.5	2370.6	(24,21)	884289500.
740	(33,29)	95.5	106.9	2379.1	(24,21)	778540500.
741	(33,30)	95.6	106.6	2323.3	(24,22)	732144900.
742	(34,30)	95.4	106.9	2320.9	(24,22)	777334000.
743	(34,30)	96.3	107.6	2325.3	(24,22)	905967600.
744	(34,30)	97.4	108.3	2352.4	(24,22)	1064525000.
745	(33,30)	97.5	108.7	2389.0	(24,22)	1164996000.
746	(33,30)	97.0	108.7	2393.4	(24,22)	1172649000.
747	(32,30)	96.5	108.6	2365.9	(23,22)	1140597000.
748	(33,29)	97.5	108.6	2315.7	(24,21)	1156411000.
749	(34,30)	97.9	109.0	2233.6	(24,22)	1270126000.
750	(35,30)	99.7	109.5	2140.9	(25,21)	1422574000
751	(35,30)	100.1	109.7	2116.5	(25,21)	1478988000.
752	(34,30)	99.2	109.3	2113.3	(24,22)	1358874000.
753	(34,30)	96.9	108.4	2108.3	(24,22)	1108944000.
754	(34,30)	94.5	107.4	2210.3	(24,22)	870531600.
755	(33,30)	93.2	106.7	2346.6	(24,22)	742460400.
756	(32,29)	93.1	106.4	2440.7	(23,21)	697890800.
757	(31,29)	92.7	106.1	2501.3	(23,21)	652457000.
758	(30,29)	92.4	105.7	2533.0	(22,21)	587657000.
759	(30,29)	92.9	105.3	2533.6	(22,21)	534083300.
760	(31,29)	92.9	105.1	2505.8	(23,21)	516323100
761	(31,29)	94.0	105.1	2479.6	(23,21)	511007200.
762	(30,29)	93.5	104.9	2502.3	(22,21)	486275100.
763	(30,29)	91.4	104.5	2498.6	(22,21)	448852500.
764	(30,29)	92.0	104.3	2463.4	(22,21)	430002400.
765	(31,30)	91.6	104.4	2383.8	(23,22)	438797100
766	(32,30)	91.3	104.6	2311.4	(23,22)	455639300.
767	(32,29)	91.0	104.6	2337.1	(23,21)	460517400.
768	(32,29)	91.0	104.6	2406.3	(23,21)	456237600.
769	(32,30)	90.7	104.5	2462.7	(23,22)	450271000
770	(31,30)	90.7	104.5	2500.7	(23,22)	442666200
771	(30,29)	90.9	104.3	2498.5	(22,21)	424765200
772	(30,29)	91.3	104.0	2505.4	(22,21)	395302400.
773	(30,29)	91.1	103.7	2507.2	(22,21)	367993300.
774	(31,29)	91.5	103.5	2524.5	(23,21)	353988400
775	(31,29)	91.9	103.4	2520.5	(23,21)	347934700.
776	(32,29)	92.5	103.2	2500.9	(23,21)	332404000.
777	(32,29)	92.3	102.8	2491.4	(23,21)	303623900.
778	(32,29)	91.4	102.4	2469.1	(23,21)	273458200.
779	(32,29)	89.8	102.1	2465.6	(23,21)	257485000.
780	(32,30)	91.5	102.1	2430.9	(23,22)	254303400.
781	(32,29)	92.5	102.0	2393.2	(23,21)	248438900.
782	(31,29)	92.3	101.6	2389.9	(23,21)	226729100.
783	(30,29)	90.9	100.8	2423.8	(22,21)	191046100.
784	(29,29)	88.2	99.9	2557.7	(22,22)	156133900.
785	(28,29)	85.1	99.4	2644.6	(21,22)	136478800.
786	(28,29)	85.7	99.3	2637.4	(21,22)	134687700.
787	(29,29)	86.3	99.5	2586.4	(22,22)	140977600.
788	(30,29)	86.9	99.6	2524.5	(22,21)	142976900.
789	(29,29)	87.6	99.4	2475.5	(22,22)	136522100.
790	(29,29)	88.1	99.0	2483.6	(22,22)	125594900.
791	(28,29)	87.9	98.6	2573.2	(21,22)	114496800.
792	(28,28)	89.5	98.2	2592.4	(21,21)	104955100.
793	(29,28)	90.5	97.8	2602.4	(22,21)	96300270.
794	(29,28)	90.6	97.4	2650.2	(22,21)	87588450.
795	(29,28)	89.7	97.0	2670.8	(22,21)	78601250

796	(29,29)	87.8	96.4	2648.4	(22,22)	69446460
797	(29,29)	85.4	95.8	2588.3	(22,22)	60841550
798	(30,29)	83.0	95.4	2543.4	(22,21)	54998820.
799	(30,30)	80.9	95.1	2495.7	(22,22)	51808750.
800	(30,30)	81.3	94.9	2469.6	(22,22)	48481790.
801	(30,30)	81.7	94.3	2454.5	(22,22)	42646900.
802	(30,30)	82.9	93.6	2491.7	(22,22).	35929230.
803	(29,30)	83.4	93.1	2531.3	(21,22)	32237330.
804	(28,29)	83.0	93.2	2546.8	(21,22)	32790510.
805	(28,29)	81.6	93.3	2620.3	(21,22)	34167040.
806	(28,29)	81.0	93.1	2666.8	(21,22)	32498020.

TRACK TRAIL FOR SPQSASH2.DA

BLOCK	(IR3D, JR3D)	AMAX	AMAXUP	RSUM	LOG COORD'S	POWER
1	(33,29)	84.5	92.8	2331.0	(24,21)	30505380
2	(34,29)	84.2	92.8	2307.7	(25,21)	30461340
3	(35,29)	83.6	92.8	2277.6	(25,21)	30482830
10	(35,29)	84.5	94.2	2139.6	(25,21)	41828220
11	(37,29)	86.7	95.8	2033.1	(26,21)	60395060
12	(38,29)	87.8	96.7	1998.1	(27,20)	74953780
13	(38,29)	87.6	96.9	1983.3	(27,20)	78176340
14	(37,29)	86.8	96.5	2034.3	(26,21)	70935390
15	(36,29)	87.0	95.9	2081.8	(26,21)	61920190
16	(36,29)	88.1	95.7	2096.9	(26,21)	58471380
17	(37,29)	88.4	95.7	2066.2	(26,21)	58938690
18	(37,29)	87.9	95.5	2022.3	(26,21)	56568400
19	(37,29)	86.6	94.9	2073.5	(26,21)	48992220
20	(36,29)	84.5	94.1	2122.5	(26,21)	40727720
21	(36,28)	83.7	93.7	2103.2	(26,20)	37534400
22	(37,29)	84.6	94.0	2133.3	(26,21)	39785250
23	(37,29)	85.5	94.4	2140.9	(26,21)	43526640
24	(37,29)	86.7	94.7	2157.4	(26,21)	46380340
25	(36,29)	87.6	94.8	2134.4	(26,21)	47724210
26	(36,29)	87.5	94.6	2073.8	(26,21)	46089180
27	(37,29)	86.6	94.1	2025.1	(26,21)	40532770
28	(36,29)	85.1	93.1	2070.7	(26,21)	32734580
31	(36,30)	84.8	93.8	2035.5	(26,21)	37731540
32	(37,30)	86.8	95.0	1988.1	(26,21)	50352020
33	(37,29)	87.3	95.5	1961.5	(26,21)	56355630
34	(36,29)	86.3	95.1	2117.7	(26,21)	51803330
35	(34,29)	84.5	94.6	2224.3	(25,21)	45700460
36	(35,29)	85.9	95.4	2193.2	(25,21)	54664690
37	(37,29)	89.6	97.7	2059.7	(26,21)	93130080
38	(40,29)	92.5	99.9	1943.2	(28,20)	154774600
39	(41,29)	94.0	101.2	1844.6	(28,20)	208918000
40	(40,29)	94.3	101.4	1890.0	(28,20)	220450300
41	(37,29)	93.3	100.6	1998.6	(26,21)	182223400
42	(34,29)	91.0	98.9	2136.7	(25,21)	121970100
43	(32,29)	87.6	96.7	2295.2	(23,21)	74923900
44	(30,29)	84.3	95.3	2426.8	(22,21)	54075260
45	(29,29)	84.0	95.0	2453.2	(22,22)	49737380
46	(30,29)	84.5	95.0	2385.4	(22,21)	50621520
47	(31,29)	84.8	95.0	2353.7	(23,21)	50519090
48	(31,29)	85.1	94.9	2344.4	(23,21)	48497860
49	(31,29)	84.5	94.6	2325.6	(23,21)	45823280
50	(30,29)	83.9	94.4	2410.8	(22,21)	43267410
51	(28,29)	83.1	94.0	2512.1	(21,22)	39967390
52	(27,29)	82.0	93.5	2558.1	(20,22)	35353420
61	(27,27)	89.7	95.3	2797.8	(20,20)	53180210
62	(27,26)	93.9	100.2	2766.2	(21,20)	164533600
63	(27,26)	98.2	104.1	2747.8	(21,20)	408765200
64	(28,26)	101.5	106.8	2702.6	(21,20)	757267700
65	(28,27)	103.9	108.8	2663.4	(21,20)	1195103000
66	(28,27)	105.6	110.6	2686.3	(21,20)	1834996000
67	(28,26)	106.6	112.2	2712.7	(21,20)	2606754000
68	(28,26)	107.2	113.0	2699.1	(21,20)	3133739000
69	(28,25)	107.5	113.0	2661.4	(21,20)	3177981000
70	(28,27)	108.3	112.9	2612.0	(21,20)	3062976000
71	(28,27)	108.6	113.1	2634.2	(21,20)	3206067000
72	(28,27)	108.7	113.4	2641.8	(21,20)	3477667000
73	(28,27)	108.8	113.5	2643.0	(21,20)	3544462000
74	(28,27)	108.8	113.5	2636.8	(21,20)	3542521000
75	(28,27)	108.8	113.8	2679.0	(21,20)	3834216000
76	(28,27)	108.7	114.2	2685.3	(21,20)	4210641000
77	(28,27)	108.6	114.3	2657.2	(21,20)	4265793000

78	(28, 27)	108.5	114.1	2619.5	(21, 20)	4094593000
79	(28, 27)	108.6	114.2	2631.2	(21, 20)	4135992000
80	(28, 27)	108.9	114.4	2647.4	(21, 20)	4329288000
81	(28, 27)	109.2	114.4	2633.8	(21, 20)	4385563000
82	(28, 27)	109.4	114.4	2626.3	(21, 20)	4391817000
83	(27, 27)	109.7	114.6	2657.0	(20, 20)	4609241000
84	(28, 27)	109.9	114.8	2656.1	(21, 20)	4837884000
85	(28, 27)	110.0	114.8	2617.2	(21, 20)	4783325000
86	(28, 28)	110.1	114.7	2619.2	(21, 21)	4651172000
87	(27, 27)	110.2	114.8	2662.2	(20, 20)	4775739000
88	(28, 27)	110.3	115.0	2663.0	(21, 20)	4990595000
89	(28, 28)	110.3	115.0	2642.7	(21, 21)	4992782000
90	(27, 28)	110.5	115.0	2659.8	(20, 21)	4962988000
91	(27, 28)	110.4	115.1	2704.5	(20, 21)	5120573000
92	(27, 28)	110.2	115.2	2702.7	(20, 21)	5214142000
93	(27, 28)	109.9	115.0	2664.7	(20, 21)	5035368000
94	(27, 28)	109.8	114.9	2665.7	(20, 21)	4943020000
95	(27, 28)	109.8	115.1	2703.0	(20, 21)	5185081000
96	(27, 28)	109.6	115.3	2700.7	(20, 21)	5357916000
97	(27, 28)	109.4	115.1	2672.6	(20, 21)	5147628000
98	(27, 28)	109.2	115.0	2672.8	(20, 21)	4975731000
99	(26, 28)	109.2	115.1	2708.6	(20, 21)	5186269000
100	(26, 28)	109.1	115.3	2706.3	(20, 21)	5354111000
101	(27, 28)	109.0	115.1	2678.7	(20, 21)	5109289000
102	(27, 28)	108.8	114.9	2678.5	(20, 21)	4879995000
103	(26, 28)	108.6	115.0	2716.2	(20, 21)	5060571000
104	(26, 28)	108.5	115.2	2717.0	(20, 21)	5247132000
105	(27, 28)	108.3	115.1	2690.2	(20, 21)	5075251000
106	(27, 28)	108.2	115.0	2691.0	(20, 21)	4967522000
107	(26, 28)	108.1	115.2	2725.3	(20, 21)	5283213000
108	(26, 28)	107.9	115.4	2725.8	(20, 21)	5553455000
109	(27, 28)	107.8	115.3	2693.4	(20, 21)	5404623000
110	(27, 28)	107.8	115.3	2680.5	(20, 21)	5331972000
111	(26, 28)	107.8	115.6	2711.3	(20, 21)	5770678000
112	(26, 28)	108.3	115.9	2709.8	(20, 21)	6190035000
113	(27, 28)	108.8	115.8	2675.4	(20, 21)	6033084000
114	(27, 28)	108.9	115.6	2658.5	(20, 21)	5701870000
115	(27, 28)	109.0	115.6	2687.8	(20, 21)	5771829000
116	(27, 28)	109.1	115.8	2693.6	(20, 21)	5956784000
117	(27, 28)	109.3	115.6	2664.6	(20, 21)	5797257000
118	(27, 28)	109.4	115.5	2650.0	(20, 21)	5629735000
119	(27, 28)	109.6	115.7	2682.5	(20, 21)	5909479000
120	(27, 28)	109.9	116.0	2684.7	(20, 21)	6279356000
121	(27, 28)	110.1	115.9	2660.4	(20, 21)	6222742000
122	(27, 28)	110.2	115.8	2648.2	(20, 21)	6090850000
123	(27, 28)	110.3	116.1	2684.4	(20, 21)	6400229000
124	(27, 28)	110.5	116.3	2692.5	(20, 21)	6812234000
125	(27, 28)	110.7	116.2	2667.7	(20, 21)	6676664000
126	(27, 28)	110.7	116.0	2650.3	(20, 21)	6267290000
127	(27, 28)	110.8	116.0	2690.6	(20, 21)	6274138000
128	(27, 28)	111.0	116.2	2702.4	(20, 21)	6620586000
129	(27, 28)	111.2	116.2	2676.5	(20, 21)	6660829000
130	(27, 28)	111.5	116.1	2647.1	(20, 21)	6439801000
131	(27, 28)	111.7	116.1	2678.1	(20, 21)	6491812000
132	(27, 28)	111.9	116.3	2697.0	(20, 21)	6752088000
133	(27, 28)	111.9	116.2	2670.7	(20, 21)	6623453000
134	(27, 28)	111.9	115.9	2630.3	(20, 21)	6118744000
135	(27, 28)	111.8	115.7	2656.0	(20, 21)	5864903000
136	(27, 28)	111.8	115.8	2685.6	(20, 21)	6027792000
137	(27, 28)	111.8	115.8	2671.3	(20, 21)	6059241000
138	(27, 28)	111.8	115.6	2630.6	(20, 21)	5795930000
139	(27, 28)	111.9	115.6	2637.9	(20, 21)	5721600000
140	(27, 28)	112.0	115.8	2669.7	(20, 21)	6008353000
141	(27, 28)	112.0	115.9	2657.3	(20, 21)	6117040000
142	(28, 28)	112.0	115.6	2618.1	(21, 21)	5778825000
143	(27, 28)	111.9	115.4	2625.4	(20, 21)	5455950000

144	(27,28)	111.7	115.4	2672.3	(20,21)	5512466000
145	(27,28)	111.5	115.5	2668.8	(20,21)	5578764000
146	(27,28)	111.3	115.2	2635.5	(20,21)	5270417000
147	(27,28)	111.2	114.9	2622.2	(20,21)	4935971000
148	(27,28)	111.1	115.0	2657.6	(20,21)	4974707000
149	(27,28)	110.9	115.1	2660.2	(20,21)	5110755000
150	(27,28)	110.6	114.9	2637.5	(20,21)	4852838000
151	(27,28)	110.2	114.5	2621.9	(20,21)	4462641000
152	(27,28)	110.0	114.5	2655.8	(20,21)	4462088000
153	(27,28)	110.1	114.8	2675.1	(20,21)	4758282000
154	(27,28)	110.1	114.8	2650.7	(20,21)	4766065000
155	(27,28)	110.0	114.5	2621.8	(20,21)	4511318000
156	(27,28)	110.0	114.5	2651.2	(20,21)	4517659000
157	(27,28)	110.1	114.9	2689.1	(20,21)	4862902000
158	(27,28)	110.3	114.9	2675.7	(20,21)	4936196000
159	(27,28)	110.2	114.5	2642.2	(20,21)	4461502000
160	(27,28)	110.0	114.0	2658.3	(20,21)	3945489000
161	(26,28)	109.7	113.8	2707.6	(20,21)	3827246000
162	(26,28)	109.6	113.8	2714.2	(20,21)	3837766000
163	(27,28)	109.4	113.5	2682.5	(20,21)	3508277000
164	(27,28)	109.0	112.8	2678.0	(20,21)	3011761000
165	(26,28)	108.5	112.4	2733.9	(20,21)	2781468000
166	(26,28)	108.1	112.5	2770.5	(20,21)	2828415000
167	(26,28)	107.8	112.4	2749.0	(20,21)	2745625000
168	(27,28)	107.6	111.9	2703.1	(20,21)	2471149000
169	(26,28)	107.5	111.7	2717.1	(20,21)	2332391000
170	(26,28)	107.4	111.9	2753.2	(20,21)	2473390000
171	(26,28)	107.3	112.1	2745.5	(20,21)	2584103000
172	(27,28)	107.1	111.8	2711.4	(20,21)	2423235000
173	(26,28)	106.9	111.5	2726.4	(20,21)	2239269000
174	(26,28)	106.7	111.7	2766.9	(20,21)	2330386000
175	(26,28)	106.6	112.1	2784.9	(20,21)	2541489000
176	(26,28)	106.3	111.9	2751.2	(20,21)	2462599000
177	(27,28)	106.0	111.2	2700.2	(20,21)	2113420000
178	(26,28)	105.7	110.8	2718.9	(20,21)	1890032000
179	(26,28)	105.6	111.0	2753.5	(20,21)	1974992000
180	(26,28)	105.7	111.2	2744.0	(20,21)	2076876000
181	(27,28)	105.3	110.8	2702.2	(20,21)	1917264000
182	(27,28)	104.9	110.2	2709.7	(20,21)	1660753000
183	(26,28)	104.8	110.1	2758.7	(20,21)	1606355000
184	(26,28)	104.8	110.4	2787.0	(20,21)	1726005000
185	(26,28)	104.8	110.4	2760.6	(20,21)	1727111000
186	(27,28)	104.8	110.0	2723.0	(20,21)	1585558000
187	(26,28)	105.0	109.9	2753.8	(20,21)	1566407000
188	(26,28)	105.2	110.5	2779.7	(20,21)	1783236000
189	(26,28)	105.4	110.9	2770.3	(20,21)	1964874000
190	(27,28)	105.2	110.6	2725.2	(20,21)	1830586000
191	(27,28)	104.9	109.8	2716.3	(20,21)	1519316000
192	(26,28)	104.5	109.4	2760.3	(20,21)	1364925000
193	(26,28)	104.2	109.5	2802.3	(20,21)	1428196000
194	(26,28)	103.7	109.6	2783.7	(20,21)	1442148000
195	(27,28)	103.3	109.0	2739.5	(20,21)	1265007000
196	(26,28)	102.9	108.3	2734.9	(20,21)	1075965000
197	(26,28)	102.9	108.4	2759.9	(20,21)	1091268000
198	(26,28)	103.2	108.9	2766.4	(20,21)	1241999000
199	(27,28)	103.2	109.1	2724.5	(20,21)	1280563000
200	(28,28)	102.8	108.7	2663.1	(21,21)	1172575000
201	(27,28)	102.4	108.5	2677.5	(20,21)	1117064000
202	(27,28)	102.6	108.9	2706.7	(20,21)	1238792000
203	(27,28)	103.1	109.4	2703.8	(20,21)	1387333000
204	(27,28)	103.0	109.3	2661.1	(20,21)	1346719000
205	(28,28)	103.2	108.7	2609.6	(21,21)	1161752000
206	(27,28)	103.3	108.3	2617.9	(20,21)	1069030000
207	(27,28)	103.5	108.7	2646.3	(20,21)	1166952000
208	(27,28)	103.8	109.1	2647.2	(20,21)	1284825000
209	(28,28)	104.0	108.9	2611.0	(21,21)	1236549000

210	(28,28)	104.0	108.2	2615.7	(21,21)	1059040000
211	(28,28)	103.7	107.7	2630.9	(21,21)	930928900
212	(28,28)	103.2	107.6	2650.1	(21,21)	913918200
213	(28,28)	102.4	107.5	2675.9	(21,21)	894036200
214	(28,28)	101.5	106.9	2666.2	(21,21)	775951600
215	(27,28)	100.8	105.8	2671.8	(20,21)	606547500
216	(27,28)	100.2	105.0	2673.9	(20,21)	497182000
217	(27,28)	99.6	104.8	2708.3	(20,21)	475213600
218	(27,28)	98.9	104.7	2722.6	(20,21)	469745700
219	(27,28)	98.2	104.3	2692.1	(20,21)	430738900
220	(27,28)	97.9	103.9	2683.9	(20,21)	388894000
221	(27,27)	97.9	104.0	2648.7	(20,20)	394982900
222	(26,27)	98.0	104.4	2642.5	(20,21)	433493500
223	(26,28)	97.7	104.4	2644.5	(20,21)	436683500
224	(27,28)	97.5	103.8	2618.1	(20,21)	379471100
225	(27,28)	97.2	103.0	2606.8	(20,21)	314298900
226	(27,28)	97.2	102.8	2588.4	(20,21)	301084400
227	(27,28)	97.6	103.2	2596.4	(20,21)	329635800
228	(27,28)	97.3	103.3	2595.3	(20,21)	337644300
229	(27,28)	95.7	102.7	2599.5	(20,21)	292233200
230	(27,28)	95.0	101.4	2651.1	(20,21)	218569700
231	(26,28)	94.7	100.2	2679.7	(20,21)	164200200
232	(26,28)	94.6	99.6	2703.3	(20,21)	145951800
233	(26,28)	94.5	99.6	2723.6	(20,21)	145032600
234	(26,28)	94.6	99.5	2733.3	(20,21)	141395100
235	(25,28)	94.6	99.2	2771.0	(19,21)	132126300
236	(25,28)	94.4	99.0	2757.9	(19,21)	126719100
237	(26,28)	94.2	99.0	2727.9	(20,21)	126796100
238	(26,28)	93.9	99.0	2744.7	(20,21)	124645000
239	(26,28)	93.5	98.6	2744.8	(20,21)	115055000
240	(26,28)	93.2	98.0	2749.0	(20,21)	100258500
241	(27,28)	93.0	97.4	2731.8	(20,21)	86752900
242	(27,29)	92.6	96.9	2682.3	(20,22)	78009060
243	(27,29)	92.5	96.6	2681.0	(20,22)	72335500
244	(27,29)	92.4	96.3	2676.3	(20,22)	67106900
245	(28,29)	92.3	95.9	2682.5	(21,22)	62326460
246	(28,29)	92.1	95.8	2642.6	(21,22)	60259780
247	(29,29)	91.5	95.9	2598.9	(22,22)	61525820
248	(28,29)	90.8	95.9	2593.4	(21,22)	62103950
249	(28,29)	90.1	95.5	2634.3	(21,22)	56497070
250	(27,29)	89.5	94.6	2668.9	(20,22)	45637730
251	(27,29)	89.1	93.6	2694.5	(20,22)	36219970
252	(28,29)	88.9	93.3	2705.5	(21,22)	33547520
253	(28,29)	88.6	93.6	2661.9	(21,22)	36001470
254	(28,29)	87.8	93.7	2697.8	(21,22)	37340240
255	(27,29)	86.3	93.3	2755.0	(20,22)	33845580
264	(29,29)	85.2	92.9	2606.4	(22,22)	30722750
265	(30,29)	84.6	93.7	2526.6	(22,21)	36789950
266	(29,29)	84.6	94.8	2610.8	(22,22)	48022640
267	(28,29)	85.3	96.3	2639.0	(21,22)	66957920
268	(29,28)	87.5	97.6	2637.9	(22,21)	91465090
269	(29,29)	88.3	98.6	2620.7	(22,22)	114723100
270	(30,29)	88.3	99.3	2559.8	(22,21)	134239700
271	(32,29)	88.3	100.0	2433.3	(23,21)	158702100
272	(34,30)	90.0	101.0	2357.9	(24,22)	200883700
273	(36,30)	92.3	102.2	2287.0	(26,21)	261683500
274	(36,29)	94.0	103.1	2235.4	(26,21)	322565900
275	(38,29)	95.0	103.6	2189.7	(27,20)	362136600
276	(38,29)	95.4	103.8	2130.4	(27,20)	380762600
277	(39,29)	95.8	104.0	2130.3	(27,20)	401317100
278	(40,30)	96.0	104.3	2109.2	(28,21)	431096800
279	(40,29)	96.5	104.5	2155.6	(28,20)	441596700
280	(39,29)	96.0	104.0	2207.3	(27,20)	401775400
281	(37,30)	94.0	103.1	2266.1	(26,21)	322751200
282	(36,30)	91.3	101.9	2283.5	(26,21)	247223000
283	(35,30)	91.4	101.0	2241.7	(25,21)	201095700

284	(35, 30)	90. 1	100. 5	2171. 5	(25, 21)	177618400
285	(37, 30)	88. 9	100. 1	2083. 1	(26, 21)	162632400
286	(38, 30)	88. 6	100. 0	1928. 7	(27, 21)	157195600.
287	(39, 30)	90. 0	100. 1	1889. 0	(27, 21)	161891800.
288	(40, 30)	90. 5	100. 2	1893. 0	(28, 21)	165016600.
289	(39, 30)	90. 0	100. 0	1915. 5	(27, 21)	159143400
290	(39, 30)	89. 1	99. 8	1894. 3	(27, 21)	152958000.
291	(39, 30)	89. 6	100. 0	1881. 6	(27, 21)	160251700.
292	(40, 31)	91. 1	100. 7	1856. 0	(28, 21)	187329700.
293	(41, 31)	92. 4	101. 6	1854. 8	(28, 21)	226872700.
294	(42, 30)	93. 1	102. 3	1838. 7	(29, 21)	266463600.
295	(43, 30)	94. 1	102. 7	1836. 4	(29, 20)	293801000.
296	(43, 30)	94. 9	102. 7	1857. 3	(29, 20)	294976500.
297	(42, 30)	94. 9	102. 2	1871. 6	(29, 21)	265535600.
298	(40, 30)	94. 1	101. 5	1936. 9	(28, 21)	221758700.
299	(39, 30)	92. 7	100. 7	1963. 4	(27, 21)	188168700.
300	(40, 31)	92. 3	100. 5	1888. 9	(28, 21)	177961500.
301	(42, 31)	93. 4	100. 7	1831. 2	(29, 21)	188230800.
302	(43, 30)	93. 5	101. 1	1771. 0	(29, 20)	206081000.
303	(42, 30)	93. 1	101. 4	1776. 2	(29, 21)	218009800.

TRACK TRAIL FOR SPZSASH3.DA

BLOCK	(IR3D, JR3D)	AMAX	AMAXUP	RSUM	LOG COORD'S	POWER
444	(38, 29)	83.5	93.0	1932.1	(27, 20)	31912130
445	(38, 29)	82.9	93.0	1969.3	(27, 20)	31666300
447	(36, 30)	84.2	92.9	1992.9	(26, 21)	30731620
448	(36, 30)	85.7	93.3	2032.2	(26, 21)	33518770
449	(36, 30)	86.1	93.3	2061.2	(26, 21)	34194820
450	(36, 30)	85.3	92.8	2105.0	(26, 21)	30164750
458	(36, 29)	82.1	93.2	2271.6	(26, 21)	32752030
459	(36, 29)	83.6	93.6	2299.4	(26, 21)	36479230
460	(35, 29)	84.1	93.6	2300.5	(25, 21)	36055060
461	(35, 29)	83.2	92.9	2297.4	(25, 21)	31095100
464	(34, 29)	85.1	93.7	2324.1	(25, 21)	37277580
465	(35, 29)	87.0	94.9	2267.8	(25, 21)	48935550
466	(36, 29)	87.6	95.5	2215.1	(26, 21)	56318560
467	(35, 29)	86.9	95.5	2223.3	(25, 21)	56045090
468	(35, 29)	85.7	95.0	2311.2	(25, 21)	50504460
469	(35, 28)	86.2	94.5	2365.6	(25, 20)	44290380
470	(35, 28)	86.1	93.9	2410.8	(25, 20)	38982500
471	(33, 28)	85.4	93.3	2471.1	(24, 20)	33498770
477	(34, 29)	87.6	93.0	2479.8	(25, 21)	31559920
478	(35, 29)	88.3	94.0	2430.1	(25, 21)	39793360
479	(36, 29)	88.6	94.6	2350.6	(26, 21)	46052940
480	(36, 29)	88.6	95.0	2337.4	(26, 21)	49862820
481	(36, 28)	88.6	95.3	2350.9	(26, 20)	53485180
482	(36, 28)	88.4	96.0	2334.0	(26, 20)	63800270
483	(36, 28)	87.8	97.2	2277.9	(26, 20)	83233470
484	(36, 28)	89.5	98.1	2225.5	(26, 20)	102373300
485	(37, 29)	90.1	98.3	2222.7	(26, 21)	106892000
486	(36, 29)	89.3	97.7	2227.6	(26, 21)	93114340
487	(34, 29)	87.5	96.7	2268.0	(25, 21)	73491380
488	(34, 29)	86.1	96.3	2316.3	(25, 21)	67706000
489	(33, 29)	86.5	97.1	2311.9	(24, 21)	80372140
490	(33, 30)	87.2	97.8	2274.1	(24, 22)	95704660
491	(33, 29)	87.4	97.9	2307.5	(24, 21)	98560190
492	(32, 29)	88.5	97.4	2420.5	(23, 21)	08056990
493	(32, 29)	89.6	96.8	2502.5	(23, 21)	75420720
494	(32, 29)	90.8	96.5	2523.3	(23, 21)	70515060
495	(32, 28)	91.6	96.7	2518.0	(23, 21)	73848260
496	(32, 28)	91.7	97.1	2568.4	(23, 21)	80479120
497	(31, 28)	91.2	97.4	2607.0	(23, 21)	87006030
498	(30, 28)	90.4	97.5	2617.6	(22, 21)	89591740
499	(30, 28)	89.2	97.5	2592.4	(22, 21)	88205460
500	(31, 28)	87.8	97.5	2563.9	(23, 21)	88935220
501	(30, 28)	88.8	97.9	2521.6	(22, 21)	96624060
502	(30, 28)	89.3	98.3	2498.5	(22, 21)	106496200
503	(30, 29)	89.0	98.5	2518.9	(22, 21)	112646700
504	(31, 29)	90.4	98.6	2519.4	(23, 21)	115793700
505	(31, 28)	93.4	98.9	2539.9	(23, 21)	123752400
506	(31, 28)	95.4	99.5	2505.0	(23, 21)	140326000
507	(32, 28)	96.7	100.1	2503.1	(23, 21)	162231300
508	(31, 28)	97.4	100.7	2540.8	(23, 21)	186498700
509	(31, 28)	97.7	101.4	2549.7	(23, 21)	219081100
510	(31, 29)	98.0	102.3	2496.0	(23, 21)	267112200
511	(33, 29)	98.0	103.1	2407.3	(24, 21)	322396400
512	(34, 29)	98.1	103.6	2367.0	(25, 21)	361760000
513	(35, 29)	97.8	103.6	2388.7	(25, 21)	358953200
514	(34, 29)	97.2	102.9	2454.4	(25, 21)	309970900
515	(32, 29)	95.9	101.8	2508.8	(23, 21)	240823200
516	(31, 29)	93.4	100.8	2550.1	(23, 21)	190912800
517	(31, 29)	89.9	100.4	2524.3	(23, 21)	174368500
518	(31, 29)	89.9	100.4	2445.2	(23, 21)	172158800
519	(30, 29)	89.5	100.0	2382.2	(22, 21)	158754600

520	(30,29)	88.3	99.2	2441.3	(22,21)	130921700
521	(29,29)	87.0	98.3	2548.3	(22,22)	107435700
522	(29,29)	88.9	98.1	2603.2	(22,22)	102331300
523	(29,29)	89.5	98.4	2594.4	(22,22)	110309600
524	(30,29)	88.9	98.6	2548.7	(22,21)	116036600
525	(31,29)	88.6	98.7	2525.9	(23,21)	116707200
526	(31,29)	87.5	98.8	2512.5	(23,21)	119275100
527	(31,29)	88.5	99.2	2439.9	(23,21)	130424900
528	(31,29)	89.9	99.6	2409.1	(23,21)	143270200
529	(31,29)	90.3	99.6	2406.7	(23,21)	145237800
530	(32,29)	89.8	99.2	2414.7	(23,21)	133201200
531	(31,28)	88.5	98.6	2477.5	(23,21)	115359100
532	(31,28)	87.5	98.0	2531.7	(23,21)	100628300
533	(31,28)	87.6	97.7	2531.0	(23,21)	93742930
534	(31,28)	89.0	97.8	2481.9	(23,21)	96511310
535	(32,28)	90.0	98.2	2464.3	(23,21)	104323400
536	(32,28)	89.7	98.4	2467.0	(23,21)	109404300
537	(32,29)	90.5	98.2	2473.4	(23,21)	104604300
538	(31,29)	91.2	97.6	2519.2	(23,21)	90230350
539	(30,29)	91.1	96.6	2606.4	(22,21)	73225230
540	(28,28)	90.6	96.0	2727.4	(21,21)	63804240
541	(28,27)	91.4	97.4	2742.8	(21,20)	87813280
542	(28,26)	93.5	100.6	2724.4	(21,20)	182291500
543	(29,27)	98.0	104.0	2685.6	(22,20)	400574500
544	(29,27)	101.6	107.1	2662.1	(22,20)	820546300
545	(29,27)	104.0	109.5	2656.0	(22,20)	1399250000
546	(29,27)	105.9	110.9	2621.1	(22,20)	1944254000
547	(30,27)	107.7	111.9	2564.0	(22,20)	2456208000
548	(31,27)	108.8	112.9	2546.1	(23,20)	3071650000
549	(31,27)	109.8	113.8	2547.9	(23,20)	3777939000
550	(31,27)	110.4	114.5	2515.1	(23,20)	4417593000
551	(31,27)	111.2	115.0	2493.9	(23,20)	5035684000
552	(30,27)	111.7	115.5	2521.7	(22,20)	5673267000
553	(30,27)	112.0	115.9	2535.5	(22,20)	6108496000
554	(30,27)	112.0	115.9	2532.2	(22,20)	6162653000
555	(30,27)	111.7	115.7	2553.5	(22,20)	5917061000
556	(29,27)	111.4	115.5	2599.6	(22,20)	5579977000
557	(29,27)	110.8	115.1	2621.8	(22,20)	5125886000
558	(29,27)	110.1	114.6	2620.8	(22,20)	4534739000
559	(29,27)	109.3	114.0	2659.8	(22,20)	3955366000
560	(28,27)	108.3	113.5	2697.4	(21,20)	3547594000
561	(28,27)	107.6	113.2	2695.7	(21,20)	3316038000
562	(28,27)	107.4	113.1	2704.4	(21,20)	3248735000
563	(28,27)	107.7	113.2	2740.0	(21,20)	3335071000
564	(28,27)	107.7	113.3	2738.4	(21,20)	3362958000
565	(28,27)	107.8	113.2	2716.3	(21,20)	3282841000
566	(28,27)	107.6	113.1	2723.7	(21,20)	3268903000
567	(28,27)	107.5	113.3	2753.4	(21,20)	3370265000
568	(28,27)	107.5	113.4	2741.4	(21,20)	3444282000
569	(28,27)	107.4	113.5	2720.6	(21,20)	3509506000
570	(28,27)	108.0	113.7	2738.4	(21,20)	3719472000
571	(27,27)	108.4	113.9	2739.7	(20,20)	3934056000
572	(28,27)	108.8	114.0	2706.9	(21,20)	4012449000
573	(28,27)	109.2	114.1	2689.2	(21,20)	4077226000
574	(27,27)	109.5	114.3	2715.4	(20,20)	4268622000
575	(28,27)	109.8	114.5	2701.0	(21,20)	4423389000
576	(28,27)	110.0	114.5	2676.4	(21,20)	4438946000
577	(28,27)	110.1	114.5	2685.2	(21,20)	4479967000
578	(27,27)	110.1	114.6	2709.4	(20,20)	4580123000
579	(28,27)	110.0	114.6	2688.3	(21,20)	4562665000
580	(28,27)	109.7	114.4	2675.1	(21,20)	4413600000
581	(27,27)	109.5	114.4	2709.2	(20,20)	4337754000
582	(27,27)	109.2	114.3	2730.2	(20,20)	4285913000
583	(28,27)	108.9	114.1	2712.1	(21,20)	4113604000
584	(28,27)	108.6	113.9	2708.9	(21,20)	3894866000
585	(27,27)	108.3	113.8	2744.9	(20,20)	3807955000

586	(27,27)	108.1	113.8	2748.2	(20,20)	3779986000
587	(27,27)	107.9	113.7	2729.4	(20,20)	3739985000
588	(27,27)	107.7	113.8	2747.2	(20,20)	3789102000
589	(27,27)	107.3	113.9	2776.6	(20,20)	3896179000
590	(27,27)	106.8	113.8	2768.8	(20,20)	3841759000
591	(27,27)	106.1	113.6	2751.8	(20,20)	3627413000
592	(27,27)	105.9	113.5	2782.6	(20,20)	3514951000
593	(26,27)	105.9	113.5	2808.2	(20,21)	3510886000
594	(27,27)	105.9	113.3	2784.5	(20,20)	3405140000
595	(27,27)	105.9	113.1	2752.0	(20,20)	3216690000
596	(27,27)	105.9	113.0	2776.1	(20,20)	3171016000
597	(26,27)	105.8	113.1	2794.8	(20,21)	3206834000
598	(27,27)	105.9	113.0	2770.7	(20,20)	3182027000
599	(27,27)	105.7	113.0	2765.0	(20,20)	3192124000
600	(26,27)	105.8	113.3	2801.1	(20,21)	3354903000
601	(26,27)	105.8	113.4	2804.3	(20,21)	3457985000
602	(27,27)	105.9	113.2	2771.0	(20,20)	3348089000
603	(26,27)	106.0	113.1	2771.3	(20,21)	3225492000
604	(26,27)	106.0	113.1	2804.4	(20,21)	3262166000
605	(26,27)	106.1	113.1	2796.6	(20,21)	3265222000
606	(27,27)	106.2	113.0	2763.1	(20,20)	3131183000
607	(26,27)	106.4	112.9	2767.4	(20,21)	3086843000
608	(26,27)	106.4	113.0	2801.7	(20,21)	3190983000
609	(26,27)	106.5	113.0	2788.6	(20,21)	3196541000
610	(26,27)	106.4	112.8	2766.6	(20,21)	3026160000
611	(26,27)	106.1	112.6	2788.4	(20,21)	2914631000
612	(26,27)	105.9	112.6	2813.8	(20,21)	2911448000
613	(26,27)	105.6	112.5	2791.7	(20,21)	2819396000
614	(26,27)	105.4	112.2	2759.4	(20,21)	2649131000
615	(26,27)	105.3	112.2	2788.9	(20,21)	2616631000
616	(26,27)	105.1	112.3	2813.9	(20,21)	2665930000
617	(26,27)	105.2	112.1	2784.4	(20,21)	2594851000
618	(27,28)	105.4	112.0	2745.5	(20,21)	2487185000
619	(26,28)	105.7	112.1	2755.6	(20,21)	2563805000
620	(26,27)	105.9	112.3	2758.2	(20,21)	2718949000
621	(26,28)	106.2	112.5	2740.9	(20,21)	2815630000
622	(26,28)	106.4	112.8	2736.3	(20,21)	2991514000
623	(26,28)	106.5	113.2	2772.4	(20,21)	3339240000
624	(26,28)	106.4	113.5	2772.8	(20,21)	3523481000
625	(27,28)	106.2	113.2	2736.9	(20,21)	3306275000
626	(27,28)	106.0	112.7	2715.0	(20,21)	2973261000
627	(26,28)	105.5	112.6	2751.0	(20,21)	2868485000
628	(26,28)	105.2	112.5	2757.5	(20,21)	2842514000
629	(27,28)	105.3	112.2	2729.4	(20,21)	2637493000
630	(27,28)	105.4	111.8	2705.4	(20,21)	2400826000
631	(26,28)	105.5	111.7	2722.1	(20,21)	2345906000
632	(26,28)	105.5	111.7	2719.9	(20,21)	2366978000
633	(27,28)	105.7	111.7	2696.2	(20,21)	2348351000
634	(26,28)	106.0	111.9	2687.8	(20,21)	2437745000
635	(26,28)	106.3	112.3	2706.2	(20,21)	2682963000
636	(26,28)	106.6	112.5	2700.0	(20,21)	2838056000
637	(27,28)	106.8	112.5	2694.5	(20,21)	2827088000
638	(26,28)	107.0	112.6	2713.5	(20,21)	2900042000
639	(26,28)	107.1	113.0	2747.5	(20,21)	3126684000
640	(26,28)	107.0	113.0	2743.9	(20,21)	3191134000
641	(27,28)	107.0	112.7	2709.7	(20,21)	2951988000
642	(27,28)	106.9	112.3	2705.0	(20,21)	2714167000
643	(26,28)	106.8	112.3	2744.7	(20,21)	2702252000
644	(26,28)	106.8	112.4	2747.7	(20,21)	2741476000
645	(27,28)	106.8	112.4	2728.1	(20,21)	2739229000
646	(26,28)	106.9	112.6	2733.1	(20,21)	2905491000
647	(26,28)	107.3	113.1	2759.4	(20,21)	3247990000
648	(26,28)	107.7	113.3	2745.6	(20,21)	3384371000
649	(27,28)	107.7	113.0	2705.9	(20,21)	3128360000
650	(27,28)	107.5	112.5	2689.6	(20,21)	2804912000
651	(26,28)	107.4	112.3	2723.8	(20,21)	2706742000

652	(26,28)	107.4	112.3	2724.3	(20,21)	2676339000
653	(27,28)	107.4	112.0	2689.9	(20,21)	2514803000
654	(27,28)	107.3	111.8	2669.8	(20,21)	2383999000
655	(26,28)	107.5	111.9	2697.8	(20,21)	2445867000
656	(27,28)	107.8	112.0	2697.1	(20,21)	2535511000
657	(27,28)	108.1	112.0	2670.4	(20,21)	2495185000
658	(27,28)	108.4	112.0	2663.1	(20,21)	2492141000
659	(26,28)	108.6	112.3	2691.1	(20,21)	2673557000
660	(27,28)	108.7	112.5	2690.7	(20,21)	2833459000
661	(27,28)	108.7	112.4	2661.7	(20,21)	2740967000
662	(27,28)	108.6	112.1	2656.7	(20,21)	2548489000
663	(26,28)	108.4	112.0	2706.3	(20,21)	2504224000
664	(26,28)	108.4	112.1	2721.2	(20,21)	2542167000
665	(27,28)	108.3	111.9	2690.9	(20,21)	2434705000
666	(27,28)	108.2	111.5	2657.7	(20,21)	2254914000
667	(26,28)	108.1	111.5	2688.9	(20,21)	2214406000
668	(26,28)	107.9	111.6	2710.9	(20,21)	2273557000
669	(27,28)	107.6	111.4	2694.7	(20,21)	2181358000
670	(27,28)	107.1	110.8	2677.7	(20,21)	1924463000
671	(26,28)	106.5	110.3	2711.9	(20,21)	1714405000
672	(26,28)	106.0	110.2	2759.4	(20,21)	1648166000
673	(26,28)	105.5	110.0	2748.8	(20,21)	1582798000
674	(27,28)	105.1	109.6	2715.0	(20,21)	1446735000
675	(26,28)	104.6	109.3	2724.0	(20,21)	1353554000
676	(26,28)	104.3	109.4	2762.8	(20,21)	1368677000
677	(26,28)	104.0	109.4	2758.8	(20,21)	1369810000
678	(27,28)	104.0	109.1	2723.3	(20,21)	1274607000
679	(26,28)	103.8	108.7	2723.2	(20,21)	1186556000
680	(26,27)	103.7	108.8	2764.0	(20,21)	1202158000
681	(26,27)	103.7	109.0	2768.1	(20,21)	1244789000
682	(27,28)	103.7	108.8	2724.5	(20,21)	1201115000
683	(27,28)	103.8	108.6	2684.5	(20,21)	1148368000
684	(26,28)	104.1	108.8	2695.5	(20,21)	1208454000
685	(26,28)	104.5	109.2	2703.6	(20,21)	1328613000
686	(27,28)	104.6	109.3	2678.0	(20,21)	1334111000
687	(27,28)	104.6	108.9	2670.2	(20,21)	1231387000
688	(26,28)	104.4	108.7	2698.2	(20,21)	1171867000
689	(26,28)	104.3	108.8	2739.2	(20,21)	1211641000
690	(26,28)	104.0	108.8	2724.3	(20,21)	1214993000
691	(27,28)	103.7	108.4	2687.5	(20,21)	1098585000
692	(27,28)	103.2	107.8	2701.3	(20,21)	956662300
693	(26,28)	102.7	107.5	2750.6	(20,21)	898083600
694	(26,28)	102.4	107.5	2758.2	(20,21)	889409300
695	(27,28)	102.4	107.4	2715.0	(20,21)	861190700
696	(27,28)	102.7	107.3	2695.4	(20,21)	859440600
697	(26,28)	102.9	107.7	2707.9	(20,21)	934648100
698	(26,28)	103.1	108.1	2722.3	(20,21)	1016513000
699	(27,28)	103.0	107.9	2694.6	(20,21)	978841100
700	(27,28)	102.7	107.3	2660.4	(20,21)	853228800
701	(26,28)	102.2	106.9	2676.8	(20,21)	772687900
702	(26,28)	101.9	106.9	2724.3	(20,21)	784750100
703	(26,28)	101.5	107.0	2718.9	(20,21)	785752100
704	(27,28)	101.3	106.5	2682.9	(20,21)	714043900
705	(27,28)	101.0	106.1	2681.5	(20,21)	639457800
706	(26,27)	100.7	106.0	2708.7	(20,21)	637184000
707	(26,27)	100.5	106.2	2720.2	(20,21)	661984000
708	(27,27)	100.2	106.0	2691.0	(20,20)	626602500
709	(27,27)	100.0	105.5	2677.5	(20,20)	556280300
710	(26,27)	99.7	105.2	2703.0	(20,21)	529652000
711	(26,27)	99.4	105.4	2749.0	(20,21)	555289900
712	(26,27)	99.0	105.4	2740.8	(20,21)	550771700
713	(27,27)	98.5	105.0	2700.0	(20,20)	496756000
714	(27,28)	98.5	104.6	2683.8	(20,21)	457172000
715	(26,28)	98.6	104.8	2713.7	(20,21)	478183900
716	(26,28)	98.7	105.0	2714.1	(20,21)	505227000
717	(27,28)	98.5	104.8	2690.1	(20,21)	474899500

718	(26,28)	98.4	104.2	2686.1	(20,21)	419553300
719	(26,28)	98.2	104.1	2678.9	(20,21)	403827500
720	(26,27)	98.0	104.3	2701.1	(20,21)	423663600
721	(26,27)	97.5	104.1	2697.4	(20,21)	410838800
722	(26,28)	97.6	103.5	2682.1	(20,21)	353396700
723	(26,28)	97.2	102.8	2685.8	(20,21)	303853300
724	(26,27)	97.2	102.8	2698.5	(20,21)	303545100
725	(26,27)	97.1	103.0	2709.9	(20,21)	318128900
726	(26,27)	96.9	102.7	2692.6	(20,21)	294728400
727	(26,27)	96.8	101.7	2695.0	(20,21)	237101000
728	(26,28)	96.6	100.8	2685.8	(20,21)	191106500
729	(26,28)	96.4	100.6	2694.9	(20,21)	181819300
730	(26,27)	96.1	100.7	2708.6	(20,21)	184807800
731	(26,28)	96.0	100.3	2693.4	(20,21)	169654600
732	(26,28)	95.7	99.3	2710.3	(20,21)	135027000
733	(27,28)	95.7	98.4	2683.2	(20,21)	108568700
734	(27,28)	95.5	98.2	2718.6	(20,21)	105013400
735	(27,28)	95.3	98.5	2715.9	(20,21)	111411600
736	(27,28)	95.2	98.4	2674.3	(20,21)	108647200
737	(28,28)	94.9	97.8	2655.1	(21,21)	94519100
738	(27,28)	94.6	97.1	2644.6	(20,21)	82068340
739	(27,28)	94.1	96.9	2664.3	(20,21)	78449200
740	(27,28)	93.9	97.0	2666.8	(20,21)	79659010
741	(27,28)	93.7	97.0	2655.2	(20,21)	80270860
742	(27,28)	93.6	97.1	2671.8	(20,21)	81498860
743	(27,29)	93.3	97.3	2667.7	(20,22)	84201970
744	(27,29)	92.6	97.2	2666.8	(20,22)	83944020
745	(28,28)	92.1	96.8	2677.5	(21,21)	76318060
746	(28,28)	91.4	96.1	2680.1	(21,21)	64103020
747	(27,28)	91.1	95.5	2741.1	(20,21)	55728610
748	(28,28)	90.8	95.4	2739.8	(21,21)	55108670
749	(28,28)	90.5	95.7	2695.4	(21,21)	58297760
750	(28,29)	89.7	95.6	2684.4	(21,22)	58140990
751	(28,29)	87.5	95.2	2713.3	(21,22)	52847040
752	(27,28)	85.0	94.7	2748.7	(20,21)	46596800
753	(26,29)	83.8	94.4	2688.2	(20,22)	43326500
754	(27,29)	85.0	94.3	2632.9	(20,22)	43103620
755	(27,29)	85.4	94.5	2675.3	(20,22)	44558270
756	(27,28)	84.8	94.8	2691.9	(20,21)	48014940
757	(28,28)	85.1	95.5	2693.5	(21,21)	56367330
758	(28,28)	86.4	96.4	2681.6	(21,21)	69897120
759	(29,28)	87.2	97.2	2674.3	(22,21)	83155010
760	(29,28)	87.8	97.5	2651.5	(22,21)	89060700
761	(29,28)	87.9	97.4	2648.3	(22,21)	86364500
762	(30,28)	88.1	97.3	2624.0	(22,21)	84630030
763	(30,28)	88.5	97.8	2559.0	(22,21)	96266670
764	(31,29)	88.7	99.0	2514.9	(23,21)	126716600
765	(33,29)	88.9	100.4	2394.8	(24,21)	172333000
766	(35,29)	92.3	101.7	2283.2	(25,21)	234283300
767	(36,29)	94.4	103.0	2194.2	(26,21)	313542400
768	(36,30)	95.4	104.0	2171.6	(26,21)	395661600
769	(36,30)	95.6	104.6	2204.5	(26,21)	454361300
770	(35,30)	95.2	104.8	2250.8	(25,21)	477809900
771	(35,30)	94.9	104.8	2268.6	(25,21)	473297700
772	(35,30)	94.2	104.5	2239.9	(25,21)	450494700
773	(36,30)	94.1	104.2	2227.4	(26,21)	416347100
774	(36,30)	93.3	103.9	2190.0	(26,21)	384994600
775	(37,30)	92.8	103.7	2102.6	(26,21)	375413800
776	(37,30)	93.0	103.9	2071.3	(26,21)	384652300
777	(37,30)	93.7	103.8	2038.8	(26,21)	380082200
778	(36,30)	93.4	103.3	1975.9	(26,21)	335975400
779	(36,29)	91.8	102.3	1991.6	(26,21)	268596000
780	(35,29)	92.0	101.5	2035.8	(25,21)	222407900
781	(35,30)	93.6	101.5	2011.6	(25,21)	221612300
782	(36,30)	94.7	101.9	2003.8	(26,21)	246501600
783	(36,30)	94.9	102.2	1981.7	(26,21)	264869900

784	(36,29)	94.1	102.2	1953.6	(26,21)	265698300.
785	(37,30)	93.5	102.1	1968.2	(26,21)	257103300.
786	(37,30)	94.2	101.9	1965.4	(26,21)	243403800.
787	(38,30)	94.4	101.5	1968.2	(27,21)	222366500.
788	(37,30)	93.7	101.0	1991.3	(26,21)	197469800.
789	(37,30)	91.9	100.6	2040.8	(26,21)	183652500.
790	(37,30)	89.5	100.9	2046.4	(26,21)	194637800.
791	(37,30)	90.0	101.5	2020.7	(26,21)	224705100.
792	(38,30)	90.5	101.9	1997.7	(27,21)	247304700
793	(37,30)	89.7	101.8	1959.3	(26,21)	237279200
794	(37,30)	88.8	101.0	1935.5	(26,21)	200270500.
795	(37,30)	89.7	100.5	1882.8	(26,21)	177343500.
796	(37,30)	92.1	101.1	1942.9	(26,21)	202966500
797	(38,30)	93.8	102.2	1986.7	(27,21)	260180500.
798	(39,30)	94.1	102.7	2013.8	(27,21)	297933600.
799	(39,30)	93.2	102.6	2020.5	(27,21)	290773000.
800	(38,30)	91.2	102.2	2057.7	(27,21)	260179400
801	(38,30)	92.3	101.8	2115.3	(27,21)	242408700.
802	(37,30)	92.5	101.9	2115.0	(26,21)	248202800
803	(38,30)	93.4	102.1	2072.5	(27,21)	256456100.
804	(39,30)	94.1	102.0	2002.5	(27,21)	251217100.
805	(40,30)	93.6	101.9	1947.6	(28,21)	245204500.
806	(42,30)	92.3	102.2	1817.3	(29,21)	262199700.
807	(44,30)	92.0	102.8	1709.9	(30,20)	303324900.
808	(44,30)	92.8	103.4	1697.3	(30,20)	350289700.
809	(42,30)	92.4	103.9	1805.5	(29,21)	388449800
810	(40,30)	93.4	104.1	1874.0	(28,21)	408564700.
811	(38,30)	94.9	104.0	1882.0	(27,21)	401044700
812	(37,30)	94.9	103.6	1888.6	(26,21)	361618900
813	(36,30)	93.6	102.9	1898.2	(26,21)	305943000.
814	(36,30)	91.0	102.2	1927.2	(26,21)	261324100
815	(37,30)	90.3	101.9	2012.2	(26,21)	246438100
816	(38,30)	91.3	102.2	1999.5	(27,21)	264060000.
817	(39,30)	94.4	102.9	1979.1	(27,21)	306490600.
818	(40,30)	96.2	103.4	1941.7	(28,21)	348520700.
819	(42,30)	96.6	103.7	1892.6	(29,21)	368543000.
820	(43,30)	95.8	103.7	1879.8	(29,20)	375710500.
821	(44,30)	95.2	104.0	1836.1	(30,20)	397650900.
822	(45,30)	95.3	104.4	1790.7	(30,20)	434510300.
823	(45,30)	96.1	104.5	1763.6	(30,20)	450605300.
824	(44,30)	95.8	104.3	1760.0	(30,20)	429047800
825	(43,30)	94.8	104.1	1813.2	(29,20)	407982800.
826	(43,31)	95.0	104.4	1841.4	(29,21)	432196100.
827	(42,30)	95.6	104.8	1834.8	(29,21)	483137300
828	(40,30)	95.1	105.0	1923.1	(28,21)	498984400.
829	(38,30)	93.9	104.5	2027.2	(27,21)	449397800.
830	(37,30)	93.6	103.7	2101.2	(26,21)	371693300.
831	(37,30)	93.5	103.2	2085.5	(26,21)	334371300.
832	(38,29)	94.2	103.6	1982.2	(27,20)	361432300
833	(41,30)	94.5	104.1	1881.7	(28,21)	410502700.
834	(43,30)	94.2	104.3	1804.7	(29,20)	424738600.
835	(42,31)	92.9	104.0	1836.6	(29,21)	393915600.
836	(39,31)	91.3	103.6	1940.0	(27,22)	360323600
837	(38,31)	91.5	103.7	1985.7	(27,22)	371240700
838	(38,30)	94.9	104.3	1937.0	(27,21)	426022100.
839	(38,30)	96.7	104.8	1937.2	(27,21)	473195000.
840	(40,30)	97.2	104.7	1923.4	(28,21)	472117200
841	(41,30)	96.5	104.4	1889.9	(28,21)	432577800
842	(42,30)	94.6	104.0	1859.8	(29,21)	399196900.
843	(42,30)	92.2	104.0	1855.5	(29,21)	401726500
844	(41,30)	93.6	104.3	1937.7	(28,21)	431042300
845	(39,30)	94.5	104.6	1972.0	(27,21)	459408600
846	(39,30)	95.4	104.7	1995.0	(27,21)	467085600
847	(39,29)	95.5	104.6	1997.6	(27,20)	454767100.
848	(39,29)	94.4	104.4	2001.2	(27,20)	433765600
849	(39,29)	92.6	104.1	2000.5	(27,20)	411122200

850	(39, 29)	92.5	104.0	1988.0	(27, 20)	393911300
851	(39, 29)	92.2	104.0	1904.1	(27, 20)	396775200.
852	(40, 29)	95.0	104.3	1845.4	(28, 20)	429820200
853	(42, 29)	96.8	104.8	1771.9	(29, 20)	477256400.
854	(42, 29)	97.2	105.0	1759.0	(29, 20)	503338200
855	(40, 29)	96.3	104.8	1793.0	(28, 20)	478689500.
856	(38, 29)	94.3	104.1	1794.7	(27, 20)	410309400.
857	(37, 29)	92.5	103.3	1852.4	(26, 21)	340359700.
858	(37, 30)	91.7	102.9	1901.8	(26, 21)	309619200.
859	(37, 30)	93.8	103.2	1883.9	(26, 21)	328961500.
860	(39, 30)	95.0	103.9	1883.0	(27, 21)	386155500.
861	(41, 30)	96.2	104.6	1862.8	(28, 21)	457170700
862	(40, 30)	98.0	105.1	1853.3	(28, 21)	508824600
863	(38, 30)	98.4	105.1	1923.4	(27, 21)	508021000.
864	(36, 29)	97.4	104.5	1976.2	(26, 21)	443508000.
865	(34, 29)	95.5	103.5	2036.6	(25, 21)	355021100.
866	(34, 29)	94.7	102.9	2093.3	(25, 21)	305647400.
867	(34, 29)	95.2	102.9	2135.4	(25, 21)	312379900.
868	(34, 29)	95.5	103.2	2135.8	(25, 21)	332110800.
869	(34, 29)	94.8	103.2	2141.8	(25, 21)	328761900.
870	(34, 29)	93.1	102.8	2156.0	(25, 21)	301952000
871	(34, 29)	92.3	102.2	2140.9	(25, 21)	264874400
872	(34, 30)	92.1	101.4	2176.3	(24, 22)	218740300
873	(33, 30)	90.7	100.1	2282.8	(24, 22)	161523800.
874	(31, 29)	87.8	98.3	2380.8	(23, 21)	107519000
875	(30, 29)	84.0	96.7	2469.8	(22, 21)	73851790.
876	(30, 29)	82.8	95.9	2492.6	(22, 21)	61196610.
877	(31, 29)	83.9	95.6	2463.9	(23, 21)	57787120.
878	(31, 29)	84.5	95.5	2437.9	(23, 21)	55794980.
879	(30, 29)	84.7	95.1	2498.2	(22, 21)	51351810
880	(29, 29)	85.0	94.5	2540.1	(22, 22)	45158720
881	(29, 29)	84.9	93.9	2532.2	(22, 22)	39052780
882	(30, 29)	84.3	93.4	2485.7	(22, 21)	34523980.
883	(31, 29)	84.1	93.0	2444.5	(23, 21)	31803380.
884	(31, 29)	83.9	92.8	2467.4	(23, 21)	30413360
886	(31, 29)	85.0	92.8	2466.9	(23, 21)	30472720
887	(30, 29)	85.7	93.0	2555.5	(22, 21)	31902480
888	(28, 29)	85.5	93.2	2634.5	(21, 22)	33008800
889	(28, 28)	84.0	93.0	2671.0	(21, 21)	31967580.

TRACK TRAIL FOR SPZASH.DA

BLOCK	(IR3D, JR3D)	AMAX	AMAXUP	RSUM	LOG COORD'S	POWER
335	(25,29)	82.4	93.3	2718.9	(19,22)	33734450
336	(25,29)	87.2	97.6	2670.1	(19,22)	90434260
337	(26,29)	90.4	100.1	2614.7	(20,22)	162417700.
338	(26,29)	92.1	101.2	2558.9	(20,22)	206695100
339	(26,29)	92.6	100.9	2527.4	(20,22)	195576300
340	(26,29)	93.0	100.0	2544.4	(20,22)	157602300.
341	(25,28)	94.6	101.1	2609.1	(19,21)	203965200
342	(25,27)	97.7	104.2	2661.0	(19,21)	419537400
343	(26,27)	100.8	106.9	2655.9	(20,21)	768872400.
344	(26,28)	103.4	108.6	2642.3	(20,21)	1140537000
345	(27,28)	105.5	109.9	2634.9	(20,21)	1552792000.
346	(26,28)	106.8	111.1	2691.5	(20,21)	2043016000.
347	(26,28)	107.1	111.9	2705.3	(20,21)	2459057000.
348	(27,28)	106.2	112.1	2680.8	(20,21)	2594430000.
349	(27,28)	105.2	112.0	2664.4	(20,21)	2504436000
350	(26,28)	105.2	111.9	2710.2	(20,21)	2438237000
351	(26,28)	105.3	112.0	2742.8	(20,21)	2489820000
352	(26,28)	105.3	112.1	2721.0	(20,21)	2579725000
353	(26,28)	106.2	112.3	2706.8	(20,21)	2705745000
354	(26,28)	107.0	112.7	2743.2	(20,21)	2949469000
355	(26,28)	107.3	113.1	2746.9	(20,21)	3210434000.
356	(26,28)	107.1	113.3	2718.5	(20,21)	3387865000
357	(26,28)	106.8	113.5	2722.3	(20,21)	3536522000
358	(26,28)	106.3	113.7	2763.7	(20,21)	3741360000
359	(26,28)	105.5	113.9	2763.5	(20,21)	3924339000
360	(26,28)	106.0	114.1	2724.7	(20,21)	4055923000.
361	(26,28)	106.7	114.2	2730.9	(20,21)	4188193000
362	(26,28)	107.3	114.3	2762.6	(20,21)	4269015000
363	(26,28)	107.4	114.2	2769.1	(20,21)	4158138000.
364	(27,28)	107.3	114.0	2732.2	(20,21)	3993610000.
365	(27,28)	107.5	114.1	2725.6	(20,21)	4061549000
366	(27,28)	107.3	114.3	2746.8	(20,21)	4301394000
367	(27,28)	107.6	114.5	2730.4	(20,21)	4510179000
368	(27,28)	108.2	114.8	2719.1	(20,21)	4799939000
369	(26,28)	108.6	115.3	2756.4	(20,21)	5342274000
370	(26,28)	108.9	115.7	2763.9	(20,21)	5833474000
371	(27,28)	108.9	115.8	2737.5	(20,21)	5968814000
372	(27,28)	109.2	115.8	2703.2	(20,21)	5971317000
373	(27,28)	109.3	115.9	2729.1	(20,21)	6159217000
374	(27,28)	109.0	116.0	2743.3	(20,21)	6256947000
375	(27,28)	108.6	115.8	2718.0	(20,21)	5991739000
376	(27,28)	108.4	115.5	2699.3	(20,21)	5666968000
377	(27,28)	108.3	115.5	2740.1	(20,21)	5642985000
378	(27,28)	108.5	115.5	2743.8	(20,21)	5659722000.
379	(27,28)	108.7	115.4	2706.1	(20,21)	5481148000.
380	(27,28)	108.8	115.3	2699.2	(20,21)	5373579000
381	(27,28)	108.7	115.4	2739.7	(20,21)	5478318000.
382	(27,28)	108.5	115.3	2739.3	(20,21)	5381468000
383	(27,28)	108.0	114.9	2722.4	(20,21)	4914852000.
384	(27,28)	107.6	114.5	2723.5	(20,21)	4516241000
385	(26,28)	107.2	114.4	2764.7	(20,21)	4406751000.
386	(26,28)	107.0	114.3	2757.4	(20,21)	4307120000
387	(27,28)	107.1	114.2	2738.9	(20,21)	4152975000
388	(27,28)	107.3	114.3	2762.3	(20,21)	4262267000
389	(26,28)	107.5	114.6	2788.0	(20,21)	4548268000.
390	(27,28)	107.9	114.6	2766.8	(20,21)	4574122000
391	(27,28)	108.2	114.4	2719.0	(20,21)	4395524000
392	(27,28)	108.3	114.5	2710.0	(20,21)	4473610000
393	(27,28)	108.3	114.7	2723.3	(20,21)	4729016000.
394	(27,28)	108.0	114.7	2714.5	(20,21)	4677566000
395	(27,28)	107.5	114.4	2700.9	(20,21)	4360737000

396	(27,28)	107.2	114.3	2729.9	(20,21)	4232449000.
397	(26,28)	107.1	114.3	2772.2	(20,21)	4270390000.
398	(26,28)	107.3	114.1	2764.1	(20,21)	4103275000.
399	(27,28)	107.5	113.8	2740.7	(20,21)	3792109000.
400	(26,28)	107.6	113.7	2752.4	(20,21)	3712193000.
401	(26,28)	107.6	113.8	2756.9	(20,21)	3799985000.
402	(26,28)	107.8	113.9	2741.2	(20,21)	3857831000.
403	(26,28)	108.1	114.1	2750.6	(20,21)	4068839000.
404	(26,28)	108.5	114.6	2777.6	(20,21)	4605932000.
405	(26,28)	108.7	115.0	2779.6	(20,21)	5055070000
406	(27,28)	109.0	115.1	2734.7	(20,21)	5118394000.
407	(27,28)	109.3	115.1	2705.2	(20,21)	5140582000.
408	(27,28)	109.6	115.4	2723.7	(20,21)	5481607000
409	(27,28)	110.0	115.6	2723.4	(20,21)	5819789000.
410	(27,28)	110.5	115.7	2700.0	(20,21)	5914259000.
411	(27,28)	110.9	115.9	2694.0	(20,21)	6154854000.
412	(27,28)	111.3	116.3	2724.1	(20,21)	6765408000.
413	(27,28)	111.5	116.6	2726.1	(20,21)	7195492000.
414	(27,28)	111.5	116.5	2701.1	(20,21)	7099789000.
415	(27,28)	111.4	116.4	2698.2	(20,21)	6961218000.
416	(27,28)	111.1	116.5	2733.2	(20,21)	7125709000.
417	(27,28)	110.7	116.5	2739.4	(20,21)	7096537000.
418	(27,28)	110.2	116.1	2721.3	(20,21)	6479806000
419	(27,28)	109.7	115.6	2720.6	(20,21)	5781864000.
420	(26,28)	109.3	115.4	2765.7	(20,21)	5527871000
421	(26,28)	109.1	115.4	2775.8	(20,21)	5473968000.
422	(27,28)	109.1	115.3	2748.4	(20,21)	5379080000.
423	(26,28)	109.2	115.5	2748.5	(20,21)	5589922000.
424	(26,28)	109.5	115.9	2771.8	(20,21)	6206484000.
425	(26,28)	109.8	116.2	2765.6	(20,21)	6601212000
426	(27,28)	110.1	116.1	2731.6	(20,21)	6394073000
427	(27,28)	110.3	115.8	2720.9	(20,21)	6082216000
428	(26,28)	110.3	115.9	2750.0	(20,21)	6122099000.
429	(26,28)	110.3	115.9	2749.7	(20,21)	6191628000.
430	(27,28)	110.3	115.8	2727.0	(20,21)	6012559000.
431	(27,28)	110.3	115.8	2732.8	(20,21)	5991539000.
432	(26,28)	110.3	116.0	2767.4	(20,21)	6373933000
433	(26,28)	110.3	116.2	2767.9	(20,21)	6637859000
434	(27,28)	110.3	116.0	2736.9	(20,21)	6365053000
435	(27,28)	110.2	115.8	2720.0	(20,21)	5964284000
436	(26,28)	110.1	115.7	2750.8	(20,21)	5913948000
437	(26,28)	110.1	115.8	2758.2	(20,21)	6001816000.
438	(27,28)	110.1	115.8	2730.8	(20,21)	6002708000
439	(27,28)	110.3	116.0	2725.8	(20,21)	6252990000
440	(26,28)	110.6	116.4	2749.9	(20,21)	6895272000
441	(27,28)	111.1	116.6	2748.6	(20,21)	7325114000
442	(27,28)	111.3	116.5	2714.9	(20,21)	7031259000
443	(27,28)	111.4	116.1	2696.6	(20,21)	6404215000.
444	(26,28)	111.3	115.8	2732.4	(20,21)	6069842000.
445	(27,28)	111.2	115.8	2742.7	(20,21)	5980541000.
446	(27,28)	111.0	115.6	2717.4	(20,21)	5807919000.
447	(27,28)	110.7	115.6	2702.5	(20,21)	5708976000.
448	(26,28)	110.7	115.7	2734.4	(20,21)	5898600000.
449	(27,28)	110.7	115.8	2739.3	(20,21)	6092960000
450	(27,28)	110.8	115.7	2711.6	(20,21)	5923021000
451	(27,28)	110.9	115.5	2689.7	(20,21)	5614576000
452	(26,28)	110.9	115.5	2723.5	(20,21)	5566026000
453	(26,28)	111.0	115.6	2730.6	(20,21)	5697954000
454	(27,28)	111.2	115.5	2705.0	(20,21)	5669560000
455	(27,28)	111.4	115.5	2690.8	(20,21)	5606777000.
456	(26,28)	111.5	115.6	2724.5	(20,21)	5806871000
457	(27,28)	111.7	115.9	2733.2	(20,21)	6125281000
458	(27,28)	111.8	115.9	2705.9	(20,21)	6192292000
459	(27,28)	111.8	115.9	2680.9	(20,21)	6134907000
460	(27,28)	111.8	116.0	2709.5	(20,21)	6309384000
461	(27,28)	111.8	116.2	2724.9	(20,21)	6599537000

462	(27,28)	111.8	116.2	2700.1	(20,21)	6580400000
463	(27,28)	111.7	116.0	2677.1	(20,21)	6315737000
464	(27,28)	111.6	115.9	2705.7	(20,21)	6224912000
465	(27,28)	111.6	116.0	2731.3	(20,21)	6348104000
466	(27,28)	111.6	116.0	2710.1	(20,21)	6307586000
467	(27,28)	111.7	115.9	2686.6	(20,21)	6124761000
468	(27,28)	111.7	115.9	2700.5	(20,21)	6176547000
469	(27,28)	111.8	116.1	2726.3	(20,21)	6481363000
470	(27,28)	111.8	116.2	2705.8	(20,21)	6590026000
471	(27,28)	111.9	116.1	2669.3	(20,21)	6467674000
472	(27,28)	112.0	116.1	2675.7	(20,21)	6512542000
473	(27,28)	112.0	116.3	2713.9	(20,21)	6771139000
474	(27,28)	112.0	116.3	2705.5	(20,21)	6763266000
475	(27,28)	111.9	116.0	2663.8	(20,21)	6334587000
476	(27,28)	111.8	115.8	2654.7	(20,21)	5966037000
477	(27,28)	111.6	115.7	2684.8	(20,21)	5939077000
478	(27,28)	111.5	115.7	2685.0	(20,21)	5908328000
479	(28,28)	111.3	115.5	2655.3	(21,21)	5621875000
480	(28,28)	111.2	115.4	2655.4	(21,21)	5472285000
481	(27,28)	111.0	115.6	2689.2	(20,21)	5718974000
482	(27,28)	110.8	115.8	2701.2	(20,21)	5964354000
483	(27,28)	110.6	115.6	2677.9	(20,21)	5756203000
484	(27,28)	110.4	115.3	2665.9	(20,21)	5417914000
485	(27,28)	110.3	115.3	2686.0	(20,21)	5425758000
486	(27,28)	110.2	115.5	2712.0	(20,21)	5632791000
487	(27,28)	110.1	115.4	2690.1	(20,21)	5494551000
488	(27,28)	110.1	115.1	2659.7	(20,21)	5080199000
489	(27,28)	109.9	114.9	2668.2	(20,21)	4858737000
490	(27,28)	109.7	114.9	2701.6	(20,21)	4913373000
491	(27,28)	109.5	114.8	2696.6	(20,21)	4800610000
492	(27,28)	109.4	114.4	2665.5	(20,21)	4413366000
493	(27,28)	109.1	114.2	2678.1	(20,21)	4144820000
494	(27,28)	109.0	114.2	2717.6	(20,21)	4187103000
495	(27,28)	109.1	114.2	2718.6	(20,21)	4211043000
496	(27,28)	109.2	114.0	2680.5	(20,21)	3966281000
497	(27,28)	109.2	113.7	2678.9	(20,21)	3735450000
498	(27,28)	109.1	113.8	2707.6	(20,21)	3795769000
499	(27,28)	109.1	114.0	2720.2	(20,21)	3951088000
500	(27,28)	109.1	113.8	2691.6	(20,21)	3840328000
501	(27,28)	109.0	113.6	2677.8	(20,21)	3601856000
502	(27,28)	108.9	113.5	2697.4	(20,21)	3559624000
503	(27,28)	108.9	113.7	2726.8	(20,21)	3691917000
504	(27,28)	109.0	113.6	2707.6	(20,21)	3630317000
505	(28,28)	109.1	113.3	2671.7	(21,21)	3355026000
506	(27,28)	109.1	113.1	2687.8	(20,21)	3211175000
507	(27,28)	109.0	113.2	2714.5	(20,21)	3343242000
508	(27,28)	109.0	113.3	2712.4	(20,21)	3422389000
509	(27,28)	108.8	113.0	2675.9	(20,21)	3183106000
510	(27,28)	108.5	112.5	2679.9	(20,21)	2841773000
511	(27,27)	108.0	112.3	2718.0	(20,20)	2695629000
512	(27,27)	107.6	112.3	2746.1	(20,20)	2668297000
513	(27,27)	107.0	111.9	2724.8	(20,20)	2447668000
514	(27,28)	106.2	111.1	2697.3	(20,21)	2063237000
515	(27,28)	105.3	110.5	2716.3	(20,21)	1787385000
516	(27,27)	104.1	110.3	2762.2	(20,20)	1698934000
517	(27,27)	102.5	109.9	2763.1	(20,20)	1564818000
518	(27,27)	100.6	109.0	2753.8	(20,20)	1248305000
519	(26,27)	100.5	107.6	2741.2	(20,21)	903705900
520	(26,27)	100.7	106.6	2763.2	(20,21)	729684000
521	(26,27)	100.8	106.4	2787.3	(20,21)	696367100
522	(27,27)	100.8	106.0	2756.9	(20,20)	634876700
523	(27,27)	100.7	104.9	2698.9	(20,20)	490918900
524	(27,28)	100.4	103.2	2652.1	(20,21)	334889500
525	(28,28)	100.0	101.9	2597.2	(21,21)	244698500
526	(29,28)	99.4	101.4	2580.1	(22,21)	217781100
527	(28,29)	99.1	101.2	2595.4	(21,22)	211242800

528	(28, 28)	98.5	100.9	2608.4	(21, 21)	197109200
529	(28, 28)	98.0	100.6	2613.9	(21, 21)	181794500
530	(28, 28)	97.3	100.4	2627.2	(21, 21)	171844400
531	(28, 29)	96.5	100.1	2619.4	(21, 22)	162849600
532	(28, 29)	96.2	99.8	2584.1	(21, 22)	151428700
533	(29, 28)	96.0	99.6	2535.3	(22, 21)	144701700
534	(29, 28)	96.2	99.8	2563.5	(22, 21)	153043800
535	(29, 29)	96.4	100.2	2553.6	(22, 22)	167737700
536	(30, 29)	96.3	100.3	2557.6	(22, 21)	169805700
537	(29, 29)	95.3	99.8	2593.5	(22, 22)	150110900
538	(29, 28)	93.7	98.8	2651.5	(22, 21)	118989500
539	(28, 28)	92.1	97.7	2661.8	(21, 21)	92285890
540	(27, 29)	90.1	96.9	2670.8	(20, 22)	77222850
541	(27, 29)	88.8	96.5	2681.5	(20, 22)	70676660
542	(27, 28)	87.4	96.3	2717.3	(20, 21)	68166320
543	(27, 28)	88.2	96.8	2740.4	(20, 21)	75283390
544	(27, 28)	89.4	97.8	2673.5	(20, 21)	95085330
545	(28, 28)	90.4	98.9	2683.0	(21, 21)	124065800
546	(28, 29)	91.6	99.9	2676.8	(21, 22)	153499000
547	(28, 29)	92.7	100.5	2642.5	(21, 22)	176287600
548	(29, 29)	93.4	100.8	2620.9	(22, 22)	192178800
549	(29, 29)	93.3	101.1	2621.6	(22, 22)	204917700
550	(30, 29)	92.7	101.6	2597.9	(22, 21)	226822700
551	(30, 29)	91.9	102.3	2551.1	(22, 21)	272137700
552	(30, 29)	93.0	103.2	2506.5	(22, 21)	332133900
553	(30, 30)	94.1	103.7	2460.4	(22, 22)	375499800
554	(30, 30)	93.8	103.9	2497.5	(22, 22)	386889200
555	(30, 29)	94.6	103.8	2563.9	(22, 21)	379092700
556	(29, 29)	95.2	103.7	2608.3	(22, 22)	375488000
557	(29, 29)	95.3	103.8	2638.3	(22, 22)	383082200
558	(29, 29)	95.0	103.9	2634.1	(22, 22)	386511400
559	(29, 29)	94.9	103.7	2629.0	(22, 22)	375674900
560	(29, 29)	94.7	103.5	2660.5	(22, 22)	353019900
561	(29, 29)	94.7	103.2	2684.4	(22, 22)	328811000
562	(29, 29)	94.6	103.0	2668.8	(22, 22)	319757100
563	(29, 29)	94.3	103.5	2619.5	(22, 22)	355502100
564	(30, 29)	93.9	104.6	2533.3	(22, 21)	457855500
565	(32, 30)	95.8	106.2	2422.2	(23, 22)	661819600
566	(34, 30)	99.4	108.0	2294.4	(24, 22)	996127000
567	(36, 30)	101.4	109.5	2139.8	(26, 21)	1411236000
568	(38, 29)	102.1	110.4	2019.4	(27, 20)	1733270000
569	(40, 29)	102.3	110.5	1954.5	(28, 20)	1765435000
570	(41, 30)	101.6	109.7	1914.7	(28, 21)	1492541000
571	(40, 30)	100.1	108.7	1883.4	(28, 21)	1171464000
572	(39, 30)	99.9	108.4	1960.2	(27, 21)	1102624000
573	(38, 30)	100.7	109.1	1983.4	(27, 21)	1292433000
574	(38, 30)	102.0	109.7	2006.8	(27, 21)	1483139000
575	(37, 30)	101.9	109.6	2021.8	(26, 21)	1449130000
576	(36, 29)	101.0	108.9	2035.6	(26, 21)	1239633000
577	(37, 29)	100.5	108.3	2048.6	(26, 21)	1065755000
578	(38, 29)	100.2	108.1	2022.5	(27, 20)	1023255000
579	(40, 29)	100.3	108.2	1952.7	(28, 20)	1043572000
580	(41, 29)	100.6	108.3	1929.1	(28, 20)	1062399000
581	(41, 29)	100.5	108.3	1911.3	(28, 20)	1059271000
582	(41, 29)	100.3	108.0	1931.8	(28, 20)	1002793000
583	(40, 29)	99.2	107.4	1981.8	(28, 20)	861792300
584	(39, 30)	96.7	106.2	2038.9	(27, 21)	661194000
585	(38, 30)	95.4	105.0	2103.0	(27, 21)	502082600
586	(38, 30)	95.6	104.7	2091.8	(27, 21)	463423700
587	(38, 30)	95.6	105.2	2042.2	(27, 21)	522914000
588	(38, 29)	95.6	105.8	2038.8	(27, 20)	604075500
589	(38, 29)	96.7	106.2	2054.7	(27, 20)	659713000
590	(38, 30)	97.0	106.4	2088.5	(27, 21)	694258400
591	(39, 30)	97.5	106.6	2085.9	(27, 21)	731512800
592	(39, 30)	97.8	106.9	2047.2	(27, 21)	767936500
593	(40, 30)	97.8	107.0	1993.5	(28, 21)	786691600

594	(41,30)	97.5	107.1	1924.7	(28,21)	812459000
595	(41,30)	98.3	107.5	1870.2	(28,21)	898349300
596	(42,30)	100.1	108.1	1876.7	(29,21)	1032453000.
597	(41,30)	101.3	108.5	1907.8	(28,21)	1114793000
598	(40,30)	101.4	108.5	1932.7	(28,21)	1115033000
599	(39,30)	100.5	108.6	1922.7	(27,21)	1136833000
600	(40,30)	99.7	109.0	1872.1	(28,21).	1251834000
601	(40,30)	101.8	109.4	1860.4	(28,21)	1391622000
602	(41,30)	102.8	109.6	1861.7	(28,21)	1436759000.
603	(42,30)	102.7	109.4	1863.5	(29,21)	1368973000
604	(42,30)	102.1	109.1	1842.3	(29,21)	1290169000.
605	(42,30)	102.3	109.1	1852.7	(29,21)	1283562000
606	(42,30)	103.0	109.2	1829.7	(29,21)	1321498000
607	(42,30)	103.1	109.2	1816.2	(29,21)	1323436000
608	(42,29)	102.3	108.9	1804.0	(29,20)	1230799000.
609	(41,29)	101.1	108.2	1808.6	(28,20)	1046241000
610	(42,29)	98.8	107.3	1844.2	(29,20)	848233000.
611	(41,29)	95.6	106.6	1923.2	(28,20)	724075800.
612	(39,29)	95.9	106.4	1993.7	(27,20)	693831700
613	(39,30)	95.2	106.6	2050.7	(27,21)	720960800
614	(38,30)	96.7	106.7	2049.8	(27,21)	745677100.
615	(38,30)	98.2	106.7	2075.5	(27,21)	737655600
616	(39,30)	98.5	106.5	2079.2	(27,21)	714641700
617	(40,30)	97.9	106.5	2052.9	(28,21)	715157500
618	(42,30)	98.1	106.8	2019.3	(29,21)	754228200
619	(44,30)	99.0	107.3	1958.4	(30,20)	847079400
620	(46,30)	99.5	107.9	1862.0	(31,20)	974378200
621	(47,29)	99.2	108.2	1752.7	(31,19)	1048596000
622	(47,30)	99.0	107.9	1786.1	(31,20)	988127200
623	(44,30)	97.8	107.1	1887.2	(30,20)	821931800
624	(41,30)	95.4	106.6	2001.3	(28,21)	718134000
625	(39,30)	97.0	107.2	2032.9	(27,21)	829028400
626	(39,30)	99.8	108.4	2048.8	(27,21)	1090074000
627	(39,30)	100.9	109.0	2031.4	(27,21)	1260881000
628	(39,30)	100.5	108.8	2052.8	(27,21)	1189969000
629	(37,30)	98.3	107.8	2123.4	(26,21)	962580200.
630	(36,31)	96.9	107.1	2179.0	(25,22)	804899800
631	(36,31)	96.2	107.3	2172.1	(25,22)	848452100.
632	(37,31)	97.2	108.0	2143.9	(26,22)	989234200.
633	(38,31)	97.5	108.1	2124.4	(27,22)	1028878000.
634	(37,30)	96.7	107.5	2121.1	(26,21)	894129900.
635	(36,30)	95.3	106.3	2171.2	(26,21)	682640100.
636	(36,30)	93.7	105.3	2215.7	(26,21)	532033800.
637	(36,30)	94.4	104.9	2184.1	(26,21)	491267600
638	(37,30)	95.1	105.2	2102.3	(26,21)	523455700
639	(37,30)	95.7	105.8	2072.1	(26,21)	605181200.
640	(38,30)	97.2	106.7	2053.0	(27,21)	735627800
641	(39,30)	98.4	107.4	2017.8	(27,21)	879114000
642	(39,30)	98.6	107.9	2052.1	(27,21)	977384200
643	(38,30)	98.9	108.1	2052.9	(27,21)	1019034000.
644	(38,31)	100.2	108.2	2023.4	(27,22)	1055739000
645	(40,31)	101.9	108.6	1973.9	(28,21)	1145475000.
646	(42,31)	103.1	109.1	1860.0	(29,21)	1290187000.
647	(42,30)	103.6	109.4	1751.6	(29,21)	1390831000.
648	(40,30)	103.1	109.2	1814.8	(28,21)	1331211000.
649	(39,30)	101.5	108.3	1891.6	(27,21)	1079775000.
650	(37,30)	98.8	106.7	1993.6	(26,21)	744353000.
651	(36,30)	94.6	104.8	2141.8	(26,21)	483143700.
652	(36,30)	93.2	103.8	2191.3	(26,21)	384524500.
653	(37,30)	94.1	104.3	2141.3	(26,21)	426376200.
654	(38,30)	96.8	105.3	2064.5	(27,21)	532259800.
655	(39,30)	98.0	106.0	2014.8	(27,21)	629283600.
656	(40,30)	97.8	106.1	2021.0	(28,21)	651256600
657	(39,30)	96.3	105.6	2016.1	(27,21)	580305200.
658	(38,30)	94.2	104.6	1974.8	(27,21)	456936700
659	(36,30)	92.8	103.3	2046.5	(26,21)	339449300

660	(35,30)	91.8	102.1	2137.2	(25,21)	255854100
661	(35,30)	89.8	101.1	2185.8	(25,21)	204347100
662	(34,30)	89.3	100.7	2212.5	(24,22)	186868400
663	(33,30)	91.5	101.2	2215.9	(24,22)	207783900
664	(33,30)	92.3	102.0	2172.3	(24,22)	249771000
665	(34,30)	92.2	102.5	2118.8	(24,22)	280697300
666	(35,30)	92.7	102.8	2112.5	(25,21)	304335600
667	(36,30)	94.2	103.7	2057.9	(26,21)	367726800
668	(37,30)	95.9	104.8	2033.5	(26,21)	474515200
669	(37,29)	96.5	105.4	2039.6	(26,21)	549729300
670	(36,29)	96.1	105.1	2095.4	(26,21)	516244500
671	(34,29)	94.6	104.0	2170.6	(25,21)	395473700
672	(34,29)	91.6	102.5	2214.4	(25,21)	281522900
673	(35,30)	90.0	101.7	2203.0	(25,21)	232249500
674	(35,30)	89.2	101.6	2204.7	(25,21)	226592900
675	(35,30)	89.8	101.4	2238.9	(25,21)	218387100
676	(34,30)	90.4	101.0	2289.7	(24,22)	197750800
677	(35,30)	90.3	100.5	2308.3	(25,21)	176245300
678	(35,29)	89.8	100.1	2296.5	(25,21)	162743600
679	(35,30)	89.1	99.9	2315.9	(25,21)	156410500
680	(35,30)	88.9	100.1	2266.6	(25,21)	163143600
681	(35,30)	91.3	100.6	2204.7	(25,21)	183977900
682	(36,30)	93.2	101.2	2142.7	(26,21)	207940000
683	(35,29)	93.9	101.5	2095.5	(25,21)	221359200
684	(35,29)	93.6	101.3	2098.5	(25,21)	214352700
685	(34,29)	93.2	100.8	2141.3	(25,21)	189832100
686	(34,29)	92.4	100.0	2188.6	(25,21)	157480600
687	(34,29)	90.7	99.1	2188.4	(25,21)	129637900
688	(34,30)	88.8	98.8	2199.3	(24,22)	119065500
689	(34,29)	88.8	99.1	2230.4	(25,21)	129563400
690	(35,30)	89.7	99.6	2243.6	(25,21)	145563600
691	(34,30)	89.8	99.8	2224.6	(24,22)	150528400
692	(34,30)	89.0	99.5	2188.2	(24,22)	140735900
693	(34,30)	89.3	98.8	2217.7	(24,22)	120821000
694	(33,30)	89.0	97.9	2275.8	(24,22)	98164980
695	(33,30)	87.8	96.9	2277.3	(24,22)	78378500
696	(34,30)	85.4	96.2	2234.7	(24,22)	65569250
697	(35,30)	83.4	95.8	2214.2	(25,21)	60658660
698	(35,30)	84.5	95.9	2165.5	(25,21)	61526820
699	(35,29)	85.9	96.2	2144.4	(25,21)	66016960
700	(35,30)	87.3	96.7	2159.6	(25,21)	73706510
701	(36,30)	89.0	97.2	2139.4	(26,21)	83933220
702	(37,30)	90.3	97.7	2113.4	(26,21)	92761410
703	(38,30)	90.9	97.8	2102.3	(27,21)	95963310
704	(38,30)	90.7	97.7	2125.9	(27,21)	93330000
705	(37,30)	89.6	97.4	2160.6	(26,21)	87556620
706	(36,30)	87.9	97.1	2187.0	(26,21)	81702130
707	(36,30)	87.6	96.9	2208.9	(26,21)	78313760
708	(36,30)	87.9	96.9	2227.3	(26,21)	77668370
709	(37,29)	88.3	96.8	2219.3	(26,21)	76649020
710	(36,29)	88.3	96.5	2213.4	(26,21)	71394190
711	(35,29)	87.1	95.8	2229.9	(25,21)	60168430
712	(35,30)	84.6	94.7	2225.1	(25,21)	47114000
713	(34,30)	83.5	93.9	2238.6	(24,22)	38915380
714	(33,30)	83.6	93.6	2288.1	(24,22)	36658540
715	(32,30)	83.5	93.6	2307.6	(23,22)	35937890
716	(32,30)	83.2	93.2	2299.9	(23,22)	33073630

TRACK TRAIL FOR SPZSASS.DA

BLOCK	(IR3D, JR3D)	AMAX	AMAXUP	RSUM	LOG COORD'S	POWER
274	(36, 29)	83.8	93.5	2180.1	(26, 21)	35189170.
275	(36, 29)	84.1	94.1	2175.8	(26, 21)	40356350.
276	(34, 29)	83.6	94.0	2204.5	(25, 21)	39873460.
277	(33, 29)	82.9	93.4	2220.8	(24, 21)	34955730.
289	(34, 29)	81.5	92.9	2289.8	(25, 21)	30891250.
290	(35, 29)	83.2	93.6	2289.7	(25, 21)	36079760.
291	(35, 29)	83.8	93.9	2274.9	(25, 21)	38823870.
292	(35, 29)	83.7	93.9	2230.4	(25, 21)	39170580.
293	(35, 29)	83.3	93.9	2219.8	(25, 21)	38478580.
294	(36, 29)	82.8	93.7	2201.4	(26, 21)	37257470.
295	(36, 29)	82.3	93.5	2172.2	(26, 21)	35636400.
296	(37, 29)	82.1	93.4	2122.2	(26, 21)	34657230.
297	(38, 29)	83.0	93.6	2059.2	(27, 20)	36190660.
298	(38, 29)	85.2	94.1	2067.4	(27, 20)	40928910.
299	(38, 29)	86.7	94.8	2112.5	(27, 20)	48147250.
300	(37, 29)	87.5	95.8	2106.3	(26, 21)	60645980.
301	(37, 29)	88.4	97.0	2109.5	(26, 21)	79410580.
302	(37, 29)	89.5	97.9	2078.0	(26, 21)	98059600
303	(36, 29)	89.7	98.4	2035.1	(26, 21)	108770400
304	(35, 29)	88.8	98.4	2116.7	(25, 21)	108838300.
305	(34, 30)	89.2	98.0	2168.6	(24, 22)	99684340.
306	(33, 30)	89.3	97.2	2235.7	(24, 22)	83538160.
307	(33, 29)	87.9	96.1	2327.8	(24, 21)	63963200.
308	(32, 29)	84.8	95.0	2416.3	(23, 21)	50307280.
309	(33, 29)	85.0	95.3	2384.8	(24, 21)	53249440.
310	(35, 29)	86.9	96.5	2251.1	(25, 21)	70071280.
311	(37, 29)	87.9	97.5	2120.9	(26, 21)	88509260.
312	(39, 29)	88.3	97.9	2071.2	(27, 20)	98426240.
313	(39, 29)	88.5	97.9	2056.1	(27, 20)	97563300.
314	(37, 29)	87.6	97.5	2149.3	(26, 21)	89832180.
315	(35, 29)	86.1	97.2	2249.9	(25, 21)	82488900.
316	(33, 29)	86.2	97.2	2329.1	(24, 21)	83378480.
317	(33, 29)	88.8	98.1	2323.1	(24, 21)	101222200.
318	(32, 29)	90.9	99.2	2291.2	(23, 21)	131150400.
319	(32, 29)	91.7	99.8	2265.5	(23, 21)	152070900
320	(31, 29)	91.2	99.7	2282.6	(23, 21)	147555100.
321	(31, 29)	89.5	98.9	2316.7	(23, 21)	122718300.
322	(31, 29)	87.8	97.9	2356.3	(23, 21)	96980880.
323	(32, 29)	88.1	97.2	2361.5	(23, 21)	82258220.
324	(31, 29)	88.2	96.7	2418.6	(23, 21)	74597570.
325	(30, 29)	87.2	96.2	2492.7	(22, 21)	65838400.
326	(29, 28)	85.2	95.6	2599.3	(22, 21)	56902930.
327	(29, 28)	84.2	95.0	2655.4	(22, 21)	50279870.
328	(29, 28)	85.1	94.6	2694.2	(22, 21)	46007280.
329	(29, 28)	86.0	94.3	2679.7	(22, 21)	42921200.
330	(29, 28)	85.7	94.0	2642.9	(22, 21)	40126350
331	(29, 28)	84.9	93.7	2637.6	(22, 21)	37180130.
332	(28, 28)	86.3	93.7	2668.0	(21, 21)	37024030.
333	(27, 27)	88.7	94.9	2782.8	(20, 20)	49396990.
334	(27, 26)	92.5	98.6	2751.3	(21, 20)	113636600.
335	(27, 26)	96.5	102.4	2746.4	(21, 20)	276417500
336	(27, 27)	99.7	105.5	2750.3	(20, 20)	563250400.
337	(28, 27)	102.7	108.5	2749.4	(21, 20)	1122898000.
338	(27, 27)	104.4	111.0	2765.5	(20, 20)	2013243000.
339	(28, 27)	105.9	112.7	2751.3	(21, 20)	2958746000.
340	(28, 27)	107.4	113.6	2711.0	(21, 20)	3597679000.
341	(28, 27)	109.0	114.0	2668.2	(21, 20)	3992778000.
342	(28, 27)	109.9	114.4	2673.1	(21, 20)	4359463000
343	(28, 27)	109.9	114.6	2693.2	(21, 20)	4605014000.
344	(28, 27)	109.6	114.6	2682.7	(21, 20)	4575789000
345	(28, 27)	108.9	114.4	2690.9	(21, 20)	4396339000

346	(28,27)	108.3	114.4	2724.6	(21,20)	4334944000
347	(28,27)	107.8	114.4	2734.7	(21,20)	4379578000.
348	(28,27)	107.9	114.6	2716.5	(21,20)	4518625000.
349	(27,27)	108.3	114.8	2736.1	(20,20)	4836983000.
350	(27,27)	109.0	115.2	2756.3	(20,20)	5220078000
351	(27,27)	109.7	115.4	2738.2	(20,20)	5437047000.
352	(27,27)	110.3	115.5	2715.4	(20,20)	5588488000.
353	(27,27)	110.8	115.8	2725.3	(20,20)	5962748000
354	(27,27)	111.2	116.0	2724.5	(20,20)	6382469000
355	(27,27)	111.6	116.2	2697.4	(20,20)	6601814000.
356	(27,27)	111.8	116.3	2686.1	(20,20)	6769848000
357	(27,27)	111.9	116.5	2712.6	(20,20)	7088042000.
358	(27,27)	111.9	116.6	2696.6	(20,20)	7311659000
359	(27,27)	111.9	116.6	2670.3	(20,20)	7271809000
360	(27,27)	112.0	116.6	2688.8	(20,20)	7216030000.
361	(27,27)	111.8	116.6	2718.0	(20,20)	7175160000.
362	(27,27)	111.7	116.4	2696.0	(20,20)	6960484000.
363	(27,27)	111.5	116.2	2691.3	(20,20)	6579364000
364	(27,27)	111.2	116.0	2724.4	(20,20)	6326743000
365	(27,27)	110.7	115.9	2746.5	(20,20)	6110265000.
366	(27,27)	110.2	115.5	2728.7	(20,20)	5685969000
367	(27,27)	109.5	115.1	2723.1	(20,20)	5166420000.
368	(27,27)	108.7	114.8	2765.4	(20,20)	4819063000
369	(27,27)	108.0	114.6	2777.2	(20,20)	4584911000
370	(27,27)	107.4	114.4	2774.3	(20,20)	4408422000
371	(26,28)	107.0	114.5	2794.4	(20,21)	4465189000.
372	(26,27)	106.5	114.7	2825.6	(20,21)	4628238000.
373	(26,27)	105.9	114.6	2813.4	(20,21)	4560892000
374	(27,28)	105.8	114.4	2781.8	(20,21)	4321190000
375	(26,28)	105.9	114.3	2800.9	(20,21)	4288499000
376	(26,27)	105.9	114.4	2826.5	(20,21)	4409455000.
377	(26,28)	106.0	114.4	2807.4	(20,21)	4405907000
378	(26,28)	106.2	114.5	2777.1	(20,21)	4421792000.
379	(26,28)	106.3	114.7	2797.9	(20,21)	4723859000
380	(26,28)	106.1	115.0	2813.9	(20,21)	4979462000
381	(26,28)	106.1	114.8	2788.3	(20,21)	4835959000.
382	(27,28)	106.0	114.6	2755.7	(20,21)	4581347000
383	(26,28)	105.9	114.7	2787.4	(20,21)	4639687000.
384	(26,28)	105.8	114.8	2795.2	(20,21)	4747473000.
385	(26,28)	106.0	114.6	2772.1	(20,21)	4553040000.
386	(26,28)	106.4	114.3	2759.8	(20,21)	4289367000
387	(26,28)	106.6	114.3	2796.7	(20,21)	4285850000.
388	(26,28)	106.9	114.4	2797.8	(20,21)	4337140000
389	(26,28)	107.3	114.3	2766.4	(20,21)	4268322000
390	(26,28)	107.8	114.4	2744.5	(20,21)	4346380000
391	(26,28)	108.1	114.7	2772.9	(20,21)	4659421000
392	(26,28)	108.5	114.8	2763.2	(20,21)	4835922000
393	(27,28)	108.8	114.8	2735.6	(20,21)	4786872000
394	(27,28)	109.0	114.9	2737.0	(20,21)	4892013000
395	(26,28)	109.2	115.2	2767.9	(20,21)	5219181000
396	(27,28)	109.4	115.2	2755.3	(20,21)	5298323000
397	(27,28)	109.5	115.0	2722.3	(20,21)	4974420000
398	(27,28)	109.6	114.7	2727.4	(20,21)	4689383000
399	(26,28)	109.6	114.7	2757.2	(20,21)	4676297000
400	(27,28)	109.7	114.7	2740.0	(20,21)	4673315000
401	(27,28)	109.9	114.6	2701.3	(20,21)	4578214000
402	(27,28)	110.1	114.7	2705.5	(20,21)	4661928000
403	(26,28)	110.1	114.9	2730.8	(20,21)	4888228000.
404	(27,28)	110.2	114.9	2709.9	(20,21)	4926484000
405	(27,28)	110.3	114.8	2672.7	(20,21)	4793655000.
406	(27,28)	110.4	114.9	2687.5	(20,21)	4861514000
407	(27,28)	110.4	115.1	2715.7	(20,21)	5087375000
408	(27,28)	110.3	115.0	2698.9	(20,21)	5064323000
409	(27,28)	110.2	114.8	2650.9	(20,21)	4802912000
410	(27,28)	110.1	114.7	2664.0	(20,21)	4722024000.
411	(27,28)	109.9	114.8	2691.0	(20,21)	4837655000

412	(27,28)	109.7	114.7	2696.1	(20,21)	4699963000.
413	(27,28)	109.8	114.3	2665.5	(20,21)	4256769000
414	(27,28)	109.7	114.0	2679.9	(20,21)	3944873000.
415	(26,28)	109.5	113.9	2721.5	(20,21)	3911043000.
416	(27,28)	109.5	113.8	2716.4	(20,21)	3798258000.
417	(27,28)	109.5	113.4	2678.0	(20,21)	3491824000.
418	(27,28)	109.5	113.2	2689.2	(20,21)	3327966000
419	(26,28)	109.5	113.3	2731.0	(20,21)	3419202000
420	(27,28)	109.5	113.3	2727.0	(20,21)	3408547000.
421	(27,28)	109.5	112.9	2696.3	(20,21)	3112846000.
422	(27,28)	109.3	112.6	2688.3	(20,21)	2858562000.
423	(26,28)	109.2	112.6	2723.3	(20,21)	2874116000.
424	(26,28)	109.0	112.7	2727.9	(20,21)	2925135000.
425	(27,28)	109.0	112.5	2702.0	(20,21)	2834675000
426	(26,28)	108.9	112.5	2711.6	(20,21)	2847640000.
427	(26,28)	108.8	112.9	2757.4	(20,21)	3101236000
428	(26,28)	108.7	113.1	2763.8	(20,21)	3271988000.
429	(26,28)	108.4	112.9	2733.6	(20,21)	3061736000.
430	(26,28)	108.0	112.4	2714.5	(20,21)	2757911000
431	(26,28)	107.6	112.4	2748.9	(20,21)	2729066000
432	(26,28)	107.2	112.5	2776.4	(20,21)	2823968000.
433	(26,28)	106.5	112.2	2758.5	(20,21)	2626824000.
434	(26,28)	106.2	111.5	2717.3	(20,21)	2231928000.
435	(26,28)	105.9	111.1	2725.7	(20,21)	2037655000.
436	(26,28)	105.7	111.2	2764.0	(20,21)	2101157000
437	(26,28)	105.4	111.1	2756.7	(20,21)	2055954000.
438	(27,28)	105.1	110.5	2717.6	(20,21)	1767730000
439	(26,28)	104.6	109.8	2723.5	(20,21)	1512137000.
440	(26,27)	104.2	109.7	2768.7	(20,21)	1476999000
441	(26,27)	103.9	109.7	2776.7	(20,21)	1482969000.
442	(26,28)	103.6	109.3	2744.2	(20,21)	1336359000
443	(26,28)	103.2	108.7	2731.6	(20,21)	1172228000
444	(26,27)	102.8	108.7	2770.6	(20,21)	1172918000.
445	(26,27)	102.7	109.0	2783.6	(20,21)	1260484000.
446	(26,28)	102.5	108.9	2755.3	(20,21)	1226842000
447	(27,28)	102.5	108.5	2731.9	(20,21)	1117930000
448	(26,27)	102.5	108.5	2747.6	(20,21)	1115147000
449	(26,27)	102.5	108.9	2785.0	(20,21)	1219056000.
450	(26,27)	102.4	108.9	2771.4	(20,21)	1221909000
451	(27,28)	102.3	108.3	2728.1	(20,21)	1074562000
452	(26,27)	102.0	107.8	2738.8	(20,21)	962389000
453	(26,27)	101.8	108.0	2789.3	(20,21)	1001115000.
454	(26,27)	101.6	108.2	2791.7	(20,21)	1056413000
455	(27,27)	101.3	107.9	2756.5	(20,20)	983618300.
456	(27,28)	101.1	107.5	2728.1	(20,21)	892275700
457	(26,28)	101.2	107.7	2738.4	(20,21)	935479300
458	(26,28)	101.2	108.2	2761.0	(20,21)	1050679000.
459	(26,28)	100.6	108.1	2738.8	(20,21)	1031733000.
460	(27,28)	100.2	107.4	2712.9	(20,21)	865191400.
461	(26,28)	99.8	106.6	2725.9	(20,21)	725538300.
462	(26,27)	99.4	106.5	2762.5	(20,21)	714897900
463	(26,27)	99.1	106.6	2779.0	(20,21)	728444400
464	(26,28)	98.4	106.1	2750.2	(20,21)	638956500.
465	(26,28)	98.0	104.9	2710.7	(20,21)	489080600.
466	(26,28)	97.8	104.0	2729.7	(20,21)	394083600
467	(25,27)	97.6	103.8	2771.7	(19,21)	380139000.
468	(26,27)	97.3	103.7	2772.3	(20,21)	369167400.
469	(26,28)	97.3	103.0	2745.9	(20,21)	318231800
470	(26,28)	97.1	102.1	2757.7	(20,21)	259858500.
471	(25,28)	97.1	101.8	2741.6	(19,21)	241804000.
472	(25,27)	97.0	102.1	2769.8	(19,21)	255534900
473	(26,28)	96.8	102.1	2739.5	(20,21)	256349400.
474	(26,28)	96.6	101.7	2706.4	(20,21)	232171600.
475	(26,28)	96.2	101.2	2704.1	(20,21)	207972900.
476	(26,28)	95.9	101.1	2679.1	(20,21)	205720400.
477	(26,28)	95.5	101.2	2706.0	(20,21)	210834900

478	(26,28)	95.2	100.9	2709.5	(20,21)	195422500
479	(26,28)	94.8	99.9	2731.8	(20,21)	154818400
480	(26,28)	94.4	98.5	2764.7	(20,21)	112366100
481	(26,28)	94.1	97.6	2743.3	(20,21)	91984380
482	(26,28)	93.7	97.8	2761.2	(20,21)	94540080
483	(26,28)	93.5	98.2	2754.9	(20,21)	105159300
484	(26,28)	93.1	98.4	2751.0	(20,21)	108922700
485	(26,28)	92.9	98.2	2745.3	(20,21)	104624000
486	(26,28)	92.5	98.0	2693.2	(20,21)	100234800
487	(26,28)	92.1	98.1	2715.9	(20,21)	102357900
488	(26,29)	91.6	98.4	2724.9	(20,22)	109295800
489	(26,28)	91.0	98.5	2727.0	(20,21)	112706900
490	(26,28)	90.4	98.3	2730.0	(20,21)	107762600
491	(26,28)	89.4	97.9	2709.7	(20,21)	97222370
492	(26,28)	90.6	97.5	2664.3	(20,21)	88362380
493	(26,28)	91.7	97.3	2609.8	(20,21)	85998210
494	(27,28)	92.6	97.6	2555.3	(20,21)	91013440
495	(27,29)	92.9	98.0	2627.8	(20,22)	100610200
496	(26,28)	92.4	98.4	2694.7	(20,21)	108925000
497	(26,28)	92.2	98.4	2715.8	(20,21)	109453700
498	(25,28)	91.0	97.9	2732.9	(19,21)	98726830
499	(25,28)	89.8	97.1	2717.8	(19,21)	81276450
500	(26,28)	88.8	96.2	2670.2	(20,21)	65328130
501	(27,28)	89.1	95.5	2639.5	(20,21)	55725310
502	(27,28)	88.9	95.1	2713.6	(20,21)	51179470
503	(26,28)	88.5	94.8	2737.8	(20,21)	47394780
504	(26,28)	88.4	94.3	2744.7	(20,21)	42506450
505	(26,27)	88.4	93.9	2751.0	(20,21)	38649920
506	(26,27)	88.3	93.8	2789.8	(20,21)	37591280
507	(26,27)	88.1	93.7	2789.7	(20,21)	37349520
508	(26,27)	88.1	93.5	2809.8	(20,21)	35275180
509	(26,27)	88.5	93.1	2831.4	(20,21)	32158320
510	(26,27)	89.0	93.1	2832.9	(20,21)	32372620
511	(27,27)	90.1	94.0	2795.7	(20,20)	39820000
512	(27,28)	91.1	95.1	2762.9	(20,21)	51275120
513	(28,28)	91.2	95.6	2696.1	(21,21)	57583390
514	(29,28)	90.3	95.2	2656.3	(22,21)	52519890
515	(29,28)	88.4	93.9	2712.1	(22,21)	39131300
520	(29,28)	90.5	93.4	2635.8	(22,21)	34896060
521	(30,28)	92.2	95.1	2560.5	(22,21)	50833780
522	(32,28)	93.4	96.6	2508.2	(23,21)	72093760
523	(34,28)	94.2	97.5	2467.5	(25,20)	90058060
524	(34;28)	94.2	97.8	2442.3	(25,20)	94994240
525	(34,28)	93.5	97.3	2417.2	(25,20)	85466300
526	(33,28)	92.3	96.4	2439.7	(24,20)	69681440
527	(32,28)	90.6	95.5	2453.5	(23,21)	56528210
528	(32,29)	88.7	94.8	2469.0	(23,21)	47908260
529	(31,29)	86.6	94.2	2496.8	(23,21)	41229500
530	(30,29)	84.2	93.5	2519.8	(22,21)	35728670
531	(30,29)	82.5	93.2	2469.7	(22,21)	33320510
532	(31,29)	81.7	93.3	2449.0	(23,21)	34000770
533	(31,29)	83.4	93.4	2398.3	(23,21)	34666560
534	(32,29)	83.7	93.2	2386.3	(23,21)	33215970
535	(31,28)	82.6	92.9	2450.5	(23,21)	30701220
538	(32,28)	85.7	93.5	2513.7	(23,21)	35866700
539	(32,28)	85.8	94.8	2474.2	(23,21)	47517420
540	(33,28)	86.1	95.9	2412.0	(24,20)	61274820
541	(34,28)	86.5	96.4	2355.5	(25,20)	69391680
542	(33,28)	86.2	96.3	2365.5	(24,20)	67162110
543	(33,28)	85.1	95.7	2400.8	(24,20)	59263020
544	(34,28)	86.0	95.8	2397.3	(25,20)	60550540
545	(34,29)	88.2	96.9	2281.0	(25,21)	78437420
546	(35,29)	89.9	98.1	2122.3	(25,21)	102754400
547	(37,29)	90.5	98.7	1995.0	(26,21)	117752000
548	(37,29)	90.4	98.6	1985.5	(26,21)	115738400
549	(37,29)	89.3	98.0	2081.5	(26,21)	100951400

550	(36,29)	87.7	97.1	2156.6	[illegible]	[illegible]
551	(35,29)	85.7	95.8	2193.5	(26,21)	80906720.
552	(35,29)	83.9	94.2	2248.4	(25,21)	59815250.
553	(35,29)	82.3	93.4	2303.8	(25,21)	41976000.
554	(35,29)	82.8	93.5	2300.0	(25,21)	34278450.
555	(35,29)	83.6	93.8	2318.0	(25,21)	35404380.
556	(34,29)	84.2	94.0	2360.3	(25,21)	38282020.
557	(34,29)	84.9	94.8	2348.3	(25,21)	40134130.
558	(35,29)	88.2	96.8	2227.4	(25,21)	48373810.
559	(37,29)	90.8	98.7	2076.6	(25,21)	75943970.
560	(36,29)	91.9	99.8	2081.7	(26,21)	118079700.
561	(35,29)	91.7	99.9	2174.4	(26,21)	150314100.
562	(34,28)	90.5	99.2	2260.8	(25,21)	153398800.
563	(33,28)	89.1	98.1	2318.7	(25,20)	131420800.
564	(33,29)	87.8	97.0	2325.3	(24,20)	102773300.
565	(33,29)	86.5	96.0	2305.5	(24,21)	79598050.
566	(35,29)	85.1	95.5	2273.9	(24,21)	62669410.
567	(37,29)	86.0	96.5	2189.2	(25,21)	56412050.
568	(39,29)	88.8	98.1	2133.9	(26,21)	70571630.
569	(39,30)	90.6	99.2	2118.3	(27,20)	102674900.
570	(38,30)	90.9	99.4	2123.6	(27,21)	132242000.
571	(37,30)	90.1	98.8	2137.8	(27,21)	138695700.
572	(37,29)	88.9	97.8	2179.3	(26,21)	120746900.
573	(35,29)	88.7	97.2	2234.0	(26,21)	96131980.
574	(35,29)	89.0	97.3	2215.6	(25,21)	83304610.
575	(36,29)	89.0	97.4	2172.1	(25,21)	84248610.
576	(36,29)	88.7	97.0	2129.2	(26,21)	86680340.
577	(36,29)	87.5	96.0	2104.3	(26,21)	79267330.
578	(35,29)	85.3	94.5	2168.6	(26,21)	62545100.
579	(34,29)	83.3	93.4	2195.4	(25,21)	44656720.
580	(36,29)	83.8	93.6	2140.4	(25,21)	34852530.
581	(37,29)	85.8	94.7	2053.0	(26,21)	36311060.
582	(38,30)	87.2	95.8	2007.0	(26,21)	46658830.
583	(37,29)	87.4	96.5	2067.5	(27,21)	60203070.
584	(37,29)	87.1	97.0	2126.4	(26,21)	70640610.
585	(37,29)	88.7	97.9	2100.3	(26,21)	78880620.
586	(40,29)	92.1	99.6	1983.0	(26,21)	97882340.
587	(43,29)	94.3	101.3	1868.5	(28,20)	144947000.
588	(45,30)	95.2	102.2	1766.9	(29,20)	213654600.
589	(45,30)	94.8	102.2	1752.3	(30,20)	265757300.
590	(43,29)	93.3	101.3	1836.3	(30,20)	264644800.
591	(41,29)	91.4	99.9	1929.1	(29,20)	214999200.
592	(39,29)	90.1	98.5	2004.4	(28,20)	154222300.
593	(38,29)	89.1	97.4	2047.0	(27,20)	112190100.
594	(36,29)	87.2	96.3	2072.1	(27,20)	88080160.
595	(35,29)	84.8	94.8	2179.6	(26,21)	67469520.
596	(34,29)	83.5	93.6	2280.6	(25,21)	47993470.
597	(34,29)	83.7	93.5	2283.1	(25,21)	36418110.
598	(35,29)	84.4	94.0	2262.9	(25,21)	35254590.
599	(35,29)	84.3	94.5	2245.6	(25,21)	39952860.
600	(36,29)	83.4	94.6	2255.8	(25,21)	44460560.
601	(36,29)	82.9	94.4	2228.0	(26,21)	45345540.
602	(36,29)	83.8	94.5	2214.3	(26,21)	44121380.
603	(36,29)	86.1	95.4	2213.6	(26,21)	45116510.
604	(37,29)	88.1	96.6	2149.3	(26,21)	54710110.
605	(38,29)	89.6	97.4	2094.4	(26,21)	72036460.
606	(39,29)	89.8	97.3	2068.2	(27,20)	86266320.
607	(38,29)	88.9	96.6	2080.9	(27,20)	85955660.
608	(37,29)	87.1	95.6	2100.3	(27,20)	71887680.
609	(37,29)	86.3	95.3	2097.0	(26,21)	56965950.
610	(37,29)	87.0	95.9	2074.7	(26,21)	53551740.
611	(38,29)	88.1	96.7	2018.9	(26,21)	62104700.
612	(38,29)	88.8	97.3	2017.6	(27,20)	74293550.
613	(37,29)	88.8	97.5	2076.2	(27,20)	84402430.
614	(36,29)	88.7	97.3	2143.9	(26,21)	88721700.
615	(35,29)	88.5	97.0	2216.6	(26,21)	86015650.
					(25,21)	78971580.

616	(34, 29)	87. 7	96. 5	2280. 8	(25, 21)	70767070.
617	(34, 29)	86. 9	95. 9	2290. 1	(25, 21)	62205810.
618	(33, 29)	86. 1	95. 2	2340. 3	(24, 21)	52262990
619	(32, 29)	84. 2	94. 1	2374. 1	(23, 21)	41036700
620	(31, 29)	82. 0	93. 1	2398. 8	(23, 21)	32611500
621	(31, 29)	83. 2	93. 0	2418. 5	(23, 21)	31403310
622	(31, 29)	84. 9	93. 7	2390. 7	(23, 21)	37144750.
623	(32, 29)	85. 9	94. 8	2312. 3	(23, 21)	47919220
624	(33, 29)	87. 0	95. 9	2271. 5	(24, 21)	61042080.
625	(35, 29)	88. 0	96. 4	2203. 4	(25, 21)	69963980.
626	(36, 29)	88. 0	96. 3	2141. 7	(26, 21)	68067220
627	(36, 29)	86. 9	95. 5	2146. 9	(26, 21)	55932670.
628	(34, 29)	85. 0	94. 2	2250. 4	(25, 21)	41513140
629	(33, 29)	83. 0	93. 1	2347. 0	(24, 21)	32613710
630	(32, 29)	82. 6	92. 8	2416. 8	(23, 21)	30140220.
631	(30, 29)	81. 8	93. 0	2518. 0	(22, 21)	31576350.
632	(30, 29)	81. 6	93. 5	2559. 0	(22, 21)	35796450.
633	(30, 29)	82. 7	94. 1	2522. 4	(22, 21)	40944080
634	(31, 28)	82. 8	94. 4	2480. 1	(23, 21)	43797310
635	(31, 28)	84. 6	94. 4	2504. 2	(23, 21)	43354500
636	(32, 28)	85. 7	94. 1	2517. 8	(23, 21)	40963200.
637	(32, 28)	86. 0	93. 8	2564. 5	(23, 21)	37600940
638	(31, 28)	85. 4	93. 2	2608. 5	(23, 21)	33403060
641	(29, 28)	82. 4	92. 9	2617. 8	(22, 21)	30978620.
642	(29, 28)	82. 5	93. 2	2592. 6	(22, 21)	32776770.
643	(29, 28)	82. 1	92. 8	2589. 3	(22, 21)	30307500

Appendix F

CTT Audio Simulation Program Listings

This appendix contains the program listings for the CTT audio simulation. It consists primarily of three modules. First, analog speech was passed through a low pass filter with a 3.8 KHz cut-off frequency. Then it was passed through a high pass filter with a 100 Hz cut-off frequency. It was then sampled at 8 Khz and digitized with sixteen bit digitization (-2^{15} to $+2^{15}$). This file of 8 Khz sampled digitized speech was the input for the first module which has the listing name "TRACKSPAC.FR". The "TRACKSPAC.FR" module performed the function of calculating the image inside the log-log 60 dB, 3900 Hz primary audio cortex (P.A.C.) window. It stores the image for each 20 msec (slid by 2 msec) window of the digitized speech file onto a second file which becomes the input for the second module.

The second module has the listing name "TRACKSR3.FR". This module functions to calculate the 2DDFTs and single-point gestalts of each P.A.C. windowed image. It saves these gestalt points in a file (see Appendix E).

This file becomes the input for the third module with the listing name "WDPTADD.FR". This module compiles all the gestalt points calculated in the second module into a single 2-D image. This is the image of the phoneme track. It then computes the 2DDFT and gestalt point from this image. The resulting gestalt point is the identity of the initial analog utterance.

```
MESSAGE "THIS PROGRAM PROCESSES A SPEECH FILE STARTING WITH THE"
MESSAGE "  AD.SV DIGITIZED SPEECH FILE.  THE DIGITIZED SPEECH FILE"
MESSAGE "  IS READ BY TRACKSPAC WHICH PRODUCES THE INFORMATION TO"
MESSAGE "  TO MAKE PRIMARY AUDIO CORTEX MAPS.  TRACKSR3 IS THEN RUN"
MESSAGE "  PRODUCING A PHONEME GESTALT TRACK ON THE SECONDARY AUDIO CORTEX"
MESSAGE "  WDPTADD IS THEN RUN IN ORDER TO COMPUTE THE GESTALT OF THE WORD"
MESSAGE " "
TRACKSPAC
TRACKSR3
PRINT TPP
WDPTADD
MESSAGE "TRACKS PROGRAM IS FINISHED"
```

```
CCCCCCCCCCCCCCCCCCCCCCCCCCCCCCCCCCCCCCCCCCCCCCCCCCCCCCCCCCCCCCCCC
C                                                               C
C       FILE NAME: TRACKSPAC.FR                                 C
C       AUTHOR: ROUTH                                           C
C       PURPOSE: TO COMPUTE THE PRIMARY AUDIO CORTEX IMAGE OF   C
C              A SPEECH FILE AND OUTPUT 1875 MSECS OF THESE     C
C              IMAGES TO A FILE TO BE PROCESSED BY TRACKSR3     C
C       LOAD LINE: USE CNLTP.MC                                 C
C       HISTORY: A REWRITE OF PAC.FR                            C
C                                                               C
CCCCCCCCCCCCCCCCCCCCCCCCCCCCCCCCCCCCCCCCCCCCCCCCCCCCCCCCCCCCCCCCC

        INTEGER FILENAME(7),SUMFILE(7), OUTFILE(7)
        DIMENSION GAIN(512),COEF(1,1)
        DIMENSION RDATA(1024),FIDATA(1024)
        DIMENSION IDATA(1024),SUM(1024),RSUM(2,1024)


CCCCCCCCCCCCCCCCCCCCCCCCCCCCCCCCCCCCCCCCCCCCCCCCCCCCCCCCCCCCCCCCCCCCCCCCCCCCC
C
C     VARIABLE INITIALIZATION
C
CCCCCCCCCCCCCCCCCCCCCCCCCCCCCCCCCCCCCCCCCCCCCCCCCCCCCCCCCCCCCCCCCCCCCCCCCCCCC
        IRUN=0       ; IRUN=0 ON FIRST PASS, =1 ON SECOND PASS
        SCLDIV=1.    ; SCLDIV IS NORMALIZATION DIVISOR FOR FIRST STAGE OF
                     ;   OF AGC SYSTEM.  CALCULATED AT END OF FIRST PASS.
3       KNT=1
        AMAXUP=0.
        IFSCL=0
        MODE=0
        NC=1
C     LOGLEN IS NUMBER OF INCREMENTS FOR LOG LENGTH
        LOGLEN=64
C     N IS FFT WINDOW SIZE
        N=1024

        IF(IRUN .EQ. 1)GO TO 8


CCCCCCCCCCCCCCCCCCCCCCCCCCCCCCCCCCCCCCCCCCCCCCCCCCCCCCCCCCCCCCCCCCCCCCCCCCCCC
C
C     OPEN FILES TO BE USED IN THIS PROGRAM
C
CCCCCCCCCCCCCCCCCCCCCCCCCCCCCCCCCCCCCCCCCCCCCCCCCCCCCCCCCCCCCCCCCCCCCCCCCCCCC
5       TYPE " "
6000    TYPE "WHAT IS THE NAME OF THE SPEECH FILE YOU WISH"
6       ACCEPT "TO PROCESS? "
        READ(11,7)FILENAME(1)
7       FORMAT(S13)
8       CALL OPEN(2,FILENAME,1,IER)
        IF (IER.EQ.1)GO TO 9
        TYPE "CANNOT OPEN BECAUSE OF ERROR",IER
        TYPE "TRY AGAIN."
```

```
        GO TO 5

C     ROOT.NM IS FILE WHICH TRACKSR3 READS TO FIND NAME OF SPEECH FILE
C      CURRENTLY BEING PROCESSED
9       CALL DFILW("ROOT.NM",IER)
        CALL CFILW("ROOT.NM",1,IER)
        CALL OPEN(1,"ROOT.NM",3,IER)
        IF(IER  .EQ. 1)GO TO 91
        TYPE "OPEN FILE ERROR",IER
        STOP

C    SUMFILE IS NAME OF FILE INTO WHICH LOG-LOG MATRICIES WILL BE WRITTEN
91      DO 10 I=2,7
          SUMFILE(I)=FILENAME(I-1)
10      CONTINUE
        SUMFILE(1)="PP"
        CALL DFILW(SUMFILE,IER)
        IF(IER .EQ. 13)GO TO 910
        IF(IER .NE. 1)TYPE "DELETE ERROR",IER
910     CALL CFILW(SUMFILE,3,600,IER)
        IF(IER .NE. 1)TYPE "CREATE FILE ERROR",IER
        CALL OPEN(4,SUMFILE,3,IER)
        IF(IER .NE. 1)TYPE "OPEN ERROR",IER
        WRITE BINARY(1)(SUMFILE(J),J=1,7)

C    NP IS NUMBER OF SPEECH FILE POINTS IN EACH 20 MSEC WINDOW OF AUDIO
        NP=160
C60102    ACCEPT "HOW MANY SPECTRUMS DO YOU WANT TO AVERAGE IN ONE PLOT? ",NS
        NS=1
C. THIS PROGRAM NOW DOES A SLIDING NP/8 MSEC WINDOW (SLIDES EVERY 2 MSEC)

C    RLL IS THE FREQUENCY OF LEFT WINDOW EDGE
        RLL=100
        RLOGLL=ALOG10(RLL)
        SCALE=LOGLEN/(ALOG10(4090./RLL))

C    VWIND IS VERTICAL WINDOW SIZE IN DB
        VWIND=60.
        INS=0


CCCCCCCCCCCCCCCCCCCCCCCCCCCCCCCCCCCCCCCCCCCCCCCCCCCCCCCCCCCCCCCCCCCCCCCCCCCCC
C
C     INITIALIZE VARIABLE ARRAYS
C
CCCCCCCCCCCCCCCCCCCCCCCCCCCCCCCCCCCCCCCCCCCCCCCCCCCCCCCCCCCCCCCCCCCCCCCCCCCCCCCC
        DO 750 J=1,N
          DO 750 K=1,NS
            RSUM(K,J)=0.
750     CONTINUE

        DO 725 J=1,NP
          IDATA(J)=0
725     CONTINUE
```

```
      DO 700 J=1,N
        SUM(J)=0
700   CONTINUE

C     RESERVE 4 DUMMY SLOTS AT BEGINNING OF FILE TO BE WRITTEN INTO LATER ON.
C         THESE DUMMY SLOTS ARE USED TO PASS FILESIZE INFO TO TRACKSR3.
      WRITE BINARY(4)AMAXUP,VWIND,LOGLEN,KNT
      READ BINARY(2,END=6025)(IDATA(J),J=1,NP-16)


C     RDATA=REAL DATA,  FIDATA=IMAGINARY DATA
      DO 60100 ICT=1,5000

      DO 6011 J=1,N
        RDATA(J)=0
        FIDATA(J)=0
6011  CONTINUE

C     THIS SLIDES 20MSEC WINDOW EVERY 2 MSECS.
      READ BINARY(2,END=6025)(IDATA(J),J=NP-15,NP)


CCCCCCCCCCCCCCCCCCCCCCCCCCCCCCCCCCCCCCCCCCCCCCCCCCCCCCCCCCCCCCCCCCCCCCCCC
C
C     APPLY HAMMING WINDOW TO INPUT DATA AND COMPUTE ENERGY(PWR)
C
CCCCCCCCCCCCCCCCCCCCCCCCCCCCCCCCCCCCCCCCCCCCCCCCCCCCCCCCCCCCCCCCCCCCCCCCCCCC
      PWR=0.
      P=NP-1
      DO 1234 J=1,NP
        RDATA(J)=FLOAT(IDATA(J))/SCLDIV
        RJ=J-1
        W=.54-.46*COS(2.*3.14159*RJ/P)
        RDATA(J)=RDATA(J)*W
        PWR=PWR+RDATA(J)*RDATA(J)
1234  CONTINUE


CCCCCCCCCCCCCCCCCCCCCCCCCCCCCCCCCCCCCCCCCCCCCCCCCCCCCCCCCCCCCCCCCCCCCCCCC
C
C     SHIFT INPUT ARRAY BY 2 MSEC
C
CCCCCCCCCCCCCCCCCCCCCCCCCCCCCCCCCCCCCCCCCCCCCCCCCCCCCCCCCCCCCCCCCCCCCCCCCCCC
      NP3QRT=NP-16
      NP1QRT=16
      DO 1235 J=1,NP3QRT
        IDATA(J)=IDATA(J+NP1QRT)
1235  CONTINUE

C     CHECK SIGNAL TO NOISE RATIO
      IF((IRUN .EQ. 0) .AND. (PWR .LT. 1.E9))GO TO 60100


CCCCCCCCCCCCCCCCCCCCCCCCCCCCCCCCCCCCCCCCCCCCCCCCCCCCCCCCCCCCCCCCCCCCCCCCC
C
```

```
C     FIND DFT AND COMPUTE MAGNITUDE SFECTRUM
C
CCCCCCCCCCCCCCCCCCCCCCCCCCCCCCCCCCCCCCCCCCCCCCCCCCCCCCCCCCCCCCCCCCCCCCCCCCCC
        CALL FFT(RDATA,FIDATA,N,1)
        DO 6015 J=1,N/2+1
        TEMP=RDATA(J)*RDATA(J)+FIDATA(J)*FIDATA(J)
        SUM(J)=SQRT(TEMP)
9913    FORMAT(15X,I4,F15.2)
6015    CONTINUE

CCCCCCCCCCCCCCCCCCCCCCCCCCCCCCCCCCCCCCCCCCCCCCCCCCCCCCCCCCCCCCCCCCCCCCCCCC
C
C     CONVERT DATA TO LOG PLOT FORM
C
CCCCCCCCCCCCCCCCCCCCCCCCCCCCCCCCCCCCCCCCCCCCCCCCCCCCCCCCCCCCCCCCCCCCCCCCCCCC
954     JP=1
        DO 800 J=1,LOGLEN
          R=J
          PRD=(4000.**(R/LOGLEN))*(RLL**((LOGLEN-R)/LOGLEN))
          PRD=PRD/4000.*N/2.
          JK=INT(PRD+.5)
          RSUM(1,J)=0.
          DO 9911 JCT=JP,JK
            RSUM(1,J)=RSUM(1,J)+SUM(JCT)
9911      CONTINUE
          DIVDR=JK-JP+1
          RSUM(1,J)=RSUM(1,J)/DIVDR
          RSUM(1,J)=20.*(ALOG10(RSUM(1,J)))
          JP=JK
9912      FORMAT(5X,5F15.3)
800     CONTINUE
        DO 802 J=1,LOGLEN
          SUM(J)=RSUM(1,J)
802     CONTINUE

CCCCCCCCCCCCCCCCCCCCCCCCCCCCCCCCCCCCCCCCCCCCCCCCCCCCCCCCCCCCCCCCCCCCCCCCCC
C
C     OUTPUT STATUS OF PROGRESS TO USER TERMINAL
C
CCCCCCCCCCCCCCCCCCCCCCCCCCCCCCCCCCCCCCCCCCCCCCCCCCCCCCCCCCCCCCCCCCCCCCCCCCCC
955     ITIME=38+ICT*2
        TYPE "MSECS OF FILE PROCESSED = ",ITIME
        KNT=ICT

C     AMAX IS USED FOR AGC
        AMAX=0.
        DO 810 J=1,LOGLEN
          IF(SUM(J) .GT. AMAX) AMAX=SUM(J)
          IF(SUM(J) .GT. AMAXUP) AMAXUP=SUM(J)
810     CONTINUE

CCCCCCCCCCCCCCCCCCCCCCCCCCCCCCCCCCCCCCCCCCCCCCCCCCCCCCCCCCCCCCCCCCCCCCCCCC
```

```
C     FIND DFT AND COMPUTE MAGNITUDE SPECTRUM
C
CCCCCCCCCCCCCCCCCCCCCCCCCCCCCCCCCCCCCCCCCCCCCCCCCCCCCCCCCCCCCCCCCCCCCCCCCC
        CALL FFT(RDATA,FIDATA,N,1)
        DO 6015 J=1,N/2+1
        TEMP=RDATA(J)*RDATA(J)+FIDATA(J)*FIDATA(J)
        SUM(J)=SQRT(TEMP)
9913    FORMAT(15X,I4,F15.2)
6015    CONTINUE

CCCCCCCCCCCCCCCCCCCCCCCCCCCCCCCCCCCCCCCCCCCCCCCCCCCCCCCCCCCCCCCCCCCCCCCC
C
C     CONVERT DATA TO LOG PLOT FORM
C
CCCCCCCCCCCCCCCCCCCCCCCCCCCCCCCCCCCCCCCCCCCCCCCCCCCCCCCCCCCCCCCCCCCCCCCCCC
954     JP=1
        DO 800 J=1,LOGLEN
          R=J
          PRD=(4000.**(R/LOGLEN))*(RLL**((LOGLEN-R)/LOGLEN))
          PRD=PRD/4000.*N/2.
          JK=INT(PRD+.5)
          RSUM(1,J)=0.
          DO 9911 JCT=JP,JK
            RSUM(1,J)=RSUM(1,J)+SUM(JCT)
9911      CONTINUE
          DIVDR=JK-JP+1
          RSUM(1,J)=RSUM(1,J)/DIVDR
          RSUM(1,J)=20.*(ALOG10(RSUM(1,J)))
          JP=JK
9912      FORMAT(5X,5F15.3)
800     CONTINUE
        DO 802 J=1,LOGLEN
          SUM(J)=RSUM(1,J)
802     CONTINUE

CCCCCCCCCCCCCCCCCCCCCCCCCCCCCCCCCCCCCCCCCCCCCCCCCCCCCCCCCCCCCCCCCCCCCCCC
C
C     OUTPUT STATUS OF PROGRESS TO USER TERMINAL
C
CCCCCCCCCCCCCCCCCCCCCCCCCCCCCCCCCCCCCCCCCCCCCCCCCCCCCCCCCCCCCCCCCCCCCCCCCC
955     ITIME=38+ICT*2
        TYPE "MSECS OF FILE PROCESSED = ",ITIME
        KNT=ICT

C     AMAX IS USED FOR AGC
        AMAX=0.
        DO 810 J=1,LOGLEN
          IF(SUM(J) .GT. AMAX) AMAX=SUM(J)
          IF(SUM(J) .GT. AMAXUP) AMAXUP=SUM(J)
810     CONTINUE

CCCCCCCCCCCCCCCCCCCCCCCCCCCCCCCCCCCCCCCCCCCCCCCCCCCCCCCCCCCCCCCCCCCCCCCC
```

```
C
C    WRITE OUT LOG-LOG PLOT OF MAGNITUDE SPECTRUM WITH AGC INFO
C
CCCCCCCCCCCCCCCCCCCCCCCCCCCCCCCCCCCCCCCCCCCCCCCCCCCCCCCCCCCCCCCCCCCCCCCCCCC
          TYPE ICT,AMAX,PWR
          WRITE BINARY(4)(SUM(J),J=1,LOGLEN),AMAX,PWR


CCCCCCCCCCCCCCCCCCCCCCCCCCCCCCCCCCCCCCCCCCCCCCCCCCCCCCCCCCCCCCCCCCCCCCCCCC
C
C    REINITIALIZE VARIABLES
C
CCCCCCCCCCCCCCCCCCCCCCCCCCCCCCCCCCCCCCCCCCCCCCCCCCCCCCCCCCCCCCCCCCCCCCCCCCC
715       DO 720 J=1,N
            SUM(J)=0.
720       CONTINUE

60100     CONTINUE



6025      REWIND 4
          WRITE BINARY(4)AMAXUP,VWIND,LOGLEN,KNT



          CALL CLOSE(2,IER)
          CALL CLOSE(1,IER)
          CALL CLOSE(4,IER)


C    FIRST RUN THROUGH WAS ONLY TO FIND SCLDIV VALUE FOR AGC NORMALIZATION
          IF(IRUN .EQ. 1)STOP

7793      IRUN=1
          TEMP=AMAXUP-112.
          SCLDIV=10.**(TEMP/20.)
          TYPE "AMAXUP=",AMAXUP,"TEMP=",TEMP,"SCLDIV=",SCLDIV
          GO TO 3


          END
```

```
CCCCCCCCCCCCCCCCCCCCCCCCCCCCCCCCCCCCCCCCCCCCCCCCCCCCCCC
C                                                     C
C                                                     C
C       NAME:  TRACKSR3.FR                            C
C       AUTHOR:  ROUTH                                C
C       PURPOSE: TAKES 2DFFT OF 64 BY 64 ARRAY.       C
C                USES OUTPUT FILES GENERATED BY TRACKSPAC C
C       LOAD LINE:                                    C
C                           USE MACRO: TR3.MC         C
C       HISTORY: REWRITE OF R3DFFT.FR                 C
C                                                     C
CCCCCCCCCCCCCCCCCCCCCCCCCCCCCCCCCCCCCCCCCCCCCCCCCCCCCCC

        INTEGER SUMFILE(7),SECFIL(7)
        DIMENSION RINP(4098)
        DIMENSION A(2,2),CRAY(64,64)

CCCCCCCCCCCCCCCCCCCCCCCCCCCCCCCCCCCCCCCCCCCCCCCCCCCCCCCCCCCCCCCCCCCCCCCCCC
C
C    INITIALIZE VARIABLES
C
CCCCCCCCCCCCCCCCCCCCCCCCCCCCCCCCCCCCCCCCCCCCCCCCCCCCCCCCCCCCCCCCCCCCCCCCCC
C   L IS THE DIMENSION OF CRAY(L,L)
        L=64
C   IADEM IS THE DIMENSION OF A(IADEM,IADEM)
        IADEM=2
C   IDEM IS THE DIMENSION RINP AND RIMP AND THE LENGTH OF FFT'S TAKEN
        IDEM=4096

        REALL=L
        SCALE=40./(ALOG10(REALL)-ALOG10(10.))

CCCCCCCCCCCCCCCCCCCCCCCCCCCCCCCCCCCCCCCCCCCCCCCCCCCCCCCCCCCCCCCCCCCCCCCCCC
C
C    SET UP FILES TO BE USED IN THIS PROGRAM
C
CCCCCCCCCCCCCCCCCCCCCCCCCCCCCCCCCCCCCCCCCCCCCCCCCCCCCCCCCCCCCCCCCCCCCCCCCC

C    TRP FILE IS THE PRINTER OUTPUT FILE FOR SECFIL DATA
        CALL DFILW("TRP",IER)
        CALL CFILW("TRP",1,IER)
        CALL OPEN(2,"TRP",3,IER)
        IF (IER .NE. 1)TYPE "OPEN FILE ERROR",IER


        CALL OPEN(4,"ROOT.NM",1,IER)
        IF(IER .EQ. 1)GO TO 8
        TYPE "OPEN FILE ERROR",IER
        STOP
8       READ BINARY(4)(SUMFILE(J),J=1,7)
        DO 81 J=1,7
          SECFIL(J)=SUMFILE(J)
81      CONTINUE
```

```
          SECFIL(1)=SECFIL(1)+768

C    SUMFILE IS NAME OF TRACKSPAC OUTPUT FILE
          CALL OPEN(1,SUMFILE,1,IER)
          IF(IER .EQ. 1)GO TO 909
          TYPE "CANNOT OPEN BECAUSE OF ERROR",IER
          STOP

C    SECFIL IS NAME OF SECOND CORTEX OUTPUT FILE ("SP-.DA")
C      SET UP HEADER FOR PRINTER OUTPUT OF SECFIL (TRP)
          WRITE(2,904)
903       FORMAT(2X,"TRACK TRAIL FOR ",S16)
904       FORMAT(//,8X,"BLOCK    (IR3D,JR3D)",6X,"AMAX",6X,"AMAXUP",8X,"RSUM",5X,
     &             "LOG COORD'S",6X,"POWER",/)
          CALL DFILW(SECFIL,IER)
          IF(IER .EQ. 13)GO TO 10
          IF(IER .NE. 1)TYPE "DELETE ERROR",IER
10        CALL CFILW(SECFIL,3,30,IER)
          IF(IER .NE. 1)TYPE "CREATE FILE ERROR",IER
          CALL OPEN(3,SECFIL,3,IER)
          IF(IER .EQ. 1)GO TO 9091
          TYPE "CANNOT OPEN BECAUSE OF ERROR",IER
          STOP

C     INITIALIZE OUTPUT ARRAY
9091      DO 300 I=1,IADEM
            DO 300 J=1,IADEM
              A(I,J)=0.
300       CONTINUE

C     READ INPUT FILE PARAMETERS
          READ BINARY(1)AMAXUP,VWIND,LOGLEN,KNT
          WRITE BINARY(3)KNT

          KNT1=KNT
C         ACCEPT "HOW MANY GRAPHS DO YOU WANT TO DO (400 FOR ENTIRE FILE)? ",KNT1
C         IF(KNT1 .EQ. 400)KNT1=KNT
          TYPE "THE FOLLOWING LIST WILL TERMINATE AFTER",KNT1,"  BLOCKS:"
          KNT=KNT1
          IF(KNT .NE. 1)GO TO 302
          TYPE
          ACCEPT "WHICH GRAPH (40 msec OVERLAPPING BLOCK) DO YOU WANT? ",KWONE
          IF(KWONE .EQ. 1)GO TO 302
          DO 301 I=1,KWONE-1
            READ BINARY(1,END=6025)(RINP(J),J=1,L),AMAX,PWR
301       CONTINUE

302       TIMER = 40.
          DO 9999 KOUNT=1,KNT

          TIMER=TIMER+1.

CCCCCCCCCCCCCCCCCCCCCCCCCCCCCCCCCCCCCCCCCCCCCCCCCCCCCCCCCCCCCCCCCCCCCCCCCCCCC
C
```

```
C     READ IN PAC PLOT AND AGC PARAMETERS
C
CCCCCCCCCCCCCCCCCCCCCCCCCCCCCCCCCCCCCCCCCCCCCCCCCCCCCCCCCCCCCCCCCCCCCCCCCCCCCC
          READ BINARY (1,END=6025)(RINP(J),J=1,L),AMAX,PWR
          IF(PWR .LT. 3.000E7)GO TO 9999

          RSUM=0.
          AMAXUP=+18. +ALOG10(PWR)*10.
          DO 6022 J=1,L
            RINP(J)=(RINP(J)-AMAXUP+VWIND)*LOGLEN/VWIND
            IF(RINP(J) .LT. 0.)RINP(J)=0.
            IF(RINP(J) .GT. 64.)RINP(J)=64
            RSUM=RSUM+RINP(J)
6022      CONTINUE

CCCCCCCCCCCCCCCCCCCCCCCCCCCCCCCCCCCCCCCCCCCCCCCCCCCCCCCCCCCCCCCCCCCCCCCCCCCCCC
C
C     BUILD 2-D WINDOWED PAC
C
CCCCCCCCCCCCCCCCCCCCCCCCCCCCCCCCCCCCCCCCCCCCCCCCCCCCCCCCCCCCCCCCCCCCCCCCCCCCCC
6024      DO 912 I=1,L
            DO 912 J=1,L
              CRAY(I,J)=0.
912       CONTINUE
          DO 920 J=1,64
            IUPLIM=RINP(J)
            IF((IUPLIM .LT. 65) .AND. (IUPLIM .GE. 0))GO TO 910
            TYPE "FOR J=",J," IUPLIM=",IUPLIM
            WRITE(2,1765)IUPLIM
1765        FORMAT(1X,"********************* IUPLIM =",I4)
            IUPLIM=64
910         IF(IUPLIM .EQ. 0)GO TO 920
C           DO 920 I=1,IUPLIM
C             CRAY(I,J)=1.
              CRAY(IUPLIM,J)=1.
920       CONTINUE

CCCCCCCCCCCCCCCCCCCCCCCCCCCCCCCCCCCCCCCCCCCCCCCCCCCCCCCCCCCCCCCCCCCCCCCCCCCCCC
C
C     APPLY 2-D HAMMING WINDOW
C
CCCCCCCCCCCCCCCCCCCCCCCCCCCCCCCCCCCCCCCCCCCCCCCCCCCCCCCCCCCCCCCCCCCCCCCCCCCCCC
          DO 7898 I=1,64
            RI=I-1
            WI=.54-.46*COS(2.*3.14159*RI/63.)
            DO 7898 J=1,64
              RJ=J-1
              WJ=.54-.46*COS(2.*3.14159*RJ/63.)
              CRAY(I,J)=CRAY(I,J)*WI*WJ
 7898     CONTINUE

C   THIS CODE WAS USED TO PUT D.C. TERM IN CENTER OF GRAPH (OUTPUT ARRAY MATRIX)
```

```
C    DO -1**(R+C) SHUFFLE BEFORE TRANSFORMING
C         DO 25 I=1,L
C           DO 24 J=1,L
C             CRAY(I,J)=CRAY(I,J)*((-1)**(I+J))
C24         CONTINUE
C25       CONTINUE


CCCCCCCCCCCCCCCCCCCCCCCCCCCCCCCCCCCCCCCCCCCCCCCCCCCCCCCCCCCCCCCCCCCCCCCCCCC
C
C     DO 2DDFST (2 DIMEN. DISCRETE FOURIER SINE TRANSFORM)
C
CCCCCCCCCCCCCCCCCCCCCCCCCCCCCCCCCCCCCCCCCCCCCCCCCCCCCCCCCCCCCCCCCCCCCCCCCCC
C    DO 2DFFT
          P=L-1
C         JDEM=IDEM/2-L/2+1
C         JDEM=IDEM/2+1
          JDEM=2
C         JTERM=JDEM+L-1
          JTERM=2*L
          DO 40 I=1,L
            DO 250 J=1,IDEM+2
              RINP(J)=0.
C             RIMP(J)=0.
250         CONTINUE
            DO 30 J=1,L
              RINP(J)=CRAY(I,J)
30          CONTINUE
C           CALL FFT(RINP,RIMP,IDEM,1)
            CALL FFA(RINP,IDEM)
            DO 35 JJ=JDEM,JTERM,2
C             J=JJ-JDEM+1
              J=JJ/2
              CRAY(I,J)=RINP(JJ)
35          CONTINUE
40        CONTINUE

          DO 60 J=24,40
            DO 450 I=1,IDEM+2
              RINP(I)=0.
450         CONTINUE
            DO 50 I=1,L
              RINP(I)=CRAY(I,J)
50          CONTINUE
C           CALL FFT(RINP,RIMP,IDEM,1)
            CALL FFA(RINP,IDEM)
            DO 55 II=JDEM,JTERM,2
C             I=II-JDEM+1
              I=II/2
              CRAY(I,J)=RINP(II)
55          CONTINUE
60        CONTINUE

CCCCCCCCCCCCCCCCCCCCCCCCCCCCCCCCCCCCCCCCCCCCCCCCCCCCCCCCCCCCCCCCCCCCCCCCCCC
```

```
C
C     FIND MAX VALUE IN ARRAY = COORDS OF GESTALT POINT
C
CCCCCCCCCCCCCCCCCCCCCCCCCCCCCCCCCCCCCCCCCCCCCCCCCCCCCCCCCCCCCCCCCCCCCCCCCC
          B=0.
          DO 70 I=1,L
            DO 70 J=1,L
              C=ABS(CRAY(I,J))
              IF(C .LE. B)GO TO 77712
              B=C
              IR3D=I
              JR3D=J
77712         CONTINUE
70        CONTINUE

CCCCCCCCCCCCCCCCCCCCCCCCCCCCCCCCCCCCCCCCCCCCCCCCCCCCCCCCCCCCCCCCCCCCCCCCCC
C
C     COMPUTE LOGGED COORDS OF GESTALT POINT
C
CCCCCCCCCCCCCCCCCCCCCCCCCCCCCCCCCCCCCCCCCCCCCCCCCCCCCCCCCCCCCCCCCCCCCCCCCC
          TEMP=IR3D*IR3D+JR3D*JR3D
          DISTCT=SQRT(TEMP)
          DISTLG=SCALE*(ALOG10(DISTCT)-1.)
          RIR3D=IR3D
          RJR3D=JR3D
          LIR3D=RIR3D/DISTCT*DISTLG+.5
          LJR3D=RJR3D/DISTCT*DISTLG+.5

CCCCCCCCCCCCCCCCCCCCCCCCCCCCCCCCCCCCCCCCCCCCCCCCCCCCCCCCCCCCCCCCCCCCCCCCCC
C
C     ADD NEW GESTALT TO PHONEME SURFACE MAP
C
CCCCCCCCCCCCCCCCCCCCCCCCCCCCCCCCCCCCCCCCCCCCCCCCCCCCCCCCCCCCCCCCCCCCCCCCCC
          IF((IR3D.LE.IADEM).AND.(JR3D.LE.IADEM))A(IR3D,JR3D)=TIMER+A(IR3D,JR3D)

          IF(KNT .NE. 1)GO TO 80
          TYPE "KNT = 1"
          DO 80 I=1,IADEM
            DO 80 J=1,IADEM
              TEMP=I*I+J*J
              DISTLG=SQRT(TEMP)
              DISTCT=10.**(DISTLG/SCALE+1.)
              RI=I
              RJ=J
              ICART=RI/DISTLG*DISTCT+.5
              JCART=RJ/DISTLG*DISTCT+.5
              A(I,J)=CRAY(ICART,JCART)
80        CONTINUE
          IF(KNT .EQ. 1)TYPE A

CCCCCCCCCCCCCCCCCCCCCCCCCCCCCCCCCCCCCCCCCCCCCCCCCCCCCCCCCCCCCCCCCCCCCCCCCC
C
```

```
C     OUTPUT RESULTS TO USER TERMINAL
C
CCCCCCCCCCCCCCCCCCCCCCCCCCCCCCCCCCCCCCCCCCCCCCCCCCCCCCCCCCCCCCCCCCCCCCCCCC
        WRITE(10,7078)KOUNT, IR3D, JR3D, AMAX, AMAXUP, PWR
7078    FORMAT(1X,I3,": (",I2,",",I2,")      AMAX=",F5.1,",   AMAXUP=",F5.1,F14.0)
        WRITE(2,7071)KOUNT, IR3D, JR3D, AMAX, AMAXUP, RSUM, LIR3D, LJR3D, PWR
7071    FORMAT(5X,I7,6X,"(",I2,",",I2,")",3F12.1,7X,"(",I2,",",I2,")",F15.0)

C     OUTPUT RESULTS TO SECFIL
        WRITE BINARY(3)KOUNT, IR3D, JR3D, AMAX, RSUM, LIR3D, LJR3D


9999    CONTINUE

CCCCCCCCCCCCCCCCCCCCCCCCCCCCCCCCCCCCCCCCCCCCCCCCCCCCCCCCCCCCCCCCCCCCCCCCCC
C
C    CLOSE FILES AND END RUN
C
CCCCCCCCCCCCCCCCCCCCCCCCCCCCCCCCCCCCCCCCCCCCCCCCCCCCCCCCCCCCCCCCCCCCCCCCCC
6025    CALL CLOSE(1,IER)
        CALL CLOSE(2,IER)
        CALL CLOSE(3,IER)
        CALL CLOSE(4,IER)
        TYPE "TRACKSR3 DONE"

        END
```

```
CCCCCCCCCCCCCCCCCCCCCCCCCCCCCCCCCCCCCCCCCCCCCCCCCCCCCCC
C                                                      C
C                                                      C
C       NAME:  WDPTADD.FR                              C
C       AUTHOR:  ROUTH                                 C
C       PURPOSE:  BUILDS A MATRIX FROM TRACKSR3 OUTPUT AND   C
C               TAKES A 2DFFT OF IT.  OUTPUTS 2DFFT IN FILE:  C
C                 TSXXXXXX.DA .   ALSO PRINTS OUT COORDINATES  C
C               OF 2DDFST HIGH POINT (WORD I.D.).      C
C       LOAD LINE:  SEE: WPTADD                        C
C                                                      C
C                                                      C
CCCCCCCCCCCCCCCCCCCCCCCCCCCCCCCCCCCCCCCCCCCCCCCCCCCCCCC


        DIMENSION A(64,64),RR(4098)
        INTEGER FILEIN(7),FILEOUT(7),TRAKOUT(7)


CCCCCCCCCCCCCCCCCCCCCCCCCCCCCCCCCCCCCCCCCCCCCCCCCCCCCCCCCCCCCCCCCCCC
C
C    INITIALIZE VARIABLES
C
CCCCCCCCCCCCCCCCCCCCCCCCCCCCCCCCCCCCCCCCCCCCCCCCCCCCCCCCCCCCCCCCCCCC
C    IDEM IS DIMENSION OF RR AND RI AND NUMBER OF PTS IN FFT
        IDEM=4096
C    IADEM IS DIMENSION OF A(IADEM,IADEM)
        IADEM=64


CCCCCCCCCCCCCCCCCCCCCCCCCCCCCCCCCCCCCCCCCCCCCCCCCCCCCCCCCCCCCCCCCCCC
C
C    SET UP FILES TO BE USED IN THIS PROGRAM
C
CCCCCCCCCCCCCCCCCCCCCCCCCCCCCCCCCCCCCCCCCCCCCCCCCCCCCCCCCCCCCCCCCCCC
        CALL DFILW("WPRT",IER)
        CALL CFILW("WPRT",1,IER)
        CALL OPEN(1,"WPRT",3,IER)
        IF(IER .NE. 1)TYPE "OPEN FILE ERROR:",IER

        CALL OPEN(2,"ROOT.NM",1,IER)
        IF(IER .EQ. 1)GO TO 8
        TYPE "OPEN ROOT.NM ERROR",IER
        STOP
8       READ BINARY(2)(FILEIN(J),J=1,7)
        FILEIN(1)=FILEIN(1)+768

        ACCEPT "WHAT IS THE INPUT FILENAME? (SP) "
        READ(11,905)FILEIN(1)
905     FORMAT(S13)
        CALL OPEN(3,FILEIN,1,IER)
        IF(IER .EQ. 1)GO TO 9
        TYPE "OPEN FILEIN ERROR",IER
        STOP
9       DO 10 J =2,7
```

```
          FILEOUT(J)=FILEIN(J)
          TRAKOUT(J)=FILEIN(J)
10      CONTINUE
        FILEOUT(1)=FILEIN(1)+259
        TRAKOUT(1)=FILEOUT(1)-1

        CALL DFILW(FILEOUT,IER)
        CALL CFILW(FILEOUT,3,35,IER)
        CALL OPEN(4,FILEOUT,3,IER)
        IF(IER .EQ. 1)GO TO 12
        TYPE "OPEN FILEOUT ERROR",IER
        STOP
12      CONTINUE


C    TRAKOUT IS 3-D PLOT GRAPHICS FILE
        CALL DFILW(TRAKOUT,IER)
        CALL CFILW(TRAKOUT,3,140,IER)
        CALL OPEN(5,TRAKOUT,3,IER)
        IF(IER .EQ. 1)GO TO 1221
        TYPE "OPEN TRAKOUT ERROR",IER
        STOP
1221    CONTINUE

CCCCCCCCCCCCCCCCCCCCCCCCCCCCCCCCCCCCCCCCCCCCCCCCCCCCCCCCCCCCCCCCCCCCCCCCC
C
C    INITIALIZE OUTPUT ARRAY
C
CCCCCCCCCCCCCCCCCCCCCCCCCCCCCCCCCCCCCCCCCCCCCCCCCCCCCCCCCCCCCCCCCCCCCCCCC
        DO 20 I=1,IADEM
          DO 20 J=1,IADEM
            A(I,J)=0.
20      CONTINUE


CCCCCCCCCCCCCCCCCCCCCCCCCCCCCCCCCCCCCCCCCCCCCCCCCCCCCCCCCCCCCCCCCCCCCCCCC
C
C     COMPUTE SINGLE CONGLOMERATE MAP OF ALL "TRACKSR3" GESTALT POINTS
C
CCCCCCCCCCCCCCCCCCCCCCCCCCCCCCCCCCCCCCCCCCCCCCCCCCCCCCCCCCCCCCCCCCCCCCCCC
        DISTMX=24.
        DISTMN=16.
        SCALE=64./(ALOG10(DISTMX)-ALOG10(DISTMN))
        ALDSMN=ALOG10(DISTMN)
        READ BINARY(3)KNT
C       ACCEPT "AT WHAT BLOCK DO YOU WANT TO BEGIN PROCESSING? ",ISTART
        ISTART=1
C       ACCEPT "AT WHAT BLOCK DO YOU WANT TO FINISH PROCESSING? ",IEND
        IEND=9000
        TIMER=1.
        DO 30 ICT = 1,KNT
          READ BINARY(3,END = 30)KOUNT,IR3D,JR3D,AMAX,RSUM,LIR3D,LJR3D
          IF((KOUNT .LT. ISTART) .OR. (KOUNT .GT. IEND))GO TO 30
          IF(RSUM .LT. 800.)GO TO 30
```

```
         LI=LIR3D
         LJ=LJR3D
         LI=IR3D
         LJ=JR3D
C        TIMER=TIMER+1
C        A(LI,LJ)=TIMER
         A(LI,LJ)=A(LI,LJ)+TIMER
       TYPE "IR3D=",IR3D,",   JR3D=",JR3D," LI,LJ=",LI,LJ,A(LI,LJ)
30     CONTINUE

CCCCCCCCCCCCCCCCCCCCCCCCCCCCCCCCCCCCCCCCCCCCCCCCCCCCCCCCCCCCCCCCCCCCCC
C
C    BUILD AND WRITE 3-D GRAPHICS MAP OF SECOND CORTEX SURFACE
C
CCCCCCCCCCCCCCCCCCCCCCCCCCCCCCCCCCCCCCCCCCCCCCCCCCCCCCCCCCCCCCCCCCCCCC
       DUMMY=0.
       DO 300 ICT=1,IADEM
         DO 3001 JCT=1,IADEM
           WRITE BINARY(5)A(ICT,JCT)
           WRITE BINARY(5)DUMMY
3001     CONTINUE
         DO 300 JCT=1,IADEM*2
           WRITE BINARY(5)DUMMY
300    CONTINUE

CCCCCCCCCCCCCCCCCCCCCCCCCCCCCCCCCCCCCCCCCCCCCCCCCCCCCCCCCCCCCCCCCCCCCC
C
C    APPLY 2-D HAMMING WINDOW TO SECOND CORTEX SURFACE IMAGE
C
CCCCCCCCCCCCCCCCCCCCCCCCCCCCCCCCCCCCCCCCCCCCCCCCCCCCCCCCCCCCCCCCCCCCCC
40     P=IADEM-1
       DO 50 I=1,IADEM
         RI=I-1
         WI=.54-.46*COS(2.*3.14159*RI/P)
         DO 50 J=1,IADEM
           RJ=J-1
           WJ=.54-.46*COS(2.*3.14159*RJ/P)
           A(I,J)=A(I,J)*WI*WJ
50     CONTINUE

CCCCCCCCCCCCCCCCCCCCCCCCCCCCCCCCCCCCCCCCCCCCCCCCCCCCCCCCCCCCCCCCCCCCCC
C
C    COMPUTE 2DDFST OF SECOND CORTEX SURFACE IMAGE
C
CCCCCCCCCCCCCCCCCCCCCCCCCCCCCCCCCCCCCCCCCCCCCCCCCCCCCCCCCCCCCCCCCCCCCC
       DO 60 I=1,IADEM
         DO 55 J=1,IDEM+2
           RR(J)=0.
55     CONTINUE
       DO 56 J=1,IADEM
         RR(J)=A(I,J)
56     CONTINUE
```

```
        CALL FFA(RR,IDEM)

        DO 58 J=1,IADEM
          A(I,J)=RR(2*J)
58      CONTINUE

60      CONTINUE

        DO 80 J=1,IADEM
          DO 75 I=1,IDEM+2
            RR(I)=0.
75        CONTINUE
          DO 76 I=1,IADEM
            RR(I)=A(I,J)
76        CONTINUE

          CALL FFA(RR,IDEM)

          DO 78 I=1,IADEM
            A(I,J)=ABS(RR(I*2))
78        CONTINUE
80      CONTINUE

CCCCCCCCCCCCCCCCCCCCCCCCCCCCCCCCCCCCCCCCCCCCCCCCCCCCCCCCCCCCCCCCCCCCCCCCCCC
C
C     FIND COORDS OF WORD GESTALT POINT
C
CCCCCCCCCCCCCCCCCCCCCCCCCCCCCCCCCCCCCCCCCCCCCCCCCCCCCCCCCCCCCCCCCCCCCCCCCCC
        B=0.
        DO 90 I=1,IADEM
          DO 90 J=1,IADEM
            C=ABS(A(I,J))
            IF(C .LE. B)GO TO 90
            B=C
            IWPT=I
            JWPT=J
90      CONTINUE

CCCCCCCCCCCCCCCCCCCCCCCCCCCCCCCCCCCCCCCCCCCCCCCCCCCCCCCCCCCCCCCCCCCCCCCCCCC
C
C     WRITE OUT GRAPHICS FILE OF 2DDFST CALCULATION
C
CCCCCCCCCCCCCCCCCCCCCCCCCCCCCCCCCCCCCCCCCCCCCCCCCCCCCCCCCCCCCCCCCCCCCCCCCCC
        DO 100 I=1,IADEM
          WRITE BINARY(4)(A(I,J),J=1,IADEM)
100     CONTINUE

CCCCCCCCCCCCCCCCCCCCCCCCCCCCCCCCCCCCCCCCCCCCCCCCCCCCCCCCCCCCCCCCCCCCCCCCCCC
C
C     OUTPUT RESULTS TO PRINTER FILE
C
```

```
CCCCCCCCCCCCCCCCCCCCCCCCCCCCCCCCCCCCCCCCCCCCCCCCCCCCCCCCCCCCCCCCCCCCCCCCCCCCCCC
      WRITE(1,903)FILEOUT(1),IWPT,JWPT
903   FORMAT(1X,//,2X,"WORD POINT COORDINATES FOR ",S14,"ARE:",1X,
     &          "(",I2,",",I2,")")

      TYPE "IWPT=",IWPT,",  JWPT=",JWPT

CCCCCCCCCCCCCCCCCCCCCCCCCCCCCCCCCCCCCCCCCCCCCCCCCCCCCCCCCCCCCCCCCCCCCCCCCCCCCCC
C
C     CLOSE FILES AND END RUN
C
CCCCCCCCCCCCCCCCCCCCCCCCCCCCCCCCCCCCCCCCCCCCCCCCCCCCCCCCCCCCCCCCCCCCCCCCCCCCCCC
      CALL RESET

      END
```

Appendix G

CTT Word Recognition Plots

This appendix presents the word recognition plots referred to in section two of Chapter Five.

The identification of the speakers are:

RLR - Richard L. Routh, male, 31 years old;

BLR - Robert L. Russel, male, 29 years old;

ENR - Edith N. Routh, female, 31 years old;

AH - Ahni Holten, female, 7 years old.

Two types of inconsistencies are presented by these data. It is believed that both types are due to oversimplifications in the engineering of the simulation, and not due to faults in CTT theory.

One type of inconsistency is the appearance of a word in the wrong group. An example of this is seen in Figure 5.14 (reproduced here as Figure G-1). The word bell is identified by the system as being closer to the "cot" group than to the "elm" group. After analysis of the data presented in Appendix E and after listening to the differences between the "ell" sound in both "bell" and the "elms" and "helm", the following explanation is presented: First, the "ell" sound in "bell" was noticeably more stocato than the emphasized "ell" sound in the other elm-group words. When combined with the characteristic that this oversimplified engineering implementation has of not watching rapid energy transitions (see section two of Chapter Five), so that it does not see the b phoneneme at the beginning of "bell", "bell" sounds more like a short e than the entire word "bell". Since for these same reasons, the "cot" group words all sound like the short o sound, it seems reasonable that a stacoto short e should be grouped psychologically closer to a stacoto short o than to the other words in the elm-group which had heavily emphasized "ell" sounds. When "bell" is carefully enunciated to emphasize the "ell" sound, such as was the case for speaker BLR, it appears in the proper word group (see Figure G-2).

The other type of inconsistency is the variation among speakers of the relative positions of each of the three major utterance groups. In the case of the "sash" group for speaker AH, the energy level for the "s" and "sh" sounds was so low in the 100-3800 Hz band, that the A.G.C. mechanism (in module TRACKSPAC) did not allow the system to differentiate them from the background noise. It is suspected that other variations, such as the apparent transposition of the "cot" and "elm" groups for RLR and BLR, is due to the oversimplification of the cortex windowing mechanisms for both the primary audio cortex (P.A.C.) and the secondary audio cortex (phoneme cortex). The P.A.C. window edges are fixed (in the simulation) at 100 Hz and 3800 Hz. This is very likely an overrestriction of the real window mechanism. There is no engineering mechanism for "focusing in" on pertinent information on the phoneme cortex. The phoneme cortex window (in the simulation) is static and views the entire phoneme cortex surface. This is also probably an overrestriction.

It is suspected that each of these surfaces has a specific window setting for each different speaker which results in completely consistent speaker independent classifications of phonemes and words.

The exact specifications of each window setting may well be significant contributing factors to the speaker identification process.

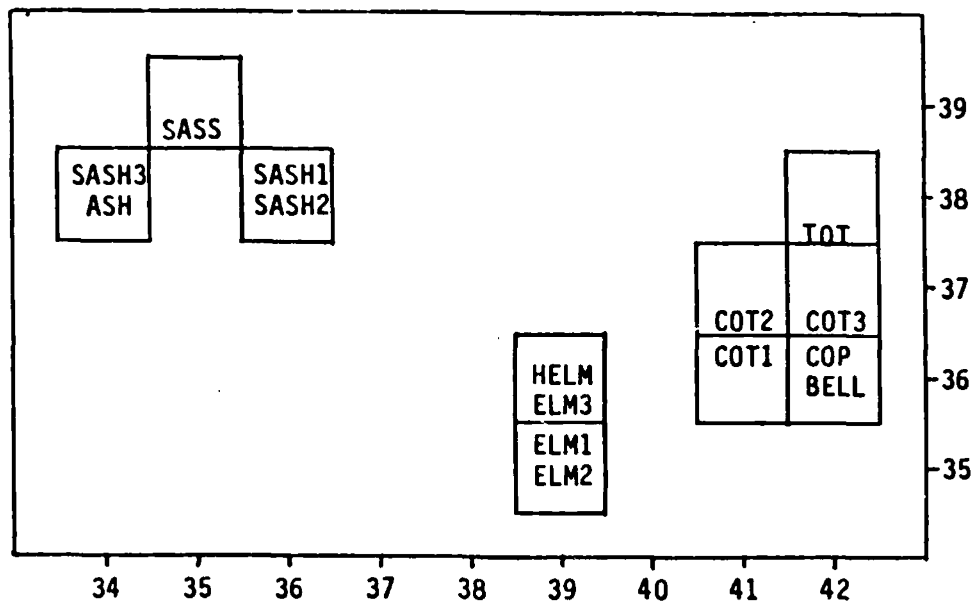

Figure G-1 - Word Gestalt Plots on the Word Local Cortex Surface for Speaker "RLR"

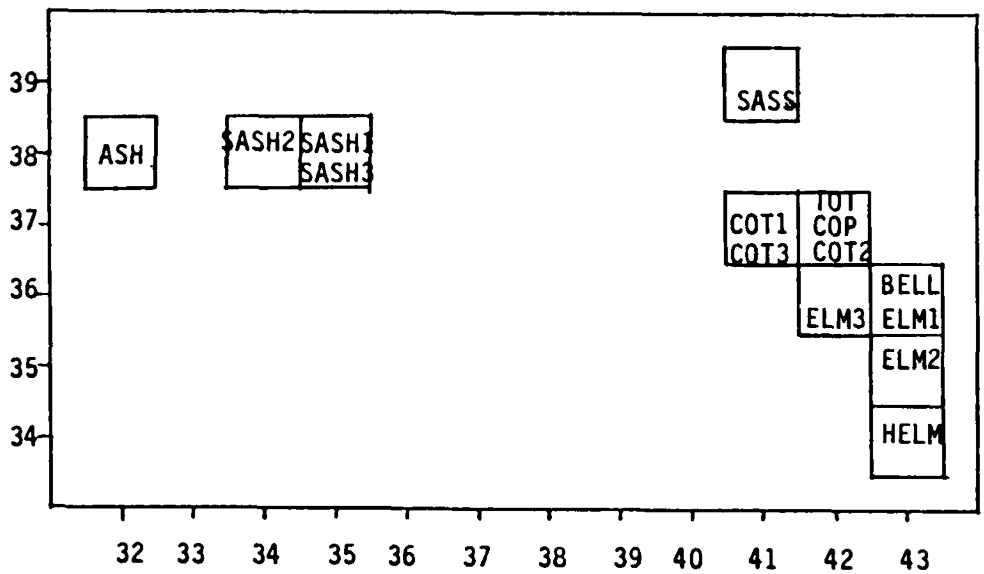

Figure G-2 - Word Gestalt Plots on the Word Local Cortex Surface for Speaker "BLR"

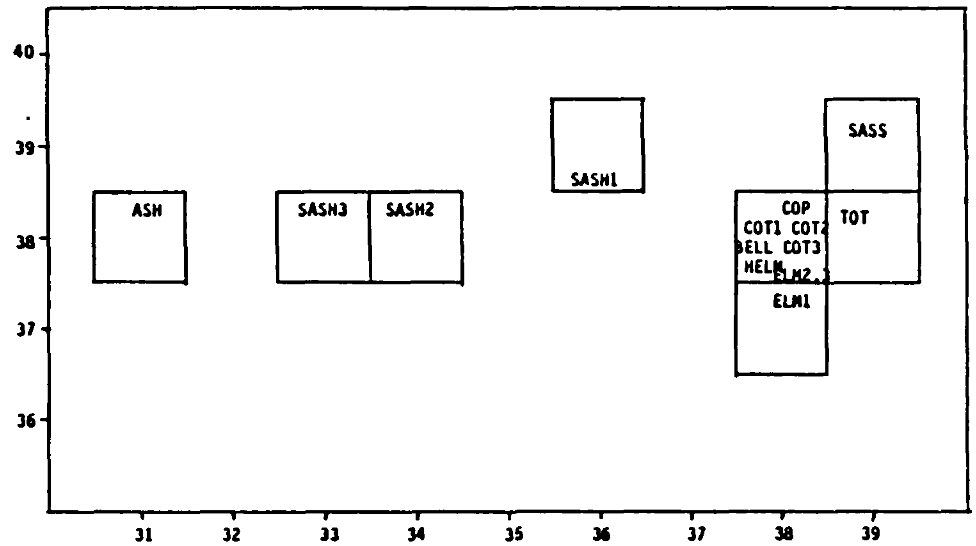

Figure G-3 - Word Gestalt Plots on the Word Local Cortex Surface for Speaker "ENR"

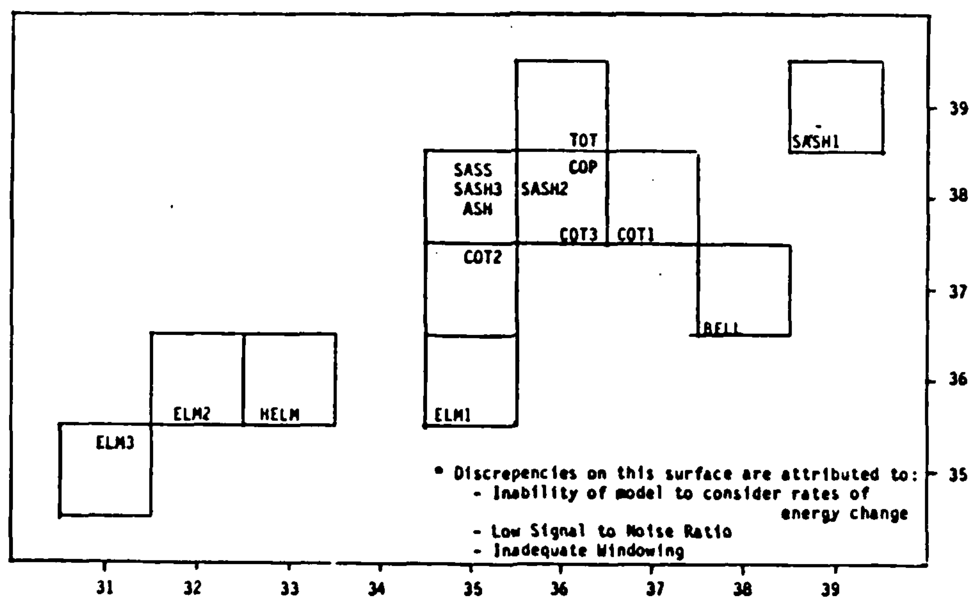

Figure G-4 - Word Gestalt Plots on the Word Local Cortex Surface for Speaker "AH"

Appendix H

Modified Phoneme Tracks Compared

In Figures H-1 and H-2, the phoneme tracks for two different utterances of "did you" are shown. In these utterances, particular care was taken to enunciate the terminal "d" in "did", the stop, and the "y" in "you". In Figures H-3 and H-4, the phoneme tracks for two different utterances of "dijew" are shown. In these utterances, particular care was taken to insure that the terminal "d" in "did", the stop, and the "y" in "you", were absent and replaced by a single "j" phoneme sound.

The similarity in phoneme tracks is apparent.

Similarly, the phoneme track for "want to" and the phoneme track for "wanna" are plotted in Figures H-5 and H-6.

The "TRP" files from the "TRACKSR3" program are also included for all six utterances.

It can be seen that this data is suggestive of the conclusion that a CTT architecture, when used to do speech recognition, is forgiving of the same types of phoneme substitutions, omissions, and modifications, of which the human speech recognition system is also apparently forgiving.

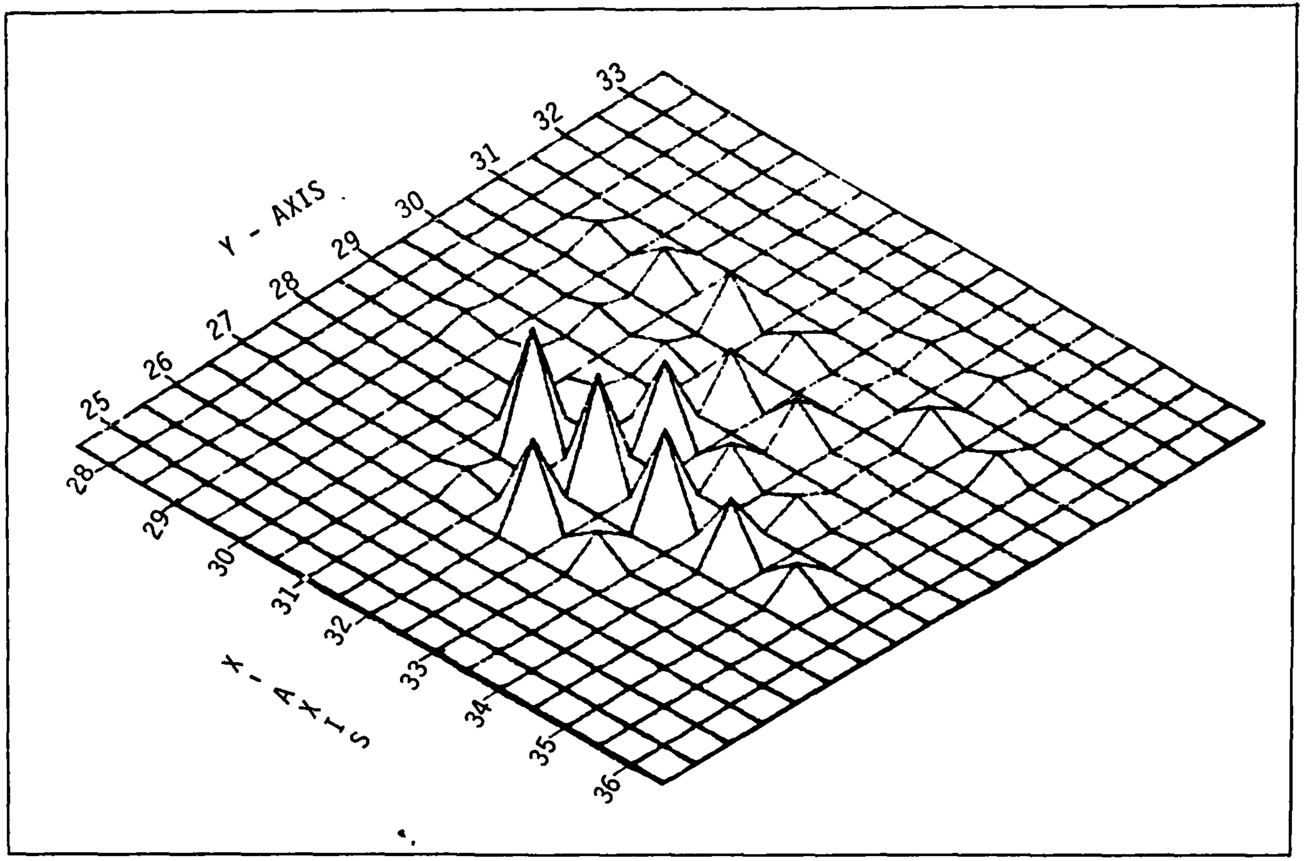

Figure H-1 - Phoneme Track for "Did You" (1^{st} Utterance)

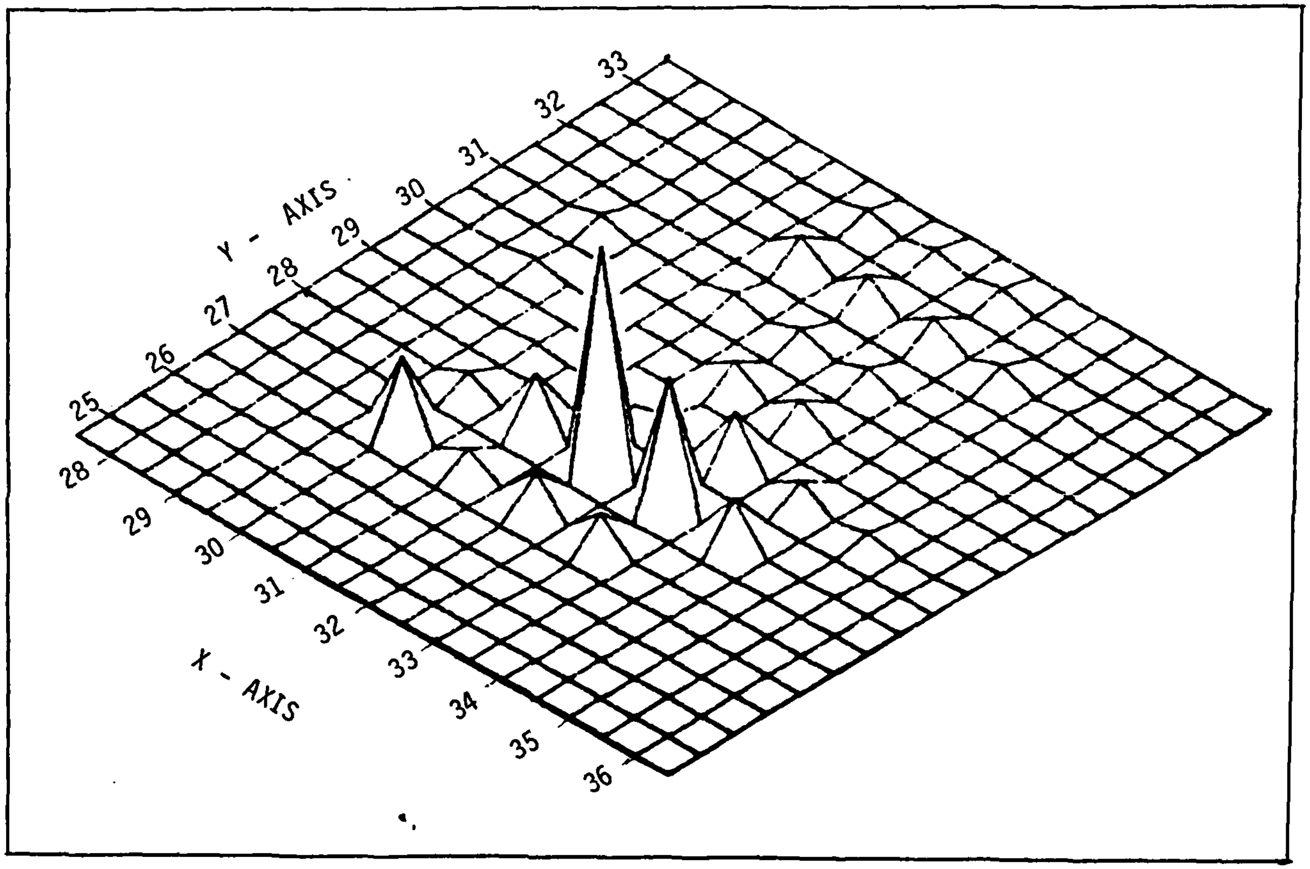

Figure H-2 - Phoneme Track for "Did You" (2^{nd} Utterance)

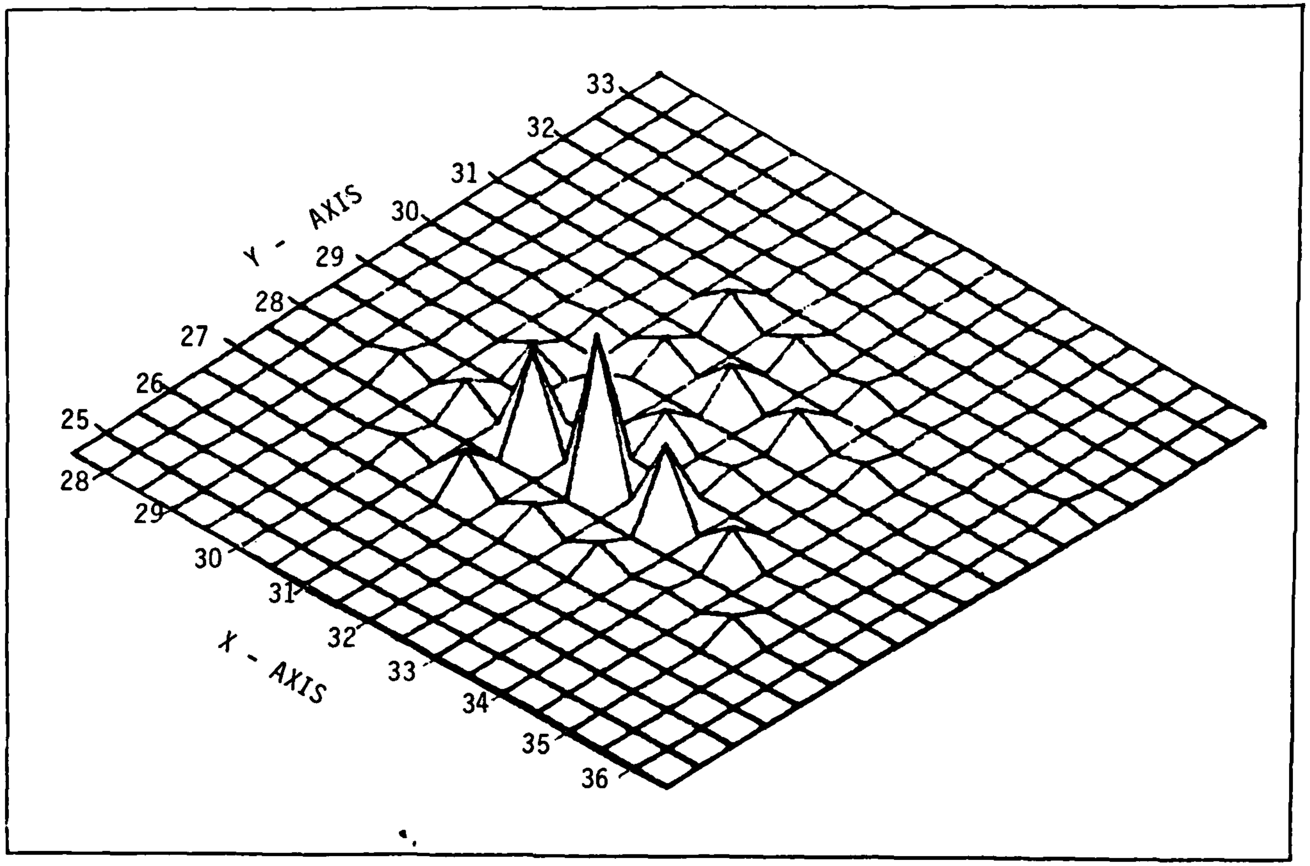

Figure H-3 - Phoneme Track for "Dijew" (1^{st} Utterance)

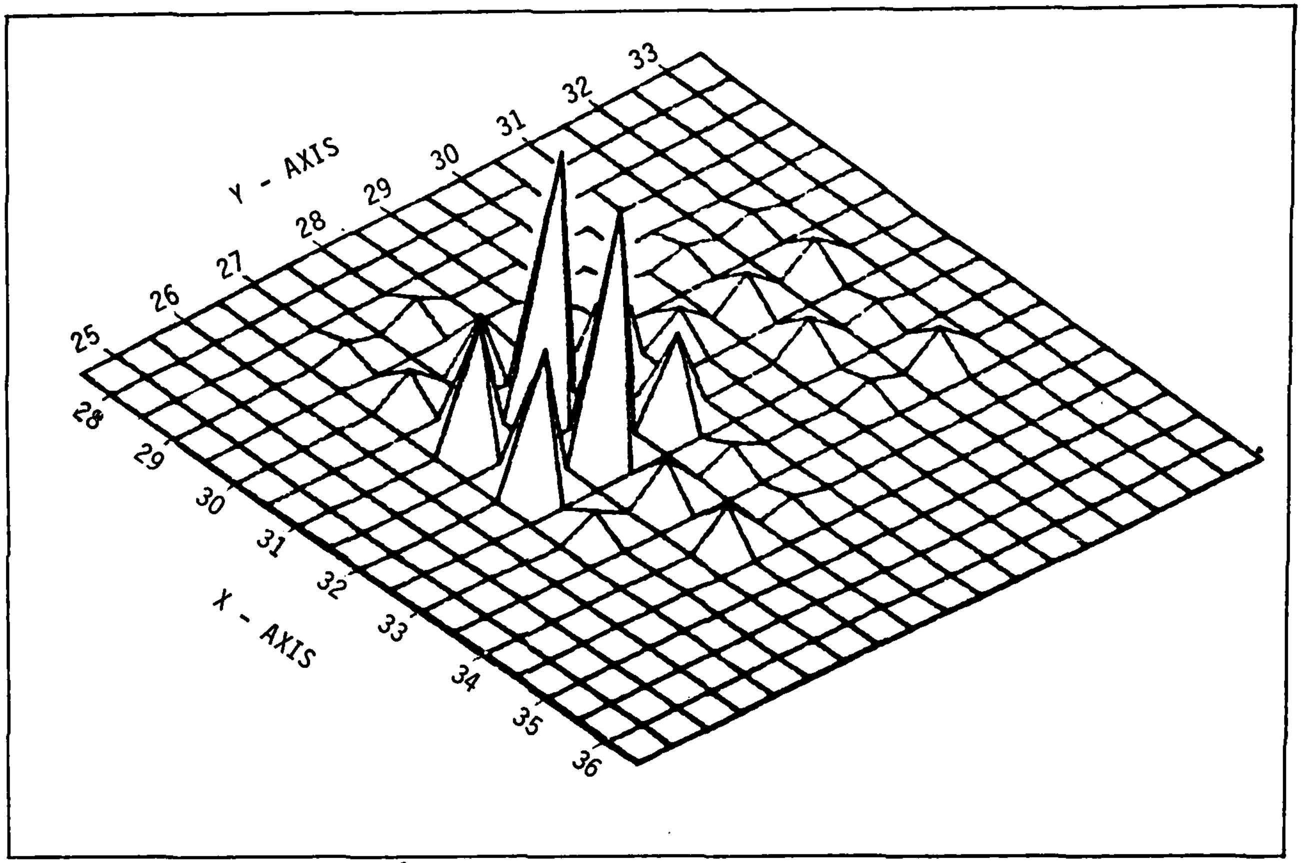

Figure H-4 - Phoneme Track for "Dijew" (2^{nd} Utterance)

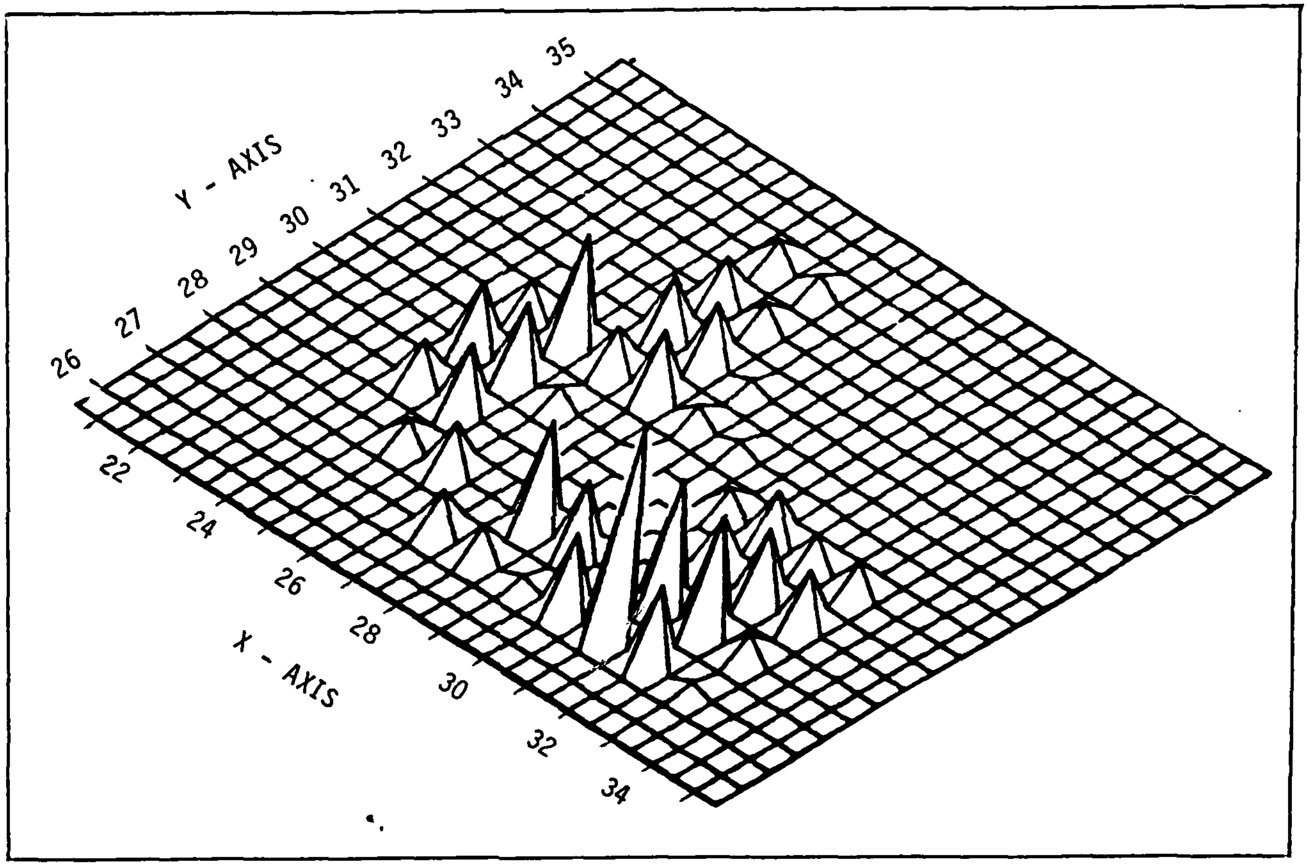

Figure H-5 - Phoneme Track for "Want To"

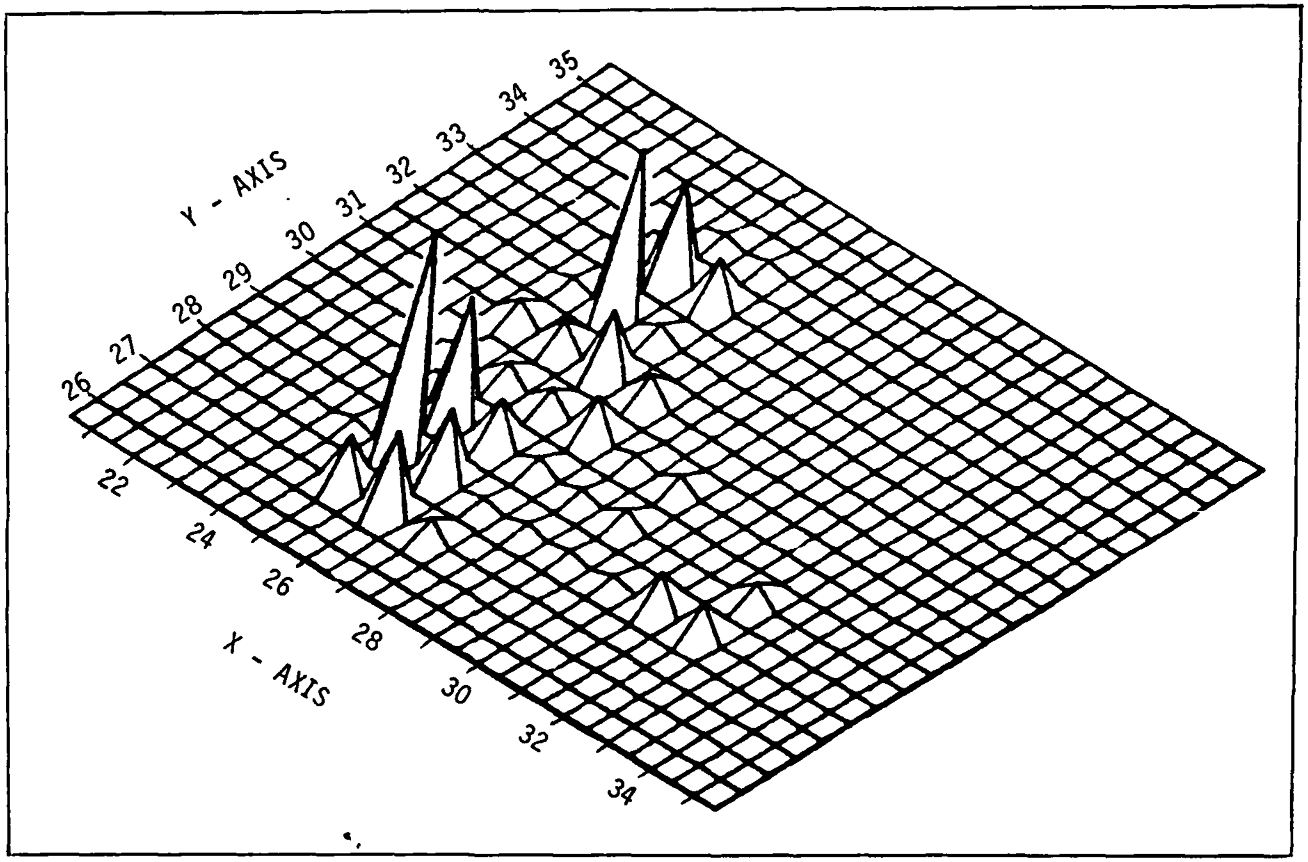

Figure H-6 - Phoneme Track for "Wanna"

TRACK TRAIL FOR SPQDY1.DA

BLOCK	(IR3D, JR3D)	AMAX	AMAXUP	RSUM	LOG COORD'S	POWER
43	(28,27)	90.2	94.5	2591.7	(21,20)	45009490.
44	(32,28)	92.9	96.4	2388.6	(23,21)	68948530.
45	(32,28)	95.2	97.9	2357.5	(23,21)	98555200.
46	(31,28)	97.3	99.8	2376.8	(23,21)	152947000.
47	(31,28)	99.4	102.1	2337.7	(23,21)	259770700.
48	(32,28)	101.0	104.0	2306.9	(23,21)	397664300.
49	(32,29)	102.0	104.9	2236.4	(23,21)	493099800.
50	(32,29)	102.8	105.1	2198.1	(23,21)	517975300.
51	(32,29)	103.4	105.5	2205.9	(23,21)	561309400.
52	(32,28)	104.0	106.5	2246.0	(23,21)	704895000.
53	(33,28)	104.7	107.5	2250.2	(24,20)	885932300.
54	(33,28)	105.5	108.0	2257.3	(24,20)	994494700.
55	(33,28)	106.3	108.4	2314.6	(24,20)	1105731000.
56	(32,28)	106.8	109.4	2361.2	(23,21)	1368720000.
57	(33,28)	107.1	110.3	2336.4	(24,20)	1691143000.
58	(33,28)	107.2	110.6	2293.6	(24,20)	1807352000.
59	(33,28)	107.3	110.4	2307.7	(24,20)	1733132000.
60	(32,28)	107.4	110.6	2331.3	(23,21)	1828560000.
61	(33,27)	107.5	111.5	2337.8	(24,20)	2215808000.
62	(33,27)	107.8	112.0	2284.6	(24,20)	2522135000.
63	(33,27)	108.2	111.9	2287.9	(24,20)	2473175000.
64	(32,28)	108.6	111.8	2302.0	(23,21)	2389937000.
65	(32,27)	109.0	112.2	2339.5	(24,20)	2635931000.
66	(32,27)	109.3	112.7	2309.3	(24,20)	2985168000.
67	(32,27)	109.6	112.8	2250.9	(24,20)	3005967000.
68	(32,28)	109.9	112.6	2264.1	(23,21)	2863448000.
69	(31,28)	110.1	112.8	2296.5	(23,21)	3019959000.
70	(32,27)	110.3	113.3	2304.7	(24,20)	3396149000.
71	(32,27)	110.6	113.4	2261.4	(24,20)	3492569000.
72	(32,28)	110.8	113.2	2250.1	(23,21)	3329325000.
73	(32,28)	111.1	113.3	2269.6	(23,21)	3422517000.
74	(32,27)	111.2	113.8	2276.6	(24,20)	3820770000.
75	(33,27)	111.4	114.0	2260.2	(24,20)	3994429000.
76	(32,28)	111.5	113.8	2266.0	(23,21)	3799598000.
77	(32,28)	111.7	113.8	2287.3	(23,21)	3776845000.
78	(32,27)	111.7	114.2	2305.9	(24,20)	4132625000.
79	(32,27)	111.8	114.4	2280.3	(24,20)	4344807000.
80	(32,28)	111.8	114.1	2275.2	(23,21)	4105799000.
81	(31,28)	111.9	113.9	2288.5	(23,21)	3917554000.
82	(31,28)	111.9	114.2	2318.7	(23,21)	4172325000.
83	(31,28)	111.9	114.5	2290.8	(23,21)	4431151000.
84	(32,28)	111.9	114.3	2268.5	(23,21)	4242823000.
85	(31,28)	111.9	114.0	2265.0	(23,21)	3973816000.
86	(31,28)	111.9	114.2	2306.2	(23,21)	4124338000.
87	(31,28)	111.9	114.4	2282.3	(23,21)	4404261000.
88	(31,28)	111.9	114.3	2240.8	(23,21)	4284389000.
89	(31,28)	112.0	114.0	2246.6	(23,21)	4010380000.
90	(31,28)	112.0	114.2	2285.7	(23,21)	4124916000.
91	(31,28)	112.0	114.5	2292.5	(23,21)	4459696000.
92	(32,28)	111.9	114.4	2269.6	(23,21)	4411273000.
93	(32,28)	112.0	114.1	2281.8	(23,21)	4086888000.
94	(31,28)	112.0	114.1	2318.3	(23,21)	4077588000.
95	(32,27)	111.9	114.4	2330.3	(24,20)	4378522000.
96	(32,27)	111.9	114.4	2293.8	(24,20)	4398170000.
97	(31,28)	111.9	114.1	2273.3	(23,21)	4068596000.
98	(31,28)	112.0	114.0	2285.7	(23,21)	3971874000.
99	(31,27)	111.9	114.3	2304.6	(23,20)	4238557000.
100	(32,27)	111.9	114.4	2282.1	(24,20)	4327932000.
101	(31,28)	111.9	114.0	2271.8	(23,21)	4026394000.
102	(31,28)	112.0	113.9	2276.8	(23,21)	3866512000
103	(31,27)	111.9	114.1	2300.1	(23,20)	4102069000

104	(31,27)	111.9	114.3	2281.3	(23,20)	4260643000.
105	(32,27)	111.9	114.1	2284.1	(24,20)	4028900000.
106	(31,28)	111.9	113.8	2292.4	(23,21)	3840635000.
107	(32,27)	111.9	114.1	2333.7	(24,20)	4043984000.
108	(32,27)	111.8	114.3	2310.2	(24,20)	4239510000.
109	(32,27)	111.8	114.0	2274.8	(24,20)	4004865000.
110	(31,28)	111.8	113.6	2271.0	(23,21)	3664712000.
111	(32,27)	111.6	113.7	2303.6	(24,20)	3678915000.
112	(32,27)	111.5	113.8	2306.9	(24,20)	3821089000.
113	(32,27)	111.2	113.6	2268.2	(24,20)	3610036000.
114	(31,28)	111.1	113.1	2266.4	(23,21)	3215416000.
115	(32,28)	110.8	112.9	2301.6	(23,21)	3111518000.
116	(32,27)	110.4	113.1	2310.1	(24,20)	3223395000.
117	(32,27)	110.0	112.8	2295.1	(24,20)	3053359000.
118	(31,28)	109.5	112.1	2295.5	(23,21)	2566937000.
119	(31,28)	109.0	111.5	2329.2	(23,21)	2252972000.
120	(31,28)	108.5	111.6	2350.4	(23,21)	2280140000.
121	(32,28)	107.9	111.5	2325.2	(23,21)	2243686000.
122	(31,28)	106.9	110.6	2268.0	(23,21)	1820724000.
123	(31,28)	105.6	109.0	2259.2	(23,21)	1255424000.
124	(31,28)	104.2	107.6	2315.4	(23,21)	910235400.
125	(31,28)	103.3	107.0	2344.1	(23,21)	793617900.
126	(31,28)	102.0	106.2	2339.6	(23,21)	662747400.
127	(30,29)	100.4	104.3	2319.9	(22,21)	428998700.
128	(30,29)	98.3	101.2	2341.7	(22,21)	208723200.
129	(29,29)	96.2	97.8	2408.3	(22,22)	95286530.
130	(29,29)	94.6	96.2	2441.0	(22,22)	66588060.
131	(31,29)	93.7	95.9	2335.3	(23,21)	62137390.
132	(32,30)	93.6	95.5	2255.7	(23,22)	56157040.
133	(32,29)	93.5	94.9	2221.8	(23,21)	49075230.
134	(32,30)	93.1	94.6	2202.7	(23,22)	45832860.
135	(32,30)	92.8	94.5	2180.2	(23,22)	44764350.
136	(32,30)	92.1	94.1	2204.4	(23,22)	41042720.
137	(31,30)	91.4	93.4	2228.7	(23,22)	34818370.
193	(33,30)	92.9	94.1	2198.0	(24,22)	40438220.
194	(34,31)	93.6	95.2	2100.5	(24,22)	52405540.
195	(35,31)	94.2	95.6	2031.0	(25,22)	57915920.
196	(34,32)	94.5	95.5	1996.0	(24,23)	55631020.
197	(34,32)	94.6	95.1	1980.7	(24,23)	51602940.
198	(35,31)	94.5	95.1	2015.2	(25,22)	51268850.
199	(35,31)	94.3	95.2	2032.8	(25,22)	52764580.
200	(35,31)	94.0	95.0	2022.1	(25,22)	50574880.
201	(34,31)	93.8	94.4	2012.8	(24,22)	43977060.
202	(34,31)	93.6	93.9	1986.5	(24,22)	38583460.
203	(33,32)	93.4	93.9	2027.0	(24,23)	38900190.
204	(34,31)	93.4	94.3	2074.6	(24,22)	42385950.
205	(34,31)	93.4	94.4	2080.6	(24,22)	43241500.
206	(34,30)	93.4	94.1	2117.1	(24,22)	40536350.
207	(33,30)	93.5	93.9	2114.6	(24,22)	39011010.
208	(33,30)	93.5	94.2	2129.3	(24,22)	41992610.
209	(34,31)	93.4	94.6	2089.7	(24,22)	45855600.
210	(34,32)	93.1	94.5	2039.7	(24,23)	44280980.
211	(33,32)	92.6	93.6	2046.5	(24,23)	36560540.
237	(33,31)	91.2	92.8	2082.8	(24,22)	30221950.
238	(35,31)	91.6	93.6	2062.3	(25,22)	36169460.
239	(34,31)	91.7	93.5	2101.2	(24,22)	35792670.
240	(31,31)	91.7	92.9	2121.1	(23,23)	31237810.
242	(31,31)	91.6	93.3	2146.9	(23,23)	33900000.
243	(32,30)	91.6	93.8	2168.8	(23,22)	38084460.
244	(32,30)	91.5	93.6	2171.3	(23,22)	36224740.
245	(33,29)	91.5	93.0	2192.9	(24,21)	31781940.
246	(33,29)	91.7	93.2	2217.4	(24,21)	32994770.
247	(33,30)	91.9	94.1	2236.5	(24,22)	40789420.
248	(32,30)	92.2	94.7	2241.5	(23,22)	47038180.
249	(31,30)	92.6	94.7	2284.2	(23,22)	46471920.
250	(31,29)	93.0	94.6	2297.4	(23,21)	46024670.

251	(32,29)	93.4	95.4	2294.4	(23,21)	54396050.
252	(33,29)	93.7	96.3	2265.5	(24,21)	67359730.
253	(33,29)	94.1	96.6	2249.8	(24,21)	72802740.
254	(32,29)	94.5	96.4	2215.9	(23,21)	69618990.
255	(32,30)	94.9	96.5	2192.9	(23,22)	70742850.
256	(33,30)	95.2	97.2	2165.7	(24,22)	82849090.
257	(33,30)	95.6	97.8	2171.7	(24,22)	94959090.
258	(33,30)	96.0	97.8	2163.4	(24,22)	95755840.
259	(32,30)	96.5	97.8	2147.9	(23,22)	96473390.
260	(33,30)	97.0	98.6	2156.5	(24,22)	115260600.
261	(34,29)	97.4	99.6	2176.6	(25,21)	145385000.
262	(33,30)	97.8	100.1	2187.9	(24,22)	161007400.
263	(32,29)	98.3	100.0	2168.0	(23,21)	157856400.
264	(32,30)	98.6	100.1	2150.4	(23,22)	163413900.
265	(32,30)	98.9	100.8	2184.0	(23,22)	192511500.
266	(32,29)	99.1	101.4	2214.5	(23,21)	220309100.
267	(32,29)	99.4	101.5	2254.3	(23,21)	221912000.
268	(32,29)	99.7	101.5	2251.9	(23,21)	222116100.
269	(33,28)	100.2	102.1	2234.4	(24,20)	258833000.
270	(34,29)	100.7	103.0	2240.9	(25,21)	317079800.
271	(33,29)	101.3	103.4	2256.9	(24,21)	348747800.
272	(32,29)	101.9	103.6	2269.9	(23,21)	360228600.
273	(32,29)	102.4	104.1	2277.2	(23,21)	410724900.
274	(33,29)	102.9	105.1	2247.2	(24,21)	507776800.
275	(33,28)	103.5	105.6	2213.6	(24,20)	581263600.
276	(32,28)	104.0	105.8	2211.6	(23,21)	600628200.
277	(32,29)	104.6	106.1	2203.8	(23,21)	644692200.
278	(32,29)	105.1	106.9	2181.4	(23,21)	774359000.
279	(32,29)	105.6	107.6	2132.9	(23,21)	917351700.
280	(32,29)	106.1	107.9	2190.7	(23,21)	977060600.
281	(32,29)	106.6	108.0	2208.8	(23,21)	1008183000.
282	(32,29)	107.0	108.5	2202.6	(23,21)	1125594000.
283	(33,29)	107.4	109.1	2189.4	(24,21)	1295024000.
284	(33,29)	107.7	109.4	2173.7	(24,21)	1376176000.
285	(32,29)	108.1	109.4	2195.2	(23,21)	1375868000.
286	(32,29)	108.4	109.6	2211.6	(23,21)	1453968000.
287	(34,28)	108.6	110.2	2218.3	(25,20)	1646096000.
288	(34,28)	108.8	110.5	2199.6	(25,20)	1783079000.
289	(33,28)	109.0	110.5	2203.5	(24,20)	1778761000.
290	(33,28)	109.2	110.5	2227.5	(24,20)	1790901000.
291	(33,28)	109.3	110.9	2215.7	(24,20)	1946440000.
292	(33,28)	109.3	111.2	2179.3	(24,20)	2108126000.
293	(33,28)	109.4	111.2	2203.7	(24,20)	2101829000.
294	(32,28)	109.5	111.1	2219.3	(23,21)	2028069000.
295	(32,28)	109.5	111.2	2220.9	(23,21)	2091644000.
296	(33,28)	109.5	111.5	2196.9	(24,20)	2247175000.
297	(32,28)	109.5	111.6	2198.3	(23,21)	2272567000.
298	(32,28)	109.6	111.4	2213.1	(23,21)	2168752000.
299	(31,28)	109.6	111.3	2224.1	(23,21)	2154934000.
300	(32,28)	109.5	111.6	2232.2	(23,21)	2283622000.
301	(33,28)	109.4	111.7	2217.3	(24,20)	2336508000.
302	(32,28)	109.4	111.4	2203.7	(23,21)	2207730000.
303	(31,28)	109.3	111.2	2246.2	(23,21)	2094343000.
304	(32,28)	109.2	111.3	2254.9	(23,21)	2161076000.
305	(32,28)	109.1	111.5	2225.9	(23,21)	2258359000.
306	(33,28)	109.0	111.4	2241.8	(24,20)	2182787000.
307	(32,27)	109.0	111.1	2256.6	(24,20)	2039681000.
308	(31,28)	109.0	111.1	2262.7	(23,21)	2060989000.
309	(32,28)	108.9	111.4	2238.8	(23,21)	2209369000.
310	(32,28)	108.8	111.5	2237.9	(23,21)	2225730000.
311	(33,27)	108.7	111.2	2254.7	(24,20)	2068890000.
312	(32,27)	108.7	111.0	2277.7	(24,20)	1973644000
313	(32,28)	108.5	111.1	2274.8	(23,21)	2055721000
314	(33,28)	108.4	111.3	2239.9	(24,20)	2117826000
315	(33,27)	108.3	111.0	2214.7	(24,20)	1993476000.
316	(33,27)	108.3	110.7	2238.6	(24,20)	1843373000

317	(32,27)	108.2	110.8	2242.7	(24,20)	1890586000.
318	(33,28)	108.1	111.1	2225.5	(24,20)	2039944000.
319	(33,28)	108.0	111.1	2201.7	(24,20)	2018551000.
320	(33,28)	108.0	110.6	2215.5	(24,20)	1828816000.
321	(33,28)	107.9	110.4	2247.5	(24,20)	1738225000.
322	(33,28)	107.8	110.7	2229.8	(24,20)	1851603000.
323	(34,28)	107.7	110.9	2198.6	(25,20)	1940979000.
324	(34,28)	107.6	110.6	2188.6	(25,20)	1813238000.
325	(34,28)	107.5	110.1	2228.8	(25,20)	1617756000.
326	(33,28)	107.4	110.0	2246.8	(24,20)	1593404000.
327	(33,28)	107.2	110.3	2206.3	(24,20)	1692743000.
328	(34,28)	107.0	110.2	2177.0	(25,20)	1668359000.
329	(34,28)	106.8	109.7	2190.6	(25,20)	1488405000.
330	(34,28)	106.7	109.4	2237.7	(25,20)	1374515000.
331	(34,28)	106.6	109.6	2234.7	(25,20)	1444172000.
332	(34,28)	106.5	109.8	2191.4	(25,20)	1521010000.
333	(35,28)	106.4	109.5	2153.2	(25,20)	1415148000.
334	(34,28)	106.2	108.9	2183.5	(25,20)	1229893000.
335	(34,28)	106.0	108.7	2222.7	(25,20)	1185057000.
336	(34,28)	105.8	109.1	2214.9	(25,20)	1274265000.
337	(34,28)	105.5	109.1	2190.5	(25,20)	1276332000.
338	(35,28)	105.3	108.4	2190.0	(25,20)	1106113000.
339	(34,28)	105.1	107.7	2197.2	(25,20)	942415400.
340	(34,28)	104.9	107.8	2227.4	(25,20)	950043600.
341	(35,28)	104.7	108.2	2187.7	(25,20)	1035712000.
342	(35,28)	104.5	108.0	2121.9	(25,20)	997638900.
343	(35,28)	104.4	107.2	2129.1	(25,20)	833089800.
344	(35,28)	104.3	106.6	2162.4	(25,20)	732441600.
345	(35,28)	104.1	107.0	2192.9	(25,20)	790127100.
346	(35,28)	103.9	107.4	2158.4	(25,20)	867848700.
347	(35,29)	103.6	107.0	2128.9	(25,21)	798916100.
348	(34,29)	103.4	106.0	2180.1	(25,21)	628171800.
349	(33,29)	103.1	105.3	2229.6	(24,21)	536568800.
350	(33,28)	102.8	105.7	2261.1	(24,20)	584852500.
351	(34,29)	102.6	106.1	2224.4	(25,21)	640845600.
352	(34,29)	102.4	105.6	2164.3	(25,21)	580192300.
353	(32,29)	102.3	104.7	2144.5	(23,21)	462932000.
354	(31,29)	102.2	104.5	2174.1	(23,21)	441620200.
355	(32,29)	102.2	105.3	2179.5	(23,21)	542923000.
356	(32,30)	102.1	106.0	2151.0	(23,22)	626033400.
357	(33,30)	101.8	105.6	2109.8	(24,22)	570528800.
358	(31,30)	101.3	104.3	2161.1	(23,22)	423422200.
359	(30,30)	100.9	103.2	2205.2	(22,22)	329218300.
360	(30,30)	100.6	103.4	2242.0	(22,22)	348808700.
361	(30,30)	100.4	104.0	2221.1	(22,22)	400239600.
362	(32,30)	100.2	103.9	2158.1	(23,22)	385647100.
363	(31,30)	99.9	102.9	2133.5	(23,22)	309558500.
364	(29,30)	99.7	102.0	2171.0	(21,22)	253980400.
365	(29,31)	99.6	102.3	2185.6	(21,23)	270155300.
366	(29,31)	99.5	103.0	2170.4	(21,23)	318517500.
367	(30,31)	99.1	103.2	2129.5	(22,23)	331038200.
368	(30,31)	98.9	102.7	2096.3	(22,23)	293146600.
369	(30,31)	98.6	101.8	2085.3	(22,23)	242419300.
370	(29,31)	98.2	101.4	2100.5	(21,23)	219637800.
371	(29,31)	98.0	101.5	2149.3	(21,23)	224209100.
372	(30,31)	97.6	101.5	2146.6	(22,23)	223728000.
373	(31,31)	96.9	101.0	2119.6	(23,23)	200845200.
374	(31,31)	96.4	100.2	2062.0	(23,23)	164923300.
375	(31,31)	96.1	99.5	2026.8	(23,23)	139916900.
376	(32,31)	96.2	99.5	2077.9	(23,22)	141997200.
377	(31,31)	96.3	100.0	2073.0	(23,23)	158089200
378	(31,31)	95.9	100.1	2064.2	(23,23)	162913600.
379	(32,31)	95.3	99.7	2076.9	(23,22)	147639700.
380	(32,31)	94.7	98.8	2074.9	(23,22)	121277400
381	(31,31)	94.3	98.0	2078.0	(23,23)	100721200
382	(31,31)	94.3	97.8	2095.1	(23,23)	95352620

383	(31,31)	94.7	97.9	2139.3	(23,23)	97595090.
384	(32,31)	94.7	97.8	2084.8	(23,22)	95660900.
385	(32,31)	94.3	97.3	2071.3	(23,22)	85095780.
386	(32,31)	93.9	96.4	2104.8	(23,22)	69604690.
387	(31,31)	93.6	95.7	2079.0	(23,23)	58992020.
388	(30,31)	93.4	95.7	2130.7	(22,23)	59209490.
389	(30,31)	93.3	96.1	2175.7	(22,23)	63928350.
390	(30,31)	92.9	96.0	2143.5	(22,23)	63076900.
391	(31,31)	92.0	95.2	2130.1	(23,23)	52816300.
392	(30,31)	90.9	93.7	2209.5	(22,23)	37423620.

TRACK TRAIL FOR SPGDY2.DA

BLOCK	(IR3D, JR3D)	AMAX	AMAXUP	RSUM	LOG COORD'S	POWER
90	(31,27)	91.9	95.6	2536.7	(23,20)	57659180.
91	(32,27)	95.2	98.6	2452.2	(24,20)	115234400.
92	(32,28)	97.8	100.6	2399.9	(23,21)	181711000.
93	(32,28)	99.6	101.6	2392.2	(23,21)	230521000.
94	(32,28)	100.8	102.3	2413.8	(23,21)	270816800.
95	(33,27)	101.9	103.5	2399.2	(24,20)	352937500.
96	(33,27)	102.8	104.9	2384.5	(24,20)	486999000.
97	(33,27)	103.5	105.8	2361.0	(24,20)	604224800.
98	(33,27)	104.2	106.2	2357.4	(24,20)	653719800.
99	(32,28)	104.9	106.6	2368.7	(23,21)	717283100.
100	(32,27)	105.5	107.5	2389.2	(24,20)	894509800.
101	(33,27)	106.0	108.5	2354.4	(24,20)	1120238000.
102	(32,28)	106.5	108.9	2313.5	(23,21)	1234020000.
103	(32,28)	107.0	109.0	2315.4	(23,21)	1254849000.
104	(32,27)	107.3	109.4	2333.0	(24,20)	1377585000.
105	(32,27)	107.6	110.1	2324.3	(24,20)	1628345000.
106	(32,27)	107.8	110.5	2300.8	(24,20)	1782084000.
107	(32,28)	108.0	110.4	2299.2	(23,21)	1739553000.
108	(32,28)	108.1	110.4	2306.4	(23,21)	1726364000.
109	(32,27)	108.1	110.8	2327.3	(24,20)	1903256000.
110	(32,27)	108.1	111.2	2284.3	(24,20)	2072365000.
111	(32,28)	108.1	111.1	2273.6	(23,21)	2029585000.
112	(32,28)	108.0	110.9	2274.1	(23,21)	1959945000.
113	(32,27)	107.9	111.2	2306.2	(24,20)	2110040000.
114	(32,27)	107.8	111.7	2283.0	(24,20)	2325166000.
115	(32,28)	107.7	111.6	2247.4	(23,21)	2304972000.
116	(32,28)	107.8	111.4	2258.5	(23,21)	2175998000.
117	(32,27)	108.0	111.6	2294.2	(24,20)	2272030000.
118	(32,27)	108.2	112.0	2288.8	(24,20)	2528012000.
119	(33,27)	108.5	112.1	2260.5	(24,20)	2571485000.
120	(33,27)	108.8	111.8	2257.4	(24,20)	2406744000.
121	(33,27)	109.0	111.8	2274.3	(24,20)	2416800000.
122	(33,27)	109.1	112.3	2274.7	(24,20)	2661055000.
123	(33,27)	109.3	112.4	2255.3	(24,20)	2762656000.
124	(33,28)	109.4	112.1	2243.6	(24,20)	2591262000.
125	(32,28)	109.6	112.0	2253.9	(23,21)	2529993000.
126	(32,28)	109.8	112.4	2267.2	(23,21)	2772129000.
127	(33,28)	109.9	112.7	2228.1	(24,20)	2970190000.
128	(32,28)	110.2	112.6	2234.1	(23,21)	2874853000.
129	(32,28)	110.4	112.5	2234.7	(23,21)	2810431000.
130	(32,28)	110.6	112.9	2273.4	(23,21)	3075450000.
131	(32,28)	110.8	113.3	2248.9	(23,21)	3370383000.
132	(32,28)	111.0	113.2	2219.4	(23,21)	3316477000.
133	(32,28)	111.2	113.0	2231.2	(23,21)	3171315000.
134	(32,28)	111.3	113.3	2255.8	(23,21)	3376960000.
135	(32,28)	111.5	113.8	2255.2	(23,21)	3761957000.
136	(32,28)	111.6	113.8	2205.8	(23,21)	3809821000.
137	(31,28)	111.7	113.5	2208.1	(23,21)	3570384000.
138	(31,28)	111.8	113.5	2236.1	(23,21)	3556463000.
139	(31,28)	111.8	113.8	2245.8	(23,21)	3839725000.
140	(32,28)	111.7	113.9	2236.7	(23,21)	3929887000.
141	(31,28)	111.6	113.6	2215.8	(23,21)	3639565000.
142	(31,28)	111.6	113.3	2239.5	(23,21)	3398439000.
143	(31,28)	111.5	113.4	2271.7	(23,21)	3490598000.
144	(31,28)	111.4	113.6	2259.7	(23,21)	3619828000
145	(31,28)	111.3	113.4	2238.7	(23,21)	3442237000.
146	(31,28)	111.2	113.0	2245.9	(23,21)	3165864000.
147	(31,28)	111.1	113.0	2287.0	(23,21)	3126521000.
148	(31,27)	111.0	113.1	2293.6	(23,20)	3237579000.

AD-A163 215 CORTICAL THOUGHT THEORY: A WORKING MODEL OF THE HUMAN GESTALT MECHANISM(U) AIR FORCE INST OF TECH WRIGHT-PATTERSON AFB OH SCHOOL OF ENGINEERING 5/5

UNCLASSIFIED R L ROUTH JUL 85 AFIT/DS/EE/85-1 F/G 5/10 NL

END
FILMED
DTIC

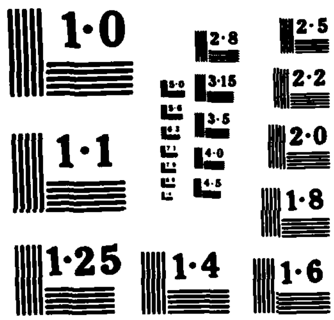

NATIONAL BUREAU OF STANDARDS
MICROCOPY RESOLUTION TEST CHART

149	(31,27)	110.9	113.0	2273.2	(23,20)	3175742000.
150	(30,28)	110.7	112.7	2267.5	(22,21)	2933844000.
151	(30,27)	110.5	112.4	2296.4	(22,20)	2775373000.
152	(30,27)	110.3	112.4	2337.4	(22,20)	2762285000.
153	(31,27)	110.0	112.3	2344.1	(23,20)	2699662000.
154	(31,27)	109.7	112.0	2329.4	(23,20)	2494283000.
155	(30,27)	109.5	111.7	2337.1	(22,20)	2338024000.
156	(30,27)	109.2	111.7	2369.9	(22,20)'	2340030000.
157	(30,27)	109.1	111.8	2375.1	(22,20)	2378273000.
158	(30,27)	109.0	111.6	2343.7	(22,20)	2294702000.
159	(30,27)	108.9	111.4	2337.2	(22,20)	2171607000.
160	(30,27)	108.9	111.4	2350.3	(22,20)	2182149000.
161	(30,27)	108.9	111.6	2384.0	(22,20)	2285432000.
162	(30,27)	108.8	111.6	2378.0	(22,20)	2300997000.
163	(30,27)	108.8	111.4	2350.0	(22,20)	2188705000.
164	(30,27)	108.8	111.3	2350.6	(22,20)	2145567000.
165	(30,27)	108.7	111.5	2364.9	(22,20)	2253823000.
166	(30,27)	108.8	111.7	2373.3	(22,20)	2362612000.
167	(30,27)	108.9	111.6	2347.4	(22,20)	2307306000.
168	(30,27)	108.9	111.4	2334.3	(22,20)	2191778000.
169	(30,27)	108.9	111.5	2358.8	(22,20)	2216095000.
170	(30,27)	108.9	111.7	2381.5	(22,20)	2334445000.
171	(30,27)	108.8	111.7	2366.0	(22,20)	2328436000.
172	(30,28)	108.7	111.3	2327.0	(22,21)	2150402000.
173	(30,27)	108.6	111.1	2324.8	(22,20)	2028082000.
174	(30,27)	108.4	111.2	2336.5	(22,20)	2071572000.
175	(30,28)	108.1	111.2	2343.4	(22,21)	2098028000.
176	(31,28)	107.7	110.8	2333.9	(23,21)	1889880000.
177	(31,27)	107.0	109.9	2352.7	(23,20)	1543233000.
178	(30,27)	106.3	109.2	2400.0	(22,20)	1327318000.
179	(30,27)	105.3	109.1	2421.6	(22,20)	1285669000.
180	(31,28)	104.3	108.8	2422.6	(23,21)	1200789000.
181	(31,28)	103.2	107.6	2375.1	(23,21)	910650100.
182	(32,28)	100.2	105.1	2358.0	(23,21)	516376300.
183	(30,28)	97.0	101.3	2405.5	(22,21)	212702700.
184	(29,28)	94.1	96.9	2514.7	(22,21)	78282910.
185	(30,28)	92.6	94.8	2479.6	(22,21)	48277440.
186	(30,29)	92.3	94.5	2369.0	(22,21)	44507650.
187	(33,29)	92.0	94.1	2265.2	(24,21)	40707780.
188	(35,29)	91.9	93.4	2209.8	(25,21)	34916350.
189	(35,29)	91.8	92.9	2174.6	(25,21)	30962050.
244	(33,28)	90.3	93.7	2354.6	(24,20)	36968980.
245	(34,29)	91.3	94.9	2229.0	(25,21)	48676910.
246	(33,30)	91.7	95.0	2170.8	(24,22)	50351220
247	(33,30)	92.0	94.4	2186.5	(24,22)	43232030.
248	(33,30)	92.0	93.7	2190.8	(24,22)	36971870.
249	(33,29)	91.7	93.7	2217.0	(24,21)	36959790.
250	(34,29)	91.2	93.8	2196.3	(25,21)	37971120.
251	(34,29)	90.7	93.2	2186.8	(25,21)	33377340.
295	(35,32)	91.6	93.2	2055.3	(25,23)	32880700.
296	(34,32)	92.2	93.7	2026.2	(24,23)	36940620.
297	(34,32)	92.7	93.8	2000.5	(24,23)	37730770.
298	(34,32)	93.0	94.0	1999.7	(24,23)	39724610.
299	(34,32)	93.2	94.5	2035.6	(24,23)	45124340.
300	(33,32)	93.4	94.9	2054.7	(24,23)	49442960.
301	(31,32)	93.5	94.9	2102.8	(22,23)	48836990.
302	(31,32)	93.7	94.8	2110.9	(22,23)	48306850.
303	(31,31)	94.0	95.3	2116.4	(23,23)	53966780.
304	(33,31)	94.2	96.0	2119.3	(24,22)	62396480.
305	(33,30)	94.6	96.2	2131.1	(24,22)	65627020.
306	(32,30)	94.9	96.2	2140.0	(23,22)	65729760.
307	(32,30)	95.3	96.6	2143.4	(23,22)	72245550.
308	(34,29)	95.5	97.3	2184.4	(25,21)	85183120
309	(33,29)	95.8	97.7	2177.4	(24,21)	93275810
310	(33,29)	96.2	97.7	2191.4	(24,21)	93532580.
311	(33,29)	96.5	97.9	2191.1	(24,21)	98564770.

312	(33, 29)	96.9	98.6	2192.4	(24, 21)	114631100.
313	(34, 29)	97.3	99.1	2171.6	(25, 21)	129486000.
314	(33, 29)	97.7	99.3	2209.9	(24, 21)	133647400.
315	(33, 29)	98.2	99.5	2203.2	(24, 21)	141178500.
316	(33, 29)	98.6	100.2	2180.2	(24, 21)	165649400.
317	(33, 29)	99.0	100.9	2171.1	(24, 21)	193164000.
318	(33, 28)	99.4	101.1	2208.3	(24, 20)	203170300.
319	(33, 28)	99.8	101.2	2206.9	(24, 20)	208145200.
320	(32, 28)	100.2	101.7	2206.7	(23, 21)	233716100.
321	(34, 28)	100.5	102.3	2249.1	(25, 20)	271729200.
322	(34, 28)	100.9	102.7	2262.1	(25, 20)	291943900.
323	(34, 28)	101.3	102.8	2281.1	(25, 20)	300742900.
324	(34, 28)	101.6	103.2	2294.7	(25, 20)	334314000.
325	(34, 28)	102.0	103.9	2284.8	(25, 20)	390553100.
326	(34, 28)	102.3	104.3	2274.9	(25, 20)	428691200.
327	(33, 28)	102.7	104.5	2291.4	(24, 20)	447423500.
328	(33, 28)	103.2	104.9	2291.9	(24, 20)	494191400.
329	(33, 28)	103.6	105.6	2289.6	(24, 20)	572549400.
330	(34, 28)	104.1	106.0	2264.4	(25, 20)	629237200
331	(33, 28)	104.6	106.2	2271.3	(24, 20)	657877800.
332	(33, 28)	105.1	106.6	2277.7	(24, 20)	725917200.
333	(33, 28)	105.5	107.3	2275.1	(24, 20)	845277700.
334	(33, 28)	105.9	107.7	2252.6	(24, 20)	932919800.
335	(32, 28)	106.3	107.8	2265.6	(23, 21)	963417600.
336	(32, 28)	106.7	108.1	2248.9	(23, 21)	1034005000.
337	(33, 28)	107.1	108.8	2280.0	(24, 20)	1188629000.
338	(33, 28)	107.5	109.2	2256.5	(24, 20)	1325149000.
339	(32, 28)	108.0	109.4	2292.1	(23, 21)	1389037000.
340	(33, 28)	108.4	109.7	2287.5	(24, 20)	1491644000.
341	(33, 28)	108.7	110.3	2303.4	(24, 20)	1694496000.
342	(33, 28)	109.0	110.7	2281.1	(24, 20)	1868517000.
343	(32, 28)	109.4	110.8	2278.8	(23, 21)	1926925000.
344	(32, 28)	109.7	111.0	2281.1	(23, 21)	2011698000.
345	(33, 28)	110.0	111.5	2290.3	(24, 20)	2227818000.
346	(33, 28)	110.2	111.9	2265.2	(24, 20)	2435401000.
347	(32, 28)	110.6	112.0	2262.3	(23, 21)	2519484000.
348	(33, 28)	110.8	112.2	2269.0	(24, 20)	2628939000.
349	(33, 28)	111.0	112.6	2277.0	(24, 20)	2873662000.
350	(33, 28)	111.2	112.9	2256.9	(24, 20)	3066479000.
351	(32, 28)	111.4	112.9	2240.1	(23, 21)	3061692000.
352	(32, 28)	111.5	112.9	2243.8	(23, 21)	3056791000.
353	(32, 28)	111.6	113.1	2261.7	(23, 21)	3234438000.
354	(33, 28)	111.6	113.3	2250.4	(24, 20)	3403729000.
355	(32, 28)	111.7	113.3	2253.4	(23, 21)	3365467000.
356	(32, 28)	111.8	113.2	2271.1	(23, 21)	3302308000.
357	(32, 28)	111.8	113.4	2287.7	(23, 21)	3431176000.
358	(32, 28)	111.8	113.6	2262.3	(23, 21)	3593317000
359	(31, 28)	111.9	113.5	2237.3	(23, 21)	3587363000.
360	(31, 28)	112.0	113.5	2260.7	(23, 21)	3574078000.
361	(31, 28)	112.0	113.7	2267.5	(23, 21)	3734298000.
362	(32, 28)	112.0	113.9	2248.9	(23, 21)	3866416000.
363	(32, 28)	111.9	113.7	2249.8	(23, 21)	3745075000.
364	(31, 28)	111.9	113.5	2271.7	(23, 21)	3564150000.
365	(32, 28)	111.7	113.5	2288.3	(23, 21)	3584357000.
366	(32, 28)	111.7	113.6	2268.5	(23, 21)	3658175000.
367	(32, 28)	111.6	113.5	2248.7	(23, 21)	3542452000.
368	(32, 28)	111.6	113.3	2249.9	(23, 21)	3384996000.
369	(32, 28)	111.5	113.4	2253.5	(23, 21)	3437055000.
370	(32, 28)	111.5	113.5	2240.7	(23, 21)	3560219000.
371	(32, 28)	111.5	113.4	2233.5	(23, 21)	3489147000.
372	(32, 28)	111.5	113.2	2242.1	(23, 21)	3333921000.
373	(32, 28)	111.4	113.3	2255.6	(23, 21)	3358484000.
374	(32, 28)	111.3	113.4	2256.7	(23, 21)	3470231000.
375	(32, 28)	111.3	113.3	2260.7	(23, 21)	3410226000.
376	(32, 28)	111.2	113.1	2282.2	(23, 21)	3263021000.
377	(32, 28)	111.2	113.2	2289.5	(23, 21)	3301798000.

378	(32,28)	111.1	113.4	2272.9	(23,21)	3457038000.
379	(32,28)	111.1	113.4	2274.9	(23,21)	3437145000.
380	(32,28)	111.1	113.2	2302.4	(23,21)	3276159000.
381	(32,28)	111.0	113.1	2314.9	(23,21)	3266568000.
382	(32,28)	111.0	113.3	2286.6	(23,21)	3403759000.
383	(32,28)	111.0	113.3	2281.9	(23,21)	3394940000.
384	(32,28)	111.0	113.1	2290.4	(23,21)	3212527000.
385	(32,28)	111.0	113.0	2315.6	(23,21)	3141670000.
386	(32,28)	110.9	113.1	2288.8	(23,21)	3248538000.
387	(32,28)	110.9	113.1	2270.9	(23,21)	3254126000.
388	(32,28)	110.9	112.9	2268.5	(23,21)	3061594000.
389	(32,28)	110.8	112.7	2299.1	(23,21)	2935861000.
390	(32,28)	110.7	112.8	2289.3	(23,21)	3019388000.
391	(33,28)	110.6	112.9	2260.1	(24,20)	3065638000.
392	(33,28)	110.5	112.6	2254.2	(24,20)	2883315000.
393	(32,28)	110.3	112.3	2295.2	(23,21)	2669777000.
394	(32,28)	110.1	112.2	2289.8	(23,21)	2649215000.
395	(33,28)	109.8	112.3	2259.1	(24,20)	2684736000.
396	(33,28)	109.6	112.0	2243.8	(24,20)	2538702000.
397	(33,28)	109.5	111.6	2262.7	(24,20)	2316397000.
398	(33,28)	109.4	111.6	2276.7	(24,20)	2268758000.
399	(33,28)	109.2	111.7	2248.5	(24,20)	2348755000.
400	(34,28)	109.0	111.6	2225.7	(25,20)	2277641000.
401	(33,28)	108.8	111.1	2219.5	(24,20)	2029273000.
402	(33,28)	108.5	110.7	2249.1	(24,20)	1852801000.
403	(33,28)	108.3	110.7	2253.3	(24,20)	1851632000.
404	(33,28)	107.9	110.6	2230.8	(24,20)	1822816000.
405	(34,28)	107.7	110.1	2212.7	(25,20)	1627740000.
406	(33,28)	107.4	109.6	2243.7	(24,20)	1432592000.
407	(33,28)	107.1	109.5	2270.4	(24,20)	1409196000.
408	(34,28)	106.9	109.6	2246.5	(25,20)	1447862000.
409	(34,28)	106.7	109.3	2232.8	(25,20)	1349870000.
410	(33,28)	106.6	108.7	2244.0	(24,20)	1181785000.
411	(33,28)	106.4	108.6	2265.6	(24,20)	1148916000.
412	(33,28)	106.2	109.0	2254.4	(24,20)	1245311000.
413	(34,28)	106.1	109.0	2211.8	(25,20)	1245052000.
414	(34,28)	105.8	108.3	2199.6	(25,20)	1067004000.
415	(33,29)	105.6	107.6	2207.6	(24,21)	920292600.
416	(33,28)	105.4	107.9	2237.6	(24,20)	972742100.
417	(34,28)	105.1	108.4	2208.0	(25,20)	1091518000.
418	(34,29)	104.8	108.2	2168.0	(25,21)	1044370000.
419	(33,29)	104.6	107.3	2176.6	(24,21)	857861900.
420	(32,29)	104.4	106.9	2178.2	(23,21)	768341000.
421	(33,29)	104.2	107.4	2201.4	(24,21)	865647100.
422	(33,29)	103.8	107.9	2148.6	(24,21)	968336400.
423	(34,29)	103.6	107.6	2099.6	(25,21)	901722900.
424	(32,30)	103.5	106.8	2110.3	(23,22)	754795300.
425	(32,29)	103.4	106.6	2126.7	(23,21)	729583400.
426	(33,29)	103.7	107.3	2135.2	(24,21)	841856000.
427	(33,29)	104.0	107.6	2095.7	(24,21)	909786900.
428	(33,30)	104.2	107.2	2070.0	(24,22)	823779100.
429	(32,30)	104.1	106.4	2080.5	(23,22)	694991600.
430	(32,30)	104.0	106.3	2104.5	(23,22)	678150400.
431	(32,30)	104.1	106.8	2108.3	(23,22)	757346600.
432	(33,30)	104.2	107.0	2090.8	(24,22)	789722900.
433	(33,30)	104.2	106.6	2021.4	(24,22)	719628300.
434	(32,31)	104.2	106.1	2000.5	(23,22)	645490200.
435	(32,30)	104.1	106.2	2039.1	(23,22)	666491900.
436	(32,31)	104.1	106.7	2047.2	(23,22)	744779000.
437	(33,31)	104.3	106.8	2037.6	(24,22)	765509100.
438	(32,31)	104.4	106.4	2008.2	(23,22)	698271000.
439	(31,31)	104.4	106.0	2000.4	(23,23)	627613200.
440	(31,31)	104.3	106.0	2015.8	(23,23)	631931900.
441	(32,31)	104.4	106.3	2012.8	(23,22)	681444100.
442	(33,31)	104.5	106.4	1996.1	(24,22)	689561900.
443	(33,31)	104.4	106.0	1935.6	(24,22)	635610900.

444	(32, 32)	104. 3	105. 7	1904. 2	(23, 23)	586123800.
445	(31, 32)	104. 4	105. 8	1922. 4	(22, 23)	600185300.
446	(31, 32)	104. 5	106. 1	1899. 8	(22, 23)	649688100.
447	(32, 32)	104. 6	106. 2	1910. 4	(23, 23)	655097300.
448	(33, 32)	104. 5	105. 7	1874. 4	(24, 23)	592423200.
449	(32, 32)	104. 3	105. 2	1870. 3	(23, 23)	521447900.
450	(31, 32)	104. 1	105. 0	1869. 8	(22, 23)	505903900
451	(31, 32)	103. 9	105. 3	1895. 9	(22, 23)	535270400.
452	(32, 32)	103. 7	105. 3	1886. 4	(23, 23)	539815400.
453	(33, 32)	103. 4	104. 8	1852. 8	(24, 23)	482424100.
454	(33, 32)	103. 2	104. 1	1835. 7	(24, 23)	405423100.
455	(32, 32)	103. 0	103. 7	1869. 9	(23, 23)	373646100.
456	(32, 32)	102. 8	104. 0	1851. 8	(23, 23)	398580700
457	(33, 32)	102. 7	104. 3	1887. 4	(24, 23)	426002400
458	(33, 32)	102. 3	104. 0	1918. 5	(24, 23)	397123100.
459	(32, 33)	101. 8	103. 0	1881. 6	(23, 24)	315706600.
460	(31, 33)	101. 1	101. 8	1857. 6	(22, 24)	237363400.
461	(31, 33)	100. 6	101. 2	1870. 2	(22, 24)	209706900.
462	(33, 33)	100. 3	101. 6	1825. 9	(23, 23)	227736900.
463	(33, 33)	100. 2	101. 9	1844. 2	(23, 23)	244523800.
464	(32, 33)	99. 7	101. 5	1862. 7	(23, 24)	222420500.
465	(32, 32)	99. 0	100. 3	1904. 2	(23, 23)	168762100.
466	(31, 33)	98. 2	98. 8	1948. 2	(22, 24)	120852700.
467	(31, 32)	97. 7	98. 3	1988. 1	(22, 23)	108243000.
468	(32, 32)	97. 6	99. 0	1968. 0	(23, 23)	126701000.
469	(32, 33)	97. 4	99. 6	1932. 2	(23, 24)	144282300.
470	(33, 33)	96. 9	99. 3	1889. 4	(23, 23)	134547000.
471	(33, 32)	95. 7	98. 0	1907. 7	(24, 23)	99338290.
472	(31, 32)	94. 0	95. 9	2034. 9	(22, 23)	62123090.
473	(29, 31)	92. 4	94. 2	2196. 2	(21, 23)	41978740.
474	(29, 30)	91. 5	93. 8	2245. 1	(21, 22)	38379470.
475	(29, 30)	91. 2	93. 8	2235. 0	(21, 22)	38298540.
476	(29, 31)	90. 6	93. 2	2183. 7	(21, 23)	32879660.
482	(29, 31)	89. 6	93. 2	2238. 3	(21, 23)	32835520.

TRACK TRAIL FOR SPGDJ1.DA

BLOCK	(IR3D, JR3D)	AMAX	AMAXUP	RSUM	LOG COORD'S	POWER
43	(25, 27)	86.6	93.2	2835.3	(19, 21)	33022510.
44	(26, 27)	87.2	93.5	2816.2	(20, 21)	35855600.
45	(26, 27)	88.6	93.3	2778.1	(20, 21)	34162670.
46	(28, 28)	90.1	93.8	2654.7	(21, 21)	37630930.
47	(31, 28)	91.6	95.7	2514.7	(23, 21)	58887950.
48	(33, 28)	93.5	98.0	2452.3	(24, 20)	99157950.
49	(32, 28)	96.2	99.6	2415.8	(23, 21)	144110600.
50	(31, 28)	98.6	100.9	2395.8	(23, 21)	193275300.
51	(31, 28)	100.6	102.5	2348.3	(23, 21)	280482300.
52	(32, 28)	101.9	104.2	2329.1	(23, 21)	416945900.
53	(32, 28)	103.3	105.4	2291.1	(23, 21)	553329700.
54	(32, 28)	104.5	106.1	2251.3	(23, 21)	648917200.
55	(32, 28)	105.5	106.9	2230.0	(23, 21)	773920300.
56	(32, 28)	106.2	108.0	2227.4	(23, 21)	1003699000.
57	(32, 28)	106.9	109.0	2224.3	(23, 21)	1255700000.
58	(32, 28)	107.5	109.5	2216.9	(23, 21)	1404803000.
59	(32, 28)	108.3	110.0	2216.6	(23, 21)	1572234000.
60	(32, 28)	108.9	111.0	2223.8	(23, 21)	1990827000.
61	(32, 28)	109.5	112.1	2198.2	(23, 21)	2543400000.
62	(32, 29)	109.9	112.6	2175.1	(23, 21)	2852530000.
63	(32, 29)	110.3	112.6	2192.6	(23, 21)	2915519000.
64	(31, 29)	110.5	113.0	2185.0	(23, 21)	3172797000.
65	(32, 28)	110.7	113.7	2181.0	(23, 21)	3717064000.
66	(32, 28)	111.0	114.1	2149.4	(23, 21)	4063241000.
67	(33, 28)	111.3	114.0	2170.3	(24, 20)	3992514000.
68	(32, 29)	111.4	114.0	2179.9	(23, 21)	3976358000.
69	(32, 28)	111.5	114.4	2197.1	(23, 21)	4318462000.
70	(32, 28)	111.5	114.6	2171.3	(23, 21)	4602253000.
71	(32, 28)	111.7	114.5	2182.1	(23, 21)	4516377000.
72	(32, 28)	111.7	114.5	2190.1	(23, 21)	4463911000.
73	(32, 28)	111.7	114.8	2218.3	(23, 21)	4765065000.
74	(32, 28)	111.7	115.0	2199.7	(23, 21)	5016662000.
75	(32, 28)	111.8	114.9	2203.6	(23, 21)	4896944000.
76	(32, 28)	111.9	114.8	2223.4	(23, 21)	4811002000.
77	(32, 28)	111.8	115.1	2252.3	(23, 21)	5072691000.
78	(31, 28)	111.8	115.2	2223.8	(23, 21)	5267927000.
79	(31, 28)	111.9	115.1	2214.4	(23, 21)	5094224000.
80	(31, 28)	111.9	115.0	2223.6	(23, 21)	4990362000.
81	(31, 28)	111.8	115.2	2246.7	(23, 21)	5256630000.
82	(32, 28)	111.8	115.3	2230.0	(23, 21)	5427061000.
83	(32, 28)	111.9	115.1	2208.8	(23, 21)	5183537000.
84	(32, 28)	111.9	115.0	2228.1	(23, 21)	5005259000.
85	(32, 28)	111.8	115.2	2247.2	(23, 21)	5228106000.
86	(32, 28)	111.9	115.3	2225.4	(23, 21)	5372027000.
87	(32, 28)	111.9	115.1	2202.8	(23, 21)	5077721000.
88	(32, 29)	111.9	114.8	2215.3	(23, 21)	4800610000.
89	(32, 28)	111.9	114.9	2238.2	(23, 21)	4913365000.
90	(32, 28)	111.9	115.0	2230.0	(23, 21)	5009904000.
91	(32, 28)	112.0	114.8	2239.7	(23, 21)	4740100000.
92	(32, 28)	112.0	114.5	2266.8	(23, 21)	4469916000.
93	(32, 28)	111.9	114.5	2292.1	(23, 21)	4512821000.
94	(32, 28)	111.9	114.5	2279.0	(23, 21)	4511171000.
95	(31, 28)	111.9	114.2	2272.5	(23, 21)	4178770000.
96	(31, 28)	111.8	113.9	2294.7	(23, 21)	3873411000.
97	(31, 28)	111.7	113.9	2311.3	(23, 21)	3885744000.
98	(31, 28)	111.5	113.9	2286.2	(23, 21)	3855672000.
99	(31, 28)	111.3	113.4	2263.3	(23, 21)	3449479000.
100	(31, 29)	111.0	112.7	2258.8	(23, 21)	2983472000.
101	(31, 28)	110.8	112.5	2275.2	(23, 21)	2847187000.
102	(31, 28)	110.5	112.5	2252.8	(23, 21)	2839235000.
103	(31, 28)	110.2	112.1	2231.6	(23, 21)	2566297000.

104	(30, 28)	109.7	111.2	2237.6	(22, 21)	2109206000.
105	(31, 28)	109.2	110.6	2315.0	(23, 21)	1816808000.
106	(31, 28)	108.5	110.3	2337.1	(23, 21)	1716367000.
107	(31, 29)	107.6	109.9	2319.7	(23, 21)	1533018000.
108	(30, 29)	106.4	108.6	2321.6	(22, 21)	1152420000.
109	(29, 28)	104.9	106.7	2352.9	(22, 21)	742724100.
110	(29, 28)	103.0	104.7	2379.7	(22, 21)	471704100.
111	(29, 29)	101.1	103.2	2389.5	(22, 22)	328989400.
112	(30, 29)	99.4	101.6	2336.9	(22, 21)	228052500.
113	(32, 30)	97.8	99.5	2244.9	(23, 22)	139988500.
114	(33, 30)	96.0	97.2	2170.7	(24, 22)	83307140.
115	(34, 30)	94.5	95.9	2213.2	(24, 22)	62200880.
116	(33, 30)	93.1	95.6	2193.6	(24, 22)	58182220.
117	(32, 31)	92.0	95.4	2158.4	(23, 22)	54438100.
118	(31, 31)	91.4	94.9	2154.2	(23, 23)	49018770.
119	(31, 31)	91.5	94.7	2143.8	(23, 23)	47214720.
120	(33, 31)	91.3	94.9	2142.6	(24, 22)	49133580.
121	(34, 30)	91.1	94.9	2170.1	(24, 22)	48525490.
122	(33, 30)	90.9	94.4	2205.5	(24, 22)	43485360.
123	(32, 30)	90.6	93.9	2208.6	(23, 22)	39347280.
124	(33, 30)	90.4	94.0	2194.8	(24, 22)	39448060.
125	(34, 31)	90.3	94.0	2161.6	(24, 22)	39652240.
126	(35, 31)	90.2	93.7	2108.2	(25, 22)	36845920.
127	(36, 31)	90.2	93.4	2063.3	(25, 22)	34685490.
128	(36, 31)	90.3	93.7	2060.0	(25, 22)	36840780.
129	(34, 33)	90.4	94.0	2034.7	(24, 23)	39902850.
130	(32, 33)	90.3	93.9	2088.0	(23, 24)	38653440.
131	(31, 32)	90.4	93.4	2122.3	(22, 23)	35068110.
132	(32, 32)	90.3	93.4	2115.3	(23, 23)	34398640.
133	(33, 31)	90.2	93.6	2116.0	(24, 22)	36549680.
134	(33, 31)	89.9	93.6	2165.3	(24, 22)	36355580.
135	(31, 31)	90.1	93.2	2208.5	(23, 23)	33016050.
136	(31, 31)	89.9	92.9	2192.9	(23, 23)	30948500.
137	(32, 31)	89.9	93.2	2188.3	(23, 22)	33045740.
138	(32, 31)	89.6	93.5	2154.9	(23, 22)	35738690.
139	(32, 31)	89.6	93.5	2172.0	(23, 22)	35101790.
140	(31, 31)	89.6	93.1	2197.8	(23, 23)	32372770.
141	(31, 31)	89.4	92.9	2206.6	(23, 23)	31025470.
142	(31, 31)	89.1	92.9	2228.9	(23, 23)	31076610.
147	(32, 31)	89.5	92.9	2190.6	(23, 22)	31152220.
175	(32, 28)	88.0	92.8	2578.2	(23, 21)	30137840.
176	(32, 28)	87.9	93.0	2580.4	(23, 21)	31334590.
177	(31, 28)	87.7	93.4	2569.7	(23, 21)	34658430.
178	(31, 28)	87.3	94.0	2574.0	(23, 21)	39786190.
179	(31, 28)	87.1	94.4	2565.6	(23, 21)	44083390.
180	(30, 28)	87.1	94.7	2569.3	(22, 21)	47209360.
181	(30, 28)	87.2	95.1	2560.7	(22, 21)	51508860.
182	(31, 28)	87.2	95.6	2546.9	(23, 21)	57128940.
183	(32, 28)	87.5	95.8	2528.7	(23, 21)	60137680.
184	(33, 28)	87.8	95.7	2526.5	(24, 20)	58539360.
185	(32, 28)	88.2	95.6	2551.0	(23, 21)	57231020.
186	(32, 28)	88.6	95.9	2583.0	(23, 21)	61614190.
187	(32, 28)	88.8	96.4	2584.8	(23, 21)	69425700.
188	(31, 28)	89.0	96.7	2626.3	(23, 21)	73938690.
189	(29, 28)	89.4	96.8	2652.1	(22, 21)	75694700.
190	(29, 28)	89.7	97.2	2640.1	(22, 21)	82991440.
191	(30, 28)	90.2	97.9	2618.6	(22, 21)	98555460.
192	(31, 28)	91.2	98.7	2562.0	(23, 21)	118370500.
193	(31, 28)	92.3	99.5	2543.4	(23, 21)	140270200.
194	(31, 28)	93.3	100.2	2548.1	(23, 21)	166709600.
195	(31, 28)	94.2	100.8	2585.4	(23, 21)	191594800.
196	(31, 28)	94.9	101.1	2594.4	(23, 21)	203989400.
197	(30, 28)	95.5	101.2	2588.1	(22, 21)	208568100.
198	(30, 28)	96.1	101.6	2569.7	(22, 21)	230934100.
199	(31, 28)	96.4	102.4	2548.3	(23, 21)	277952000.
200	(31, 27)	96.7	103.0	2555.0	(23, 20)	316449800

201	(31,27)	97.2	103.0	2560.9	(23,20)	317988400.
202	(31,27)	97.8	102.9	2581.2	(23,20)	309102100.
203	(31,27)	98.2	103.4	2589.5	(23,20)	343945700.
204	(31,27)	98.7	104.2	2597.5	(23,20)	417948700.
205	(31,27)	99.1	104.7	2606.2	(23,20)	468909100.
206	(30,27)	99.5	104.7	2627.5	(22,20)	470994700.
207	(30,28)	100.1	104.9	2625.4	(22,21)	486333200.
208	(30,27)	100.4	105.5	2632.1	(22,20)	557852900.
209	(31,27)	100.8	106.0	2609.6	(23,20)	629166600.
210	(31,27)	101.1	106.0	2591.6	(23,20)	626841100.
211	(30,28)	101.4	105.8	2565.4	(22,21)	595794400.
212	(30,27)	101.7	106.1	2549.0	(22,20)	644808200.
213	(31,27)	102.0	106.8	2535.7	(23,20)	762143700.
214	(31,27)	102.4	107.1	2511.3	(23,20)	820513800.
215	(31,27)	102.8	106.9	2514.0	(23,20)	775974400.
216	(31,28)	103.3	106.8	2509.4	(23,21)	758383100.
217	(31,27)	103.5	107.3	2519.3	(23,20)	856749100.
218	(32,27)	103.8	107.9	2493.7	(24,20)	970591700.
219	(33,27)	104.1	107.8	2482.6	(24,20)	965550100.
220	(33,27)	104.4	107.6	2476.5	(24,20)	917028100.
221	(32,27)	104.7	108.0	2487.4	(24,20)	994857500.
222	(32,27)	104.9	108.7	2483.5	(24,20)	1166362000.
223	(32,27)	105.3	108.9	2448.5	(24,20)	1233142000.
224	(32,27)	105.6	108.6	2461.1	(24,20)	1158085000.
225	(32,27)	105.9	108.7	2464.4	(24,20)	1168155000.
226	(33,27)	106.1	109.4	2465.5	(24,20)	1373799000.
227	(33,27)	106.3	109.9	2423.9	(24,20)	1565321000.
228	(33,27)	106.4	109.8	2409.8	(24,20)	1527282000.
229	(33,27)	106.6	109.5	2413.6	(24,20)	1411967000.
230	(34,27)	106.8	109.7	2406.8	(25,20)	1494899000.
231	(35,27)	107.0	110.4	2368.8	(25,20)	1726960000.
232	(35,27)	107.2	110.6	2326.3	(25,20)	1817595000.
233	(34,28)	107.3	110.4	2352.7	(25,20)	1721642000.
234	(34,28)	107.5	110.4	2361.5	(25,20)	1720399000.
235	(35,27)	107.5	110.8	2349.2	(25,20)	1920092000.
236	(35,28)	107.5	111.2	2309.8	(25,20)	2067602000.
237	(35,27)	107.6	110.9	2304.1	(25,20)	1969254000.
238	(34,28)	107.8	110.7	2313.1	(25,20)	1841002000.
239	(34,28)	107.8	110.9	2341.5	(25,20)	1941903000.
240	(35,27)	107.9	111.3	2316.1	(25,20)	2141354000.
241	(35,27)	107.9	111.3	2304.4	(25,20)	2133454000.
242	(34,27)	108.0	110.9	2305.6	(25,20)	1965217000.
243	(33,28)	108.1	110.9	2330.3	(24,20)	1960383000.
244	(34,28)	108.0	111.4	2328.5	(25,20)	2164077000.
245	(34,28)	108.0	111.5	2267.1	(25,20)	2263074000.
246	(34,28)	108.1	111.2	2268.2	(25,20)	2098007000.
247	(33,28)	108.0	110.9	2286.8	(24,20)	1938230000.
248	(33,28)	107.9	111.1	2305.4	(24,20)	2019657000.
249	(33,28)	107.7	111.3	2283.7	(24,20)	2157170000.
250	(34,28)	107.5	111.1	2260.0	(25,20)	2061591000.
251	(33,28)	107.4	110.7	2295.6	(24,20)	1843297000.
252	(33,28)	107.3	110.6	2329.3	(24,20)	1816679000.
253	(33,28)	107.1	111.0	2319.6	(24,20)	1973386000.
254	(33,28)	107.1	111.0	2298.3	(24,20)	1998323000.
255	(33,28)	107.0	110.5	2315.7	(24,20)	1796913000.
256	(32,28)	106.9	110.2	2361.7	(23,21)	1662878000.
257	(32,28)	106.7	110.5	2374.3	(23,21)	1776817000.
258	(33,28)	106.6	110.8	2322.9	(24,20)	1903657000.
259	(33,28)	106.5	110.5	2276.5	(24,20)	1772268000.
260	(33,28)	106.5	109.8	2286.4	(24,20)	1523906000.
261	(32,28)	106.4	109.7	2319.0	(23,21)	1463870000.
262	(33,28)	106.2	110.0	2308.4	(24,20)	1577088000.
263	(33,28)	106.0	109.9	2276.0	(24,20)	1565451000.
264	(33,28)	105.8	109.3	2239.6	(24,20)	1339475000.
265	(32,28)	105.6	108.7	2256.3	(23,21)	1170240000.
266	(32,28)	105.4	108.9	2291.1	(23,21)	1239302000

267	(33, 28)	105.2	109.3	2278.3	(24, 20)	1356170000.
268	(33, 28)	105.1	109.0	2247.6	(24, 20)	1256627000.
269	(33, 28)	105.0	108.1	2245.9	(24, 20)	1015288000.
270	(32, 28)	104.9	107.6	2265.3	(23, 21)	914613200.
271	(33, 28)	104.6	108.1	2288.6	(24, 20)	1012398000.
272	(34, 28)	104.3	108.3	2248.8	(25, 20)	1073722000.
273	(34, 28)	104.2	107.7	2207.8	(25, 20)	936558600.
274	(33, 28)	104.1	106.8	2235.2	(24, 20)	753911800.
275	(32, 28)	103.9	106.7	2232.4	(23, 21)	741899300.
276	(33, 28)	103.7	107.4	2251.3	(24, 20)	864908500.
277	(33, 28)	103.4	107.5	2240.4	(24, 20)	901043700.
278	(33, 28)	103.2	106.8	2248.7	(24, 20)	763199200.
279	(32, 28)	103.0	105.8	2304.2	(23, 21)	607614500.
280	(31, 28)	102.8	105.8	2307.7	(23, 21)	601744100.
281	(32, 28)	102.6	106.5	2305.9	(23, 21)	702747600.
282	(32, 28)	102.2	106.6	2275.6	(23, 21)	732702200
283	(33, 29)	101.9	106.0	2234.0	(24, 21)	625184300.
284	(31, 29)	101.6	105.0	2260.9	(23, 21)	497959200
285	(30, 29)	101.6	104.9	2283.6	(22, 21)	491004400.
286	(31, 29)	101.7	105.7	2292.3	(23, 21)	584497200.
287	(32, 29)	101.5	106.0	2251.9	(23, 21)	632166700.
288	(33, 29)	101.2	105.5	2202.3	(24, 21)	557721900.
289	(32, 28)	101.1	104.4	2261.2	(23, 21)	441331500.
290	(31, 28)	100.9	104.2	2299.6	(23, 21)	413788900.
291	(31, 28)	101.1	104.9	2309.6	(23, 21)	489783000.
292	(32, 29)	101.0	105.4	2285.3	(23, 21)	552121900.
293	(33, 29)	100.6	105.1	2234.5	(24, 21)	507504600.
294	(32, 29)	100.0	103.9	2241.1	(23, 21)	391984400.
295	(31, 29)	99.7	103.0	2310.6	(23, 21)	316408100.
296	(30, 29)	99.8	103.2	2309.0	(22, 21)	334188800.
297	(31, 29)	100.0	103.8	2301.2	(23, 21)	383994400.
298	(32, 29)	99.8	103.8	2250.7	(23, 21)	379255800.
299	(32, 29)	99.6	102.9	2214.9	(23, 21)	312443600.
300	(31, 29)	99.5	102.0	2249.8	(23, 21)	252106700
301	(31, 29)	99.2	102.2	2253.0	(23, 21)	262038000
302	(31, 29)	99.2	103.1	2258.9	(23, 21)	321310000
303	(32, 29)	98.9	103.5	2234.3	(23, 21)	351166500.
304	(32, 30)	98.6	103.0	2174.2	(23, 22)	314917900.
305	(31, 30)	98.5	102.0	2175.9	(23, 22)	253142500
306	(30, 29)	98.5	101.8	2216.3	(22, 21)	238706000.
307	(30, 30)	98.9	102.6	2218.7	(22, 22)	290041100
308	(31, 30)	99.2	103.4	2208.7	(23, 22)	345418200.
309	(32, 30)	98.8	103.3	2146.3	(23, 22)	339260700.
310	(33, 30)	98.5	102.3	2095.0	(24, 22)	272023800.
311	(32, 30)	98.0	101.1	2130.4	(23, 22)	202527500.
312	(32, 30)	97.7	100.8	2136.4	(23, 22)	189570600.
313	(32, 30)	97.8	101.6	2133.3	(23, 22)	228019400.
314	(33, 30)	98.0	102.1	2119.1	(24, 22)	259304900.
315	(34, 30)	97.7	101.9	2098.3	(24, 22)	243171300.
316	(35, 30)	97.3	100.8	2073.5	(25, 21)	190426600.
317	(33, 30)	97.0	99.7	2114.2	(24, 22)	147361900.
318	(32, 30)	96.9	99.7	2129.4	(23, 22)	147230600.
319	(32, 30)	96.9	100.4	2104.1	(23, 22)	173030400.
320	(32, 30)	96.7	100.6	2080.4	(23, 22)	182708100.
321	(33, 30)	96.2	100.0	2082.6	(24, 22)	158275100.
322	(33, 30)	95.7	98.7	2057.5	(24, 22)	116872400.
323	(31, 30)	95.5	97.7	2088.4	(23, 22)	94024670.
324	(31, 30)	95.8	98.3	2123.4	(23, 22)	107300900.
325	(31, 30)	96.1	99.3	2140.6	(23, 22)	135338000.
326	(31, 31)	96.0	99.6	2054.7	(23, 23)	143468300.
327	(32, 31)	95.1	98.7	2074.0	(23, 22)	118557200.
328	(31, 31)	93.8	96.8	2162.0	(23, 23)	76029260.
329	(30, 30)	92.4	94.3	2233.6	(22, 22)	42908590.
330	(29, 30)	91.5	93.2	2282.3	(21, 22)	33224830.
331	(30, 29)	91.4	93.9	2331.0	(22, 21)	39342900.
332	(31, 30)	91.7	94.7	2250.9	(23, 22)	46516960.
333	(32, 30)	91.6	94.5	2205.4	(23, 22)	45162270.
334	(31, 30)	90.6	93.5	2241.6	(23, 22)	35194500.

TRACK TRAIL FOR SPGDJ2.DA

BLOCK	(IR3D, JR3D)	AMAX	AMAXUP	RSUM	LOG COORD'S	POWER
54	(29,27)	88.5	93.2	2661.7	(22,20)	33253630.
55	(30,28)	90.4	96.0	2520.4	(22,21)	62804130.
56	(31,28)	92.1	97.8	2460.0	(23,21)	96340540.
57	(31,28)	95.3	99.3	2401.2	(23,21)	134763200.
58	(31,28)	98.2	101.3	2354.5	(23,21)	212077500.
59	(31,28)	100.2	103.4	2318.4	(23,21)	347827200.
60	(32,28)	101.7	104.9	2277.0	(23,21)	493326300.
61	(31,29)	103.2	105.7	2240.7	(23,21)	589497600.
62	(31,29)	104.5	106.4	2206.7	(23,21)	692219100.
63	(31,29)	105.6	107.6	2224.5	(23,21)	912364500.
64	(32,29)	106.6	108.9	2191.8	(23,21)	1220311000.
65	(32,29)	107.5	109.7	2107.9	(23,21)	1481858000.
66	(31,30)	108.3	110.4	2068.6	(23,22)	1719822000.
67	(31,29)	109.0	111.1	2102.4	(23,21)	2045548000.
68	(30,30)	109.4	111.8	2055.0	(22,22)	2373894000.
69	(31,30)	109.8	112.0	2051.3	(23,22)	2537377000.
70	(32,29)	110.0	112.2	2094.1	(23,21)	2642821000.
71	(32,29)	110.3	112.6	2113.0	(23,21)	2896229000.
72	(32,29)	110.4	113.0	2108.9	(23,21)	3190138000.
73	(32,29)	110.6	113.2	2123.8	(23,21)	3312943000.
74	(31,29)	110.7	113.3	2146.7	(23,21)	3363794000.
75	(31,29)	110.8	113.5	2179.5	(23,21)	3549910000.
76	(31,29)	111.0	113.7	2164.1	(23,21)	3743451000.
77	(32,29)	111.0	113.8	2175.9	(23,21)	3771143000.
78	(31,29)	111.1	113.8	2186.3	(23,21)	3787535000.
79	(31,29)	111.2	114.0	2194.1	(23,21)	3945311000.
80	(31,29)	111.4	114.1	2174.4	(23,21)	4053052000.
81	(32,29)	111.5	114.0	2190.0	(23,21)	4018272000.
82	(32,28)	111.6	114.1	2215.5	(23,21)	4051637000.
83	(31,28)	111.7	114.2	2219.7	(23,21)	4194130000.
84	(32,28)	111.8	114.3	2203.4	(23,21)	4232516000.
85	(32,28)	111.9	114.2	2217.3	(23,21)	4144583000.
86	(31,28)	112.0	114.2	2250.6	(23,21)	4132482000.
87	(31,28)	112.0	114.2	2243.1	(23,21)	4157580000.
88	(32,28)	112.0	114.0	2237.5	(23,21)	4022241000.
89	(32,28)	112.0	113.8	2253.4	(23,21)	3806772000.
90	(31,28)	111.9	113.7	2267.9	(23,21)	3736822000.
91	(31,28)	111.9	113.7	2258.2	(23,21)	3704269000.
92	(32,28)	111.8	113.5	2258.5	(23,21)	3513145000.
93	(31,28)	111.7	113.1	2288.5	(23,21)	3271527000.
94	(31,28)	111.4	113.0	2299.6	(23,21)	3126876000.
95	(31,28)	111.0	112.7	2276.3	(23,21)	2935348000.
96	(30,29)	110.4	112.1	2274.1	(22,21)	2547761000.
97	(30,29)	109.6	111.2	2312.5	(22,21)	2111631000.
98	(30,29)	108.6	110.5	2322.4	(22,21)	1784580000.
99	(31,28)	107.2	109.7	2330.5	(23,21)	1470876000.
100	(31,28)	105.3	108.2	2365.6	(23,21)	1037828000.
101	(30,28)	102.8	105.7	2403.4	(22,21)	584460300.
102	(29,28)	99.7	102.4	2452.1	(22,21)	277782800.
103	(29,28)	96.8	99.5	2525.6	(22,21)	140909300.
104	(30,28)	94.3	97.4	2478.9	(22,21)	86176980.
105	(31,30)	92.7	95.8	2296.3	(23,22)	60366320.
106	(32,31)	92.6	95.3	2186.7	(23,22)	53973230.
107	(32,31)	92.7	95.5	2155.4	(23,22)	56433350.
108	(31,32)	93.1	95.5	2129.5	(22,23)	56458060.
109	(31,32)	93.3	95.2	2074.7	(22,23)	52544740.
110	(31,32)	93.1	95.0	2094.7	(22,23)	49685460.
111	(33,32)	92.6	94.8	2080.7	(24,23)	48147550.
112	(33,32)	92.2	94.5	2058.5	(24,23)	44524880.

113	(33,32)	91.6	94.0	2057.4	(24,23)	39479280.
114	(33,31)	91.2	93.7	2073.5	(24,22)	37506590.
115	(32,32)	90.9	93.8	2077.2	(23,23)	38256430.
116	(31,31)	90.8	93.7	2112.0	(23,23)	37551520.
117	(30,31)	90.6	93.4	2093.1	(22,23)	34602350.
118	(31,31)	90.4	93.2	2115.8	(23,23)	33087200.
119	(32,31)	90.0	93.3	2106.5	(23,22)	33801920.
120	(31,31)	89.7	93.2	2150.5	(23,23)	33399340.
121	(30,32)	89.4	92.8	2128.8	(22,23)	30489250.
152	(31,28)	87.3	92.8	2537.6	(23,21)	30245140.
153	(32,28)	88.7	94.1	2539.4	(23,21)	41138030.
154	(33,28)	89.8	95.3	2511.6	(24,20)	54231760.
155	(32,28)	90.7	96.0	2553.0	(23,21)	62882220.
156	(30,28)	91.4	96.4	2626.6	(22,21)	68768260.
157	(30,27)	92.2	97.2	2635.8	(22,20)	82962350.
158	(30,27)	93.0	98.4	2634.6	(22,20)	108408300.
159	(30,27)	93.6	99.2	2614.2	(22,20)	132074000.
160	(31,27)	94.3	99.6	2608.1	(23,20)	143119000.
161	(31,27)	95.3	99.9	2598.1	(23,20)	155872900.
162	(31,27)	96.3	100.9	2569.1	(23,20)	194322200.
163	(32,27)	97.3	102.0	2555.1	(24,20)	251406100.
164	(32,27)	98.1	102.6	2513.6	(24,20)	289908000.
165	(32,27)	98.8	102.8	2504.3	(24,20)	303293400.
166	(31,27)	99.5	103.4	2503.2	(23,20)	345204200.
167	(31,27)	100.1	104.5	2497.5	(23,20)	447685900.
168	(31,27)	100.6	105.4	2458.2	(23,20)	551956500.
169	(32,27)	101.1	105.6	2468.6	(24,20)	579335700.
170	(32,27)	101.6	105.5	2472.4	(24,20)	564757800.
171	(31,27)	102.1	106.0	2466.0	(23,20)	632202500.
172	(32,27)	102.6	107.0	2469.6	(24,20)	798202100.
173	(32,27)	102.8	107.6	2437.2	(24,20)	914773200.
174	(32,27)	103.0	107.4	2400.7	(24,20)	874230800.
175	(32,27)	103.2	107.0	2420.8	(24,20)	792292600.
176	(31,27)	103.3	107.2	2444.4	(23,20)	841304300.
177	(32,27)	103.3	107.9	2434.2	(24,20)	984549100.
178	(32,27)	103.4	108.1	2385.8	(24,20)	1019319000.
179	(32,27)	103.5	107.5	2390.8	(24,20)	890842600.
180	(32,27)	103.5	107.0	2404.2	(24,20)	794943700.
181	(32,27)	103.5	107.4	2437.3	(24,20)	874871000.
182	(33,27)	103.4	108.0	2391.7	(24,20)	1002640000.
183	(33,27)	103.4	107.9	2353.0	(24,20)	972513500.
184	(32,28)	103.3	107.1	2375.5	(23,21)	821188600.
185	(31,28)	103.2	106.8	2395.2	(23,21)	764891900.
186	(31,28)	102.9	107.3	2422.8	(23,21)	860787700.
187	(32,28)	102.8	107.7	2383.6	(23,21)	926514900.
188	(32,28)	102.7	107.2	2358.8	(23,21)	831541200.
189	(31,28)	102.8	106.5	2395.3	(23,21)	711864800.
190	(31,27)	102.7	106.7	2424.5	(23,20)	744729900.
191	(31,27)	102.7	107.4	2412.3	(23,20)	870790100.
192	(32,27)	102.5	107.4	2361.1	(24,20)	877746700.
193	(32,28)	102.3	106.6	2339.8	(23,21)	721366800.
194	(31,28)	102.3	105.8	2366.6	(23,21)	596584200.
195	(31,28)	102.1	106.1	2418.1	(23,21)	639486200.
196	(31,28)	102.0	106.7	2392.8	(23,21)	742907400.
197	(32,28)	101.8	106.6	2354.8	(23,21)	725190400.
198	(32,28)	101.7	105.8	2363.5	(23,21)	598450900.
199	(31,28)	101.6	105.3	2382.5	(23,21)	533100300.
200	(30,28)	101.4	105.8	2399.9	(22,21)	601838600.
201	(31,28)	101.1	106.4	2363.3	(23,21)	684428500.
202	(32,28)	100.8	106.1	2320.9	(23,21)	646203100.
203	(31,28)	100.6	105.2	2349.8	(23,21)	519689500.
204	(31,27)	100.4	104.5	2398.0	(23,20)	443234800.
205	(31,27)	100.1	104.7	2418.9	(23,20)	472140800.
206	(31,27)	100.2	105.2	2387.7	(23,20)	523445500.
207	(32,28)	100.3	105.0	2317.6	(23,21)	506135000.
208	(32,28)	99.7	104.3	2303.6	(23,21)	431136000.

209	(31,28)	99.0	103.8	2339.2	(23,21)	376938500.
210	(31,28)	99.1	103.8	2318.2	(23,21)	383447600.
211	(31,28)	99.2	104.1	2319.3	(23,21)	406152700.
212	(32,28)	98.9	103.9	2280.1	(23,21)	386397200.
213	(32,28)	98.2	103.1	2244.8	(23,21)	323184600.
214	(32,28)	97.3	102.2	2263.4	(23,21)	263832700.
215	(31,28)	97.1	102.0	2284.6	(23,21)	250491600.
216	(32,28)	97.2	102.3	2302.8	(23,21)	268027400.
217	(32,28)	96.7	102.3	2274.4	(23,21)	267424800.
218	(32,29)	96.1	101.6	2193.6	(23,21)	229509800.
219	(31,29)	95.9	100.5	2166.3	(23,21)	175820900.
220	(31,29)	95.4	99.6	2208.3	(23,21)	145020000.
221	(31,29)	95.4	99.8	2238.8	(23,21)	149922700.
222	(32,28)	95.5	100.1	2265.0	(23,21)	163058300.
223	(33,28)	94.8	99.9	2226.3	(24,20)	154113800.
224	(33,29)	94.2	98.8	2181.7	(24,21)	120088800.
225	(33,29)	93.9	97.2	2222.6	(24,21)	82579760.
226	(32,28)	93.4	96.3	2246.6	(23,21)	67982780.
227	(32,28)	93.3	96.9	2249.2	(23,21)	78449540.
228	(33,28)	92.9	97.6	2225.6	(24,20)	90875680.
229	(34,28)	92.5	97.3	2184.4	(25,20)	85782000.
230	(34,29)	91.8	96.0	2185.2	(25,21)	63048160.
231	(33,28)	90.8	93.9	2257.9	(24,20)	38634240.
233	(32,28)	89.9	93.2	2289.7	(23,21)	33352000.
234	(34,28)	89.7	94.1	2255.4	(25,20)	40678140
235	(34,28)	89.0	94.0	2215.9	(25,20)	40206660
236	(34,28)	87.6	92.8	2212.3	(25,20)	30270960.

TRACK TRAIL FOR SPTWANTTO.DA

BLOCK	(IR3D, JR3D)	AMAX	AMAXUP	RSUM	LOG COORD'S	POWER
256	(30, 30)	91.8	93.2	2196.4	(22, 22)	33270580
257	(30, 30)	92.8	94.6	2192.0	(22, 22)	45704910
258	(30, 30)	93.7	96.0	2212.0	(22, 22)	62702290
259	(29, 31)	94.5	96.8	2153.0	(21, 23)	75545620.
260	(28, 31)	95.2	97.2	2162.3	(21, 23)	82878780.
261	(27, 31)	95.9	98.0	2156.1	(20, 23)	77133020
262	(27, 31)	96.4	99.2	2189.2	(20, 23)	130387600.
263	(28, 31)	97.0	100.1	2203.2	(21, 23)	162442500
264	(28, 32)	97.6	100.7	2099.4	(21, 23)	185021300.
265	(27, 32)	98.3	101.7	2088.0	(20, 24)	235431100.
266	(26, 32)	98.8	103.5	2010.6	(19, 24)	354078500.
267	(28, 30)	100.5	105.0	2171.3	(21, 22)	503100900
268	(26, 33)	101.9	105.8	2005.6	(19, 24)	597759500
269	(26, 33)	103.1	106.1	2000.4	(19, 24)	649182200
270	(26, 33)	104.5	107.1	1994.5	(19, 24)	808249100
271	(26, 32)	105.6	108.5	2039.3	(19, 24)	1121923000
272	(27, 32)	106.6	109.6	2086.5	(20, 24)	1430985000
273	(26, 33)	107.6	110.0	1998.9	(19, 24)	1596412000
274	(26, 34)	108.4	110.6	1947.1	(19, 25)	1825874000
275	(26, 34)	109.4	111.7	1927.7	(19, 25)	2371358000.
276	(26, 34)	110.5	112.9	1932.5	(19, 25)	3080001000
277	(27, 33)	111.3	113.4	1976.9	(20, 24)	3495322000.
278	(27, 34)	111.8	113.5	1902.6	(20, 25)	3554081000
279	(27, 34)	112.0	113.7	1919.3	(20, 25)	3695274000
280	(27, 33)	111.9	114.1	1991.4	(20, 24)	4112031000
281	(26, 33)	111.6	114.4	1974.8	(19, 24)	4354716000
282	(27, 33)	110.9	114.1	2007.8	(20, 24)	4035317000
283	(27, 32)	110.0	113.4	2029.7	(20, 24)	3475303000
284	(27, 32)	108.9	113.1	2101.2	(20, 24)	3259024000
285	(27, 32)	108.2	113.1	2123.1	(20, 24)	3265308000
286	(27, 32)	108.0	112.9	2121.4	(20, 24)	3067395000
287	(27, 32)	107.6	112.3	2140.2	(20, 24)	2689383000
288	(27, 31)	107.0	112.0	2133.1	(20, 23)	2515425000.
289	(27, 31)	106.4	112.1	2144.8	(20, 23)	2592142000
290	(27, 31)	105.8	112.1	2195.4	(20, 23)	2560376000
291	(27, 31)	105.5	111.8	2192.7	(20, 23)	2372031000
292	(27, 31)	106.1	111.7	2228.3	(20, 23)	2323460000
293	(26, 31)	106.9	112.0	2265.9	(19, 23)	2495263000
294	(26, 31)	107.6	112.1	2241.8	(19, 23)	2593495000
295	(27, 31)	108.2	112.1	2188.7	(20, 23)	2551694000
296	(26, 32)	108.6	112.2	2158.7	(19, 24)	2622690000
297	(26, 32)	108.7	112.5	2184.9	(19, 24)	2840930000
298	(26, 32)	108.8	112.6	2183.4	(19, 24)	2894854000
299	(26, 32)	108.7	112.4	2175.6	(19, 24)	2727357000.
300	(26, 32)	108.5	112.2	2202.2	(19, 24)	2654520000
301	(26, 31)	108.1	112.4	2258.8	(19, 23)	2765952000
302	(25, 31)	107.7	112.3	2275.0	(19, 23)	2722492000
303	(26, 31)	107.0	111.8	2294.5	(19, 23)	2386660000
304	(26, 31)	106.4	111.3	2289.5	(19, 23)	2120422000.
305	(26, 30)	105.9	111.3	2354.8	(19, 22)	2153989000.
306	(25, 30)	105.5	111.5	2328.5	(19, 23)	2219295000
307	(25, 31)	105.2	111.2	2336.1	(19, 23)	2086792000
308	(26, 30)	105.2	111.0	2316.0	(19, 22)	2008973000
309	(25, 30)	104.9	111.4	2381.1	(19, 23)	2108461000
310	(25, 30)	104.9	111.7	2356.5	(19, 23)	2371167000
311	(25, 31)	104.7	111.6	2341.1	(19, 23)	2290481000
312	(25, 31)	104.8	111.4	2331.7	(19, 23)	2204122000
313	(25, 30)	104.7	111.8	2356.3	(19, 23)	2382583000
314	(25, 30)	104.7	112.2	2364.1	(19, 23)	2606999000

315	(25,30)	104.6	112.1	2395.8	(19,23)	2549842000
316	(25,31)	104.8	111.9	2328.9	(19,23)	2447150000.
317	(25,31)	105.2	112.2	2358.5	(19,23)	2637991000.
318	(25,31)	105.5	112.7	2352.4	(19,23)	2951667000
319	(25,31)	105.7	112.8	2388.7	(19,23)	2993813000
320	(25,31)	105.8	112.7	2329.8	(19,23)	2931602000
321	(25,31)	105.7	113.0	2354.4	(19,23)	3137209000.
322	(24,31)	105.9	113.4	2373.7	(18,23)	3474761000.
323	(25,31)	106.3	113.5	2360.1	(19,23)	3540949000.
324	(25,31)	106.7	113.5	2331.4	(19,23)	3536958000
325	(24,31)	107.0	113.9	2352.1	(18,23)	3898553000.
326	(24,31)	107.3	114.4	2385.4	(18,23)	4405866000.
327	(24,31)	107.4	114.5	2397.9	(18,23)	4449804000.
328	(25,31)	107.5	114.2	2377.0	(19,23)	4169313000
329	(25,30)	107.6	114.2	2395.3	(19,23)	4215638000
330	(24,30)	107.6	114.6	2437.8	(18,23)	4578267000.
331	(24,30)	107.5	114.6	2453.8	(18,23)	4589887000.
332	(25,30)	107.3	114.2	2452.7	(19,23)	4166484000.
333	(24,30)	107.1	114.0	2464.3	(18,23)	3964657000
334	(24,30)	106.8	114.2	2493.7	(18,23)	4169780000
335	(24,30)	106.4	114.3	2502.3	(18,23)	4225498000
336	(24,30)	106.2	114.0	2488.5	(18,23)	3937446000
337	(25,30)	106.3	113.9	2476.3	(19,23)	3856414000
338	(24,30)	106.4	114.2	2497.0	(18,23)	4164421000
339	(24,30)	106.4	114.3	2509.1	(18,23)	4310512000
340	(25,29)	106.2	114.0	2506.2	(19,22)	3906801000
341	(25,29)	106.1	113.6	2515.7	(19,22)	3671728000
342	(24,29)	106.0	113.7	2551.5	(18,22)	3698917000
343	(24,29)	105.9	113.7	2571.8	(18,22)	3703329000
344	(24,29)	105.8	113.2	2558.2	(18,22)	3314570000.
345	(25,29)	105.8	112.5	2546.2	(19,22)	2827434000
346	(24,29)	105.8	112.2	2572.3	(18,22)	2610010000
347	(24,29)	105.8	112.0	2601.4	(18,22)	2533510000
348	(25,29)	105.7	111.7	2599.2	(19,22)	2327312000
349	(25,29)	105.6	111.3	2581.5	(19,22)	2119466000
350	(25,29)	105.4	111.2	2587.4	(19,22)	2101544000
351	(25,29)	105.2	111.3	2611.8	(19,22)	2137599000
352	(25,29)	105.0	111.0	2597.2	(19,22)	1994723000
353	(26,28)	104.8	110.4	2579.4	(20,21)	1744697000
354	(25,28)	104.5	109.9	2592.2	(19,21)	1565559000
355	(25,28)	104.1	109.6	2638.1	(19,21)	1436304000
356	(25,28)	103.6	108.9	2637.1	(19,21)	1227991000
357	(26,28)	103.3	107.9	2606.0	(20,21)	983610600
358	(26,28)	102.5	107.2	2588.7	(20,21)	824762100
359	(26,28)	101.5	106.7	2608.5	(20,21)	742676700
360	(26,28)	99.9	106.0	2605.1	(20,21)	628121600
361	(26,28)	98.8	104.7	2572.2	(20,21)	471743000.
362	(28,28)	97.6	103.4	2516.9	(21,21)	348748500
363	(28,27)	96.6	102.6	2483.0	(21,20)	287827500
364	(28,27)	95.5	101.8	2476.1	(21,20)	241111100
365	(29,27)	95.2	100.4	2481.5	(22,20)	173427500
366	(29,28)	94.2	98.0	2452.0	(22,21)	101064500
367	(29,28)	92.8	95.4	2452.6	(22,21)	55010610
368	(29,28)	91.8	94.0	2474.9	(22,21)	40189490.
369	(31,28)	91.2	94.0	2444.0	(23,21)	39829300
370	(31,28)	91.0	93.9	2395.5	(23,21)	39295020.
371	(31,28)	90.4	93.0	2308.0	(23,21)	31692130
482	(28,28)	86.0	93.8	2680.2	(21,21)	37741580
483	(28,28)	87.4	94.7	2651.1	(21,21)	47219900
484	(28,28)	88.0	95.5	2626.1	(21,21)	56734050
485	(28,28)	87.6	96.2	2651.0	(21,21)	65406180
486	(27,27)	86.5	96.6	2676.5	(20,20)	71622960
487	(28,27)	85.9	96.6	2671.2	(21,20)	73076640.
488	(28,28)	88.1	96.5	2643.1	(21,21)	71196270
489	(29,28)	89.6	96.5	2610.2	(22,21)	70570510
490	(29,28)	90.3	96.7	2643.8	(22,21)	74202460

491	(29,28)	90.7	96.9	2645.2	(22,21)	78364080.
492	(28,28)	90.8	96.8	2672.8	(21,21)	76500400.
493	(28,28)	90.7	96.3	2717.2	(21,21)	68339380.
494	(27,27)	90.6	95.9	2756.5	(20,20)	61662270.
495	(27,27)	90.7	95.9	2764.4	(20,20)	62354160.
496	(27,27)	91.5	96.3	2776.2	(20,20)	66954690.
497	(27,27)	92.8	96.5	2739.1	(20,20)	71245440.
498	(28,27)	93.7	96.9	2701.8	(21,20)	77587330.
499	(28,28)	94.4	97.5	2720.5	(21,21)	89524720.
500	(28,28)	94.9	98.1	2705.8	(21,21)	103329500.
501	(28,28)	95.1	98.5	2683.3	(21,21)	111156600.
502	(28,28)	95.1	98.4	2661.9	(21,21)	108489800.
503	(28,28)	95.0	97.9	2651.9	(21,21)	97299920.
504	(29,28)	94.7	97.2	2616.9	(22,21)	83954220.
505	(29,28)	94.4	96.9	2604.0	(22,21)	77201440.
506	(29,28)	93.8	97.3	2624.4	(22,21)	85253870.
507	(30,27)	94.6	98.9	2625.9	(22,20)	123822300.
508	(30,27)	96.4	101.2	2569.9	(22,20)	207958300.
509	(30,27)	97.4	103.0	2538.9	(22,20)	319111900.
510	(30,27)	99.7	104.2	2484.2	(22,20)	412339200.
511	(30,28)	101.9	105.0	2426.1	(22,21)	501625300.
512	(31,28)	103.5	106.3	2381.0	(23,21)	680780500
513	(32,28)	104.8	107.9	2355.7	(23,21)	967620400
514	(33,28)	105.8	108.9	2297.7	(24,20)	1221661000
515	(33,28)	106.7	109.4	2313.6	(24,20)	1374414000.
516	(32,28)	107.3	110.0	2337.8	(23,21)	1586146000
517	(32,28)	107.8	110.9	2365.8	(23,21)	1952614000
518	(33,27)	108.2	111.5	2334.6	(24,20)	2261239000
519	(32,27)	108.6	111.7	2350.3	(24,20)	2353014000
520	(31,28)	109.1	112.0	2377.6	(23,21)	2492333000
521	(31,27)	109.6	112.7	2424.3	(23,20)	2924852000
522	(32,27)	109.9	113.3	2393.5	(24,20)	3363267000
523	(32,27)	110.4	113.3	2353.5	(24,20)	3384532000
524	(32,27)	110.8	113.1	2372.4	(24,20)	3204003000
525	(31,27)	111.0	113.2	2407.4	(23,20)	3319167000
526	(31,27)	111.1	113.6	2404.8	(23,20)	3669798000
527	(32,27)	110.9	113.7	2366.0	(24,20)	3718324000
528	(31,27)	110.6	113.2	2377.3	(23,20)	3347934000
529	(31,27)	110.4	112.8	2432.5	(23,20)	3023624000
530	(31,27)	110.2	112.8	2466.0	(23,20)	2992752000
531	(31,27)	109.9	112.8	2452.4	(23,20)	2991101000
532	(31,27)	109.3	112.4	2413.3	(23,20)	2743840000
533	(30,27)	108.6	111.9	2418.7	(22,20)	2429077000
534	(30,27)	108.1	111.6	2455.9	(22,20)	2284090000
535	(30,27)	107.9	111.6	2473.3	(22,20)	2266616000
536	(31,27)	107.6	111.4	2434.0	(23,20)	2164812000
537	(31,27)	107.0	110.9	2414.7	(23,20)	1949442000
538	(30,27)	106.5	110.5	2432.4	(22,20)	1788193000
539	(30,27)	106.1	110.4	2469.2	(22,20)	1750462000
540	(30,27)	105.8	110.4	2473.1	(22,20)	1737767000
541	(31,27)	105.4	110.1	2442.9	(23,20)	1627714000
542	(31,27)	104.9	109.7	2410.5	(23,20)	1472843000.
543	(31,27)	104.5	109.5	2425.7	(23,20)	1412667000
544	(31,27)	104.5	109.7	2447.7	(23,20)	1477165000
545	(31,27)	104.3	109.9	2443.3	(23,20)	1540067000
546	(31,27)	104.5	109.7	2397.7	(23,20)	1483734000
547	(31,27)	104.8	109.3	2377.8	(23,20)	1352838000
548	(31,27)	104.9	109.1	2389.7	(23,20)	1291025000
549	(31,27)	104.9	109.3	2412.2	(23,20)	1348240000
550	(31,27)	104.8	109.5	2411.5	(23,20)	1411770000
551	(31,27)	104.7	109.3	2369.4	(23,20)	1357972000
552	(31,27)	104.6	108.8	2348.0	(23,20)	1210541000
553	(31,27)	104.4	108.4	2355.2	(23,20)	1101789000
554	(31,27)	104.1	108.4	2336.8	(23,20)	1100941000
555	(32,27)	103.8	108.5	2362.4	(24,20)	1132837000
556	(32,27)	103.8	108.4	2320.0	(24,20)	1100005000

557	(32,27)	103.9	108.1	2324.2	(24,20)	1019267000.
558	(31,27)	103.6	108.0	2369.1	(23,20)	999531800.
559	(31,27)	103.7	108.3	2356.8	(23,20)	1081861000.
560	(31,27)	103.6	108.6	2366.1	(23,20)	1158880000.
561	(32,27)	104.0	108.5	2317.0	(24,20)	1110231000.
562	(32,28)	104.1	107.8	2233.2	(23,21)	952522200.
563	(31,28)	104.0	107.2	2263.4	(23,21)	832780500
564	(31,28)	103.9	107.3	2270.2	(23,21)	856154400.
565	(32,27)	103.9	107.8	2303.4	(24,20)	946860800.
566	(32,28)	103.8	107.8	2252.7	(23,21)	954942700
567	(33,28)	103.7	107.3	2210.6	(24,20)	843602900.
568	(32,28)	103.3	106.6	2243.2	(23,21)	721104100.
569	(31,28)	103.1	106.6	2260.1	(23,21)	718455800
570	(31,28)	103.0	107.1	2290.5	(23,21)	809116400
571	(32,28)	102.9	107.3	2266.1	(23,21)	845457200
572	(32,28)	102.7	106.7	2209.7	(23,21)	748745200
573	(32,28)	102.3	105.7	2221.8	(23,21)	590080500
574	(31,28)	101.9	105.1	2284.2	(23,21)	510674200.
575	(31,28)	101.7	105.4	2285.7	(23,21)	550686200.
576	(32,28)	101.7	105.9	2292.2	(23,21)	611042300.
577	(32,28)	101.6	105.7	2232.6	(23,21)	594814500
578	(32,28)	101.5	105.1	2182.9	(23,21)	511034400.
579	(31,28)	101.3	104.6	2242.1	(23,21)	453522700.
580	(31,28)	101.3	104.8	2215.3	(23,21)	483897600
581	(31,28)	101.2	105.4	2204.6	(23,21)	547554800.
582	(32,28)	101.0	105.4	2170.1	(23,21)	548880600.
583	(32,29)	100.9	104.7	2155.6	(23,21)	464049200.
584	(32,28)	100.2	103.6	2192.1	(23,21)	365758200
585	(31,28)	100.0	103.4	2232.1	(23,21)	345411300.
586	(31,28)	99.9	104.0	2270.0	(23,21)	398950400
587	(32,28)	99.9	104.4	2242.7	(23,21)	439902500
588	(33,29)	100.4	104.1	2156.0	(24,21)	410913800
589	(33,29)	100.0	103.3	2162.2	(24,21)	335011100
590	(31,29)	99.3	102.6	2233.5	(23,21)	291068200
591	(31,29)	99.1	103.0	2234.8	(23,21)	316896000.
592	(31,29)	99.2	103.6	2227.8	(23,21)	364476400
593	(32,29)	99.3	103.6	2171.8	(23,21)	366898700
594	(33,29)	99.1	102.9	2104.2	(24,21)	311427300
595	(33,29)	98.5	101.9	2148.6	(24,21)	248131000.
596	(32,29)	98.1	101.8	2192.2	(23,21)	237535500
597	(32,29)	98.0	102.4	2175.6	(23,21)	275082000
598	(32,29)	97.8	102.8	2170.8	(23,21)	300306700.
599	(33,29)	97.9	102.4	2120.3	(24,21)	273645800
600	(33,29)	97.3	101.2	2108.0	(24,21)	209853600
601	(32,29)	96.2	100.1	2197.3	(23,21)	162253200
602	(31,29)	95.9	100.2	2234.3	(23,21)	165442200.
603	(32,29)	95.9	100.9	2223.9	(23,21)	196007100
604	(32,29)	95.9	101.2	2190.6	(23,21)	207627500
605	(33,29)	96.2	100.6	2157.1	(24,21)	181543700
606	(32,30)	95.7	99.3	2126.3	(23,22)	135480100.
607	(31,29)	94.6	98.2	2201.1	(23,21)	105802600.
608	(30,29)	93.9	98.4	2190.4	(22,21)	109619000.
609	(31,29)	93.9	99.1	2228.8	(23,21)	127975600.
610	(32,29)	94.1	99.3	2181.7	(23,21)	133910100.
611	(31,30)	94.4	98.8	2158.8	(23,22)	119503600
612	(31,30)	93.3	97.8	2170.2	(23,22)	96289570.
613	(31,30)	92.5	97.2	2209.4	(23,22)	82603040.
614	(31,30)	93.2	97.2	2230.9	(23,22)	83571950
615	(31,30)	93.2	97.5	2221.2	(23,22)	88243380
616	(31,30)	92.2	97.4	2161.0	(23,22)	87439060
617	(32,30)	92.9	97.0	2149.0	(23,22)	80205120
618	(32,30)	92.9	96.4	2114.2	(23,22)	69979040
619	(33,30)	91.9	95.9	2149.1	(24,22)	62073900
620	(33,30)	91.7	95.7	2194.0	(24,22)	58684340
621	(33,30)	92.0	95.5	2202.7	(24,22)	56302900
622	(33,30)	91.6	95.1	2194.3	(24,22)	51057150
623	(32,30)	90.7	94.2	2216.9	(23,22)	41716560
624	(31,29)	89.4	93.0	2294.5	(23,21)	31781070

TRACK TRAIL FOR SPTWANNA.DA

BLOCK	(IR3D, JR3D)	AMAX	AMAXUP	RSUM	LOC COORD'S	POWER
236	(28, 29)	89.5	93.6	2323.4	(21, 22)	36708800.
237	(29, 29)	90.7	94.6	2355.8	(22, 22)	45451310.
238	(29, 29)	92.6	95.5	2346.0	(22, 22)	55930720.
239	(28, 30)	94.1	96.4	2298.7	(21, 22)	69707630.
240	(29, 30)	95.3	97.3	2268.5	(21, 22)	84442700.
241	(29, 30)	96.0	97.9	2270.1	(21, 22)	97069920.
242	(27, 30)	96.7	98.5	2251.6	(20, 22)	112639600.
243	(27, 30)	97.3	99.5	2251.5	(20, 22)	140310400.
244	(26, 31)	97.7	100.5	2276.1	(19, 23)	176929200.
245	(27, 31)	98.1	101.1	2265.3	(20, 23)	204634000.
246	(27, 30)	98.2	101.4	2285.7	(20, 22)	218691400.
247	(27, 30)	98.6	102.0	2300.5	(20, 22)	249763800.
248	(26, 30)	98.9	103.0	2273.0	(19, 22)	316095700
249	(27, 29)	99.2	103.8	2321.1	(20, 22)	383092500.
250	(26, 31)	99.4	104.0	2247.2	(19, 23)	398959900.
251	(27, 31)	99.6	103.8	2207.5	(20, 23)	383714000
252	(26, 31)	100.0	104.3	2201.6	(19, 23)	427902000.
253	(26, 31)	100.2	105.4	2217.5	(19, 23)	551408600.
254	(26, 31)	100.4	106.1	2235.5	(19, 23)	652816900.
255	(26, 31)	100.9	106.1	2230.4	(19, 23)	644424200.
256	(27, 31)	101.7	105.9	2220.6	(20, 23)	623437100.
257	(27, 31)	102.6	106.7	2198.7	(20, 23)	742844700.
258	(26, 31)	103.3	107.8	2208.3	(19, 23)	962472400.
259	(26, 30)	104.1	108.3	2241.5	(19, 22)	1078486000.
260	(26, 31)	104.7	108.2	2173.1	(19, 23)	1040649000.
261	(26, 31)	105.5	108.5	2150.7	(19, 23)	1116161000.
262	(26, 31)	106.1	109.7	2117.8	(19, 23)	1469679000.
263	(26, 30)	106.7	110.7	2205.9	(19, 22)	1865476000.
264	(25, 32)	107.2	110.9	2127.7	(19, 24)	1952262000.
265	(26, 32)	107.6	110.7	2131.4	(19, 24)	1845536000
266	(26, 32)	108.1	111.1	2101.9	(19, 24)	2051577000.
267	(25, 32)	108.7	112.3	2094.3	(19, 24)	2691094000.
268	(25, 32)	109.1	113.1	2128.9	(19, 24)	3245401000.
269	(25, 32)	109.1	113.0	2123.0	(19, 24)	3197960000.
270	(25, 33)	108.6	112.5	2072.4	(18, 24)	2805266000
271	(25, 33)	108.1	112.4	2060.1	(18, 24)	2724079000.
272	(25, 32)	107.6	112.9	2100.6	(19, 24)	3085992000.
273	(25, 31)	107.1	113.2	2159.2	(19, 23)	3332034000
274	(25, 33)	106.9	112.9	2082.0	(18, 24)	3126049000.
275	(25, 33)	107.5	112.8	2084.4	(18, 24)	3010891000
276	(25, 33)	107.9	113.5	2080.1	(18, 24)	3543747000.
277	(25, 33)	108.5	114.4	2093.7	(18, 24)	4345217000.
278	(25, 33)	108.8	114.6	2122.4	(18, 24)	4528665000.
279	(25, 33)	109.0	114.2	2108.0	(18, 24)	4190246000.
280	(26, 33)	109.2	114.5	2084.2	(19, 24)	4418650000
281	(25, 33)	110.1	115.4	2106.2	(18, 24)	5549244000
282	(25, 33)	110.9	116.1	2106.8	(18, 24)	6481605000
283	(25, 34)	111.1	116.0	2056.5	(18, 25)	6255047000
284	(26, 34)	111.4	115.6	2040.7	(19, 25)	5705548000
285	(26, 33)	111.7	115.9	2066.9	(19, 24)	6115971000
286	(25, 33)	111.9	116.5	2096.0	(18, 24)	7135913000
287	(26, 33)	112.0	116.7	2102.1	(19, 24)	7331275000
288	(26, 33)	111.9	116.1	2106.2	(19, 24)	6478201000
289	(26, 33)	111.8	115.8	2087.8	(19, 24)	6094905000
290	(25, 33)	111.7	116.4	2124.5	(18, 24)	6861742000
291	(25, 33)	111.6	116.8	2151.2	(18, 24)	7557763000
292	(26, 33)	111.4	116.4	2149.1	(19, 24)	6993744000
293	(26, 33)	111.3	115.8	2129.6	(19, 24)	6075929000
294	(25, 32)	111.1	115.9	2159.6	(19, 24)	6236860000

295	(25, 32)	111.0	116.5	2190.8	(19, 24)	7155094000
296	(25, 33)	110.9	116.6	2180.1	(18, 24)	7268770000
297	(25, 33)	110.7	116.1	2182.0	(18, 24)	6413578000
298	(25, 32)	110.7	115.8	2177.9	(19, 24)	6014329000
299	(25, 32)	110.7	116.2	2212.2	(19, 24)	6651675000
300	(25, 32)	110.6	116.6	2217.6	(19, 24)	7204524000
301	(25, 32)	110.5	116.3	2222.7	(19, 24)	6704189000
302	(25, 32)	110.5	115.8	2182.6	(19, 24)	6075609000
303	(25, 32)	110.7	116.1	2190.3	(19, 24)	6441882000
304	(25, 32)	110.9	116.6	2240.3	(19, 24)	7309013000
305	(25, 32)	111.0	116.6	2226.0	(19, 24)	7308325000
306	(25, 32)	111.0	116.2	2216.1	(19, 24)	6584459000
307	(25, 32)	111.1	116.1	2202.0	(19, 24)	6481195000
308	(25, 32)	111.1	116.6	2250.9	(19, 24)	7289631000
309	(25, 32)	111.1	116.9	2218.4	(19, 24)	7833919000
310	(25, 32)	111.1	116.7	2209.4	(19, 24)	7430328000
311	(25, 32)	111.4	116.6	2205.4	(19, 24)	7212687000
312	(25, 32)	111.6	117.0	2219.5	(19, 24)	8021258000
313	(24, 32)	111.8	117.5	2230.3	(18, 24)	8971563000
314	(25, 32)	111.7	117.4	2238.5	(19, 24)	8689000000
315	(25, 32)	111.7	116.9	2211.8	(19, 24)	7771652000
316	(25, 32)	111.8	116.9	2230.9	(19, 24)	7715729000
317	(25, 31)	111.9	117.3	2302.6	(19, 23)	8502256000
318	(25, 31)	111.8	117.4	2298.7	(19, 23)	8617939000
319	(25, 32)	111.7	116.9	2265.7	(19, 24)	7686234000
320	(25, 31)	111.6	116.6	2284.3	(19, 23)	7190966000
321	(24, 31)	111.5	117.0	2307.8	(18, 23)	7857861000
322	(24, 31)	111.4	117.3	2320.9	(18, 23)	8481026000
323	(24, 31)	111.0	116.9	2341.2	(18, 23)	7779283000
324	(25, 30)	110.7	116.3	2357.9	(19, 23)	6739681000
325	(25, 30)	110.5	116.3	2394.1	(19, 23)	6825288000
326	(24, 30)	110.3	116.9	2419.5	(18, 23)	7688962000
327	(25, 29)	109.9	116.9	2460.7	(19, 22)	7676207000
328	(25, 30)	109.5	116.2	2434.9	(19, 23)	6672777000
329	(25, 29)	109.1	115.9	2461.9	(19, 22)	6106698000
330	(25, 29)	109.0	116.2	2492.4	(19, 22)	6570156000
331	(24, 29)	108.9	116.4	2501.5	(18, 22)	6938620000
332	(25, 29)	108.5	116.0	2491.9	(19, 22)	6263218000
333	(25, 29)	108.2	115.4	2490.4	(19, 22)	5442507000
334	(25, 28)	108.1	115.4	2515.6	(19, 21)	5543453000
335	(25, 28)	108.2	115.9	2528.9	(19, 21)	6140588000
336	(25, 28)	107.9	115.7	2537.2	(19, 21)	5952991000
337	(25, 28)	107.4	115.0	2539.9	(19, 21)	5047259000
338	(25, 28)	107.0	114.6	2551.8	(19, 21)	4534444000
339	(25, 27)	107.1	114.8	2590.6	(19, 21)	4823765000
340	(25, 27)	107.1	115.0	2602.7	(19, 21)	5035430000
341	(25, 28)	107.0	114.5	2584.8	(19, 21)	4457251000
342	(26, 28)	106.9	113.6	2593.3	(20, 21)	3672364000
343	(26, 27)	106.7	113.4	2621.7	(20, 21)	3462717000
344	(25, 27)	106.4	113.6	2661.3	(19, 21)	3631850000
345	(25, 27)	105.7	113.2	2664.3	(19, 21)	3349401000
346	(26, 27)	105.3	111.8	2643.7	(20, 21)	2422154000
347	(26, 28)	105.0	109.5	2582.2	(20, 21)	1417504000
348	(27, 28)	104.7	107.6	2517.8	(20, 21)	910426100
349	(29, 28)	104.9	107.4	2489.8	(22, 21)	874510800
350	(31, 28)	105.3	107.7	2361.4	(23, 21)	927775500
351	(31, 28)	105.8	107.5	2321.4	(23, 21)	892328200
352	(31, 28)	106.2	107.3	2356.4	(23, 21)	848254700
353	(31, 28)	106.4	107.6	2382.6	(23, 21)	915726600
354	(32, 28)	106.5	108.2	2370.4	(23, 21)	1040952000
355	(32, 29)	106.6	108.3	2327.6	(23, 21)	1066810000
356	(32, 29)	106.6	107.9	2323.8	(23, 21)	968175400
357	(32, 28)	106.5	107.4	2364.4	(23, 21)	880982300
358	(32, 28)	106.4	107.5	2381.0	(23, 21)	895463700
359	(32, 28)	106.2	107.7	2353.1	(23, 21)	933333000
360	(32, 29)	106.2	107.5	2317.1	(23, 21)	892430300

361	(32, 28)	106. 2	107. 1	2342. 3	(23, 21)	812771600.
362	(31, 28)	106. 2	107. 1	2379. 7	(23, 21)	814728700.
363	(31, 28)	106. 4	107. 6	2416. 3	(23, 21)	912262700.
364	(30, 28)	106. 4	108. 0	2492. 6	(22, 21)	1006812000.
365	(28, 28)	106. 5	108. 4	2615. 8	(21, 21)	1105172000
366	(27, 27)	106. 6	109. 1	2682. 1	(20, 20)	1302845000.
367	(27, 27)	106. 4	110. 0	2681. 2	(20, 20)	1572759000.
368	(27, 27)	106. 1	110. 4	2668. 4	(20, 20)	1725034000.
369	(26, 27)	105. 7	110. 4	2658. 7	(20, 21)	1737991000.
370	(26, 27)	105. 4	110. 9	2685. 9	(20, 21)	1950085000.
371	(26, 27)	105. 2	112. 1	2678. 1	(20, 21)	2560082000.
372	(26, 27)	105. 8	113. 0	2679. 9	(20, 21)	3183031000
373	(26, 27)	105. 7	113. 1	2665. 2	(20, 21)	3239089000.
374	(26, 27)	105. 0	112. 4	2641. 4	(20, 21)	2778940000.
375	(26, 27)	104. 7	112. 0	2663. 9	(20, 21)	2491309000.
376	(25, 27)	104. 7	112. 4	2679. 2	(19, 21)	2752585000.
377	(25, 27)	104. 7	112. 9	2698. 6	(19, 21)	3095024000.
378	(26, 27)	104. 5	112. 6	2689. 0	(20, 21)	2899453000
379	(26, 27)	104. 5	111. 7	2667. 3	(20, 21)	2320350000.
380	(26, 27)	104. 6	111. 2	2670. 8	(20, 21)	2079911000
381	(25, 27)	104. 6	111. 9	2675. 1	(19, 21)	2450430000
382	(25, 27)	104. 4	112. 6	2701. 1	(19, 21)	2866114000.
383	(26, 27)	104. 3	112. 3	2682. 6	(20, 21)	2714587000.
384	(26, 28)	104. 5	111. 4	2648. 0	(20, 21)	2187576000.
385	(26, 28)	104. 8	111. 1	2632. 9	(20, 21)	2035987000.
386	(25, 28)	105. 4	112. 0	2624. 9	(19, 21)	2529271000.
387	(25, 28)	105. 8	112. 9	2647. 2	(19, 21)	3058884000.
388	(26, 28)	105. 7	112. 7	2635. 1	(20, 21)	2941028000.
389	(26, 28)	105. 2	111. 5	2605. 5	(20, 21)	2261196000
390	(26, 28)	104. 9	110. 5	2575. 3	(20, 21)	1772800000
391	(25, 28)	105. 1	110. 9	2556. 2	(19, 21)	1935652000
392	(25, 28)	105. 3	111. 7	2563. 6	(19, 21)	2367781000
393	(25, 28)	105. 8	111. 8	2568. 3	(19, 21)	2403623000.
394	(26, 28)	105. 6	110. 8	2552. 6	(20, 21)	1910580000.
395	(25, 29)	105. 0	109. 4	2538. 2	(19, 22)	1387053000.
396	(25, 28)	104. 8	109. 3	2549. 5	(19, 21)	1339247000
397	(25, 28)	105. 1	110. 2	2520. 4	(19, 21)	1677411000.
398	(25, 29)	105. 3	110. 7	2539. 7	(19, 22)	1873663000.
399	(25, 29)	105. 0	110. 2	2529. 5	(19, 22)	1649981000.
400	(25, 29)	104. 3	108. 8	2527. 2	(19, 22)	1202420000.
401	(25, 28)	103. 4	107. 8	2581. 3	(19, 21)	964768500.
402	(25, 28)	103. 1	108. 4	2597. 8	(19, 21)	1089725000.
403	(25, 28)	103. 3	109. 1	2544. 2	(19, 21)	1296616000.
404	(25, 28)	103. 2	109. 0	2556. 7	(19, 21)	1267423000.
405	(25, 29)	101. 9	107. 8	2545. 2	(19, 22)	964279800
406	(25, 29)	99. 7	105. 9	2525. 1	(19, 22)	623250900.
407	(25, 28)	98. 1	104. 8	2556. 2	(19, 21)	479373600.
408	(25, 28)	97. 4	105. 2	2530. 2	(19, 21)	527997400.
409	(24, 28)	97. 9	105. 7	2561. 5	(18, 21)	583137800.
410	(25, 28)	97. 4	105. 2	2580. 0	(19, 21)	523669500
411	(25, 29)	96. 3	103. 7	2576. 2	(19, 22)	368505600.
412	(25, 28)	94. 6	101. 6	2587. 4	(19, 21)	230867300
413	(25, 28)	93. 6	100. 9	2604. 4	(19, 21)	194817100
414	(25, 28)	93. 9	101. 8	2607. 4	(19, 21)	237694000
415	(25, 28)	94. 5	102. 4	2563. 4	(19, 21)	277049600
416	(25, 28)	94. 2	102. 1	2577. 3	(19, 21)	259447300
417	(25, 28)	93. 2	100. 8	2606. 1	(19, 21)	192746500
418	(26, 28)	92. 5	99. 0	2628. 2	(20, 21)	126645200
419	(26, 28)	92. 4	98. 1	2667. 1	(20, 21)	102033500
420	(25, 28)	92. 5	98. 7	2675. 3	(19, 21)	117804600
421	(25, 28)	93. 4	99. 7	2634. 2	(19, 21)	147583800
422	(25, 28)	93. 8	100. 2	2612. 2	(19, 21)	164609700
423	(25, 29)	93. 1	99. 9	2599. 8	(19, 22)	155886600
424	(25, 29)	91. 7	99. 1	2592. 2	(19, 22)	128297200.
425	(25, 29)	90. 7	98. 0	2592. 9	(19, 22)	100955100
426	(25, 29)	91. 1	97. 5	2548. 4	(19, 22)	88290990

427	(25,29)	[illegible]	97.5	2481.5	(19,22)	89050270.
428	(25,29)	89.5	97.7	2502.0	(19,22)	93327950.
429	(25,29)	89.5	97.7	2545.0	(19,22)	93581170.
430	(26,29)	90.4	97.5	2547.4	(20,22)	88411230.
431	(26,29)	90.3	97.0	2540.6	(20,22)	78704460.
432	(26,[illegible])	89.9	96.3	2546.8	(20,22)	67539310.
433	([illegible],29)	90.7	95.9	2493.6	(20,22)	61449520.
434	(26,29)	91.8	96.2	2424.0	(20,22)	65957020.
435	(27,30)	93.0	97.0	2426.1	(20,22)	78679260.
436	(27,30)	93.9	97.6	2382.5	(20,22)	90603980.
437	(27,29)	94.2	97.8	2410.7	(20,22)	94667570.
438	(26,29)	93.7	97.6	2509.1	(20,22)	90267250.
439	(26,28)	92.5	97.0	2599.6	(20,21)	79857310.
440	(25,28)	90.8	96.2	2653.8	(19,21)	66663620.
441	(25,28)	89.0	95.3	2670.4	(19,21)	54112540.
442	(25,28)	87.4	94.4	2654.8	(19,21)	44005120.
443	(25,28)	85.7	93.5	2576.7	(19,21)	35783410.
447	(25,28)	85.4	93.2	2591.1	(19,21)	32836400.
448	(25,28)	87.0	93.7	2552.3	(19,21)	36744670.
449	(26,29)	87.7	93.4	2507.7	(20,22)	34944110.

Appendix J

The pictures appearing in this appendix are examples of the pictures used to obtain the results shown in Figure 5.15, section four, Chapter Five.

These pictures were taken, digitized, and provided courtesy of Robert L. Russel.

NORM

JOHNSON

HULTEN

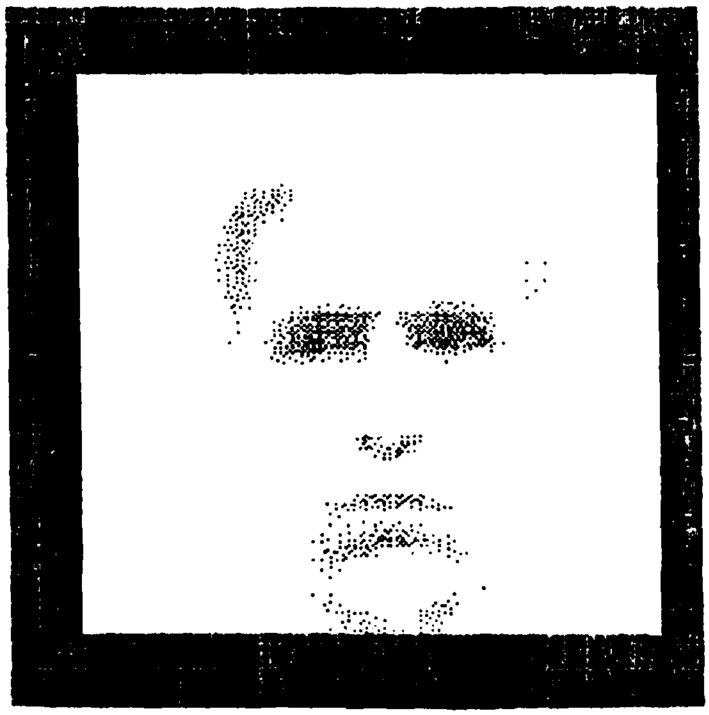

KABRISKY

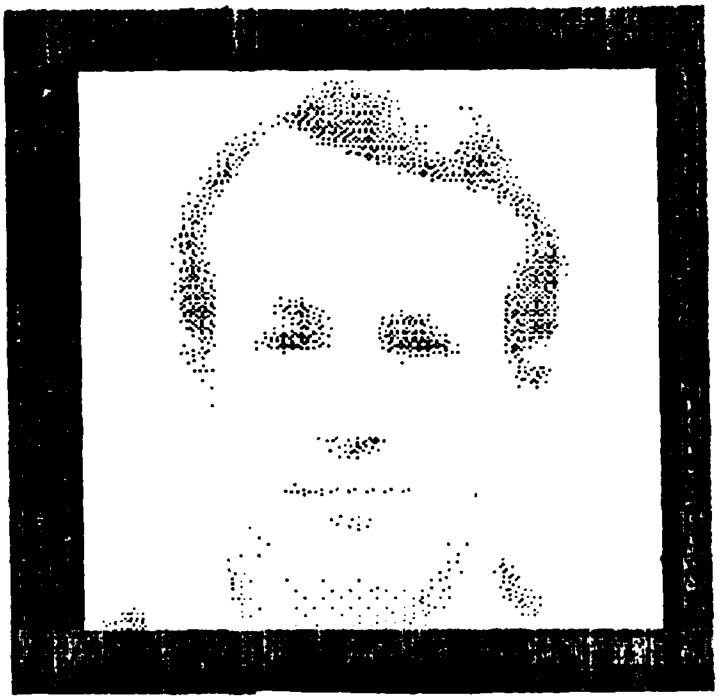

GRIFFIN

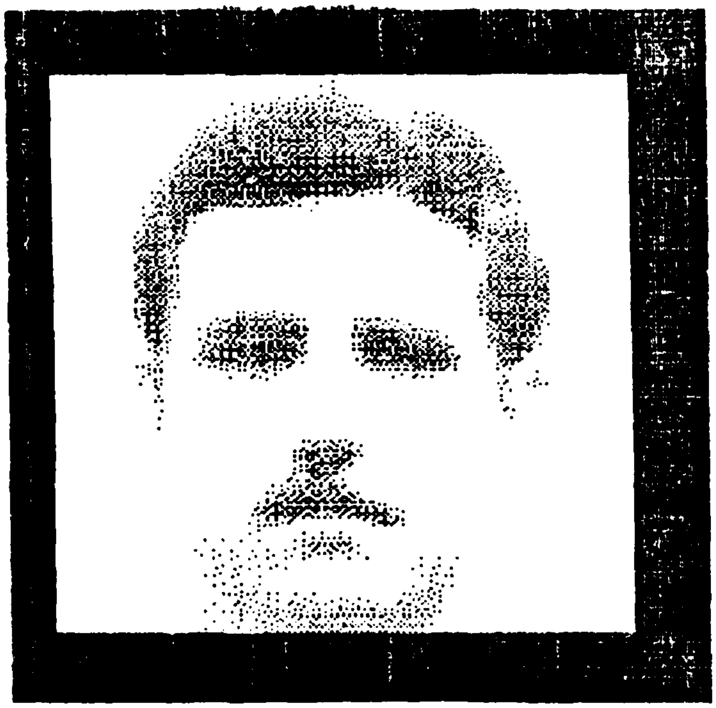

HALL

DONNER

JIMMY

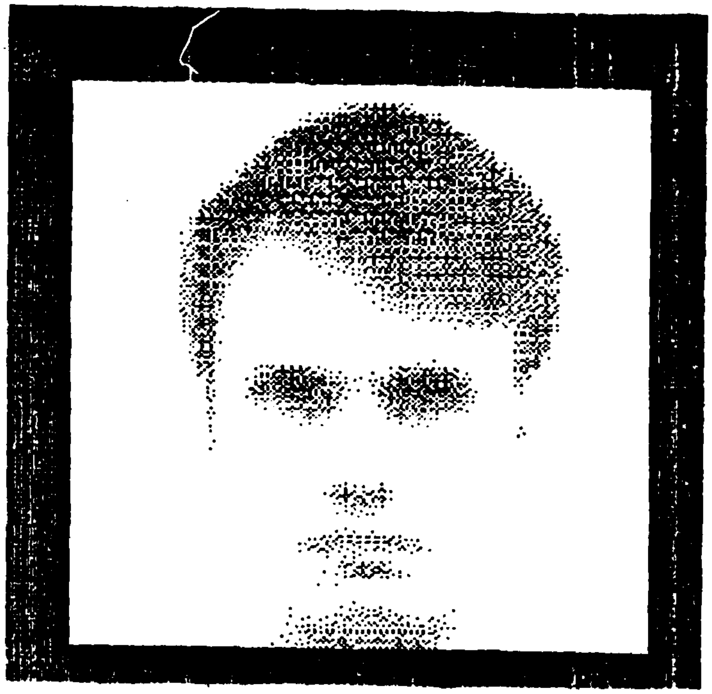

RUSSEL

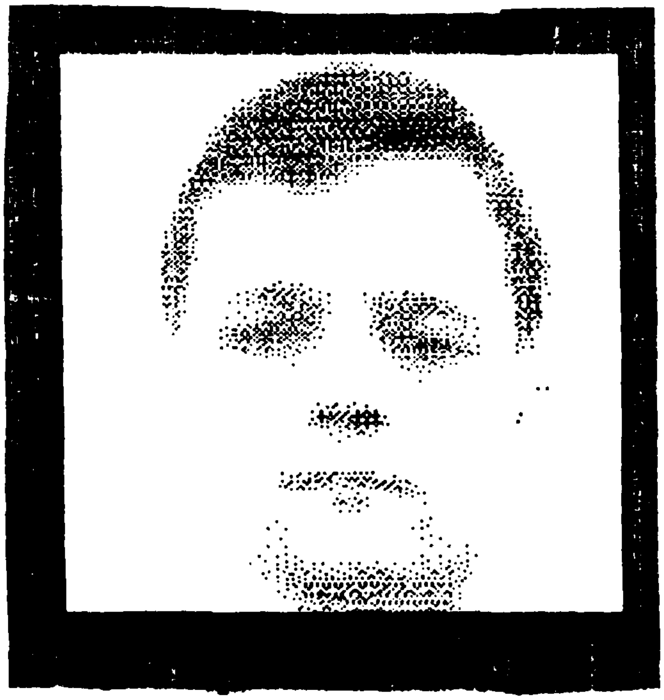

ROUTH

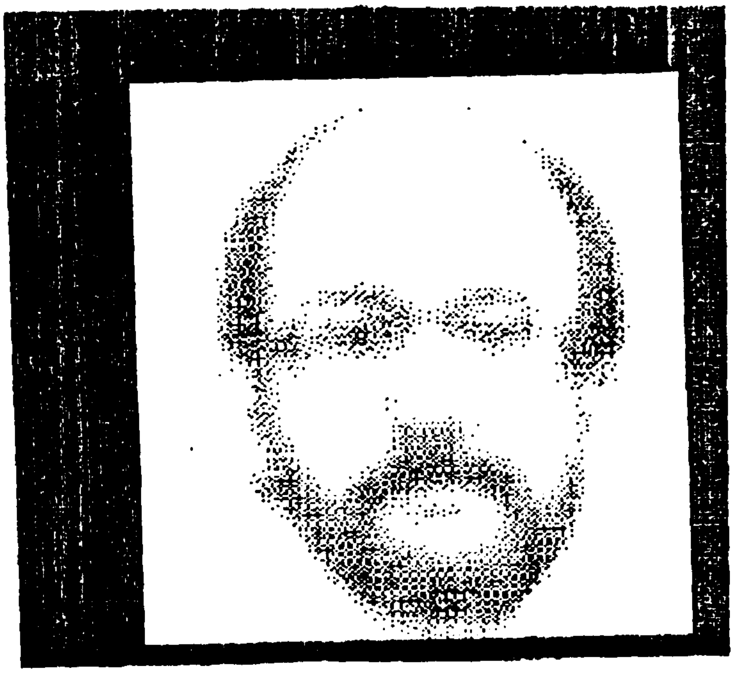

ZAMBON

CARL

GERACE

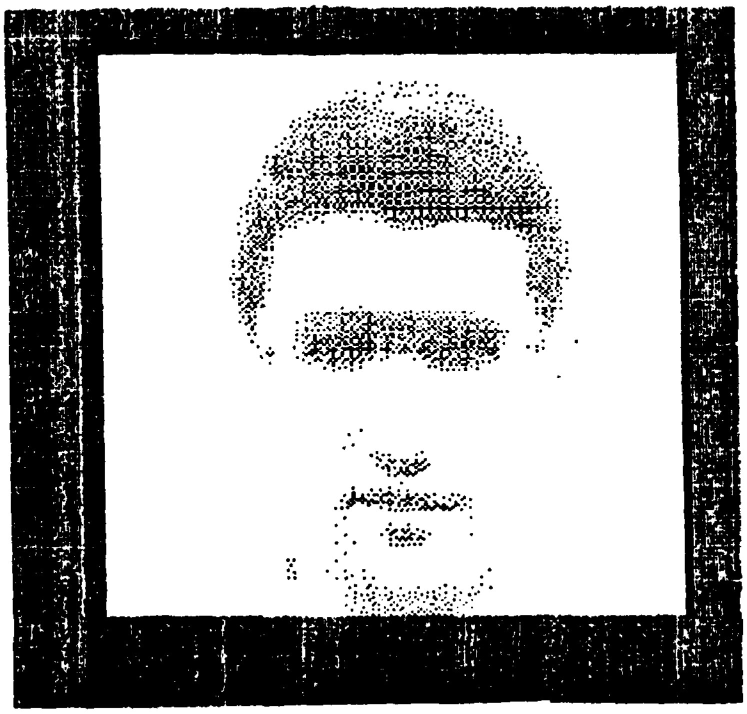

CRON

MONA

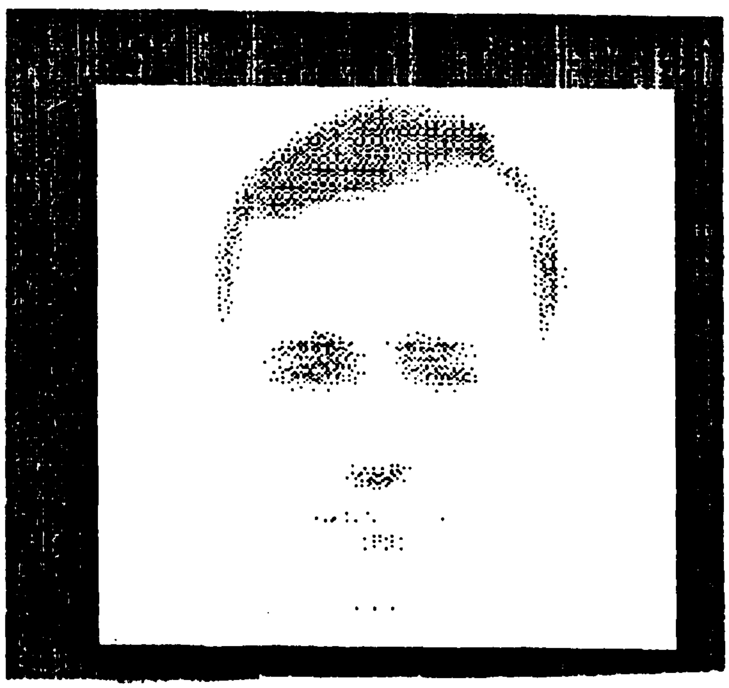

STIERWALT

VITA

Richard LeRoy Routh graduated from the United States Military Academy in 1978 with a B.S. in Applied Engineering with areas of concentration in Nuclear Engineering and Computer Science. He graduated from the University of Phoenix in 1982 with an M.A. in Management. He graduated from the Air Force Institute of Technology in 1983 with an M.S. in Computer Systems.

He currently holds the rank of Captain in the U.S. Army, Signal Corps.

He is married to the former Edith Caroline Nichols of Savannah, Georgia.

His permanent address is:

135 Desert Inn Way
Colorado Springs, CO 80908

UNCLASSIFIED

SECURITY CLASSIFICATION OF THIS PAGE

REPORT DOCUMENTATION PAGE

1a. REPORT SECURITY CLASSIFICATION: UNCLASSIFIED	1b. RESTRICTIVE MARKINGS: N/A
2a. SECURITY CLASSIFICATION AUTHORITY	3. DISTRIBUTION/AVAILABILITY OF REPORT: APPROVED FOR PUBLIC RELEASE; DISTRIBUTION UNLIMITED.
2b. DECLASSIFICATION/DOWNGRADING SCHEDULE	
4. PERFORMING ORGANIZATION REPORT NUMBER(S)	5. MONITORING ORGANIZATION REPORT NUMBER(S)
6a. NAME OF PERFORMING ORGANIZATION: School of Engineering, Air Force Instit. of Technlgy — 6b. OFFICE SYMBOL (If applicable): AFIT/ENG	7a. NAME OF MONITORING ORGANIZATION
6c. ADDRESS (City, State and ZIP Code): Wright-Patterson AFB, OH 45433	7b. ADDRESS (City, State and ZIP Code)
8a. NAME OF FUNDING/SPONSORING ORGANIZATION — 8b. OFFICE SYMBOL (If applicable)	9. PROCUREMENT INSTRUMENT IDENTIFICATION NUMBER
8c. ADDRESS (City, State and ZIP Code)	10. SOURCE OF FUNDING NOS.: PROGRAM ELEMENT NO. / PROJECT NO. / TASK NO. / WORK UNIT NO.
11. TITLE (Include Security Classification): see box 19	
12. PERSONAL AUTHOR(S): Richard LeRoy Routh, Captain, U.S. Army	
13a. TYPE OF REPORT: PhD Dissertation — 13b. TIME COVERED: FROM ____ TO ____	14. DATE OF REPORT (Yr., Mo., Day): July 1985 — 15. PAGE COUNT: 409
16. SUPPLEMENTARY NOTATION: in back	

17. COSATI CODES

FIELD	GROUP	SUB. GR.
06	16	
09	02	

18. SUBJECT TERMS (Continue on reverse if necessary and identify by block number)
BRAIN, COMPUTERS, CEREBRAL CORTEX, BIONICS, REASONING, COMBINATORIAL ANALYSIS, LEARNING, PSYCHOLOGY, (continued on back)

19. ABSTRACT (Continue on reverse if necessary and identify by block number)

Title: CORTICAL THOUGHT THEORY: A WORKING MODEL OF THE HUMAN GESTALT MECHANISM

Thesis Chairman: Matthew Kabrisky, PhD
Professor of Electrical Engineering

Approved for public release: IAW AFR 190-1.
LYNN E. WOLAVER 16 Oct 85
Dean for Research and Professional Development
Air Force Institute of Technology (AFIT)
Wright-Patterson AFB OH 45433

20. DISTRIBUTION/AVAILABILITY OF ABSTRACT: UNCLASSIFIED/UNLIMITED ☒ SAME AS RPT. ☐ DTIC USERS ☐	21. ABSTRACT SECURITY CLASSIFICATION: UNCLASSIFIED
22a. NAME OF RESPONSIBLE INDIVIDUAL: Matthew Kabrisky, Professor, GS-15	22b. TELEPHONE NUMBER (Include Area Code): 513-255-5876 — 22c. OFFICE SYMBOL: AFIT/ENG

DD FORM 1473, 83 APR — EDITION OF 1 JAN 73 IS OBSOLETE.

UNCLASSIFIED

SECURITY CLASSIFICATION OF THIS PAGE

UNCLASSIFIED

SECURITY CLASSIFICATION OF THIS PAGE

ABSTRACT:

A new unified theory of human brain function called Cortical Thought Theory (CTT) was developed which integrates the disciplines of Artificial Intelligence, neurophysiology, perceptual psychology, and theory of computation, to develop the theoretical constraints which determine the form of the solution of the computing architecture which the human brain uses to process information. It was shown that the human gestalt mechanism is probably a singular mechanism of classification and comparison which is used in all domains and at all levels of abstraction of human information processing in the cortex. This gestalt mechanism is central to the operation of human memory access and human inferencing. Most significantly, it was shown that the cardinality of the gestalt feature vector set is two.

This new computing architecture was implemented by simulation and used to process audio (speech) and visual (human face images) inputs. The results were shown to be psychologically compatible with human speech and image perception.

A complete human-like information processing architecture capable of multiple levels of abstract human inferencing was developed which accounts for the human characteristic of direct memory access to the desired information or inference.

The theory also accounts for various types of human learning.

Continued from block 18 - Subject Terms:

ARTIFICIAL INTELLIGENCE
COMPUTER ARCHITECTURE
SPEECH RECOGNITION
IMAGE PROCESSING
PERCEPTION (psychology)

UNCLASSIFIED

SECURITY CLASSIFICATION OF THIS PAGE

UNCLASSIFIED

SECURITY CLASSIFICATION OF THIS PAGE

REPORT DOCUMENTATION PAGE

1a. REPORT SECURITY CLASSIFICATION UNCLASSIFIED	1b. RESTRICTIVE MARKINGS N/A
2a. SECURITY CLASSIFICATION AUTHORITY	3. DISTRIBUTION/AVAILABILITY OF REPORT APPROVED FOR PUBLIC RELEASE; DISTRIBUTION UNLIMITED.
2b. DECLASSIFICATION/DOWNGRADING SCHEDULE	
4. PERFORMING ORGANIZATION REPORT NUMBER(S)	5. MONITORING ORGANIZATION REPORT NUMBER(S)
6a. NAME OF PERFORMING ORGANIZATION School of Engineering Air Force Instit.of Techngy 6b. OFFICE SYMBOL (If applicable) AFIT/ENG	7a. NAME OF MONITORING ORGANIZATION
6c. ADDRESS (City, State and ZIP Code) Wright-Patterson AFB, OH 45433	7b. ADDRESS (City, State and ZIP Code)
8a. NAME OF FUNDING/SPONSORING ORGANIZATION 8b. OFFICE SYMBOL (If applicable)	9. PROCUREMENT INSTRUMENT IDENTIFICATION NUMBER
8c. ADDRESS (City, State and ZIP Code)	10. SOURCE OF FUNDING NOS. PROGRAM ELEMENT NO. / PROJECT NO. / TASK NO. / WORK UNIT NO.
11. TITLE (Include Security Classification) see box 19	

12. PERSONAL AUTHOR(S)
Richard LeRoy Routh, Captain, U.S. Army

13a. TYPE OF REPORT	13b. TIME COVERED	14. DATE OF REPORT (Yr., Mo., Day)	15. PAGE COUNT
PhD Dissertation	FROM ____ TO ____	July 1985	409

16. SUPPLEMENTARY NOTATION

17. COSATI CODES			18. SUBJECT TERMS (Continue on reverse if necessary and identify by block number)
FIELD	GROUP	SUB. GR.	BRAIN, COMPUTERS, CEREBRAL CORTEX,
06	16		BIONICS, REASONING, COMBINATORIAL ANALYSIS,
09	02		LEARNING, PSYCHOLOGY (continued on back)

19. ABSTRACT (Continue on reverse if necessary and identify by block number)

Title: CORTICAL THOUGHT THEORY: A WORKING MODEL OF THE HUMAN GESTALT MECHANISM

Thesis Chairman: Matthew Kabrisky, PhD
Professor of Electrical Engineering

Approved for public release: IAW AFR 190-1.
LYNN E. WOLAVER 16 Oct 85
Dean for Research and Professional Development
Air Force Institute of Technology (ATC)
Wright-Patterson AFB OH 45433

20. DISTRIBUTION/AVAILABILITY OF ABSTRACT	21. ABSTRACT SECURITY CLASSIFICATION
UNCLASSIFIED/UNLIMITED ☒ SAME AS RPT. ☐ DTIC USERS ☐	UNCLASSIFIED

22a. NAME OF RESPONSIBLE INDIVIDUAL	22b. TELEPHONE NUMBER (Include Area Code)	22c. OFFICE SYMBOL
Matthew Kabrisky, Professor, GS-15	513-255-5876	AFIT/ENG

DD FORM 1473, 83 APR EDITION OF 1 JAN 73 IS OBSOLETE.

UNCLASSIFIED

SECURITY CLASSIFICATION OF THIS PAGE

END

FILMED

2-86

DTIC